Development of Synthetic Methods for the Functionalized Tacrines, 1,2,3,4-Tetrahydroacridines, Acridin-4-yl(aryl)methanones, Carbazoles, and β-Carbolines

Thesis

Submitted in partial fulfilment of the requirement

For the Degree of

DOCTOR OF PHILOSOPHY

(In Chemistry)

To

NATIONAL INSTITUTE OF TECHNOLOGY

WARANGAL

By

T. Shirisha

(Roll No. 718165)

Under the supervision of

Dr. Dhurke Kashinath

Professor

Department of Chemistry

National Institute of Technology, Warangal-506004, India

June 2024

DECLARATION

I hereby declare that the research work presented in this thesis entitled ***"Development of Synthetic Methods for the Functionalized Tacrines, 1,2,3,4-Tetrahydroacridines, Acridin-4-yl(aryl)methanones, Carbazoles, and β-Carbolines"*** has been carried out by me under the supervision of **Dr. D. Kashinath**, Professor, Department of Chemistry, National Institute of Technology Warangal. I declare that this work is original and has not been submitted in part or full, for any degree or diploma to this or any other Institute/University.

NIT Warangal **(T. Shirisha)**

28.06.2024

रसायन शास्त्र विभाग
राष्ट्रीय प्रौद्योगिकी संस्थान, वरंगल
तेलंगाना, भारत, पिन-५०४००६
फ़ोन नंबर: +९१-८७०-२४६-२६७७
+९१-८३३-२९६-९५०२
E-mail: kashinath@nitw.ac.in

Department of Chemistry
National Institute of Technology, Warangal
Telangana, INDIA, PIN-506004
Ph. No. +91-870-246-2677
+91-833-296-9502
E-mail: kashinath@nitw.ac.in

Dr. D. Kashinath
Professor

CERTIFICATE

I certify that **Ms. T. Shirisha**, a bonafide student of Ph. D. degree in National Institute of Technology, Warangal, has carried out research work under my direct supervision. The investigations, observations and the conclusions reported by her in this thesis entitled ***"Development of Synthetic Methods for the Functionalized Tacrines, 1,2,3,4-Tetrahydroacridines, Acridin-4-yl(aryl)methanones, Carbazoles, and β-Carbolines"*** being submitted for the award of Ph. D. degree in Chemistry are her original contributions to the Chemical Sciences. It is also certified that she has not submitted the same in part or in full to this or any other University for the award of a degree or diploma.

Date: 28-06-2024 **(Dr. D. Kashinath)**

Residence address: # 401, Vasundhara Mayfair, Chaitanyapuri Colony, Hanamkonda, Warnagal-506 004

ACKNOWLEDGEMENT

It has been a long and wonderful journey since I started my research career in the Organic Research Lab, Department of Chemistry, National Institute of Technology, Warangal. Although, the first year of my Ph.D. was a bit challenging due to new working atmosphere but I was fortunate to join the Department that helped me to overcome and improve my curiosity towards research. Completion of this thesis was impossible without the support and guidance of the people mentioned here.

It gives me immense pleasure to express my sincere gratitude and respect for my supervisor Dr. D. Kashinath, Professor, Department of Chemistry, National Institute of Technology, Warangal for his guidance and unconditional support throughout different stages of my doctoral studies.

I express my sincere thanks to the Directors, National Institute of Technology, Warangal, for giving me the opportunity to carry out my research work. I thank the faculty-in-charges of NMR, LC-HRMS, FT-IR instruments and the staff of the CRIF for their help of recording the analytical data. I am grateful to MoE for providing the fellowship during my Ph. D. tenure.

I express my heartfelt gratitude to former Heads, Department of Chemistry (Prof. Vishnu Shanker and Prof. P. V. Srilakshmi) for their timely help to get fellowship and provided facilities in time to my research.

I express my sincere thanks to my DSC members Prof. V. Rajeswer Rao, Dr. K. Hari Prasad, and Dr. S. Nagarajan of Department of Chemistry and Prof. Prof. Sonawane Shirish Hari of Department of Chemical Engineering for their constructive suggestions and assessing my work progress throughout the tenure of my Ph. D. period.

I take this opportunity to express thanks to the faculty members of the Department of Chemistry, Prof. A. Ramachandraiah, Prof. K. Laxma Reddy, Prof. V. Rajeswer Rao, Prof. K. V. Gobi, Prof. P. V. Srilakshmi, Prof. Vishnu Shankar, Prof. Venkatathri Narayanan, Dr. B. Srinivas, Dr. K. Hari Prasad, Dr. Raghu Chitta, Dr. S. Nagarajan, Dr. M. Raghasudha, Dr. C. Jugun Prakash, Dr. Ravinder Pawar, Dr. Mukul Pradhan, Dr. Rajeshkhanna Gaddam, and Dr. V. Rajeshkumar for their valuable advice, encouragement and moral support.

I would like to express my thanks to Dr. K. Divakar, Department of Biotechnology, Sri Venkateshwara College of Engineering, for his help in the evaluation of cholinesterase and α-glucosidase inhibition activity.

The thesis would not have come to a successful completion, without the help of my lab mates (group members) Dr. S. Nagaraju, Dr. B. Paplal, Dr. K. Sathish, Dr. N. Satyanarayana, Subir Majhi, Bhuvaneshwari, Ankita Parida. Also thankful to co-Scholars Dr. P. Soumya, Dr. G. Shivaparwathi, Dr. A. Naveen, Dr. T. Sanjeeva, Dr. M. Shireesha, Dr. J. Parameshwara Chary, Dr. Ch. Raju, Dr. P. Vinay, Dr. K. Ramaiah, Dr. G. Ambedkar, Dr. P. Babji, Dr. A. Bhargav sai, Dr. T. Dhanunjay Rao, Dr. B. Prasanth, Dr. Ramesh, B. Sravanthi, J. Swathi, R. Vara prasad, R. Arun, K. Madhu, Anjaiha Yadav, Akanksha Ashok Sangolkar, and all the non-teaching staff of the Department of Chemistry.

I also gratefully acknowledge to Venkana, Venu, Shirshindu Mondal (NMR technicians, CRIF, NITW), Srinivas, Naveen (HRMS technicians, CRIF, NITW) for analyses help during my Ph. D. tenure.

I would like to thank my son M. Saikrishna, for his endless patience and understanding while I focused on my Ph.D. His unwavering support kept me going, even on the toughest days. I couldn't have done it without him. The completion of this thesis would not have been possible without the unwavering support, encouragement and affection from my husband Mr. M. Shankara Chary, my beloved parents Mrs. T. Vijayalaxmi, Mr. T. Kishan Rao. My deepest gratitude to my brother Mr. T. Naresh Kumar for always having my back throughout my Ph.D. I would like to express my gratitude to my sister Mrs. K. Harika Vinod, sister-in-law Mrs. T. Sushma, mother-in-law Mrs. Ramamani, niece Lakshmi Sathwika, nephews Pragnan Maruthi, Anirudh Sai, relatives, well-wishers for their caring and constant support during my Ph.D. tenure.

(T. Shirisha)

List of Abbreviations

Aβ	β-Amyloid
AcOH	Acetic acid
ACN	Acetonitrile
AChE	Acetylcholinesterase
AD	Alzheimer's disease
AHMA	3-(9-acridinylamino)-5-hydroxymethylaniline
ARG	Arginine
BBB	Blood-brain barrier
^{t}BuOH	*tert*-butanol
ChCl	Choline chloride
CH_3CN	Acetonitrile
CuI	Copper(I) iodide
$CuSO_4$	Copper sulphate
$Cu(OTf)_2$	Copper(II) triflate
$(NCCl)_3$	Cyanuric chloride
CNS	Central nervous system
^{13}C NMR	Carbon nuclear magnetic resonance
$CDCl_3$	Deuterated chloroform
DABCO	1,4-Diazabicyclo[2.2.2]octane
DACA	Acridine carboxamide
DBU	1,8-Diazabicyclo(5.4.0)undec-7-ene
DCE	1,2-Dichloroethane
DCM	Dichloromethane
DIPEA	*N,N*-Diisopropylethylamine
DESs	Deep Eutectic Solvents
DMAP	4-Dimethylaminopyridine
DMF	Dimethylformamide
DMP	Dess–Martin periodinane
DMSO	Dimethyl sulfoxide
1,3-DMU	1,3-Dimethylurea (N,N'-dimethylurea)

EDCl	l-(3-Dimethylamino-propyl)-ethyl-carbodiimide Hydrochloride
d	Doublets
dd	Doubly doublet
EtOAc	Ethyl acetate
ESI	Electronic supplementary information
Equiv	Equivalent
$FeCl_3$	Iron(III) chloride
h	Hours
HIS	Histidine
H_2O_2	Hydrogen peroxide
HOBT	Hydroxybenzotriazole
HRMS	High-Resolution Mass Spectrometry
Hz	Hertz
I_2	Iodine
IC_{50}	Half maximal inhibitory concentration
IR	Infrared spectroscopy
J	Coupling constant
$K_2S_2O_8$	Potassium persulfate
K_m	Michaelis constant of the enzyme
L-(+)-TA	L-(+)-Tartaric acid
LYS	Lysine
m	Multiplet
m-AMSA	m-Amsacrine
m-CPBA	*meta*-Chloroperoxybenzoic acid
MCRs	Multicomponent reactions
MD	molecular dynamics
MePhos	2-(Dicyclohexylphosphino)-2'-methylbiphenyl
mL	Millilitre
min	Minutes
mg	milligram
μM	Micromolar
mmol	Millimoles

MP	Melting point
MW	Micro wave
Mwt	Molecular weight
NaOAc	Sodium acetate
NH_4OAc	Ammonium acetate
nm	Nanometre
nM	Nanomolar
NMR	Nuclear magnetic resonance
ns	Nanosecond
PDB	Protein Data Bank
$Pd(OAc)_2$	Palladium(II) acetate
Ph	Phenyl
PHE	Phenylalanine
$Ph(IOAc)_2$	(Diacetoxyiodo)benzene
Ph_3P	Triphenyl Phosphine
PTSA	*p*-Toluene sulfonic acid
q	Quartet
QSAR	Quantitative structure-activity relationship
rt	Room temperature
RMSD	Root Mean Square Deviation
s	Singlet
$SnCl_2$	Stannous(II) chloride
t	Triplet
TBAI	Tetrabutylammonium iodide
TBHP	*tert*-Butyl hydroperoxide
TEMPO	(2,2,6,6-Tetramethylpiperidin-1-yl)oxyl
THF	Tetrahydrofuran
TLC	Thin layer chromatography
Et_3N	Triethylamine
TRP	Tryptophan
TYR	Tyrosine
V_{MAX}	Maximal value of reaction rate of an enzyme catalysed reaction

CONTENTS

CHAPTER-1

Chapter-1

Introduction

Abstract

Heterocyclic compounds are important structures in organic chemistry owing to their extensive applications in the synthetic organic chemistry, pharmaceutical and materials chemistry fields. Particularly the presence of hetero atom (nitrogen, oxygen or a combination of these hetero atoms) in five or six-membered carbocycles helps in enhancing the biological efficacy of the molecule. Acridines/tetrahydroacridines are one of the distinguished class of heterocycles predominantly found in natural alkaloids. Many synthetic molecules based on tetrahydroacridines are known for cholinesterase inhibition (Alzheimer's disease). However, there are a few gaps in exploring the chemistry and biology of tacrine (9-amino-1,2,3,4-tetrahydroacrindine). In this background, we have described the design and synthesis of potential acridine and tetrahydroacridine derivatives synthesis via C(sp^3)-H activation under deep eutectic solvent and assessing their potential as cholinesterase and α-glucosidase inhibitory activity in the present thesis. Thus, in this chapter-1, a brief introduction of cholinesterase, α-glucosidase inhibitors, C(sp^3)-H activation and deep eutectic solvent along with an outline of the present work is discussed.

1.1 Introduction to cholinesterase inhibitors

Alzheimer's disease (AD) is a multifactorial age-dependent, chronic neurodegenerative disorder triggered by a diverse set of neurochemical factors and characterized by progressive cholinergic dysfunction, and neuronal loss. This leads to a decline in cognitive abilities, primarily memory, accompanied by altered thinking, behaviour and psychological symptoms of dementia.[1,2] The primary neuropathological feature of brain of AD patients are the misfolding and intracellular accumulation of neurofibrillary tangles of hyperphosphorylated Tau protein or extracellular deposition of senile plaques of amyloid-β-peptide.[3] These pathological changes contribute to a loss of cholinergic neurons in the basal forebrain, resulting in decreased levels of neurotransmitters like acetylcholine, which play a crucial role in cognitive function.[4] Due to the etiopathogenesis of AD involving many targets and signalling pathways, various mechanisms/hypotheses including the acetylcholine hypothesis, amyloid deposition hypothesis, oxidative stress hypothesis and metal ion homeostasis imbalance hypothesis have been described in the literature as shown in **Figure 1.1a**.

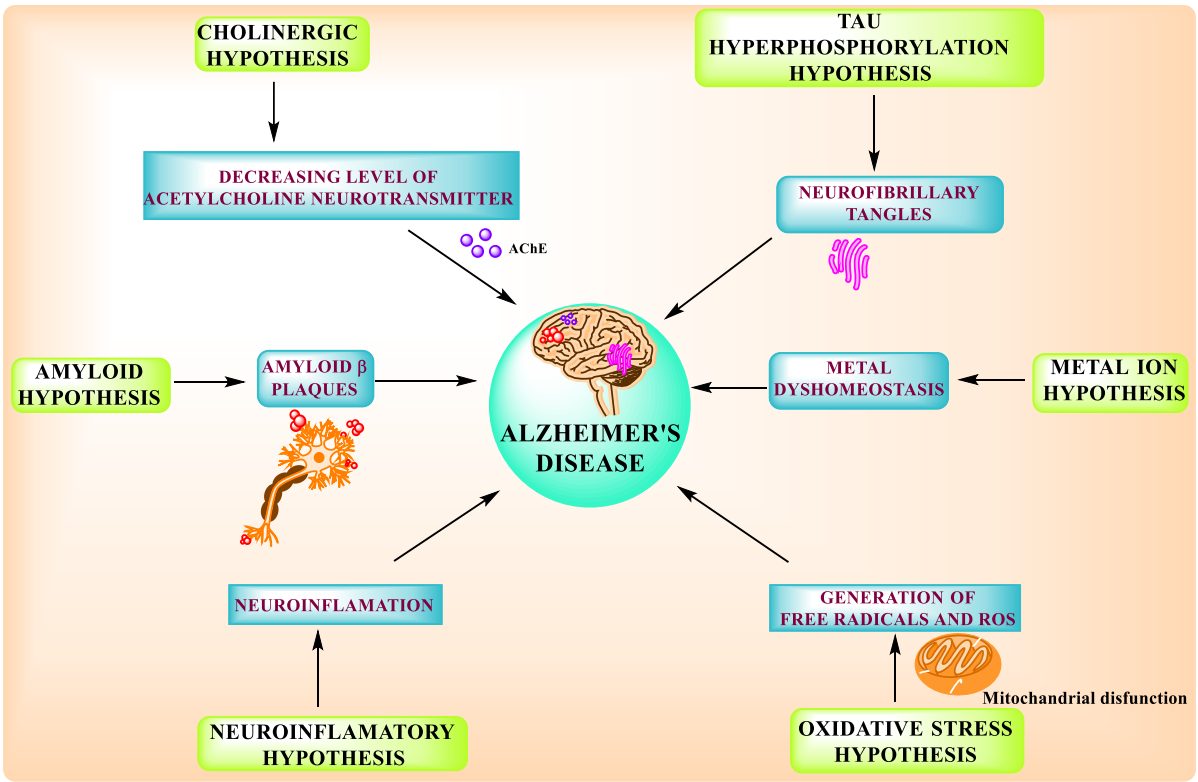

Figure 1.1a Pathophysiology of Alzheimer's Disease

Among the approaches explored for the treatment of AD, i.e., inhibition of acetylcholinesterase (AChE)/butyrylcholinesterase (BChE) using natural/synthetic cholinesterase (ChE) inhibitors were approved as a therapeutic strategy to alleviate the symptoms of AD and delay its progression.[5] Tacrine, donepezil, rivastigmine, and galantamine are the acetylcholinesterase inhibitors that have been approved for commercial use (**Figure 1.1b)**. These drugs promote cholinergic neurotransmission through elevation of acetylcholine (ACh) levels in the central nervous system.[6] Among them, tacrine is approved as an initial cholinesterase inhibitor that acts noncompetitively for Alzheimer's disease. However, its poor pharmacokinetics and toxic effects on the liver led to its withdrawal from the market.[7]

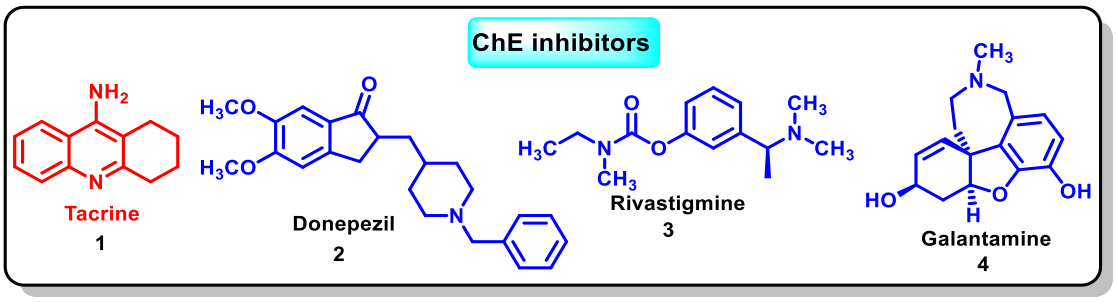

Figure 1.1b FDA approved cholinesterase inhibitors for the treatment of Alzheimer's disease

The AChE enzyme consists of the catalytic binding site (CS) and the peripheral anionic binding site, these active sites are responsible for enzymatic function. AChE inhibitors block the AChE by interacting amino acid residues in the CS (competitive inhibitors) and PAS (non-competitive inhibitors) **Figure 1.1c**.[8]

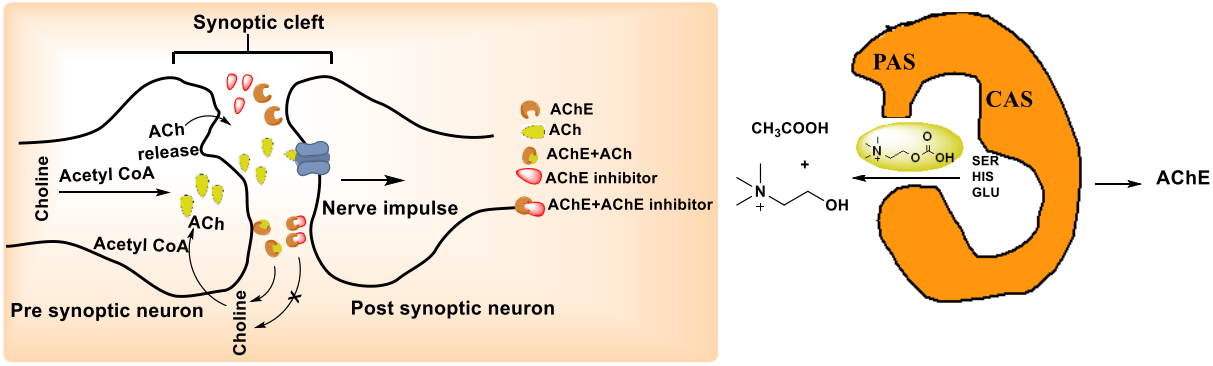

Figure 1.1c Cholinergic hypothesis for the treatment of Alzheimer's disease

Tacrine acts as a specific inhibitor at the catalytic anionic site (CAS) within the CS of AChE. Nevertheless, the inhibitors that promote the dual interaction with the catalytic binding site and peripheral anionic binding site exhibit significantly better inhibitory efficiency.[9] Furthermore,

recent studies demonstrated that the PAS of AChE is important in the formation of Aβ-aggregates, BChE knockout animal model also demonstrated that BChE deficiency reduces the Aβ deposition in Alzheimer's disease.[10] In this context, the development of dual binding site AChE and BChE inhibitors has received great attention to increase inhibitory activity and prevent Aβ-aggregation.[11] However, several dual-binding inhibitors have been synthesized, evaluated and particular emphasis has been paid to the tacrine-based derivatives to profit from tacrine's anti-cholinesterase activity and get rid of associated adverse effects[12] (**Figure 1.1d**).

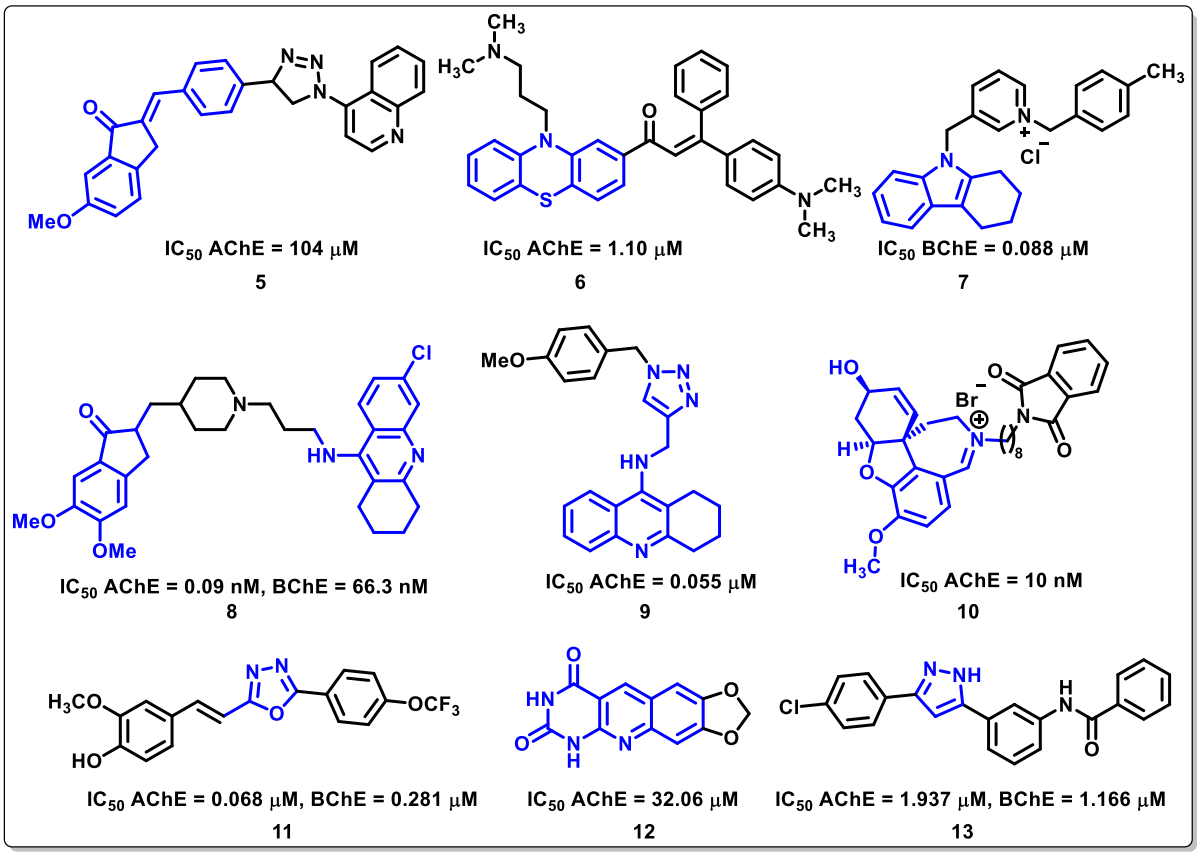

Figure 1.1d Examples of potent cholinesterase inhibitors reported in the literature

1.2 α-Glucosidase inhibitors

Hyperglycaemia or abnormal blood glucose levels, is a metabolic disorder known as Diabetes mellitus. Among various types of diabetes, type 2 diabetes accounts for approximately 90%. The therapeutic treatment for type 2 diabetes encompasses the use of dipeptidyl peptidase-IV (DPP-IV) inhibitors and α-glucosidase inhibitors, glucagon-like peptide-1 (GLP-1) agonists.[13] α-Glucosidase enzyme plays a crucial role in the degradation of carbohydrates into glucose by hydrolysing 1,4-α-glucopyranosidic bonds in oligosaccharide and disaccharide, which are then absorbed and enter into the bloodstream.[14] By inhibiting the α-glucosidase enzyme, the

breakdown of carbohydrates is delayed leading to a decrease in blood glucose levels. As a result, α-glucosidase inhibitors are regarded as an effective and safe treatment for type 2 diabetes. α -Glucosidase inhibitors like acarbose, voglibose and miglitol (**Figure 1.2a**) are used effectively for the treatment of type 2 diabetes.[15]

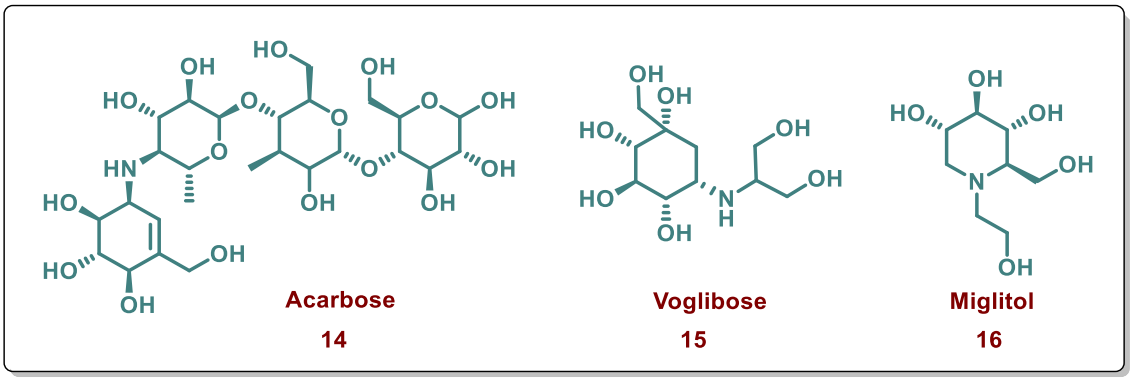

Figure 1.2a α-Glucosidase inhibitors used for the treatment of type 2 diabetes

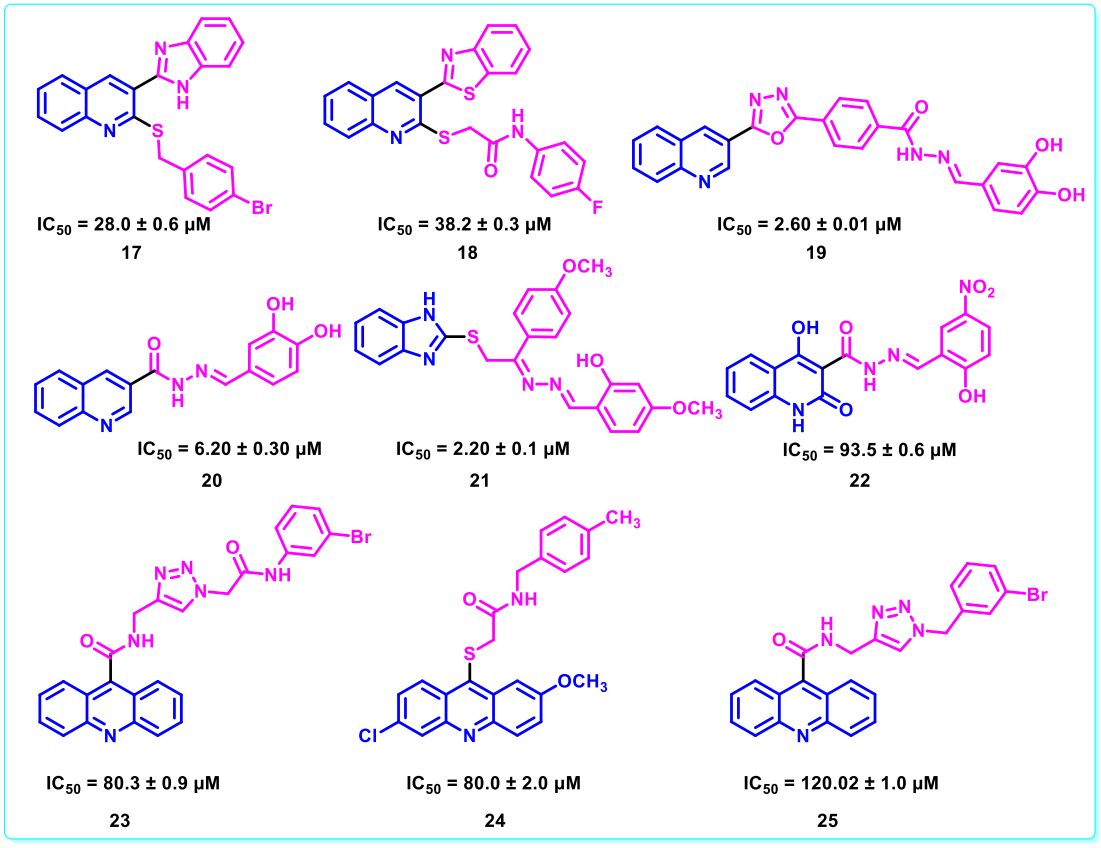

Figure 1.2b Representative examples of α-glucosidase inhibitors

The heterocycle-based α-glucosidase inhibitors have gained attention in the last few years. Many types of scaffolds including benzofuran,[16] triazoles,[17] benzimidazoles,[18] quinolones,[19]

benzothiazoles,[20] imidazoles,[21] isatins,[22] imidazopyridines.[23] quinolines have been proven as effective pharmacophores for α-glucosidase inhibition, providing promising leads with easy synthesis and structural diversity, making them as ideal candidates for antidiabetic drug development.[24] Tricyclic aromatic heterocycles such as acridine,[25] xanthones[26] are also known for their efficacy in inhibiting the enzyme that plays a significant role in carbohydrate hydrolysis. In this regard, a representative example of α-glucosidase inhibitors are shown in **Figure 1.2b**.

1.3 C(sp^3)-H activation

The construction of C-C and C-X bonds (X=N, O, S) is a fundamental objective in organic synthesis. Achieving this through direct C-H activation is considered both atom-economical and in alignment with the principles of green chemistry.[27] In comparison to the more established cross-coupling reactions, C-H activation/functionalization can avoid the pre-functionalization of substrates, hence decreasing step-count. Consequently, the use of precious metal catalysts in high loadings, stoichiometric metal-based oxidants, high temperature and directing group manipulations can be reduced.[28] Towards this, continuous efforts to increase the power of the C–H activation approach by the merger of resource-economical electrochemistry or photochemistry with C–H activation, by employing green solvents are going on.

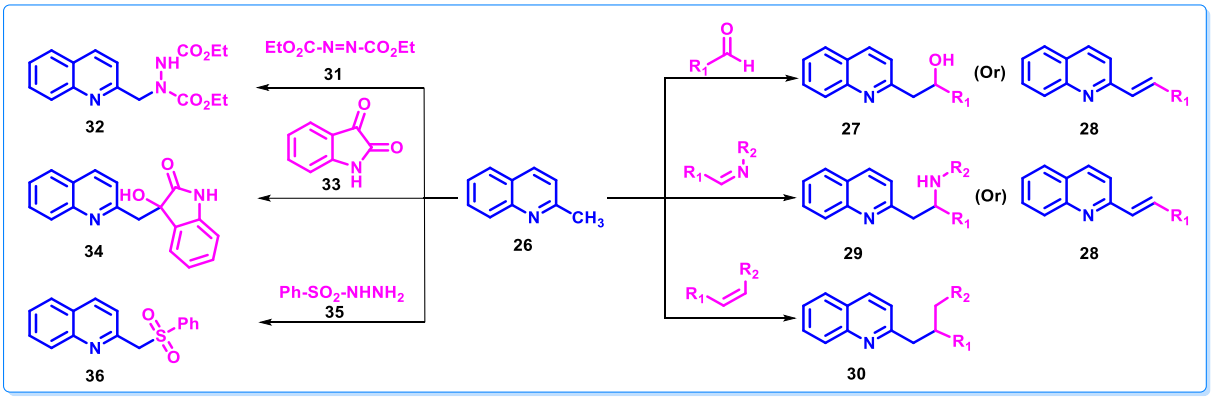

Figure 1.3a Methods for the C(sp^3)-H activation of 2-methyl quinoline

As shown above, the C(sp^3)-H activation/functionalization has been utilised for functionalisation of various scaffolds, including 2-methylquinoline (aza-arenes). The functionalization of the C(sp^3)-H bond in methyl azaarenes is a good approach for the synthesis of biologically active *N*-heterocyclic compounds.[29] Thus, several derivatives of 2-methyl quinoline were synthesised through C(sp^3)-H bond functionalisation. Methyl azarenes, due to

their nucleophilic character, readily react with various activated electrophiles. For instance, the reactions with aldehyde yield β-hydroxy azaarenes,[30] 2-styrylazaarenes,[31] and β-aryl 1,3-bisazaarenes to give functionalized derivatives.[32] In a similar fashion, methyl azarenes react with imines to afford β-amino azaarenes and styryl-azaarenes,[33] while with isatin provide 3-hydroxy azaarenyl indolinones[34] and with ethyl glyoxalates they furnish β-hydroxy esters of azaarenes.[35] Additionally, azaarenes react with dialkyl azodicarboxylates to afford azaarene-containing hydrazines,[36] react with electron-deficient olefins *via* an aza-ene reaction to form C–C bonds,[37] 2-sulfolmethyl quinoline were synthesised *via* C(sp^3)-H sulfonylation of 2-methylquinoline with sulfonating agents (**Figure 1.3a)**.[38] Notably, the C(sp^3)-H activation/ C-X (X = C, N, O, S) bond formation reactions of 2- methylquinoline are facilitated by various catalysts including transition metal catalysts, alkali earth metal catalysts, Lewis's acids, Bronsted acids, ionic liquids.[39]

Styrylazaarenes are distinct among the activated azaarene derivatives due to their potent biological activity. Various synthetic strategies have been devised for the synthesis of 2-styrylquinolines, which relay on the nucleophilicity of 2-methylquinolines (attributed to their ability to adopt an enamine tautomeric form), with various electrophiles like aldehydes, benzyl alcohols, benzyl amines and *N*-benzylidene-4-methylbenzenesulfonamides. Among the synthetic methods for 2-styrylquinolines, some involve the aldol-type condensation of 2-methylquinoline with aldehydes, facilitated by $Ca(OTf)_2$,[40] $InCl_3$,[41] $Fe(OAc)_2$[42] or through the synergistic organocatalysis of 1,3-dimethylbarbituric acid combined with AcOH[43] and catalyst-free activation methods employing 1,4-dioxane[44] or water[45] as reaction medium. Another approach involves alkenylation of 4-methylbenzenesulfonamides with 2-methyl-quinoline facilitated by catalyst $Fe(OAc)_2$,[46] $Cu(OTf)_2$,[47] $Pd(OAc)_2$.[48] Oxidative system like NaCl/TBHP, MnO_2, Pt/Al_2O_3 or microwave condition enables benzyl alcohols to react with 2-methyl quinoline.[49] Similarly, benzylamines also participate in azaarene activation with 2-methyl quinoline to offer 2-styrylquinoline[50] (**Figure 1.3b**).

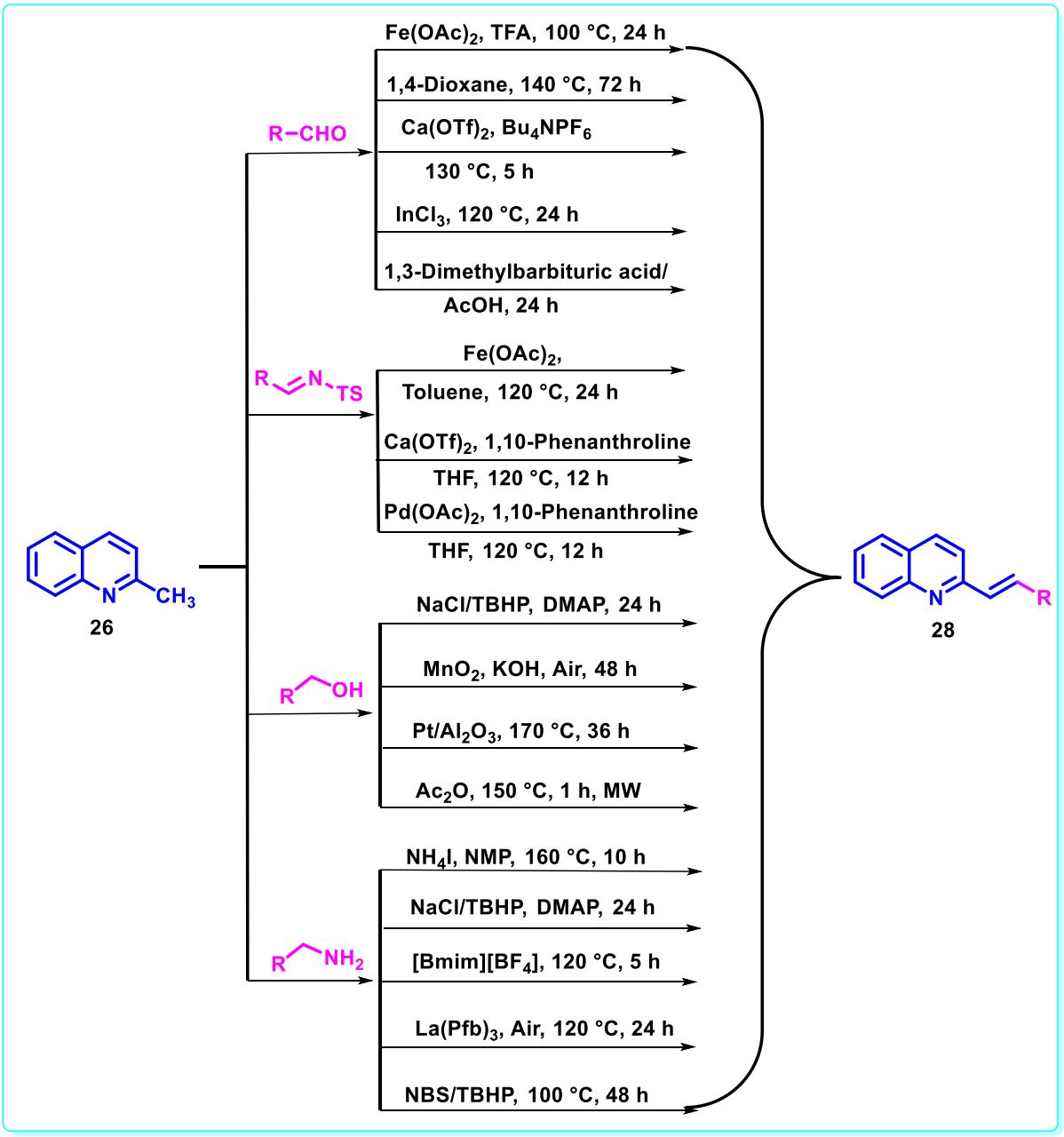

Figure 1.3b Reported methods for the synthesis of 2-Styrylquinolines *via* C(sp^3)-H functionalisation

1.4 Biologically active 1,2,3,4-tetrahydroacridine and acridine molecules

Acridine and 1,2,3,4-tetrahydroacridine derivatives constitute a prominent group of nitrogen-containing heterocycles due to their enormous range of biological activities.[51] Numerous natural and synthetic acridines have been extensively investigated as prospective therapeutic agents for the treatment of cancer,[52] Alzheimer's disease, bacterial and protozoan infections,[53] anti-tuberculosis,[54] anti-herpes[55] and α-glucosidase inhibition[56] (**Figure 1.4**). Beyond their biological activities, these acridines have garnered significant attention in recent years in the

area of materials science because of their promising photophysical and electrochemical characteristics as organic electronic devices and organic light-emitting diodes.[57]

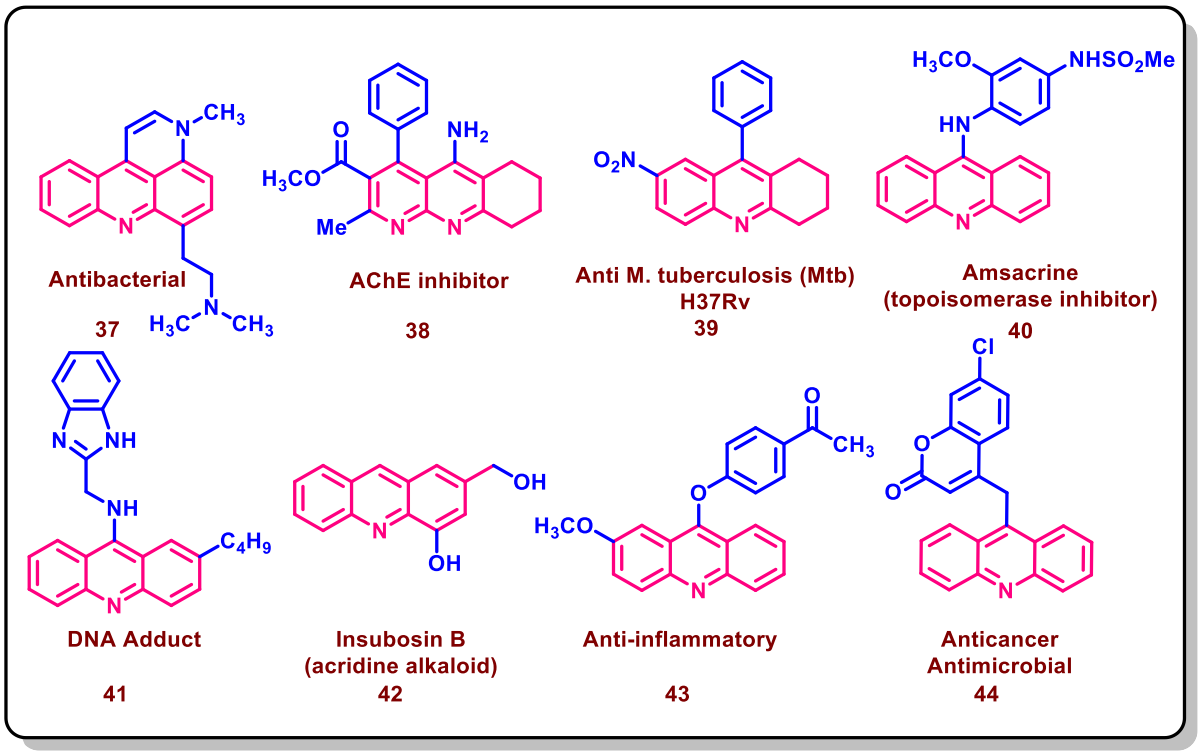

Figure 1.4 Biologically active tetrahydroacridine and acridine derivatives

1.5 Deep Eutectic Solvents

Deep eutectic solvents (DESs) popularly known as 21st century solvents have emerged as a new class of solvents exhibiting significant potential for sustainable applications in synthetic chemistry.[58] DESs offer an environmentally benign alternative to conventional organic solvents. They exhibit distinct physical and chemical characteristics such as non-toxicity, biodegradability, and use of inexpensive/ readily available reagents for the preparation.[59] These are formed by mixing hydrogen bond donor and hydrogen bond acceptor (**Figure 1.5**), which are capable of having self-association with intermolecular hydrogen bonding. These two components collectively form a transparent liquid at or below 100 °C whose melting points are higher than that of two independent components.[60] DESs have been used in various applications, including organic transformations, metal-catalyzed organic reactions, biotransformations, polymerization reactions, metal processing applications, biomass processing, biodiesel synthesis, and separation processes.[61] The DES mixture enhances the reactivity of the reaction mixture with the formation of strong hydrogen bonding with the

starting materials. Thus, they became the preferred reaction media and catalysts in organic synthesis.

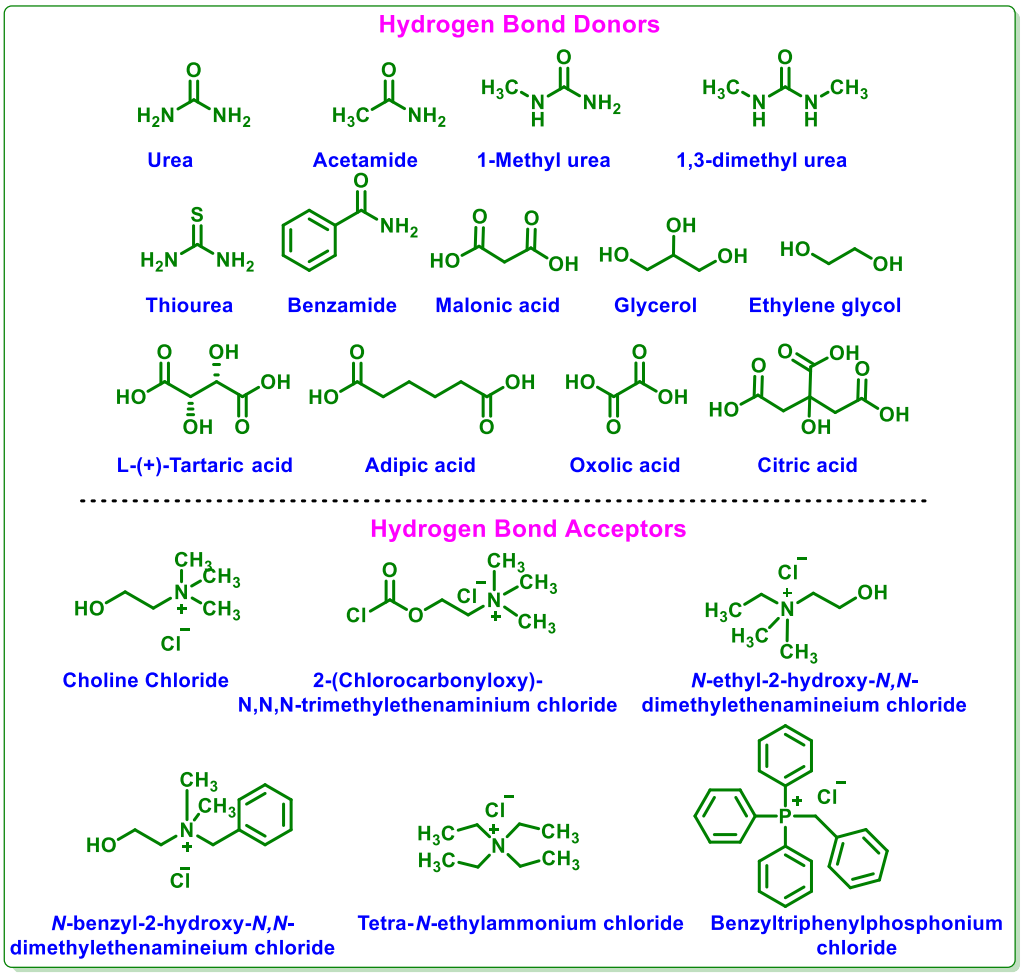

Figure 1.5 Representative examples of hydrogen bond donors (HBDs) and hydrogen bond acceptors (HBAs) used in the preparation of DES

1.6 General objectives of the thesis: Alzheimer's disease (AD) is a brain (neuronal) disorder. The symptoms of the disease are gradual decreases in memory leading to the behavioural changes that affect a person's ability to function. About 55 million people around the globe are suffering from this disease and the addition of new cases is alarming. Many researchers are working in medicinal chemistry to find new molecules for AD and associated diseases. In this regard, we planned the synthesis of new molecules in the present thesis with the following objectives

a) Identification of the gaps in the literature for possible modifications of known molecules like **tacrine/1,2,3,4-tetrahydroacridine** using molecular docking studies
b) Synthesis of new molecules based on the results of molecular docking studies

c) Evaluation of the newly synthesized molecules for the acetyl/butyrylcholinesterase inhibition (one of the ways of treating AD)
d) In addition to this, testing of the synthesized molecules for other therapeutic areas like type 2 diabetes (α-Glucosidase inhibition)
e) Development of new methods for the synthesis of other biological scaffolds like **Acridines**, **Carbazoles,** and **β-Carbolines**
f) Use of "aza-arene activation" [i.e. C(sp^3)-H functionalization of aza-arene under metal-free conditions] and green chemistry concepts [Deep Eutectic Solvents] as reaction medium for the synthesis of the molecules

With the above objectives and based on the findings, the thesis has been titled ***"Development of synthetic methods for the functionalized Tacrines, 1,2,3,4-Tetrahydroacridines, Acridin-4-yl(aryl)methanones, Carbazoles, and β-Carbolines"*** and divided into **four chapters** as follows

Chapter-I: Introduction to Cholinesterase and α-Glucosidase inhibitors, Metal-based and metal-free C(sp^3)-H activation/functionalization, Deep Eutectic Solvents (DES)

Chapter-II: Synthesis of functionalized tacrine/1,2,3,4-tetrahydroacridine, Pfitzinger acid derivatives and their evaluation for dual cholinesterase and α-glucosidase inhibition

Chapter-III: Part-A: Metal-free C4 C(sp^3)-H functionalization of 1,2,3,4-tetrahydroacridines using dialkyl azodicarboxylates and *N*-phenylmaleimide in Deep Eutectic Solvent

Chapter-III: Part-B: TBHP-TBAI Mediated synthesis of 2,3-dihydroacridin-4(*1H*)-ones *via* C4 C(sp^3)-H sulfonylation and desulfonylation of 1,2,3,4-tetrahydroacridines

Chapter-III: Part-C: DDQ Mediated synthesis of acridin-4-yl(aryl)methanones *via* aromatization-C(sp^2)-H oxidation sequence of C4-functionalized 1,2,3,4-tetrahydroacridine derivatives

Chapter-IV ~~(Appendix)~~: One-Pot Synthesis of Functionalized Carbazoles and *β*-Carbolines *via* Diethyl Azodicarboxylate Mediated Dehydrogenative Aromatization in Deep Eutectic Solvent

In correlation with the objectives/titles, a brief discussion on the biologically active molecules of respective chapters, the synthetic methods reported along with the detailed discussion on the results obtained in the present investigation including biological activity will be discussed in the thesis.

1.7 References

(1) (a) Hussein, W.; Sağlık, B. N.; Levent, S.; Korkut, B.; Ilgın, S.; Özkay, Y.; Kaplancıklı, Z. A. *Molecules* **2018,** *23*, 2033. (b) Vitorović-Todorović, M. D.; Juranić, I. O.; Mandić, L. M.; Drakulić, B. J. *Bioorg. Med. Chem.* **2010**, *18*, 1181–1193.

(2) Singh, M.; Kaur, M.; Chadha, N.; Silakari, O. *Mol. Divers.* **2016**, *20*, 271–297.

(3) (a) Mroueh, M.; Faour, W. H.; Shebaby, W. N.; Daher, C. F.; Ibrahim, T. M.; Ragab, H. M. *Bioorg. Chem.* **2020**, *100*, 103895. (b) Wang, Y.; Wang, F.; Yu, J.-P.; Jiang, F.-C.; Guan, X.-L.; Wang, C.-M.; Li, L.; Cao, H.; Li, M.-X.; Chen, J.-G. *Bioorg. Med. Chem.* **2012**, *20* (21), 6513–6522.

(4) (a) Gao, H.; Jiang, Y.; Zhan, J.; Sun, Y. *Bioorg. Chem.* **2021**, *114*, 105149. (b) Chen, Y.; Lin, H.; Zhu, J.; Gu, K.; Li, Q.; He, S.; Lu, X.; Tan, R.; Pei, Y.; Wu, L.; Bian, Y.; Sun, H. *RSC Adv.* **2017**, *7*, 33851–33867. (c) Vecchio, I.; Sorrentino, L.; Paoletti, A.; Marra, R.; Arbitrio, M. *J. Cent. Nerv. Syst. Dis.* **2021**, *13*, 1–13.

(5) (a) Girek, M.; Szymański, P. *Chem. Pap.* **2019**, *73*, 269–289. (b) Zhang, C.; Du, Q. Y.; Chen, L. D.; Wu, W. H.; Liao, S. Y.; Yu, L. H.; Liang, X. T. *Eur. J. Med. Chem.* **2016**, *116*, 200–209. (b) Więckowska, A.; Kołaczkowski, M.; Bucki, A.; Godyń, J.; Marcinkowska, M.; Więckowski, K.; Zaręba, P.; Siwek, A.; Kazek, G.; Głuch-Lutwin, M.; Mierzejewski, P.; Bienkowski, P.; Sienkiewicz-Jarosz, H.; Knez, D.; Wichur, T.; Gobec, S.; Malawska, B. *Eur. J. Med. Chem.* **2016**, *124*, 63–81. (c) Zhang, P.; Xu, S.; Zhu, Z.; Xu, J. *Eur. J. Med. Chem.* **2019**, *176*, 228–247.

(6) (a) Obaid, R. J.; Naeem, N.; Mughal, E. U.; Al-Rooqi, M. M.; Sadiq, A.; Jassas, R. S.; Moussa, Z.; Ahmed, S. A. *RSC Adv.* **2022**, *12*, 19764–19855. (b) Eghtedari, M.; Sarrafi, Y.; Nadri, H.; Mahdavi, M.; Moradi, A.; Homayouni Moghadam, F.; Emami, S.; Firoozpour, L.; Asadipour, A.; Sabzevari, O.; Foroumadi, A. *Eur. J. Med. Chem.* **2017**, *128*, 237–246.

(7) (a) Jalili-Baleh, L.; Nadri, H.; Moradi, A.; Bukhari, S. N. A.; Shakibaie, M.; Jafari, M.; Golshani, M.; Homayouni Moghadam, F.; Firoozpour, L.; Asadipour, A.; Emami, S.; Khoobi, M.; Foroumadi, A. *Eur. J. Med. Chem.* **2017**, *139*, 280–289.

(8) Najafi, Z.; Mahdavi, M.; Saeedi, M.; Karimpour-Razkenari, E.; Asatouri, R.; Vafadarnejad, F.; Moghadam, F. H.; Khanavi, M.; Sharifzadeh, M.; Akbarzadeh, T. *Eur. J. Med. Chem.* **2017**, *125*, 1200–1212.

(9) Mohammadi-Khanaposhtani, M.; Mahdavi, M.; Saeedi, M.; Sabourian, R.; Safavi, M.; Khanavi, M.; Foroumadi, A.; Shafiee, A.; Akbarzadeh, T. *Chem. Biol. Drug Des.* **2015**, *86*, 1425–1432.

(10) Wu, W. Y.; Dai, Y. C.; Li, N. G.; Dong, Z. X.; Gu, T.; Shi, Z. H.; Xue, X.; Tang, Y.-P.; Duan, J. A. *J. Enzyme Inhib. Med. Chem.* **2017**, *32*, 572–587.

(11) Sameem, B.; Saeedi, M.; Mahdavi, M.; Shafiee, A. *Eur. J. Med. Chem.* **2017**, *128*, 332–345.

(12) (a) Obaid, R. J.; Naeem, N.; Mughal, E. U.; Al-Rooqi, M. M.; Sadiq, A.; Jassas, R. S.; Moussa, Z.; Ahmed, S. A. *RSC Adv.* **2022**, *12*, 19764–19855. (b) Mantoani, S.; Chierrito, T.; Vilela, A.; Cardoso, C.; Martínez, A.; Carvalho, I. *Molecules* **2016**, *21*, 193. (c) Tran, T. S.; Le, M. T.; Nguyen, T. C. V.; Tran, T. H.; Tran, T. D.; Thai, K. M. *Molecules* **2020**, *25*, 3916. (d) Ghobadian, R.; Mahdavi, M.; Nadri, H.; Moradi, A.; Edraki, N.; Akbarzadeh, T.; Sharifzadeh, M.; Bukhari, S. N. A.; Amini, M. *Eur. J. Med. Chem.* **2018**, *155*, 49–60. (e) Najafi, Z.; Mahdavi, M.; Saeedi, M.; Karimpour-Razkenari, E.; Asatouri, R.; Vafadarnejad, F.; Moghadam, F. H.; Khanavi, M.; Sharifzadeh, M.; Akbarzadeh, T. *Eur. J. Med. Chem.* **2017**, *125*, 1200–1212. (f) Tripathi, A.; Choubey, P. K.; Sharma, P.; Seth, A.; Saraf, P.; Shrivastava, S. K. *Bioorg. Chem.* **2020**, *95*, 103506.

(13) Moghadam Farid, S.; Noori, M.; Nazari Montazer, M.; Khalili Ghomi, M.; Mollazadeh, M.; Dastyafteh, N.; Irajie, C.; Zomorodian, K.; Mirfazli, S. S.; Mojtabavi, S.; Faramarzi, M. A.; Larijani, B.; Iraji, A.; Mahdavi, M. *Sci. Rep.* **2023**, *13*, 4392.

(14) Dhameja, M.; Gupta, P. *Eur. J. Med. Chem.* **2019**, *176*, 343–377.

(15) Ghani, U. *Eur. J. Med. Chem.* **2015**, *103*, 133–162.

(16) Azimi, F.; Azizian, H.; Najafi, M.; Khodarahmi, G.; Saghaei, L.; Hassanzadeh, M.; Ghasemi, J. B.; Faramarzi, M. A.; Larijani, B.; Hassanzadeh, F.; Mahdavi, M. *Sci. Rep.* **2021**, *11*, 20776.

(17) Iraji, A.; Shareghi-Brojeni, D.; Mojtabavi, S.; Faramarzi, M. A.; Akbarzadeh, T.; Saeedi, M. *Sci. Rep.* **2022**, *12*, 8647.

(18) Rahim, F.; Zaman, K.; Taha, M.; Ullah, H.; Ghufran, M.; Wadood, A.; Rehman, W.; Uddin, N.; Shah, S. A. A.; Sajid, M.; Nawaz, F.; Khan, K. M. *Bioorg. Chem.* **2020**, *94*, 103394.

(19) Shayegan, N.; Haghipour, S.; Tanideh, N.; Moazzam, A.; Mojtabavi, S.; Faramarzi, M. A.; Irajie, C.; Parizad, S.; Ansari, S.; Larijani, B.; Hosseini, S.; Iraji, A.; Mahdavi, M. *Sci. Rep.* **2023**, *13*, 6304.

(20) Ghomi, M. K.; Dastyafteh, N.; Montazer, M. N.; Noori, M.; Mojtabavi, S.; Faramarzi, M. A.; Hashemi, S. M.; Mahdavi, M. *Sci. Rep.* **2024**, *14*, 501.

(21) Naureen, S.; Chaudhry, F.; Munawar, M. A.; Ashraf, M.; Hamid, S.; Khan, M. A. *Bioorg. Chem.* **2018**, *76*, 365–369.

(22) Rahim, F.; Malik, F.; Ullah, H.; Wadood, A.; Khan, F.; Javid, M. T.; Taha, M.; Rehman, W.; Ur Rehman, A.; Khan, K. M. *Bioorg. Chem.* **2015**, *60*, 42–48.

(23) (a) Taha, M.; Sultan, S.; Imran, S.; Rahim, F.; Zaman, K.; Wadood, A.; Rehman, A. U.; Uddin, N.; Mohammed Khan, K. *Bioorg. Med. Chem.* **2019**, *27*, 4081–4088. (b) Taha, M.; Ismail, N. H.; Imran, S.; Wadood, A.; Rahim, F.; Ali, M.; Rehman, A. U. *Med. Chem. Comm.* **2015**, *6*, 1826–1836.

(24) (a)Asgari, M. S.; Tahmasebi, B.; Mojtabavi, S.; Faramarzi, M. A.; Rahimi, R.; Ranjbar, P. R.; Biglar, M.; Larijani, B.; Rastegar, H.; Mohammadi-Khanaposhtani, M.; Mahdavi, M. *J. Heterocycl. Chem.* **2020**, *57*, 4348–4357. (c) Narayanaswamy, L.; Yarrappagaari, S.; Cheemanapallia, S.; Saddala, R. R.; Vijayakumar, V. *Struct. Chem.* **2020**, *31*, 2063–2074. (d) Sepehri, N.; Asemanipoor, N.; Mousavianfard, S. A.; Hoseini, S.; Faramarzi, M. A.; Adib, M.; Biglar, M.; Larijani, B.; Hamedifar, H.; Mohammadi-Khanaposhtani, M.; Mahdavi, M. *Med. Chem. Res.* **2020**, *29*, 1836–1845.

(25) Mohammadi-Khanaposhtani, M.; Rezaei, S.; Khalifeh, R.; Imanparast, S.; Faramarzi, M. A.; Bahadorikhalili, S.; Safavi, M.; Bandarian, F.; Nasli Esfahani, E.; Mahdavi, M.; Larijani, B. *Bioorg. Chem.* **2018**, *80*, 288–295.

(26) Santos, C. M. M.; Freitas, M.; Fernandes, E. *Eur. J. Med. Chem.* **2018**, *157*, 1460–1479.

(27) (a) Gao, Q.H.; Fei, Z.; Zhu, Y.-P.; Lian, M.; Jia, F. C.; Liu, M. C.; She, N. F.; Wu, A. X. *Tetrahedron* **2013**, *69* (1), 22-28. (b) Khake, S. M.; Chatani, N. *Chem* **2020**, *6*, 1056–1081. (c) Mishra, A. A.; Subhedar, D.; Bhanage, B. M. *Chem. Rec.* **2019**, *19*, 1829–1857.

(28) Dalton, T.; Faber, T.; Glorius, F. *ACS Cent. Sci.* **2021**, *7*, 245–261.

(29) Latha, D. S.; Yaragorla, S. *Eur. J. Org. Chem.* **2020**, *2020*, 2155–2179.

(30) Nageswara Rao, N.; Meshram, H. M. *Tetrahedron Lett.* **2013**, *54*, 5087–5090.

(31) Mao, D.; Hong, G.; Wu, S.; Liu, X.; Yu, J.; Wang, L. *Eur. J. Org. Chem.* **2014**, *2014*, 3009-3019.

(32) Jin, J.; Wang, D.; Niu, H.; Wu, S.; Qu, G.; Zhang, Z.; Guo, H. *Tetrahedron* **2013**, *69*, 6579–6584.

(33) Yan, Y.; Xu, K.; Fang, Y.; Wang, Z. *J. Org. Chem.* **2011**, *76*, 6849–6855.

(34) Kumari, K.; Allam, B. K.; Singh, K. N. *RSC Adv* **2014**, *4*, 19789–19793.

(35) Jin, J. J.; Niu, H. Y.; Qu, G. R.; Guo, H. M.; Fossey, J. S. *RSC Adv.* **2012**, *2*, 5968.

(36) Liu, J. Y.; Niu, H. Y.; Wu, S.; Qu, G. R.; Guo, H. M. *Chem. Commun.* **2012**, *48*, 9723.

(37) Li, H. Y.; Xing, L. J.; Xu, T.; Wang, P.; Liu, R. H.; Wang, B. *Tetrahedron Lett.* **2013**, *54*, 858–860.

(38) Xiao, F.; Chen, S.; Chen, Y.; Huang, H.; Deng, G.-J. *Chem. Commun.* **2015**, *51*, 652–654.

(39) (a) Singh, G.; Yaragorla, S. *RSC Adv.* **2017**, *7*, 18874–18882. (b)Zhang, X.-Y.; Dong, D.-Q.; Yue, T.; Hao, S.-H.; Wang, Z.-L. *Tetrahedron Lett.* **2014**, *55*, 5462–5464. (c) Niu, R.; Xiao, J.; Liang, T.; Li, X. *Org. Lett.* **2012**, *14*, 676–679. (d) Komai, H.; Yoshino, T.; Matsunaga, S.; Kanai, M. *Org. Lett.* **2011**, *13*, 1706–1709. (e) Yaragorla, S.; Dada, R.; Singh, G. *Synlett* **2015**, *27*, 912–918.

(40) Yaragorla, S.; Singh, G.; Dada, R. *Tetrahedron Lett.* **2015**, *56*, 5924–5929.

(41) Jamal, Z.; Teo, Y.-C.; Lim, G. S. *Tetrahedron* **2016**, *72*, 2132–2138.

(42) Pi, D.; Jiang, K.; Zhou, H.; Sui, Y.; Uozumi, Y.; Zou, K. *RSC Adv.* **2014**, *4*, 57875–57884.

(43) (a) Liang, E.; Wang, J.; Wu, Y.; Huang, L.; Yao, X.; Tang, X. *Adv. Synth. Catal.* **2019**, *361*, 3619–3623. (b) Yan, Y.; Xu, K.; Fang, Y.; Wang, Z. *J. Org. Chem.* **2011**, *76*, 6849–6855.

(44) Xu, L.; Shao, Z.; Wang, L.; Zhao, H.; Xiao, J. *Tetrahedron Lett.* **2014**, *55*, 6856–6860.

(45) Fu, S.; Wang, L.; Dong, H.; Yu, J.; Xu, L.; Xiao, J. *Tetrahedron Lett.* **2016**, *57*, 4533–4536.

(46) Qian, B.; Xie, P.; Xie, Y.; Huang, H. *Org. Lett.* **2011**, *13*, 2580–2583.

(47) Rueping, M.; Tolstoluzhsky, N. *Org. Lett.* **2011**, *13*, 1095–1097.

(48) Qian, B.; Guo, S.; Shao, J.; Zhu, Q.; Yang, L.; Xia, C.; Huang, H. *J. Am. Chem. Soc.* **2010**, *132*, 3650–3651.

(49) (a) Zhang, C.; Li, Z.; Fang, Y.; Jiang, S.; Wang, M.; Zhang, G.; *Tetrahedron* **2020**, *76*, 130968. (b) Chaudhari, C.; Hakim Siddiki, S. M. A.; Shimizu, K. *Tetrahedron Lett.* **2013**, *54*, 6490–6493. (c) Hazra, S.; Tiwari, V.; Verma, A.; Dolui, P.; Elias, A. J. *Org. Lett.* **2020**, *22*, 5496–5501. (d) Staderini, M.; Cabezas, N.; Bolognesi, M.; Menéndez, J. *Synlett* **2011**, *2011*, 2577–2579.

(50) (a) Gong, L.; Xing, L.-J.; Xu, T.; Zhu, X.-P.; Zhou, W.; Kang, N.; Wang, B. *Org. Biomol. Chem.* **2014**, *12*, 6557–6560. (b) Li, X.; Huang, B.; Wang, J.; Zhang, Y.; Liao, W. *J. Chem. Res.* **2021**, *45*, 903–910. (c) Mao, D.; Zhu, X.; Hong, G.; Wu, S.; Wang, L. *Synlett* **2016**, *27*, 2481–2484. (d) Sharma, R.; Abdullaha, M.; Bharate, S. B. *J. Org. Chem.* **2017**, *82*, 9786-9793.

(51) Kowalewska, M. G.; Cholewiński, G.; Dzierzbicka, K. *RSC Adv*. **2017**, *7*, 15776–15804.

(52) (a) Arya, S.; Kumar, A.; Kumar, N.; Roy, P.; Sondhi, S. M. *Med. Chem. Res.* **2015**, *24*, 1942–1951. (b) Patel, M. M.; Mali, M. D.; Patel, S. K. *Bioorg. Med. Chem. Lett.* **2010**, *20*, 6324–6326.

(53) (a) Zhang, B.; Li, X.; Li, B.; Gao, C.; Jiang, Y. *Expert Opin. Ther. Patents*. **2014**, *24*, 6. (b) Fathhalla, O. A.; Mohamed, M. S.; Farag, M. A.; Ismail, R. S. A. *Res. Chem. Intermed*. **2013**, *39*, 3487–3505. (c) Singh, M.; Kaur, M.; Chadha, N.; Silakari, O. *Mol. Divers*. **2016**, *20*, 271–297. (d) Prameela, S.; Nawaz Khan, F. R. *Eur. J. Org. Chem*. **2020**, *33*, 5394–5410.

(54) Muscia, G. C.; Buldain, G. Y.; Asís, S. E. *Eur. J. Med. Chem.* **2014**, *73*, 243–249.

(55) Goodell, J. R.; Madhok, A. A.; Hiasa, H.; Ferguson, D. M. *Bioorg. Med. Chem.* **2006**, *14*, 5467-5480.

(56) (a) Asgari, M. S.; Tahmasebi, B.; Mojtabavi, S.; Faramarzi, M. A.; Rahimi, R.; Ranjbar, P. R.; Biglar, M.; Larijani, B.; Rastegar, H.; Khanaposhtani, M. M.; Mahdavi, M. *J. Heterocycl. Chem*. **2020,** *57*, 4348–4357. (b) Sepehri, N.; Asemanipoor, N.; Mousavianfard, S. A.; Hoseini, S.; Faramarzi, M. A.; Adib, M.; Biglar, M.; Larijani, B.; Hamedifar, H.; Khanaposhtani, M. M.; Mahdavi, M. *Med. Chem. Res*. **2020**, *29*, 1836–1845.

(57) (a) Tka, N.; Ayed, M. A. H.; Braiek, M. B.; Jabli, M.; Chaaben, N.; Kamel, A.; Stefan, J.; Langer, P. *Beilstein J. Org. Chem*. **2021**, *17*, 1629–1640.

(58) Hansen, B. B.; Spittle, S.; Chen, B.; Poe, D.; Zhang, Y.; Klein, J. M.; Horton, A.; Adhikari, L.; Zelovich, T.; Doherty, B. W.; Gurkan, B.; Maginn, E. J.; Ragauskas, A.; Dadmun, M.; Zawodzinski, T. A.; Baker, G. A.; Tuckerman, M. E.; Savinell, R. F.; Sangoro, J. R. *Chem. Rev.* **2021**, *121*, 1232–1285.

(59) Zhang, Q.; De Oliveira Vigier, K.; Royer, S.; Jérôme, F. *Chem. Soc. Rev.* **2012**, *41*, 7108.

(60) Smith, E. L.; Abbott, A. P.; Ryder, K. S. *Chem. Rev.* **2014**, *114*, 11060–11082.

(61) (a) Hooshmand, S. E.; Afshari, R.; Ramón, D. J.; Varma, R. S. *Green Chem.* **2020**, *22*, 3668–3692. (b) Longo Jr., L.; Craveiro, M. *J. Braz. Chem. Soc.* **2018**, *29*, 1999-2025. (c) Alonso, D. A.; Baeza, A.; Chinchilla, R.; Guillena, G.; Pastor, I. M.; Ramón, D. J. *Eur. J. Org. Chem.* **2016**, *2016*, 612–632. (d) Ling, J. K. U.; Hadinoto, K. *Int. J. Mol. Sci.* **2022**, *23*, 3381.

CHAPTER-2

Chapter-2

Synthesis of Functionalized Tacrine/1,2,3,4-Tetrahydroacridine, Pfitzinger Acid Derivatives and Their Evaluation for Dual Cholinesterase and α-Glucosidase Inhibition

Abstract

Tacrine (9-amino-1,2,3,4-tetrahydroacridine) is approved as initial cholinesterase inhibitor used for the treatment of Alzheimer's disease. Due to its sub-optimal pharmacokinetics and toxic effects on the liver led to its withdrawn from the market. However, tacrine remains a compound of interest for AD treatment. Researchers designed and synthesised various derivatives of tacrine as potent cholinesterase inhibitors. Following this approach, we intended to develop C4 functionalised tacrine/tetrahydroacridine derivatives as potent cholinesterase inhibitors. Thus, in this chapter, we have described an efficient strategy for the synthesis of C4 arylidenes, C9 modified (N-aryl, triazoles, acids, esters, and amides) tetrahydroacridine/tacrine derivatives and biological evaluation for dual cholinesterase and α-glucosidase inhibitory activity.

2. Introduction

Tacrine (9-amino-1,2,3,4-tetrahydroacridine; **TA**), a competitive cholinesterase inhibitor is the first drug used for the treatment of AD[1] that complexes with AChE through Vander Waals interactions and charge-transfer involving π electrons at the peripheral site on the enzyme. It also interacts with the catalytic site of AChE through electrostatic interactions with tryptophan, phenylamine and hydrogen bonds with histidine. Unfortunately, poor pharmacokinetics and hepatotoxicity associated with the administration of TA led to its withdrawal from the market.[2] Notably, tacrine induced liver toxicity is closely related to the free primary amine group.[3]

2.1 Literature reports

Despite its limitations, tacrine holds significant promise for Alzheimer's treatment. Its potent AChE inhibition, favourable ligand efficiency, synthetic accessibility, and the possibility of structural modification make it an attractive starting point for further research to find safer tacrine analogues and explore it in multi-target-directed ligand strategies involving hepatoprotective agents to treat AD. Therefore, significant efforts have been made towards the development of tacrine derivatives/hybrids that exhibit enhanced inhibitory activity with minimum hepatotoxic effects by AChE/BChE inhibition. The majority of these molecules are based on the modification of aromatic ring A or by conjugating the $–NH_2$ moiety (at 9^{th} position) of tacrine with other pharmacophore moieties to generate an array of hybrid molecules (**Figure 2.1a**).

In the quest to find new anti-cholinesterase agents with therapeutic potential, Hu et al., showed that linking two tacrine molecules with alkylene linker lengths 6-8 carbons [tacrine homodimers (**I**)] significantly increased their potency.[4] These *bis*-tacrines were 1000 times more potent than tacrine due to their dual interaction with cholinesterase. Encouraged by the promising results of linking tacrine molecules, Fernandez-Bachiller co-workers investigated new compounds combining tacrine with 8-hydroxy quinoline (**II**), 4-oxo-4H-chromene (**III**). These new derivatives exhibited strong activity against multiple targets (inhibit AChE, *β*-amyloid aggregation, antioxidant properties).[5] In a similar way, a series of novel tacrine-coumarin hybrids (**IV**) was synthesized and evaluated for potent inhibitory activity toward AChE and BuChE, and selectively inhibited MAO-B enzyme.[6] In another report, tacrine-ferulic acid hybrids (**V**) connected by alkyldiamine spacer were synthesised and citing ferulic acid's role towards hepatoprotective effect in addition to anti-oxidative stress.[7]

Similar to the multi-targeted approach mentioned before, Keri et al. expanded the scope of AD treatment by investigating natural-based tacrine hybrids with *S*-allylcysteine (**VI**). These compounds inhibit AChE activity and offer neuroprotective effects against Aβ-and ROS-induced toxicity, alongside antioxidant capabilities.[8] Similarly, L.X. Wan et al. designed and developed new *N*-aryltacrine (**VII**) derivatives *via* metal-catalysed reactions. The synthesized molecules by these methods show better inhibitory activity (IC_{50}: AChE = 1.77±0.22 μM, BChE = 19.0±0.43 μM) than tacrine.[9]

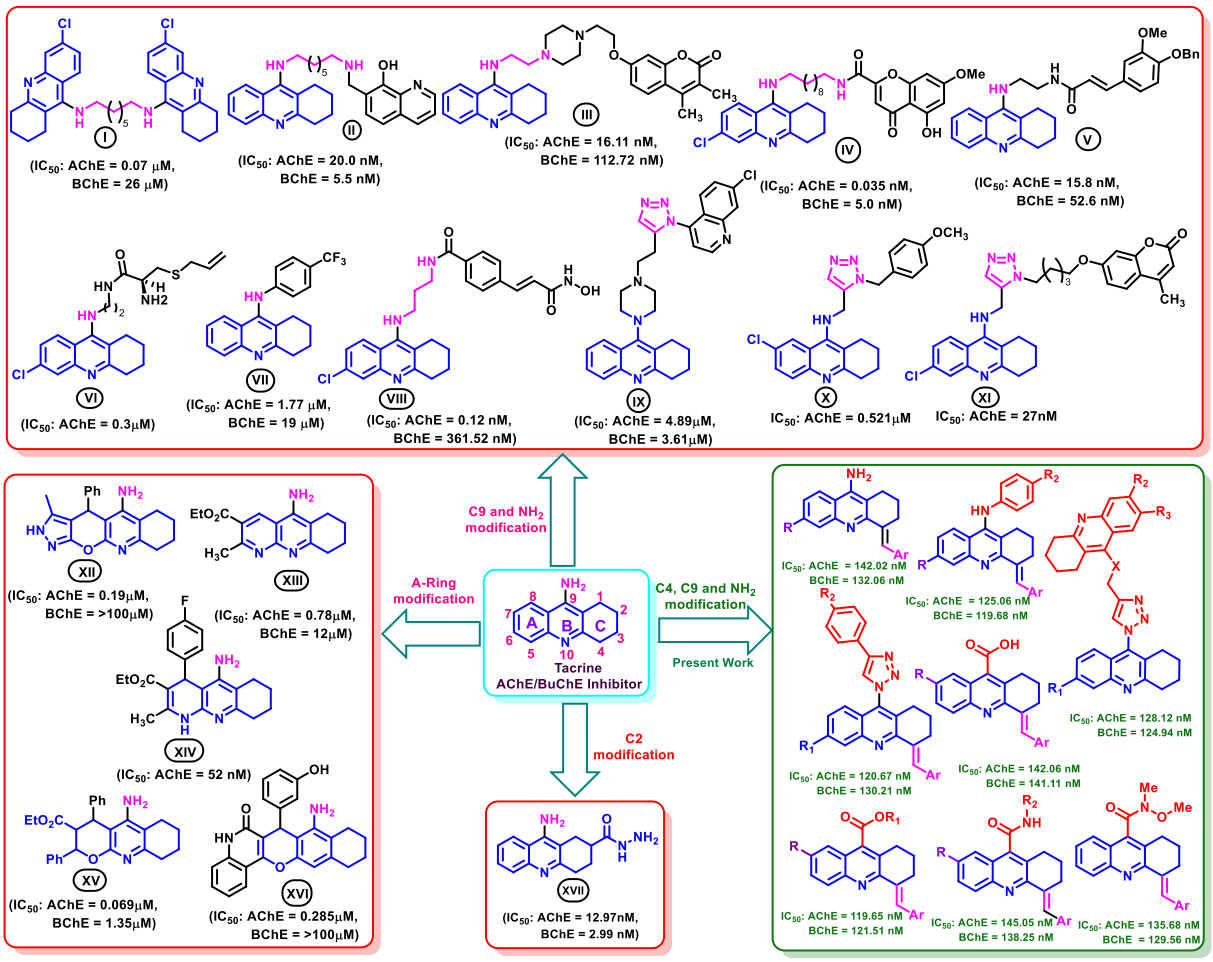

Figure 2.1a Reported Tacrine-based AChE and BChE inhibitors and present investigation (tested values of tacrine in the present investigation: AChE IC_{50} = 203.57 nM; BChE IC_{50} = 204.01 nM)

In the search for finding new potent anti-cholinesterase agents, Khoobi's group explored different approach to achieve potent anti-cholinesterase activity. They synthesised tetracyclic-tacrine analogues, replacing the benzene ring of tacrine with aryl-dihydropyrano[3,2-

c]pyrazoles (**XII**) *via* multi-component reaction and subsequent Friedlander reaction between the obtained pyrano[2,3-c]pyrazoles and cyclohexanone and achieved potent and selective anti-AChE activity.[10] In search for non-hepatotoxic tacrine derivatives, Marco-Contelles et al. designed juxtaposed structures between Tacrine and 1,4-dihydropyridine (**XIII**), pyridine (**XIV**) to obtain multi-target directed ligands for AD. The reported derivatives showed potent inhibition towards AChE inhibitors, excellent neuroprotective profile and mild calcium channel blockage effect.[11] Eghtedari et al. designed and synthesized 5-amino-2-phenyl-4*H*-pyrano[2,3-*b*] quinoline-3-carboxylates (**XV**), a new group of tacrine-derived AChE inhibitors.[12] Sadafi and co-workers took a step further in the realm of cholinesterase inhibitors. They crafted quinolotacrine hybrids (**XVI**) and assessed them as anti-cholinesterase (ChE) agents. Where the hybrids showed significant potency against AChE in the range of 0.285 μM.[13] Similarly, Najafi,[14] Wu,[15] groups reported a new series of tacrine-triazole hybrids (**IX, X, XI**) and evaluated as potent dual cholinesterase inhibitors for the treatment of AD. Anwar and his group reported the C2-substituted tacrine derivatives (**XVII**) and are aimed to achieve interaction with the peripheral anionic site of AChE. These synthesised compounds showed inhibitory activity towards AChE (IC_{50}: AChE = 12.97 nM, BChE = 2.99 nM).[16] Majority of these reports discuss the dual interaction (cationic and peripheral anionic sites) of cholinesterase enzyme.

The above discussion indicates that there are many variations of *N*-alkyl/aryl derivatives and aromatic ring modifications and only a couple of reports for the cyclohexane modification at the C2 position of tacrine. However, there are no reports found in the literature for the functionalization of the C4 position of the tacrine. To fill the gap in the SAR of tacrine analogues, we decided to carry on our work on 9-amino-1,2,3,4-tetrahydroacridine based AChE/BChE inhibitors by synthesizing and testing a series of tacrine derivatives substituted at C4, C6 and modification at C9 i.e. -NH_2 group (**Figure 2.1a**).

Functionalization of 2-methyl quinolines/azaarenes *via* C(sp^3)–H at the 2nd position got attention in recent times (**Figure 2.1b**). Similarly, 1,2,3,4-tetrahydroacridine could undergo azaarene activation at C4 position.[17] As well as, *N*-aryl tacrine's were synthesized *via* metal-catalysed reactions such as Buchwald-Hartwig[18] and Ullmann amination reactions (**Figure-2.1c**).[19] However, these methods require more reaction time and use metal-based catalysts. Deep eutectic solvents (DESs) popularly known as 21st century solvents exhibit distinct physical and chemical characteristics such as non-toxicity, biodegradability, and use of inexpensive/ readily available reagents for the preparation.[20] Thus, they became preferred

reaction media and catalysts in organic synthesis. In this context, we have reported a metal-free, one-pot synthesis of functionalized styrylquinolines employing deep eutectic solvents (DES) as the reaction medium.[21]

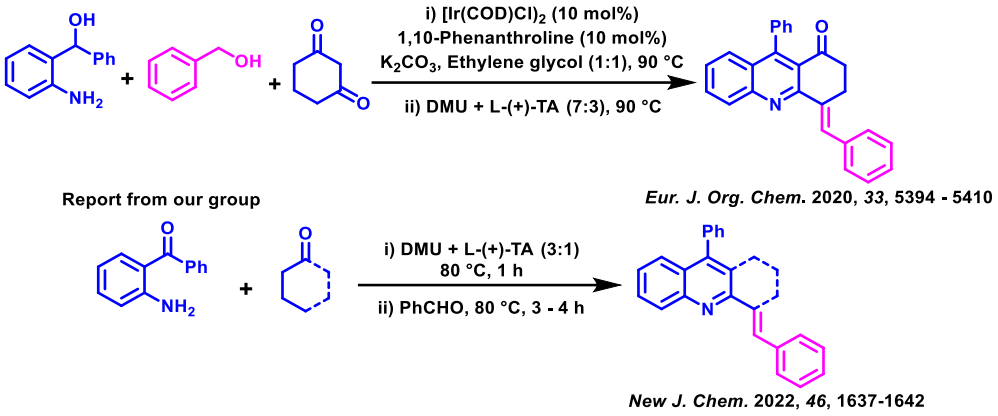

Figure 2.1b Previous reports for the new C–C bond formation *via* C(sp^3)–H functionalization

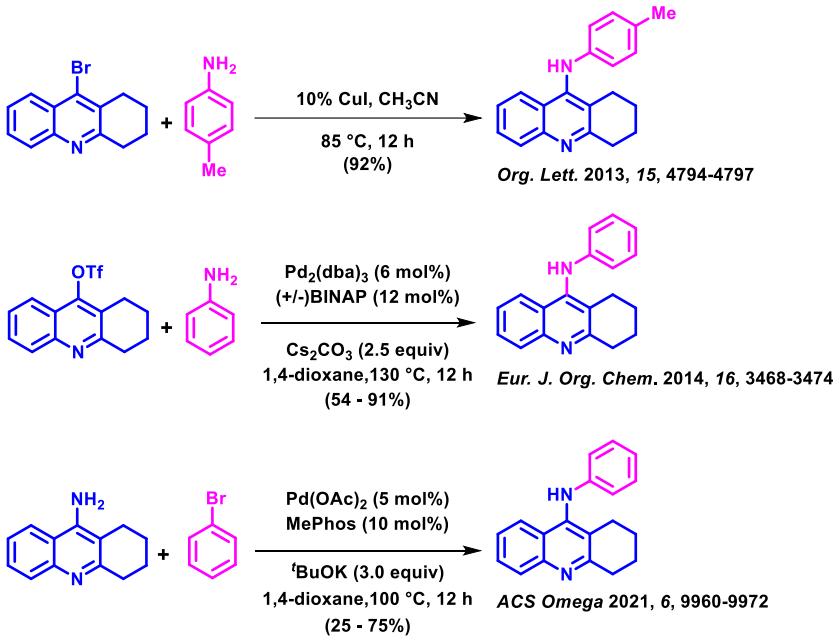

Figure 2.1c Reported methods for the synthesis of *N*-aryl tacrine derivatives

2.2 Present study

2.2.1 Metal-free synthesis of functionalized tacrine derivatives and their evaluation for acetyl/butyrylcholinesterase and α-glucosidase inhibition

Towards achieving the objectives i.e. C4 functionalisation of tacrine derivatives and to understand possible synthetic modifications (**Figure 2.2.1a**), molecular docking studies were performed on tacrine to the active site of the AChE or BChE and observed a void space below the C4 position of tacrine after binding (**Figure 2.2.1b**). This could be used for designing and

synthesizing new compounds to improve the binding between the compound and protein in its active site.

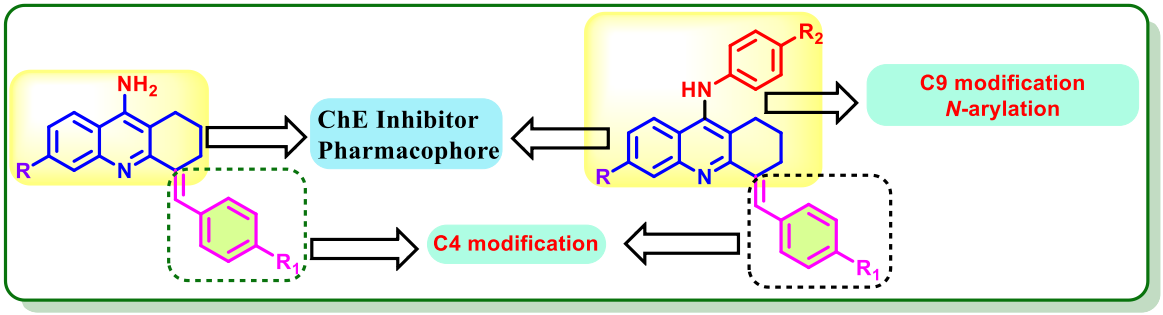

Figure 2.2.1a Design strategy for the synthesis of C4 functionalised tacrine derivatives

A)

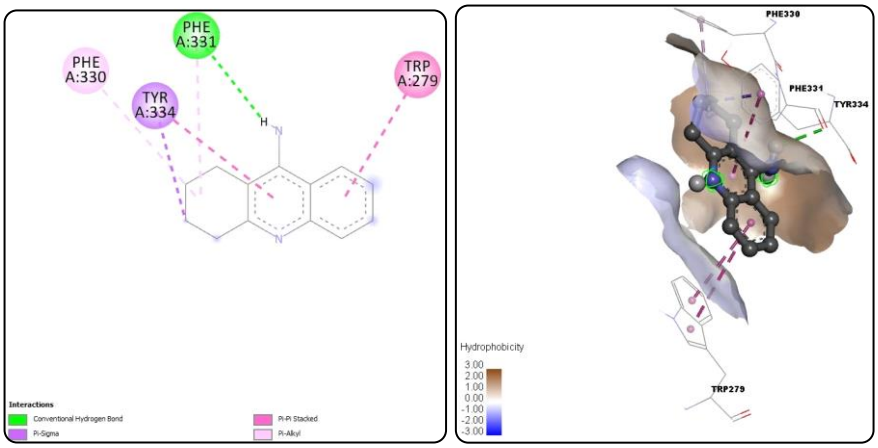

B)

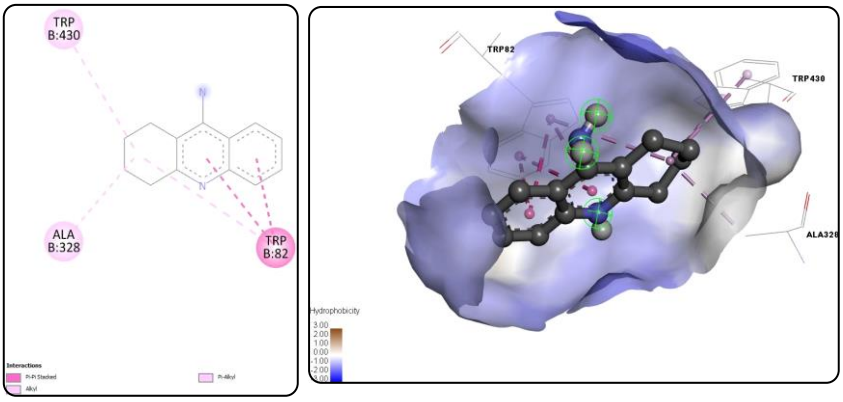

Figure 2.2.1b 2D, 3D docking interactions of tacrine with protein A) **1DX6,** B) **6EMI**

Based on the substitutions that gave better interaction/dock scores, compounds were synthesized and tested for *in vitro* activities. So, in this chapter we have discussed an attempt to introduce substitutions in the C4 position of tacrine/tetrahydroacridine derivatives using

metal-free C–C bond formation *via* C(sp^3)–H functionalization using DES as reaction medium. Along with C4 activation, we aimed to describe a more economical and environmentally friendly approach for the synthesis of *N*-aryl tacrine through a metal-free C–N bond formation reaction, facilitated by deep eutectic solvent.

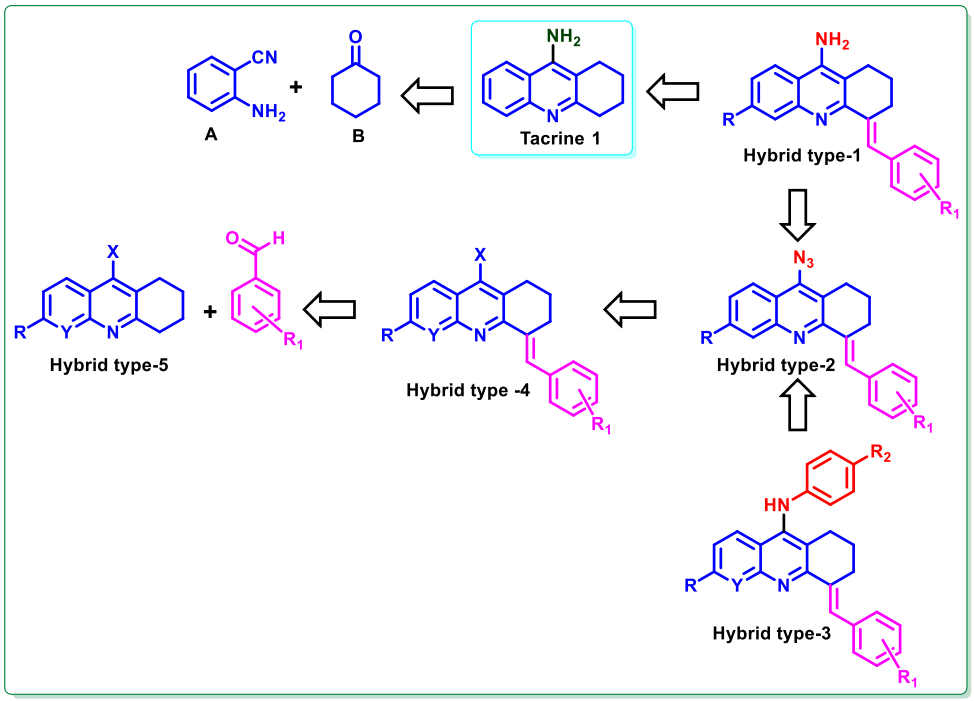

Scheme 2.2.1a Retrosynthetic plan for the synthesis of C4 functionalised tacrine derivatives

2.2.1.1 Results and Discussion

2.2.1.2 Chemistry

To achieve the goal i.e., C(sp^3)–H functionalization of tacrine at the C4 position, initially tacrine **(1)** was treated with benzaldehyde (**2a**) under known acidic and basic conditions. However, there was no product (**3a**) formation observed (**Scheme 2.2.1b**).

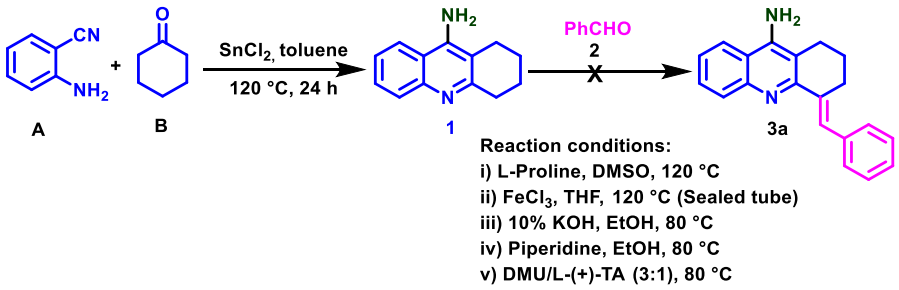

Scheme 2.2.1b Initial attempts for the C(sp^3)–H functionalization of Tacrine at C4 position

Later, an alternative method was envisaged to use tacrine analogue i.e., 9-chloro-1,2,3,4-tetrahydroacridine (**4a**). Accordingly, (**4a**) was reacted with benzaldehyde (**2a**) using known methods as indicated in **Table 2.2.1** (entries 1-7). To our surprise, all these methods failed to give the desired product **(5a)**. At this juncture, an attempt was made using a strong Lewis acid $SnCl_2$ in THF at 120 °C to give the desired product (**5a**) in 75% yield (**Table 2.2.1**; entry 8). The structure of compound **5a** was confirmed by ^1H, ^{13}C-NMR, and mass spectral data. Encouraged by this result, to improve the reaction conditions further and with our previous experience in C(sp^3)–H functionalization of azaarenes in deep eutectic solvent,[21] the DES was selected as the reaction medium. Thus, initially, the reaction was carried out using *N,N'*-dimethylurea (DMU), and L(+)-tartaric acid (L-(+)-TA) (in a 3:1 ratio at 80 °C) as DES* which resulted in the desired product (**5a**) in 85% yield, (**Table 2.2.1**; entry 10). Later, a series of experiments were conducted to identify the best suitable conditions as indicated in **Table 2.2.1** (Entries 10-26) and found DMU + L-(+)-TA (3:1) at 80 °C as effective due to the acidic nature (approx. pH = 3.7) of the melt.[22]

Table 2.2.1 Optimisation of reaction condition[a]

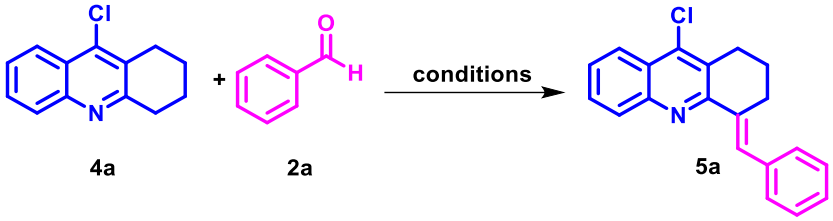

S. No.	Catalyst	Solvent	Temp (°C)	Time (h)	Yield (%)[c]
1	Piperidine	EtOH	80	24	5
2	TEA	EtOH	80	24	10
3	L-Proline	DMSO	RT, RF	24	ND
4	DBU	EtOH	RT, RF	24	ND
5	DABCO	EtOH	RT, RF	24	ND
6	DMAP	EtOH	RT, RF	24	ND
7	DIPEA	EtOH	RT, RF	24	ND
8	$SnCl_2$[b]	THF	120	8	75
9	$FeCl_3$[b]	THF	120	4	60
10		**DMU/ L-(+)-TA (3:1)**	**80**	**2**	**85**
11		ChCl/$SnCl_2$	80	4	30

12		$ChCl/FeCl_3$	80	4	ND
13		DMU/ L-(+)-TA (2:1)	80	3	60
14		DMU/ L-(+)-TA (1:1)	80	3	30
15		DMU/Citric acid (2:1)	80	2	30
16		DMU/Citric acid (3:1)	80	2	50
17		DMU/Oxalic acid (2:1)	80	2	60
18		DMU/ Oxalic acid (3:1)	80	2	70
19		DMU/ L-(+)-TA (3:1)	100	2	60
20		DMU/ L-(+)-TA (3:1)	90	2	55
21		Ch-Cl/ L-(+)-TA (2:1)	80	2	10
22		Ch-Cl/ L-(+)-TA (3:1)	80	2	20
23		Ch-Cl/$ZnCl_2$ (3:1)	80	2	35
24		DMU/Ch-Cl (3:1)	80	2	55
25		Urea/Ch-Cl (3:1)	80	2	15
26		DMU/Citric acid (2:1)	80	2	30

[a]All the reactions were performed with 0.46 mmol of **4a** and 0.46 mmol of **2a**, DES is prepared by heating the hydrogen bond acceptor and hydrogen bond donor. [b]Sealed tube. [c]Isolated yield.

After establishing the optimal reaction condition, our attention shifted towards exploring the range of substrates. Thus, a diverse set of aldehydes (**2a-2m**) and substituted 9-chloro-1,2,3,4-tetrahydroacridines **(4a-4f)** were screened as shown in **Figure 2.2.1c**. Aromatic aldehydes, bearing electron-withdrawing group as well as electron donating groups along with hetero aromatic aldehydes, polycyclic aldehydes exhibited favourable reactivity with compounds **4a-4f** yielding the corresponding products **5a-5af** in good to high yields (73%-94%).

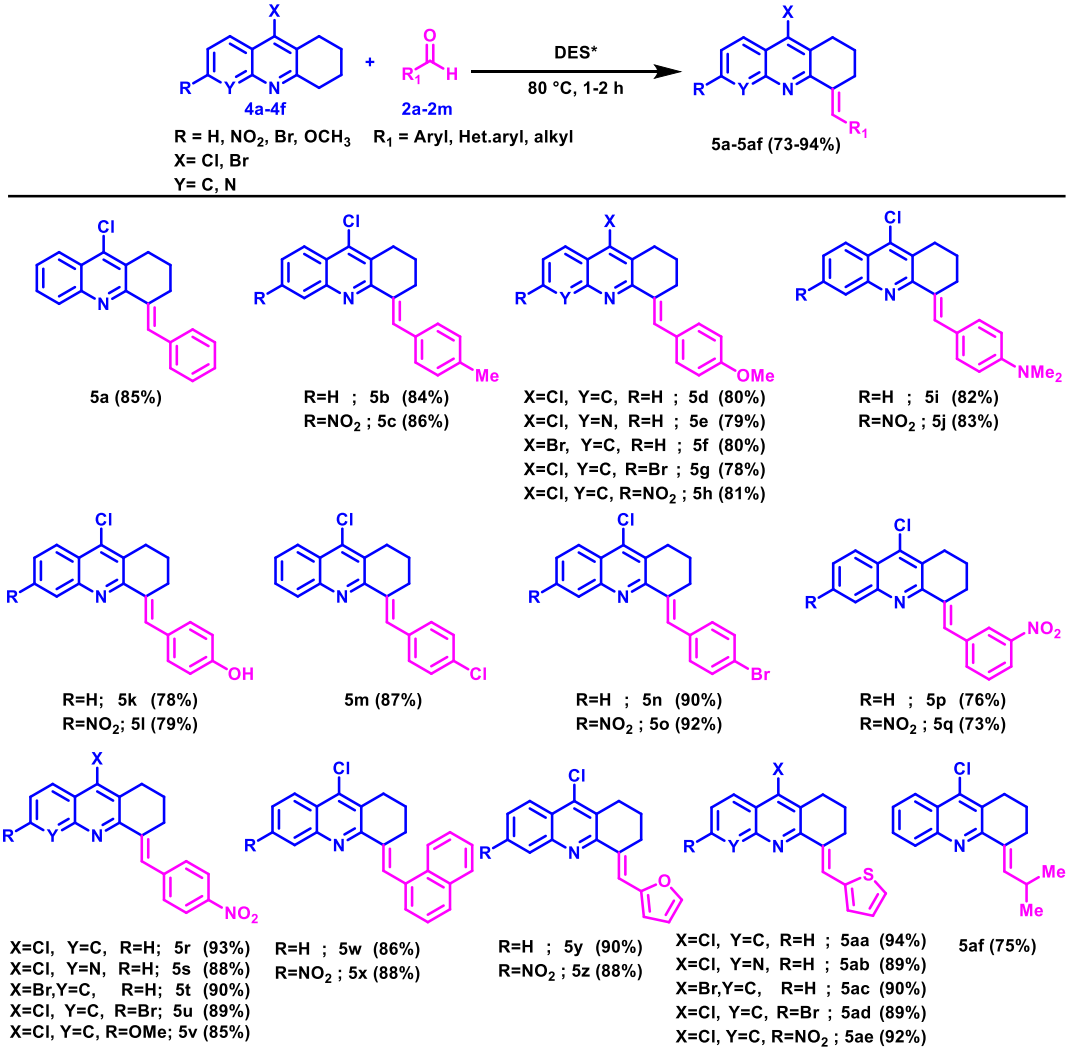

Figure 2.2.1c Synthesis of 9-chloro-1,2,3,4-tetrahydroacridine derivatives (**5a-5af**)

After the successful synthesis of functionalized 9-chloro-1,2,3,4-tetrahydroacridine derivatives (at C4-position), our next task was to convert these compounds to functionalized tacrine derivatives. To achieve this, unsaturated derivatives of 9-chloro-1,2,3,4-tetrahydroacridines **(5a–5i)** were converted into 9-azido-1,2,3,4-tetrahydroacridines **(6a–6i)** in the presence of DES* and then reduced into amines **(3a–3i)** using Staudinger conditions [23] in moderate to good yields (50-72%) (**Scheme 2.2.1c**).

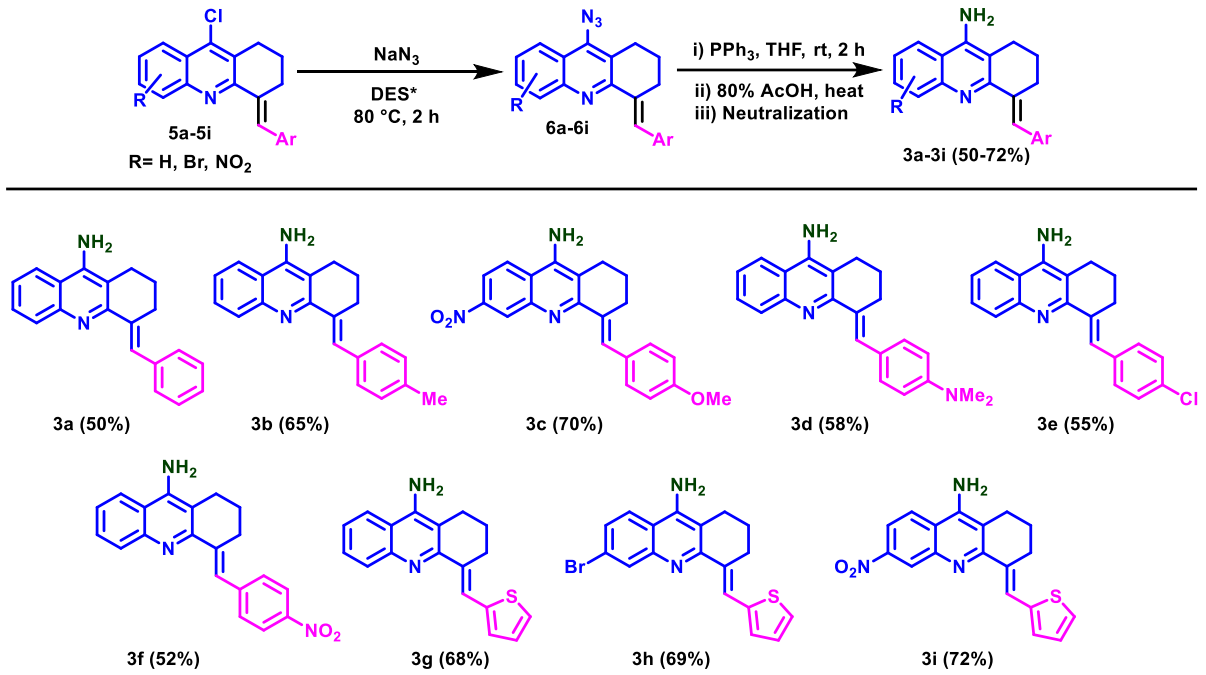

Scheme 2.2.1c Synthesis of functionalized tacrine derivatives (**3a-3i**). All the reactions were performed with **5** (1 mmol), NaN_3 (5 mmol), **6** (0.32 mmol), and PPh_3 (0.96 mmol)

Inspired by the successful synthesis of functionalized tacrine derivatives, we attempted to prepare *N*-aryl tacrine derivatives by the reaction of compound **(5a)** with toluidine **(7a)** in the presence of CuI (10 mol%), CH_3CN at 85 °C for 24 h (**Scheme 2.2.1d**) to give the desired product **(8a)** with 45% yield. The product structure was confirmed by ^{1}H, ^{13}C, and mass spectral analysis. To enhance the reaction rate and to improve the desired product yield, optimization reactions were performed. Interestingly, the DES* i.e., DMU+L-(+)-TA (3:1) at 80 °C was the best condition to give the desired product in good yield (76%) in less time (catalyst-free conditions) (**Table 2.2.2**; entry 6). With the optimized reaction conditions at our disposal, we conducted a screening of a range of substituted 9-chloro-1,2,3,4-tetrahydroacridine derivatives and substituted anilines. Notably, the compound featuring a $-NO_2$ group on the benzene ring (**8s**) exhibited decreased reactivity, whereas the compound with $-NO_2$ substitution on acridine moiety (**8c, 8g, 8m**) displayed enhanced reactivity towards -Cl substitution, as illustrated in **Figure 2.2.1d**.

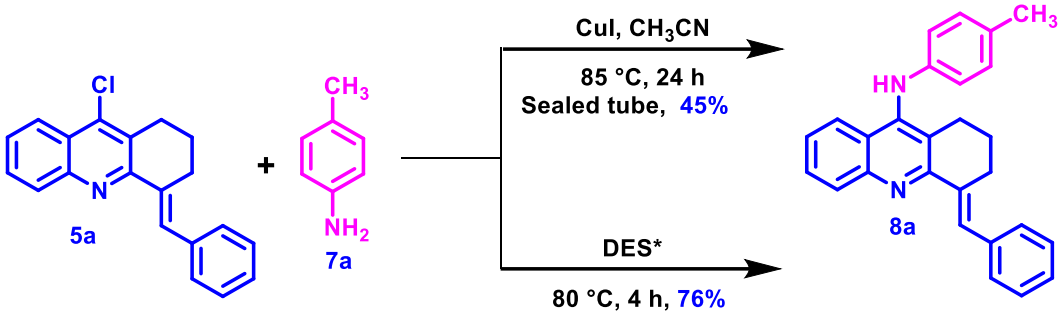

Scheme 2.2.1d Initial attempts for the Synthesis of functionalised *N*-aryl tacrine derivatives

Table 2.2.2 Optimization of the reaction condition[a]

S. No.	Catalyst (10 mol%)	solvent	Temp (°C)	Time (h)	Yield (%) [c]
1	CuI [b]	CH_3CN	85	24	45
2	CuI [b]	CH_3CN	100	24	45
3	$Cu(OAC)_2$ [b]	CH_3CN	80	24	ND
4	Cu_2O [b]	NMP	100	24	ND
5	$CuSO_4$ [b]	CH_3CN	80	24	ND
6		**DMU/ L-(+)-TA (3:1)**	**80**	**4**	**76**
7		DMU/ L-(+)-TA (2:1)	70	12	40
8		DMU/ L-(+)-TA (3:1)	100	12	70
9		DMU/ L-(+)-TA (3:1)	90	12	72
10		Gly/Ch-Cl (2:1)	80	24	ND
11		Ch-Cl/ L-(+)-TA (3:1)	80	24	ND
12		$ZnCl_2$/Ch-Cl (1:3)	80	24	ND
13		Ch-Cl/DMU (1:3)	80	24	20
14		Urea/Ch-Cl (3:1)	80	24	15

[a] Reaction condition: **5a** (0.32 mmol), **7a** (1 mmol), DES prepared by heating hydrogen bond donor and acceptor at 80 °C. [b] Sealed tube. [c] Isolated yield.

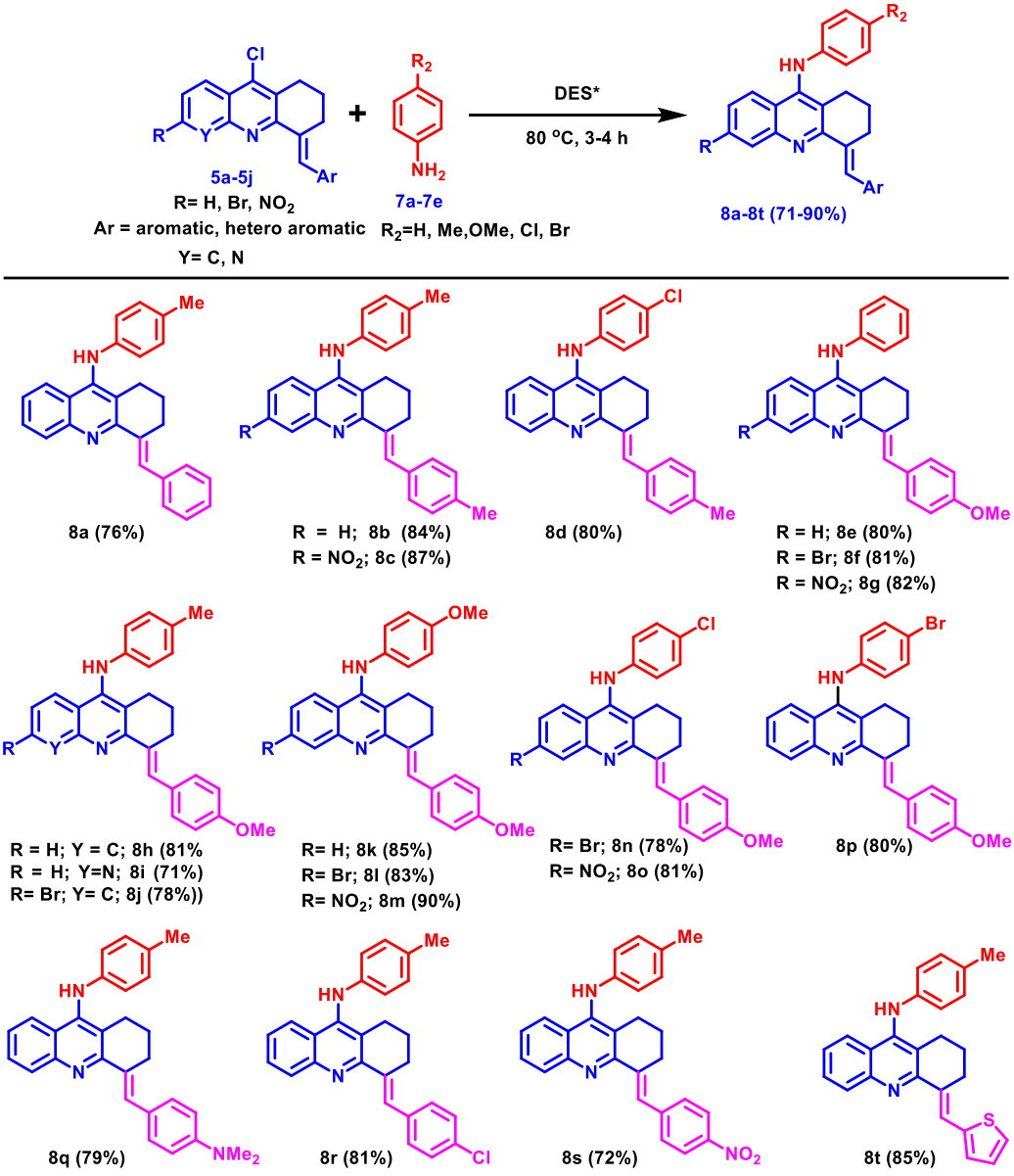

Figure 2.2.1d Synthesis of functionalised *N*-aryl tacrine derivatives (**8a-8t**)

To check the feasibility of one-pot synthesis of the functionalized *N*-aryl tacrine, compounds (**4a**) and (**2a**) were reacted in DES* [i.e., *N,N'*- Dimethyl urea and L-(+)-TA at 80 °C] to give (**5a**) followed by the addition of (to the same reaction pot) *p*-toluidine (**7a**) at 80 °C gave the desired product (**8a**) in good yield (76%) (**Scheme 2.2.1e**).

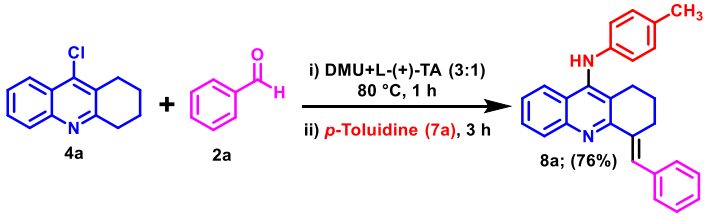

Scheme 2.2.1e One-pot synthesis of functionalized *N*- aryl tacrine (**8a**)

2.2.1.3 Plausible mechanism

Based on the experimental observations, a plausible mechanism is proposed following the literature reports.[20] At first, the DES is prepared by heating *N,N'*-Dimethyl urea, and L-(+)-TA (3:1) at 80 °C. DES is formed through the intermolecular hydrogen bonding association between components. The DES interacts with the aromatic nitrogen of 1,2,3,4-tetrahydroacridine moiety *via* hydrogen bonding to produce an enamine-type intermediate (**II**). Simultaneously, the DES also activates aldehyde and enamine intermediate (**II**) to provide the C(sp^3)–H functionalization product (**III**) followed by the elimination of water to produce an unsaturated product (**5a**) (**Figure 2.2.1e**). For the C–N bond formation (*N*-arylation), DES activates **5a** through hydrogen bonding to enhance the reactivity of condensed compound (**IV**) and aryl amine through the hydrogen bonding leading to the facilitation of faster attack of aryl amine on the condensed product, which results in the formation final product (**8a**) (**Figure 2.2.1f**).

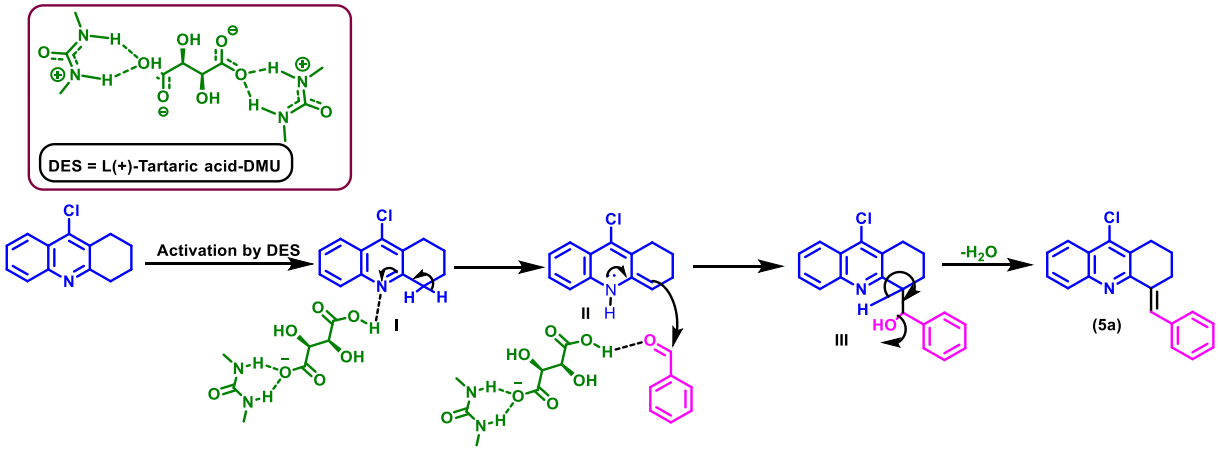

Figure 2.2.1e Proposed mechanism for the synthesis of C(sp^3)–H functionalized 9-chloro-1,2,3,4-tetrahydroacridine (**5a**)

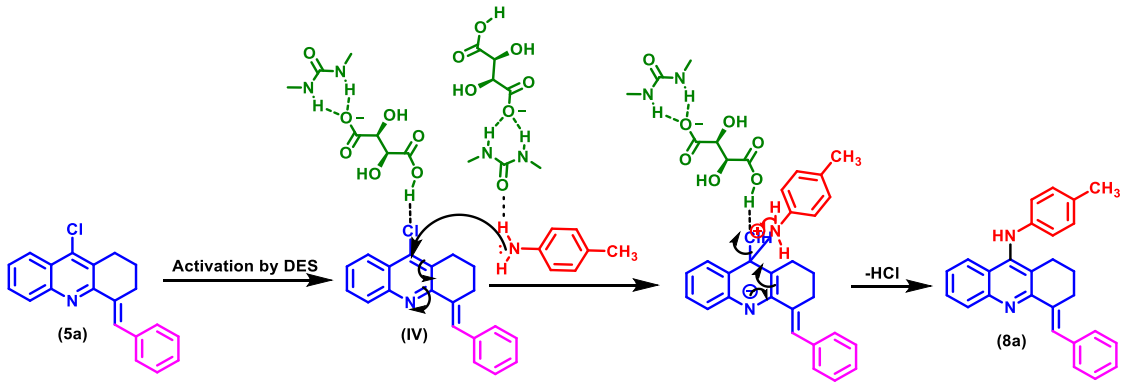

Figure 2.2.1f Proposed mechanism for the formation of *N*-aryl tacrine derivatives (**8a**)

2.2.1.4 Biological assay materials and methods

2.2.1.4a AChE and BChE assay

Ellman's spectrophotometric method with some modifications was used to determine acetylcholinesterase inhibitory activity using acetylcholine chloride as a substrate for AChE (from electric eel) and BChE (from equine serum). All the synthesized compounds were dissolved in DMSO (0.01 M concentration) and diluted in double distilled water (0.001 M concentration). In a 96-well plate 60 µL phosphate buffer saline (PBS), 10 µL enzyme (AChE or BChE), and synthesized compounds (10 µL) were added in sequence. After mixing the reaction components, the plate was incubated for 10 min at 37 °C, and absorbance was recorded at 405 nm. Further, 10 µL of the substrate (0.5 nM acetylcholine chloride) was added to the reaction mixture then 110 µL DTNB (5,5′-dithiobis-2-nitrobenzoic acid was dissolved in 50 nM Tris–HCl, pH 8, containing 0.1 M NaCl and 0.02 M $MgCl_2.6H_2O$) added to the reaction mixture. The reaction mixtures in the plate were mixed well, then the plate was incubated for 5 min at 37 °C, and absorbance was recorded every 60 s at 405 nm consecutively for 5 times in a microplate reader (BioTek). Experiments were performed in triplicate with their respective controls. The reference drug, Tacarine (0.1 nM/well) was used as a positive control. The percentage of acetylcholinesterase inhibition was calculated by using the following formula:

$$\boldsymbol{Percent\ inhibition} = \mathbf{1} - (\boldsymbol{At/Ac}) \times \mathbf{100}$$

At is the absorbance of enzymatic reaction at 405 nm with inhibitor and Ac is the absorbance of enzymatic reaction at 405 nm without inhibitors.

To calculate IC_{50}, the dependency of At/Ac versus inhibitor concentration was constructed and IC_{50} was then calculated from the derived equation of the regression curve for y = 2 (coming from the definition of IC_{50}). The IC_{50} values obtained for all tested compounds are shown in following **Table 2.2.3**.

2.2.1.4b α-Glucosidase assay

The calorimetric analysis was used to determine the catalytic activity of α-glucosidase using 4-nitrophenyl glucopyranoside (4-NPG). The enzymatic reaction was initiated by adding 25µl of α-glucosidase (2mg dissolved in 1ml of 10mM cTris-HCl pH 7.0) to 25µl of 4-NPG (substrate stock solution) and 950µl deionized H_2O and then the reaction mixture was incubated for 10 min at 37 °C. By comparing the liberated 4-nitrophenol absorbance at 405 nm against a blank without any enzyme, the enzyme activity was determined. For investigations involving enzyme

inhibition, the enzyme was pre-incubated with synthesized compounds for 30 min before the addition of substrate solution. The quantity of enzyme required to release 1μg of 4-nitrophenol per minute under standard test conditions was used to define 1 unit (U) of glycolytic activity.

2.2.1.4c Molecular Docking

The three-dimensional (3D) structures of proteins α-glucosidase, AChE, and BChE were obtained from RCSB-PDB and were used as receptor or target proteins. The PDB IDs of the proteins α-glucosidase, AChE, and BChE were 3TOP, 1DX6, and 6EMI respectively. A PyRx virtual screening tool was used for docking protein with the prepared compound. BIOVIA Discovery Studio was used for the visualization of 2D and 3D patterns of compound–target protein interactions.

2.2.1.4d Molecular Dynamics Simulation

Classical molecular dynamics (MD) simulations were performed using GROMACS 2019[24] to assess binding interactions and stability of synthesized compounds with Acetylcholinesterase (AChE, PDB ID: 1DX6), Butyrylcholinesterase (BChE, PDB ID:6EMI), and α-glucosidase (PDB ID:3TOP). The protein-ligand complexes obtained from the docking study served as the starting point for the MD simulation investigation. The compounds underwent parameterization with the general amber force field (GAFF). For the generation of protein topology and coordinate files, the Amber99SB force field provided in GROMACS was employed.[25] The protein-ligand complex was enclosed within a dodecahedron and immersed in TIP3P water. Counter ions were introduced to neutralize the solvated system, followed by a rapid energy minimization utilizing the steepest descent minimization algorithm. Subsequently, the system underwent equilibration in the restrained constant number of particles, volume, and temperature (NVT) ensemble for 1 ns, followed by a constant number of particles, pressure, and temperature (NPT) ensemble for 2 ns. Monitoring thermodynamic properties, including pressure, density, potential energy, and temperature, ensured sufficient equilibration before the commencement of the production run. Long-range electrostatics were computed using the particle mesh Ewald method. Temperature and pressure coupling utilized the Modified Berendsen thermostat and Parrinello-Rahman barostat, respectively. Finally, unrestrained production simulations spanning 200 ns were conducted for the systems, maintaining a temperature of 310 K and a pressure of 1 bar atmospheric pressure.

2.2.1.4e Blood Brain Barrier Prediction

To predict the blood-brain barrier (BBB) of ligand molecules which gave significant AChE and BChE *in vitro* inhibitory activity was predicted using the BBB predictor module of ALzPlatform. [26] BBB predictor was used to identify whether a ligand can cross the blood-brain barrier (BBB+) or not (BBB−) based on a threshold value of 0.2 and compared with the SVM_MACCSFP BBB Score of tested compounds.

2.2.1.4f QSAR Analysis

QSAR analysis was conducted by using the open-source tool QSAR-Co. The model was created using linear discriminant analysis (LDA). The following model aspects were taken into account for assessing the developed model accuracy, specificity, sensitivity, precision, AUROC (Area Under the Receiver Operating Characteristic curve), and MCC (Matthews Correlation Coefficient). PaDEL tool was used to calculate the molecular descriptors. The Monte Carlo optimization approach as implemented in the correlation and logic (CORAL) tool was used to assess components that affect the compound's inhibitory activity.

2.2.1.5 Biological assay Results and discussion

Table 2.2.3 *In vitro* and *In silico* molecular docking study of synthesised compounds

	In vitro	***In silico***	***In vitro***	***In silico***	***In vitro***	***In silico***
Compound No.	**AChE - IC_{50} nM**	**Dock score**	**BChE - IC_{50} nM**	**Dock score**	**α-Glucosidase - IC_{50} nM**	**Dock Score**
5a	197.23	-7.43	197.23	-7.43	34940	-6.94
5b	189.02	-7.43	189.02	-7.45	33920	-6.83
5c	199.13	-7.82	199.13	-7.54	21200	-7.92
5d	204.91	-6.43	204.91	-6.65	35430	-7.43
5e	213.12	-6.12	213.12	-6.45	38540	-7.54
5f	189.34	-7.63	196.21	-7.36	39040	-7.02
5g	197.49	-7.31	186.35	-7.84	21400	-7.33
5h	150.32	-7.52	145.94	-7.54	31200	-7.46
5i	241.93	-4.43	235.32	-4.36	32.940	-6.93
5j	233.18	-6.12	223.21	-6.54	30930	-7.01
5k	198.32	-7.5	201.95	-7.35	33480	-6.81

5l	210.72	-6.02	206.45	-6.87	22300	-7.32
5m	211.93	-6.43	223.15	-6.4	34320	-6.83
5n	189.04	-7.03	185.64	-7.65	30260	-7.03
5o	191.99	-7.45	190.35	-7.28	**22400**	-7.14
5p	229.32	-4.53	235.21	-4.49	31040	-6.99
5q	203.48	-5.43	210.35	-5.36	30940	-6.93
5r	205.92	-5.76	206.45	-5.37	33020	-6.83
5s	198.3	-7.01	201.32	-7.49	31030	-7.03
5t	196.85	-7.11	195.32	-7.16	32040	-6.98
5u	204.92	-5.94	213.65	-5.67	29480	-7.43
5v	212.43	-5.23	209.32	-5.05	28030	-7.65
5w	171.41	-7.74	169.37	-7.42	37020	-6.83
5x	183.05	-7.12	180.34	-7.38	31100	-7.11
5y	193.32	-7.41	191.45	-7.37	36540	-6.83
5z	189.87	-7.39	190.35	-7.72	39230	-6.78
5aa	203.75	-6.18	201.54	-6.23	36030	-6.43
5ab	205.83	-5.39	203.21	-5.43	39350	-6.34
5ac	210.18	-5.23	212.48	-5.15	40320	-6.04
5ad	204.04	-5.4	206.34	-5.34	26300	-7.1
5ae	201.93	-5.21	213.02	-5.46	33100	-6.91
5af	276.93	-4.32	257.32	-4.64	38040	-6.53
3a	201.43	-6.92	186.32	-6.89	39540	-6.9
3b	221.63	-6.99	198.32	-7.13	39540	-6.81
3c	**142.02**	**-7.71**	**132.06**	**-7.8**	**30250**	-7.56
3d	205.81	-6.96	199.02	-7.05	37590	-6.9
3e	232.12	-4.32	224.76	-4.65	38430	-6.82
3f	228.9	-4.23	226.81	-4.44	39290	-6.98
3g	229.41	-4.65	219.35	-4.68	33640	-7.21
3h	169.72	-7.21	159.05	-7.23	40210	-7.63
3i	186.44	-7.1	176.75	-7.15	35140	-7.59

8a	145.64	-5.23	154.32	-7.72	29030	-7.84
8b	143.04	-5.23	140.65	-7.37	31030	-7.24
8c	165.93	-7.93	131.25	-8.12	23300	-7.32
8d	135.32	-7.93	152.34	-7.78	34950	-6.83
8e	149.68	-7.8	138.66	-7.8	35010	-7.46
8f	152.32	-7.63	141.03	-7.65	31250	-7.41
8g	139.02	-7.81	129.03	-7.85	43460	-7.72
8h	145.93	-5.64	138.02	-7.95	33920	-6.89
8i	175.18	-7.82	134.38	-7.97	37060	-6.93
8j	140.92	-8.03	134.02	-8.13	**19400**	-7.55
8k	**133.61**	**-7.92**	**121.04**	**-7.91**	29540	-7.56
8l	136.05	-7.83	123.68	-7.9	23570	-7.59
8m	**125.06**	**-7.82**	**119.68**	**-7.89**	41050	-7.42
8n	140.21	-7.81	130.55	-7.86	29650	-7.92
8o	**131.02**	**-7.81**	**122.66**	**-7.87**	40280	-7.91
8p	146.84	-7.73	139.64	-7.81	31050	-6.32
8q	144.53	-5.54	157.32	-5.32	30210	-7.43
8r	171.43	-7.91	181.05	-7.11	31490	-7.02
8s	159.03	-7.92	197.32	-7.37	30940	-7.22
8t	173.94	-7.82	170.32	-7.39	35380	-6.98
Tacrine	**203.57**	**-7.76**	**204.01**	**-7.71**	**-**	**-**
Acarbose					**23100**	**-7.89**

The tacrine molecule was reported to inhibit the AChE and BChE. Based on the structural and chemical features of tacrine-based molecules in the previous reports and molecular docking studies, we sought to improve the biological activity profile by substituting various functional groups in the top (C9) and bottom (C4) positions of tacrine. *In vitro* and *in silico* studies performed for the synthesized compounds showed improved AChE and BChE inhibitory activity and binding efficiency. The *in vitro* and *in silico* results for all the synthesised compounds are mentioned in **Table 2.2.3**. By studying the inhibition pattern and kinetics of inhibition of AChE and BChE, compounds **8m, 8k,** and **8o** were found to exhibit maximum inhibitory activity among the tested compounds. The 2D, 3D binding interactions and Lineweaver–Burk plot of potent compounds were mentioned in **Figure 2.2.1g- Figure 2.2.1i**. From the Lineweaver–Burk double reciprocal plot, it was observed that the presence of **8m**, **8k,** and **8o** greatly affected the K_m and V_{max} values (**Table 2.2.4**). For all the compounds decreasing trend for V_{max} value with an increase in substrate concentration was observed, but there is no significant change was observed for K_m. This reveals that the tested compounds exhibit a non-competitive mode of inhibition against AChE and BChE. Lima et al.[27] reported a similar inhibition pattern for benzyltetrahydroprotoberberine alkaloids against AChE. The molecular docking studies revealed that the tested compounds **8m**, **8k**, and **8o** are interacting with the target protein by hydrogen bonding and aromatic (π-π stacking) interactions. The interactions are between hydrophobic amino acids present in the active site pocket of both AChE and BChE, methoxy group substitution attached to the aromatic ring. Among the tested compounds the substitution of the phenyl methoxy group in the R_1 position improved the activity, also methoxy substitution in the R_2 position of the Ar moiety improved the inhibitory activity of the enzyme. It was evident from the *in silico* 2D interaction representation that the hydrophobic amino acids have interaction with the methoxy group of the molecules. The amine group of compound **3c** was found to interact with the serine residue away from the active site pocket of AChE, but no interaction with the amine group was found when docked with BChE. However, the NO_2 group found in **3c** was found to form hydrogen bonds with aromatic amino acids in the hydrophobic pocket of the BChE. **3c** with an amine group exhibits distinct interaction behaviour among the investigated compounds. While docking with AChE, the amine group of **3c** is found to interact with a serine residue situated away from the active site pocket. Surprisingly, no significant interaction with the amine group is observed when **3c** is docked with BChE. This disparity in interaction patterns underscores the selectivity and specificity of the compounds toward different cholinesterase enzymes. The compound having more π-π interaction showed a better docking score that indicates the significant role

hydrophobic moiety introduced in the synthesized compounds (**8m**) thus giving better results with good IC_{50} values.

The Tested compounds **8j, 8c**, and **8l** showed good inhibitory activity against α-D-glucosidase. Substitution of Bromine or Nitro group in the R position along with methyl or methoxy moiety in R_1 enhanced the inhibitory activity. The compounds having the above combination of Br or Nitro and methyl /methoxy showed inhibitory activity, this clearly shows the requirement of respective substitutions in the R, R_1, and R_2. The compounds with other substitutions in this position or the presence of only one of the above substitutions did not enhance the inhibitory activity. The compounds **8o** and **8m** having nitro substitution in the R position did not show significant inhibitory activity because of the absence of methyl group in the R_2 position. Similarly, **8k** having methoxy substitution in the R_1 position lacks Nitro/Bromo substitution in the R position did not show significant inhibitory activity when compared to the best hits found among the tested compound. *In vitro* studies performed for compounds functionalized at the C4 position of tacrine showed improved AChE and BChE inhibitory activity and binding efficiency than the reference drug tacrine.

2.2.1.5a Molecular Dynamics Simulation

The analysis of Protein Backbone Root Mean Square Deviation (RMSD) values was a pivotal aspect of our molecular dynamics (MD) simulations, providing valuable insights into the stability of ligand-protein complexes and the corresponding apo-protein systems over the simulated time course, extending up to 200 nanoseconds (ns). The RMSD profiles of each ligand-protein complex and the apo-protein were logged and plotted against the simulation time in nanoseconds (**Table 2.2.4**). Remarkably, the collective observation revealed that the average RMSD values for all protein-ligand complexes closely resembled those of the apo-protein, indicating a notable stability enhancement in the presence of compounds. The stability of the apo-protein system was evident up to 200 ns, albeit with a slightly higher average RMSD compared to the protein-ligand complexes. Specifically focusing on the Acetylcholinesterase (AChE, PDB ID: 1DX6) and Butyrylcholinesterase (BChE, PDB ID: 6EMI) protein-ligand complexes, their average RMSD values fell within the range of 1.7 Å to 2.25 Å, similar to the RMSD of the apo-protein complex. It was observed that the compounds **8m** and **8o**, exhibited an average RMSD value consistently below 2 Å. This observation underscores the increased stability of these specific compound within the complex with the target protein compared to the apo-protein. On the other side, for the α-glucosidase (PDB ID: 3TOP) protein-ligand

complexes, the average RMSD values were found to hover within the range of 2 Å to 3.2 Å, again aligning with the RMSD of the apo-protein complex. Of particular significance were the protein-ligand complexes involving compounds **8j** and **8k**, both demonstrating an average RMSD value consistently below 2.6 Å. This compelling observation reinforces the conclusion that these specific hits exhibit enhanced stability within the complex with the target protein compared to the apo-protein. The RMSD profiles not only serve as indicators of structural stability but also shed light on the dynamic behaviour of the protein-ligand complexes in comparison to the apo-protein. The fact that certain compounds, such as compounds **8m**, **8o**, **8j**, and **8k**, consistently demonstrate lower average RMSD values in their complexes with target proteins suggests a robust and stable binding interaction. This stability is crucial for the potential development of these compounds as effective inhibitors.

Table 2.2.4 IC_{50}, K_m, V_{max} and modes of inhibition of selected compounds

Compound	**Enzyme**	**IC_{50} nM**	**Km nM**	**Vmax nM/min**	**Mode of inhibition**
			Inhibitor concentration of 25 nM		
8m	AChE	125.06±2.54	321.25	0.34	Non-Competitive
	BChE	119.68±2.7	310.96	0.43	Non-Competitive
	α-glucosidase	41050±1230	3140	3850	Non-Competitive
8k	AChE	133.61±2.65	321.65	0.39	Non-Competitive
	BChE	121.04±2.07	305.25	0.46	Non-Competitive
	α-glucosidase	29540±104	3170	3210	Non-Competitive
8o	AChE	131.02±3.28	335.85	0.38	Non-Competitive
	BChE	122.66±3.28	302.54	0.44	Non-Competitive
	α-glucosidase	40280±2840	3190	3320	Non-Competitive
3c	AChE	142.02±2.97	365.25	0.38	Un-competitive
	BChE	132.06±3.67	324.60	0.49	Un-competitive
	α-glucosidase	30250±1600	3120	3150	Competitive
8j	AChE	140.92±3.03	367.25	0.37	Un-competitive
	BChE	134.02±3.16	320.60	0.48	Un-competitive
	α-glucosidase	19400±1700	3150	3150	Competitive

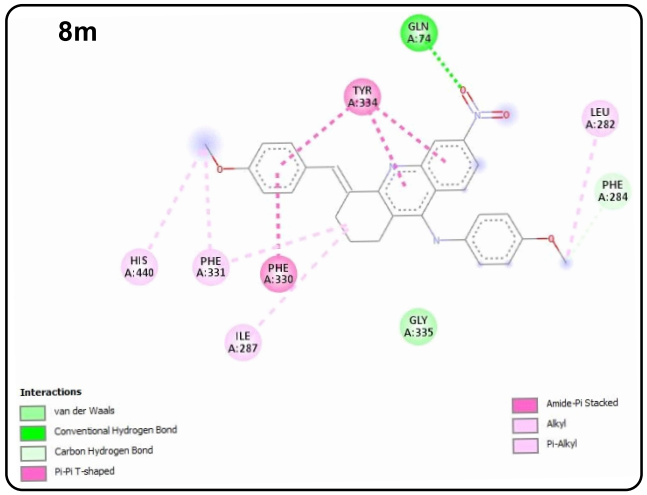
8m
GLN A:74
TYR A:334
LEU A:282
PHE A:284
HIS A:440
PHE A:331
PHE A:330
GLY A:335
ILE A:287
Interactions
van der Waals
Conventional Hydrogen Bond
Carbon Hydrogen Bond
Pi-Pi T-shaped
Amide-Pi Stacked
Alkyl
Pi-Alkyl

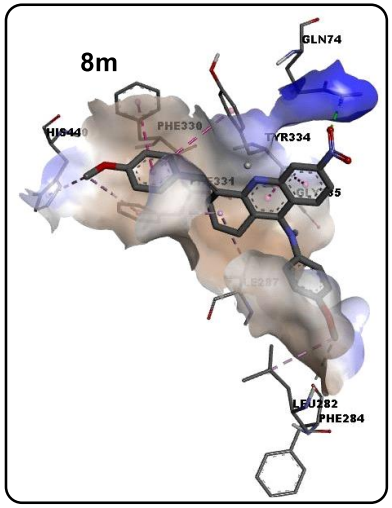
8m
GLN74
PHE330
TYR334
LEU282
PHE284

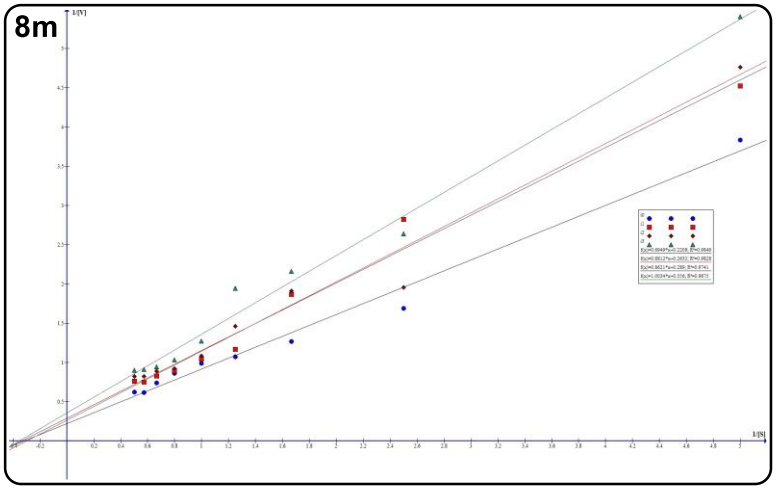
8m
1/[V]
1/[S]

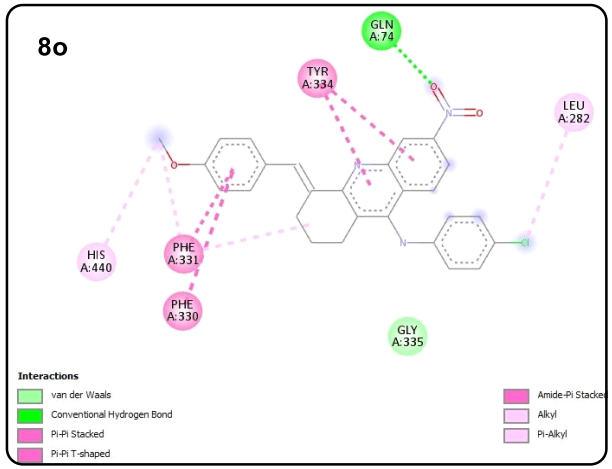
8o
GLN A:74
TYR A:334
LEU A:282
HIS A:440
PHE A:331
PHE A:330
GLY A:335
Interactions
van der Waals
Conventional Hydrogen Bond
Pi-Pi Stacked
Pi-Pi T-shaped
Amide-Pi Stacked
Alkyl
Pi-Alkyl

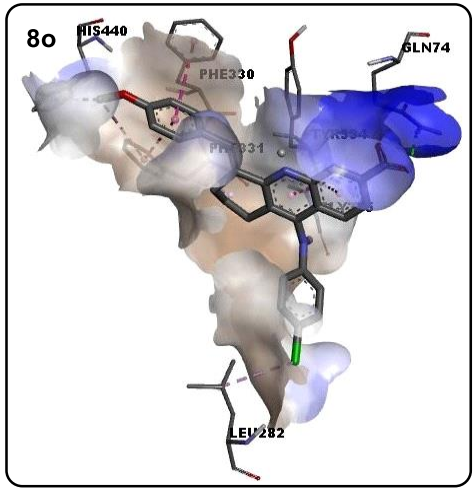
8o
HIS440
GLN74
PHE330
LEU282

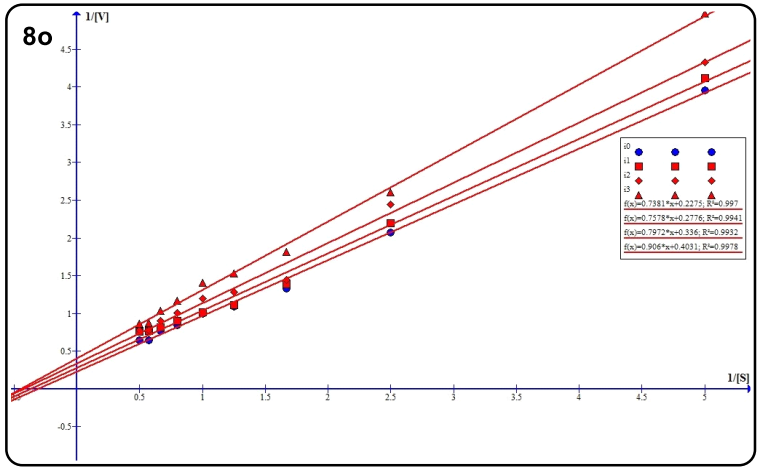
8o
1/[V]
1/[S]

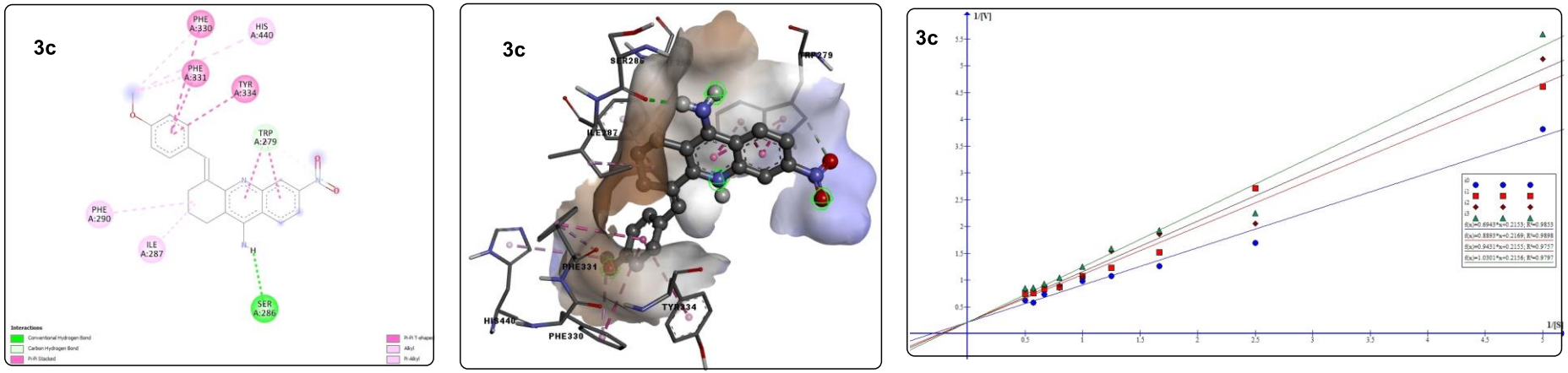

Figure 2.2.1g 2D, 3D docking interactions of compound **8m, 8o, 3c** with protein **1DX6**, Lineweaver–Burk plot for understanding the interaction of AChE with compounds **8m, 8o, 3c**

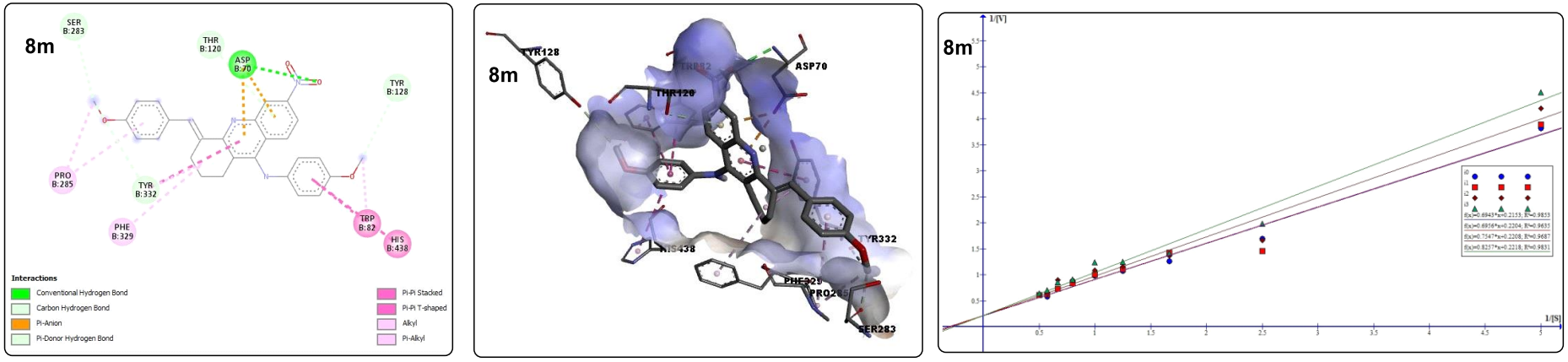

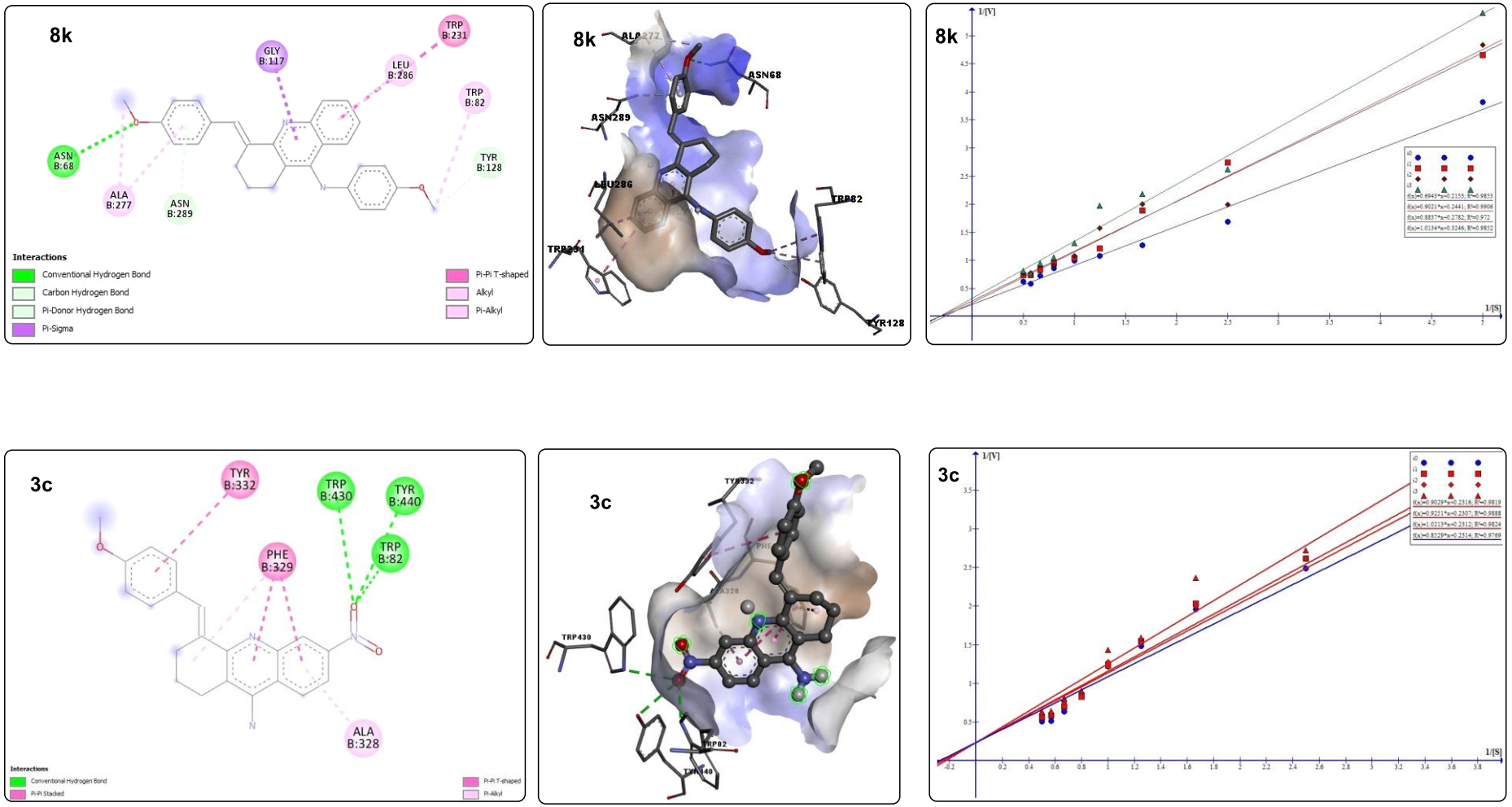

Figure 2.2.1h 2D, 3D docking interactions of compounds **8m, 8k, 3c** with protein **6EMI**, Lineweaver–Burk plot for understanding interactions of BChE with compounds **8m, 8k, 3c**

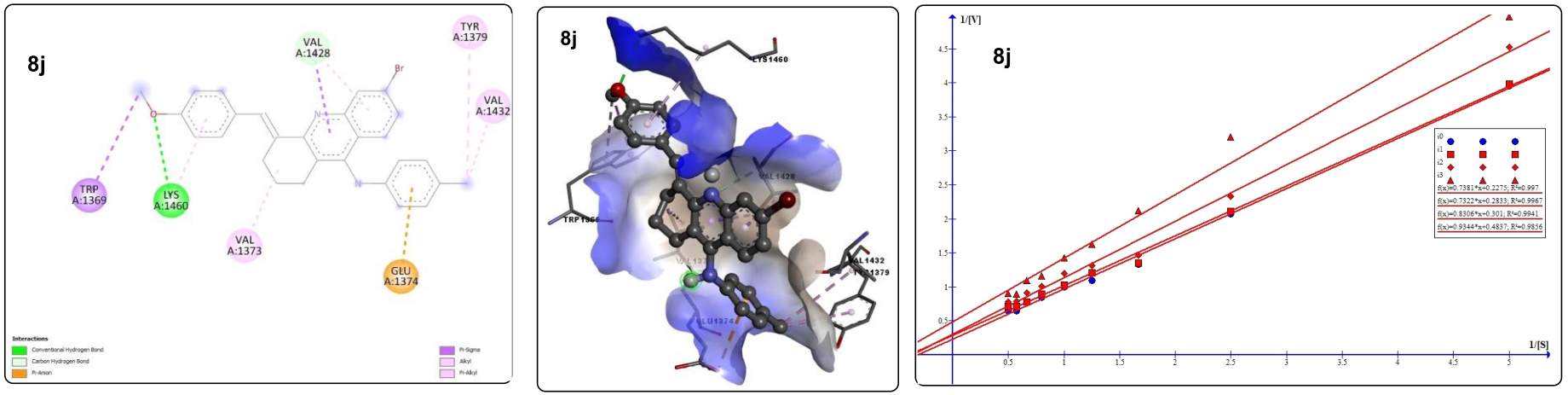

Figure 2.2.1i 2D, 3D docking interactions of compound **8j** with protein **3TOP**, Lineweaver–Burk plot for understanding the interaction of α-glucosidase with compound **8j**

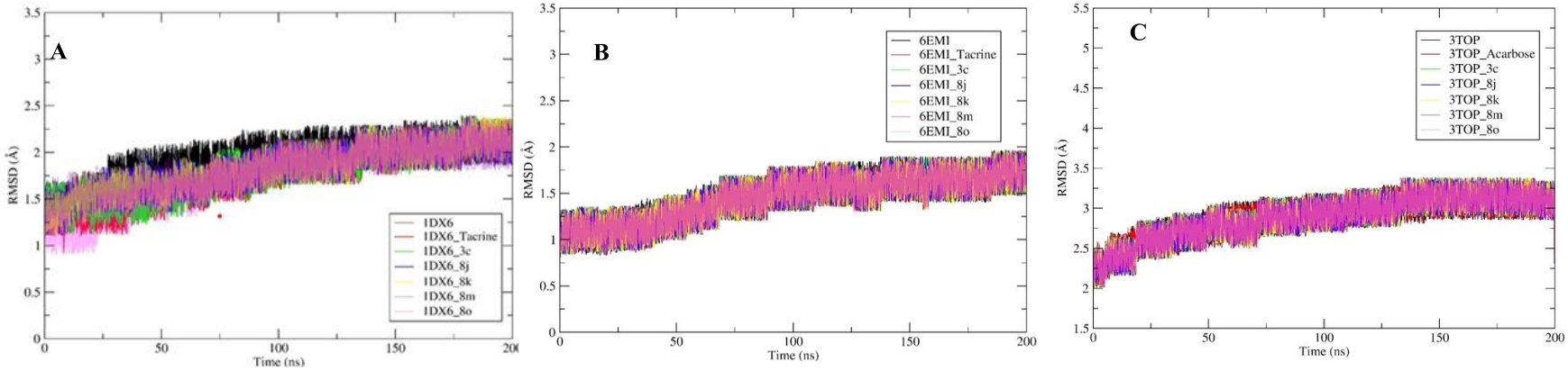

Figure 2.2.1j RMSD plot of apo-protein, co-ligands and ligand-protein complexes systems. A) 1DX6-AChE, B) 6EMI-BChE, C) 3TOP- α-glucosidase

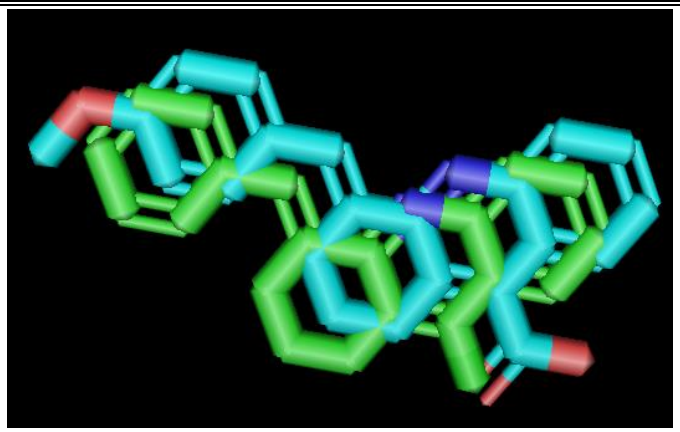

Figure 2.2.1k Superimposed structures of the **8m, 8o, 3c** compounds showed maximum AChE and BChE inhibitory activity

2.2.1.5b Blood Brain Barrier Prediction

Penetration across the blood–brain barrier BBB is an important property for compounds developed for Alzheimer's Disease or any drug targeting the central nervous system. The predicted data obtained from the BBB predictor module of ALzPlatform showed all the tested compounds chosen based on AChE and BChE *in vitro* inhibitory activity are found to be BBB+, this shows these molecules are BBB permeable and they can cross the blood-brain barrier. The predicted properties are listed in **Table 2.2.5**.

Table 2.2.5 BBB Prediction of Compounds by ALzPlatform

Compound	SVM_MACCSFP BBB Score	BBB Permeability
8m	0.055	BBB+
8o	0.061	BBB+
8k	0.080	BBB+
8d	0.081	BBB+
8l	0.076	BBB+
8g	0.082	BBB+
8n	0.078	BBB+
8j	0.068	BBB+
3c	0.088	BBB+
Tacrine	0.120	BBB+

2.2.1.5c Prediction of Drug-Like Property

The drug-like property was predicted based on Lipinski Rule of Five, the property of the drug was predicted based on the molecular mass of the compounds less than 500 Dalton, lipophilicity (based on LogP less than 5), hydrogen bond donors (less than 5), hydrogen bond acceptors (Less than 10), Molar refractivity in the range 40-150. The drug-likeness prediction was carried out using the SwissADME tool.[28] Based on analysis it was observed that the compounds showing better inhibitory activity for α-glucosidase, AChE, and BChE do not violate the Lipinski Rule of Five, hence having drug-like properties (**Table 2.2.6**).

Table 2.2.6 Drug-Like property

Compound	Molecular Mass (g/mol)	High Lipophilicity Log Po/w	Hydrogen Bond Donors	Hydrogen Bond Acceptors	Molar Refractivity
8m	467.52	4.11	1	5	140.93
8k	422.52	4.52	1	3	132.11
8o	471.93	4.53	1	4	139.45
3c	361.39	2.98	1	4	109.30
8j	485.41	4.88	1	2	138.28

2.2.1.5d QSAR analysis

Table 2.2.7 Statistical parameters of the GA-LDA

Parameters	Training Set	Test Set
No. of Compounds	30	15
Sensitivity (%)	66.3	74.2
Specificity (%)	66.4	73.7
Accuracy (%)	88.0	94.1
Precision (%)	73.4	78.1
MCC	0.561	0.544
AUROC	0.876	0.893

For comparable structures, docking analyses were carried out to ascertain the biological importance. A QSAR model was developed, and the docking score acquired for a set of substances with comparable structural/functional groupings was used to determine the biological activity. A combination of nitro at the R position and methoxy groups at the R_1 and R_2 positions in the substance showed a good correlation with the inhibitory effect. The compounds with aryl methoxy (R_2) and methoxy (R_1) also exhibited an inhibitory activity effect. However, the inhibitory properties were lacking for the compounds with chloro/bromo substitutions at the R_2 position alone. The compounds with high TPSA and high hydrophobicity showed good interaction with the AChE and BChE.

According to interactions obtained in docking studies and assumptions made by using the QSAR studies, it can be elucidated that these functional groups exhibit the inhibitory effect due to the hydrophilic basic nature of amino acids (HIS239, HIS279, LYS155, ARG312) that are present in the core binding cavity of α-glucosidase. For AChE TYR332 was found to interact with the top substituted aryl methoxy groups and PHE329 was found to interact with the Nitro or Bromo substitution in the R position.

2.2.1.6 Conclusions

In conclusion, we have designed and synthesized functionalized tacrine derivatives using DMU and L-(+)-TA as a green protocol. Based on the docking studies/binding interactions, the synthesized compounds were evaluated for inhibitory activity (*in vitro*) against AChE, BChE and α-glucosidase enzymes. The majority of the compounds efficiently showed inhibitory activity against AChE, BChE and α-glucosidase in the nanomolar range. Among the tested compounds, **8m** was found to be most potent with IC_{50} = **125.06** nM and **119.68** nM towards AChE and BChE respectively. Compound **8j** showed promising inhibitory activity against α-glucosidase enzyme with an IC_{50} value of **19400** nM. Kinetic studies indicated that compounds **8m**, **8k**, and **8o** exhibit a non-competitive mode of inhibition against AChE and BChE (because if hydrophobic amino acids present in the active pocket of AChE, BChE and methoxy substitution at R_1 position). The compound **8j** is more potent towards α-glucosidase enzyme exhibiting the competitive mode of inhibition. Additionally, the generated QSAR model provides an assumption that the nitro group at R position and methoxy group at R_1 and R_2 position in the compound exhibit good inhibitory activity. The molecular docking and dynamics simulation studies of compounds **8m**, **8k**, **8o**, and **3c** with AChE and BChE reveal binding interactions involved and stability of the bound complex that extend beyond simple ligand-protein associations. The interplay of hydrogen bonding, aromatic interactions, and the

influence of specific substituents on the compounds collectively contribute to the understanding of their inhibitory potential. These findings not only advance our knowledge of the molecular basis of enzyme inhibition but also pave the way for rational drug design and the development of novel therapeutic agents targeting cholinesterase.

2.2.2 Synthesis of 1,2,3,4-tetrahydroacridine based-1,2,3-triazole derivatives and their evaluation as dual cholinesterase and α-glucosidase inhibitors

Encouraged by the above results, and in continuation of our interest in searching for tacrine-based potential cholinesterase and α-glucosidase inhibitors, we aimed to replace C9-NH_2 with a 1,2,3-triazole moiety as bioisostere (a rigid unit at C9). Accordingly, the docking studies were performed. These studies indicated the interaction of one of the nitrogens with the active site in the enzyme.

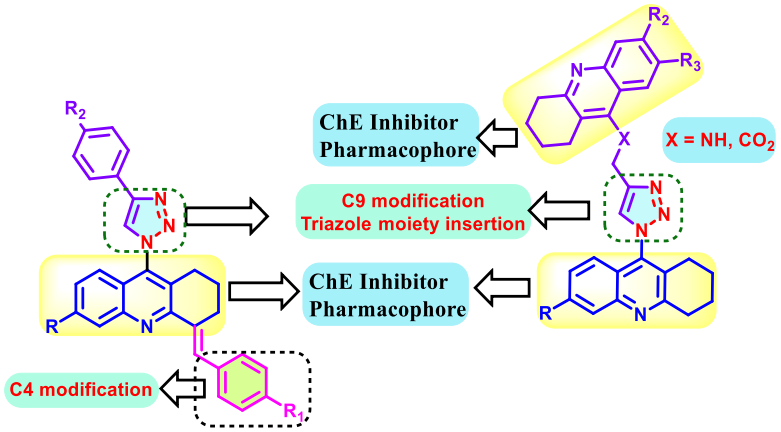

Figure 2.2.2a Design of new tetrahydroacridine - 1,2,3-triazole hybrids

2.2.2.1 Results and Discussion

Based on the molecular docking studies, the design and synthesis of 1,2,3-triazole hybrids-1 and 1,2,3-triazole hybrids-2 were planned using Cu(I)-catalysed alkyne-azide 1,3-dipolar cycloaddition (CuAAC) as a key step as shown in retrosynthetic analysis in **Scheme 2.2.2a**.

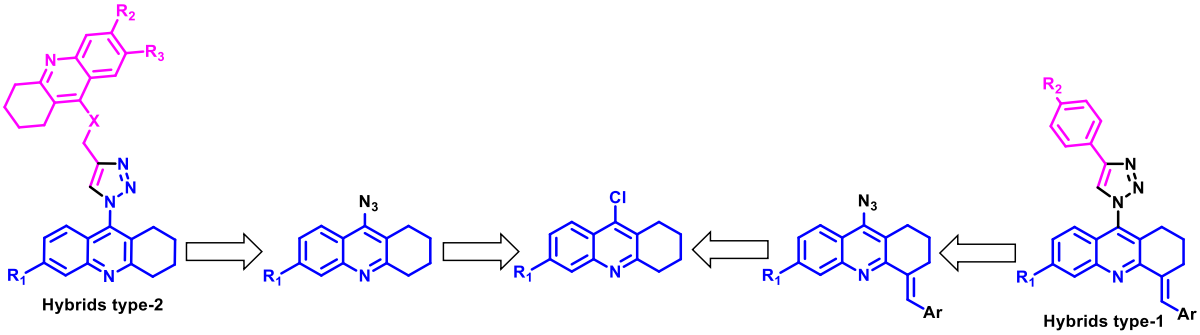

Scheme 2.2.2a Retrosynthetic plan for the Tetrahydroacridine-1,2,3-triazole hybrids type-1 and type-2

Towards achieving the objectives, initially 9-chloro-1,2,3,4-tetrahydroacridine (**1a**) was treated with benzaldehyde under DES* to obtain C(sp^3)-H functionalised derivatives **5a**. The addition of NaN_3 to the same reaction pot gave the 9-azido-1,2,3,4-tetrahydracridine derivative **6a**. Then compound **6a** was treated with phenylacetylene (**9**) in H_2O: ^{t}BuOH (1:1) in the presence of Et_3N, $CuSO_4$ and sodium ascorbate at room temperature for 3–4 h to give **10a** 90% yield (**Scheme 2.2.2b**). The structure of **10a** was confirmed using ^{1}H-, ^{13}C-NMR and HRMS spectroscopy.

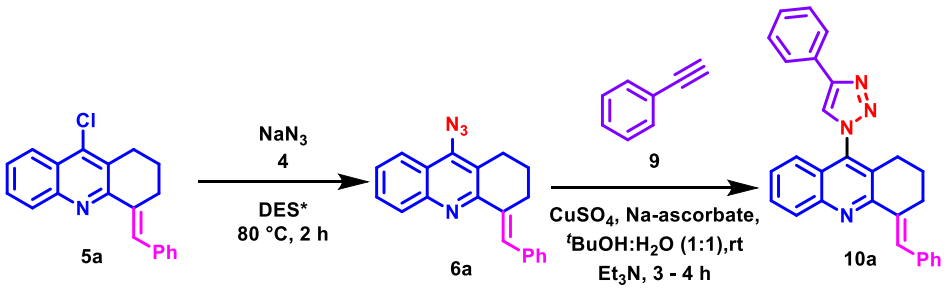

Scheme 2.2.2b Synthesis of 1,2,3-triazole containing tacrine derivative **10a** by Click reaction of azide (**6a**) with phenylacetylene (**9**)

After confirming the structure of the compound **10a**, we next studied the substrate scope by the reaction with differently substituted C(sp^3)-H functionalised 1,2,3,4-tetrahydroacridines (**5a-5h**), substituted phenylacetylenes (**9a-9c**) as illustrated in **Figure 2.2.2b**. The NO_2 substituted acridine derivatives reacted well with phenylacetylene derivatives affording the products in excellent yield (**10c and 10k**).

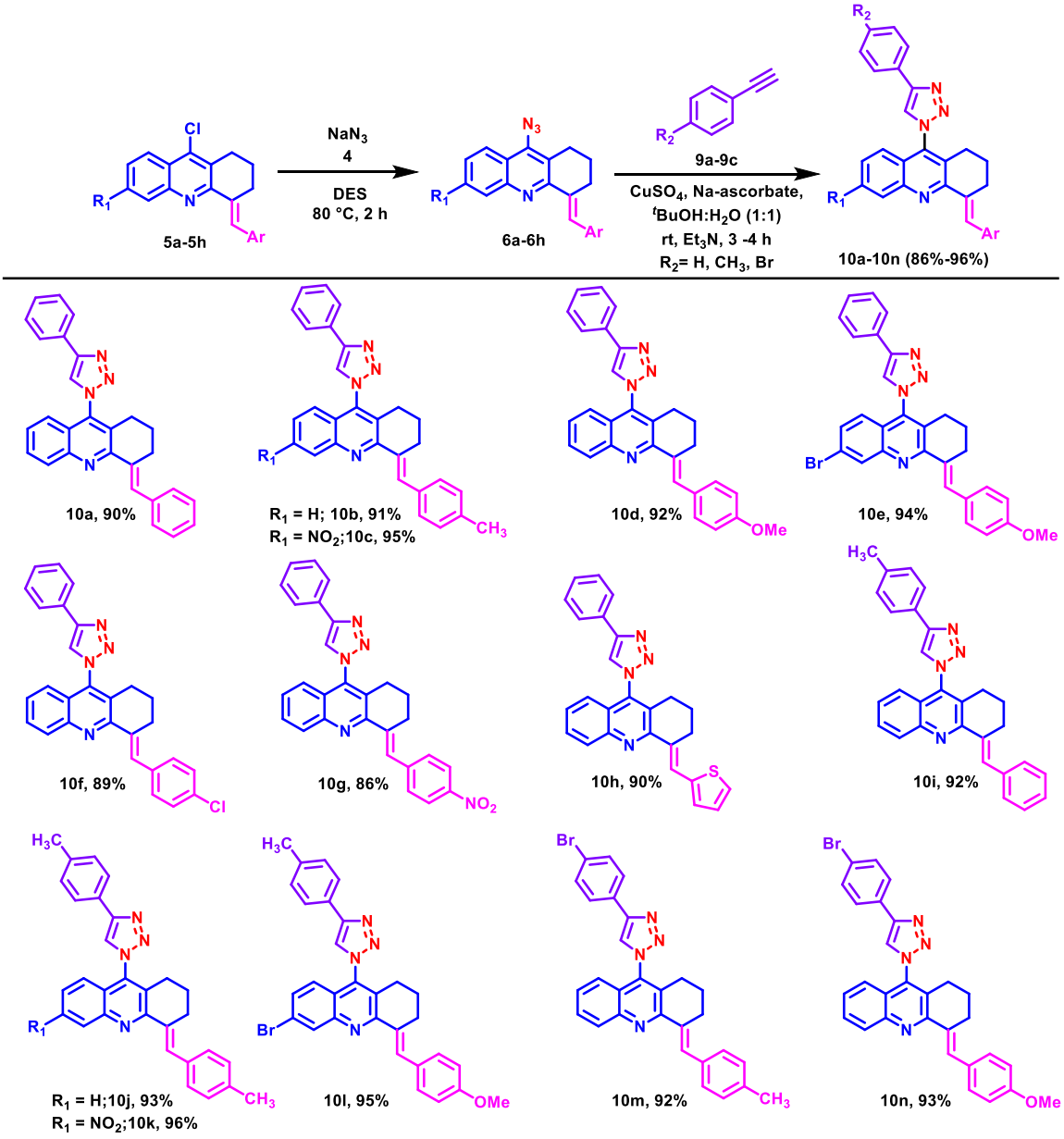

Figure 2.2.2b Synthesis of 1,2,3-triazole containing tacrine derivatives (**10a-10n**)

As described in the introduction, there are a few examples of dimeric tacrine derivatives linked by a biodegradable spacer[4] that show better activity than tacrine as a single molecule. Also, it is well known in the literature that molecular hybridization can lead to enhanced biological (often synergistic effect)/materials properties. Based on this we attempted to synthesise dimeric 1,2,3,4-tetrahydroacridine derivatives with triazole as a linker (**13**) by adopting above described click chemistry conditions. Towards this, 9-azido-1,2,3,4-tetrahydroacridines (**11a-11c**) were reacted with 1,2,3,4-tetrahydroacridine-based terminal alkyne (**12a-12d**) under click conditions to give the desired 1,2,3,4-tetrahydroacridine derivatives **13a-13h** with triazole linker in good to excellent yield (**Scheme 2.2.2c**).

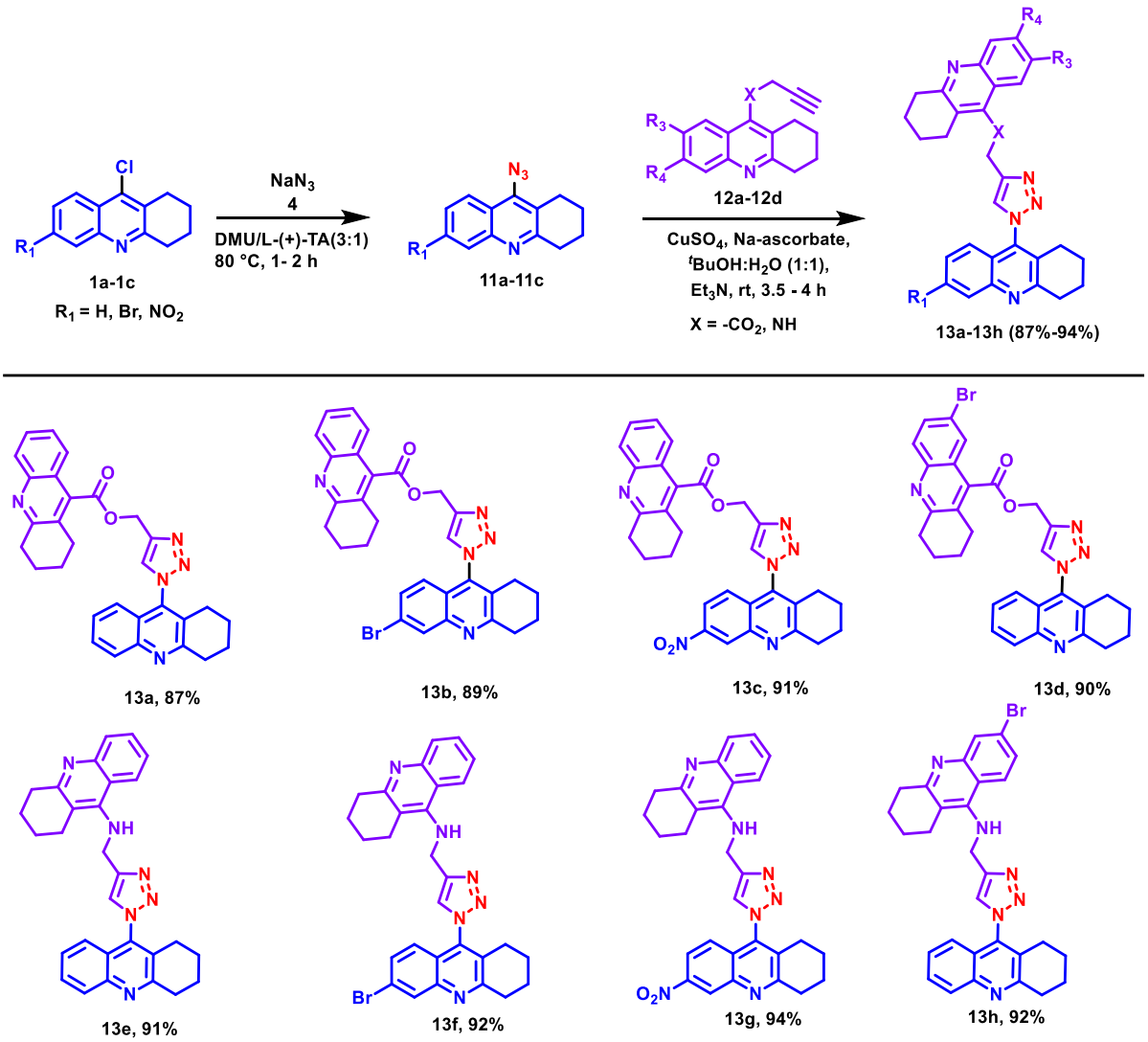

Scheme 2.2.2c Synthesis of dimerized 1,2,3,4-tetrahydroacridine derivatives (**13a-13h**) with triazole as a linker

2.2.2.2 Biological assay Result and discussion

The *in silico* and *in vitro* studies were performed for the resulting products both **10** and **13** series for the acetyl/butyrylcholinesterase and α-glucosidase inhibition. **Table 2.2.8** below indicates that most of the compounds tested here show good activity compared to the standard drug tacrine.

Table 2.2.8 *In vitro* and *In silico* molecular docking study of synthesised compounds

		In vitro	*In silico*	*In vitro*	*In silico*	*In vitro*	*In silico*
S.No.	**Compound**	**AChE - IC_{50} nM**	**Dock score**	**BChE - IC_{50} nM**	**Dock score**	**Glucosidase - IC_{50} nM**	**Dock Score**
1	**10a**	153.12	-8.03	149.32	-7.98	37490	-6.98
2	**10b**	212.21	-7.1	165.32	-7.87	38930	-6.39
3	10c	141.98	-8.01	134.05	-8.03	33100	-7.21
4	10d	223.1	-7.2	156.35	-7.98	36460	-6.76
5	**10e**	140.25	-9.8	142.65	-9.3	38650	-6.82
6	10f	189.32	-7.34	196.35	-7.36	31700	-7.3
7	**10g**	**121.02**	**-11.1**	**132.75**	**-10.6**	37050	-6.93
8	**10h**	135.2	-10.7	**130.45**	-10.3	50350	-6.05
9	**10i**	**130.54**	**-10.7**	**130.21**	**-10.1**	42310	-6.22
10	**10j**	**120.67**	**-11.2**	**132.05**	**-10.6**	40650	-6.31
11	**10k**	138.02	-10.2	140.24	-9.8	47310	-6.54
12	**10l**	132.45	-10	147.03	-9.7	45260	-6.12
13	**10m**	134.25	-10.5	**131.08**	-10.2	44650	-6.47
14	**10n**	132.54	-10	143.05	-9.6	41950	-6.3
15	**13a**	169.51	-7.61	160.53	-7.65	28480	-7.62
16	**13b**	163.54	-7.71	156.67	-7.73	**22390**	**-7.47**
17	**13c**	**128.54**	**-12.9**	**133.54**	**-11.65**	29450	-7.31
18	**13d**	**129.26**	**-12.3**	**130.15**	**-11.54**	29170	-7.59
19	**13e**	**131.65**	**-7.95**	**124.94**	**-7.92**	26570	-7.41
20	**13f**	**131.25**	**-11.6**	**131.58**	**-12.6**	28450	-7.68
21	**13g**	**135.64**	**-11.4**	**136.57**	**-11.5**	26070	-7.64
22	**13h**	**128.12**	**-12.6**	**129.45**	**-11.8**	27980	-7.05
23	**Tacrine**	201.05	-7.76	202.14	-7.71	-	-
24	**Acarbose**	--	--		--	23100	-7.89

Tacrine-1,2,3-triazole based hybrids are developed to show potent anti-cholinesterase activity. As the triazole moiety is capable of interacting with biomolecular targets through H-bonding, π-π stacking and dipole interaction and improves the pharmacokinetics. In this aspect we designed the tacrine-1,2,3-triazole based hybrids by replacing C9-NH_2 by 1,2,3-triazole moiety. *In vitro* and *in silico* studies performed for the synthesized compounds showed improved cholinesterase and α-glucosidase inhibitory activity and binding efficiency. The *in vitro* and *in silico* results for all the synthesised compounds were mentioned in **Table 2.2.8**. Among the synthesised compounds compound **10j**, **10g**, **10i**,**13h**, **13e** are showing better inhibitory activity

and the 2D and 3D binding interactions of potent compounds were mentioned in **Figure 2.2.2c-2.2.2e**. The molecular docking study revealed that the tested compounds **10j**, **10g**, **10i**,**13h**, and **13e** are interacting with the target protein by hydrogen bonding and π-π stacking interactions. The interactions are between hydrophobic amino acids present in the active site pocket of both AChE and BChE, 1,2,3,4-tetrahydroacridine moiety and C4 aryl moiety in compounds (**10j**, **10i**). Compound **13e** shows hydrogen bonding interaction through NH moiety with BChE active site. The compound having more π-π interaction showed better docking score with good IC_{50} values. The compound **13b** showed good inhibitory activity against α-D-glucosidase. The 1,2,3,4-tetrahydroacridine moieties of compound **13b** showed π-π interaction with hydrophobic amino acids at the enzyme active site and one of the nitrogen of 1,2,3-triazole showed hydrogen bonding.

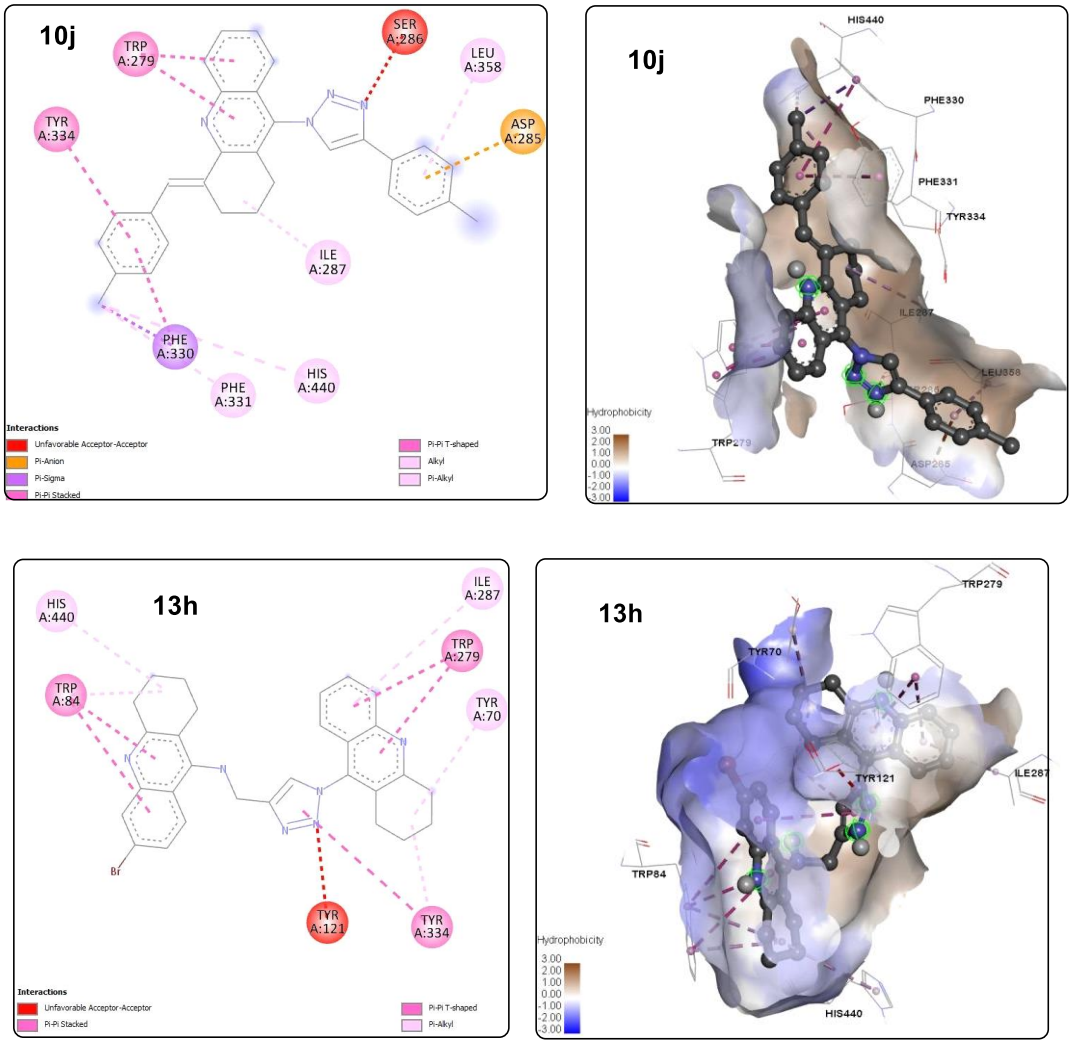

Figure 2.2.2c 2D, 3D docking interactions of compound **10j, 13h** with protein **1DX6**

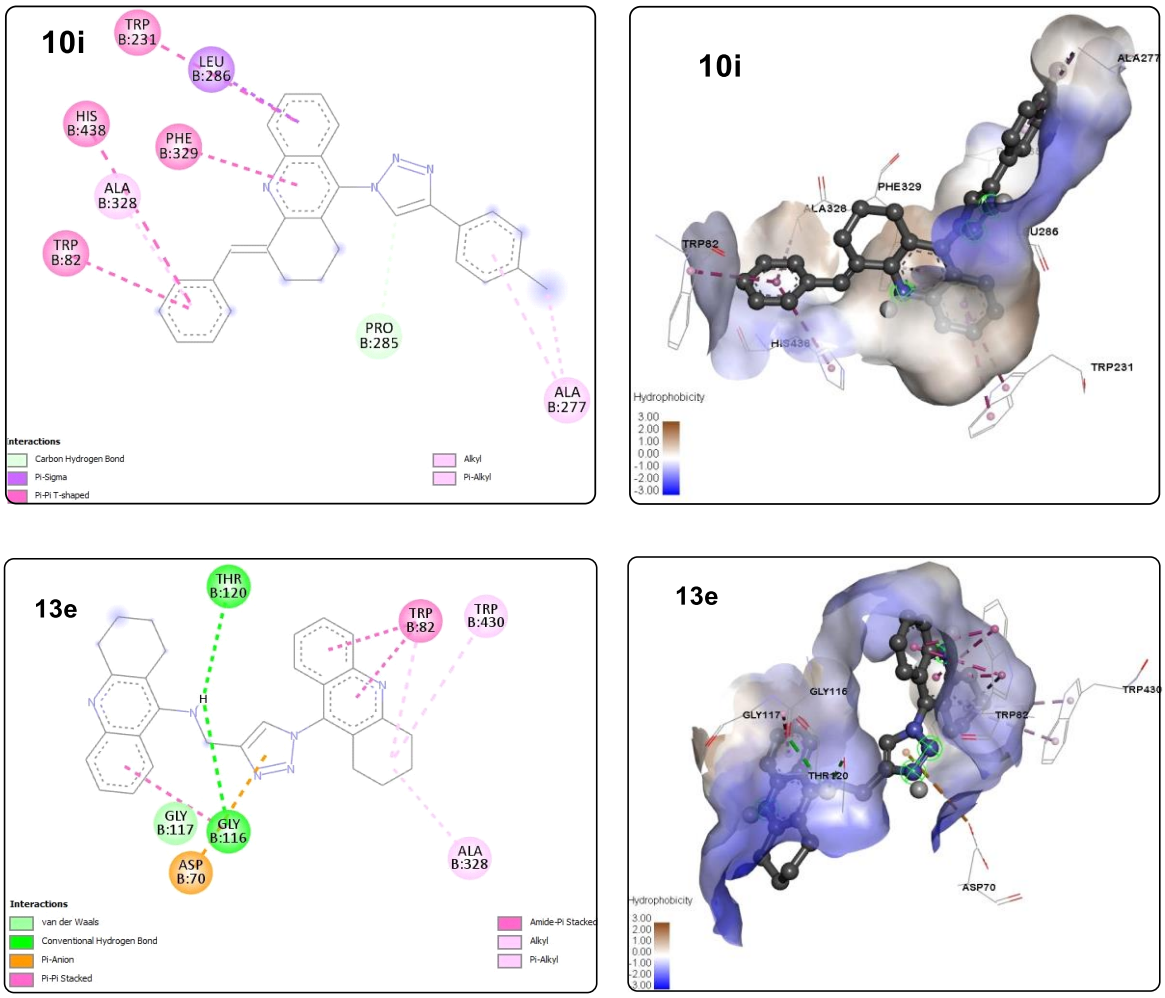

Figure 2.2.2d 2D, 3D docking interactions of compounds **10i, 13e** with protein **6EMI**

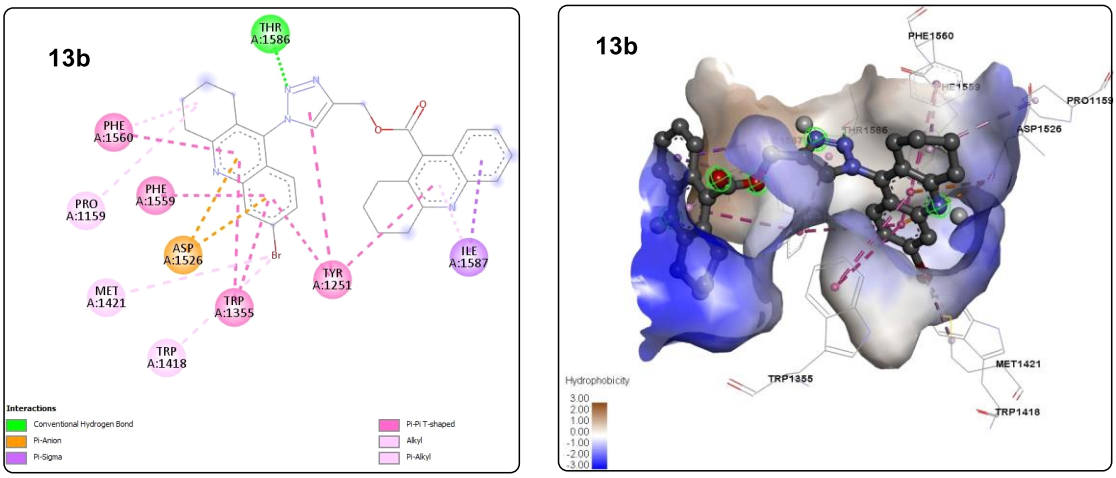

Figure 2.2.2e 2D, 3D docking interactions of compound **13b** with protein **3TOP**

2.2.2.2a Blood Brain Barrier Prediction

The ability to penetrate the blood-brain barrier (BBB) is a crucial characteristic for compounds designed for Alzheimer's Disease treatment or any drug targeting the central nervous system. According to the predicted data from the BBB predictor module of ALzPlatform, all the tested compounds selected based on their *in vitro* inhibitory activity against AChE and BChE were determined to be BBB+. This indicates that these molecules possess BBB permeability and can traverse the blood-brain barrier. The predicted properties are detailed in **Table 2.2.9**.

Table 2.2.9 BBB Prediction of Compounds by ALzPlatform

Compound	SVM_MACCSFP BBB Score	BBB Permeability
10i	0.101	BBB+
10j	0.093	BBB+
10h	0.098	BBB+
10m	0.073	BBB+
10g	0.116	BBB+
13b	0.051	BBB+
13e	0.101	BBB+
13c	0.054	BBB+
13d	0.051	BBB+
13f	0.072	BBB+
13h	0.072	BBB+
Tacrine	0.120	BBB+

2.2.2.2b Prediction of Drug-Like Property

The drug-like property was predicted based on Lipinski Rule of Five, the property of the drug was predicted based on the molecular mass of the compounds less than 500 Dalton, lipophilicity (based on LogP less than 5), hydrogen bond donors (less than 5), hydrogen bond acceptors (Less than 10), Molar refractivity in the range 40-150. The drug-likeness prediction was carried out using the SwissADME tool. Based on analysis it was observed that the compounds showing better inhibitory activity for α - glucosidase, AChE, and BChE do not violate the Lipinski Rule of Five, hence having drug-like properties (**Table 2.2.10**).

Table 2.2.10 Drug likeness and *in silico* ADME properties

Compound	Molecular Mass (g/mol)	Lipophilicity Log Po/w	Hydrogen Bond Donors	Hydrogen Bond Acceptors	Molecular Refractivity	TPSA
10i	428.53	5.79	0	3	134.9	43.6
10j	442.55	6.11	0	3	139.86	43.6
10h	420.53	5.44	0	3	127.81	71.84
10m	507.42	6.39	0	3	142.6	43.6
10g	459.5	4.72	0	5	138.75	89.42
13b	568.46	5.66	0	6	150.29	82.79
13e	460.57	5.06	1	4	140.62	68.52
13c	534.57	4.31	0	8	151.41	128.61
13d	568.46	5.65	0	6	150.29	82.79
13f	539.47	5.61	1	4	148.32	68.52
13h	539.47	5.67	1	4	148.32	68.52

2.2.2.2c QSAR analysis

Table 2.2.11 Statistical parameters of the GA-LDA

Parameters	Training Set	Test Set
No. of Compounds	45	15
Sensitivity (%)	68.83	73.9
Specificity (%)	69.32	74.5
Accuracy (%)	90.0	95.2
Precision (%)	75.5	76.3
MCC	0.548	0.541
AUROC	0.896	0.883

For comparable structures, docking analyses were carried out to ascertain the biological importance. A QSAR model was developed, and the docking score acquired for a set of substances with comparable structural/functional groupings was used to determine the biological activity. The compounds with aryl methyl at R_2 position and with aryl substitution at C4 showed a good interaction with better inhibitory activity. A combination of Br at the R_1 position and aryl substitution at C4 positions in the substance showed a good correlation with the inhibitory effect. However, the inhibitory properties were lacking for the compounds without substitutions at the R_2 position. In dimerized 1,2,3,4-tetrahydroacridine derivatives, the compounds either with Br or NO_2 substitution at R_3 or R_4 are exhibiting good interaction showing better inhibition activity.

According to interactions obtained in docking studies and assumptions made by using the QSAR studies, it can be elucidated that for AChE and BChE TRP239 was found to interact with the 1,2,3,4-tetrahydroacridine moiety.

2.2.2.3 Conclusions

In conclusion, we have designed and synthesized the tacrine-1,2,3-triazole hybrids under click reaction conditions. The synthesized compounds were evaluated for inhibitory activity against AChE, BChE, and α- glucosidase enzymes. Among the tested compounds, compounds **10j, 10g,** and **13h** were found to be most potent with IC_{50} = **120.67** nM, **121.02** nM and **128.12** nM towards AChE, compound **10i, 10h, and 13e** with IC_{50} = **130.21** nM, **130.45** nM and **124.94** nM towards BChE, compound **13b** with IC_{50} = **22390** nM towards α- glucosidase. The developed QSAR model provides assumptions that the 1,2,3,4-tetrahydroacridine moiety and aryl methyl at the R_2 position in the compound exhibit potent inhibitory activity.

2.2.3 Deep Eutectic Solvent mediated synthesis of C4 functionalized Pfitzinger acid derivatives and their evaluation as dual cholinesterase and α-glucosidase inhibitors

In continuation with the above results and in quest for finding even better compounds for the AChE, BChE inhibition and α-glucosidase, further docking studies were performed by varying the functional groups at C9-position of 1,2,3,4-tetrahydroacridine with carboxylic acids (-COOH), esters (-COOR), and amides (-COONHR) in the place of $–NH_2$ group. Interestingly, it was found that the space available at the top (in the binding pockets) can be used for introducing the hydrophobic groups. In this context, we envisaged synthesizing a series of 1,2,3,4-tetrahydroacridine based compounds with -COOH, -COOR or -COONHR at the C9 position and along with substitutions at the C4 position and C7 position to exert influence on the cholinesterase inhibitory activity. Thus, we describe here the DES-mediated synthesis of C4 functionalised C9 substituted 1,2,3,4-tetrahydroacridine through C(sp^3)-H functionalization (**Scheme 2.2.3a**), *in vitro* and *in silico* studies of synthesised compounds for AD therapy.

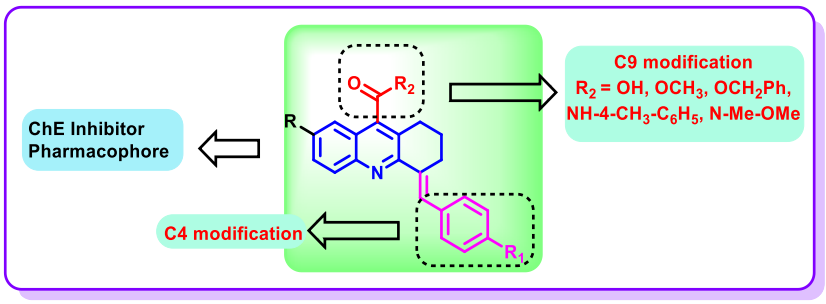

Figure 2.2.3a Design of C4 functionalised Pfitzinger acid derivatives

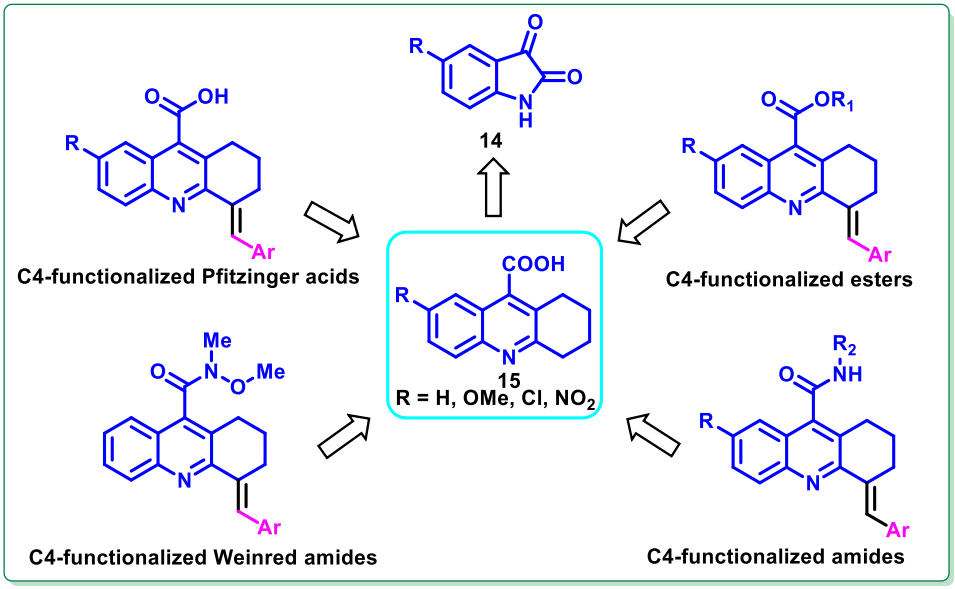

Scheme 2.2.3a Retrosynthetic plan for the C4 functionalised Pfitzinger acid derivatives

2.2.3.1 Results and Discussion

2.2.3.2 Chemistry

Towards achieving the goal, 1,2,3,4-tetrahydroacridine-9-carboxylic acid (**15**) was prepared by Pfitzinger reaction of isatin (**14**) followed by the C4 functionalization using optimized DES*conditions to give the C4-functionalized Pfitzinger acid derivatives **16a-16d** with 42%-50% yields **(Figure 2.2.3b)**. These compounds were tested for acetyl/butyrylcholinesterase and α-glucosidase inhibition. However, the results were promising compared to standard drugs (*the biology results are given in the following section;* **Table 2.2.12**). At this juncture, it was decided to explore further the C9 modification of C4-functionalized derivatives (**16a-16d**) to understand the structure-activity relationship (SAR) and hydrophobic pockets at the top position. In this direction, as an initial attempt, the carboxylic acid **15** was converted into its corresponding methyl ester **18a** which was then treated for the C(sp^3)-H bond functionalisation at C4 position with aromatic aldehyde (**2a**) under DES* at 80 °C to give (**19a**) in excellent yield and structure was confirmed by ^{1}H, ^{13}C NMR and mass spectral data. The resulting compound was tested for acetyl/butyrylcholinesterase and found better than the corresponding carboxylic acid **16a**.

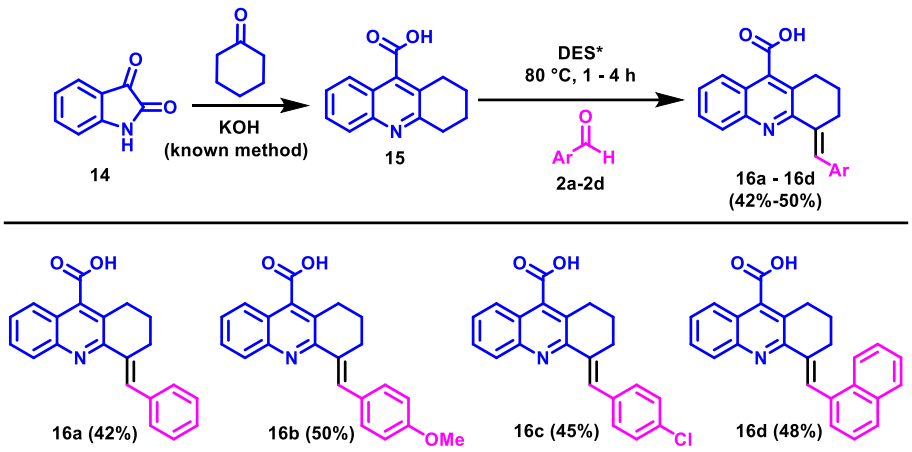

Figure 2.2.3b Synthesis of (*E*)-4-Benzylidene-1,2,3,4-tetrahydroacridine-9-carboxylic acid derivatives (**16a-16d**)

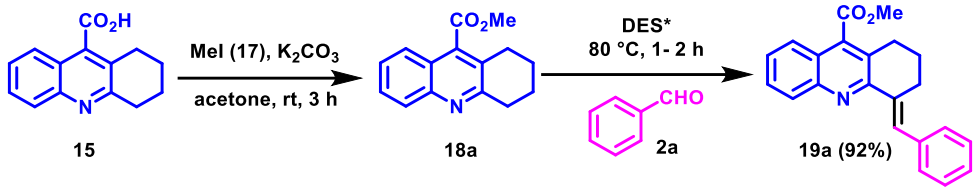

Scheme 2.2.3b Synthesis of (*E*)-4-Benzylidene-1,2,3,4-tetrahydroacridine-9-carboxylic acid derivatives

Further, the Pfitzinger acids with substitution on the aromatic ring (**15a-15d**) were converted to corresponding esters (**18a-18f**) and then treated with the aldehydes (**2a-2j**) under DES* reaction conditions to provide the corresponding C4-functionalized products (**19a-19y**) in good to excellent yields (75-95%) as illustrated in **Figure 2.2.3c**. Interestingly, it was observed that the aromatic aldehydes with electron-withdrawing groups (EWGs) at the *p*-position react faster with the substrates and result in excellent yields of the desired product (**19k-19l**) under optimized conditions. On the other hand, aromatic aldehydes containing electron-donating groups (EDGs) at the *p*-position were found to react at slower rates to offer the desired products in good yields. All the synthesized compounds were tested for biological activity (acetyl/butyrylcholinesterase and α-glucosidase inhibition) and found that majority of the compounds showed good IC_{50} values (**Table 2.2.12**).

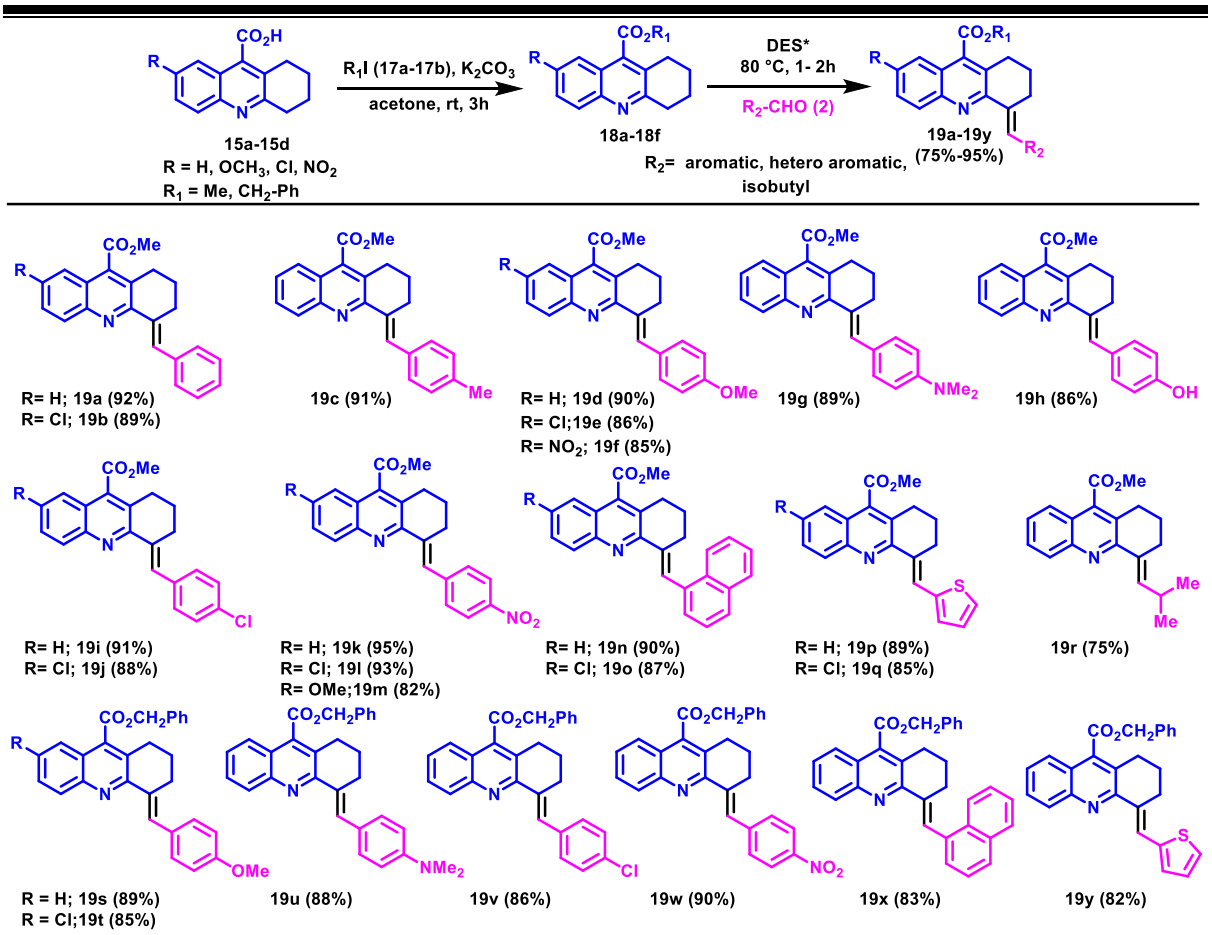

Figure 2.2.3c Synthesis of methyl or benzyl 1,2,3,4-tetrahydroacridine-9-carboxylate derivatives

Encouraged by the above results and with the optimized DES system in hand (for the C4-functionalization), we intended to extend the scope of the modifications of C9 –COOH moiety to amides and Weinreb amides. Accordingly, the *N*-aryl-1,2,3,4-tetrahydroacridine-9-carboxamides (**21a-21c**) were prepared using literature methods. Then they were treated for the C(sp^3)-H functionalization in DES* at 80 °C. To our delight desired products **22a-22m** obtained in good to excellent yield (**Figure 2.2.3d)**. Similar to this, *N*-methoxy-*N*-methyl-1,2,3,4-tetrahydroacridine-9-carboxamide (**24**) was prepared and used to generate **25a-25d** in good to excellent yield (89%-95%) (**Figure 2.2.3e)**. All the resulting products were characterized by using ^{1}H, ^{13}C, and HRMS spectroscopic techniques. All the compounds **22a-22m** and **25a-25c** were screened for biological activity and found that some of the compounds are showing good inhibitory activity as mentioned in **Table 2.2.12**.

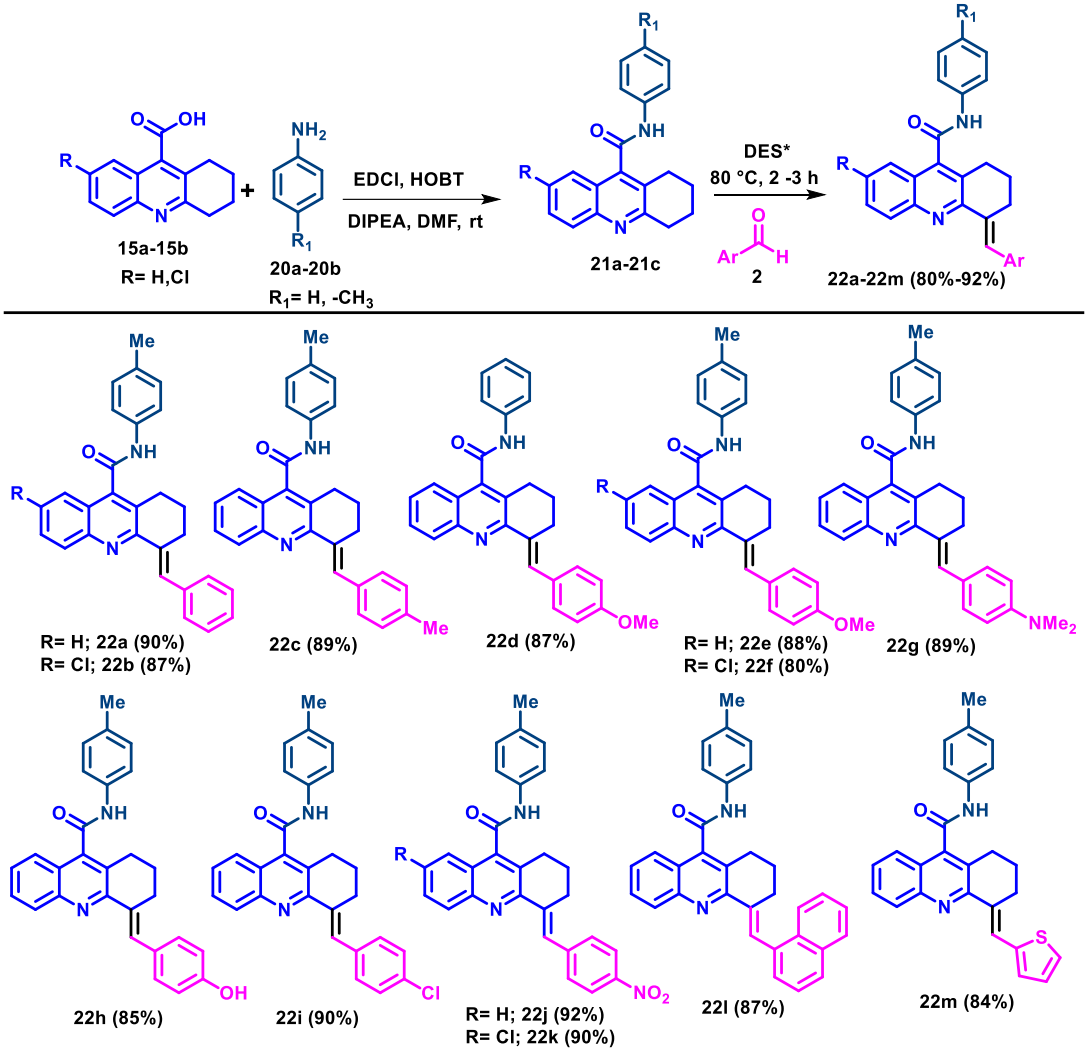

Figure 2.2.3d Synthesis of functionalise *N*-aryl-1,2,3,4-tetrahydroacridine-9-carboxamide (**21a-21c**)

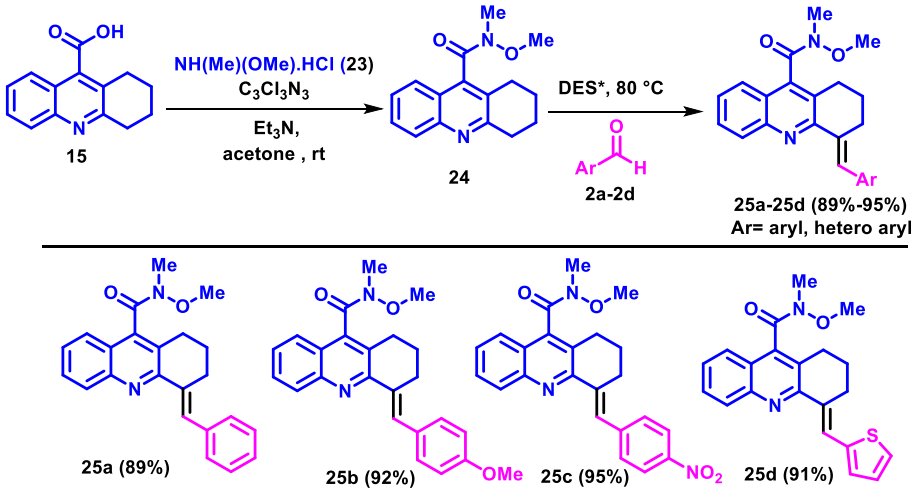

Figure 2.2.3e Synthesis of C4 functionalised *N*-methoxy-*N*-methyl-1,2,3,4-tetrahydroacridine-9-carboxamide (**25a-25d**)

2.2.3.3 Biological assay Results and discussion

Table 2.2.12 ***In vitro*** **and** ***In silico*** **molecular docking study of synthesised compounds**

	In vitro	*In silico*	*In vitro*	*In silico*	*In vitro*	*In silico*
Compound	**AChE - IC_{50} nM**	**Dock score**	**BChE - IC_{50} nM**	**Dock score**	**Glucosidase - IC_{50} nM**	**Dock Score**
16a	210.77	-6.34	209.32	-6.35	29631	-7.53
16b	**142.06**	**-7.68**	**141.11**	**-7.7**	**31254**	**-7.82**
16c	160.14	-7.58	155.44	-7.63	31655	-7.68
16d	193.02	-7.41	186.32	-7.46	45382	-7.58
19a	173.71	-7.53	168.14	-7.56	53187	-7.45
19b	155.62	-7.55	150.47	-7.59	50154	-7.92
19c	166.35	-7.39	161.5	-7.42	32152	-7.46
19d	132.17	-7.9	121.54	-7.92	41078	-7.56
19e	**121.32**	**-7.91**	**122.56**	**-7.92**	**44152**	**-7.59**
19f	**119.65**	**-7.92**	**121.58**	**-7.98**	**41541**	**-7.42**
19g	184.32	-7.41	178.54	-7.46	26453	-7.92
19h	186.02	-7.42	174.19	-7.48	33148	-7.46
19i	156.14	-7.66	146.31	-7.65	51073	-7.64
19j	132.25	-7.87	121.06	-7.9	28347	-7.95
19k	133.57	-7.84	125.83	-7.89	27062	-6.34
19l	**120.58**	**-7.96**	**125.56**	**-7.96**	**35658**	**-7.65**
19m	**122.54**	**-7.91**	**121.85**	**-7.94**	**31154**	**-7.79**
19n	186.35	-7.61	170.28	-7.65	54120	-7.41
19o	175.34	-7.62	169.11	-7.69	27664	-7.83
19p	211.49	-6.51	204.26	-6.54	33717	-7.89
19q	195.34	-6.61	190.14	-6.67	53452	-7.91
19r	212.05	-6.42	209.43	-6.42	42379	-7.61
19s	154.42	-7.65	150.01	-7.69	51842	-7.95
19t	**119.45**	**-7.91**	**118.69**	**-7.93**	**54580**	**-6.51**
19u	176.03	-7.61	171.06	-7.65	26374	-6.61
19v	**124.65**	**-7.9**	**118.25**	**-7.95**	**31574**	**-7.58**
19w	**121.87**	**-7.91**	**118.65**	**-7.93**	**45210**	**-7.68**
19x	167.11	-7.64	155.14	-7.68	40212	-7.41
19y	173.62	-7.53	163.24	-7.59	39057	-7.68
22a	173.25	-7.51	167.12	-7.54	33273	-7.55
22b	164.18	-7.43	154.08	-7.49	41053	-7.69
22c	199.67	-7.31	195.03	-7.32	41338	-7.41
22d	161.84	-7.65	155.11	-7.69	29172	-7.43
22e	**153.64**	**-7.62**	**149.61**	**-7.65**	**22149**	**-7.86**
22f	**145.05**	**-7.65**	**138.25**	**-7.69**	**25364**	**-7.83**
22g	**198.54**	**-7.38**	**193.43**	**-7.41**	**21442**	**-7.94**
22h	199.63	-7.4	195.01	-7.43	26243	-7.61
22i	163.47	-7.64	159.44	-7.66	34569	-7.41
22j	**148.21**	**-7.68**	**143.64**	**-7.72**	**33183**	**-7.62**

22k	159.22	-7.64	152.75	-7.63	41354	-7.66
22l	187.48	-7.4	181.49	-7.43	43141	-7.72
22m	196.86	-7.31	196.25	-7.32	24689	-7.4
25a	138.25	-7.56	137.65	-7.61	26840	-7.91
25b	142.83	-9.1	146.14	-8.6	35418	-7.91
25c	**135.68**	**-7.85**	**129.56**	**-7.91**	**28364**	**-7.91**
Tacrine	201.05	-7.76	202.14	-7.71	-	-
Acarbose	--	--		--	23124	-7.89

Based on the structural and chemical features of tetrahydroacridine (tacrine) based molecules in the previous reports and molecular docking studies, we sought to improve the biological activity profile by substituting various functional groups in the top (C9) and bottom (C4) positions of tetrahydroacridine.

Hasan et al.[29] reported the aryl substitutions to chalcones showed improved cholinesterase inhibitory activity. Aryl substitution was made at C4 of tetrahydroacridine and compounds were tested for *in vitro* choline esterase activity. These aryl substitutions at the bottom of the tacrine were found to increase the *in vitro* inhibitory activity. Based on this, compounds were designed and synthesised by including the electron-withdrawing group and electron-donating to the aromatic ring. From *in silico* and *in vitro* studies it was observed that the substituting electron-withdrawing group to aryl moiety increased the inhibitory activity. From the analysis, it was observed that the aromatic substitution at the bottom position was found to have an interaction with the amino acids in the active site of the enzyme.

From inhibition pattern and kinetics of inhibition of AChE and BChE compounds**19f, 19t, 19v**, and **19w** were found to exhibit maximum inhibitory activity among the tested compounds. The *in vitro* and *in silico* results for all the synthesised compounds were mentioned in **Table 2.2.12** and the 2D, 3D binding interactions along with Lineweaver–Burk double reciprocal plot of potent compounds were mentioned in **Figure 2.2.3f - 2.2.3h**. From the Lineweaver–Burk double reciprocal plot, it was observed that the presence of **19f**, **19t, 19v, and 19w** greatly affected the K_m and V_{max} values. For all the compounds decreasing trend for V_{max} value with an increase in substrate concentration was observed, but there is no significant change was observed for K_m. This reveals that the tested compounds exhibit a non-competitive or mixed-competitive mode of inhibition against AChE and BChE.

The molecular docking studies revealed that the tested compounds **19f, 19t, and 22f** are interacting with the target protein by hydrogen bonding and aromatic (π-π stacking)

interactions. The interactions are between hydrophobic amino acids present in the active site pocket of both AChE and BChE, methoxy group substitution attached to the aromatic ring at C4 position. It was evident from the *in silico* 2D interaction representation that the hydrophobic amino acids have interaction with the methoxy group of the molecules. In compounds **19t**, **19v**, **22f** the aromatic ring at the C9 position is showing aromatic (π-π stacking) interactions with hydrophobic amino acids in the active site pocket of AChE, BChE. Surprisingly, no significant interaction with the methyl ester at C9 is observed when **19f** is docked with AChE and BChE. The compound having more π-π interaction showed a better docking score that indicates the significant role of hydrophobic moiety introduced in the synthesized compounds (**19f**) thus giving better results with good IC_{50} values.

The Tested compounds **22g** and **22e** showed good inhibitory activity against α-D-glucosidase. Substitution of *N,N*-dimethyl, methoxy group in the aromatic ring at C4 position along with *N*-aryl amide at C9 enhanced the inhibitory activity. The compounds with other substitutions at the C9 position did not enhance the inhibitory activity. *In vitro* studies performed for compounds functionalized at the C4 position and C9 substitution with ester or amide group showed improved AChE and BChE inhibitory activity and binding efficiency than the reference drug tacrine.

2.2.3.3a Molecular Dynamics Simulation

Focusing specifically on the Acetylcholinesterase (AChE, PDB ID: 1DX6) and Butyrylcholinesterase (BChE, PDB ID: 6EMI) protein-ligand complexes, their average RMSD values ranged between 1.2 Å to 3.25 Å, similar to the RMSD of the apo-protein complex. Notably, compounds **19e**, **19f,** and **19l** consistently exhibited an average RMSD value below 2 Å within the complex, indicating increased stability compared to the apo-protein. Conversely, for the α-glucosidase (PDB ID: 3TOP) protein-ligand complexes, the average RMSD values fluctuated within the range of 2 Å to 3 Å, aligning with the RMSD of the apo-protein complex. Particularly noteworthy were the protein-ligand complexes involving compounds **19l** and **22f,** both consistently demonstrating an average RMSD value below 2.25 Å. This noteworthy observation reinforces the conclusion that these specific hits exhibit enhanced stability within the complex compared to the apo-protein. These RMSD profiles not only serve as indicators of structural stability but also furnish valuable insights into ligand-protein interactions.

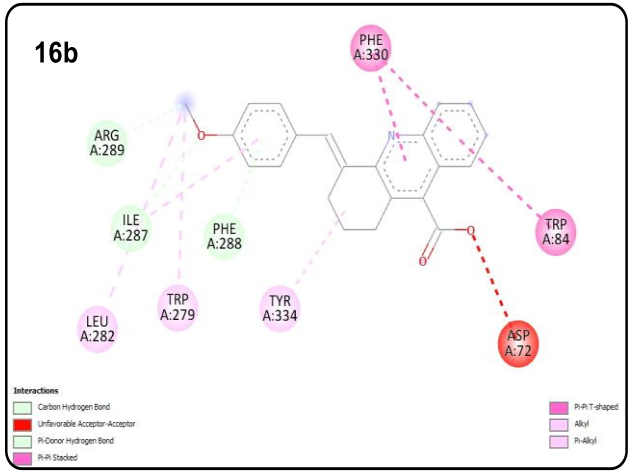
16b
PHE A:330
ARG A:289
ILE A:287
PHE A:288
TRP A:84
LEU A:282
TRP A:279
TYR A:334
ASP A:72
Interactions
Carbon Hydrogen Bond
Unfavorable Acceptor-Acceptor
Pi-Donor Hydrogen Bond
Pi-Pi Stacked
Pi-Pi T-shaped
Alkyl
Pi-Alkyl

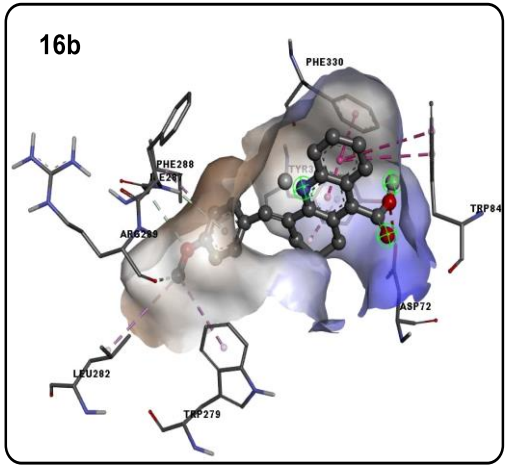
16b
PHE330
PHE288
ARG289
TRP84
ASP72
LEU282
TRP279

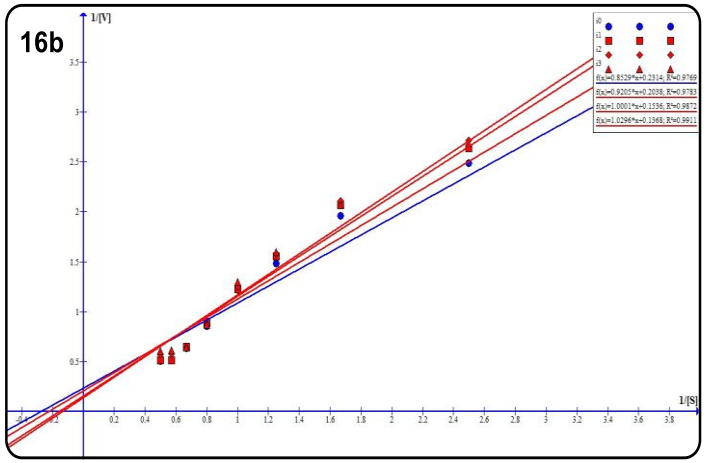
16b
1/[V]
1/[S]

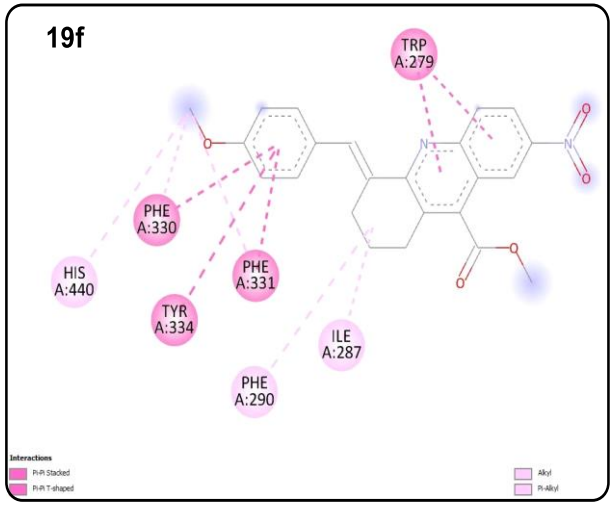
19f
TRP A:279
PHE A:330
HIS A:440
PHE A:331
TYR A:334
ILE A:287
PHE A:290
Interactions
Pi-Pi Stacked
Pi-Pi T-shaped
Alkyl
Pi-Alkyl

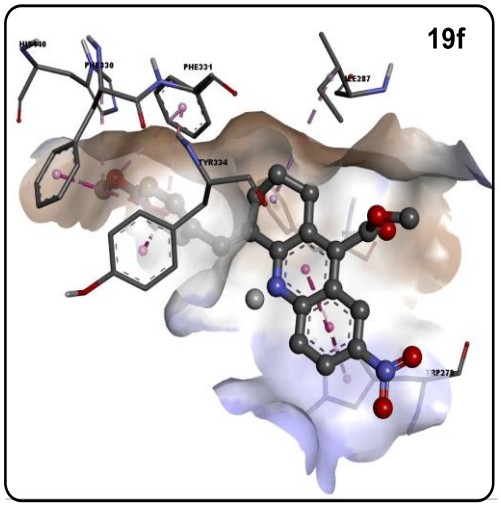
19f
PHE331
TYR334

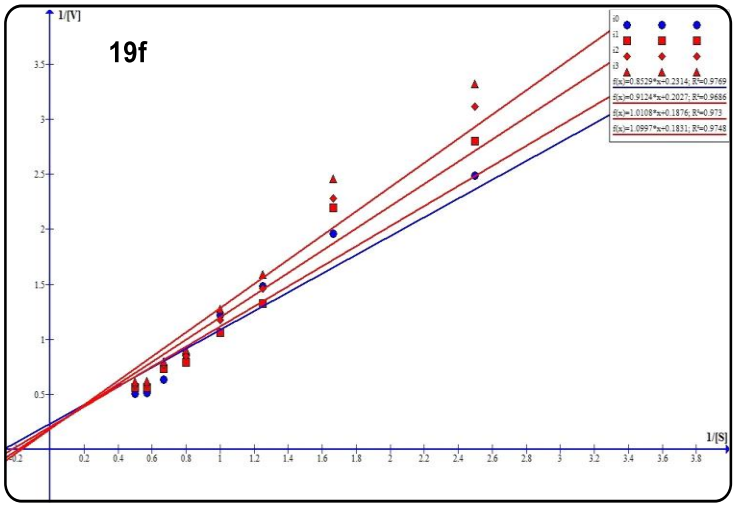
19f
1/[V]
1/[S]

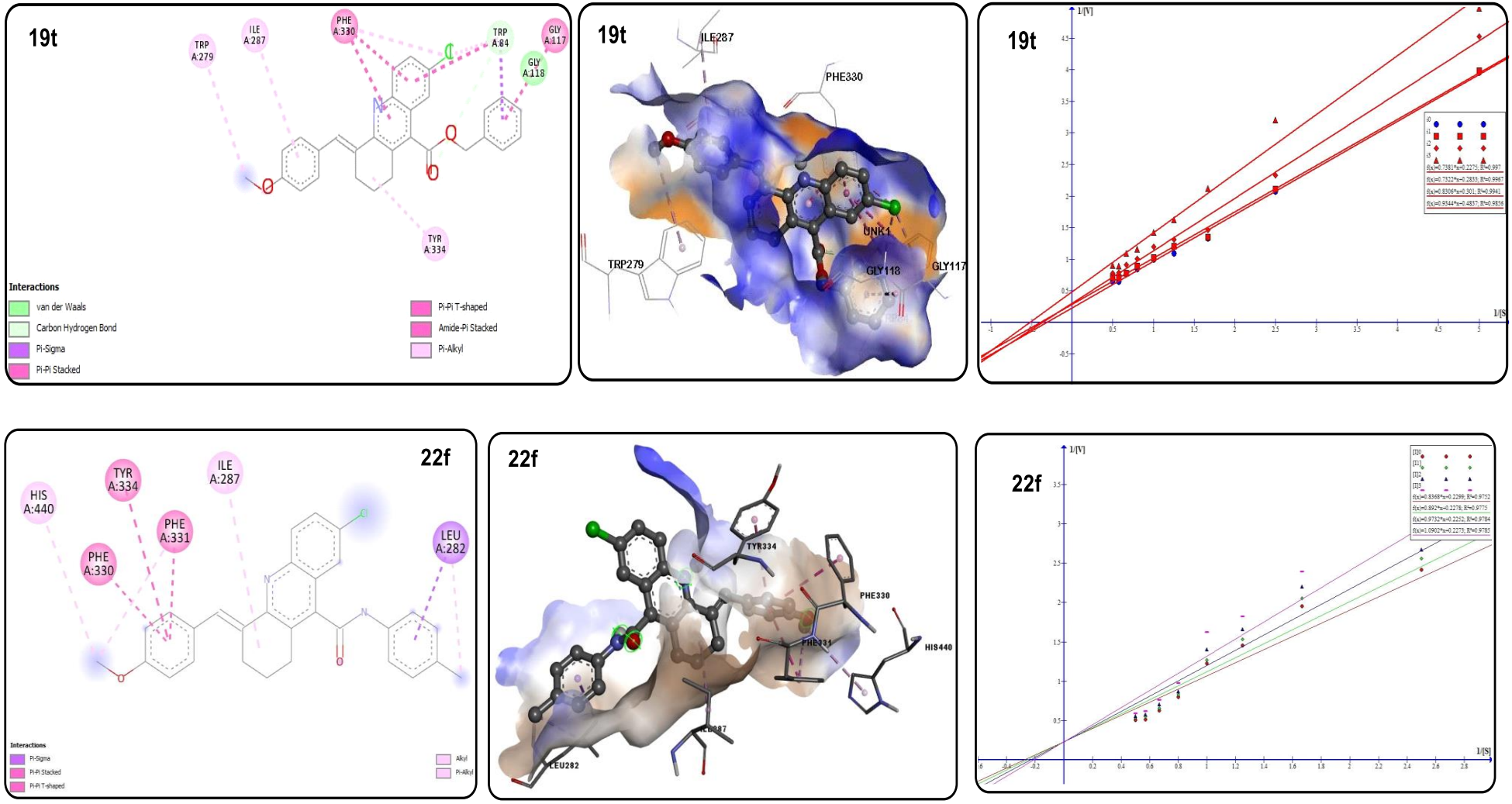

Figure 2.2.3f 2D, 3D docking interactions of compound **16b, 19f, 19t, 22f** with protein **1DX6**, **Lineweaver–Burk** plot for understanding the interaction of AChE with compounds **16b, 19f, 19t, 22f**

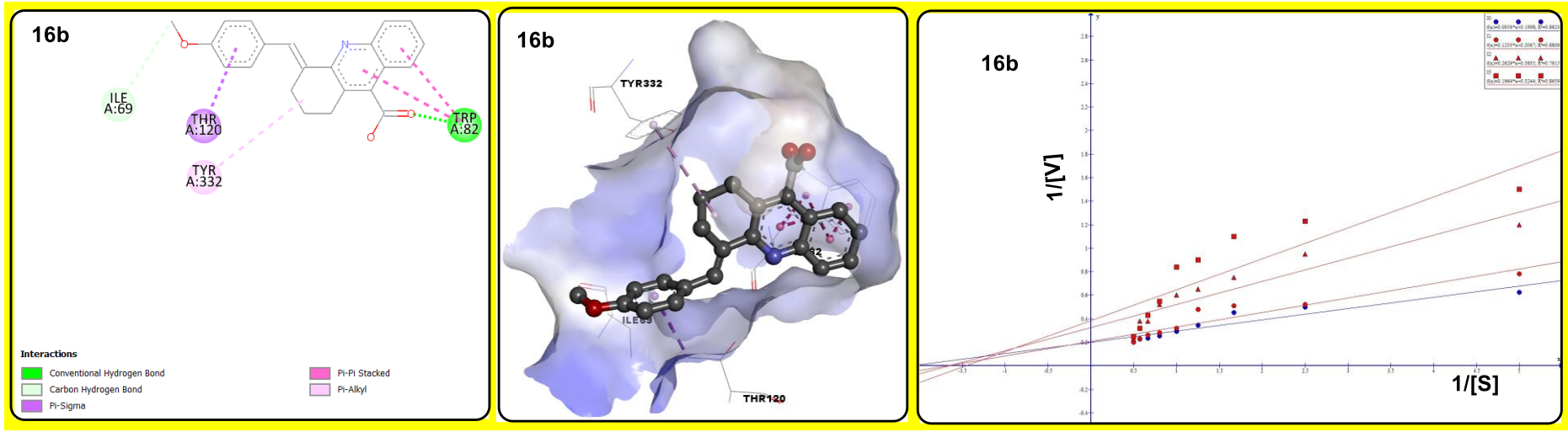
16b
ILE A:69
THR A:120
TYR A:332
TRP A:82
Interactions
Conventional Hydrogen Bond
Carbon Hydrogen Bond
Pi-Sigma
Pi-Pi Stacked
Pi-Alkyl
16b
TYR332
THR120
16b
1/[V]
1/[S]

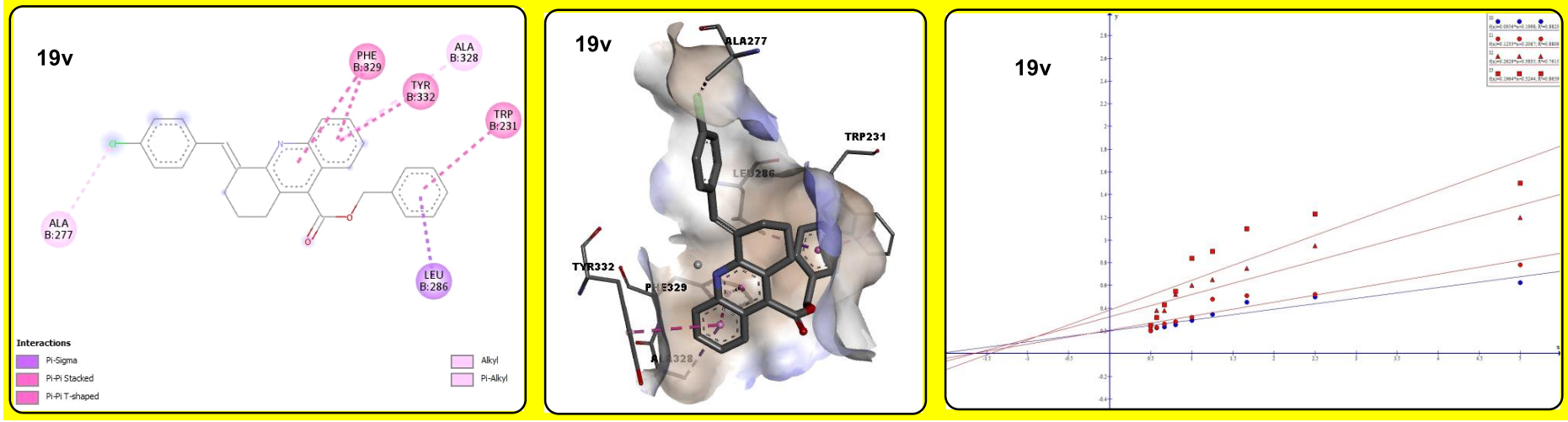
19v
PHE B:329
ALA B:328
TYR B:332
TRP B:231
ALA B:277
LEU B:286
Interactions
Pi-Sigma
Pi-Pi Stacked
Pi-Pi T-shaped
Alkyl
Pi-Alkyl
19v
ALA277
TRP231
TYR332
19v

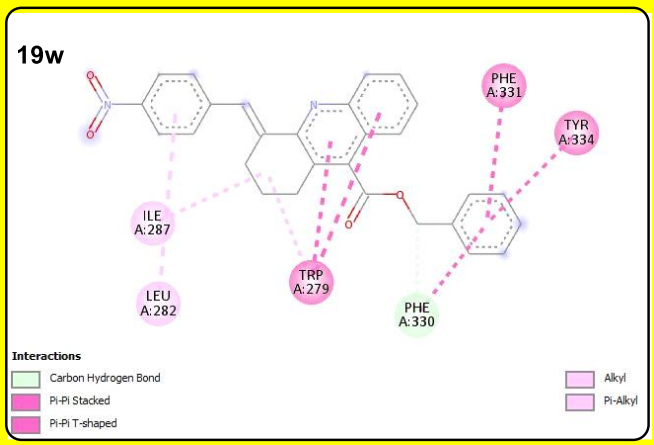
19w
PHE A:331
TYR A:334
ILE A:287
TRP A:279
LEU A:282
PHE A:330
Interactions
Carbon Hydrogen Bond
Pi-Pi Stacked
Pi-Pi T-shaped
Alkyl
Pi-Alkyl

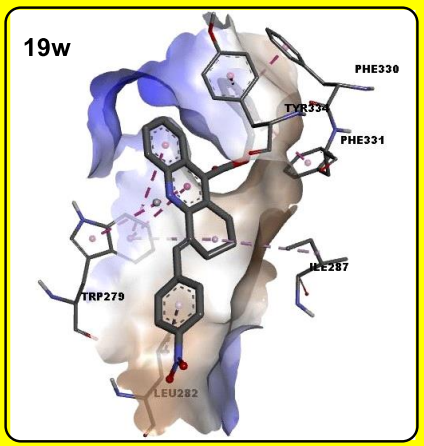
19w
PHE330
TYR334
PHE331
ILE287
TRP279
LEU282

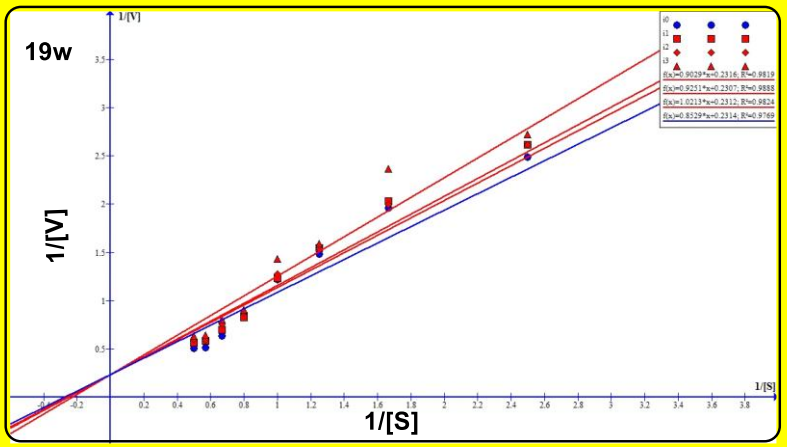
19w
1/[V]
1/[S]

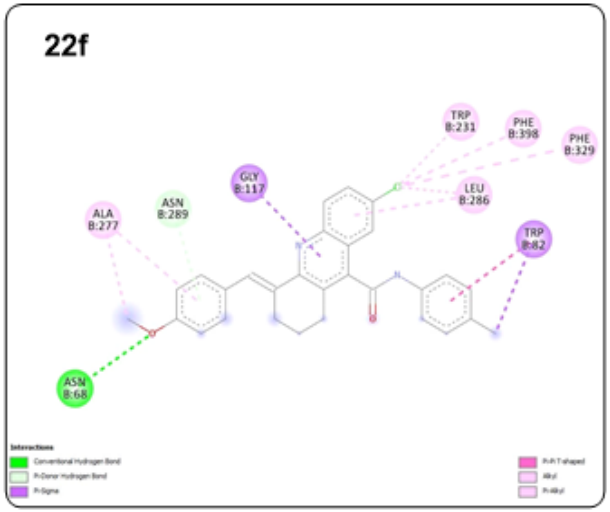
22f
TRP B:231
PHE B:398
PHE B:329
GLY B:117
LEU B:286
ALA B:277
ASN B:289
TRP B:82
ASN B:68

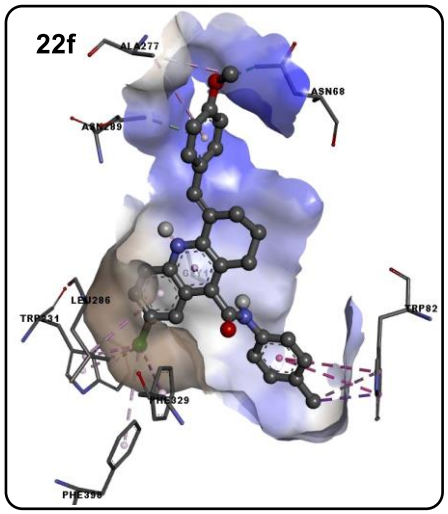
22f
ALA277
ASN68
ASN289
LEU286
TRP231
TRP82
PHE329
PHE330

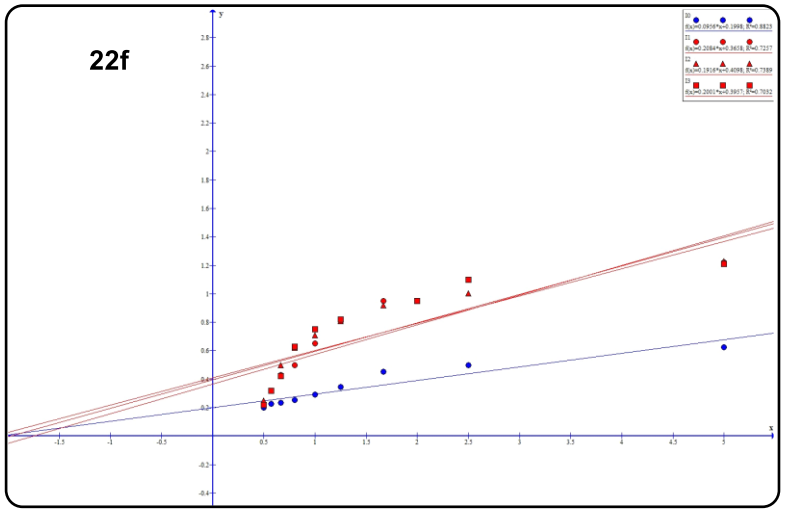
22f

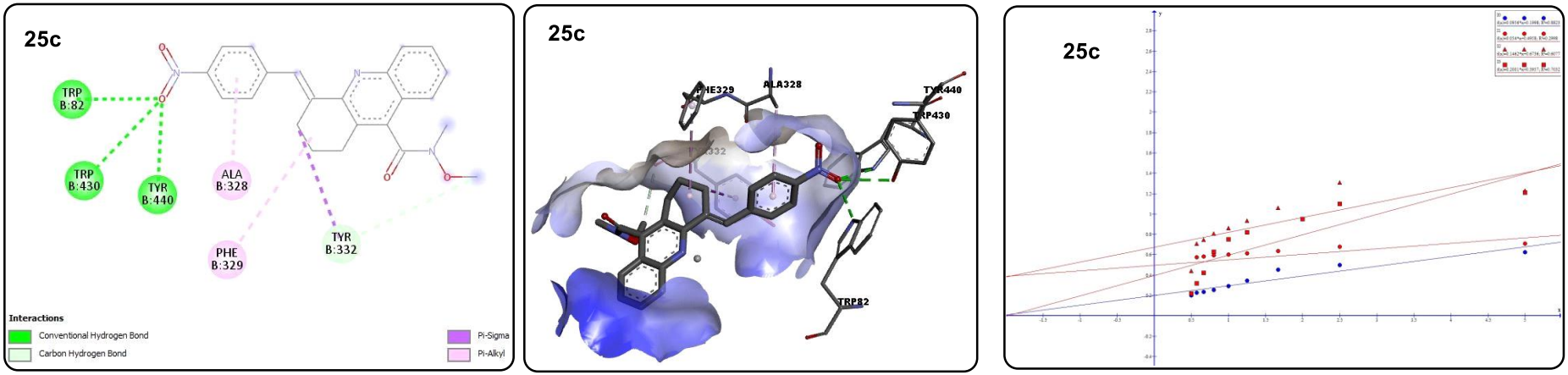

Figure 2.2.3g 2D, 3D docking interactions of compound **16b, 19v, 19w, 22f, 25c** with protein **6EMI**, Lineweaver–Burk plot for understanding the interaction of BChE with compounds **16b, 19v, 19w, 22f, 25c**

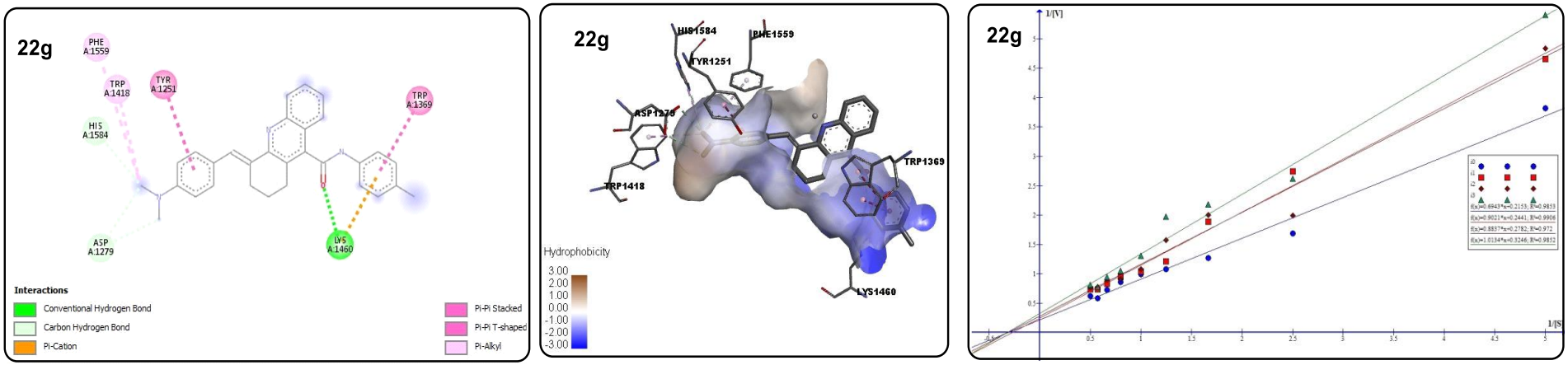

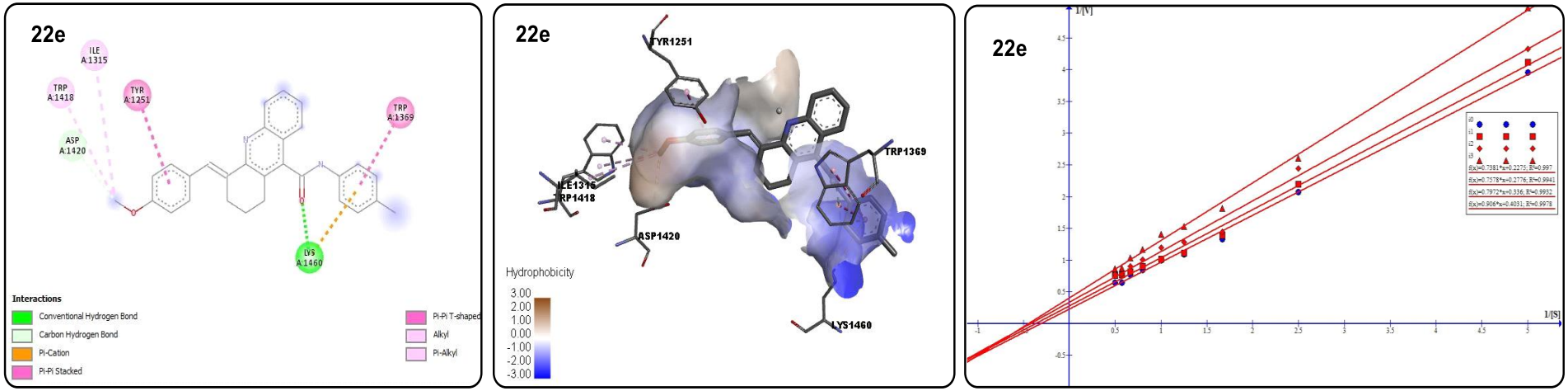

Figure 2.2.3h 2D, 3D docking interactions of compound **22e, 22g** with protein **3TOP**, Lineweaver–Burk plot for understanding the interaction of α-Glucosidase with compounds **22e, 22g**

2.2.3.3b Blood Brain Barrier Prediction

The ability to penetrate the blood-brain barrier (BBB) is a crucial characteristic for compounds designed for Alzheimer's Disease treatment or any drug targeting the central nervous system. According to the predicted data from the BBB predictor module of ALzPlatform, all the tested compounds selected based on their *in vitro* inhibitory activity against AChE and BChE were determined to be BBB+. This indicates that these molecules possess BBB permeability and can traverse the blood-brain barrier. The predicted properties are detailed in **Table 2.2.13**.

Table 2.2.13 BBB Prediction of Compounds by ALzPlatform

Compound	SVM_MACCSFP BBB Score	BBB Permeability
16b	0.085	BBB+
19e	0.097	BBB+
19f	0.042	BBB+
19l	0.035	BBB+
19m	0.042	BBB+
19v	0.140	BBB+
19w	0.083	BBB+
22f	0.127	BBB+
22j	0.091	BBB+
25a	0.115	BBB+
25b	0.072	BBB+
25c	0.080	BBB+
Tacrine	0.120	BBB+

2.2.3.3c Prediction of Drug-Like Property

The drug-like property was predicted based on Lipinski Rule of Five, the property of the drug was predicted based on the molecular mass of the compounds less than 500 Dalton, lipophilicity (based on LogP less than 5), hydrogen bond donors (less than 5), hydrogen bond acceptors (Less than 10), Molar refractivity in the range 40-150. The drug-likeness prediction was carried out using the SwissADME tool. Based on analysis it was observed that the compounds showing better inhibitory activity for α - glucosidase, AChE, and BChE do not violate the Lipinski Rule of Five, hence having drug-like properties (**Table 2.2.14**).

Table 2.2.14 Drug-like property

Compound	Molecular Mass (g/mol)	Lipophilicity Log Po/w	Hydrogen Bond Donors	Hydrogen Bond Acceptors	Molar Refractivity
16b	345.39	3.82	1	4	103.03
19e	393.86	5.03	0	4	112.36
19f	404.42	3.76	0	6	116.17
19l	408.83	4.29	0	5	114.69
19m	404.42	3.76	0	6	116.17
19v	439.93	6.26	0	3	130.36
19w	450.49	4.97	0	5	134.17
22f	468.97	6.13	1	3	140.26
22j	483.95	5.39	1	4	142.59
25a	358.43	4.21	0	3	108.56
25b	388.46	4.19	0	4	115.05
25c	403.43	3.49	0	5	117.38

2.2.3.3d QSAR analysis

Table 2.2.15 Statistical parameters of the GA-LDA

Parameters	Training Set	Test Set
No. of Compounds	45	15
Sensitivity (%)	68.83	73.9
Specificity (%)	69.32	74.5
Accuracy (%)	90.0	95.2
Precision (%)	75.5	76.3
MCC	0.548	0.541
AUROC	0.896	0.883

Docking analyses were conducted on structurally comparable entities to assess their biological significance. A QSAR model was formulated, utilizing docking scores obtained for a selection of substances with similar structural/functional arrangements to gauge their biological activity. Notably, a combination of nitro at the aromatic ring of 1,2,3,4-tetrahydroacridine and aryl

methoxy groups at C4 position demonstrated a strong correlation with inhibitory effects. Compounds featuring nitro and chloro at C4 aryl moiety also displayed inhibitory activity. However, compounds without any substitutions in the aromatic ring at C4 position lacked inhibitory properties. Compounds exhibiting high total polar surface area (TPSA) and hydrophobicity exhibited favorable interactions with both AChE and BChE.

The interactions observed in docking studies, coupled with assumptions derived from QSAR studies, suggest that these functional groups induce inhibitory effects due to the hydrophilic nature of specific amino acids (HIS239, HIS279, LYS155, ARG312) situated in the core binding cavity of α-glucosidase. In the case of AChE, TYR332 was found to interact with the predominant aryl methoxy groups, while PHE329 interacted with Nitro or chloro substitutions in aryl moiety at the C4 position.

Table 2.2.15 IC_{50}, K_m, V_{max} and modes of inhibition of selected compounds

Compound	**Enzyme**	**IC_{50} (nM)**	**K_m (nM)**	**V_{max} (nM/min)**	**Mode of inhibition**
			Inhibitor concentration of 25 nM		
16b	AChE	142.06±3.14	345.34	0.43	Non-Competitive
	BChE	141.11±3.5	334.54	0.41	Non-Competitive
	α-glucosidase	31254±1523	3140	3850	Non-Competitive
19e	AChE	121.32±2.65	321.18	0.21	Non-Competitive
	BChE	122.56±3.78	332.5	0.25	Non-Competitive
	α-glucosidase	44152.42±1658	3845	3395	Non-Competitive
19f	AChE	119.65±2.37	352.25	0.25	Non-Competitive
	BChE	121.58±3.55	348.14	0.27	Non-Competitive
	α-glucosidase	41541±1354	3656	3511	Non-Competitive
19l	AChE	120.58±3.25	323.43	0.24	Un-competitive
	BChE	125.56±2.15	325.15	0.28	Un-competitive
	α-glucosidase	35658±1568	3548	3328	Competitive
19m	AChE	122.54±2.65	315.11	0.25	Un-competitive
	BChE	121.85±3.84	354.28	0.27	Un-competitive
	α-glucosidase	31154±1259	3187	3947	Competitive
19t	AChE	119.45±2.87	308.54	0.21	Mixed-competitive
	BChE	118.69±3.25	305.28	0.19	Mixed-competitive
	α-glucosidase	54580±3547	4584	4105	Non-Competitive
19v	AChE	124.65±2.71	319.25	0.27	Mixed-competitive
	BChE	118.25±3.54	300.25	0.21	Mixed-competitive
	α-glucosidase	31574±1354	3254	3145	Non-Competitive
19w	AChE	121.87±3.24	311.94	0.25	Mixed-competitive
	BChE	118.65±2.58	304.18	0.21	Mixed-competitive
	α-glucosidase	45210±1257	3548	3154	Non-Competitive
22g	α-glucosidase	21442±1004	2241	2170	Competitive
22f	AChE	145.05±5.14	358.24	0.31	Un-competitive
	BChE	138.25±3.05	365.17	0.29	Un-competitive

	α-glucosidase	25364±1568	3264	2314	Mixed-competitive
25a	AChE	138.25±2.58	345.37	0.29	Mixed-competitive
	BChE	137.65±2.87	354.2	0.27	Mixed-competitive
	α-glucosidase	26840±1687	3254	3214	Non-Competitive
25b	AChE	142.83±3.25	354.2	0.27	Un-competitive
	BChE	146.14±3.91	349.12	0.28	Un-competitive
	α-glucosidase	35418±2191	3254	3114	Mixed-competitive
25c	AChE	135.68±3.71	325.21	0.29	Mixed-competitive
	BChE	129.56±2.65	348.96	0.28	Mixed-competitive
	α-glucosidase	28364±1248	3319	2834	Non-Competitive

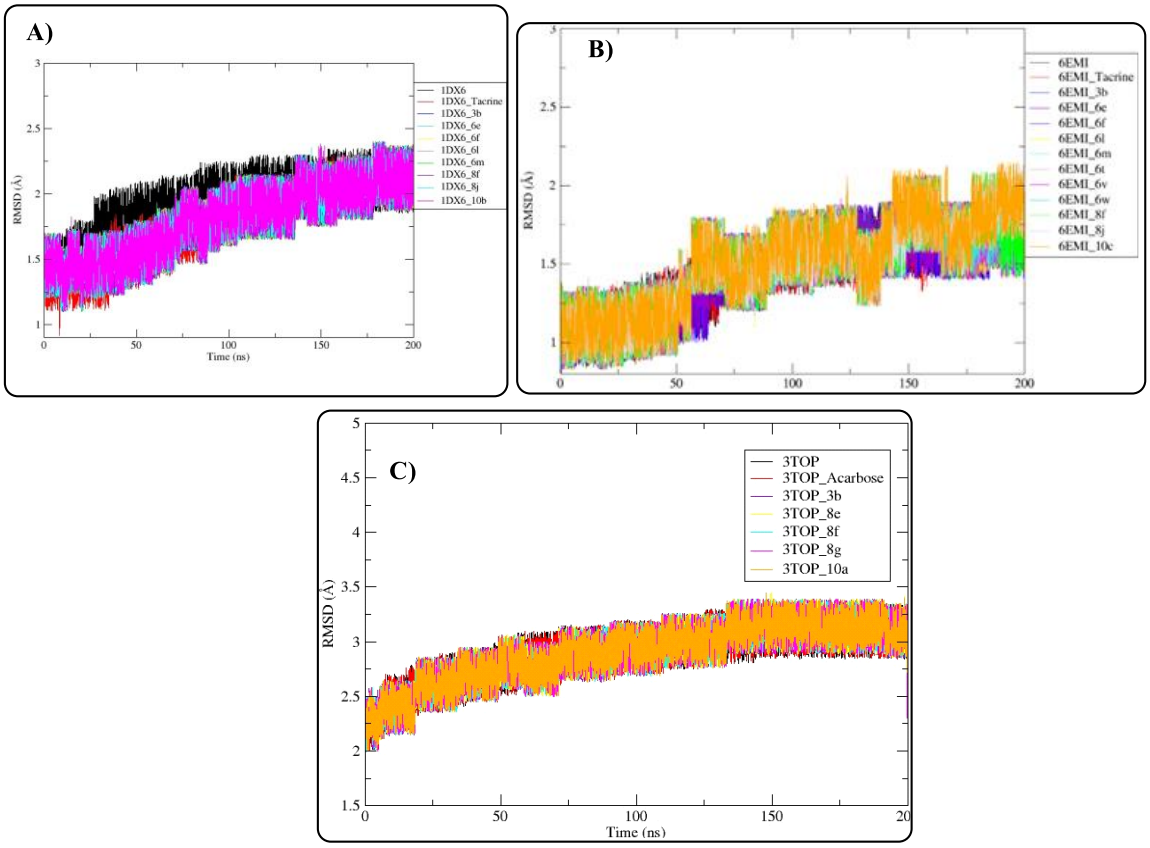

Figure 2.2.3i RMSD plot of apo-protein, co-ligands and compound-protein complexes system. A) **1DX6**-AChE, B) **6EMI**-BChE, C) **3TOP** α-glucosidase.

2.2.3.4 Conclusions

A series of compounds of 1,2,3,4-tetrahydroacridine derivatives substituted with acid, esters and amide moieties were synthesised under the green condition through utilisation of DMU+ L-(+)-TA based DES. All the newly synthesised compounds were evaluated for *in vitro* inhibitory activity against AChE, BChE, and α-glucosidase enzymes. Most of the compounds efficiently showed inhibitory activity against AChE and BChE in the nanomolar range. Among the tested compounds, **19f** showed potent inhibitory activity with IC_{50} = **119.65** nM towards

AChE and compound **19v** showed better inhibitory activity with IC_{50} = **118.25** nM towards BChE respectively. Compound **22g** showed promising inhibitory activity against α-glucosidase enzyme with an IC_{50} value of **21442** nM. From kinetic studies compound **19f** exhibited a non-competitive mode of inhibition against AChE and compound **19v** exhibited a mixed-competitive mode of inhibition against BChE, compound **22g** exhibit a competitive mode of inhibition towards α-glucosidase enzyme. The molecular docking and dynamics simulation studies of compounds **19e, 19f** and **19l** with AChE and BChE reveal binding interactions and stability of the bound complex that extend beyond simple ligand-protein associations. The generated QSAR model assumes that the compound with methoxy group in the aromatic ring at the C4 position and ester group at the C9 position exhibit good inhibitory activity towards cholinesterase enzyme.

2.3 Experimental section

2.3.1 General procedure for synthesis of compound (4):

To an ice-cooled solution of anthranilic acid (3.2 g, 3 mmol) and cyclohexanone (2.65 mL, 27 mmol) was added dropwise $POCl_3$ with a constant pressure dropping funnel. Then, the reaction was heated at reflux for 3 h. The solvent was reduced in a vacuum and the residue was dissolved in ethyl acetate and washed with 1N K_2CO_3 solution, brine and dried (Na_2SO_4). The residue was purified by silica gel chromatography using ethyl acetate: hexane = 10: 90 to yield the desired compound (**4**) as a yellow solid.

2.3.2 General procedure for synthesis of compound (5):

The deep eutectic solvent was prepared by heating *N, N*'-Dimethyl urea + L-(+)-Tartaric acid (3:1 ratio) at 80 °C for 30 min. To this, 9-Chloro-1,2,3,4-tetrahydroacridine (1.0 mmol) and aromatic aldehyde (1.0 mmol) were added and heating continued for another 2- 3 hours at 80 °C. The completion of the reaction was monitored by TLC. After completion of the reaction the crude products obtained were purified by column chromatography on silica gel using petroleum ether-ethyl acetate as eluent to give the compound **5.**

2.3.3 General procedure for synthesis of compound (3):

Deep eutectic solvent was prepared by heating *N, N*'-Dimethyl urea + L-(+)-Tartaric acid (3:1 ratio) at 80 °C for 30 min. To this, 9-Chloro-1,2,3,4-tetrahydroacridine (1.0 mmol) and sodium azide (5.0 equiv.) were added and stirred at 80 °C for 2 h. After completion of the reaction, to the reaction mixture water was added and the resulting precipitate was collected by filtration

and recrystallized to get 9-Azido-1,2,3,4-tetrahydroacridine (6). A stirred mixture of azide (1.0 equiv.) and PPh_3 (3.0 equiv.) in THF was refluxed for 5 h. The residue was purified by column chromatography to get phosphazene. A stirred solution of phosphazene (1.0 equiv.) in 80% acetic acid was boiled under reflux for 7 h. After completion of the reaction, the residue was purified by column chromatography to obtain the compound (**3**).

2.3.4 General procedure for synthesis of compound (8):

Deep eutectic solvent was prepared by heating *N, N'*-Dimethyl urea + L-(+)-Tartaric acid (3:1 ratio) at 80 °C for 30 min. To this, compound **5** (1.0 mmol) and *p*-Toluidine (1.0 mmol) were added and heating continued for another 3 - 4 hours at 80 °C. The completion of the reaction was monitored by TLC. After completion of the reaction the crude products obtained were purified by column chromatography on silica gel using petroleum ether-ethyl acetate as eluent to give the compound (**8**).

2.4 Characterization data for synthesized compounds

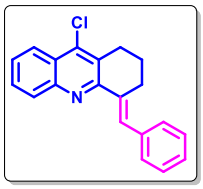

(E)-4-Benzylidene-9-chloro-1,2,3,4-tetrahydroacridine (5a): Yield= 85%, light Yellow solid; M. P: 119-119.9 °C; **IR (KBr, cm^{-1})**: 3041, 2948, 2821, 1569, 1305, 1191, 833; **^{1}H NMR (400 MHz, $CDCl_3$) δ** 8.23 (s, 1H), 8.17 (dd, *J* = 8.4, 1.2 Hz, 1H), 8.09 (d, *J* = 8.4 Hz, 1H), 7.68 (ddd, *J* = 8.4, 6.8, 1.4 Hz, 1H), 7.55 (ddd, *J* = 8.4, 6.8, 1.2 Hz, 1H), 7.49 (d, *J* = 7.2 Hz, 2H), 7.41 (t, *J* = 7.6 Hz, 2H), 7.30 (t, *J* = 7.4 Hz, 1H), 3.13 (t, *J* = 6.4 Hz, 2H), 2.99 – 2.95 (t, *J* = 6.4 Hz, 2H), 1.95 (qui, *J* = 6.4 Hz, 2H). **^{13}C NMR (100 MHz, $CDCl_3$) δ** 154.66, 147.01, 141.03, 137.66, 135.77, 129.88 (t, *J* = 18.0 Hz), 129.39 (s), 129.00 (s), 128.18 (s), 127.19 (s), 126.81 (s), 125.68 (s), 123.74, 27.90, 27.60, 22.53. **Mass (ESI-MS):** m/z Calculated $C_{20}H_{16}ClN$ for: 305.0971; Observed: 306.1043 $[M+H]^+$.

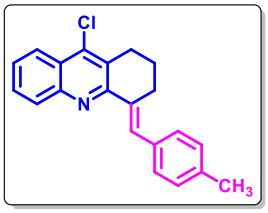

(E)-9-Chloro-4-(4-methylbenzylidene)-1,2,3,4-tetrahydroacridine (5b): Yield= 84%, Yellow solid; M. P: 91-92 °C; **IR (KBr, cm^{-1})**: 3101, 2950, 2816, 1536, 1245, 1092, 825; **^{1}H NMR (400 MHz, $CDCl_3$) δ** 8.12 (s, 1H), 8.07 (dd, *J* = 8.4, 0.8 Hz, 1H), 8.02 (d, *J* = 8.4 Hz, 1H), 7.59 (tdd, *J* = 8.3, 7.0, 1.3 Hz, 1H), 7.45 (tdd, *J* = 8.2, 6.9, 1.1 Hz, 1H), 7.31 (d, *J* = 8.0 Hz, 2H), 7.13 (d, *J* = 7.9 Hz, 2H), 3.04 (t, *J* = 6.4 Hz, 2H), 2.91 – 2.85 (td, *J* = 12.6, 6.4 Hz, 2H), 2.31 (s, 3H), 1.86 (quin, *J* = 6.4Hz, 2H). **^{13}C NMR (100 MHz, $CDCl_3$) δ** 154.82, 146.92, 141.03, 137.14, 134.90, 134.76, 130.32, 129.90, 129.58, 129.41, 129.00,

128.94, 126.75, 125.61, 123.73, 27.89, 27.67, 22.50, 21.34. **Mass (ESI-MS):** m/z Calculated $C_{21}H_{18}ClN$ for: 319.1128; Observed: 320.1201 $[M+H]^+$.

(E)-9-Chloro-4-(4-methylbenzylidene)-6-nitro-1,2,3,4-tetrahydroacridine (5c):

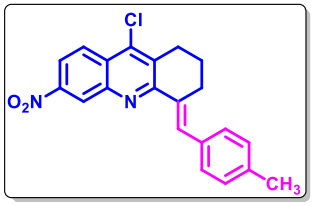

Yield=86%,Yellow solid; M. P: 205.1-205.6 °C; **IR (KBr, cm^{-1})**: 3201, 2974, 2825, 1549, 1362, 1102, 819; ^{1}H NMR (400 MHz, $CDCl_3$) δ 8.92 (s, 1H), 8.28 – 8.23 (m, 3H), 7.40 (d, *J* = 8.0 Hz, 2H), 7.23 (d, *J* = 8.0 Hz, 2H), 3.13 (t, *J* = 6.4 Hz, 2H), 2.98 (td, *J* = 6.4, 1.6 Hz, 2H), 2.40 (s, 3H), 1.99 – 1.92 (quin, *J* = 6.4 Hz, 2H). **^{13}C NMR (100 MHz, $CDCl_3$) δ** 157.39, 148.11, 145.83, 140.85, 137.79, 134.20, 133.90, 132.38, 132.03, 130.00, 129.08, 128.58, 125.69, 119.73, 28.20, 27.47, 22.00, 21.40. **Mass (ESI-MS):** m/z Calculated $C_{21}H_{17}ClN_2O_2$ for: 364.0979; Observed: 365.1095 $[M+H]^+$.

(E)-9-Chloro-4-(4-methoxybenzylidene)-1,2,3,4-tetrahydroacridine (5d): Yield= 80%,

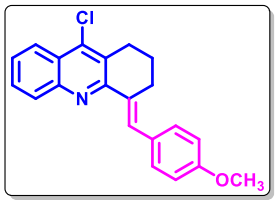

Yellow solid; M. P: 93.5-93.8 °C; **IR (KBr, cm^{-1})**: 3092, 2935, 2861, 1545, 1249, 1098, 823; **^{1}H NMR (400 MHz, $CDCl_3$) δ** 8.09 (s, 1H), 8.07 (dd, *J* = 8.8, 0.8 Hz, 1H), 8.00 (d, *J* = 8.4 Hz, 1H), 7.61 – 7.56 (td,J= 8.2, 1.2 HZ 1H), 7.45 (ddd, *J* = 8.2, 6.8, 1.2 Hz, 1H), 7.37 (d, *J* = 8.4 Hz, 2H), 6.86 (d, *J* = 8.8 Hz, 2H), 3.77 (s, 3H), 3.03 (t, *J* = 6.4 Hz, 2H), 2.88 (td, *J* = 6.6, 1.6 Hz, 2H), 1.89 – 1.83 (quin, J= 6.4 HZ2H). **^{13}C NMR (100 MHz, $CDCl_3$) δ** 158.93, 154.90, 146.60, 141.24, 133.55, 131.47, 130.50, 130.14, 129.58, 129.23, 129.04, 126.77, 125.51, 123.77, 113.69, 55.31, 27.84, 27.67, 22.44. **Mass (ESI-MS):** m/z Calculated $C_{21}H_{18}ClNO$ for: 335.1077; Observed: 336.1159 $[M+H]^+$.

(E)-5-Chloro-9-(4-methoxybenzylidene)-6,7,8,9-tetrahydrobenzo[b][1,8]naphthyridine (5e):

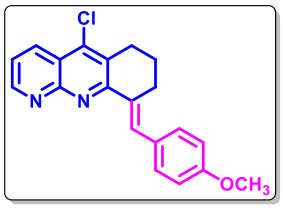

Yield= 79%, red solid; M. P: 124.5-125 °C; **IR (KBr, cm^{-1})**: 3099, 2910, 2856, 1591, 1539, 1249, 799; **^{1}H NMR (400 MHz, $CDCl_3$) δ** 9.07 (dd, *J* = 4.4, 2.0 Hz, 1H), 8.51 (dd, *J* = 8.2, 1.8 Hz, 1H), 8.47 (s, 1H), 7.48 (d, *J* = 5.2 Hz, 2H), 7.45 (d, *J* = 4.4 Hz, 1H), 6.97 – 6.92 (m, 2H), 3.85 (s, 3H), 3.12 (t, *J* = 6.4 Hz, 2H), 3.03 – 2.97 (td, J= 7.4, 1.2 Hz 2H), 1.99 – 1.93 (quin, J= 6.4 HZ, 2H). **^{13}C NMR (100 MHz, $CDCl_3$) δ** 159.12, 158.16, 154.48, 153.55, 140.98, 133.31, 132.63, 132.18, 131.61, 130.20, 129.98, 121.65, 120.44, 113.76, 55.30, 27.84, 27.68, 22.07. **Mass (ESI-MS):** m/z Calculated $C_{20}H_{17}ClN_2O$ for: 336.1029; Observed: 337.1099 $[M+H]^+$.

(E)-9-Bromo-4-(4-methoxybenzylidene)-1,2,3,4-tetrahydroacridine (5f): Yield= 80%, Yellow solid; M. P: 98.1-98.5 °C; **IR (KBr, cm^{-1})**: 3081, 2965, 2856, 1591, 1249, 1102, 650; **^{1}H NMR (400 MHz, CDCl$_3$) δ** 8.18 (s, 1H), 8.16 (s, 1H), 8.08 (d, *J* = 8.4 Hz, 1H), 7.71 – 7.66 (m, 1H), 7.58 – 7.53 (m, 1H), 7.47 (d, *J* = 8.8 Hz, 2H), 6.97 (d, *J* = 8.8 Hz, 2H), 3.88 (s, 3H), 3.15 (t, *J* = 6.4 Hz, 2H), 3.02 – 2.95 (t, *J* = 6.4 Hz, 2H), 2.01 – 1.94 (quin, *J* = 6.4 Hz, 2H). **^{13}C NMR (100 MHz, CDCl$_3$) δ** 158.86, 155.03, 147.02, 146.12, 131.37, 130.97, 130.29, 129.57, 129.35, 129.12, 127.30, 126.91, 126.50, 126.21, 113.67, 112.84, 55.30, 31.26, 27.73, 22.80. **Mass (ESI-MS):** m/z Calculated $C_{21}H_{18}BrNO$ for: 379.0572; Observed:380.0647 $[M+H]^+$.

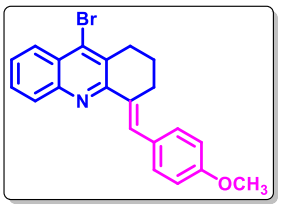

(E)-6-Bromo-9-chloro-4-(4-methoxybenzylidene)-1,2,3,4-tetrahydroacridine (5g): Yield= 78%, Yellow solid; M. P: 104.4-105.1 °C; **IR (KBr, cm^{-1})**: 3015, 2936, 2832, 1518, 1255, 1105, 1029, 844, 599; **^{1}H NMR (400 MHz, CDCl$_3$) δ** 8.28 (d, *J* = 1.6 Hz, 1H), 8.18 (s, 1H), 8.03 (d, *J* = 8.8 Hz, 1H), 7.62 (dd, *J* = 8.8, 2.0 Hz, 1H), 7.47 (d, *J* = 8.4 Hz, 2H), 6.99 – 6.96 (dd, *J* =8.8, 2.0 Hz 2H), 3.88 (s, 3H), 3.11 (t, *J* = 6.4 Hz, 2H), 3.00 – 2.96 (m, 2H), 1.99 – 1.94 (m, 2H). **^{13}C NMR (100 MHz, CDCl$_3$) δ** 149.58, 147.77, 147.53, 144.20, 219.44, 131.12, 149.58, 132.11, 138.40, 131.12 – 130.17, 129.97, 125.23, 113.72, 55.31, 29.71, 27.85, 22.30. **Mass (ESI-MS):** m/z Calculated $C_{21}H_{17}BrClNO$ for: 413.0182; Observed: 414.0247 $[M+H]^+$.

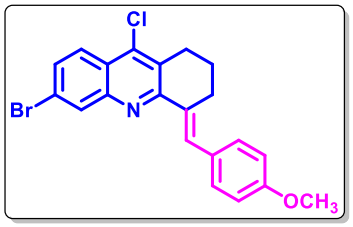

(E)-9-Chloro-4-(4-methoxybenzylidene)-6-nitro-1,2,3,4-tetrahydroacridine(5h): Yield= 81%, red solid; M. P: 172.9-173.8 °C; **IR (KBr, cm^{-1})**: 3015, 2936, 2832, 1555, 1380, 1105, 833; **^{1}H NMR (400 MHz, CDCl$_3$) δ** 8.90 (s, 1H), 8.23 (s, 3H), 7.46 (d, *J* = 8.8 Hz, 2H), 6.95 (d, *J* = 8.8 Hz, 2H), 3.86 (s, 3H), 3.12 (t, *J* = 6.4 Hz, 2H), 3.02 – 2.94 (m, 2H), 1.95 (quin, *J* = 6.4 Hz, 2H). **^{13}C NMR (100 MHz, CDCl$_3$) δ** 153.38, 147.33, 145.72, 141.05, 136.89, 131.78, 129.52, 129.04, 128.54, 128.38, 126.98, 125.01, 122.79, 121.91, 120.76, 64.02, 61.86, 26.66, 25.11, 19.38. **Mass (ESI-MS):** m/z Calculated $C_{21}H_{17}ClN_2O_3$ for: 380.0928; Observed: 381.1012 $[M+H]^+$.

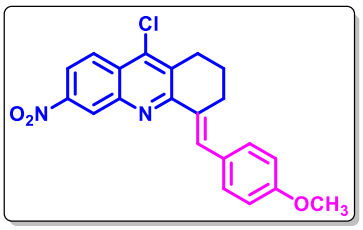

(E)-4-((9-Chloro-2,3-dihydroacridin-4(1H)-ylidene)methyl)-N,N-dimethylaniline (5i): Yield= 82%, Yellow solid; M. P: 185.5-186.5 °C; **IR (KBr, cm^{-1})**: 3109, 2998, 2878, 1604, 1474, 1156, 1066, 889, 740; **^{1}H NMR (400 MHz, CDCl$_3$) δ** 8.09 (s, 1H), 8.05 (t, *J* = 7.2 Hz,

2H), 7.58 (ddd, *J* = 8.2, 6.8, 1.2 Hz, 1H), 7.43 (ddd, *J* = 8.2, 7.0, 1.0 Hz, 1H), 7.38 (d, *J* = 8.8 Hz, 2H), 6.67 (d, *J* = 8.8 Hz, 2H), 3.02 (t, *J* = 6.4 Hz, 2H), 2.93 (s, 8H), 1.89 – 1.83 (quin, J= 6.4 HZ, 2H). **^{13}C NMR (100 MHz, CDCl$_3$) δ** 155.46, 149.65, 146.82, 140.75, 131.53, 131.23, 129.35, 129.23, 128.97, 126.37, 125.82, 125.32, 123.73, 111.85, 40.36, 27.94, 27.87, 22.47. **Mass (ESI-MS):** m/z Calculated $C_{22}H_{21}ClN_2$ for: 348.1393; Observed: 349.1473 $[M+H]^+$.

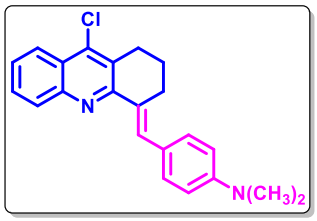

(E)-4-((9-Chloro-6-nitro-2,3-dihydroacridin-4(1H)-ylidene)methyl)-N,N-dimethylaniline (5j): Yield= 83%, red solid; M. P: 185.5-186.5 °C; **IR (KBr, cm^{-1})**: 3112, 2982, 2861, 1554, 1360, 1188, 1064, 812, 768; **^{1}H NMR (400 MHz, CDCl$_3$) δ** 8.94 (s, 1H), 8.26 (s, 1H), 8.26 (d, *J* = 2.0 Hz, 2H), 7.49 (d, *J* = 8.8 Hz, 2H), 6.78 (d, *J* = 8.8 Hz, 2H), 3.17 – 3.13 (m, 2H), 3.05 (s, 8H), 2.01 – 1.96 (m, 2H). **^{13}C NMR (100 MHz, CDCl$_3$)** δ 162.58, 158.06, 149.93, 148.06, 145.99, 145.54, 141.31, 140.26, 132.78, 132.27, 131.73, 130.49, 128.33, 125.46, 125.01, 119.77, 119.20, 111.76, 40.26, 34.26, 28.16, 21.97. **Mass (ESI-MS):** m/z Calculated $C_{22}H_{20}ClN_3O_2$ for: 393.1244; Observed: 394.1324 $[M+H]^+$.

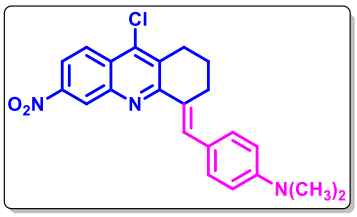

(E)-4-((9-Chloro-2,3-dihydroacridin-4(1H)-ylidene)methyl)phenol (5k): Yield= 78%, orange solid; M. P:148.4-148.5 °C; **IR (KBr, cm^{-1})**: 2982, 2870, 1730, 1604, 1194, 1043, 837; **^{1}H NMR (400 MHz, CDCl$_3$) δ** 8.09 (dd, *J* = 8.4, 0.9 Hz, 2H), 8.06 (s, 1H), 7.62 (t, *J* = 8.2 Hz, 1H), 7.48 (t, *J* = 8.4 Hz, 1H), 7.29 (d, *J* = 8.4 Hz, 2H), 6.79 (d, *J* = 8.4 Hz, 2H), 5.59 (s, 1H), 3.05 (t, *J* = 6.4 Hz, 2H), 2.88 (t, *J* = 6.8 Hz, 2H), 1.91 – 1.86 (quin, *J* = 6.4 Hz, 2H). **^{13}C NMR (100 MHz, CDCl$_3$) δ** 154.95, 131.86, 130.30, 129.31, 127.15, 125.44, 123.92, 115.51, 27.6, 22.29. **Mass (ESI-MS):** m/z Calculated $C_{20}H_{16}ClNO$ for: 321.0920; Observed:322.1000 $[M+H]^+$.

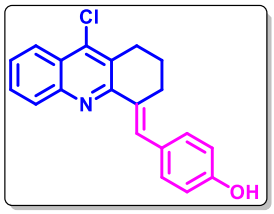

(E)-4-((9-Chloro-6-nitro-2,3-dihydroacridin-4(1H)-ylidene)methyl)phenol (5l): Yield= 79% ,Yellow solid; M. P: 165-166 °C; **IR (KBr, cm^{-1})**: 3028, 2935, 2857, 1604, 1440, 1171, 1053, 839; **^{1}H NMR (400 MHz, CDCl$_3$) δ** 8.95 (s, 1H), 8.28 (d, *J* = 2.7 Hz, 2H), 8.23 (s, 1H), 7.42 (d, *J* = 8.8 Hz, 2H), 6.90 (d, *J* = 8.8 Hz, 2H), 5.06 (s, 1H), 3.15 (t, *J* = 6.2 Hz, 2H), 3.01 – 2.96 (t, J= 5.4 Hz, 2H), 2.01 – 1.94 (quin, J= 6.2

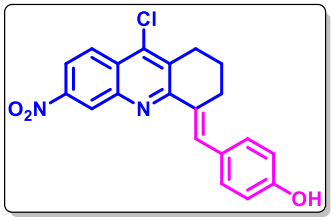

Hz, 2H). **^{13}C NMR (100 MHz, $CDCl_3$) δ** 157.55, 155.31, 148.19, 145.92, 140.79, 132.92, 132.35, 131.74, 129.90, 128.58, 125.66, 119.69, 115.34, 28.16, 27.50, 22.01. **Mass (ESI-MS):** m/z Calculated $C_{20}H_{15}ClN_2O_3$ for: 366.0771; Observed: 367.0849 $[M+H]^+$.

(E)-9-Chloro-4-(4-chlorobenzylidene)-1,2,3,4-tetrahydroacridine (5m): Yield= 87%, white solid; M. P: 142.1-143 °C; **IR (KBr, cm^{-1})**: 3010, 2931, 1567, 1366, 1009, 910, 844; **^{1}H NMR (400 MHz, $CDCl_3$) δ** 8.17 (d, *J* = 0.8 Hz, 1H), 8.15 (s, 1H), 8.07 (d, *J* = 8.4 Hz, 1H), 7.68 (ddd, *J* = 8.4, 7.0, 1.4 Hz, 1H), 7.55 (ddd, *J* = 8.2, 6.9, 1.2 Hz, 1H), 7.42 – 7.38 (m, 2H), 7.38 – 7.34 (m, 2H), 3.13 (t, *J* = 6.4 Hz, 2H), 2.95 – 2.89 (td, J= 6.4, 1.6 HZ 2H), 1.95 (dt, *J* = 12.6, 6.4 Hz, 2H). **^{13}C NMR (100 MHz, $CDCl_3$) δ** 154.29, 146.95, 141.16, 136.29, 136.07, 132.97, 131.09, 129.63, 129.49, 128.99, 128.78, 128.40, 126.96, 125.73, 123.76, 27.81, 27.59, 22.45. **Mass (ESI-MS):** m/z Calculated $C_{20}H_{15}Cl_2N$ for: 339.0582; Observed: 340.0667 $[M+H]^+$.

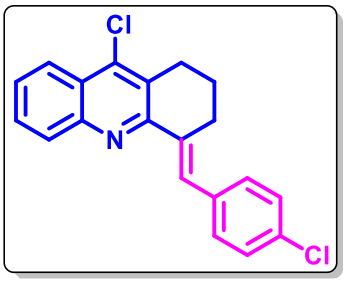

(E)-4-(4-Bromobenzylidene)-9-chloro-1,2,3,4-tetrahydroacridine (5n): Yield= 90%, white solid; M. P: 134-135.2 °C; **IR (KBr, cm^{-1})**: 3069, 2954, 1567, 1470, 1073, 519; **^{1}H NMR (400 MHz, $CDCl_3$) δ** 8.23 (d, *J* = 6.3 Hz, 2H), 8.21 (d, *J* = 8.4 Hz, 1H), 7.75 (td, *J* = 8.0 Hz, 1H), 7.61 (td, *J* = 8.0 Hz, 1H), 7.55 (d, *J* = 8.4 Hz, 2H), 7.39 (d, *J* = 8.4 Hz, 2H), 3.16 (t, *J* = 6.4 Hz, 2H), 2.98 – 2.92 (m, 2H), 2.02 – 1.95 (quin, 2H). **^{13}C NMR (100 MHz, $CDCl_3$) δ** 154.24, 136.50, 131.41, 131.37, 131.18, 130.49, 129.64, 129.57, 129.02, 127.01, 125.74, 123.78, 121.23, 27.81, 27.59, 22.43. **Mass (ESI-MS):** m/z Calculated C20H15BrClN for: 383.0076; Observed: 384.0154 $[M+H]^+$.

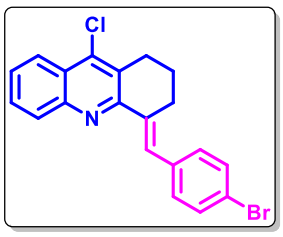

(E)-4-(4-Bromobenzylidene)-9-chloro-6-nitro-1,2,3,4-tetrahydroacridine (5o): Yield= 92%, white solid; M. P: 197.4-198 °C; **IR (KBr, cm^{-1})**: 3100, 2984, 1467, 1270, 1053, 553; **^{1}H NMR (400 MHz, $CDCl_3$) δ** 8.95 (s, 1H), 8.30 (d, *J* = 1.6 Hz, 2H), 8.22 (s, 1H), 7.55 (d, *J* = 8.4 Hz, 2H), 7.35 (d, *J* = 8.4 Hz, 2H), 3.17 (t, *J* = 6.4 Hz, 2H), 2.97 – 2.92 (td, J= 6.4 ,1.2 Hz, 2H), 2.01 – 1.95 (quin, J= 6.4 Hz, 2H). **^{13}C NMR (100 MHz, $CDCl_3$) δ** 156.85, 148.25, 145.85, 141.12, 135.97, 135.31, 132.37, 131.52, 131.44, 130.62, 128.69, 125.76, 125.73, 121.78, 120.00, 28.13, 27.39, 21.96. **Mass (ESI-MS):** m/z Calculated $C_{20}H_{14}BrClN_2O_2$ for: 427.9927; Observed: 428.9998 $[M+H]^+$.

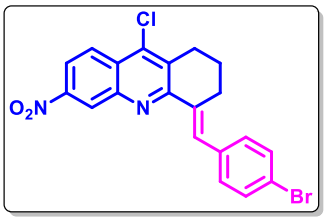

(E)-9-Chloro-4-(3-nitrobenzylidene)-1,2,3,4-tetrahydroacridine (5p): Yield= 76%, Light Yellow solid; M. P:129.8-130 °C; **IR (KBr, cm^{-1})**: 3010, 2984, 1547, 1350, 1073, 818; **^{1}H NMR (400 MHz, CDCl$_3$) δ** 8.33 (s, 1H), 8.26 (s, 1H), 8.19 (d, *J* = 8.4 Hz, 1H), 8.15 (d, *J* = 8.0 Hz, 1H), 8.08 (d, *J* = 8.4 Hz, 1H), 7.78 (d, *J* = 7.6 Hz, 1H), 7.71 (t, *J* = 7.6 Hz, 1H), 7.61 – 7.58 (m, 1H), 7.56 (d, *J* = 8.0 Hz, 1H), 3.16 (t, *J* = 6.4 Hz, 2H), 2.99 – 2.94 (t, J= 5.4 HZ HZ2H), 2.02 – 1.96 (quin, J=6.4 HZ 2H). **^{13}C NMR (100 MHz, CDCl$_3$)** δ 153.39, 148.26, 139.08, 135.88, 130.04, 129.20, 127.51, 125.90, 124.23, 123.86, 122.02, 27.71, 27.51, 22.30. **Mass (ESI-MS):** m/z Calculated $C_{20}H_{15}ClN_2O_2$ for: 350.0822; Observed: 351.0894 $[M+H]^+$.

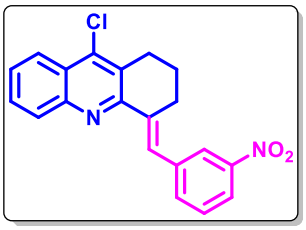

(E)-9-Chloro-6-nitro-4-(3-nitrobenzylidene)-1,2,3,4-tetrahydroacridine (5q): Yield= 73%, Light Yellow solid; M. P:146.8-147.0 °C; **IR (KBr, cm^{-1})**: 3109, 2989, 1552, 1360, 1037, 817; **^{1}H NMR (400 MHz, CDCl$_3$) δ** 8.97 (dd, *J* = 1.8, 1.0 Hz, 1H), 8.36 – 8.33 (m, 2H), 8.33 – 8.32 (m, 2H), 8.18 (ddd, *J* = 8.2, 1.9, 1.0 Hz, 1H), 7.81 – 7.78 (m, 1H), 7.61 (t, *J* = 8.0 Hz, 1H), 3.20 (t, *J* = 6.4 Hz, 2H), 3.02 – 2.97 (td, J= 6.6, 1.6 Hz, 2H), 2.05 – 1.99 (quin, J= 6.4 Hz, 2H). **^{13}C NMR (100 MHz, CDCl$_3$) δ** 156.12, 148.28, 145.79, 141.44, 138.72, 137.20, 135.87, 132.47, 129.36, 128.99, 128.86, 125.86, 125.83, 124.24, 122.33, 120.33, 28.07, 27.37, 21.91. **Mass (ESI-MS):** m/z Calculated $C_{20}H_{14}ClN_3O_4$ for: 395.0673; Observed: 396.0742 $[M+H]^+$.

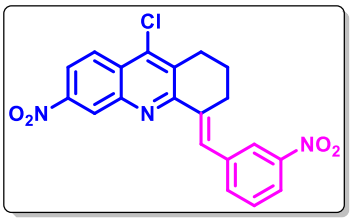

(E)-9-Chloro-4-(4-nitrobenzylidene)-1,2,3,4-tetrahydroacridine (5r): Yield= 93%, Yellow solid; M. P: 141.8-142.1 °C; **IR (KBr, cm^{-1})**: 3100, 2984, 1550, 1370, 1084, 714; **^{1}H NMR (400 MHz, CDCl$_3$) δ** 8.26 (d, *J* = 2.0 Hz, 1H), 8.25 (d, *J* = 2.8 Hz, 1H), 8.24 (s, 1H), 8.19 (dd, *J* = 8.4, 0.9 Hz, 1H), 8.08 (dd, *J* = 8.4, 0.5 Hz, 1H), 7.71 (t, *J* = 8.4 Hz, 1H), 7.61 (s, 1H), 7.61 – 7.59 (m, 1H), 7.57 (dd, *J* = 7.0, 1.3 Hz, 1H), 3.16 (t, *J* = 6.4 Hz, 2H), 2.97 – 2.93 (m, 2H), 1.98 (dt, *J* = 12.6, 6.4 Hz, 2H). **^{13}C NMR (100 MHz, CDCl$_3$) δ** 153.41, 146.95, 146.43, 144.45, 141.44, 139.22, 130.37, 130.08, 129.73, 129.14, 127.44, 125.94, 123.82, 123.54, 122.78, 27.75, 22.39. **Mass (ESI-MS):** m/z Calculated $C_{20}H_{15}ClN_2O_2$ for: 350.0822; Observed: 351.0894 $[M+H]^+$.

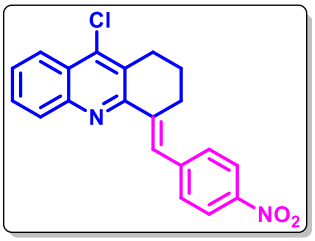

(E)-5-Chloro-9-(4-nitrobenzylidene)-6,7,8,9-tetrahydrobenzo[b][1,8]naphthyridine (5s): Yield= 88%, Yellow solid; M. P: 218.3-218.9 °C; **IR (KBr, cm^{-1})**: 3069, 2954, 1567, 1470,

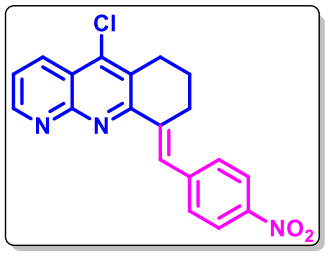

1073, 519; **^{1}H NMR (400 MHz, $CDCl_3$) δ** 9.13 (dd, *J* = 4.0, 2.0 Hz, 1H), 8.57 (dd, *J* = 8.4, 2.0 Hz, 1H), 8.55 (s, 1H), 8.27 (d, *J* = 8.8 Hz, 2H), 7.63 (d, *J* = 8.4 Hz, 2H), 7.55 (dd, *J* = 8.4, 4.2 Hz, 1H), 3.18 (t, *J* = 6.4 Hz, 2H), 3.00 (dd, *J* = 6.4Hz, 2H), 2.06 – 2.00 (m, 2H). **^{13}C NMR (100 MHz, $CDCl_3$) δ** 156.54, 154.25, 154.02, 146.59, 144.04, 141.77, 137.91, 133.41, 130.45, 129.60, 123.57, 122.39, 120.98, 27.67, 21.98. **Mass (ESI-MS):** m/z Calculated $C_{19}H_{14}ClN_3O_2$ for: 351.0775; Observed: 352.0844 $[M+H]^+$.

(E)-9-Bromo-4-(4-nitrobenzylidene)-1,2,3,4-tetrahydroacridine (5t): Yield= 90%, Yellow solid; M. P: 169.2-169.9 °C; **IR (KBr, cm^{-1})**: 3082, 2965, 1470, 1306, 769, 527; **^{1}H NMR (400 MHz, $CDCl_3$) δ** 8.29 (s, 1H), 8.27 (s, 1H), 8.27 (s, 1H), 8.20 (dd, *J* = 8.5, 0.9 Hz, 1H), 8.09 (dd, *J* = 8.4, 0.6 Hz, 1H), 7.75 – 7.70 (m, 1H), 7.64 (s, 1H), 7.63 – 7.58 (m, 2H), 3.17 (t, *J* = 6.4 Hz, 2H), 2.99 – 2.94 (m, 2H), 2.04 – 1.97 (quin, *J* = 6.4 Hz, 2H).

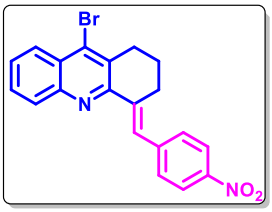

^{13}C NMR (100 MHz, $CDCl_3$) δ 153.44, 146.95, 146.43, 144.47, 139.23, 135.97, 131.52, 130.37, 129.73, 127.64, 126.57, 123.53, 31.10, 27.80, 22.69. **Mass (ESI-MS):** m/z Calculated $C_{20}H_{15}BrN_2O_2$ for: 394.0317; Observed: 395.0395 $[M+H]^+$.

(E)-6-Bromo-9-chloro-4-(4-nitrobenzylidene)-1,2,3,4-tetrahydroacridine (5u): Yield= 89%, Yellow solid; M. P: 170.2 -171.5 °C; **IR (KBr, cm^{-1})**: 3106, 2974, 1545, 1416, 1346,830, 754, 514; **^{1}H NMR (400 MHz, $CDCl_3$) δ** 8.27 (dd, *J* = 3.6, 2.0 Hz, 2H), 8.25 (t, *J* = 2.4 Hz, 2H), 8.03 (d, *J* = 9.0 Hz, 1H), 7.64 (dd, *J* = 9.0, 2.0 Hz, 1H), 7.61 – 7.58 (m, 2H), 3.12 (t, *J* = 6.4 Hz, 2H), 2.96 – 2.91 (m, 2H), 1.98 (m, 2H). **^{13}C NMR (100 MHz, $CDCl_3$) δ** 154.40, 147.36, 146.54, 144.17, 141.55, 138.71, 131.82, 130.71, 130.39, 129.58, 128.20, 125.29, 124.64, 123.94, 123.57, 27.69, 22.19. **Mass (ESI-MS):** m/z Calculated $C_{20}H_{14}BrClN_2O_2$ for: 427.9927; Observed: 429.0002 $[M+H]^+$.

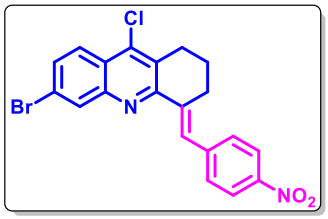

(E)-9-Chloro-6-methoxy-4-(4-nitrobenzylidene)-1,2,3,4-tetrahydroacridine (5v): Yield= 85%, Light Yellow solid; M. P: 165.4-166 °C; **IR (KBr, cm^{-1})**: 3092, 2975, 1565, 1362, 1164, 1023, 842; **^{1}H NMR (400 MHz, $CDCl_3$) δ** 8.29 (s, 1H), 8.28 (s, 1H), 8.27 (s, 2H), 7.92 (d, *J* = 8.8 Hz, 1H), 7.64 (d, *J* = 8.6 Hz, 2H), 7.59 (dd, *J* = 8.8, 2.0 Hz, 1H), 4.01 (s, 3H), 3.08 – 3.03 (m, 2H), 3.02 – 2.97 (m, 2H), 1.95 (m, 2H). **^{13}C NMR (100 MHz,**

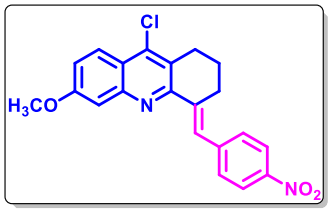

$CDCl_3$) δ 161.02, 155.65, 148.82, 146.41, 144.41, 139.20, 131.81, 131.36, 130.38, 130.03, 129.55, 127.46, 123.78 – 123.30, 123.12, 122.82, 121.57, 61.61, 28.23, 23.63, 22.29. **Mass (ESI-MS):** m/z Calculated $C_{23}H_{21}N_5O_4$ for: 380.0928; Observed: 381.0995 $[M+H]^+$.

(E)-9-Chloro-4-(naphthalen-1-ylmethylene)-1,2,3,4-tetrahydroacridine (5w): Yield= 86%, Yellow solid; M. P: 137-138 °C; **IR (KBr, cm^{-1})**: 3051, 2947, 2836, 1569, 1394, 860, 720; **^{1}H NMR (400 MHz, $CDCl_3$) δ** 8.76 (s, 1H), 8.3 (d, J= 6 Hz, 1H), 8.24 (dd, J = 8.4 Hz, 1H), 8.15 (dd, *J* = 5.4, 4.3 Hz, 1H), 7.94 – 7.89 (m, 1H), 7.88 – 7.83 (m, 1H), 7.76 (t, *J* = 7.5 Hz, 1H), 7.63 (dd, *J* = 11.3, 3.9 Hz, 1H), 7.55 (t, *J* = 2.7 Hz, 1H), 7.54 (d, *J* = 1.6 Hz, 1H), 7.53 – 7.50 (m, 2H), 3.18 (t, *J* = 6.4 Hz, 2H), 2.87 – 2.76 (m, 2H), 1.94 (quin, *J* = 12.6, 6.4 Hz, 2H). **^{13}C NMR (100 MHz, $CDCl_3$) δ** 154.45, 147.08, 141.29, 137.51, 135.10, 133.61, 132.38, 129.85, 129.42, 128.95, 128.46, 128.12, 127.75, 126.97, 126.90, 126.01, 125.91, 125.83, 125.36, 125.25, 123.74, 28.12, 27.79, 22.71. **Mass (ESI-MS):** m/z Calculated $C_{23}H_{21}N_5O_4$ for: 355.1128; Observed: 356.1207 $[M+H]^+$.

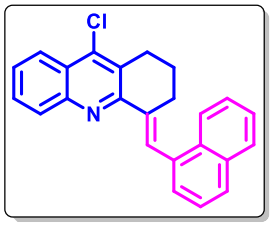

(E)-9-Chloro-4-(naphthalen-1-ylmethylene)-6-nitro-1,2,3,4-tetrahydroacridine (5x): Yield= 88%, Yellow solid; M. P: 200-201 °C; **IR (KBr, cm^{-1})**: 3102, 2986, 2852, 1543, 1364, 1018, 833; **^{1}H NMR (400 MHz, $CDCl_3$) δ** 9.00 (dd, *J* = 2.0, 0.8 Hz, 1H), 8.78 (s, 1H), 8.33 (dd, *J* = 9.0, 0.6 Hz, 1H), 8.30 (dd, *J* = 9.2, 2.0 Hz, 1H), 8.12 – 8.07 (m, 1H), 7.93 – 7.88 (m, 1H), 7.85 (d, *J* = 8.0 Hz, 1H), 7.53 (dd, *J* = 4.8, 1.6 Hz, 2H), 7.51 (d, *J* = 6.8 Hz, 1H), 7.48 (d, *J* = 6.8 Hz, 1H), 3.18 (t, *J* = 6.4 Hz, 2H), 2.86 – 2.79 (td, J= 6.2, 1.6Hz, 2H), 1.94 (quin, *J* = 6.2 Hz, 2H). **^{13}C NMR (100 MHz, $CDCl_3$) δ** 157.02, 148.21, 145.92, 141.27, 136.42, 134.45, 133.60, 132.38, 132.26, 130.01, 128.79, 128.54, 128.19, 126.93, 126.24, 126.06, 125.91, 125.68, 125.18, 125.08, 119.94, 28.44, 27.55, 22.21. **Mass (ESI-MS):** m/z Calculated $C_{23}H_{21}N_5O_4$ for: 400.0979; Observed: 401.1042 $[M+H]^+$.

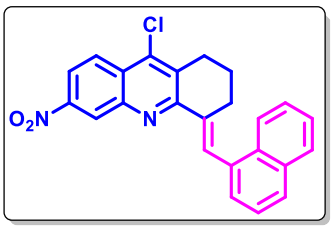

(E)-9-Chloro-4-(furan-2-ylmethylene)-1,2,3,4-tetrahydroacridine(5y): Yield= 90%, Green solid; M. P: 114-115.1 °C; **IR (KBr, cm^{-1})**: 3095, 2983, 2856, 1571, 1390, 1192, 1022, 927, 794; **^{1}H NMR (400 MHz, $CDCl_3$) δ** 8.08 (dd, *J* = 8.4, 0.4 Hz, 2H), 8.03 (s, 1H), 7.65 – 7.59 (dt, J= 8, 0.8 Hz 1H), 7.51 – 7.47 (m, 1H), 7.46 (d, *J* = 1.4 Hz, 1H), 6.56 (d, *J* = 2 Hz, 1H), 6.44 (dd, *J* = 3.2, 2 Hz, 1H), 3.05 (dd, *J* = 12.4, 6.4 Hz, 4H), 1.97 – 1.89 (m, J = 12.8, 6.4 Hz, 2H). **^{13}C NMR (100 MHz, $CDCl_3$) δ** 154.34, 153.83, 146.96, 142.81, 140.67,

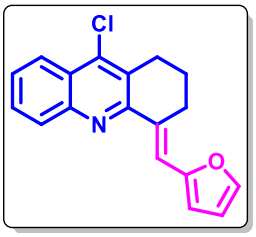

132.71, 129.46, 129.42, 129.25, 126.70, 125.51, 123.81, 117.75, 112.69, 111.85, 27.89, 27.66, 21.77. **Mass (ESI-MS):** m/z Calculated $C_{23}H_{21}N_5O_4$ for: 295.0764; Observed: 296.0845 $[M+H]^+$.

(E)-9-Chloro-4-(furan-2-ylmethylene)-6-nitro-1,2,3,4-tetrahydroacridine (5z): Yield= 88%, Yellow solid; M. P: 192-193 °C; **IR (KBr, cm^{-1})**: 3104, 2992, 2863, 1552, 1365, 1151, 1025, 920, 839; **^{1}H NMR (400 MHz, $CDCl_3$) δ** 8.93 (dd, *J* = 2.0, 0.8 Hz, 1H), 8.30 – 8.24 (m, 2H), 8.11 (t, *J* = 1.8 Hz, 1H), 7.56 (d, *J* = 1.6 Hz, 1H), 6.66 (d, *J* = 3.6 Hz, 1H), 6.54 (dd, *J* = 3.4, 1.8 Hz, 1H), 3.18 – 3.12 (m, 4H), 2.04 – 2.01 (m, 2H). **^{13}C NMR (100 MHz, $CDCl_3$) δ** 156.92, 153.45, 148.15, 145.92, 143.42, 140.47, 132.52, 131.53, 128.47, 125.68, 125.55, 119.62, 119.08, 113.82, 112.06, 27.97, 27.55, 21.30. **Mass (ESI-MS):** m/z Calculated $C_{23}H_{21}N_5O_4$ for: 340.0615; Observed: 341.0694 $[M+H]^+$.

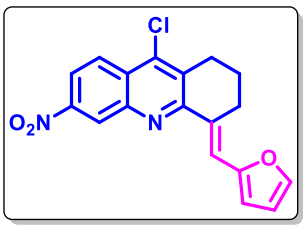

(E)-9-Chloro-4-(thiophen-2-ylmethylene)-1,2,3,4-tetrahydroacridine (5aa): Yield= 94%, Yellow solid; M. P: 112.6-113.1 °C; **IR (KBr, cm^{-1})**: 3075, 2932, 2864, 1541, 1499, 1148, 903, 838; **^{1}H NMR (400 MHz, $CDCl_3$) δ** 8.35 (s, 1H), 8.07 (dd, *J* = 8.4, 0.8 Hz, 1H), 8.01 (d, *J* = 8.4 Hz, 1H), 7.63 – 7.58 (td J=8.4 HZ, 1H), 7.48 – 7.43 (td, J=8 HZ 1H), 7.35 (d, *J* = 5.2 Hz, 1H), 7.27 (d, *J* = 3.6 Hz, 1H), 7.05 (dd, *J* = 5.2, 3.6 Hz, 1H), 3.07 – 3.03 (t, J=6.4HZ, 2H), 2.98 – 2.93 (dt, J= 5.6 Hz, 1.6 HZ,2H), 1.98 – 1.92 (quin, J= 6.4 HZ, 2H). **^{13}C NMR (100 MHz, $CDCl_3$) δ** 154.50, 147.11, 141.00, 140.49, 132.58, 130.19, 129.53, 129.40, 129.25, 127.27, 127.15, 126.69, 125.47, 123.86, 123.48, 28.24, 27.55, 21.82. **Mass (ESI-MS):** m/z Calculated $C_{23}H_{21}N_5O_4$ for: 311.0535; Observed: 312.0608 $[M+H]^+$.

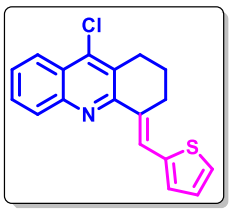

(E)-5-Chloro-9-(thiophen-2-ylmethylene)-6,7,8,9-tetrahydrobenzo[b][1,8]naphthyridine (5ab): Yield= 89%, Yellow solid; M. P: 146.8-147.1 °C; **IR (KBr, cm^{-1})**: 3079, 2945, 2872, 1531, 1421, 1247, 901, 758;**^{1}H NMR (400 MHz, $CDCl_3$) δ** 8.99 (dd, *J* = 4.2, 2.0 Hz, 1H), 8.65 (s, 1H), 8.43 (dd, *J* = 8.4, 2.0 Hz, 1H), 7.41 – 7.36 (m, 2H), 7.32 (d, *J* = 3.4 Hz, 1H), 7.07 (dd, *J* = 5.2, 3.8 Hz, 1H), 3.08 – 3.04 (m, 2H), 2.99 – 2.95 (m, 2H), 1.96 (m, 2H). **^{13}C NMR (100 MHz, $CDCl_3$) δ** 157.80, 154.44, 153.51, 140.69, 133.53, 131.24, 130.50, 127.97, 127.43, 125.85, 121.68, 120.47, 28.01, 27.50, 21.43. **Mass (ESI-MS):** m/z Calculated $C_{23}H_{21}N_5O_4$ for: 312.0488; Observed: 313.0561 $[M+H]^+$.

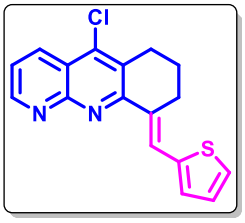

E)-9-Bromo-4-(thiophen-2-ylmethylene)-1,2,3,4-tetrahydroacridine (5ac): Yield= 90%, Yellow solid; M. P: 92.8-93.2 °C; **IR (KBr, cm^{-1})**: 3012, 2987, 2847, 1532, 1478, 1306, 1148, 910, 820, 592; **^{1}H NMR (400 MHz, CDCl$_3$) δ** 8.44 (s, 1H), 8.16 (d, *J* = 8.4 Hz, 1H), 8.08 (d, *J* = 8.4 Hz, 1H), 7.69 (ddd, *J* = 8.3, 6.9, 1.3 Hz, 1H), 7.58 – 7.53 (m, 1H), 7.45 (d, *J* = 5.2 Hz, 1H), 7.37 (d, *J* = 3.2 Hz, 1H), 7.16 (dd, *J* = 5.2, 3.4 Hz, 1H), 3.18 – 3.13(t, *J* = 6.4 Hz, 2H), 3.05 (t, *J* = 6.4 Hz, 2H), 2.05 (t, *J* = 6.4 Hz, 2H). **^{13}C NMR (100 MHz, CDCl$_3$) δ** 154.56, 147.17, 141.03, 135.00, 132.58, 131.71, 130.20, 129.46, 127.13, 126.65, 123.64, 30.96, 28.32, 22.09. **Mass (ESI-MS):** m/z Calculated $C_{20}H_{15}BrN_2O_2$ for: 355.0030; Observed:356.0107 $[M+H]^+$.

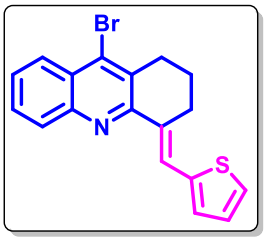

(E)-6-Bromo-9-chloro-4-(thiophen-2-ylmethylene)-1,2,3,4-tetrahydroacridine (5ad): Yield= 89%, Yellow solid; M. P: 133.7-134 °C; **IR (KBr, cm^{-1})**: 3087, 2954, 2868, 1541, 1310, 1152, 904, 832, 524; **^{1}H NMR (400 MHz, CDCl$_3$) δ** 8.39 (s, 1H), 8.23 (d, *J* = 1.6 Hz, 1H), 7.96 (d, *J* = 9.2 Hz, 1H), 7.57 (dd, *J* = 9.2, 2.0 Hz, 1H), 7.43 (d, *J* = 5.2 Hz, 1H), 7.33 (d, *J* = 3.4 Hz, 1H), 7.13 (dd, *J* = 5.2, 3.6 Hz, 1H), 3.08 – 3.04 (t, J=6.4 Hz, 2H), 3.02 – 2.97 (m, 2H), 2.03 – 1.97 (m, 2H). **^{13}C NMR (100 MHz, CDCl$_3$) δ** 155.45, 147.56, 140.79, 134.27, 132.04, 131.58, 130.55, 129.93, 129.62, 127.44, 125.32, 124.15, 123.59, 28.09, 27.51, 21.60. **Mass (ESI-MS):** m/z Calculated $C_{23}H_{21}N_5O_4$ for: 388.9641; Observed: 389.9710 $[M+H]^+$.

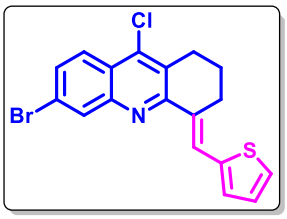

(E)-9-Chloro-6-nitro-4-(thiophen-2-ylmethylene)-1,2,3,4-tetrahydroacridine (5ae): Yield= 92%, Yellow solid; M. P: 167-168 °C; **IR (KBr, cm^{-1})**: 3109, 2975, 2845, 1567, 1360, 1207, 845; **^{1}H NMR (400 MHz, CDCl$_3$) δ** 8.95 (d, *J* = 0.8 Hz, 1H), 8.52 (s, 1H), 8.28 (s, 2H), 7.50 (d, *J* = 5.2 Hz, 1H), 7.41 (d, *J* = 3.6 Hz, 1H), 7.19 (dd, *J* = 5.0, 3.8 Hz, 1H), 3.19 – 3.15 (t, J= 6.4 Hz, 2H), 3.06 (t, *J* = 6.2 Hz, 2H), 2.10 – 2.04 (quin, J=6.4 Hz, 2H). **^{13}C NMR (100 MHz, CDCl$_3$) δ** 157.06, 148.19, 146.00, 140.49, 140.39, 132.53, 131.29, 131.13, 128.46, 128.11, 127.48, 125.75, 125.56, 125.24, 119.66, 27.93, 27.84, 21.34. **Mass (ESI-MS):** m/z Calculated $C_{23}H_{21}N_5O_4$ for: 356.0386; Observed: 357.0463 $[M+H]^+$.

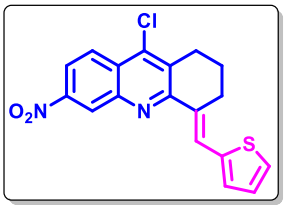

(E)-9-Chloro-4-(2-methylpropylidene)-1,2,3,4-tetrahydroacridine (5af): Yield= 75%, Yellow Oily compound; **IR (KBr, cm^{-1})**: 3010, 2982, 2854, 1536, 1174, 835; **^{1}H NMR (400 MHz, $CDCl_3$) δ** 8.15 – 8.10 (m, 1H), 8.04 – 7.99 (m, 1H), 7.64 (ddd, *J* = 8.4, 6.8, 1.6 Hz, 1H), 7.50 (ddd, *J* = 8.4, 6.8, 1.6 Hz, 1H), 7.01 (dt, *J* = 9.6, 1.6 Hz, 1H), 3.10 – 3.06 (m, 2H), 2.80 – 2.75 (m, 1H), 2.70 – 2.66 (m, 2H), 1.96 – 1.92 (m, 2H), 1.14 (d, *J* = 6.8 Hz, 6H).

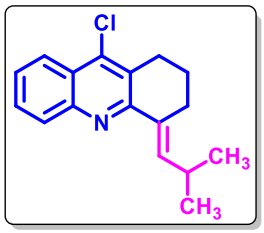

^{13}C NMR (100 MHz, $CDCl_3$) δ 154.92,146.99, 139.35, 129.60, 129.09, 126.39, 123.64, 28.02, 27.60, 26.03, 22.71, 22.28. **Mass (ESI-MS):** m/z Calculated $C_{17}H_{18}ClN$ for: 271.1128; Observed: 272.1203 $[M+H]^+$.

(E)-4-Benzylidene-1,2,3,4-tetrahydroacridin-9-amine (3a): Yield= 50%, white gummy compound; **IR (KBr, cm^{-1}):** 3312.45, 3192.05, 2922.85, 1635.01, 1495.88, 1181.01, 1011.21, 851.87, 756.46; **^{1}H NMR (400 MHz, $CDCl_3$) δ** 8.16 (s, 1H), 8.00 (d, *J* = 8.4 Hz, 1H), 7.68 (d, *J* = 8.4 Hz, 1H), 7.60 – 7.56 (m, 1H), 7.45 (d, *J* = 7.2 Hz, 2H), 7.40 – 7.35 (m, 3H), 7.26 (t, *J* = 7.2 Hz, 1H), 4.69 (s, 2H), 2.92 – 2.88 (m, 2H), 2.70 (t, *J* = 6.4 Hz, 2H), 1.95 (m, 2H). **^{13}C NMR (100 MHz, $CDCl_3$) δ** 153.63, 146.87, 146.42, 138.14, 136.96, 129.90, 129.66, 128.61, 128.33, 128.06, 126.73, 124.23, 119.54, 117.46, 111.11, 27.38, 24.17, 22.78. **Mass (ESI-MS):** m/z Calculated $C_{20}H_{18}N_2$ for: 286.1470; Observed: 287.1542 $[M+H]^+$.

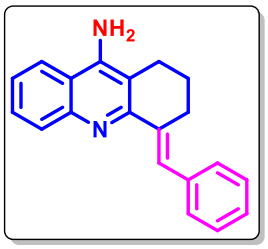

(E)-4-(4-Methylbenzylidene)-1,2,3,4-tetrahydroacridin-9-amine (3b): Yield= 65%, white solid; M. P: 146.5-147.7 °C; **IR (KBr, cm^{-1}):** 3340.42, 3246.46, 2922.23, 2850.43, 1652.65, 1518.87, 1167.43, 1.22.05, 842.40, 741.42; **^{1}H NMR (400 MHz, DMSO) δ** 8.52 (d, *J* = 8.4 Hz, 1H), 8.34 (s, 2H), 8.22 (d, *J* = 8.4 Hz, 1H), 7.91 (d, *J* = 8.0 Hz, 1H), 7.88 (s, 1H), 7.63 (t, *J* = 8.4 Hz, 1H), 7.49 (d, *J* = 8.4 Hz, 2H), 7.35 (d, *J* = 8.0 Hz, 2H), 2.92 – 2.88 (m, 2H), 2.75 (t, *J* = 6.4 Hz, 2H), 2.42 (s, 3H), 1.94 (quint, *J* = 6.4 Hz, 2H). **^{13}C NMR (100 MHz, DMSO) δ** 154.87, 152.71, 148.18, 143.26 (s), 138.36, 133.60, 133.15, 131.33, 130.22, 129.65, 125.70, 123.42, 115.67, 110.98, 110.66, 108.47, 26.64, 23.59, 22.21, 21.41. **Mass (ESI-MS):** m/z Calculated $C_{21}H_{20}N_2$ for 300.1626; Observed: 301.1700 $[M+H]^+$.

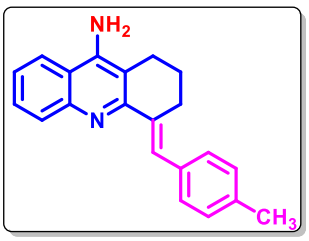

(E)-4-(4-Methoxybenzylidene)-6-nitro-1,2,3,4-tetrahydroacridin-9-amine (3c): Yield= 70%, red solid; M. P: 136.1-137.2 °C; **IR (KBr, cm^{-1}):** 3348.42, 3245.28, 2926.46, 2851.49, 2100.46, 1604.78, 1466.90, 1176.43, 1029.05, 894.19, 842.40; **^{1}H NMR (400 MHz, $CDCL_3$+DMSO) δ** 8.74 (d, *J* = 2.3 Hz, 1H), 8.19 (d, *J* = 9.2 Hz, 1H), 8.12 (s, 1H), 8.02 (dd, *J* = 9.2, 2.4 Hz, 1H), 7.41 (d, *J* = 8.8 Hz, 2H), 6.94 (d, *J* = 8.8 Hz, 2H), 5.91 (s, 2H), 3.85 (s, 3H), 2.94 – 2.89 (m, 2H), 2.74 (t, *J* = 6.4 Hz, 2H), 1.96 (quin, *J* = 6.4 Hz, 2H). **^{13}C NMR (100 MHz, $CDCL_3$+DMSO) δ** 158.69, 155.61, 148.30, 147.52, 145.67, 134.56, 131.17, 130.13, 128.94, 124.94, 123.56, 120.67, 116.08, 113.68, 113.01, 55.27, 27.28, 24.30, 22.39. **Mass (ESI-MS):** m/z Calculated $C_{21}H_{19}N_3O_3$ for 361.1426; Observed: 362.1500 $[M+H]^+$.

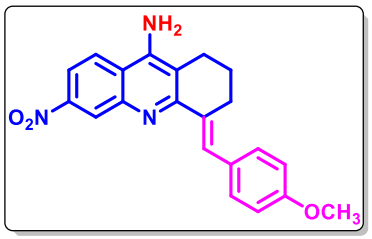

(E)-4-(4-(Dimethylamino)benzylidene)-1,2,3,4-tetrahydroacridin-9-amine (3d): Yield=58%, red solid; M. P:154.7-155.5 °C; **IR (KBr, cm^{-1}):** 3358.56, 3192.82, 2922.76, 1679.02, 1523.03, 1367.83, 1187.81, 812.23, 754.89; **^{1}H NMR (400 MHz, $CDCl_3$) δ** 8.14 (s, 2H), 7.99 (t, *J* = 8.4 Hz, 2H), 7.77 (s, 1H), 7.41 (d, *J* = 7.6 Hz, 1H), 7.38 (d, *J* = 8.8 Hz, 2H), 7.27 (s, 3H), 7.24 (d, *J* = 7.2 Hz, 1H), 6.69 (d, *J* = 8.8 Hz, 2H), 3.02 (s, 6H), 2.71 – 2.64 (m, 2H), 2.37 (t, *J* = 6.4 Hz, 2H), 1.77 – 1.71 (m, 2H). **^{13}C NMR (100 MHz, $CDCl_3$) δ** 177.31, 153.52, 150.18, 148.60, 138.82, 134.41, 131.88, 131.36, 130.56, 125.72, 124.60, 124.26, 122.21, 121.13, 115.01, 111.66, 108.82, 40.22, 26.74, 23.01, 21.88. **Mass (ESI-MS):** m/z Calculated $C_{22}H_{23}N_3$ for 329.1892; Observed: 330.1970 $[M+H]^+$.

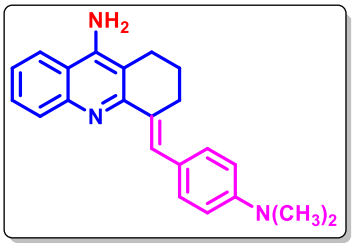

(E)-4-(4-Chlorobenzylidene)-1,2,3,4-tetrahydroacridin-9-amine (3e): Yield= 55%, white; M. P:169.7- 170.2 °C; **IR (KBr, cm^{-1}):** 3329.01, 3214.23, 2928.76, 1679.02, 1603.69, 1523.03, 1107.11, 812.45, 752.31; **^{1}H NMR (400 MHz, $CDCl_3$) δ** 8.10 (s, 1H), 7.98 (d, *J* = 8.4 Hz, 1H), 7.67 (d, *J* = 8.4 Hz, 1H), 7.59 (ddd, *J* = 8.4, 6.8, 1.2 Hz, 1H), 7.38 (dd, *J* = 6.8, 1.2 Hz, 1H), 7.37 – 7.31 (m, 4H), 4.64 (s, 2H), 2.89 – 2.83 (m, 2H), 2.70 (t, *J* = 6.4 Hz, 2H), 1.96 (quint, *J* = 6.4 Hz, 2H). **^{13}C NMR (100 MHz, $CDCl_3$) δ** 154.47, 153.93, 138.83, 137.68, 132.31, 131.28, 130.71, 128.62, 124.91, 122.69, 120.80, 114.96, 108.47, 38.48, 24.23, 22.89. **Mass (ESI-MS):** m/z Calculated $C_{20}H_{17}ClN_2$ for 320.1080; Observed: 321.1153 $[M+H]^+$.

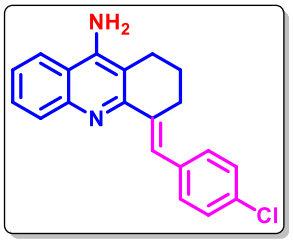

(E)-4-(4-Nitrobenzylidene)-1,2,3,4-tetrahydroacridin-9-amine (3f): Yield= 52%, red solid; M. P: 178.9-179.3 °C; **IR (KBr, cm^{-1}):** 3342.25, 3157.05, 2926.85, 1634.01, 1495.88, 1189.47, 1010.21, 84.87, 757.46; **^{1}H NMR (400 MHz, CDCL$_3$+DMSO) δ** 8.11 (s, 1H), 7.88 (d, *J* = 4.9 Hz, 2H), 7.86 – 7.84 (m, 2H), 7.53 (d, *J* = 8.4 Hz, 2H), 7.49 (d, *J* = 7.2 Hz, 1H), 7.31 – 7.26 (m, 1H), 5.46 (s, 2H), 2.92 – 2.87 (m, 2H), 2.67 (t, *J* = 6.4 Hz, 2H), 1.89 (quint, *J* = 6.4 Hz, 2H). **^{13}C NMR (100 MHz, CDCl$_3$) δ** 152.21, 150.47, 147.23, 146.20, 140.58, 138.23, 129.96, 128.88, 127.99, 126.38, 123.26, 122.12, 120.35, 117.00, 110.25, 27.17, 23.54, 22.21. **Mass (ESI-MS):** m/z Calculated $C_{20}H_{17}N_3O_2$ for 331.1321; Observed: 332.1394 $[M+H]^+$.

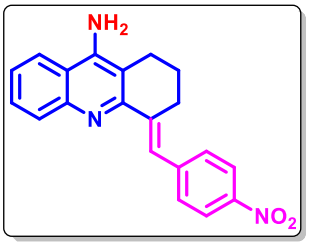

(E)-4-(Thiophen-2-ylmethylene)-1,2,3,4-tetrahydroacridin-9-amine (3g): Yield= 68%, Yellow solid; M. P:98.7-99.5 °C; **IR (KBr, cm^{-1}):** 3390.01, 3294.31, 29545.64, 1599.97, 1483.27, 1183.42, 1045.47, 925.55, 851.21; **^{1}H NMR (400 MHz, CDCl$_3$) δ** 8.36 (s, 1H), 7.98 (d, *J* = 8.0 Hz, 1H), 7.66 (dd, *J* = 8.4, 0.8 Hz, 1H), 7.57 (ddd, *J* = 8.4, 6.8, 1.2 Hz, 1H), 7.36 (d, *J* = 6.0 Hz, 1H), 7.35 – 7.32 (m, 1H), 7.28 (d, *J* = 3.6 Hz, 1H), 7.09 (dd, *J* = 5.2, 3.6 Hz, 1H), 4.70 (s, 2H), 3.01 – 2.96 (m, 2H), 2.68 (t, *J* = 6.4 Hz, 2H), 2.00 (m, 2H). **^{13}C NMR (100 MHz, CDCL$_3$+DMSO) δ** 152.27, 148.54, 146.38, 141.09, 134.04, 129.43, 128.69, 127.41, 126.67, 123.53, 121.80, 121.10, 117.41, 110.79, 28.12, 23.89, 22.22. **Mass (ESI-MS):** m/z Calculated $C_{18}H_{16}N_2S$ for 292.1034; Observed: 293.1109 $[M+H]^+$.

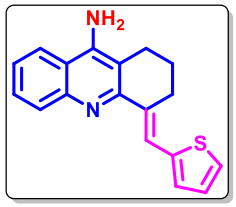

(E)-6-Bromo-4-(thiophen-2-ylmethylene)-1,2,3,4-tetrahydroacridin-9-amine(3h): Yield= 69%, red solid; M. P: 185.8-186.4 °C; **IR (KBr, cm^{-1})**: 3320.02, 3225.31, 2925.94, 1638, 1599.97, 1483.27, 1219.36, 1066.47, 851.80; **^{1}H NMR (400 MHz, CDCl$_3$) δ** 8.35 (s, 1H), 8.16 (s, 1H), 7.49 (d, *J* = 8.8 Hz, 1H), 7.41 – 7.36 (m, 2H), 7.29 (d, *J* = 3.6 Hz, 1H), 7.10 (dd, *J* = 5.4, 3.6 Hz, 1H), 4.64 (s, 2H), 2.98 (t, *J* = 5.4 Hz, 2H), 2.65 (t, *J* = 6.4 Hz, 2H), 2.00 (q, *J* = 6.4 Hz, 2H). **^{13}C NMR (100 MHz, CDCl$_3$) δ** 154.23, 147.67, 146.28, 141.10, 133.52, 131.82, 129.82, 127.23, 126.59, 122.65, 122.25, 121.27, 115.96, 111.80, 27.86, 23.79, 21.90. **Mass (ESI-MS):** m/z Calculated $C_{18}H_{15}BrN_2S$ for: 370.0139; Observed: 371.0212 $[M+H]^+$.

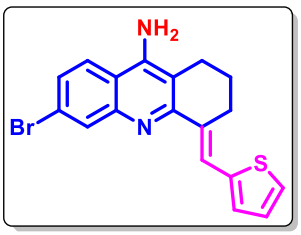

(E)-6-Nitro-4-(thiophen-2-ylmethylene)-1,2,3,4-tetrahydroacridin-9-amine (3i): Yield= 72%, Yellow solid; M. P: 156.6-157.4 °C; **IR (KBr, cm^{-1}):** 3492.68, 3467.68, 3104.96, 2926.16, 2854.26, 1631.12, 1518.78, 1184.57, 1071.24, 894.13, 739.96; **^{1}H NMR (400 MHz, CDCL$_3$+DMSO) δ** 8.77 (d, *J* = 2.2 Hz, 1H), 8.40 (s, 1H), 8.08 (d, *J* = 9.2 Hz, 1H), 8.03 (d, *J* = 9.2 Hz, 1H), 7.41 (d, *J* = 5.2 Hz, 1H), 7.32 (d, *J* = 3.6 Hz, 1H), 7.12 (dd, *J* = 5.2, 3.6 Hz, 1H), 5.62 (s, 2H), 3.03 – 2.98 (m, 2H), 2.73 (t, *J* = 6.4 Hz, 2H), 2.06 – 2.00 (quin, *J* = 6.4 Hz, 2H). **^{13}C NMR (100 MHz, CDCL$_3$+DMSO) δ** 155.28, 147.55, 145.88, 140.86, 133.27, 129.90, 126.84, 125.24, 123.12, 122.49, 120.62, 116.23, 113.46, 27.74, 23.96, 21.72. **Mass (ESI-MS):** m/z Calculated $C_{18}H_{15}N_3O_2S$ for: 337.0885; Observed: 338.0968 $[M+H]^+$.

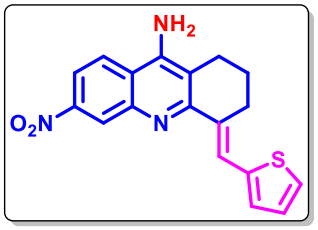

(E)-4-Benzylidene-N-(p-tolyl)-1,2,3,4-tetrahydroacridin-9-amine (8a): Yield=76%, Yellow solid; M. P: 101.2-102 °C; **IR (KBr, cm−1):** 3375, 3060, 2932, 2860, 1614, 1574, 1241; **^{1}H NMR (400 MHz, CDCl$_3$) δ** 8.32 (s, 1H), 7.81 (d, *J* = 8.4 Hz, 1H), 7.63 – 7.58 (m, 1H), 7.53 (d, *J* = 7.6 Hz, 2H), 7.39 (t, *J* = 7.6 Hz, 2H), 7.35 – 7.26 (m, 3H), 7.06 (d, *J* = 8.4 Hz, 2H), 6.74 (d, *J* = 8.0 Hz, 2H), 6.40 (s, 1H), 2.95 – 2.90 (t, *J* =5.6 Hz, 2H), 2.72 (t, *J* = 6.0 Hz, 2H), 2.30 (s, 3H), 1.85 – 1.80 (m, 2H). **^{13}C NMR (100 MHz, CDCl$_3$) δ** 154.41, 145.60, 141.81, 137.81, 135.52, 131.05, 130.43, 130.38, 129.86, 128.98, 128.34, 127.36, 122.97, 117.74 (s), 28.06, 26.32, 22.81, 20.85. **Mass (ESI-MS):** m/z Calculated $C_{27}H_{24}N_2$ for: 376.1939; Observed: 377.2013 $[M+H]^+$.

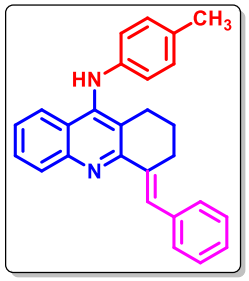

(E)-4-(4-Methylbenzylidene)-N-(p-tolyl)-1,2,3,4-tetrahydroacridin-9-amine (8b): Yield= 84%, Yellow solid; M. P: 212.3-213 °C; **IR (KBr, cm−1):** 3196, 3018, 2918, 2865, 1573, 1509, 1396, 1250, 811; **^{1}H NMR (400 MHz, DMSO) δ** 8.34 (s, 1H), 8.14 (s, 1H), 8.00 – 7.96 (m, 2H), 7.67 – 7.62 (m, 1H), 7.43 – 7.39 (m, 3H), 7.24 (d, *J* = 8.0 Hz, 2H), 6.98 (d, *J* = 8.4 Hz, 2H), 6.61 (d, *J* = 8.4 Hz, 2H), 2.91 – 2.85 (m, 2H), 2.63 (t, *J* = 6.0 Hz, 2H), 2.33 (s, 3H), 2.20 (s, 3H), 1.74 – 1.66 (m, 2H). **^{13}C NMR (100 MHz, DMSO) δ** 154.32, 147.07, 144.44, 142.96, 137.08, 135.52, 134.76, 129.96, 129.37, 128.67, 125.43, 123.75, 123.60, 116.66, 28.31, 26.72, 22.61, 21.33, 20.67. **Mass (ESI-MS):** m/z Calculated $C_{28}H_{26}N_2$ for: 390.2096; Observed: 391.2172 $[M+H]^+$.

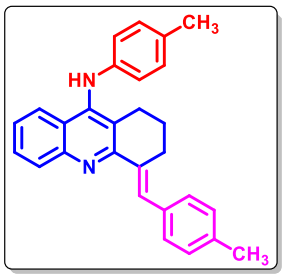

(E)-4-(4-Methylbenzylidene)-6-nitro-N-(p-tolyl)-1,2,3,4-tetrahydroacridin-9-amine (8c):

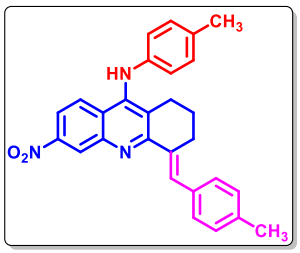

Yield= 87%, Yellow solid; M. P: 205.5-206 °C; **IR (KBr, cm−1):** 3376, 2938, 2917, 1536, 1340, 1246; **^{1}H NMR (400 MHz, $CDCl_3$) δ** 8.95 (s, 1H), 8.29 (s, 1H), 8.01 (d, *J* = 9.2 Hz, 1H), 7.86 (d, *J* = 9.2 Hz, 1H), 7.41 (d, *J* = 8.0 Hz, 2H), 7.23 (d, *J* = 8.0 Hz, 2H), 7.05 (d, *J* = 8.4 Hz, 2H), 6.66 (d, *J* = 8.4 Hz, 2H), 5.98 (s, 1H), 2.99 – 2.95 (m, 2H), 2.80 (t, *J* = 6.0 Hz, 2H), 2.39 (s, 3H), 2.30 (s, 3H), 1.88 (q, *J* = 12.4, 6.2 Hz, 2H). **^{13}C NMR (100 MHz, $CDCl_3$) δ** 157.50, 147.71, 146.57, 142.50, 141.36, 137.43, 134.60, 131.37, 130.30, 129.75, 129.02, 125.96, 125.31, 124.94 – 124.75, 118.34, 117.74, 27.79, 26.16, 22.33, 21.35, 20.66. **Mass (ESI-MS):** m/z Calculated $C_{28}H_{25}N_3O_2$ for: 435.1947; Observed: 436.2019 $[M+H]^+$.

(E)-N-(4-Chlorophenyl)-4-(4-methylbenzylidene)-1,2,3,4-tetrahydroacridin-9-amine (8d):

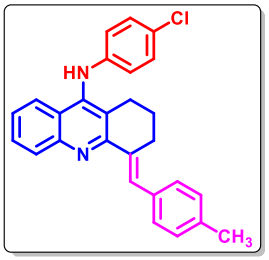

Yield= 80%, Yellow solid; M. P: 173.5-174 °C; **IR (KBr, cm−1):** 3307,2944, 2867, 1598, 1494, 819; **^{1}H NMR (400 MHz, $CDCl_3$) δ** 8.21 (s, 1H), 8.11 (d, *J* = 8.4 Hz, 1H), 7.73 (d, *J* = 8.0 Hz, 1H), 7.60 (m, 1H), 7.39 (d, *J* = 8.0 Hz, 2H), 7.36 – 7.31 (m, 1H), 7.19 (d, *J* = 8.0 Hz, 2H), 7.15 – 7.11 (m, 2H), 6.61 – 6.57 (m, 2H), 5.93 (s, 1H), 2.92 (t, *J* = 5.4 Hz, 2H), 2.71 (t, *J* = 6.2 Hz, 2H), 2.37 (s, 3H), 1.83 – 1.76 (m, 2H). **^{13}C NMR (100 MHz, $CDCl_3$) δ** 155.27, 147.56, 143.34, 142.24, 137.01, 135.34, 134.88, 130.13, 128.97, 128.97, 125.61, 125.07, 124.71, 123.58, 122.55, 117.20, 28.07, 26.10, 22.62, 21.36. **Mass (ESI-MS):** m/z Calculated $C_{27}H_{23}ClN_2$ for: 410.1550; Observed: 411.1620 $[M+H]^+$.

(E)-4-(4-Methoxybenzylidene)-N-phenyl-1,2,3,4-tetrahydroacridin-9-amine(8e):

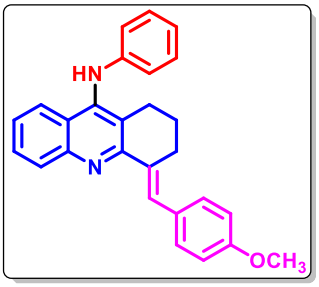

Yield=80%, Yellow solid; M. P: 160.3-161.4 °C; **IR (KBr, cm−1):** 3280,3030,2951, 2870, 1560, 1513,1189; **^{1}H NMR (400 MHz, $CDCl_3$) δ** 8.19 (s, 1H), 8.09 (d, *J* = 8.4 Hz, 1H), 7.80 (d, *J* = 9.2 Hz, 1H), 7.61 (ddd, *J* = 8.4, 6.8, 1.2 Hz, 1H), 7.46 (d, *J* = 8.4 Hz, 2H), 7.34 (ddd, *J* = 8.4, 6.8, 1.2 Hz, 1H), 7.21 (td, *J* = 7.6, 2.0 Hz, 2H), 6.94 (d, *J* = 8.8 Hz, 2H), 6.89 (t, *J* = 7.6 Hz, 1H), 6.70 (d, *J* = 7.6 Hz, 2H), 5.93 (s, 1H), 3.84 (s, 3H), 2.98 – 2.93 (m, 2H), 2.77 (t, *J* = 6.0 Hz, 2H), 1.86 – 1.81 (m, 2H). **^{13}C NMR (100 MHz, $CDCl_3$) δ** 158.67, 155.37, 147.70, 144.69, 142.45, 134.66, 131.32, 130.54, 129.86, 129.32, 129.05, 128.80, 125.33, 124.41, 123.64, 122.62, 120.40, 116.18, 113.64, 55.29, 28.15, 26.12, 22.71. **Mass (ESI-MS):** m/z Calculated $C_{27}H_{24}N_2O$ for: 392.1889; Observed: 393.1963 $[M+H]^+$.

(E)-6-Bromo-4-(4-methoxybenzylidene)-N-phenyl-1,2,3,4-tetrahydroacridin-9-amine(8f):

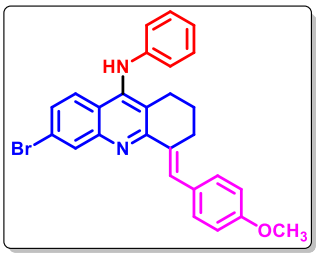

Yield= 81%, Yellow solid; M. P: 171.9-172.6 °C; **IR (KBr, cm−1):** 3302, 3044, 2926, 2853, 1569, 1174, 1023, 832; ^{1}H NMR (400 MHz, $CDCl_3$) δ 8.27 (d, *J* = 2.0 Hz, 1H), 8.18 (s, 1H), 7.60 (d, *J* = 9.2 Hz, 1H), 7.44 (d, *J* = 8.4 Hz, 2H), 7.36 (dd, *J* = 9.2, 2.0 Hz, 1H), 7.23 – 7.18 (m, 2H), 6.95 – 6.92 (m, 2H), 6.89 (d, *J* = 7.6 Hz, 1H), 6.68 (d, *J* = 7.6 Hz, 2H), 5.91 (s, 1H), 3.84 (s, 3H), 2.94 – 2.90 (m, 2H), 2.72 (t, *J* = 6.2 Hz, 2H), 1.84 – 1.79 (m, 2H). **^{13}C NMR (100 MHz, $CDCl_3$) δ** 158.82, 156.34, 148.34, 144.40, 142.83, 134.23, 131.83, 131.40, 130.28, 129.70, 129.40, 128.43, 124.50, 122.85, 122.12, 120.78, 116.40, 113.71, 55.33, 28.01, 25.99, 22.52. **Mass (ESI-MS):** m/z Calculated $C_{27}H_{23}BrN_2O$ for: 470.0994; Observed: 471.1072 $[M+H]^+$.

(E)-4-(4-Methoxybenzylidene)-6-nitro-N-phenyl-1,2,3,4-tetrahydroacridin-9-amine(8g):

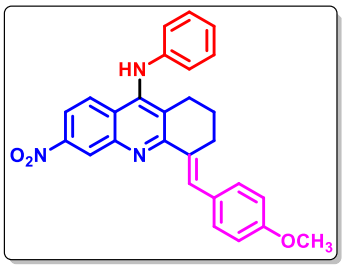

Yield= 82%, Yellow solid; M. P: 179.8-180.4 °C; **IR (KBr, cm^{-1})**: 3366, 3017, 2924, 2853, 1491, 1340, 1173; **^{1}H NMR (400 MHz, $CDCl_3$)** δ 8.94 (d, *J* = 2.4 Hz, 1H), 8.27 (s, 1H), 8.03 (dd, *J* = 9.2, 2.4 Hz, 1H), 7.88 (d, *J* = 9.2 Hz, 1H), 7.48 (d, *J* = 8.4 Hz, 2H), 7.26 – 7.21 (m, 2H), 6.98 – 6.93 (m, 3H), 6.71 (d, *J* = 7.6 Hz, 2H), 6.00 (s, 1H), 3.86 (s, 3H), 2.98 (t, *J* = 5.2 Hz, 2H), 2.81 (t, *J* = 6.0 Hz, 2H), 1.86 (q, *J* = 6.0 Hz, 2H). **^{13}C NMR (100 MHz, $CDCl_3$)** δ 159.06, 157.88, 147.74, 146.64, 144.01, 142.84, 133.61, 131.50, 130.75, 129.99, 129.52, 129.30, 126.81, 126.51, 125.89, 124.86, 121.37, 118.58, 118.12, 116.74, 115.13, 113.80, 55.34, 27.88, 26.21, 22.29. **Mass (ESI-MS):** m/z Calculated $C_{27}H_{23}N_3O_3$ for: 437.1739; Observed: 438.1817 $[M+H]^+$.

(E)-4-(4-Methoxybenzylidene)-N-(p-tolyl)-1,2,3,4-tetrahydroacridin-9-amine (8h): Yield= 81%, Yellow solid; M. P: 227.2-227.9 °C; IR (KBr, cm−1): 3356, 2922, 1591, 1519, 1104; **^{1}H NMR (400 MHz, $CDCL_3$+DMSO) δ** 8.18 (s, 1H), 8.14 (d, *J* =8.0 Hz, 1H), 7.87 (d, *J* = 8.8 Hz, 1H), 7.61 (t, *J* = 8.4 Hz, 1H), 7.48 (d, *J* = 8.8 Hz, 2H), 7.35 (d, *J* = 7.0 Hz, 1H), 7.25 (d, *J* = 8.8 Hz, 2H), 7.18 (d, *J* = 8.4 Hz, 2H), 7.03 (d, *J* = 8.0 Hz, 2H), 6.01 (s, 1H), 3.85 (s, 3H), 2.95 (t, *J* = 5.6 Hz, 2H), 2.73 (t, *J* = 6.4 Hz, 2H), 2.28 (s, 3H), 1.83 (t, *J* = 6.4 Hz, 2H). **^{13}C NMR (100 MHz, $CDCL_3$+DMSO) δ** 173.95, 158.69, 154.74, 142.00, 138.62, 131.30, 131.00, 130.28, 129.72, 129.65, 129.28, 128.95, 128.75, 125.96,

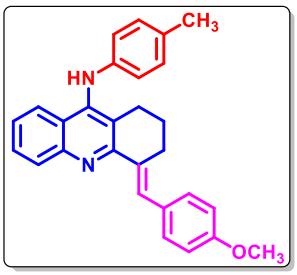

125.03, 122.96, 117.08, 113.61, 55.23, 30.88, 28.06, 26.20, 22.61, 21.14. **Mass (ESI-MS):** m/z Calculated $C_{28}H_{26}N_2O$ for: 406.2045; Observed: 407.2130 $[M+H]^+$.

(E)-9-(4-Methoxybenzylidene)-N-(p-tolyl)-6,7,8,9-tetrahydrobenzo[b][1,8]naphthyridin-5-amine (8i): Yield= 71%, Yellow solid; M. P: 260.7-270.1 °C; **IR (KBr, cm−1):** 3231, 2910, 2856, 1591, 1539, 1249; **^{1}H NMR (400 MHz, $CDCl_3$) δ** 8.96 (dd, *J* = 4.0, 1.6 Hz, 1H), 8.46 (s, 1H), 8.14 (dd, *J* = 8.4, 2.0 Hz, 1H), 7.46 (d, *J* = 8.4 Hz, 2H), 7.18 (dd, *J* = 8.0, 4.0 Hz, 1H), 7.03 (d, *J* = 8.4 Hz, 2H), 6.93 (d, *J* = 8.8 Hz, 2H), 6.67 (d, *J* = 8.4 Hz, 2H), 6.15 (s, 1H), 3.83 (s, 3H), 2.97 – 2.92 (m, 2H), 2.75 (t, *J* = 6.0 Hz, 2H), 2.29 (s, 3H), 1.84 (p, *J* = 6.0 Hz, 2H). **^{13}C NMR (100 MHz, $CDCl_3$) δ** 158.87, 158.07, 155.24, 152.86, 144.45, 141.78, 133.44, 132.84, 131.50, 130.97, 130.90, 130.27, 129.93, 123.54, 119.83, 117.42, 117.34, 113.70, 55.30, 28.00, 25.98, 22.37, 20.64. **Mass (ESI-MS):** m/z Calculated $C_{27}H_{25}N_3O$ for: 407.1998; Observed: 408.2074 $[M+H]^+$.

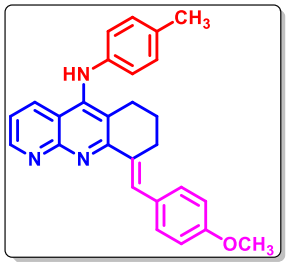

(E)-6-Bromo-4-(4-methoxybenzylidene)-N-(p-tolyl)-1,2,3,4-tetrahydroacridin-9-amine (8j): Yield= 78%, Yellow solid; M. P: 205.5-206 °C; **IR (KBr, cm−1):** 3304, 2924, 2853,1597, 1250, 539; **^{1}H NMR (400 MHz, $CDCl_3$) δ** 8.28 (s, 1H), 8.18 (s, 1H), 7.62 (d, *J* = 8.8 Hz, 1H), 7.46 (d, *J* = 8.4 Hz, 2H), 7.37 (dd, *J* = 8.8, 2.0 Hz, 1H), 7.03 (d, *J* = 8.0 Hz, 2H), 6.96 – 6.93 (m, 2H), 6.64 (d, *J* = 8.4 Hz, 2H), 5.90 (s, 1H), 3.85 (s, 3H), 2.98 – 2.91 (m, 2H), 2.73 (t, *J* = 6.4 Hz, 2H), 2.29 (s, 3H), 1.84 (q, *J* = 6.4 Hz, 3H). **^{13}C NMR (100 MHz, $CDCl_3$) δ** 158.81, 156.13, 143.51, 141.81, 131.38, 131.10, 130.75, 130.30, 129.89, 129.79, 128.58, 128.28, 124.46, 123.38, 122.84, 121.64, 121.54, 120.91, 117.13, 113.68, 112.92, 55.30, 27.96, 25.95, 22.56, 20.63. **Mass (ESI-MS):** m/z Calculated $C_{28}H_{25}BrN_2O$ for: 484.1150; Observed: 485.1125 $[M+H]^+$.

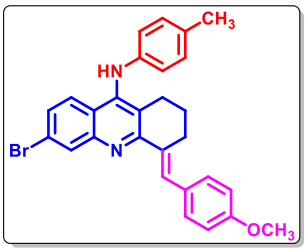

(E)-4-(4-Methoxybenzylidene)-N-(4-methoxyphenyl)-1,2,3,4-tetrahydroacridin-9-amine(8k): Yield= 85%, Yellow solid; M. P: 183.2-183.8 °C; **IR (KBr, cm−1):** 3342, 3069, 2982,2865, 1510, 1393, 1246, 1172; **^{1}H NMR (400 MHz, $CDCl_3$) δ** 8.18 (s, 1H), 8.07 (d, *J* = 8.0 Hz, 1H), 7.74 (d, *J* = 8.4 Hz, 1H), 7.58 (ddd, *J* = 8.4, 6.8, 1.6 Hz, 1H), 7.45 (d, *J* = 8.4 Hz, 2H), 7.30 (ddd, *J* = 8.4, 6.8, 1.2 Hz, 1H), 6.93 (d, *J* = 8.8 Hz, 2H), 6.78 (d, *J* = 9.2 Hz, 2H), 6.71 (d, *J* = 9.2 Hz, 2H), 5.88 (s, 1H), 3.83 (s, 3H), 3.76 (s, 3H), 2.96 – 2.91 (m, 2H), 2.70 (t, *J* = 6.0 Hz, 2H), 1.82 (t, *J* = 6.0 Hz, 2H). **^{13}C NMR (100 MHz, $CDCl_3$) δ** 158.62,

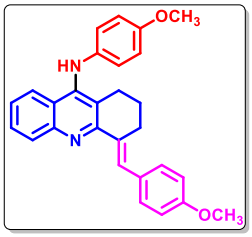

155.17, 154.47, 147.75, 143.65, 138.17, 134.87, 131.29, 130.61, 129.90, 128.78, 128.64, 124.94, 122.77, 122.54, 122.36, 118.98, 114.63, 113.63, 55.62, 55.30, 28.11, 26.11, 22.80. **Mass (ESI-MS):** m/z Calculated $C_{28}H_{26}N_2O_2$ for: 422.1994; Observed: 423.2065 $[M+H]^+$.

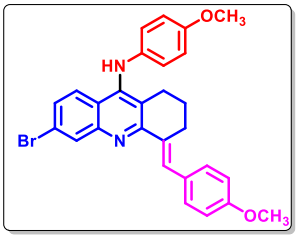

(E)-6-Bromo-4-(4-methoxybenzylidene)-N-(4-methoxyphenyl)-1,2,3,4-tetrahydroacridin-9-amine(8l): Yield= 83%, Yellow solid; M. P: 173.8-174.2 °C; **IR (KBr, cm−1):** 3367, 3109, 2942,2845, 1568, 1335, 1236, 1182; ^{1}H NMR (400 MHz, $CDCl_3$) δ 8.27 (s, 1H), 8.18 (s, 1H), 7.58 (d, *J* = 9.2 Hz, 1H), 7.45 (d, *J* = 8.4 Hz, 2H), 7.33 (dd, *J* = 8.8, 2.0 Hz, 1H), 6.95 – 6.92 (m, 2H), 6.81 – 6.78 (m, 2H), 6.76 – 6.72 (m, 2H), 5.95 (s, 1H), 3.84 (s, 3H), 3.77 (s, 3H), 2.95 – 2.90 (m, 2H), 2.69 (t, *J* = 6.4 Hz, 2H), 1.84 (t, *J* = 6.4 Hz, 2H). **^{13}C NMR (100 MHz, $CDCl_3$) δ** 158.81, 154.91, 144.27, 137.62, 131.37, 130.29, 128.03, 124.45, 122.82, 121.92, 120.90, 119.61, 114.68, 113.69, 55.61, 55.31, 27.90, 25.94, 22.60. **Mass (ESI-MS):** m/z Calculated $C_{28}H_{25}BrN_2O_2$ for: 500.1099; Observed: 501.1173 $[M+H]^+$.

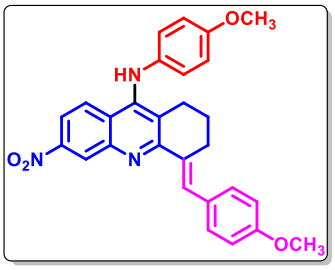

(E)-4-(4-Methoxybenzylidene)-N-(4-methoxyphenyl)-6-nitro-1,2,3,4-tetrahydroacridin-9-amine(8m): Yield= 90%, Yellow solid; M. P: 162.8-163.4 °C; **IR (KBr, cm^{-1})**: 3372, 3019, 2932,2834, 1508, 1343, 1236, 1172; **^{1}H NMR (400 MHz, $CDCl_3$)** δ 8.89 (d, *J* = 2.4 Hz, 1H), 8.25 (s, 1H), 7.96 (dd, *J* = 9.2, 2.4 Hz, 1H), 7.80 (d, *J* = 9.2 Hz, 1H), 7.46 (d, *J* = 8.8 Hz, 2H), 6.95 (d, *J* = 8.8 Hz, 2H), 6.81 (d, *J* = 9.2 Hz, 2H), 6.75 (d, *J* = 9.2 Hz, 2H), 5.97 (s, 1H), 3.85 (s, 3H), 3.78 (s, 3H), 2.95 (t, *J* = 6.2 Hz, 2H), 2.74 (t, j= 6.2 Hz, 2H), 1.86 (q, *J* = 6.2 Hz, 2H).**^{13}C NMR (100 MHz, $CDCl_3$)** δ 158.99, 157.51, 155.22, 147.57, 146.71, 144.12, 137.29, 133.81, 131.44, 130.42, 130.06, 125.87, 125.41, 124.85, 124.29, 119.89, 117.58, 114.79, 113.77, 55.61, 55.33, 27.79, 26.09, 22.38. **Mass (ESI-MS):** m/z Calculated $C_{28}H_{25}N_3O_4$ for: 467.1845; Observed: 468.1917 $[M+H]^+$.

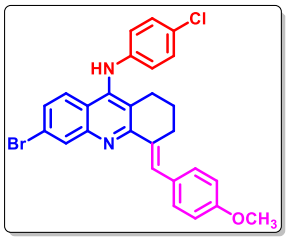

(E)-6-Bromo-N-(4-chlorophenyl)-4-(4-methoxybenzylidene)-1,2,3,4-tetrahydroacridin-9-amine(8n): Yield= 78%, Yellow solid; M. P: 87.0-87.8 °C; **IR (KBr, cm−1):** 3380, 3295, 2932,1599, 1250, 1173, 1089, 815; ^{1}H NMR (400 MHz, $CDCl_3$) δ 8.27 (s, 1H), 8.18 (s, 1H), 7.57 (dd, *J* = 9.2, 4.4 Hz, 1H), 7.45 (d, *J* = 8.8 Hz, 2H), 7.38 (dd, *J* = 9.2, 2.0 Hz, 1H), 7.15 (d, *J* = 8.8 Hz, 2H), 6.94 (d, *J* = 8.8 Hz, 2H), 6.59 (dd, *J* = 8.9, 2.2 Hz, 2H), 5.86 (s, 1H), 3.84 (s, 3H), 2.96 – 2.91 (m, 2H), 2.70 (t, *J* = 6.2 Hz, 2H), 1.82 (t, *J* = 6.2

Hz, 2H). **^{13}C NMR (100 MHz, $CDCl_3$) δ** 158.88, 156.45, 148.37, 143.08, 142.30, 134.03, 131.95, 131.39, 130.19, 129.90, 129.34, 128.68, 125.46, 124.79, 124.20, 122.96, 122.07, 117.34, 113.73, 55.32, 27.98, 26.00, 22.46. **Mass (ESI-MS):** m/z Calculated $C_{27}H_{22}BrClN_2O$ for: 504.0604; Observed: 505.0668 $[M+H]^+$.

(E)-N-(4-Chlorophenyl)-4-(4-methoxybenzylidene)-6-nitro-1,2,3,4-tetrahydroacridin-9-amine(8o): Yield= 81%, Yellow solid; M. P: 162.8 – 163.4 °C; **IR (KBr, cm^{-1}):** 3382, 3101, 2972,2843, 1567, 1356, 1264, 1092; **^{1}H NMR (400 MHz, $CDCl_3$)** δ 8.94 (d, *J* = 2.4 Hz, 1H), 8.26 (s, 1H), 8.04 (dd, *J* = 9.2, 2.4 Hz, 1H), 7.85 (d, *J* = 9.2 Hz, 1H), 7.48 (d, *J* = 8.4 Hz, 2H), 7.18 (d, *J* = 8.8 Hz, 2H), 6.96 (d, *J* = 8.8 Hz, 2H), 6.64 (d, *J* = 8.8 Hz, 2H), 6.04 (s, 1H), 3.86 (s, 3H), 2.97 (m, 2H), 2.79 (t, *J* = 6.2 Hz, 2H), 1.90 – 1.84 (m, 2H). **^{13}C NMR (100 MHz, $CDCl_3$)** δ 159.14, 157.93, 147.81, 146.54, 142.64, 142.44, 133.28, 131.53, 131.09, 129.87, 129.48, 129.12, 127.15, 126.41, 126.15, 125.82, 124.62, 118.37, 117.74, 116.24, 113.82, 55.34, 27.85, 26.28, 22.21. **Mass (ESI-MS):** m/z Calculated $C_{27}H_{22}ClN_3O_3$ for: 471.1350; Observed: 472.1429 $[M+H]^+$.

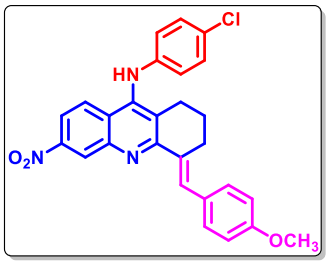

(E)-N-(4-Bromophenyl)-4-(4-methoxybenzylidene)-1,2,3,4-tetrahydroacridin-9-amine(8p): Yield= 80%,Yellow solid; M. P: 176.4-177.0 °C; **IR (KBr, cm^{-1}):** 3354, 3097, 2979, 2865, 1589, 1343, 1236, 1162; **^{1}H NMR (400 MHz, $CDCl_3$)** δ 8.19 (s, 1H), 8.10 (d, *J* = 8.4 Hz, 1H), 7.76 (d, *J* = 8.8 Hz, 1H), 7.62 (t, *J* = 8.4 Hz, 1H), 7.46 (d, *J* = 8.8 Hz, 2H), 7.39 – 7.34 (m, 1H), 7.29 (d, *J* = 8.8 Hz, 2H), 7.22 (d, *J* = 8.8 Hz, 1H), 6.94 (d, *J* = 8.8 Hz, 2H), 6.55 (dd, *J* = 8.8, 2.4 Hz, 3H), 5.89 (s, 1H), 3.85 (s, 3H), 2.98 – 2.92 (m, 2H), 2.75 (t, *J* = 6.2 Hz, 2H), 1.87 – 1.81 (m, 2H). **^{13}C NMR (100 MHz, $CDCl_3$)** δ 158.73, 155.46, 147.70, 145.44, 143.88, 141.84, 134.42, 132.15, 132.02, 131.34, 130.42, 129.92, 129.28, 128.95, 125.59, 124.88, 123.62, 122.44, 117.48, 116.72, 113.67, 112.18, 110.21, 55.31, 28.12, 26.10, 22.63. **Mass (ESI-MS):** m/z Calculated $C_{27}H_{23}BrN_2O$ for: 470.0994; Observed: 471.1069 $[M+H]^+$.

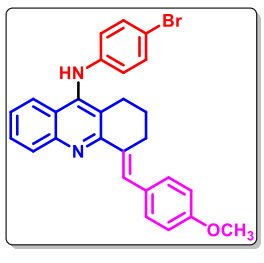

(E)-4-(4-(Dimethylamino)benzylidene)-N-(p-tolyl)-1,2,3,4-tetrahydroacridin-9-amine (8q): Yield= 79%, Yellow solid; M. P: 187.1-187.6 °C; **IR (KBr, cm−1):** 3303,3010,2941, 2868, 1569, 1523,1209; **^{1}H NMR (400 MHz, $CDCl_3$) δ** 8.16 (s, 1H), 8.10 (d, *J* = 8.0 Hz, 1H), 7.76 (d, *J* = 8.4 Hz, 1H), 7.58 (t, *J* = 7.6

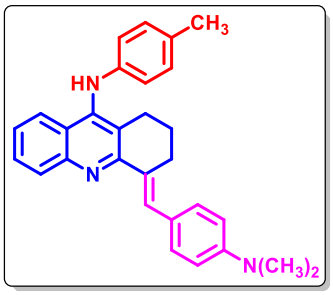

Hz, 1H), 7.46 (d, *J* = 8.4 Hz, 2H), 7.30 (t, *J* = 7.6 Hz, 1H), 7.01 (d, *J* = 8.0 Hz, 2H), 6.74 (d, *J* = 8.4 Hz, 2H), 6.63 (d, *J* = 8.0 Hz, 2H), 5.92 (s, 1H), 2.99 (s, 6H), 2.97 (t, *J* = 5.6 Hz, 2H), 2.71 (t, *J* = 5.6 Hz, 2H), 2.27 (s, 3H), 1.84 – 1.78 (m, 2H). **^{13}C NMR (101 MHz, $CDCl_3$) δ** 155.92, 149.64, 147.73, 142.96, 142.42, 132.73, 131.55, 130.13, 129.96, 129.72, 126.29, 125.09, 123.80, 123.35, 122.75, 116.83, 112.04, 40.56, 28.53, 26.31, 22.90, 20.79. **Mass (ESI-MS):** m/z Calculated $C_{27}H_{23}ClN_2$ for: 410.1550; Observed: 411.1620 $[M+H]^+$.

(E)-4-(4-Chlorobenzylidene)-N-(p-tolyl)-1,2,3,4-tetrahydroacridin-9-amine (8r): Yield= 81%, Yellow solid; M. P: 205.2-205.8 °C; **IR (KBr, cm^{-1}):** 3198, 3012, 2929, 2967, 1510, 812; **^{1}H NMR (400 MHz, $CDCl_3$) δ** 8.22 (s, 1H), 8.13 (d, *J* = 8.4 Hz, 1H), 7.82 (d, *J* = 9.2 Hz, 1H), 7.67 – 7.62 (m, 1H), 7.45 (d, *J* = 8.4 Hz, 2H), 7.39 (m, 3H), 7.06 (d, *J* = 8.0 Hz, 2H), 6.68 (d, *J* = 8.4 Hz, 2H), 5.96 (s, 1H), 2.96 – 2.91 (m, 2H), 2.78 (t, *J* = 6.2 Hz, 2H), 2.32 (s, 3H), 1.87 (q, *J* = 6.4 Hz, 2H). **^{13}C NMR (100 MHz, $CDCl_3$) δ** 154.50, 143.37, 141.97, 136.97, 136.34, 132.69, 131.12, 130.38, 129.84, 128.94, 128.36, 127.93, 125.43, 123.36, 122.66, 116.95, 28.03, 26.09, 22.68, 20.65. **Mass (ESI-MS):** m/z Calculated $C_{27}H_{23}ClN_2$ for: 410.1550; Observed: 411.1620 $[M+H]^+$.

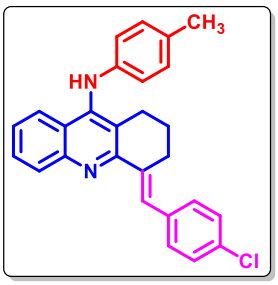

(E)-4-(4-Nitrobenzylidene)-N-(p-tolyl)-1,2,3,4-tetrahydroacridin-9-amine (8s): Yield= 72%, Yellow solid; M. P: 189.7-190 °C; **IR (KBr, cm^{-1}):** 3379, 2927, 2864, 1589, 1513, 1336; **^{1}H NMR (400 MHz, $CDCl_3$) δ** 8.29 (s, 1H), 8.25 (d, *J* = 8.8 Hz, 2H), 8.09 (d, *J* = 8.4 Hz, 1H), 7.81 (d, *J* = 7.6 Hz, 1H), 7.64 (m, 2H), 7.61 (m, 1H), 7.38 (ddd, *J* = 8.2, 6.8, 1.2 Hz, 1H), 7.04 (d, *J* = 8.0 Hz, 2H), 6.67 (d, *J* = 8.4 Hz, 2H), 5.97 (s, 1H), 2.97 – 2.92 (m, 2H), 2.78 (t, *J* = 6.2 Hz, 2H), 2.29 (s, 3H), 1.90 – 1.85 (m, 2H). **^{13}C NMR (100 MHz, $CDCl_3$) δ** 153.67, 147.62, 146.25, 144.82, 143.66, 141.85, 140.12, 130.58, 130.34, 129.93, 129.08, 126.71, 125.77, 123.48, 122.68, 117.10, 28.25, 26.05, 22.65, 20.64. **Mass (ESI-MS):** m/z Calculated $C_{27}H_{23}N_3O_2$ for: 421.1790; Observed: 422.1866 $[M+H]^+$.

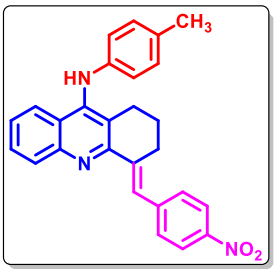

(E)-4-(Thiophen-2-ylmethylene)-N-(p-tolyl)-1,2,3,4-tetrahydroacridin-9-amine (8t): Yield= 85%, Yellow solid; M. P: 188.9-189.4 °C; **IR (KBr, cm^{-1}):** 3301,3100,2931, 2860, 1570, 1513,1209;**^{1}H NMR (400 MHz, $CDCl_3$) δ** 8.33 (s, 1H), 8.02 (d, *J* = 8.4 Hz, 1H), 7.70 (d, *J* = 8.0 Hz, 1H), 7.52 (t, *J* = 7.0 Hz, 1H), 7.31 (d, *J* = 5.1 Hz, 1H), 7.27 – 7.23 (m, 2H), 7.03 (dd, *J* = 5.1, 3.7 Hz, 1H), 6.94 (d, *J* = 8.2 Hz, 2H), 6.55 (d, *J* = 8.4 Hz,

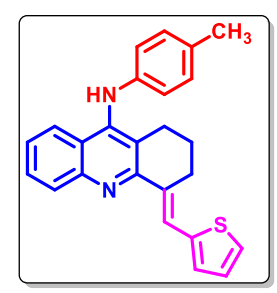

2H), 5.89 (s, 1H), 2.89 (t, *J* = 5.5 Hz, 2H), 2.63 – 2.58 (m, 2H), 2.19 (s, 3H), 1.82 – 1.76 (m, 2H). **^{13}C NMR (100 MHz, CDCl$_3$) δ** 154.99, 147.67, 142.69, 142.14, 141.29, 133.55, 130.16, 130.16, 128.86, 127.23, 126.84, 125.30, 123.93, 123.28, 122.86, 122.43, 116.70, 28.63, 26.11, 22.11, 20.64. **Mass (ESI-MS):** m/z Calculated $C_{25}H_{22}N_2S$ for: 382.1502; Observed: 383.1578 $[M+H]^+$.

2.3.5 General procedure for synthesis of compound (10 or 13):

To the azide derivatives **6** or **12** (1.0 mmol) H_2O/t-BuOH (1:1), phenylacetylene or terminal alkyne containing 1,2,3,4-tetrahydroacridine (1.0 mmol) was added in the presence of Et_3N along with a catalytic amount of $CuSO_4$ and sodium ascorbate at room temperature for 2–4 h. Completion of reaction checked through TLC. After completion of reaction the crude products obtained were purified by column chromatography on silica gel using petroleum ether-ethyl acetate as eluent to give the compound **10 or 13** in good excellent yield.

(E)-4-Benzylidene-9-(4-phenyl-1H-1,2,3-triazol-1-yl)-1,2,3,4-tetrahydroacridine (10a):

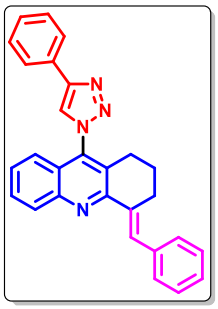

Yield= 90%, white solid; M. P: 225.2-2259 °C ; **IR (KBr, cm^{-1})**: 3110, 3081, 2939, 1580, 1437, 1199, 1033; **^{1}H NMR (400 MHz, CDCl$_3$) δ** 8.32 (s, 1H), 8.19 (d, *J* = 8.4 Hz, 1H), 8.06 (s, 1H), 7.99 – 7.96 (m, 2H), 7.72 (ddd, *J* = 8.4, 6.8, 1.2 Hz, 1H), 7.53 (s, 1H), 7.51 (s, 2H), 7.49 (m, 1H), 7.47 (m,1H), 7.45 – 7.43 (m, 1H), 7.42 (d, *J* = 1.6 Hz, 1H), 7.39 (dd, *J* = 5.6, 1.6 Hz, 1H), 7.31 (t, *J* = 7.2 Hz, 1H), 7.22 (d, *J* = 8.4 Hz, 1H), 3.01 (t, *J* = 5.2 Hz, 2H), 2.82 – 2.59 (m, 2H), 1.86 (p, *J* = 6.0 Hz, 2H). **^{13}C NMR (100 MHz, CDCl$_3$) δ** 155.14, 148.09, 147.37, 138.71, 137.37, 135.00, 130.87, 129.94, 129.88, 129.71, 129.08, 128.70, 128.28, 128.02, 127.77, 127.46, 125.94, 123.57, 122.06, 121.63, 27.82, 25.52, 22.17. **HRMS (ESI-MS):** m/z Calculated for $C_{28}H_{22}N_4$ $[M+H]^+$: 415.1917; Observed: 415.1912.

(E)-4-(4-Methylbenzylidene)-9-(4-phenyl-1H-1,2,3-triazol-1-yl)-1,2,3,4-tetrahydroacridine (10b): Yield= 91%, white solid; M. P: 258.4-258.9 °C ; **IR (KBr, cm^{-1})**: 3080, 2920, 2855, 1269, 1126, 1019, 818; **^{1}H NMR (400 MHz, CDCl$_3$)** δ 8.29 (s, 1H), 8.19 (d, *J* = 8.4 Hz, 1H), 8.05 (s, 1H), 7.98 (d, *J* = 7.2 Hz, 2H), 7.72 (td, *J* = 7.6, 1.2 Hz, 1H), 7.49 (q, *J* = 7.3 Hz, 3H), 7.44 – 7.41 (m, 3H), 7.25 – 7.20 (m, 3H), 3.02 (t, *J* = 6.4 Hz, 2H), 2.80 – 2.65 (m, 2H), 2.40 (s, 3H), 1.86 (p, *J* = 6.4 Hz, 2H). **^{13}C NMR (100 MHz, CDCl$_3$) δ** 155.36, 148.08, 147.40, 138.62, 137.44, 134.51, 134.26, 130.96, 129.96, 129.83, 129.67, 129.07, 129.02, 128.68, 128.00, 127.65,

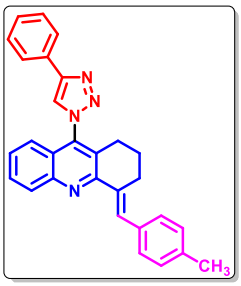

125.94, 123.50, 122.03, 121.61, 27.89, 25.52, 22.16, 21.35. **HRMS (ESI-MS):** m/z Calculated for $C_{29}H_{24}N_4$ $[M+H]^+$: 429.2074; Observed: 429.2075.

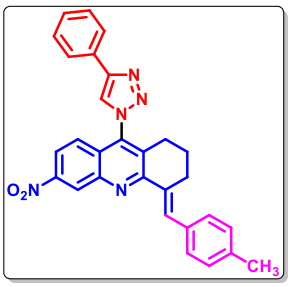

(E)-4-(4-Methylbenzylidene)-6-nitro-9-(4-phenyl-1H-1,2,3-triazol-1-yl)-1,2,3,4-tetrahydroacridine (10c): Yield= 95%, white solid; M. P: 259.6-260.1 °C ; **IR (KBr, cm^{-1})**: 3046, 2925, 2852, 1592, 1439, 1178, 1071, 905; **^{1}H NMR (400 MHz, $CDCl_3$) δ** 9.06 (d, *J* = 2.0 Hz, 1H), 8.38 (s, 1H), 8.20 (dd, *J* = 9.2, 2.4 Hz, 1H), 8.09 (s, 1H), 7.98 (d, *J* = 7.2 Hz, 2H), 7.51 (d, *J* = 7.6 Hz, 2H), 7.46 (s, 1H), 7.44 (d, *J* = 6.4 Hz, 2H), 7.38 (d, *J* = 9.2 Hz, 1H), 7.27 (s, 1H), 7.25 (s, 1H), 3.08 – 3.03 (m, 2H), 2.79 – 2.73 (m, 2H), 2.41 (s, 3H), 1.92 – 1.86 (m, 2H). **^{13}C NMR (100 MHz, $CDCl_3$) δ** 158.11, 148.53, 148.40, 146.28, 138.60, 138.16, 133.97, 133.17, 133.02, 131.44, 130.12, 129.56, 129.17, 128.97, 126.51, 125.99, 125.68, 123.72, 121.89, 120.67, 27.73, 25.90, 21.68, 21.40. **HRMS (ESI-MS):** m/z Calculated for $C_{28}H_{22}N_4$ $[M+H]^+$: 415.1917; Observed: 415.1912.

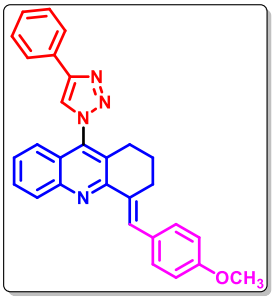

(E)-4-(4-Methoxybenzylidene)-9-(4-phenyl-1H-1,2,3-triazol-1-yl)-1,2,3,4-tetrahydroacridine (10d): Yield= 92%, white solid; M. P: 221.6-221.9 °C ; **IR (KBr, cm^{-1})**: 3050, 2945, 2842, 1545, 1265, 1122, 853; **^{1}H NMR (400 MHz, $CDCl_3$) δ** 8.26 (s, 1H), 8.17 (d, *J* = 8.4 Hz, 1H), 8.06 (s, 1H), 7.98 – 7.96 (m, 2H), 7.73 – 7.68 (m, 1H), 7.49 (d, *J* = 7.2 Hz, 2H), 7.46 (d, *J* = 3.6 Hz, 2H), 7.44 – 7.41 (m, 1H), 7.41 – 7.37 (m, 1H), 7.19 (d, *J* = 8.0 Hz, 1H), 6.95 (d, *J* = 8.8 Hz, 2H), 3.84 (s, 3H), 2.99 (t, *J* = 5.6 Hz, 2H), 2.78 – 2.60 (m, 2H), 1.85 (q, *J* = 6.0 Hz, 2H). **^{13}C NMR (100 MHz, $CDCl_3$) δ** 159.03, 155.46, 148.05, 147.38, 138.53, 133.18, 131.50, 130.65, 129.99, 129.81, 129.58, 129.08, 128.68, 127.95, 127.54, 126.07, 125.94, 123.42, 122.12, 121.62, 113.77, 55.33, 27.92, 25.48, 22.13. **HRMS (ESI-MS):** m/z Calculated for $C_{28}H_{22}N_4$ $[M+H]^+$: 415.1917; Observed: 415.1912.

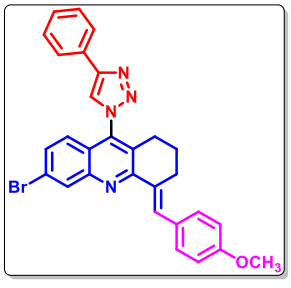

(E)-6-Bromo-4-(4-methoxybenzylidene)-9-(4-phenyl-1H-1,2,3-triazol-1-yl)-1,2,3,4-tetrahydroacridine (10e): Yield= 94%, white solid; M. P: 177-177.5 °C ; **IR (KBr, cm^{-1})**: 3141, 3064, 2936, 2863, 1594, 1450, 1202, 1163, 1040, 810; **^{1}H NMR (400 MHz, $CDCl_3$) δ** 8.29 (d, *J* = 2.0 Hz, 1H), 8.18 (s, 1H), 7.97 (s, 1H), 7.90 (d, *J* = 1.5 Hz, 1H), 7.88 (s, 1H), 7.44 (d, *J* = 3.3 Hz, 1H), 7.42 (d, *J* = 1.3 Hz, 2H), 7.40 (d, *J* = 2.8 Hz, 2H), 7.34 (d, *J* = 7.2 Hz, 1H), 7.00 (d, *J* = 8.8 Hz, 1H), 6.88 (d, *J* =

8.8 Hz, 2H), 3.78 (s, 3H), 2.93 (t, *J* = 6.0 Hz, 2H), 2.59 (s, 2H), 1.77 (t, *J* = 6.0 Hz, 2H). **^{13}C NMR (100 MHz, $CDCl_3$) δ** 159.21, 156.58, 148.20, 147.86, 138.61, 132.72, 131.75, 131.59, 131.46, 130.80, 129.81, 129.77, 129.10, 128.79, 128.32, 125.95, 124.01, 123.14, 122.09, 122.01, 113.84, 55.34, 27.86, 25.54, 21.94. **HRMS (ESI-MS):** m/z Calculated for $C_{28}H_{22}N_4$ $[M+H]^+$: 415.1917; Observed: 415.1912.

(E)-4-(4-Chlorobenzylidene)-9-(4-phenyl-1H-1,2,3-triazol-1-yl)-1,2,3,4-tetrahydroacridine (10f): Yield= 89%, white solid; M. P: 99.6- 100.5 °C ; **IR (KBr, cm^{-1})**: 3101, 3064, 2942, 2845, 1551, 1493, 1307, 1109, 972; **^{1}H NMR (400 MHz, $CDCl_3$) δ** 8.26 (s, 1H), 8.19 (d, *J* = 8.3 Hz, 1H), 8.06 (s, 1H), 7.98 (dt, *J* = 8.4, 1.6 Hz, 2H), 7.76 – 7.71 (m, 1H), 7.53 – 7.48 (m, 3H), 7.46 (m, 1H), 7.44 (s, 1H), 7.43 – 7.41 (m, 1H), 7.40 (m, 1H), 7.39 – 7.37 (m, 1H), 7.23 (d, *J* = 8.0 Hz, 1H), 3.00 – 2.95 (m, 2H), 2.81 – 2.63 (m, 2H), 1.90 – 1.84 (m, 2H). **^{13}C NMR (100 MHz, $CDCl_3$) δ** 154.79, 148.13, 147.37, 138.78, 135.80, 135.55, 133.24, 131.17, 129.97, 129.92, 129.69, 129.53, 129.09, 128.73, 128.50, 128.01, 127.91, 125.94, 123.62, 122.01, 121.65, 27.81, 25.46, 22.11. **HRMS (ESI-MS):** m/z Calculated for $C_{28}H_{22}N_4$ $[M+H]^+$: 415.1917; Observed: 415.1912.

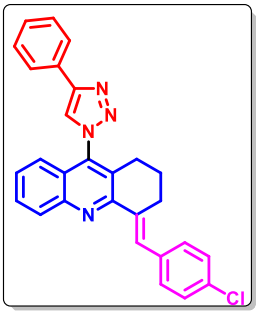

(E)-4-(4-Nitrobenzylidene)-9-(4-phenyl-1H-1,2,3-triazol-1-yl)-1,2,3,4-tetrahydroacridine (10g): Yield= 86%, white solid; M. P: 267.8-268.2 °C; **IR (KBr, cm^{-1})**: 3021, 2922, 2852, 1561, 1513, 1448, 1176, 1073, 882; **^{1}H NMR (400 MHz, $CDCl_3$) δ** 9.06 (s, 1H), 8.38 (s, 1H), 8.20 (d, *J* = 9.2 Hz, 1H), 8.09 (s, 1H), 7.98 (d, *J* = 7.2 Hz, 2H), 7.51 (d, *J* = 7.6 Hz, 2H), 7.46 (s, 1H), 7.45 (s, 1H), 7.44 (d, *J* = 6.0 Hz, 1H), 7.38 (d, *J* = 9.2 Hz, 1H), 7.27 (s, 1H), 7.25 (s, 1H), 3.07 – 3.03 (m, 2H), 2.79 – 2.73 (m, 2H), 1.92 – 1.86 (m, 2H). **^{13}C NMR (100 MHz, $CDCl_3$) δ** 158.11, 148.53, 148.40, 146.28, 138.60, 138.16, 133.97, 133.17, 133.02, 131.44, 130.12, 129.56, 129.17, 128.97, 126.51, 125.99, 125.68, 123.72, 121.89, 120.67, 27.73, 25.90, 21.40. **HRMS (ESI-MS):** m/z Calculated for $C_{28}H_{21}N_5O_2$ $[M+H]^+$: 460.1768; Observed: 460.1762.

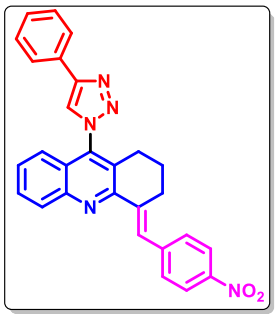

(E)-9-(4-Phenyl-1H-1,2,3-triazol-1-yl)-4-(thiophen-2-ylmethylene)-1,2,3,4-tetrahydroacridine (10h): Yield= 92%, white solid; M. P: 244-244.5 °C ; **IR (KBr, cm^{-1})**: 3011, 2916, 2862, 1561, 1345, 1176, 757; **^{1}H NMR (400 MHz, $CDCl_3$) δ** 8.51 (s, 1H), 8.18 (d, *J* = 8.4 Hz, 1H), 8.06 (s, 1H), 7.98 (d, *J* = 7.2 Hz, 2H), 7.72 (t, *J* = 8.4 Hz, 1H), 7.50 (t, *J* = 7.6 Hz, 2H), 7.47 – 7.37 (m, 4H), 7.22 (d, *J* = 8.4 Hz, 1H), 7.17 – 7.13 (m, 1H), 3.09 – 3.02 (m, 2H), 2.67 (s, 2H), 1.95 (p, *J* = 6.0 Hz, 2H). **^{13}C NMR (100 MHz, $CDCl_3$) δ** 155.10, 148.08, 147.47, 140.79, 138.26, 131.85, 130.59, 129.96, 129.88, 129.54, 129.08, 128.70, 128.25, 127.61, 127.39, 125.95, 124.23, 123.32, 122.16, 121.70, 28.29, 25.34, 21.57. **HRMS (ESI-MS):** m/z Calculated for $C_{26}H_{20}N_4S$ $[M+H]^+$: 421.1481; Observed: 421.1488.

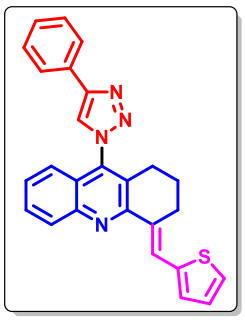

(E)-4-Benzylidene-9-(4-(p-tolyl)-1H-1,2,3-triazol-1-yl)-1,2,3,4-tetrahydroacridine (10i): Yield= 92%, white solid; M. P: 159.6-160.2 °C ; **IR (KBr, cm^{-1})**: 3097, 2937, 2870, 1615, 1556, 1423, 1223, 1025, 849; **^{1}H NMR (400 MHz, $CDCl_3$) δ** 8.32 (s, 1H), 8.19 (d, *J* = 8.4 Hz, 1H), 8.01 (s, 1H), 7.86 (d, *J* = 8.4 Hz, 2H), 7.72 (t, *J* = 8.4 Hz, 1H), 7.52 (d, *J* = 7.2 Hz, 2H), 7.47 (d, *J* = 8.4 Hz, 1H), 7.42 (t, *J* = 7.6 Hz, 2H), 7.33 – 7.28 (m, 3H), 7.23 (dd, *J* = 8.4, 2.0 Hz, 1H), 3.04 – 2.99 (m, 2H), 2.72 (s, 2H), 2.42 (s, 3H), 1.86 (p, *J* = 6.0 Hz, 2H). **^{13}C NMR (100 MHz, $CDCl_3$) δ** 155.14, 148.17, 147.38, 138.77, 138.62, 137.39, 135.03, 130.85, 129.93, 129.85, 129.74, 129.69, 128.26, 128.02, 127.73, 127.44, 127.13, 125.85, 123.60, 121.68, 27.82, 25.52, 22.18, 21.37. **HRMS (ESI-MS):** m/z Calculated for $C_{29}H_{24}N_4$ $[M+H]^+$: 429.2074; Observed: 429.2078.

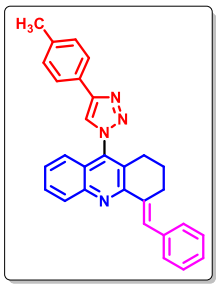

(E)-4-(4-Methylbenzylidene)-9-(4-(p-tolyl)-1H-1,2,3-triazol-1-yl)-1,2,3,4-tetrahydroacridine (10j): Yield= 93%, white solid; M. P: 220.1-220.6 °C ; **IR (KBr, cm^{-1})**: 3058, 2945, 2854, 1593, 1444, 1315, 1246, 1167, 849; **^{1}H NMR (400 MHz, $CDCl_3$) δ** 8.28 (s, 1H), 8.17 (d, *J* = 8.4 Hz, 1H), 8.01 (s, 1H), 7.85 (d, *J* = 8.4 Hz, 2H), 7.70 (t, *J* = 8.4 Hz, 1H), 7.44 (d, *J* = 8.4 Hz, 3H), 7.29 (d, *J* = 8.4 Hz, 2H), 7.22 (dd, *J* = 8.4, 4.8 Hz, 3H), 3.03 – 2.97 (m, 2H), 2.69 (s, 2H), 2.41 (s, 3H), 2.39 (s, 3H), 1.84 (t, *J* = 6.4 Hz, 2H). **^{13}C NMR (100 MHz, $CDCl_3$) δ** 155.34, 148.14, 147.38, 138.67, 138.60, 137.42, 134.52, 134.28, 130.92, 129.96, 129.80, 129.74, 129.63, 129.02, 127.99, 127.61, 127.15, 125.85, 123.53, 121.72, 121.67, 27.90, 25.51, 22.15, 21.38, 21.36. **HRMS (ESI-MS):** m/z Calculated for $C_{30}H_{26}N_4$ $[M+H]^+$: 443.2230; Observed: 443.2234.

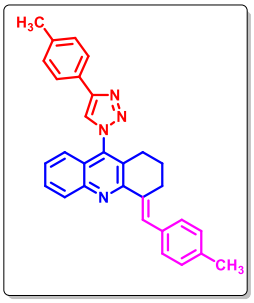

(E)-4-(4-Methylbenzylidene)-6-nitro-9-(4-(p-tolyl)-1H-1,2,3-triazol-1-yl)-1,2,3,4-tetrahydroacridine (10k): Yield= 96%, white solid; M. P: 176.3-176.9 °C; **IR (KBr, cm^{-1})**: 3061, 2915, 1585, 1430, 1231, 1186, 1075, 768; **^{1}H NMR (400 MHz, CDCl$_3$) δ** 9.04 (s, 1H), 8.38 (s, 1H), 8.19 (d, *J* = 9.2 Hz, 1H), 8.04 (s, 1H), 7.86 (d, *J* = 8.4 Hz, 2H), 7.45 (d, *J* = 8.4 Hz, 2H), 7.37 (d, *J* = 9.2 Hz, 1H), 7.31 (d, *J* = 8.4 Hz, 2H), 7.27 (s, 1H), 7.25 (s, 1H), 3.04 (t, *J* = 5.2 Hz, 2H), 2.75 (s, 2H), 2.43 (s, 3H), 2.41 (s, 3H), 1.88 (t, *J* = 6.0 Hz, 2H). **^{13}C NMR (100 MHz, CDCl$_3$) δ** 158.09, 148.60, 148.38, 146.27, 138.94, 138.66, 138.14, 133.98, 133.19, 132.97, 131.43, 130.11, 129.81, 129.17, 126.74, 126.53, 125.89, 125.65, 123.76, 121.53, 120.62, 27.73, 25.90, 21.69, 21.39. **HRMS (ESI-MS):** m/z Calculated for $C_{30}H_{25}N_5O_2$ $[M+H]^+$: 488.2081; Observed: 415.1912.

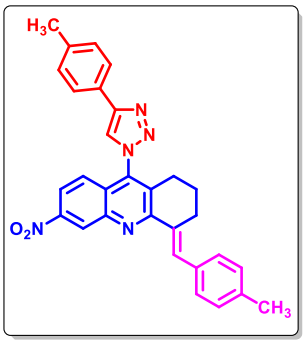

(E)-6-Bromo-4-(4-methoxybenzylidene)-9-(4-(p-tolyl)-1H-1,2,3-triazol-1-yl)-1,2,3,4-tetrahydroacridine (10l): Yield= 95%, white solid; M. P: 181.4-181.9 °C; **IR (KBr, cm^{-1})**: 3130, 2926, 2835, 1600, 1580, 1308, 1027, 893; **^{1}H NMR (400 MHz, CDCl$_3$) δ** 8.36 (d, *J* = 2.1 Hz, 1H), 8.26 (s, 1H), 8.00 (s, 1H), 7.85 (d, *J* = 8.4 Hz, 2H), 7.53 – 7.50 (m, 1H), 7.48 (d, *J* = 8.8 Hz, 2H), 7.30 (d, *J* = 8.8 Hz, 2H), 7.08 (d, *J* = 8.8 Hz, 1H), 6.96 (d, *J* = 8.8 Hz, 2H), 3.86 (s, 3H), 3.03 – 2.98 (m, 2H), 2.66 (s, 2H), 2.42 (s, 3H), 1.85 (t, *J* = 6.4 Hz, 2H). **^{13}C NMR (100 MHz, CDCl$_3$) δ** 159.20, 156.59, 148.29, 147.87, 138.73, 138.68, 132.77, 131.74, 131.59, 131.43, 130.78, 129.77, 128.32, 126.97, 125.85, 123.99, 123.19, 122.13, 121.62, 113.83, 55.34, 27.87, 25.55, 21.96, 21.39. **HRMS (ESI-MS):** m/z Calculated for $C_{30}H_{25}BrN_4O$ $[M+H]^+$: 537.1285; Observed: 537.1286.

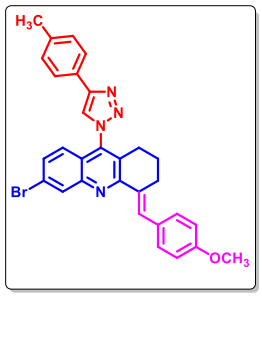

(E)-9-(4-(4-Bromophenyl)-1H-1,2,3-triazol-1-yl)-4-(4-methylbenzylidene)-1,2,3,4-tetrahydroacridine (10m): Yield= 92%, white solid; M. P: 202.3-202.8 °C; **IR (KBr, cm^{-1}):** 3124, 2914, 2812, 1580, 1506, 1478, 1246, 1067, 829; **^{1}H NMR (400 MHz, CDCl$_3$) δ** 8.28 (s, 1H), 8.18 (d, *J* = 8.4 Hz, 1H), 8.06 (s, 1H), 7.84 (d, *J* = 8.4 Hz, 2H), 7.72 (t, *J* = 7.6 Hz, 2H), 7.62 (d, *J* = 8.4 Hz, 2H), 7.42 (d, *J* = 8.0 Hz, 2H), 7.23 (d, *J* = 8.0 Hz, 3H), 3.01 (t, *J* = 5.2 Hz, 2H), 2.69 (s, 2H), 2.39 (s, 3H), 1.87 – 1.82 (m, 2H). **^{13}C NMR (100 MHz, CDCl$_3$) δ** 155.37, 147.37, 147.07, 138.46, 137.49, 134.45, 134.15, 132.24, 131.09, 129.96, 129.89, 129.68, 129.21, 129.03, 127.97, 127.70, 127.47,

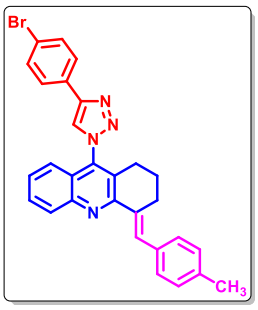

123.39, 122.62, 122.16, 121.49, 27.87, 25.52, 22.13, 21.36. **HRMS (ESI-MS):** m/z Calculated for $C_{29}H_{23}BrN_4$ $[M+H]^+$: 507.1179; Observed: 507.1183.

(E)-9-(4-(4-Bromophenyl)-1H-1,2,3-triazol-1-yl)-4-(4-methoxybenzylidene)-1,2,3,4-tetrahydroacridine (10n): Yield= 93%, white solid; M. P: 195.6-196.2 °C; **IR (KBr, cm^{-1})**: 3126, 2924, 2851, 1607, 1583, 1478, 1173, 1098, 829; **^{1}H NMR (400 MHz, $CDCl_3$) δ** 8.26 (s, 1H), 8.17 (d, *J* = 7.6 Hz, 1H), 8.06 (s, 1H), 7.84 (d, *J* = 8.4 Hz, 2H), 7.73 – 7.68 (m, 1H), 7.61 (d, *J* = 8.8 Hz, 2H), 7.48 (d, *J* = 8.4 Hz, 2H), 7.43 (d, *J* = 8.8 Hz, 1H), 7.18 (d, *J* = 8.4 Hz, 1H), 6.95 (d, *J* = 8.8 Hz, 2H), 3.85 (s, 3H), 3.04 – 2.97 (m, 2H), 2.67 (s, 2H), 1.85 (q, *J* = 6.0 Hz, 2H). **^{13}C NMR (100 MHz, $CDCl_3$) δ** 159.07, 155.47, 147.39, 147.05, 138.37, 133.10, 132.23, 131.50, 131.07, 130.75, 129.96, 129.85, 129.63, 128.97, 127.91, 127.59, 127.46, 123.32, 122.60, 122.19, 121.50, 113.78, 112.94, 55.33, 27.90, 25.50, 22.11. **HRMS (ESI-MS):** m/z Calculated for $C_{29}H_{23}BrN_4O$ $[M+H]^+$: 523.1128; Observed: 523.1130.

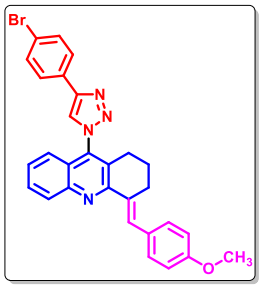

(1-(1,2,3,4-Tetrahydroacridin-9-yl)-1H-1,2,3-triazol-4-yl)methyl 1,2,3,4-tetrahydroacridine-9-carboxylate (13a): Yield= 92%, white solid; M. P: 123.7-124.2 °C ; **IR (KBr, cm^{-1})**: 3128, 2937, 2874, 1736, 1621, 1498, 1166, 967; **^{1}H NMR (400 MHz, $CDCl_3$) δ** 8.10 (d, *J* = 8.4 Hz, 1H), 8.05 (s, 1H), 8.01 (d, *J* = 8.0 Hz, 1H), 7.72 (t, *J* = 8.0 Hz, 1H), 7.67 – 7.62 (m, 2H), 7.46 (t, *J* = 7.2 Hz, 2H), 7.09 (d, *J* = 8.0 Hz, 1H), 5.80 (s, 2H), 3.24 (t, *J* = 6.4 Hz, 2H), 3.15 (t, *J* = 6.4 Hz, 2H), 2.91 (t, *J* = 6.4 Hz, 2H), 2.69 – 2.52 (m, 2H), 2.05 – 1.95 (m, 6H), 1.89 (d, *J* = 6.4 Hz, 2H). **^{13}C NMR (100 MHz, $CDCl_3$) δ** 167.87, 160.15, 159.17, 147.07, 146.24, 142.58, 138.72, 136.99, 129.86, 129.14, 128.85, 127.75, 127.60, 127.38, 126.67, 126.64, 123.85, 123.26, 122.90, 121.23, 58.45, 33.89, 33.85, 26.90, 24.83, 22.64, 22.52, 22.47, 22.10. **HRMS (ESI-MS):** m/z Calculated for $C_{30}H_{27}N_5O_2$ $[M+H]^+$: 490.2238; Observed: 490.2247.

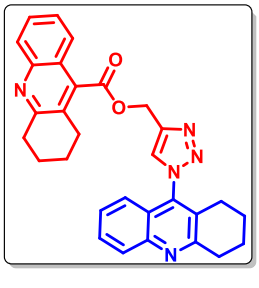

(1-(6-Bromo-1,2,3,4-tetrahydroacridin-9-yl)-1H-1,2,3-triazol-4-yl)methyl 1,2,3,4-tetrahydroacridine-9-carboxylate (13b): Yield= 89%, white solid; M. P: 123.7-124.2 °C ; **IR (KBr, cm^{-1})**: 3141, 3064, 2936, 2863, 1730, 1594, 1348, 1202, 1104, 810; **^{1}H NMR (400 MHz, $CDCl_3$) δ** 8.27 (d, *J* = 2.2 Hz, 1H), 8.04 (s, 1H), 8.00 (d, *J* = 8.1 Hz, 1H), 7.63 (d, *J* = 8.1 Hz, 2H), 7.51 (d, *J* = 8.9 Hz, 1H), 7.44 (t, *J* = 7.6 Hz, 1H), 6.95 (d, *J* =

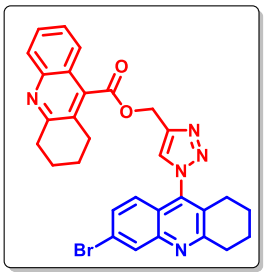

8.9 Hz, 1H), 5.79 (s, 2H), 3.21 (t, *J* = 6.5 Hz, 2H), 3.15 (t, *J* = 6.5 Hz, 2H), 2.90 (t, *J* = 6.5 Hz, 2H), 2.57 (s, 2H), 1.99 (q, *J* = 6.5 Hz, 4H), 1.85 (dt, *J* = 17.9, 5.8 Hz, 4H). **^{13}C NMR (100 MHz, $CDCl_3$) δ** 167.82, 161.57, 159.16, 147.54, 146.23, 142.71, 138.75, 136.92, 131.21, 131.00, 129.14, 128.87, 128.16, 127.37, 126.66, 126.58, 124.00, 123.81, 122.87, 122.75, 121.95, 58.39, 33.88, 26.90, 24.86, 22.63, 22.46, 22.36, 21.96. **HRMS (ESI-MS):** m/z Calculated for $C_{30}H_{26}BrN_5O_2$ $[M+H]^+$: 568.1343; Observed: 568.1356.

(1-(6-Nitro-1,2,3,4-tetrahydroacridin-9-yl)-1H-1,2,3-triazol-4-yl)methyl 1,2,3,4-tetrahydroacridine-9-carboxylate (13c): Yield= 91%, white solid; M. P: 123.7-124.2 °C ; **IR (KBr, cm^{-1})**: 2928, 2859, 1789, 1526, 1450, 1246, 901; **^{1}H NMR (400 MHz, $CDCl_3$) δ** 8.97 (s, 1H), 8.19 (dd, *J* = 9.2, 2.4 Hz, 1H), 8.09 (s, 1H), 8.01 (d, *J* = 8.4 Hz, 1H), 7.65 (td, *J* = 8.4, 1.6 Hz, 2H), 7.45 (t, *J* = 8.4 Hz, 1H), 7.24 (d, *J* = 9.2 Hz, 1H), 5.81 (s, 2H), 3.28 (t, *J* = 6.8 Hz, 2H), 3.16 (t, *J* = 6.4 Hz, 2H), 2.91 (t, *J* = 6.4 Hz, 2H), 2.65 (d, *J* = 5.2 Hz, 2H), 2.05 – 1.98 (m, 4H), 1.89 (dd, *J* = 5.2, 4.0 Hz, 4H). **^{13}C NMR (100 MHz, $CDCl_3$) δ** 167.83, 163.40, 159.18, 148.20, 146.20, 145.95, 143.03, 138.64, 136.89, 131.43, 129.22, 128.89, 127.41, 126.70, 126.55, 126.39, 125.14, 123.77, 123.35, 122.86, 120.87, 58.36, 33.96, 33.86, 26.94, 25.21, 22.62, 22.48, 22.17, 21.77. **HRMS (ESI-MS):** m/z Calculated for $C_{30}H_{26}N_6O_4$ $[M+H]^+$: 535.2088; Observed: 535.2087.

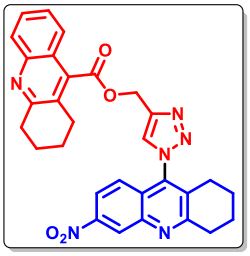

(1-(1,2,3,4-Tetrahydroacridin-9-yl)-1H-1,2,3-triazol-4-yl)methyl 7-bromo-1,2,3,4-tetrahydroacridine-9-carboxylate (13d): Yield= 90%, white solid; M. P: 202.2-202.8 °C ; **IR (KBr, cm^{-1})**: 3141, 2945, 2863, 1734, 1594, 1551, 1040, 810; **^{1}H NMR (400 MHz, $CDCl_3$) δ** 8.10 (d, *J* = 8.8 Hz, 1H), 8.05 (s, 1H), 7.95 – 7.85 (m, 1H), 7.84 – 7.69 (m, 2H), 7.68 – 7.55 (m, 1H), 7.46 (t, *J* = 7.6 Hz, 1H), 7.10 (d, *J* = 8.4 Hz, 1H), 5.80 (s, 2H), 3.23 (t, *J* = 6.4 Hz, 2H), 3.15 – 3.09 (m, 2H), 2.91 (t, *J* = 6.4 Hz, 2H), 2.62 (s, 2H), 2.03 – 1.96 (m, 4H), 1.90 – 1.83 (m, 4H). **^{13}C NMR (100 MHz, $CDCl_3$) δ** 167.23, 160.15, 159.61, 147.06, 144.82, 142.36, 138.69, 135.87, 132.61, 130.58, 130.07, 129.84, 128.82, 127.62, 126.61, 126.21, 124.04, 123.23, 122.88, 121.28, 120.70, 58.60, 33.87, 27.01, 24.82, 22.52, 22.49, 22.35, 22.11, 22.10. **HRMS (ESI-MS):** m/z Calculated for $C_{30}H_{26}BrN_5O_2$ $[M+H]^+$: 568.1343; Observed: 468.1352.

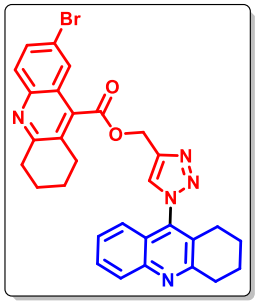

N-((1-(1,2,3,4-Tetrahydroacridin-9-yl)-1H-1,2,3-triazol-4-yl)methyl)-1,2,3,4-tetrahydroacridin-9-amine(13e): Yield= 91%, white solid; M. P: 140.2-141 °C ; **IR (KBr, cm^{-1}):** 3369, 3115, 3060, 2931, 2856, 1582, 1234, 831; **^{1}H NMR (400 MHz, CDCL$_3$+DMSO) δ** 8.15 (d, *J* = 8.4 Hz, 1H), 7.93 (d, *J* = 7.6 Hz, 1H), 7.86 (d, *J* = 8.4 Hz, 1H), 7.68 (s, 1H), 7.62 – 7.58 (m, 1H), 7.52 (t, *J* = 7.2 Hz, 1H), 7.36 – 7.30 (m, 2H), 6.73 (d, *J* = 7.2 Hz, 1H), 5.88 (s, 1H), 4.94 (s, 2H), 3.08 (t, *J* = 6.4 Hz, 2H), 2.98 (d, *J* = 6.4 Hz, 2H), 2.80 (t, *J* = 6.4 Hz, 2H), 2.26 (t, *J* = 7.2 Hz, 2H), 1.90 – 1.86 (m, 2H), 1.85 – 1.81 (m, 4H), 1.71 – 1.67 (m, 2H). **^{13}C NMR (101 MHz, CDCL$_3$+DMSO) δ** 159.99, 157.06, 151.13, 146.77, 145.85, 145.15, 138.78, 129.66, 129.25, 128.52, 127.67, 127.40, 126.67, 124.81, 124.52, 123.34, 123.18, 121.37, 43.26, 33.75, 32.75, 25.05, 24.44, 22.75, 22.43, 22.32, 21.97. **HRMS (ESI-MS):** m/z Calculated for $C_{29}H_{28}N_6$ $[M+H]^+$: 461.2448; Observed: 461.2446.

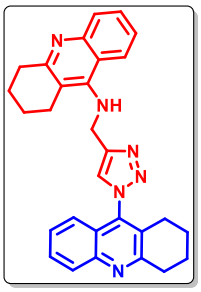

N-((1-(6-Bromo-1,2,3,4-tetrahydroacridin-9-yl)-1H-1,2,3-triazol-4-yl)methyl)-1,2,3,4-tetrahydroacridin-9-amine(13f): Yield= 92%, white solid; M. P: 151.8-152.3 °C; **IR (KBr, cm^{-1})**: 3354, 3138, 3062, 2932, 2860, 1588, 1404, 1037, 982; **^{1}H NMR (400 MHz, CDCl$_3$) δ** 8.20 (d, *J* = 2.0 Hz, 1H), 8.00 (dd, *J* = 8.4, 1.6 Hz, 1H), 7.93 (dd, *J* = 8.4, 1.2 Hz, 1H), 7.57 (ddd, *J* = 8.4, 6.4, 1.2 Hz, 1H), 7.44 (dd, *J* = 8.8, 2.0 Hz, 1H), 7.39 (ddd, *J* = 8.4, 6.4, 1.2 Hz, 1H), 7.28 (s, 1H), 6.58 (d, *J* = 9.2 Hz, 1H), 4.87 (s, 2H), 4.78 (s, 1H), 3.13 (t, *J* = 6.6 Hz, 2H), 3.05 (t, *J* = 6.4 Hz, 2H), 2.81 (t, *J* = 6.4 Hz, 2H), 2.27 (m, 2H), 1.95 – 1.86 (m, 6H), 1.73 (t, *J* = 6.0 Hz, 2H). **^{13}C NMR (100 MHz, CDCl$_3$) δ** 161.45, 158.96, 149.28, 147.39, 147.13, 145.81, 138.67, 131.04, 130.87, 128.90, 128.55, 128.06, 124.59, 123.87, 123.71, 122.66, 122.37, 121.84, 121.17, 119.21, 43.65, 33.95, 33.80, 24.94, 24.55, 22.91, 22.75, 22.31, 21.87. **HRMS (ESI-MS):** m/z Calculated for $C_{29}H_{27}BrN_6$ $[M+H]^+$:539.1553; Observed: 539.1553.

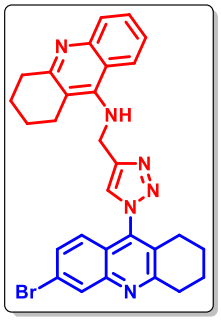

N-((1-(6-Nitro-1,2,3,4-tetrahydroacridin-9-yl)-1H-1,2,3-triazol-4-yl)methyl)-1,2,3,4-tetrahydroacridin-9-amine(13g): Yield= 94%, white solid; M. P: 151.8-152.3 °C; **IR (KBr, cm^{-1})**: 3346, 2928, 2859, 1584, 1342, 1246, 1166, 861; **^{1}H NMR (400 MHz, CDCl$_3$) δ** 8.86 (d, *J* = 10.8 Hz, 1H), 8.11 – 8.05 (m, 1H), 8.03 (d, *J* = 8.8 Hz, 1H), 7.93 (d, *J* = 10.8 Hz, 1H), 7.56 (t, *J* = 9.5 Hz, 1H), 7.42 – 7.36 (m, 2H), 6.89 (d, *J* = 9.2 Hz, 1H), 4.94 (s, 2H), 3.22 – 3.17 (m, 2H), 3.08 – 3.02 (m, 2H), 2.84 – 2.79 (m, 2H), 2.31 (s, 2H), 2.00 – 1.94 (m, 2H), 1.88 (q, *J* = 3.2 Hz, 4H), 1.78 (m, 2H). **^{13}C**

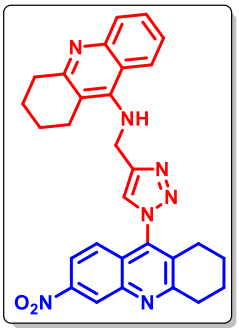

NMR (100 MHz, $CDCl_3$) δ 163.31, 158.38, 149.78, 147.98, 145.98, 145.71, 138.54, 131.35, 129.43, 128.91, 128.04, 126.28, 124.89, 124.68, 123.94, 123.30, 122.50, 122.48, 120.71, 120.66, 118.59, 115.63, 43.49, 33.88, 33.31, 24.94, 24.89, 22.81, 22.54, 22.10, 21.66. **HRMS (ESI-MS):** m/z Calculated for $C_{29}H_{27}N_7O_2$ $[M+H]^+$: 506.2299; Observed: 506.2305.

6-Bromo-N-((1-(1,2,3,4-tetrahydroacridin-9-yl)-1H-1,2,3-triazol-4-yl)methyl)-1,2,3,4-tetrahydroacridin-9-amine(13h): Yield= 92%, white solid; M. P: 158.4-158.8 °C; **IR (KBr, cm^{-1})**: 3377, 3116, 2927, 2855, 1633, 1583, 1497, 1335, 1041, 829; **^{1}H NMR (400 MHz, $CDCl_3$) δ** 8.15 (s, 1H), 8.05 (d, *J* = 8.4 Hz, 1H), 8.00 (d, *J* = 9.2 Hz, 1H), 7.70 – 7.66 (m, 1H), 7.57 (s, 1H), 7.46 – 7.39 (m, 2H), 6.83 (dd, *J* = 8.4, 1.6 Hz, 1H), 5.55 (s, 1H), 5.04 (s, 2H), 3.19 (t, *J* = 6.4 Hz, 2H), 3.07 (d, *J* = 6.4 Hz, 2H), 2.84 – 2.80 (m, 2H), 2.37 (s, 2H), 2.00 – 1.95 (m, 2H), 1.90 (q, *J* = 3.6 Hz, 4H), 1.79 (d, *J* = 6.4 Hz, 2H). **^{13}C NMR (100 MHz, $CDCl_3$) δ** 160.08, 158.01, 151.16, 146.97, 144.95, 138.62, 129.78, 128.73, 127.96, 127.65, 127.54, 124.78, 124.23, 123.72, 123.14, 121.15, 118.30, 117.44, 43.67, 33.80, 32.43, 24.70, 24.66, 22.54, 22.49, 22.06, 22.02. **HRMS (ESI-MS):** m/z Calculated for $C_{29}H_{27}BrN_6$ $[M+H]^+$: 539.1553; Observed: 539.1549.

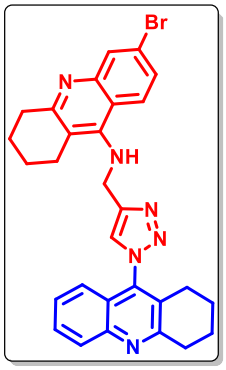

2.3.6 General procedure for synthesis of compound (16a):

Deep eutectic solvent was prepared by heating *N,N'*-dimethyl urea + L-tartaric acid (3:1 ratio) at 80 °C for 30 min. To this, 1,2,3,4-tetrahydroacridine-9-carboxylic acids (**15a**) (1 mmol) and benzaldehyde (**2a**) (1 mmol) were added and heating continued for another 2-3 h at 80 °C. The completion of reaction was monitored by TLC. After completion of reaction the crude products obtained were purified by column chromatography on silica gel using petroleum ether-ethyl acetate as eluent to give the compound **16a**.

2.3.7 General procedure for synthesis of compound (18a):

Deep eutectic solvent was prepared by heating *N,N'*-dimethyl urea + L-tartaric acid (3:1 ratio) at 80 °C for 30 min. To this, methyl 1,2,3,4-tetrahydroacridine-9-carboxylate (**17a**) (1 mmol) and benzaldehyde (**2a**) (1 mmol) were added and heating continued for another 2-3 h at 80 °C. The completion of reaction was monitored by TLC. After completion of reaction the crude products obtained were purified by column chromatography on silica gel using petroleum ether-ethyl acetate as eluent to give the compound **19a**.

2.3.8 General procedure for synthesis of compound (22a):

Deep eutectic solvent was prepared by heating *N,N'*-dimethyl urea + L-tartaric acid (3:1 ratio) at 70 °C for 30 min. To this, *N*-aryl-1,2,3,4-tetrahydroacridine-9-carboxamide (**21a**) (1 mmol) and benzaldehyde (**2a**) (1 mmol) were added and heating continued for another 2-3 h at 80 °C. The completion of reaction was monitored by TLC. After completion of reaction the crude products obtained were purified by column chromatography on silica gel using petroleum ether-ethyl acetate as eluent to give the compound **22a**.

2.3.9 General procedure for synthesis of compound (25a):

Deep eutectic solvent was prepared by heating *N,N'*-dimethyl urea + L-tartaric acid (3:1 ratio) at 80 °C for 30 min. To this, *N*-methoxy-*N*-methyl-1,2,3,4-tetrahydroacridine-9-carboxamide (**24a**) (1 mmol) and benzaldehyde (**2a**) (1 mmol) were added and heating continued for another 2-3 h at 80 °C. The completion of reaction was monitored by TLC. After completion of reaction the crude products obtained were purified by column chromatography on silica gel using petroleum ether-ethyl acetate as eluent to give the compound **25a**.

(E)-4-Benzylidene-1,2,3,4-tetrahydroacridine-9-carboxylic acid (16a): Yield= 42%, white solid; M. P: 132.2-132.9 °C ; **IR (KBr, cm^{-1})**: 2942, 1724, 1571, 1549, 1492, 1221, 1169, 961, 763; **^{1}H NMR (400 MHz, DMSO)** δ 14.09 (s, 1H), 8.18 (s, 1H), 8.06 (d, *J* = 8.0 Hz, 1H), 7.76 (t, *J* = 7.6 Hz, 2H), 7.61 (t, *J* = 7.6 Hz, 1H), 7.53 (d, *J* = 7.6 Hz, 2H), 7.45 (t, *J* = 7.6 Hz, 2H), 7.34 (t, *J* = 7.2 Hz, 1H), 2.98 (m, 4H), 1.86 (p, *J* = 6.4 Hz, 2H). **^{13}C NMR (100 MHz, DMSO)** δ 169.07, 153.87, 146.33, 139.87, 137.30, 135.60, 130.15, 129.98, 129.67, 129.41, 128.89, 127.90, 127.59, 126.77, 124.69, 122.85, 27.99, 27.50, 22.42. **HRMS (ESI, m/z): Calcd.** for $C_{21}H_{17}NO_2$ $[M+H]^+$: 316.1332; Observed 316.1337

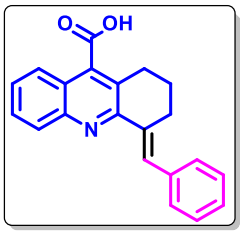

(E)-4-(4-Methoxybenzylidene)-1,2,3,4-tetrahydroacridine-9-carboxylic acid (16b): Yield= 50%, white solid; M. P: 224.9-225.4 °C ; **IR (KBr, cm^{-1})**: 2942, 1724, 1571, 1549, 1492, 1221, 1169, 961, 763; **^{1}H NMR (400 MHz, DMSO) δ** 8.12 (s, 1H), 8.03 (dd, *J* = 8.8, 1.2 Hz, 1H), 7.73 (dd, *J* = 8.8, 6.4 Hz, 2H), 7.58 (ddd, *J* = 8.4, 6.8, 1.2 Hz, 1H), 7.52 – 7.47 (m, 2H), 7.05 – 6.98 (m, 2H), 3.81 (s, 3H), 2.99 – 2.93 (m, 4H), 1.90 – 1.80 (m, 2H). **^{13}C NMR (100 MHz, DMSO) δ** 169.13, 159.10, 154.21, 146.43, 139.75, 133.59, 131.74, 129.83, 129.61, 129.26, 127.28, 126.64, 124.72, 122.75, 114.38, 55.62, 28.10, 27.55, 22.43. **HRMS (ESI, m/z):** Calcd. for $C_{22}H_{19}NO_3$ $[M+H]^+$: 346.1348; Observed: 346.1441

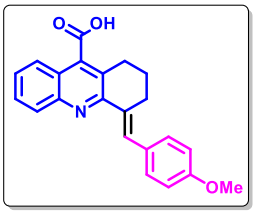

(E)-4-(4-Chlorobenzylidene)-1,2,3,4-tetrahydroacridine-9-carboxylic acid (16c): Yield= 45%, white solid; M. P: 189.190.5 °C ; **IR (KBr, cm^{-1})**: 2942, 1724, 1571, 1549, 1492, 1221, 1169, 961, 763; **^{1}H NMR (400 MHz, DMSO)** δ 8.13 (s, 1H), 8.05 (d, *J* = 8.8 Hz, 1H), 7.78 – 7.73 (m, 2H), 7.60 (t, *J* = 8.4 Hz, 1H), 7.55 (d, *J* = 8.8 Hz, 2H), 7.49 (d, *J* = 8.8 Hz, 2H), 3.00 – 2.96 (m, 2H), 2.95 – 2.91 (m, 2H), 1.86 (p, *J* = 6.4 Hz, 2H). **^{13}C NMR (100 MHz, DMSO)** δ 169.10, 153.59, 146.33, 140.01, 136.40, 136.15, 132.39, 131.88, 130.03, 129.67, 128.87, 128.00, 127.68, 126.79, 124.70, 122.90, 27.92, 27.43, 22.34. **HRMS (ESI, m/z):** Calcd. for $C_{22}H_{19}NO_3$ $[M+H]^+$: 350.0942; Observed: 350.0943

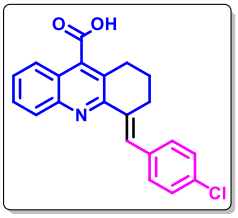

***(E)-4-(Naphthalen-1-ylmethylene)-1,2,3,4-tetrahydroacridine-9-carboxylic acid (16d)*:** Yield= 48%, Liquid; **IR (KBr, cm^{-1})**: 2942, 1724, 1571, 1549, 1492, 1221, 1169, 961, 763; **^{1}H NMR (400 MHz, DMSO) δ** 13.66 (s, 1H), 8.63 (s, 1H), 8.32 (s, 1H), 8.11 (d, *J* = 8.4 Hz, 1H), 8.03 (dd, *J* = 6.8, 3.6 Hz, 1H), 7.99 (d, *J* = 8.4 Hz, 2H), 7.94 (d, *J* = 8.0 Hz, 1H), 7.78 (t, *J* = 8.8 Hz, 2H), 7.73 (d, *J* = 8.4 Hz, 1H), 7.65 – 7.61 (m, 1H), 7.42 (t, *J* = 7.6 Hz, 1H), 3.03 (t, *J* = 6.4 Hz, 2H), 2.78 (s, 2H), 1.87 – 1.80 (m, 2H). **^{13}C NMR (100 MHz, DMSO) δ** 169.13, 153.60, 146.35, 140.21, 137.46, 134.44, 133.68, 132.07, 130.07, 129.77, 129.01, 128.26, 127.88, 127.72, 127.29, 126.98, 126.92, 126.58, 125.92, 125.14, 124.96, 124.69, 123.00, 119.49, 110.08, 28.03, 27.55, 22.52. **HRMS (ESI, m/z):** Calcd. for $C_{25}H_{19}NO_2$ $[M+H]^+$: 346.1348; Observed: 346.1441.

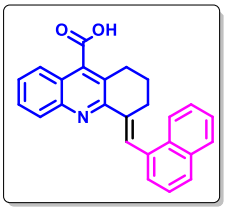

Methyl (E)-4-benzylidene-1,2,3,4-tetrahydroacridine-9-carboxylate (19a):

Yield= 92%, white solid; M. P: 99.6- 100.5 °C ; **IR (KBr, cm^{-1})**: 2942, 1724, 1571, 1549, 1492, 1221, 1169, 961, 763; **^{1}H NMR (400 MHz, $CDCl_3$) δ** 8.22 (s, 1H), 8.11 (d, *J* = 8.4 Hz, 1H), 7.67 (t, *J* = 7.6 Hz, 2H), 7.49 (td, *J* = 6.8, 1.6 Hz, 3H), 7.41 (t, *J* = 7.6 Hz, 2H), 7.29 (t, *J* = 7.2 Hz, 1H), 4.07 (s, 3H), 3.03 – 2.97 (m, 4H), 1.93 (p, *J* = 6.4 Hz, 2H). **^{13}C NMR (100 MHz, $CDCl_3$) δ** 168.42, 154.27, 146.73, 137.63, 137.56, 135.49, 130.18, 129.90, 129.82, 129.16, 128.19, 127.69, 127.20, 126.90, 124.06, 123.37, 52.54, 27.98, 27.80, 22.56. **HRMS (ESI, m/z):** Calcd. for $C_{22}H_{19}NO_2$ $[M+H]^+$: 330.1489; Observed 330.1495.

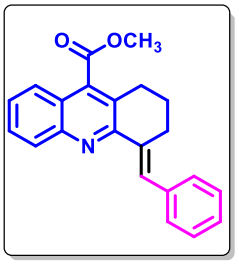

Methyl (E)-4-benzylidene-7-chloro-1,2,3,4-tetrahydroacridine-9-carboxylate (19b): Yield= 89%, light Yellow solid; M. P: 99 - 99.3 °C; **IR (KBr, cm^{-1})**: 2958, 1732, 1586, 1539, 1486, 1214, 1089, 978, 856; **^{1}H NMR (400 MHz, $CDCl_3$) δ** 8.20 (s, 1H), 8.02 (d, *J* = 9.0 Hz, 1H), 7.67 (d, *J* = 2.2 Hz, 1H), 7.59 (dd, *J* = 9.0, 2.2 Hz, 1H), 7.48 (d, *J* = 7.6 Hz, 2H), 7.40 (t, *J* = 7.6 Hz, 2H), 7.29 (t, *J* = 7.6 Hz, 1H), 4.07 (s, 3H), 3.00 (t, *J* = 6.0 Hz, 2H), 2.97 (t, *J* = 6.0 Hz, 2H), 1.91 (p, *J* = 6.0 Hz, 2H). **^{13}C NMR (100 MHz, $CDCl_3$) δ** 167.82, 154.58, 145.11, 137.45, 136.62, 135.14, 132.72, 131.35, 130.58, 130.17, 129.89, 128.84, 128.23, 127.35, 123.91, 123.08, 52.72, 27.91, 27.88, 22.39; **HRMS (ESI, m/z):** Calcd. for, $C_{22}H_{18}ClNO_2$ $[M+H]^+$: 364.1099; Observed 364.1113.

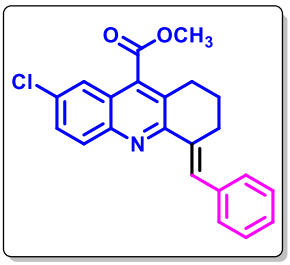

Methyl (E)-4-(4-methylbenzylidene)-1,2,3,4-tetrahydroacridine-9-carboxylate (19c): Yield= 91%, light Yellow solid; M. P: 137.6-138 °C; **IR (KBr, cm^{-1})**: 2946, 1730, 1575, 1557, 1338, 1187, 1076, 974, 898; **^{1}H NMR (400 MHz, $CDCl_3$) δ** 8.17 (s, 1H), 8.09 (dd, *J* = 9.1, 1.1 Hz, 1H), 7.68 – 7.63 (m, 2H), 7.48 (td, *J* = 7.5, 1.2 Hz, 1H), 7.40 (d, *J* = 8.0 Hz, 2H), 7.21 (d, *J* = 7.9 Hz, 2H), 4.06 (s, 3H), 3.01 (dd, *J* = 8.3, 2.8 Hz, 2H), 2.97 (d, *J* = 6.4 Hz, 2H), 2.39 (s, 3H), 1.92 (p, *J* = 6.3 Hz, 2H). **^{13}C NMR (100 MHz, $CDCl_3$) δ** 168.45, 154.47, 146.75, 137.46, 137.13, 134.76, 130.24, 129.91, 129.79, 129.11, 128.94, 127.69, 126.80, 124.05, 123.30, 52.52, 28.05, 27.82, 22.55, 21.33; **HRMS (ESI, m/z):** Calcd. for, $C_{23}H_{21}NO_2$ $[M+H]^+$: 344.1645; Observed 344.1651.

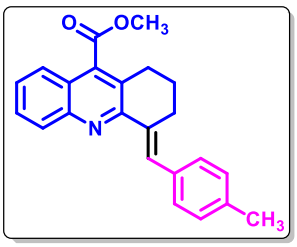

Methyl (E)-4-(4-methoxybenzylidene)-1,2,3,4-tetrahydroacridine-9-carboxylate (19d): Yield= 90%, light Yellow solid; M. P: 139.2-139.4 °C; **IR (KBr, cm^{-1})**: 2935, 2835, 1736, 1603, 1573, 1550, 1284, 1029, 975, 835; **^{1}H NMR (400 MHz, $CDCl_3$) δ** 8.15 (s, 1H), 8.09 (d, *J* = 8.0 Hz, 1H), 7.67 – 7.62 (m, 2H), 7.48 (d, *J* = 8.2 Hz, 2H), 7.45 (s, 1H), 6.96 – 6.92 (m, 2H), 4.05 (s, 3H), 3.83 (s, 3H), 3.01 – 2.98 (m, 2H), 2.98 – 2.94 (m, 2H), 1.92 (p, *J* = 6.4 Hz, 2H). **^{13}C NMR (100 MHz, $CDCl_3$) δ** 168.46, 158.85, 154.61, 146.77, 137.37, 133.72, 131.40, 130.27, 129.96, 129.73, 129.09, 127.67, 126.71, 124.05, 123.24, 113.69, 55.29, 52.52, 28.09, 27.82, 22.54; **HRMS (ESI, m/z)**: Calcd. For $C_{23}H_{21}NO_3$ $[M+H]^+$: 360.1594; Observed 360.1602.

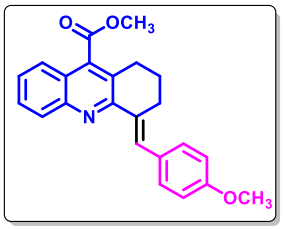

Methyl (E)-7-chloro-4-(4-methoxybenzylidene)-1,2,3,4-tetrahydroacridine-9-carboxylate (19e): Yield= 86%, light Yellow solid; M. P: 149.8 - 151 °C; **IR (KBr, cm^{-1})**: 3007, 2940, 2863, 1726, 1603, 1570, 1544, 1219, 1033, 985, 828, 534; **^{1}H NMR (400 MHz, $CDCl_3$) δ** 8.14 (s, 1H), 8.01 (d, *J* = 9.0 Hz, 1H), 7.65 (d, *J* = 2.2 Hz, 1H), 7.58 (dd, *J* = 9.0, 2.2 Hz, 1H), 7.45 (d, *J* = 8.7 Hz, 2H), 6.94 (d, *J* = 8.7 Hz, 2H), 4.07 (s, 3H), 3.84 (s, 3H), 3.01 – 2.97 (m, 2H), 2.95 (d, *J* = 6.4 Hz, 2H), 1.91 (p, *J* = 6.3 Hz, 2H). **^{13}C NMR (100 MHz, $CDCl_3$) δ** 167.86, 158.97, 154.92, 145.14, 136.42, 133.34, 132.47, 131.43, 131.25, 130.38, 130.08, 128.81, 123.77, 123.07, 113.73, 55.30, 52.69, 28.00, 27.92, 22.36; **HRMS (ESI, m/z):** Calcd. for $C_{23}H_{20}ClNO_3$ $[M+H]^+$: 394.1205; Observed 394.1210.

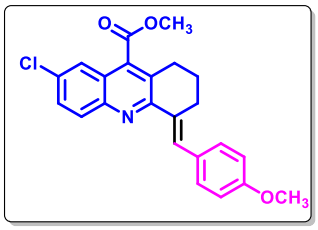

Methyl (E)-4-(4-methoxybenzylidene)-7-nitro-1,2,3,4-tetrahydroacridine-9-carboxylate (19f): Yield= 85%, light Yellow solid; M. P: 119-119.9 °C; **IR (KBr, cm^{-1})**: 2923, 2852, 1724, 1603, 1574, 1026, 801, 535; **^{1}H NMR (400 MHz, $CDCl_3$) δ** 8.33 (dd, *J* = 8.4, 1.3 Hz, 1H), 8.19 (s, 1H), 8.01 (dd, *J* = 7.6, 1.3 Hz, 1H), 7.69 (dd, *J* = 8.6, 7.6 Hz, 1H), 7.49 (d, *J* = 8.7 Hz, 2H), 6.96 (d, *J* = 8.9 Hz, 2H), 3.92 (s, 3H), 3.86 (s, 3H), 3.13 – 3.09 (m, 2H), 3.03 – 2.99 (m, 2H), 1.94 – 1.89 (m, 2H).**^{13}C NMR (100 MHz, $CDCl_3$) δ** 166.24, 159.25, 135.64, 132.93, 132.57, 131.79, 131.59, 129.75, 126.93, 123.98, 113.83, 55.33, 52.04, 29.71, 28.37, 27.84, 22.21; **HRMS (ESI, m/z):** Calcd. for $C_{23}H_{20}N_2O_5$ $[M+H]^+$: 405.1445; Observed 405.1455.

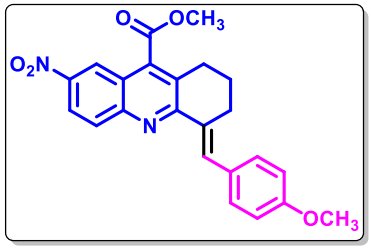

Methyl (E)-4-(4-(dimethylamino)benzylidene)-1,2,3,4-tetrahydroacridine-9-carboxylate (19g): Yield= 89%, light Yellow solid; M. P: 151.4 -152.5 °C; **IR (KBr, cm^{-1})**: 2926, 2857, 1726, 1577, 1517, 1349, 1178, 973, 818; **^{1}H NMR (400 MHz, $CDCl_3$) δ** 8.12 (s, 1H), 8.08 (d, *J* = 8.0 Hz, 1H), 7.65 (s, 1H), 7.62 (dd, *J* = 6.8, 1.2 Hz, 1H), 7.47 (s, 1H), 7.46 – 7.41 (m, 2H), 6.75 (d, *J* = 8.9 Hz, 2H), 4.06 (s, 3H), 3.06 – 3.02 (t, J= 7.2 Hz, 2H), 3.01 (s, 6H), 2.97 – 2.93 (t, J= 6.4 Hz, 2H), 1.95 – 1.89 (quin, J= 6.4 Hz, 2H). **^{13}C NMR (100 MHz, $CDCl_3$) δ** 168.58, 155.18, 149.61, 146.83, 137.06, 131.66, 131.47, 130.86, 129.62, 128.95, 127.69, 126.37, 125.85, 124.00, 123.03, 111.83, 111.01, 52.47, 40.34, 28.32, 27.89, 22.54; **HRMS (ESI, m/z):** Calcd. for $C_{24}H_{24}N_2O_2$ $[M+H]^+$: 373.1911; Observed 373.1918.

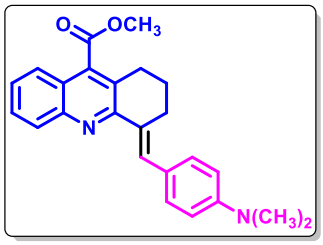

Methyl (E)-4-(4-hydroxybenzylidene)-1,2,3,4-tetrahydroacridine-9-carboxylate (19h): Yield= 86%, light Yellow solid; M. P: 169.4 – 170.6 °C; **IR (KBr, cm^{-1})**: 3416, 3065, 2943, 1731, 1583, 1549, 1344, 1034, 925, 838, 759; **^{1}H NMR (400 MHz, $CDCl_3$) δ** 8.10 (d, *J* = 8.2 Hz, 1H), 8.08 (s, 1H), 7.66 (t, *J* = 7.7 Hz, 2H), 7.51 – 7.46 (m, 1H), 7.36 (d, *J* = 8.5 Hz, 2H), 6.84 (d, *J* = 8.6 Hz, 2H), 5.83 (s, 1H), 4.07 (s, 3H), 2.98 (d, *J* = 5.1 Hz, 2H), 2.95 (d, *J* = 6.4 Hz, 2H), 1.92 (p, *J* = 6.3 Hz, 2H). **^{13}C NMR (100 MHz, $CDCl_3$) δ** 168.53, 155.39, 155.04, 146.62, 137.45, 133.31, 131.57, 130.67, 129.26, 127.90, 126.81, 124.08, 123.26, 115.37, 115.33, 52.62, 28.02, 27.76, 22.51**; HRMS (ESI, m/z)**: Calcd. for $C_{22}H_{19}NO_3$ $[M+H]^+$: 346.1438; Observed 346.1446.

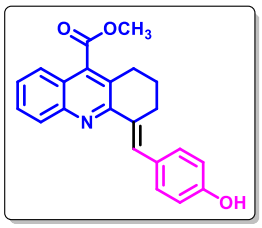

Methyl (E)-4-(4-chlorobenzylidene)-1,2,3,4-tetrahydroacridine-9-carboxylate (19i): Yield= 91%, light Yellow solid; M. P: 136.6 - 137 °C; **IR (KBr, cm^{-1})**: 2945, 2878, 1738, 1575, 1489, 1279, 1094, 973, 832, 763; **^{1}H NMR (400 MHz, $CDCl_3$) δ** 8.15 (s, 1H), 8.09 (dd, *J* = 9.8, 1.2 Hz, 1H), 7.69 (s, 1H), 7.66 (dd, *J* = 6.8, 1.6 Hz, 1H), 7.50 (ddd, *J* = 8.2, 6.8, 1.2 Hz, 1H), 7.42 (d, *J* = 8.4 Hz, 2H), 7.38 – 7.35 (m, 2H), 4.07 (s, 3H), 2.99 (d, *J* = 6.2 Hz, 2H), 2.97 – 2.94 (m, 2H), 1.93 (p, *J* = 6.4 Hz, 2H). **^{13}C NMR (100 MHz, $CDCl_3$) δ** 168.33, 153.89, 146.71, 137.64, 136.05, 132.96, 131.13, 129.79, 129.25, 128.81, 128.41, 127.67, 127.04, 124.09, 123.42, 52.56, 27.97, 27.72, 22.48; **HRMS (ESI, m/z):** Calcd. for $C_{22}H_{18}ClNO_2$ $[M+H]^+$: 364.1099; Observed 364.1102.

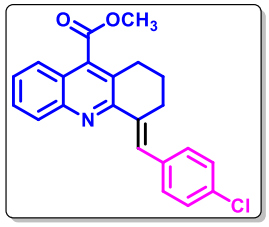

Methyl (E)-7-chloro-4-(4-chlorobenzylidene)-1,2,3,4-tetrahydroacridine-9-carboxylate (19j): Yield= 88%, light Yellow solid; M. P: 127.6 – 128.2 °C; **IR (KBr, cm^{-1})**: 2958, 2896, 1723, 1564, 1490, 1028, 976, 835, 745; **^{1}H NMR (400 MHz, $CDCl_3$) δ** 8.14 (s, 1H), 8.02 (d, *J* = 8.8 Hz, 1H), 7.67 (d, *J* = 2.4 Hz, 1H), 7.60 (dd, *J* = 9.2, 2.4 Hz, 1H), 7.41 (d, *J* = 8.8 Hz, 2H), 7.37 (d, *J* = 8.8 Hz, 2H), 4.08 (s, 3H), 3.01 – 2.97 (m, 2H), 2.97 – 2.93 (m, 2H), 1.93 (q, *J* = 6.4 Hz, 2H). **^{13}C NMR (100 MHz, $CDCl_3$) δ** 167.73, 154.21, 145.08, 136.70, 135.87, 135.69, 133.13, 132.87, 131.31, 131.12, 130.26, 129.21, 128.82, 128.45, 123.96, 123.10, 52.74, 30.92, 27.88, 22.31; **HRMS (ESI, m/z):** Calcd. for $C_{22}H_{17}Cl_2NO_2$ $[M+H]^+$: 398.0709; Observed 398.0709.

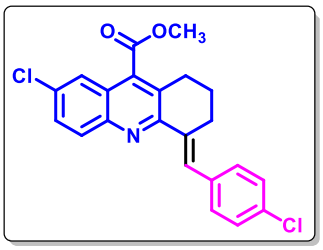

Methyl (E)-4-(4-nitrobenzylidene)-1,2,3,4-tetrahydroacridine-9-carboxylate (19k): Yield= 95%, light Yellow solid; M. P: 175.9 -176.8 °C; **IR (KBr, cm^{-1})**: 3110, 2949, 1729, 1588,

1508, 1285, 1107, 1031, 975, 920, 840; **^{1}H NMR (400 MHz, $CDCl_3$) δ** 8.29 (s, 2H), 8.27 (s, 1H), 8.13 (dd, *J* = 9.2, 1.2 Hz, 1H), 7.75 – 7.70 (m, 2H), 7.64 (d, *J* = 8.4 Hz, 2H), 7.58 – 7.54 (m, 1H), 4.11 (s, 3H), 3.07 – 3.03 (m, 2H), 3.03 – 2.99 (m, 2H), 1.99 (p, *J* = 6.4 Hz, 2H). **^{13}C NMR (100 MHz, $CDCl_3$) δ** 168.15, 153.01, 146.69, 146.39, 144.38, 138.97, 137.94, 130.38, 129.86, 129.47, 127.80, 127.58, 127.48, 124.17, 123.64, 123.52, 52.64, 28.14, 27.61, 22.43; **HRMS (ESI, m/z):** Calcd. For $C_{22}H_{18}N_2O_4$ $[M+H]^+$: 375.1340; Observed 375.1345.

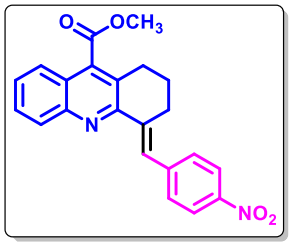

Methyl (E)-7-chloro-4-(4-nitrobenzylidene)-1,2,3,4-tetrahydroacridine-9-carboxylate (19l): Yield= 93%, light Yellow solid; M. P: 129.9 -132.5 °C; **IR (KBr, cm^{-1})** : 2989, 2932, 1732, 1567, 1543, 1293, 1039, 984, 720; **^{1}H NMR (400 MHz, $CDCl_3$) δ** 8.26 (s, 1H), 8.24 (s, 2H), 8.03 (d, *J* = 9.2 Hz, 1H), 7.69 (d, *J* = 2.4 Hz, 1H), 7.64 (d, *J* = 2.4 Hz, 1H), 7.61 (d, *J* = 8.0 Hz, 2H), 4.09 (s, 3H), 3.04 – 3.00 (m, 2H), 3.00 – 2.96 (m, 2H), 1.95 (p, *J* = 6.4 Hz, 2H). **^{13}C NMR (100 MHz, $CDCl_3$) δ** 167.56, 153.33, 146.49, 145.06, 144.19, 138.60, 137.00, 133.38, 131.40, 130.51, 130.39, 128.95, 127.95, 124.19, 123.56, 123.17, 52.82, 28.04, 27.72, 22.27; **HRMS (ESI, m/z):** Calcd. for $C_{22}H_{17}ClN_2O_4$ $[M+H]^+$: 409.0950; Observed 409.0958.

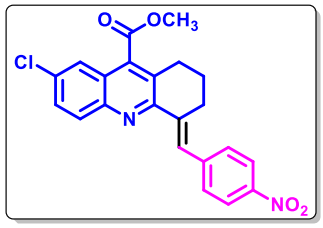

Methyl (E)-7-methoxy-4-(4-nitrobenzylidene)-1,2,3,4-tetrahydroacridine-9-carboxylate (19m): Yield= 82%, light Yellow solid; M. P: 118.9 -119.8 °C; **IR (KBr, cm^{-1})**: 3090, 2956, 2863, 1722, 1587, 1545, 1287, 1095, 952; **^{1}H NMR (400 MHz, $CDCl_3$) δ** 8.27 – 8.23 (m, 2H), 8.18 (s, 1H), 8.00 (d, *J* = 9.2 Hz, 1H), 7.62 – 7.59 (m, 2H), 7.36 (dd, *J* = 9.2, 2.8 Hz, 1H), 6.95 (d, *J* = 2.8 Hz, 1H), 4.08 (s, 3H), 3.93 (s, 3H), 3.01 (t, *J* = 5.2 Hz, 2H), 2.97 (d, *J* = 5.2 Hz, 2H), 1.95 (t, *J* = 6.4 Hz, 2H). **^{13}C NMR (100 MHz, $CDCl_3$) δ** 168.39, 158.67, 150.39, 146.28, 144.62, 143.12, 139.10, 136.48, 131.43, 130.32, 130.00, 128.22, 126.39, 124.77, 123.53, 122.77, 122.47, 101.83, 55.56, 52.56, 28.18, 27.76, 22.50; **HRMS (ESI, m/z):** Calcd. for $C_{23}H_{20}N_2O_5$ $[M+H]^+$: 405.1445; Observed 405.1452.

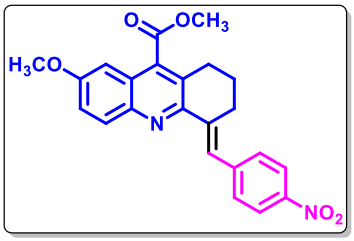

Methyl (E)-4-(naphthalen-1-ylmethylene)-1,2,3,4-tetrahydroacridine-9-carboxylate (19n): Yield= 90%, light Yellow solid; M. P: 106.0 -106.8 °C; **IR (KBr, cm^{-1})**: 2935, 2865, 1723, 1592, 1520, 1214, 1056, 985; **^{1}H NMR (400 MHz, $CDCl_3$) δ** 8.75 (s, 1H), 8.22 – 8.16 (m,

2H), 7.95 – 7.91 (m, 1H), 7.86 (dd, *J* = 6.8, 2.4 Hz, 1H), 7.78 – 7.71 (m, 2H), 7.57 (dd, *J* = 8.4, 1.8 Hz, 2H), 7.54 (d, *J* = 2.4 Hz, 3H), 4.12 (s, 3H), 3.07 (t, *J* = 6.4 Hz, 2H), 2.88 – 2.84 (m, 2H), 1.92 (q, *J* = 6.4 Hz, 2H). **^{13}C NMR (100 MHz, $CDCl_3$) δ** 168.45, 154.00, 146.81, 137.90, 137.31, 135.09, 133.64, 132.40, 130.00, 129.23, 128.49, 128.19, 127.78, 127.54, 127.02, 126.93, 126.05, 125.94, 125.37, 125.27, 124.13, 123.56, 52.58, 28.09, 27.92, 22.76; **HRMS (ESI, m/z):** Calcd. for $C_{26}H_{21}NO_2$ $[M+H]^+$: 380.1645; Observed 380.1651.

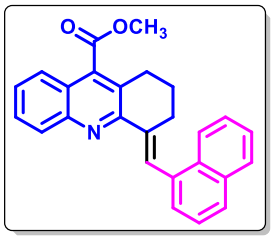

Methyl (E)-7-chloro-4-(naphthalen-1-ylmethylene)-1,2,3,4-tetrahydroacridine-9-carboxylate (19o): Yield= 87%, light Yellow solid; M. P: 136.1 – 137.0 °C; **IR (KBr, cm^{-1})**: 2925, 2853, 1711, 1583, 1515, 1079, 985, 784; **^{1}H NMR (400 MHz, $CDCl_3$) δ** 8.67 (s, 1H), 8.12 – 8.08 (m, 1H), 8.07 (d, *J* = 8.8 Hz, 1H), 7.91 – 7.87 (m, 1H), 7.82 (d, *J* = 7.6 Hz, 1H), 7.69 (d, *J* = 2.2 Hz, 1H), 7.62 (dd, *J* = 8.8, 2.4 Hz, 1H), 7.52 (d, *J* = 2.2 Hz, 1H), 7.51 – 7.49 (m, 2H), 7.48 – 7.46 (m, 1H), 4.08 (s, 3H), 3.01 (t, *J* = 6.0 Hz, 2H), 2.83 – 2.79 (m, 2H), 1.86 (q, *J* = 6.0 Hz, 2H). **^{13}C NMR (100 MHz, $CDCl_3$) δ** 167.84, 154.30, 145.14, 136.94, 136.92, 134.87, 133.60, 132.80, 132.30, 131.50, 130.21, 128.66, 128.59, 128.48, 127.86, 126.87, 126.06, 125.94, 125.25, 125.22, 124.06, 123.09, 52.74, 28.00, 27.96, 22.56; **HRMS (ESI, m/z):** Calcd. for $C_{26}H_{20}ClNO_2$ $[M+H]^+$: 414.1256; Observed 414.1258.

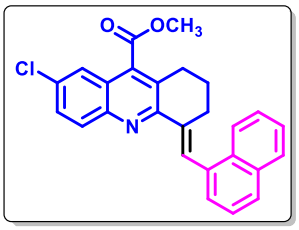

Methyl (E)-4-(thiophen-2-ylmethylene)-1,2,3,4-tetrahydroacridine-9-carboxylate (19p): Yield= 89%, light Yellow solid; M. P: 102.6 -102.8 °C; **IR (KBr, cm^{-1})**: 2940, 1722, 1572, 1543, 1281, 1032, 973, 926, 758; **^{1}H NMR (400 MHz, $CDCl_3$) δ** 8.41 (s, 1H), 8.09 (d, *J* = 8.0 Hz, 1H), 7.66 (t, *J* = 8.0 Hz, 2H), 7.48 (td, *J* = 8.0, 1.2 Hz, 1H), 7.43 (d, *J* = 5.2 Hz, 1H), 7.35 (d, *J* = 3.6 Hz, 1H), 7.13 (dd, *J* = 5.2, 3.6 Hz, 1H), 4.07 (s, 3H), 3.05 (t, *J* = 6.4, Hz, 2H), 2.97 – 2.92(t, *J* = 6.4, Hz, 2H), 2.04 – 1.98 (m, 2H). **^{13}C NMR (100 MHz, $CDCl_3$) δ** 168.38, 154.23, 146.87, 141.02, 137.07, 132.37, 130.20, 129.67, 129.16, 128.11, 127.29, 127.23, 126.79, 124.13, 123.57, 123.18, 52.55, 28.51, 27.79, 21.90; **HRMS (ESI, m/z):** Calcd. for $C_{20}H_{17}NO_2S$ $[M+H]^+$: 336.1053; Observed 336.1058.

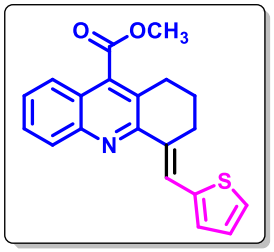

Methyl (E)-7-chloro-4-(thiophen-2-ylmethylene)-1,2,3,4-tetrahydroacridine-9-carboxylate (19q): Yield= 85%, light Yellow solid; M. P: 111.3-112.0 °C; **IR (KBr, cm^{-1})**: 3093, 2933,

1726, 1610, 1570, 1277, 1080, 973, 822,721; **^{1}H NMR (400 MHz, $CDCl_3$) δ** 8.39 (s, 1H), 8.01 (d, *J* =8.8 Hz, 1H), 7.66 (d, *J* = 2.4 Hz, 1H), 7.59 (dd, *J* = 8.8, 2.4 Hz, 1H), 7.44 (d, *J* = 4.8 Hz, 1H), 7.35 (d, *J* = 3.6 Hz, 1H), 7.13 (dd, *J* = 4.8, 3.6 Hz, 1H), 4.07 (s, 3H), 3.06 – 3.00 (m, 2H), 2.96 – 2.91 (m, 2H), 2.00 (p, *J* = 6.4 Hz, 2H). **^{13}C NMR (100 MHz, $CDCl_3$) δ** 167.79, 154.56, 145.24, 140.86, 136.13, 132.57, 131.98, 131.17, 130.40, 130.15, 129.24, 127.50, 127.34, 123.94, 123.73, 123.14, 52.73, 28.38, 27.88, 21.73; **HRMS (ESI, m/z):** Calcd. for $C_{20}H_{16}ClNO_2S$ $[M+H]^+$: 370.0663; Observed 370.0668.

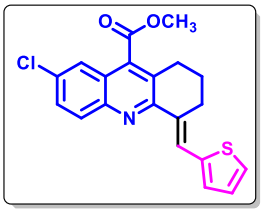

Methyl (E)-4-(2-methylpropylidene)-1,2,3,4-tetrahydroacridine-9-carboxylate (19r): Yield= 75%, light Yellow solid; M. P: 111.3-112.0 °C; **IR (KBr, cm^{-1})**: 3010, 2982, 2854, 1752, 1589, 1536, 1174, 835; **^{1}H NMR (400 MHz, $CDCl_3$) δ** 8.04 (d, *J* = 8.0 Hz, 1H), 7.66 – 7.60 (m, 2H), 7.45 (t, *J* = 7.2 Hz, 1H), 7.01 (d, *J* = 9.6 Hz, 1H), 4.05 (s, 3H), 2.92 (t, *J* = 6.2 Hz, 2H), 2.77 (dt, *J* = 9.6, 6.8 Hz, 1H), 2.73 – 2.68 (m, 2H), 1.91 (q, *J* = 6.4 Hz, 2H), 1.14 (d, *J* = 6.8 Hz, 6H). **^{13}C NMR (100 MHz, $CDCl_3$) δ** 168.54, 154.51, 146.66, 139.55, 131.58, 129.71, 128.86, 127.28, 126.48, 123.95, 123.07, 52.46, 27.97, 27.52, 26.18, 22.62, 22.26; **HRMS (ESI, m/z):** Calcd. for $C_{19}H_{21}NO_2$ $[M+H]^+$: 296.1645; Observed 296.1652.

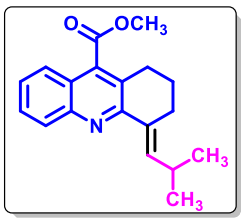

Benzyl (E)-4-(4-methoxybenzylidene)-1,2,3,4-tetrahydroacridine-9-carboxylate (19s): Yield= 89%, light Yellow solid; M. P: 119-119.9 °C; **IR (KBr, cm^{-1})**: 3034, 2925, 2854, 1730, 1573, 1494, 1280, 1024, 964, 762; **^{1}H NMR (400 MHz, $CDCl_3$) δ** 8.14 (s, 1H), 8.07 (d, *J* = 8.4 Hz, 1H), 7.61 (d, *J* = 6.8 Hz, 2H), 7.50 – 7.44 (m, 3H), 7.44 – 7.41 (m, 2H), 7.41 – 7.35 (m, 3H), 6.95 – 6.90 (m, 2H), 5.52 (s, 2H), 3.83 (s, 3H), 3.01 – 2.95 (m, 2H), 2.91 (t, *J* = 6.0 Hz, 2H), 1.87 (p, *J* = 6.0 Hz, 2H). **^{13}C NMR (100 MHz, $CDCl_3$) δ** 167.87, 158.85, 154.61, 146.76, 137.22, 135.17, 133.73, 131.40, 130.28, 129.95, 129.72, 129.07, 128.76, 127.62, 126.71, 123.98, 123.25, 113.69, 67.56, 55.30, 28.05, 27.71, 22.51; **HRMS (ESI, m/z):** Calcd. for $C_{29}H_{25}NO_3$ $[M+H]^+$: 436.1907; Observed 436.1908.

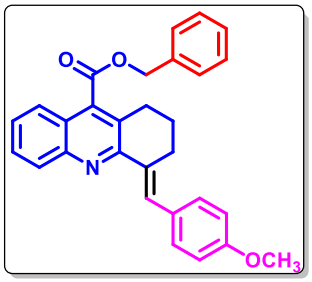

Benzyl (E)-7-chloro-4-(4-methoxybenzylidene)-1,2,3,4-tetrahydroacridine-9-carboxylate (19t): Yield= 85%, light Yellow solid; M. P: 96.7 -97.7 °C; **IR (KBr, cm^{-1})**: 2960, 2838, 1726, 1604, 1574, 1509, 1029, 829, 736; **^{1}H NMR (400 MHz, $CDCl_3$) δ** 8.12 (s, 1H), 7.98 (d, *J* = 8.8 Hz, 1H), 7.59 – 7.53 (m, 2H), 7.49 (dd, *J* = 8.0, 1.6 Hz, 2H), 7.45 – 7.42 (m,

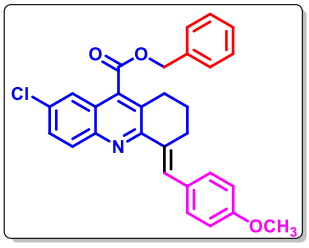

3H), 7.41 – 7.37 (m, 2H), 6.93 (d, *J* = 8.8 Hz, 2H), 5.51 (s, 2H), 3.83 (s, 3H), 2.98 – 2.93 (m, 2H), 2.90 (t, *J* = 6.0 Hz, 2H), 1.89 – 1.83 (m, 2H). **^{13}C NMR (100 MHz, $CDCl_3$) δ** 167.26, 158.96, 154.92, 145.12, 136.23, 134.99, 133.34, 132.44, 131.43, 131.20, 130.35, 130.08, 130.05, 128.89, 128.85, 128.76, 123.79, 123.03, 113.73, 67.81, 55.30, 27.96, 27.78, 22.33; **HRMS (ESI, m/z):** Calcd. for $C_{29}H_{24}ClNO_3$ $[M+H]^+$: 470.1518; Observed 470.1519.

Benzyl (E)-4-(4-(dimethylamino)benzylidene)-1,2,3,4-tetrahydroacridine-9-carboxylate (19u): Yield= 88%, light Yellow solid; M. P: 155.2 -155.6 °C; **IR (KBr, cm^{-1})**: 2926, 2857, 1725, 1604, 1576, 1518, 1225, 972, 893; **^{1}H NMR (400 MHz, $CDCl_3$) δ** 8.03 (s, 1H), 7.99 (d, *J* = 8.4 Hz, 1H), 7.56 – 7.50 (m, 2H), 7.40 (dd, *J* = 8.0, 1.6 Hz, 2H), 7.37 (d, *J* = 8.4 Hz, 2H), 7.33 – 7.28 (m, 3H), 6.68 – 6.63 (m, 2H), 5.43 (s, 2H), 2.96 – 2.92 (m, 2H), 2.92 (s, 6H), 2.82 (t, *J* = 6.4 Hz, 2H), 1.83 – 1.77 (m, 2H);**^{13}C NMR (100 MHz, $CDCl_3$) δ** 190.35, 167.97, 155.17, 149.61, 146.78, 136.94, 135.21, 130.93, 129.56, 128.95, 128.75, 128.69, 127.67, 126.38, 125.85, 123.94, 123.04, 111.84, 67.51, 40.35, 28.29, 27.78, 22.51; **HRMS (ESI, m/z):** Calcd. for $C_{30}H_{28}N_2O_2$ $[M+H]^+$: 449.2224; Observed 449.2234.

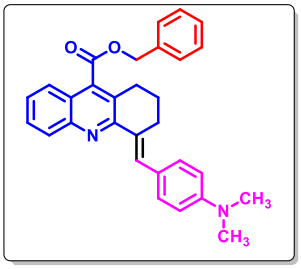

Benzyl (E)-4-(4-nitrobenzylidene)-1,2,3,4-tetrahydroacridine-9-carboxylate (19v): Yield= 90%, light Yellow solid; M. P: 141.9 – 142.0 °C; **IR (KBr, cm^{-1})**: 3034, 2933, 2446, 1727, 1590, 1517, 1186, 1028, 967, 843; **^{1}H NMR (400 MHz, $CDCl_3$) δ** 8.26 (s, 1H), 8.24 (s, 2H), 8.09 (d, *J* = 8.4 Hz, 1H), 7.70 – 7.63 (m, 2H), 7.61 (d, *J* = 8.4 Hz, 2H), 7.51 – 7.46 (m, 3H), 7.45 – 7.37 (m, 3H), 5.53 (s, 2H), 2.97 (t, *J* = 6.4 Hz, 4H), 1.92 (p, *J* = 6.4 Hz, 2H**). ^{13}C NMR (100 MHz, $CDCl_3$) δ** 167.56, 153.01, 146.69, 146.41, 144.40, 138.98, 137.79, 135.03, 130.38, 129.86, 129.43, 128.81, 127.74, 127.57, 127.47, 124.08, 123.53, 67.72, 28.09, 27.48, 22.41; **HRMS (ESI, m/z):** Calcd. for $C_{28}H_{22}N_2O_4$ $[M+H]^+$: 451.1653; Observed 451.1652.

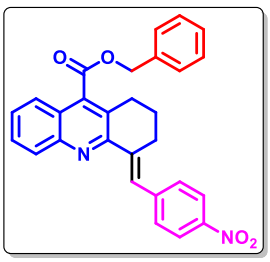

Benzyl (E)-4-(4-chlorobenzylidene)-1,2,3,4-tetrahydroacridine-9-carboxylate (19w): Yield= 86%, light Yellow solid; M. P: °C; **IR (KBr, cm^{-1})**: 3034, 2948, 2926, 1724, 1575, 1489, 1224, 1188, 970, 825, 734; **^{1}H NMR (400 MHz, $CDCl_3$) δ** 8.13 (s, 1H), 8.07 (d, *J* = 8.0 Hz, 1H), 7.64 (q, *J* = 6.8 Hz, 2H), 7.49 (dd, *J* = 8.0, 1.6 Hz, 2H), 7.47 – 7.42 (m, 2H), 7.42 – 7.38 (m, 4H), 7.38 – 7.34 (m, 2H), 5.52 (s, 2H), 2.93 (t, *J* = 6.4 Hz, 4H),

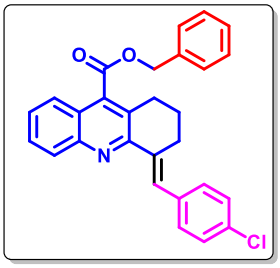

1.89 (p, *J* = 6.4 Hz, 2H). **^{13}C NMR (100 MHz, CDCl$_3$) δ** 167.75, 153.89, 146.70, 137.49, 136.05, 135.09, 132.95, 131.14, 129.78, 129.24, 128.79, 128.41, 127.63, 127.05, 124.02, 123.43, 67.64, 27.93, 27.61, 22.46; **HRMS (ESI, m/z):** Calcd. for $C_{28}H_{22}ClNO_2$ $[M+H]^+$: 440.1412; Observed 440.1417.

Benzyl (E)-4-(naphthalen-1-ylmethylene)-1,2,3,4-tetrahydroacridine-9-carboxylate (19x): Yield= 83%, light Yellow solid; M. P: 119-119.9 °C; **IR (KBr, cm^{-1})**: 3023, 2926, 2845, 1732, 1584, 1494, 1175, 1025, 24, 762; **^{1}H NMR (400 MHz, CDCl$_3$) δ** 8.66 (s, 1H), 8.15 – 8.11 (m, 1H), 8.11 – 8.07 (m, 1H), 7.88 – 7.84 (m, 1H), 7.80 (dd, *J* = 7.2, 1.6 Hz, 1H), 7.67 – 7.63 (m, 2H), 7.49 (d, *J* = 2.4 Hz, 3H), 7.46 (d, *J* = 6.4 Hz, 4H), 7.42 (dd, *J* = 7.2, 1.6 Hz, 1H), 7.38 (dd, *J* = 7.2, 1.6 Hz, 2H), 5.52 (s, 2H), 2.96 (t, *J* = 6.4 Hz, 2H), 2.79 – 2.75 (m, 2H), 1.84 – 1.79 (m, 2H). **^{13}C NMR (100 MHz, CDCl$_3$) δ** 167.86, 154.00, 146.78, 137.71, 137.31, 135.16, 135.09, 133.62, 132.37, 129.96, 129.18, 128.79, 128.46, 128.20, 127.74, 127.47, 127.00, 126.90, 126.02, 125.92, 125.37, 125.25, 124.03, 123.54, 67.62, 28.02, 27.78, 22.72; **HRMS (ESI, m/z):** Calcd. for $C_{32}H_{25}NO_2$ $[M+H]^+$: 456.1958; Observed 456.1964.

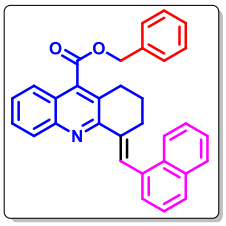

Benzyl (E)-4-(thiophen-2-ylmethylene)-1,2,3,4-tetrahydroacridine-9-carboxylate (19y): Yield= 82%, light Yellow solid; M. P: 115.8-116.2 °C; **IR (KBr, cm^{-1})**: 3033, 2935, 2855, 1731, 1605, 1571, 1496, 1218, 1025, 965, 696; **^{1}H NMR (400 MHz, CDCl$_3$) δ** 8.39 (s, 1H), 8.08 (d, *J* = 8.4 Hz, 1H), 7.66 – 7.60 (m, 2H), 7.49 (dd, *J* =8.0, 1.6 Hz, 2H), 7.46 – 7.42 (m, 2H), 7.42 – 7.37 (m, 3H), 7.34 (d, *J* = 3.5 Hz, 1H), 7.13 (dd, *J* = 5.2, 3.6 Hz, 1H), 5.52 (s, 2H), 3.02 (td, *J* = 6.4, 1.6 Hz, 2H), 2.92 – 2.87 (m, 2H), 1.97 (p, *J* = 6.4 Hz, 2H). **^{13}C NMR (100 MHz, CDCl$_3$) δ** 167.78, 154.22, 146.87, 141.02, 136.92, 135.14, 132.38, 130.18, 129.66, 129.13, 128.76, 128.73, 128.06, 127.28, 127.21, 126.78, 124.05, 123.53, 123.19, 67.58, 28.47, 27.67, 21.86; **HRMS (ESI, m/z):** Calcd. for $C_{26}H_{21}NO_2S$ $[M+H]^+$: 412.1366; Observed 412.1369.

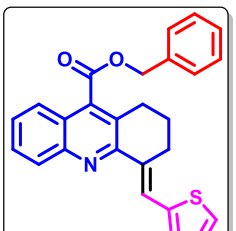

(E)-4-Benzylidene-N-(p-tolyl)-1,2,3,4-tetrahydroacridine-9-carboxamide (22a): Yield= 90%, light Yellow solid; M. P: 208.5-209.2 °C; **IR (KBr, cm^{-1})**: 3244, 3028, 2921, 2864, 1673, 1597, 1529, 1178, 924, 815; **^{1}H NMR (400 MHz, DMSO) δ** 10.69 (s, 1H), 8.21 (s, 1H), 8.08 (d, *J* = 7.6 Hz, 1H), 7.97 – 7.95 (m, 1H), 7.78 – 7.74 (m, 2H), 7.69 – 7.66 (m, 2H), 7.56 (d, *J* = 7.2 Hz, 2H), 7.46 (t, *J* = 7.6 Hz, 2H), 7.35 (t, *J* = 7.3 Hz, 1H),

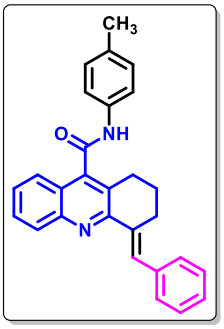

7.21 (d, *J* = 8.4 Hz, 2H), 3.00 (t, *J* = 6.4 Hz, 4H), 2.31 (s, 3H), 1.88 (m, 2H). **^{13}C NMR (100 MHz, DMSO) δ** 167.79, 165.50, 153.98, 146.54, 142.24, 137.38, 136.57, 135.76, 133.69, 133.32, 131.23, 130.18, 129.85, 129.75, 129.73, 129.66, 129.29, 129.03, 128.89, 127.87, 127.44, 127.13, 124.87, 123.86, 120.27, 28.16, 27.27, 22.51, 21.00; **HRMS (ESI, m/z):** Calcd. for $C_{28}H_{24}N_2O$ $[M+H]^+$: 405.1962; Observed 405.1967.

(E)-4-Benzylidene-7-chloro-N-(p-tolyl)-1,2,3,4-tetrahydroacridine-9-carboxamide (22b):

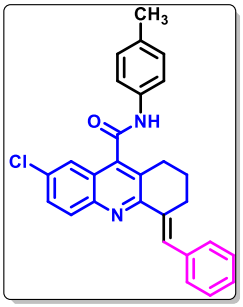

Yield= 87%, light Yellow solid; M. P: 192.8-193.1 °C; **IR (KBr, cm^{-1})**: 3431, 2927, 2852, 1652, 1603, 1176, 1035, 820; **^{1}H NMR (400 MHz, DMSO) δ** 10.73 (s, 1H), 8.20 (s, 1H), 8.11 (d, *J* = 9.2 Hz, 1H), 7.78 (dd, *J* = 9.2, 2.4 Hz, 1H), 7.68 (d, *J* = 2.0 Hz, 1H), 7.67 – 7.65 (m, 2H), 7.56 (d, *J* = 7.2 Hz, 2H), 7.47 (t, *J* = 7.2 Hz, 2H), 7.36 (d, *J* = 7.2 Hz, 1H), 7.22 (d, *J* = 7.2 Hz, 2H), 3.00 (s, 4H), 2.32 (s, 3H), 1.88 (s, 2H). **^{13}C NMR (100 MHz, DMSO) δ** 164.79, 154.69, 144.96, 141.36, 137.21, 136.36, 135.46, 133.93, 131.92, 131.77, 130.47, 130.23, 129.92, 129.82, 128.93, 128.43, 128.04, 124.46, 123.32, 120.33, 28.04, 27.37, 22.30, 21.00; **HRMS (ESI, m/z):** Calcd. for $C_{28}H_{23}ClN_2O$ $[M+H]^+$: 439.1572; Observed 439.1577;

(E)-4-(4-Methylbenzylidene)-N-(p-tolyl)-1,2,3,4-tetrahydroacridine-9-carboxamide (22c):

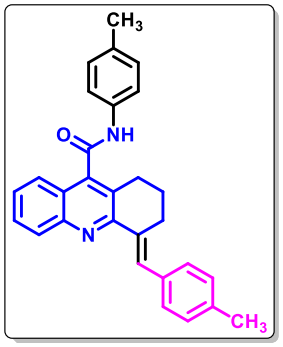

Yield= 89%, light Yellow solid; M. P: 260.3-260.6 °C; **IR (KBr, cm^{-1})**: 3430, 3057, 2920, 2860, 1644, 1606, 1548, 1174, 1018, 817, 759; **^{1}H NMR (400 MHz, DMSO) δ** 10.68 (s, 1H), 8.17 (s, 1H), 8.09 – 8.05 (m, 1H), 7.77 – 7.73 (m, 2H), 7.67 (d, *J* = 8.4 Hz, 2H), 7.60 – 7.56 (m, 1H), 7.46 (d, *J* = 8.0 Hz, 2H), 7.27 (d, *J* = 8.0 Hz, 2H), 7.21 (d, *J* = 8.4 Hz, 2H), 2.98 (t, *J* = 6.0 Hz, 4H), 2.36 (s, 3H), 2.31 (s, 3H), 1.93 – 1.79 (m, 2H). **^{13}C NMR (100 MHz, DMSO) δ** 165.53, 154.15, 146.55, 142.14, 137.36, 136.57, 134.95, 134.53, 133.69, 130.20, 129.81, 129.75, 129.62, 129.52, 129.35, 127.34, 127.08, 124.86, 123.79, 120.27, 28.23, 27.29, 22.49, 21.36, 21.00; **HRMS (ESI, m/z):** Calcd. for $C_{29}H_{26}N_2O$ $[M+H]^+$: 419.2118; Observed 419.2123;

(E)-4-(4-Methoxybenzylidene)-N-phenyl-1,2,3,4-tetrahydroacridine-9-carboxamide (22d):

Yield= 87%, light Yellow solid; M. P: 250.6-250.9 °C; **IR (KBr, cm^{-1})**: 3238, 3059, 2929, 1669, 1601, 1540, 1251, 1031, 831, 757; **^{1}H NMR (400 MHz, DMSO) δ** 10.78 (s, 1H), 8.16 (s, 1H), 8.07 (d, *J* = 7.2 Hz, 1H), 7.79 (d, *J* = 7.2 Hz, 2H), 7.75 (d, *J* = 5.6 Hz, 2H), 7.58 (d, *J*

= 6.8 Hz, 1H), 7.53 (d, *J* = 7.6 Hz, 2H), 7.41 (t, *J* = 6.8 Hz, 2H), 7.17 (t, *J* = 6.8 Hz, 1H), 7.03 (d, *J* = 7.2 Hz, 2H), 3.82 (s, 3H), 2.98 (s, 4H), 1.94 – 1.82 (m, 2H). **^{13}C NMR (100 MHz, DMSO) δ** 165.87, 159.10, 154.37, 146.55, 141.87, 138.97, 133.70, 131.78, 129.83, 129.55, 129.21, 127.27, 127.05, 124.78, 123.64, 120.30, 114.42, 55.64, 28.23, 27.29, 22.44; **HRMS (ESI, m/z):** Calcd. for $C_{28}H_{24}N_2O_2$ $[M+H]^+$: 421.1911; Observed 421.1914;

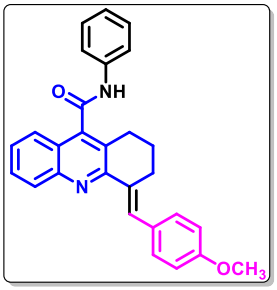

(E)-4-(4-Methoxybenzylidene)-N-(p-tolyl)-1,2,3,4-tetrahydroacridine-9-carboxamide (22e): Yield= 88%, light Yellow solid; M. P: 119-119.9 °C; **IR (KBr, cm^{-1})**: 3246, 2942, 2714, 1670, 1551, 1312, 1165, 1065, 812, 756; **^{1}H NMR (400 MHz, DMSO) δ** 10.67 (s, 1H), 8.14 (s, 1H), 8.05 (d, *J* = 8.4 Hz, 1H), 7.75 – 7.71 (m, 2H), 7.66 (d, *J* = 8.4 Hz, 2H), 7.58 – 7.54 (m, 1H), 7.52 (d, *J* = 8.4 Hz, 2H), 7.20 (d, *J* = 8.4 Hz, 2H), 7.02 (d, *J* = 8.4 Hz, 2H), 3.81 (s, 3H), 2.97 (t, *J* = 6.0 Hz, 4H), 2.30 (s, 3H), 1.87 (m, 2H). **^{13}C NMR (100 MHz, DMSO) δ** 165.55, 159.11, 154.34, 146.58, 142.04, 136.59, 133.71, 133.67, 131.78, 129.87, 129.75, 129.56, 129.18, 127.20, 127.02, 124.86, 123.71, 120.26, 114.42, 55.65, 28.26, 27.31, 22.48, 21.01; **HRMS (ESI, m/z):** Calcd. for $C_{29}H_{26}N_2O_2$ $[M+H]^+$: 435.2067; Observed 435.2070.

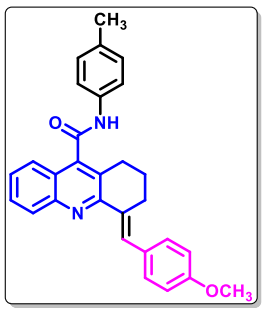

(E)-7-chloro-4-(4-methoxybenzylidene)-N-(p-tolyl)-1,2,3,4-tetrahydroacridine-9-carboxamide (22f): Yield= 80%, light Yellow solid; M. P: 223.2-224 °C; **IR (KBr, cm^{-1})**: 3224, 2956, 2879, 1652, 1235, 1098, 951, 823; **^{1}H NMR (400 MHz, DMSO) δ** 10.72 (s, 1H), 8.14 (s, 1H), 8.08 (d, *J* = 8.8 Hz, 1H), 7.76 (dd, *J* = 8.8, 2.4 Hz, 1H), 7.67 – 7.64 (m, 3H), 7.52 (d, *J* = 8.8 Hz, 2H), 7.21 (d, *J* = 8.8 Hz, 2H), 7.03 (d, *J* = 8.8 Hz, 2H), 3.81 (s, 3H), 2.97 (s, 4H), 2.31 (s, 3H), 1.88 (s, 2H). **^{13}C NMR (100 MHz, DMSO) δ** 164.88, 159.23, 155.06, 145.00, 141.13, 136.36, 133.93, 133.37, 131.86, 131.51, 129.81, 129.71, 128.33, 124.31, 123.30, 120.33, 114.44, 55.65, 28.13, 27.40, 22.26, 20.99; **HRMS (ESI, m/z):** Calcd. for $C_{29}H_{25}ClN_2O_2$ $[M+H]^+$: 469.1678; Observed 469.1689.

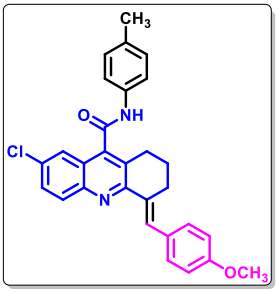

(E)-4-(4-(Dimethylamino)benzylidene)-N-(p-tolyl)-1,2,3,4-tetrahydroacridine-9-carboxamide (22g): Yield= 89%, light Yellow solid; M. P: 119-119.9 °C; **IR (KBr, cm^{-1}):** 3236, 3025, 2917, 2820, 1532, 1165, 1065, 825; **^{1}H NMR (400 MHz, DMSO) δ** 10.67 (s, 1H), 8.11 (s, 1H), 8.03 (dd, *J* = 8.0, 1.6 Hz, 1H), 7.71 (dd, *J* = 8.0, 1.6 Hz, 2H), 7.68 – 7.66 (m, 2H), 7.56 – 7.51 (m, 1H), 7.45 (d, *J* = 8.8 Hz, 2H), 7.21 (d, *J* = 8.8 Hz, 2H), 6.79 (d, *J* = 8.8 Hz, 2H), 3.00 (s, 2H), 2.98 (s, 6H), 2.94 (d, *J* = 6.0 Hz, 2H), 2.31 (s, 3H), 1.92 – 1.81 (m, 2H). **^{13}C NMR (100 MHz, DMSO) δ** 165.67, 154.88, 150.05, 146.66, 141.73, 136.61, 133.64, 131.69, 131.19, 130.19, 129.74, 129.64, 129.43, 126.92, 126.84, 125.11, 124.82, 123.50, 120.25, 112.36, 40.32, 28.53, 27.39, 22.48, 21.00; **HRMS (ESI, m/z):** Calcd. for $C_{30}H_{29}N_3O$ $[M+H]^+$: 448.2384; Observed 448.2388.

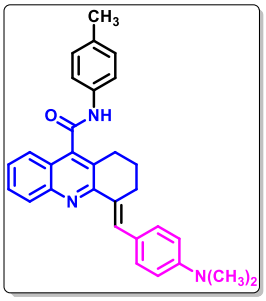

(E)-4-(4-Hydroxybenzylidene)-N-(p-tolyl)-1,2,3,4-tetrahydroacridine-9-carboxamide (22h): Yield= 85%, light Yellow solid; M. P: 272.1-272.9 °C; 3479, 3237, 3066, 2928, 1652, 1544, 1513, 1258, 1170, 815; **IR (KBr, cm^{-1}):** **^{1}H NMR (400 MHz, DMSO) δ** 10.68 (s, 1H), 9.72 (s, 1H), 8.11 (s, 1H), 8.05 (d, *J* = 8.8 Hz, 1H), 7.73 (d, *J* = 7.2 Hz, 2H), 7.67 (d, *J* = 8.0 Hz, 2H), 7.56 (t, *J* = 7.6 Hz, 1H), 7.42 (d, *J* = 8.8 Hz, 2H), 7.21 (d, *J* = 8.4 Hz, 2H), 6.86 (d, *J* = 8.8 Hz, 2H), 2.96 (t, *J* = 6.4 Hz, 4H), 2.31 (s, 3H), 1.89 (s, 2H). **^{13}C NMR (100 MHz, DMSO) δ** 165.55, 157.58, 154.55, 146.42, 142.05, 136.58, 133.68, 132.61, 131.97, 129.81, 129.74, 129.36, 128.29, 127.14, 127.03, 124.86, 123.64, 120.27, 115.85, 28.29, 27.32, 22.46, 21.01; **HRMS (ESI, m/z):** Calcd. for $C_{28}H_{24}N_2O_2$ $[M+H]^+$: 421.1911; Observed 421.1920.

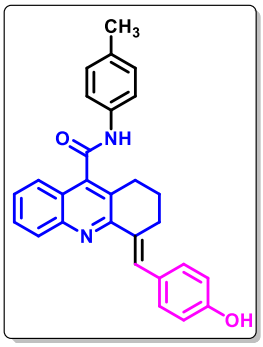

(E)-4-(4-Chlorobenzylidene)-N-(p-tolyl)-1,2,3,4-tetrahydroacridine-9-carboxamide (22i): Yield= 90%, light Yellow solid; M. P: 119-119.9 °C; **IR (KBr, cm^{-1}):** 3421, 2989, 2842, 1652, 1251, 1037, 925; **^{1}H NMR (400 MHz, DMSO) δ** 10.68 (s, 1H), 8.16 (s, 1H), 8.07 (d, *J* = 8.8 Hz, 1H), 7.74 (d, *J* = 7.6 Hz, 2H), 7.66 (d, *J* = 8.4 Hz, 2H), 7.58 (d, *J* = 8.8 Hz, 3H), 7.50 (d, *J* = 8.4 Hz, 2H), 7.20 (d, *J* = 8.4 Hz, 2H), 2.97 (q, *J* = 8.4 Hz, 4H), 2.30 (s, 3H), 1.87 (q, *J* = 5.8 Hz, 2H). **^{13}C NMR (100 MHz, DMSO) δ** 165.45, 153.70, 146.52, 142.28, 136.54, 136.23, 133.73, 132.39, 131.93, 129.92, 129.75, 129.66, 128.90, 127.92, 127.56, 127.18, 124.88, 123.90, 120.29, 28.10, 27.21, 22.44, 21.00; **HRMS (ESI, m/z):** Calcd. for $C_{28}H_{23}ClN_2O$ $[M+H]^+$: 439.1572; Observed 439.1585.

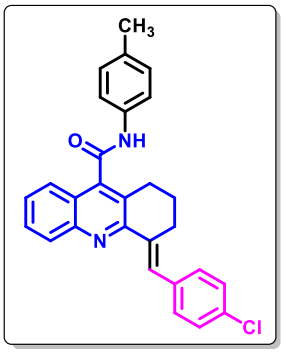

(E)-4-(4-Nitrobenzylidene)-N-(p-tolyl)-1,2,3,4-tetrahydroacridine-9-carboxamide (22j):

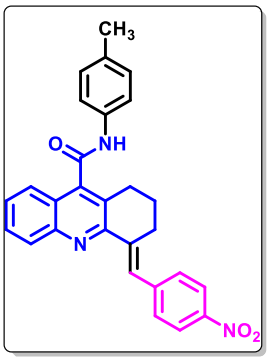

Yield= 92%, light Yellow solid; M. P: 259.7-260.3 °C; **IR (KBr, cm^{-1})**: 3284, 3027, 2945, 1868, 1673, 1596, 1295, 1189, 856; **^{1}H NMR (400 MHz, DMSO) δ** 10.71 (s, 1H), 8.30 (d, *J* = 8.8 Hz, 2H), 8.28 (s, 1H), 8.11 (d, *J* = 8.4 Hz, 1H), 7.83 (d, *J* = 8.8 Hz, 2H), 7.77 (d, *J* = 9.2 Hz, 2H), 7.66 (d, *J* = 8.4 Hz, 2H), 7.65 – 7.61 (m, 1H), 7.21 (d, *J* = 8.8 Hz, 2H), 3.06 – 2.98 (t, *J* = 6.4 Hz, 4H), 2.31 (s, 3H), 1.91 (s, 2H). **^{13}C NMR (100 MHz, DMSO) δ** 165.34, 153.12, 146.52, 146.43, 144.33, 142.50, 139.54, 136.53, 133.75, 131.22, 130.07, 129.76, 127.92, 127.47, 127.09, 124.93, 124.10, 124.01, 120.30, 28.26, 27.14, 22.43, 21.00; **HRMS (ESI, m/z):** Calcd. for $C_{28}H_{23}N_3O_3$ $[M+H]^+$: 450.1812; Observed 450.1817.

(E)-7-Chloro-4-(4-nitrobenzylidene)-N-(p-tolyl)-1,2,3,4-tetrahydroacridine-9-carboxamide (22k): Yield= 90%, light Yellow solid; M. P: 119-119.9 °C; **IR (KBr, cm^{-1})**: 3275, 2922, 1731, 1665, 1244, 1190, 902, 840; **^{1}H NMR (400 MHz, DMSO) δ** 10.75 (s, 1H), 8.29 (d, *J* = 8.8 Hz, 2H), 8.27 (s, 1H), 8.13 (d, *J* = 9.2 Hz, 1H), 7.84 – 7.79 (m, 3H), 7.71 (s, 1H), 7.66 (d, *J* = 8.4 Hz, 2H), 7.22 (d, *J* = 8.4 Hz, 2H), 3.02 (s, 4H), 2.31 (s, 3H), 1.90 (s, 2H). **^{13}C NMR (100 MHz, DMSO) δ** 164.64, 153.82, 146.52, 144.93, 144.13, 141.61, 139.19, 136.31, 133.99, 132.29, 132.03, 131.26, 130.70, 129.82, 129.61, 128.76, 127.67, 124.69, 124.03, 123.38, 120.36, 118.70, 28.12, 27.24, 22.22, 21.00; **HRMS (ESI, m/z):** Calcd. for $C_{28}H_{22}ClN_3O_3$ $[M+H]^+$: 484.1423; Observed 484.1428.

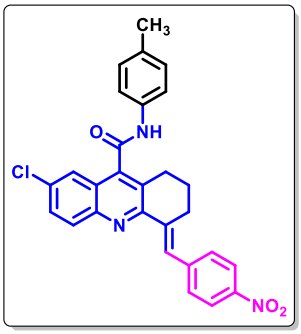

(E)-4-(Naphthalen-1-ylmethylene)-N-(p-tolyl)-1,2,3,4-tetrahydroacridine-9-carboxamide (22l): Yield= 87%, light Yellow solid; M. P: 119-119.9 °C; **IR (KBr, cm^{-1})**: 3226, 3035, 2918, 1670, 1529, 1245, 1196, 825, 776; **^{1}H NMR (400 MHz, DMSO) δ** 10.70 (s, 1H), 8.65 (s, 1H), 8.13 (dd, *J* = 8.8, 1.2 Hz, 1H), 8.04 – 7.99 (m, 2H), 7.94 (d, *J* = 8.0 Hz, 1H), 7.81 – 7.78 (m, 1H), 7.78 – 7.76 (m, 1H), 7.69 – 7.66 (m, 2H), 7.64 – 7.62 (m, 1H), 7.61 – 7.59 (m, 2H), 7.59 – 7.56 (m, 2H), 7.21 (d, *J* = 8.4 Hz, 2H), 3.03 (t, *J* = 6.8 Hz, 2H), 2.80 (s, 2H), 2.31 (s, 3H), 1.84 (d, *J* = 6.0 Hz, 2H). **^{13}C NMR (100 MHz, DMSO) δ** 165.50, 153.68, 146.56, 142.56, 137.62, 136.56, 134.52, 133.72, 132.13, 129.92, 129.76, 129.05, 128.25, 127.57, 127.28, 126.93, 126.57, 125.93, 124.92, 124.03,

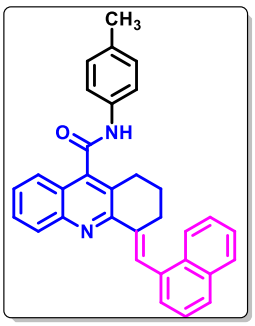

120.28, 29.49, 28.18, 22.64, 21.01; **HRMS (ESI, m/z):** Calcd. for $C_{32}H_{26}N_2O$ $[M+H]^+$: 455.2118; Observed 455.2120.

(E)-4-(Thiophen-2-ylmethylene)-N-(p-tolyl)-1,2,3,4-tetrahydroacridine-9-carboxamide (22m): Yield= 84%, light Yellow solid; M. P: 227.5-228.3 °C; **IR (KBr, cm^{-1})**: 3230, 3029, 2954, 2876, 1596, 1295, 1189, 856; **^{1}H NMR (400 MHz, DMSO) δ** 10.69 (s, 1H), 8.42 (s, 1H), 8.07 (d, *J* = 8.4 Hz, 1H), 7.77 – 7.75 (m, 1H), 7.74 (s, 1H), 7.74 – 7.71 (m, 1H), 7.66 (d, *J* = 8.4 Hz, 2H), 7.57 (ddd, *J* = 8.0, 6.8, 1.1 Hz, 1H), 7.50 (d, *J* = 3.5 Hz, 1H), 7.23 (dd, *J* = 5.1, 3.6 Hz, 1H), 7.21 (s, 1H), 7.19 (s, 1H), 3.03 – 2.97 (m, 2H), 2.95 (t, *J* = 6.0 Hz, 2H), 2.31 (s, 3H), 1.96 (t, *J* = 6.0 Hz, 2H). **^{13}C NMR (100 MHz, DMSO) δ** 165.50, 153.96, 146.62, 141.82, 140.54, 136.51, 133.76, 132.59, 131.17, 129.91, 129.76, 129.48, 128.93, 128.28, 127.42, 127.36, 124.89, 123.70, 122.85, 120.29, 28.56, 27.19, 21.90, 20.99; HRMS (ESI, m/z): Calcd. for $C_{26}H_{22}N_2OS$ $[M+H]^+$: 411.1526; Observed 411.1529.

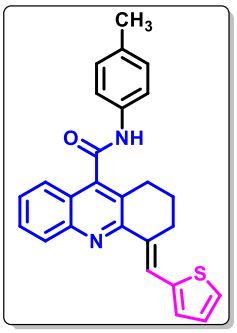

(E)-4-Benzylidene-N-methoxy-N-methyl-1,2,3,4-tetrahydroacridine-9-carboxamide (25a): Yield= 89%, Liquid; **IR (KBr, cm^{-1})**: 2942, 1724, 1571, 1549, 1492, 1221, 1169, 961, 763; **^{1}H NMR (400 MHz, $CDCl_3$) δ** 8.24 (s, 1H), 8.10 (d, *J* = 8.4 Hz, 1H), 7.66 (d, *J* = 7.6 Hz, 2H), 7.50 (d, *J* = 8.0 Hz, 2H), 7.46 (d, *J* = 8.4 Hz, 1H), 7.39 (d, *J* = 8.0 Hz, 2H), 7.29 (d, *J* = 7.6 Hz, 1H), 3.50 (s, 3H), 3.30 (s, 3H), 3.02 – 2.86 (m, 4H), 1.93 (m, 2H). **^{13}C NMR (100 MHz, $CDCl_3$) δ** 169.09, 154.04, 146.65, 140.05, 137.70, 135.66, 129.97, 129.89, 129.76, 129.02, 128.18, 127.15, 126.61, 124.17, 123.76, 61.77, 32.29, 28.12, 27.46, 22.56. **HRMS (ESI, m/z):** Calcd. for $C_{23}H_{22}N_2O_2$ $[M+H]^+$: 359.1754; Observed 359.1760.

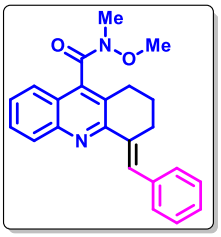

(E)-N-methoxy-4-(4-methoxybenzylidene)-N-methyl-1,2,3,4-tetrahydroacridine-9-carboxamide (25b): Yield= 92%, white solid; M. P: 147.7-148.2 °C ; **IR (KBr, cm^{-1})**: 2942, 1724, 1571, 1549, 1492, 1221, 1169, 961, 763; **^{1}H NMR (400 MHz, $CDCl_3$) δ** 8.18 (s, 1H), 8.08 (d, *J* = 8.8 Hz, 1H), 7.67 – 7.62 (m, 2H), 7.47 (dd, *J* = 8.4, 1.6 Hz, 3H), 6.96 – 6.93 (m, 2H), 3.85 (s, 3H), 3.50 (s, 3H), 3.30 (s, 3H), 3.02 – 2.85 (m, 4H), 1.96 – 1.90 (m, 2H). **^{13}C NMR (100 MHz, $CDCl_3$) δ** 169.15, 158.79, 154.35, 146.70, 139.81, 133.94, 131.38, 130.34, 129.66, 128.93, 127.11, 126.41, 124.15, 123.63, 113.67, 61.76, 55.30, 32.28, 28.22,

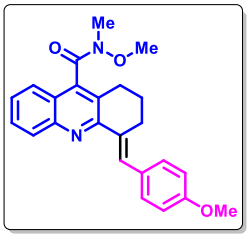

27.48, 22.54. **HRMS (ESI, m/z):** Calcd. for $C_{24}H_{24}N_2O_3$ $[M+H]^+$: 389.1860; Observed 389.1865.

(E)-N-methoxy-N-methyl-4-(4-nitrobenzylidene)-1,2,3,4-tetrahydroacridine-9-carboxamide (25c): Yield= 95%, white solid; M. P: 151.2-152.1 °C ; **IR (KBr, cm^{-1})**: 2942, 1724, 1571, 1549, 1492, 1221, 1169, 961, 763; **^{1}H NMR (400 MHz, $CDCl_3$) δ** 8.21 (s, 1H), 8.19 – 8.17 (m, 2H), 8.05 – 8.01 (m, 1H), 7.63 – 7.59 (m, 2H), 7.56 – 7.54 (m, 2H), 7.44 (ddd, *J* = 8.2, 6.8, 1.3 Hz, 1H), 3.44 (s, 3H), 3.24 (s, 3H), 2.95 – 2.82 (m, 4H), 1.88 (t, *J* = 5.2 Hz, 2H). **^{13}C NMR (100 MHz, $CDCl_3$) δ** 168.77, 152.78, 146.60, 146.39, 144.50, 140.53, 139.18, 130.39, 129.81, 129.34, 127.41, 127.30, 127.17, 124.26, 124.02, 123.54, 61.79, 32.29, 28.28, 27.24, 22.44. **HRMS (ESI, m/z):** Calcd. for $C_{23}H_{22}N_2O_3^+$ $[M+H]^+$: 404.1605; Observed 404.1623.

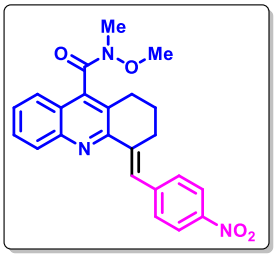

(E)-N-methoxy-N-methyl-4-(thiophen-2-ylmethylene)-1,2,3,4-tetrahydroacridine-9-carboxamide (25d): Yield= 91%, Liquid; **IR (KBr, cm^{-1})**: 2942, 1724, 1571, 1549, 1492, 1221, 1169, 961, 763; **^{1}H NMR (400 MHz, $CDCl_3$) δ** 8.44 (s, 1H), 8.10 (d, *J* = 9.6 Hz, 1H), 7.66 – 7.64 (m, 1H), 7.63 (dd, *J* = 4.4, 2.8 Hz, 1H), 7.46 (ddd, *J* = 8.0, 6.8, 1.2 Hz, 1H), 7.41 (d, *J* = 5.2 Hz, 1H), 7.35 (d, *J* = 3.6 Hz, 1H), 7.13 – 7.11 (m, 1H), 3.50 (s, 3H), 3.29 (s, 3H), 3.05 (td, *J* = 6.4, 2.4 Hz, 2H), 2.90 (m, 2H), 2.00 (t, *J* = 6.4 Hz, 2H). **^{13}C NMR (100 MHz, $CDCl_3$) δ** 168.99, 154.00, 146.77, 141.07, 130.11, 129.58, 129.04, 127.51, 127.28, 127.18, 126.51, 124.25, 123.60, 123.41, 61.79, 32.27, 28.63, 27.48, 21.91. **HRMS (ESI, m/z):** Calcd. for $C_{22}H_{22}N_2O_2S^+$ $[M+H]^+$: 365.1318; Observed 365.1325.

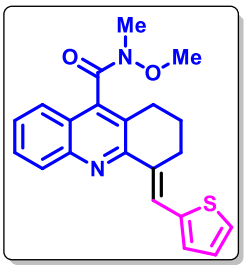

2.4 References

(1) (a) Proctor, G. R.; Harvey, A. L. *Curr. Med. Chem.* **2000**, *7*, 295–302. (b) Camps, P.; Achab, R. El.; Morral, J.; Muñoz-Torrero, D.; Badia, A.; Baños, J. E.; Vivas, N. M.; Barril, X.; Orozco, M.; Luque, F. J. *J. Med. Chem.* **2000**, *43*, 4657-4666.

(2) Paul, B.; Watkins, MD; Hyman, J.; Zimmerman, MD; Margaret, J.; Knapp,; Stephen, I.; Gracon, D. V. M.; Karen, W.; Lewis, M. S. *JAMA.* **1994**, *271*, 992–998.

(3) Wu, W-Y.; Dai, Y-C.; Li, N-G.; Dong, Z-X.; Gu, T.; Shi, Z-H.; Xue, X.; Tang, Y-P.; Duan, J-A. *J. Enzyme Inhib. Med. Chem.* **2017**, *32*, 572–587.

(4) Hu, M-K.; Wu, L-J.; Hsiao, G.; Yen, M-H. *J. Med. Chem.* **2002**, *45*, 2277-2282.

(5) Isabel, F -B, M.; Concepcion, P.; Gema C. G -M.; Conde, S.; Manuela, G. L.; Villarroya, M.; Antonio, G. G.; Isabel R-F. M. *J. Med. Chem.* **2010**, *53*, 4927–4937.

(6) Xie, S-S.; Wang, X.; Jiang, N.; Yu, W.; Kelvin, D.G.; Wang; Lan, J-S.; Li, Z-R.; Kong, L-Y. *Eur. J. Med. Chem.* **2015**, *95*, 153–165.

(7) Fang, L.; Kraus, B.; Lehmann, J.; Heilmann, J.; Zhangb, Y.; Deckera, M. *Bioorg. Med. Chem. Lett*. **2008,** *18*, 2905–2909.

(8) Keri, R. S.; Quintanova, C.; Chaves, S.; Silva, D. F.; Cardoso, S. M.; Santos, M. A. *Chem. Biol. Drug. Des.* **2016**, *87*, 101–111.

(9) Wan, L-X.; Zhen, Y-Q.; He, Z-X.; Zhang, Y.; Zhang, L.; Li, X.; Gao, F.; Zhou, X-L. *ACS Omega* **2021**, *6*, 9960−9972.

(10) Khoobi, M.; Ghanoni, F.; Nadri, H.; Moradi, A.; Hamedani, M. P.; Moghadam, F. H.; Emami, S.; Vosooghi, M.; Zadmard, R.; Foroumadi, A.; Shafiee, A. *Eur. J. Med. Chem.* **2015**, *89*, 296−303.

(11) (a) Cristobal de los R.; Jose M-C.; *Eur. J. Med. Chem.* **2019**, *166*, 381−389.
(b)Jose, M-C.; Rafael, L.; Cristobal de los R.; Guglietta, A.; Terencio, J.; Manuela, G. L.; Garci, A. G.; Villarroya, M. *J. Med. Chem.* **2006**, *49*, 7607−7610.

(12) Eghtedari, M.; Sarrafi, Y.; Nadri, H.; Mahdavi, M.; Moradi, A.; Homayouni, F.; Moghadam; Emami, S.; Firoozpour, L.; Asadipour, A.; Sabzevari, O.; Foroumadi, A. *Eur. J. Med. Chem.* **2017**,*128*, 237−246.

(13) Kohnehshahri, M. S.; Chehardoli, G.; Bahiraei, M.; Akbarzadeh, T.; Ranjbar, A.; Rastegari, A.; Najaf, Z. *Mol. Divers.* **2022**, *26*, 489–503.

(14) (a)Najafi, Z.; Mahdavi, Md.; Saeedi, M.; Karimpour-Razkenari, E.; Asatouri, R.; Vafadarnejad, F.; Homayouni, F.; Moghadam, Khanavi, M.; Sharifzadeh, M.; Akbarzadeh, T. *Eur. J. Med. Chem.* **2017**,*125*, 1200−1212 (b) Najafia, Z.; Mahdavic, M.; Saeedid, M.; Karimpour-Razkenarie, E.; Edrakif, N.; Sharifzadehg, M.; Khanavih, M.; Akbarzadeha, T. *Bioorg. Chem.* **2019**, *83*, 303–316.

(15) Wu, G.; Gao, Y.; Kang, D.; Huang, B.; Huo, Z.; Liu, H.; Poongavanam, V.; Zhan, P.; Liu, X. *Med. Chem. Commun.* **2018**, *9*, 149.

(16) Reddy, E. K.; Remya, C.; Mantosh, K.; Sajith, A. M.; Omkumar, R.V.; Sadasivan, C.; Anwar, S. K. *Eur. J. Med. Chem.* **2017**, *139*, 367–377.

(17) Prameela, S.; Nawaz Khan, F-R. *Eur. J. Org. Chem*, **2020,** *33*, 5394-5410.

(18) Sousa D. J.; Brown, R. C. D.; Baati, R. *Eur. J. Org. Chem*, **2014**, *16*, 3468–3474.

(19) Yong, W.; Chen, C.; Zhang, S.; Zhenbang, L.; Su, X.; Wen, L.; Li, M. *Org. Lett*. **2013**, *15*, 18.

(20) Liu, P.; Hao, J. W.; Mo, L. P.; Zhang, Z. H. *RSC Adv*. **2015**, *5*, 48675.

(21) Satyanarayana, N.; Sathish, K.; Nagaraju, S.; Pawar, R.; Faizan, M.; Arumugavel, M.; Shirisha, T.; Kashinath, D. *New J. Chem.* **2022**, *46*, 1637-1642.

(22) Krishnakumar, V.; Vindhya, N. G.; Mandal, B. K.; Nawaz Khan, F. R. *Ind. Eng. Chem. Res.* **2014**, *53*, 10814-10819.

(23) Mphahlele, M. J.; Mtshemla, V. *J. Heterocyclic Chem.* **2008**, *45*, 1343-1350.

(24) Lindahl, E.; Hess, B.; Spoel, D. V. *J. Mol. Mod.* **2001**, *7*, 306-317.

(25) Maier, J.A.; Martinez, C.; Kasavajhala, K.; Wickstrom, L.; Hauser K.E.; Simmerling, C. *J. Chem. Theory Comput* **2015**, *11*, 3696-3713.

(26) Liu, H.; Wang, L.; Lv, M.; Pei, R.; Li, P.; Pei, Z.; Wang, Y.; Su, W.; Xie, X.-Q. *J Comput Info Modeling*. **2014**, *54*,1050-1060.

(27) De Lima, B. R.; Lima, J. M.; Maciel, J. B.; Valentim, C. Q.; De Cássia, R.; Nunomura, S.; Emerson; Lima, S.; Koolen, H. H.; Souza, A. D. L.; Pinheiro, M. L. B.; Cass, Q. B.; Silva, F. M. A. *Front. Chem*. **2019**, *7*, 629.

(28) Daina, A.; Michielin, O.; Zoete, V. *Sci. Rep.* **2017**, *7*, 42717.

(29) Hasan, A. H.; Murugesan, S.; Amran, S. I.; Chander, S.; Alanazi, M. M.; Hadda, T. B.; Shakya, S.; Pratama, M. R. F.; Das, B.; Biswas, S.; Jamalis, J. *Bioorg. Chem.* **2022**, *119*, 105572.

2.5 Selected Spectra

(E)-4-Benzylidene-9-chloro-1,2,3,4-tetrahydroacridine (5a):

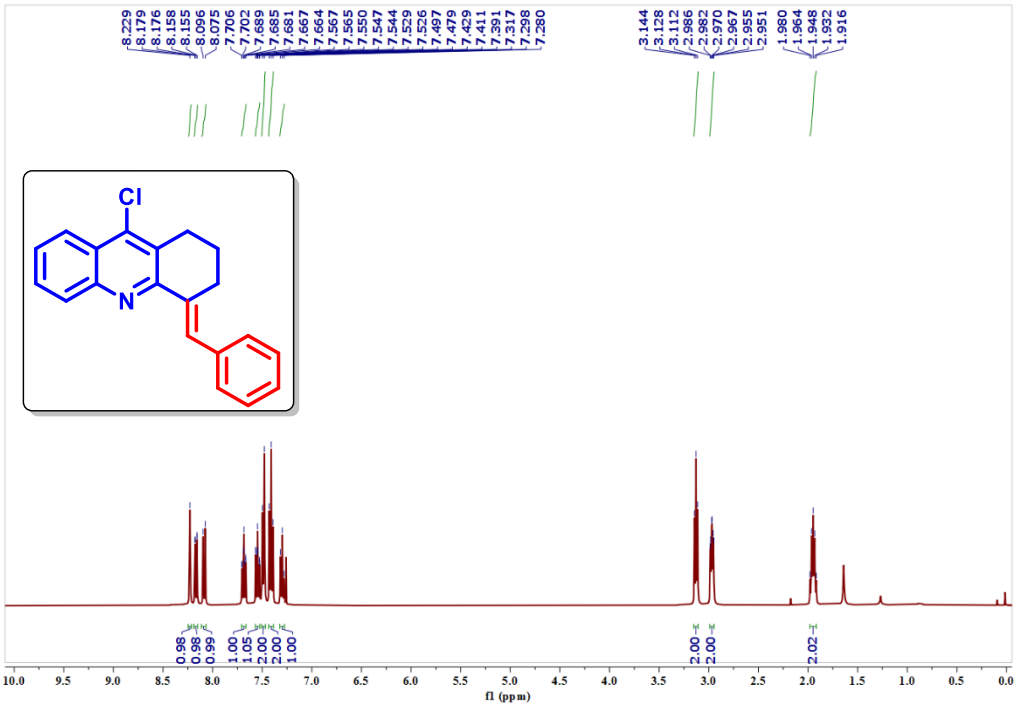

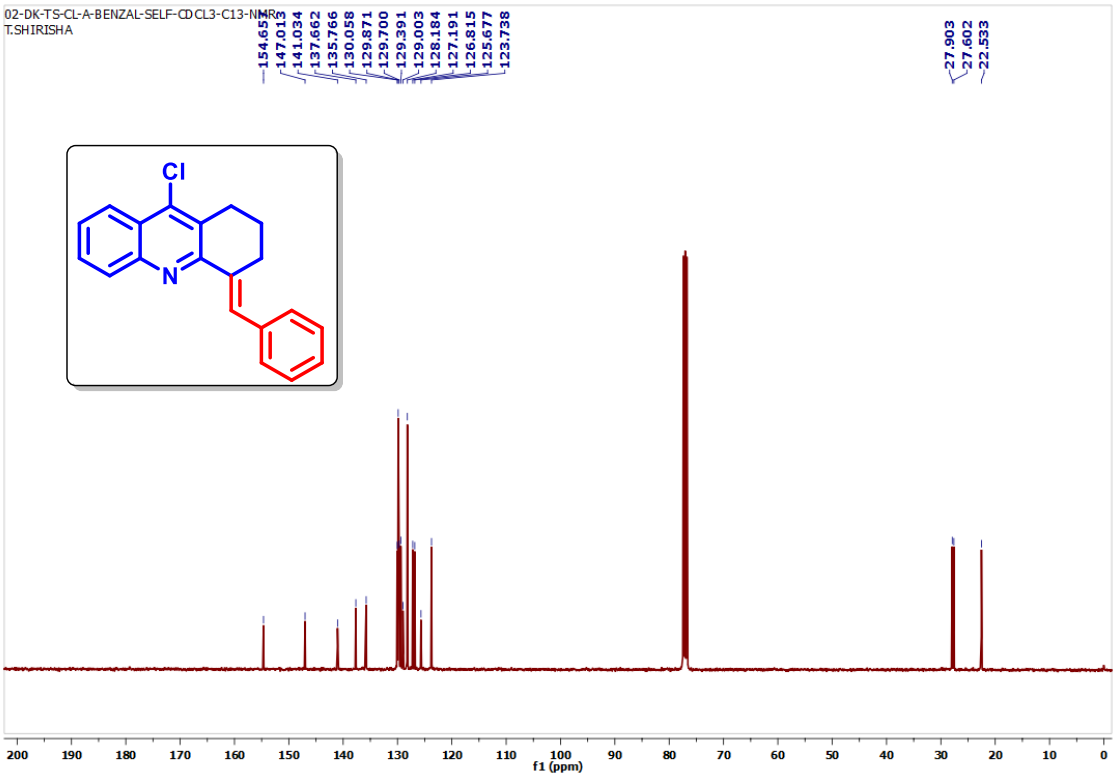

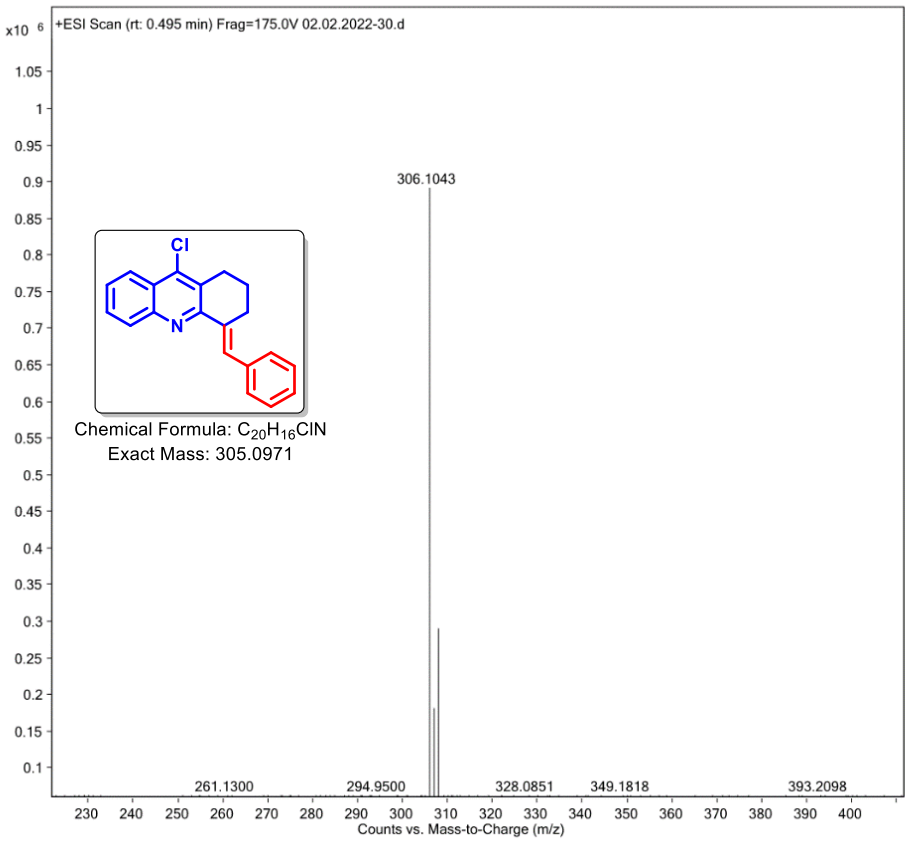

(E)-4-Benzylidene-1,2,3,4-tetrahydroacridin-9-amine (3a)

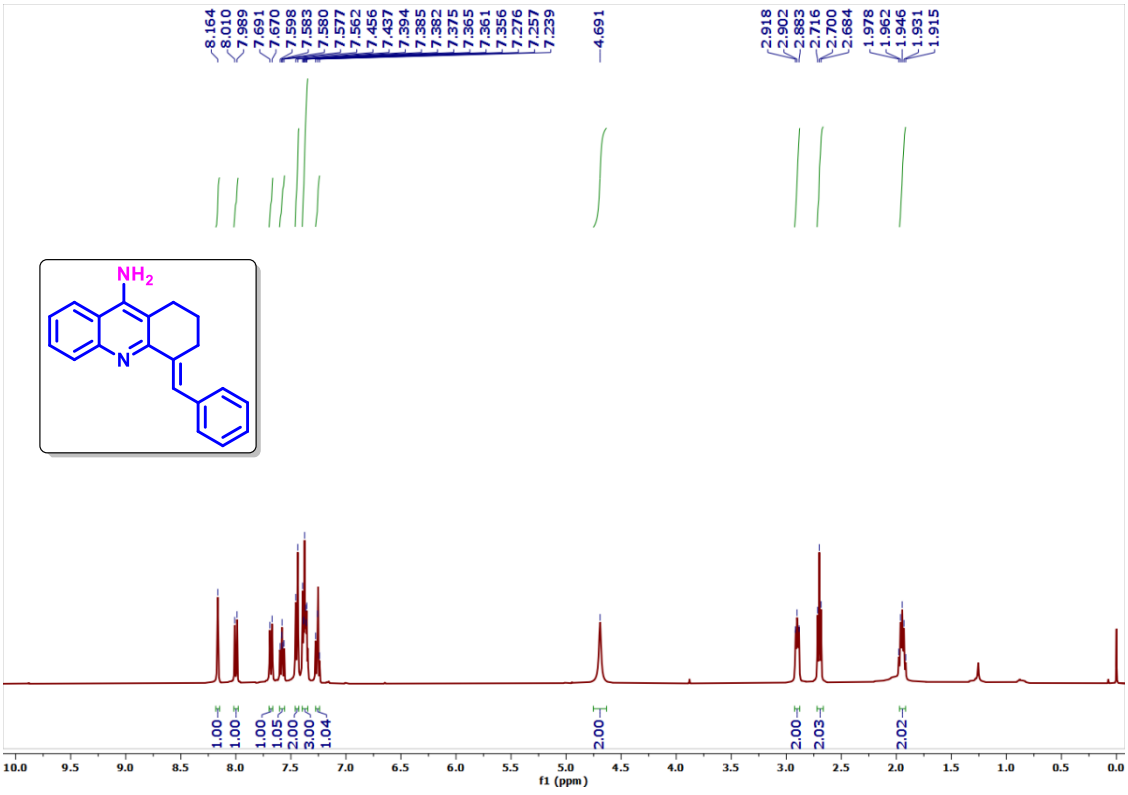

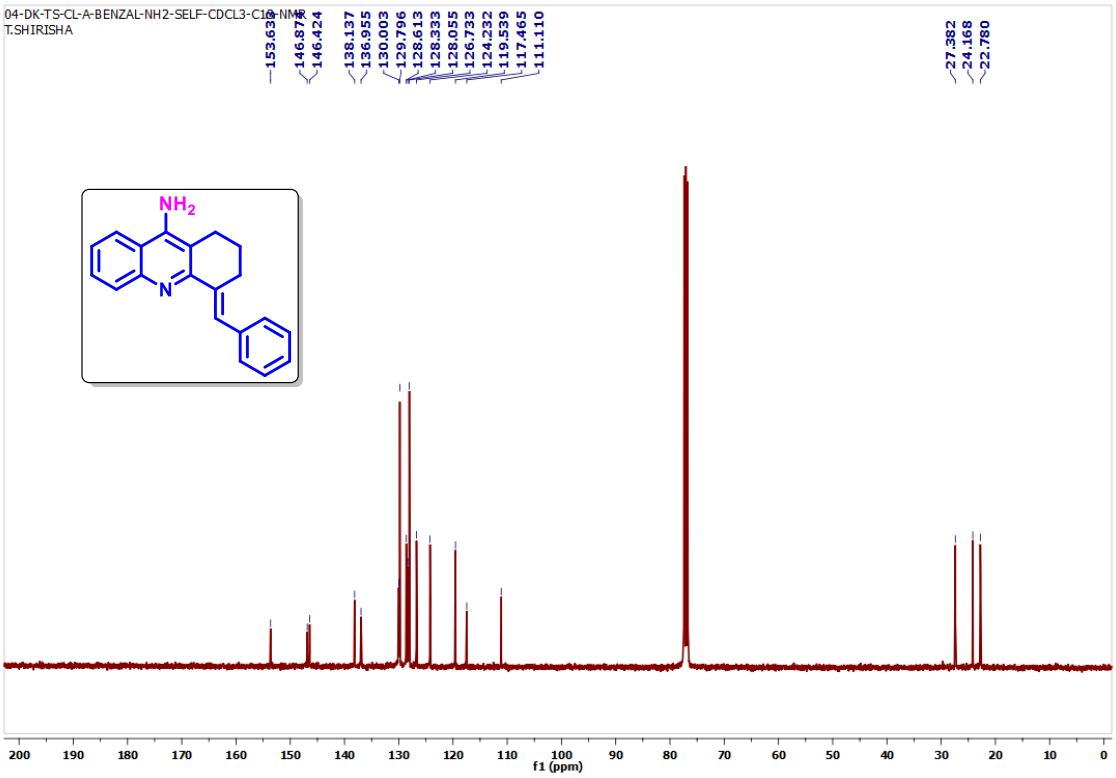
04-DK-TS-CL-A-BENZAL-NH2-SELF-CDCL3-C13-NMR
T.SHIRISHA
153.634
146.874
146.424
138.137
136.955
130.003
129.796
128.613
128.333
128.055
126.733
124.232
119.539
117.465
111.110
27.382
24.168
22.780
NH2
N
f1 (ppm)

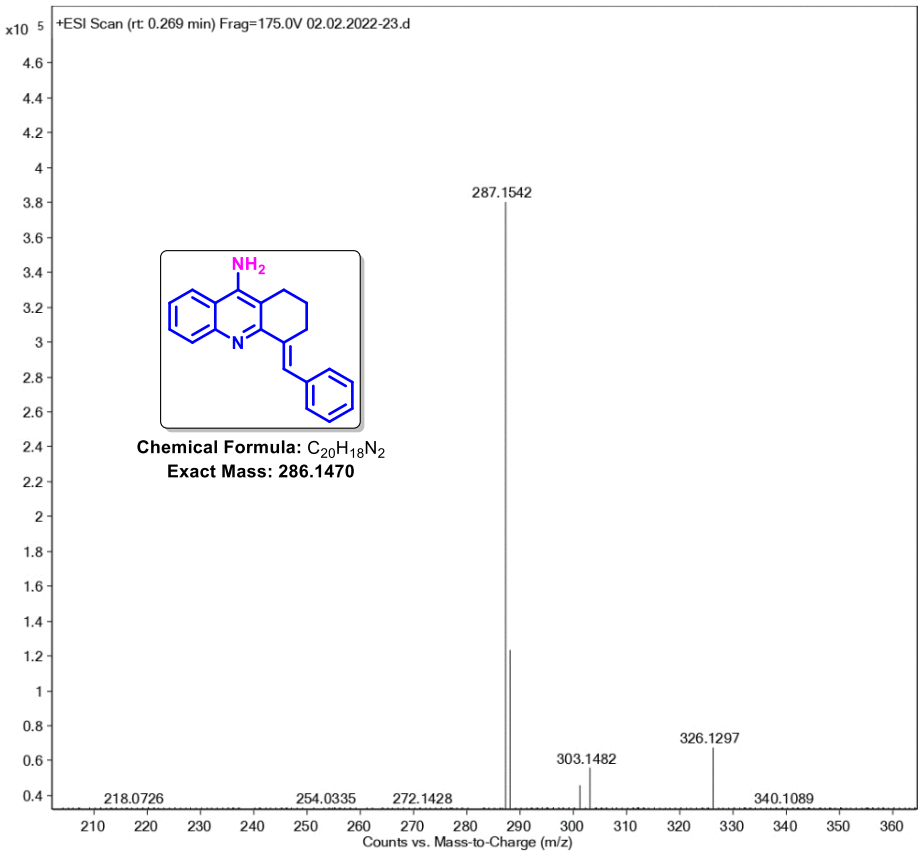
+ESI Scan (rt: 0.269 min) Frag=175.0V 02.02.2022-23.d
x10 5
287.1542
NH2
N
Chemical Formula: C20H18N2
Exact Mass: 286.1470
326.1297
303.1482
218.0726
254.0335
272.1428
340.1089
Counts vs. Mass-to-Charge (m/z)

(E)-N-(4-Chlorophenyl)-4-(4-methylbenzylidene)-1,2,3,4-tetrahydroacridin-9-amine (8d):

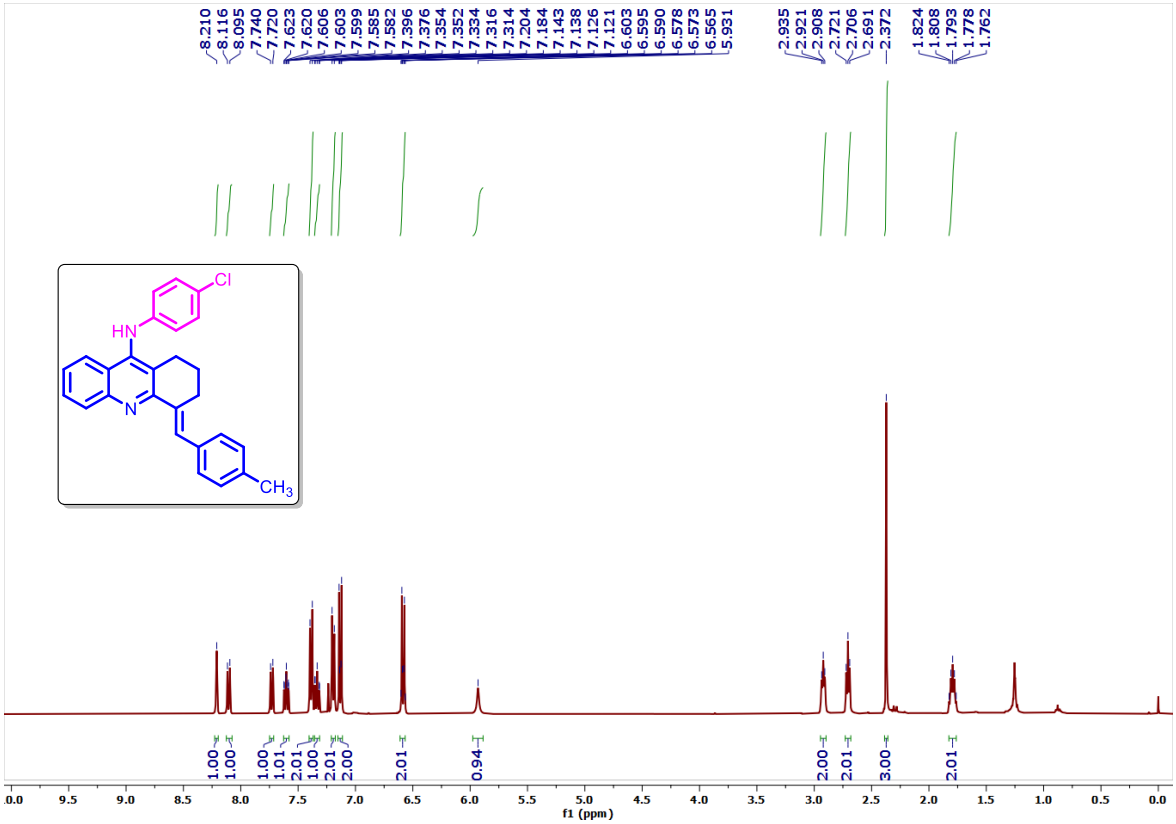

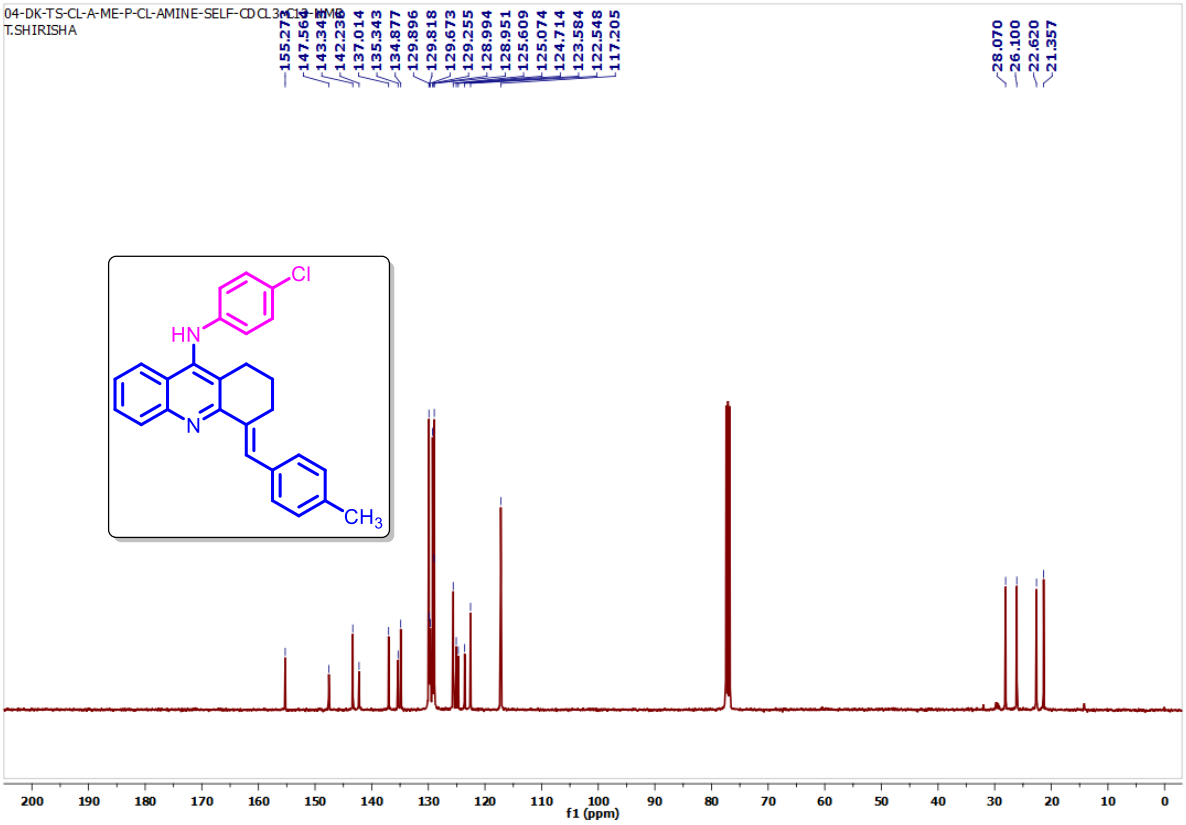

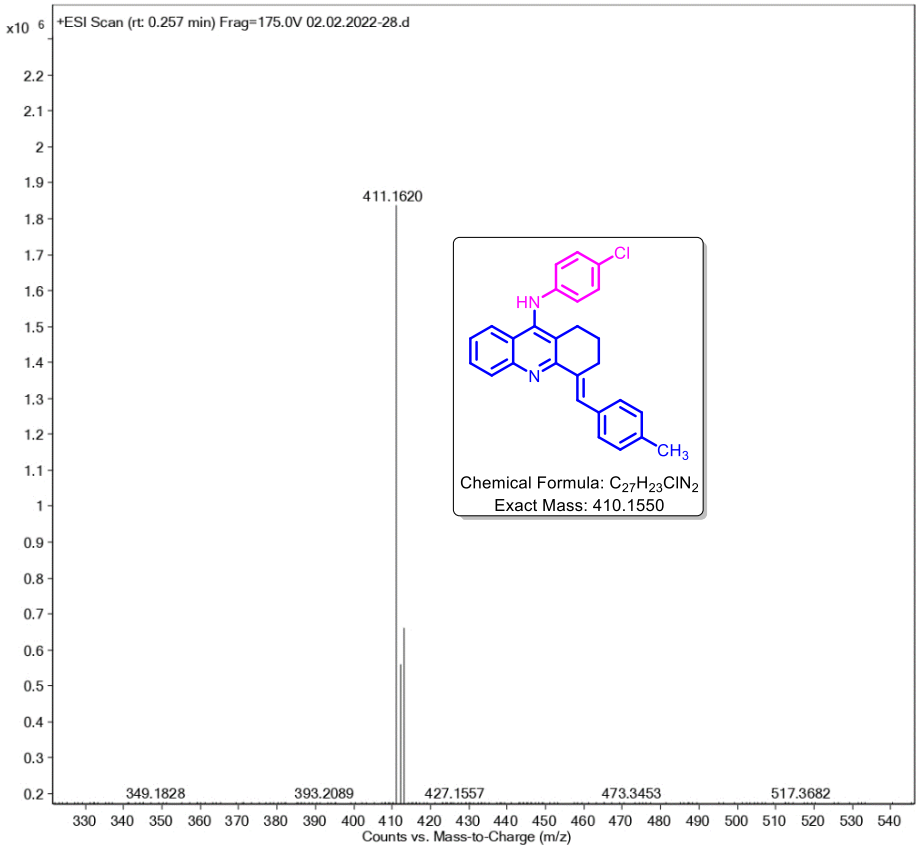

(E)-4-(4-Methylbenzylidene)-9-(4-(p-tolyl)-1H-1,2,3-triazol-1-yl)-1,2,3,4-tetrahydroacridine (10j):

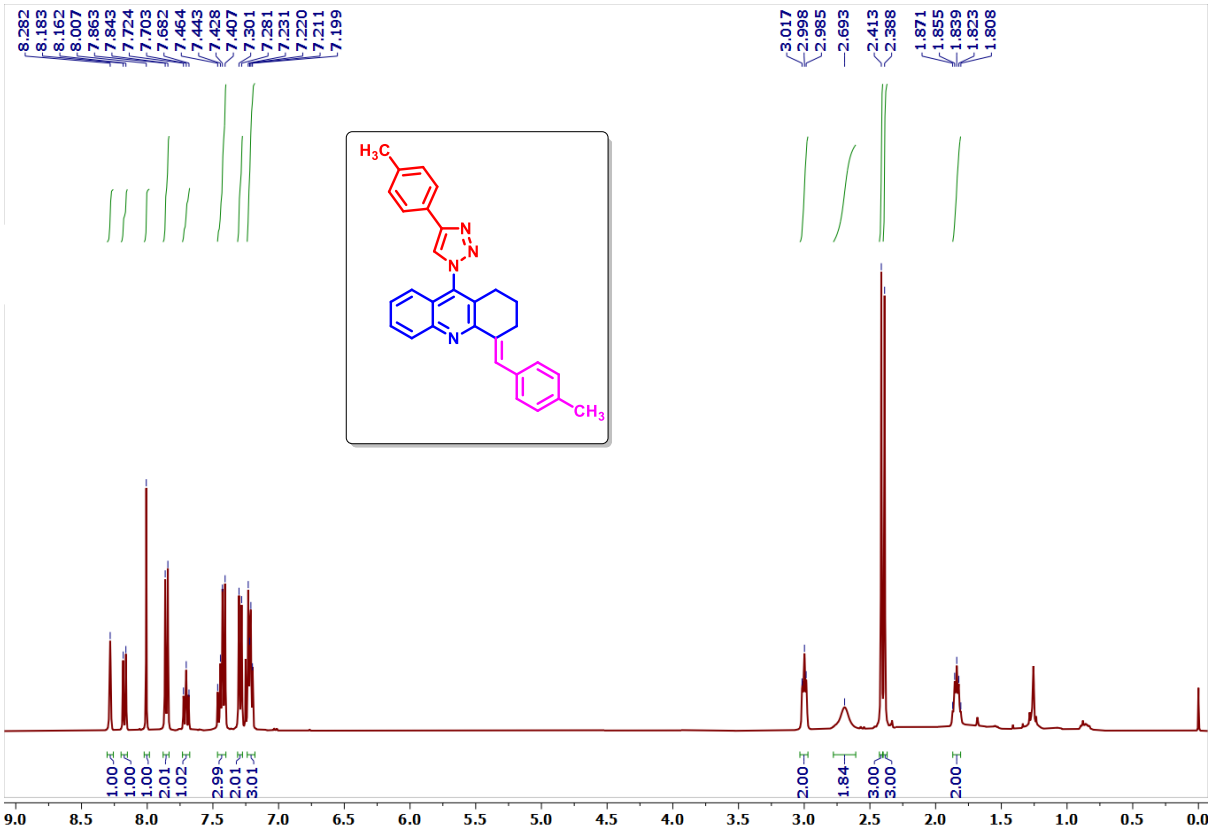

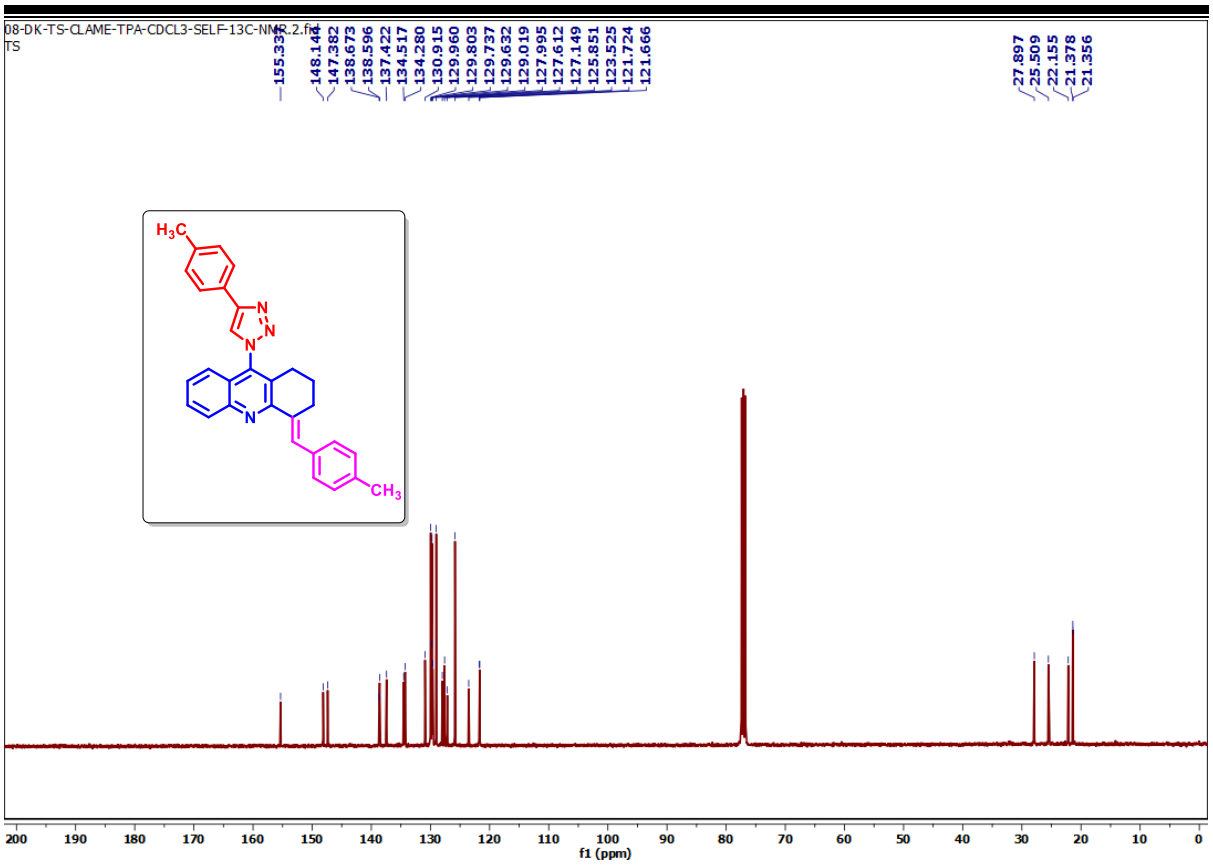
08-DK-TS-CLAME-TPA-CDCL3-SELF-13C-NMR-2.fid
TS
155.339
148.144
147.382
138.673
138.596
137.422
134.517
134.280
130.915
129.960
129.803
129.737
129.632
129.019
127.995
127.612
127.149
125.851
123.525
121.724
121.666
27.897
25.509
22.155
21.378
21.356
H3C
CH3
f1 (ppm)

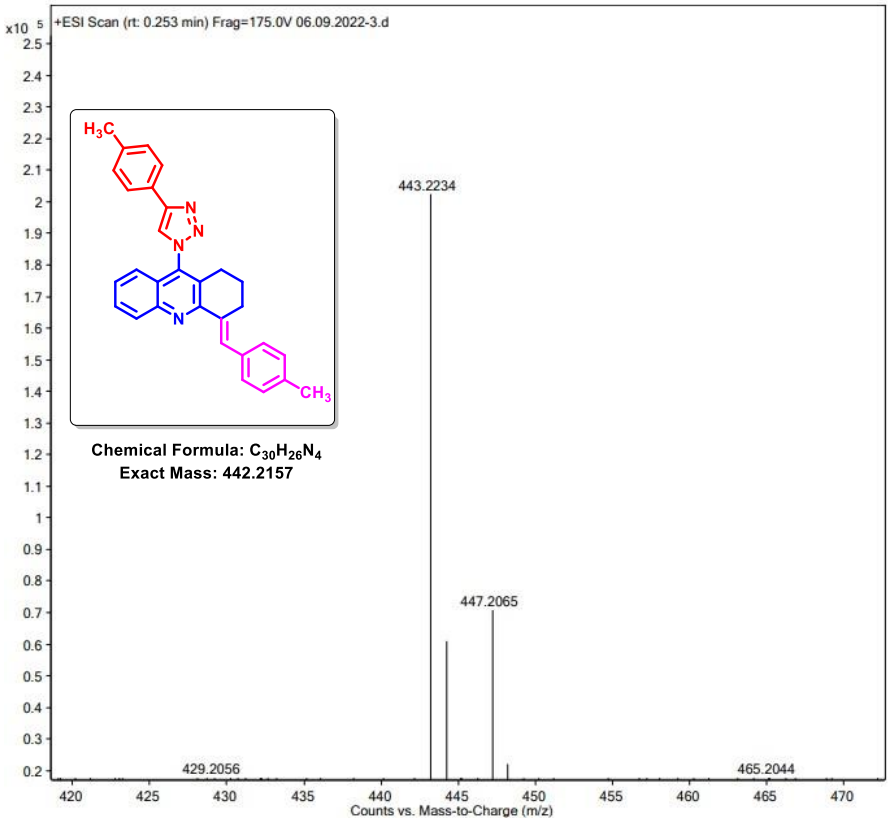
+ESI Scan (rt: 0.253 min) Frag=175.0V 06.09.2022-3.d
x10 5
H3C
CH3
Chemical Formula: C30H26N4
Exact Mass: 442.2157
443.2234
447.2065
429.2056
465.2044
Counts vs. Mass-to-Charge (m/z)

(1-(6-Nitro-1,2,3,4-tetrahydroacridin-9-yl)-1H-1,2,3-triazol-4-yl)methyl 1,2,3,4-tetrahydroacridine-9-carboxylate (13c):

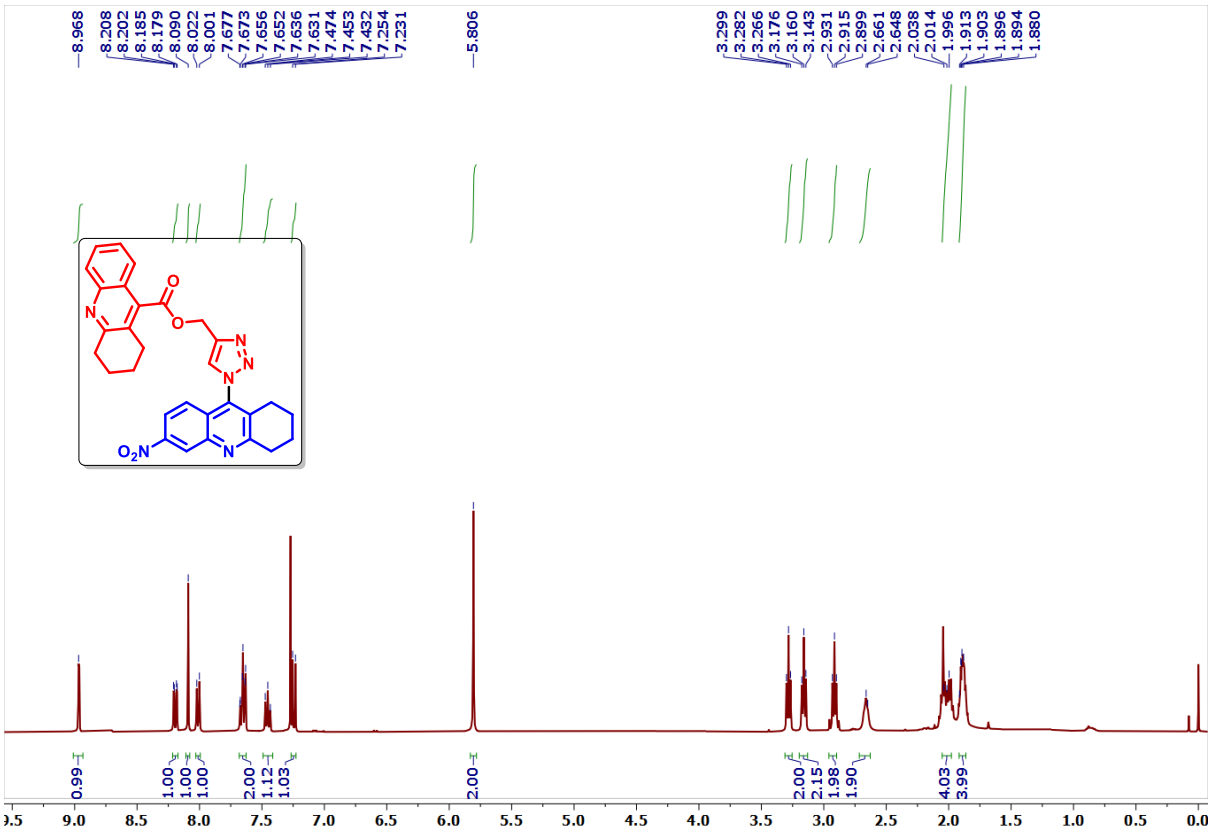

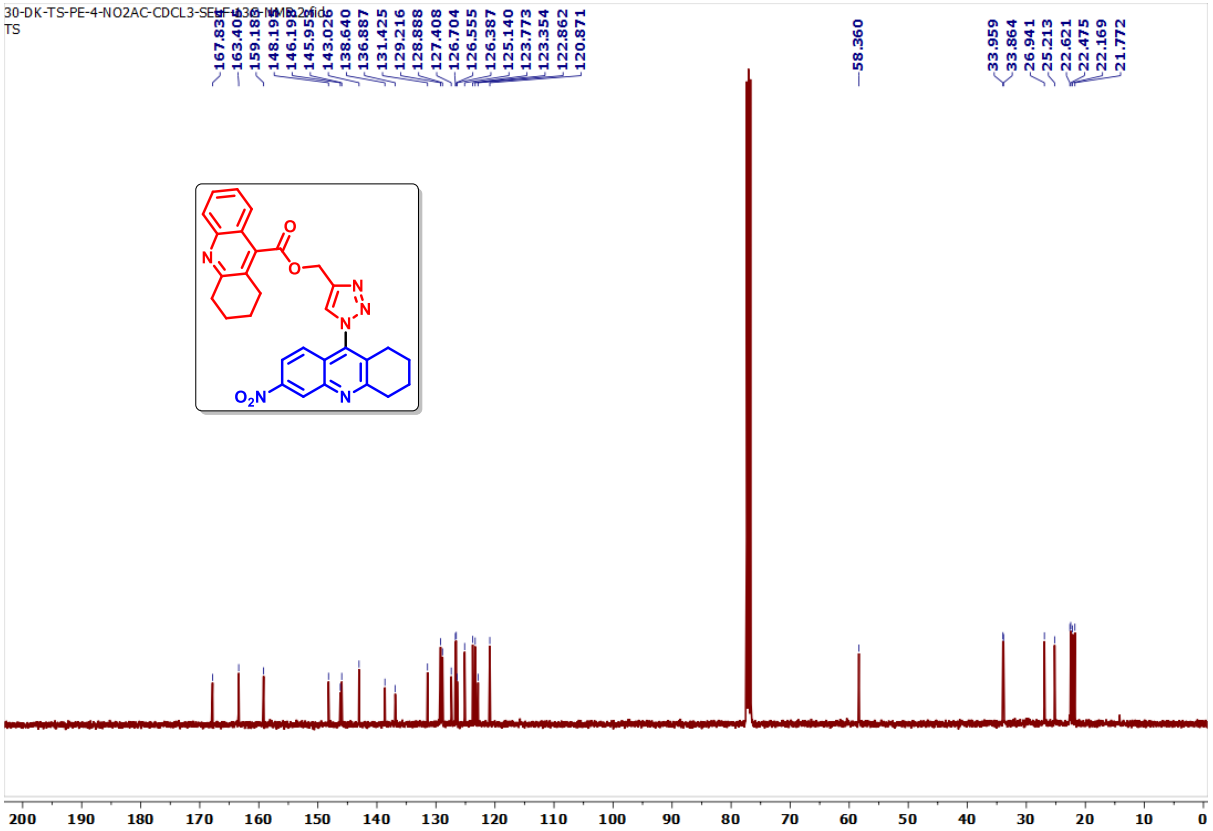

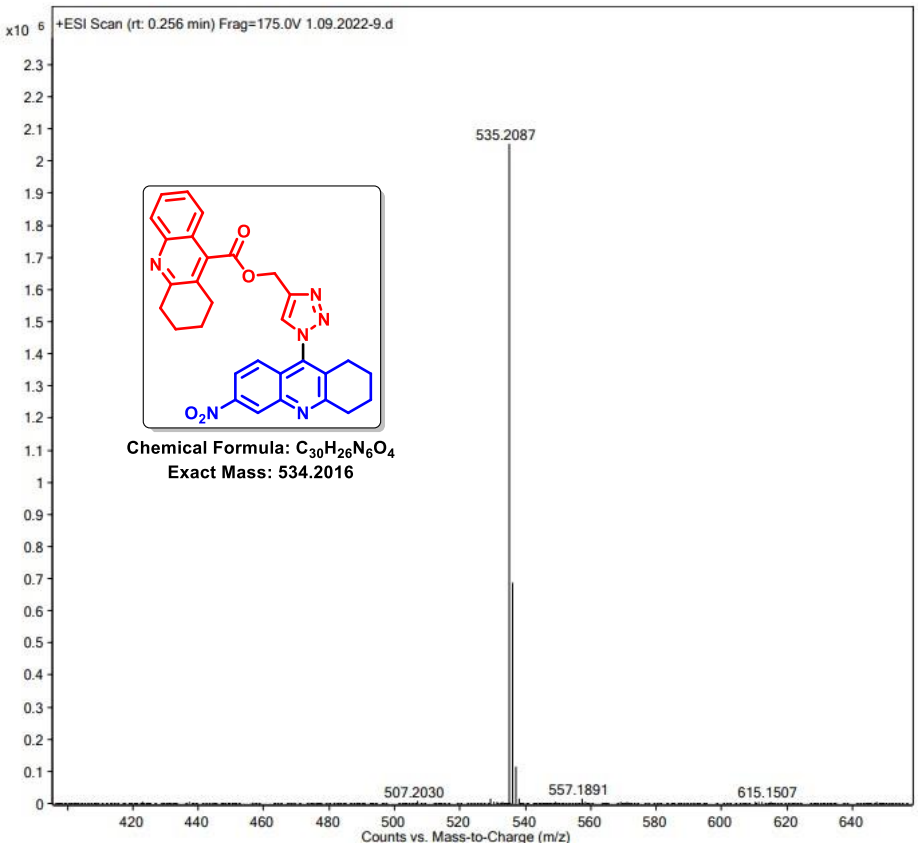

(E)-4-(4-Methoxybenzylidene)-1,2,3,4-tetrahydroacridine-9-carboxylic acid (16b):

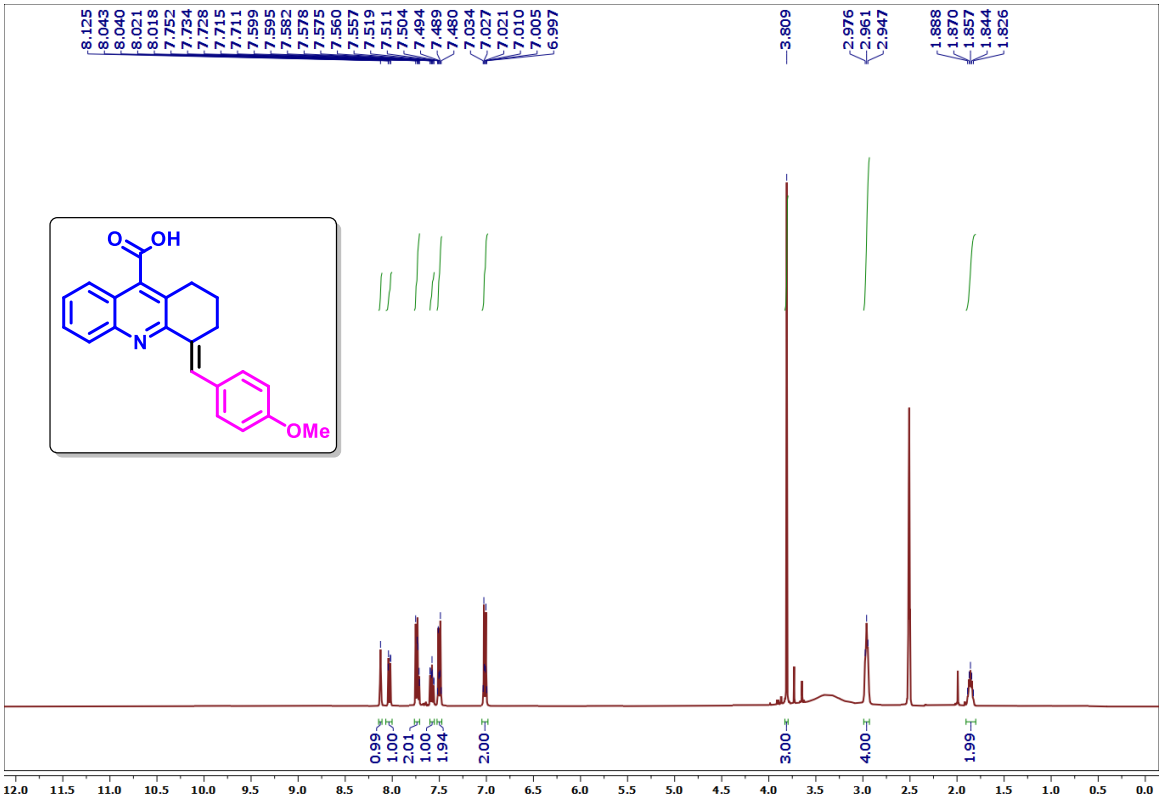

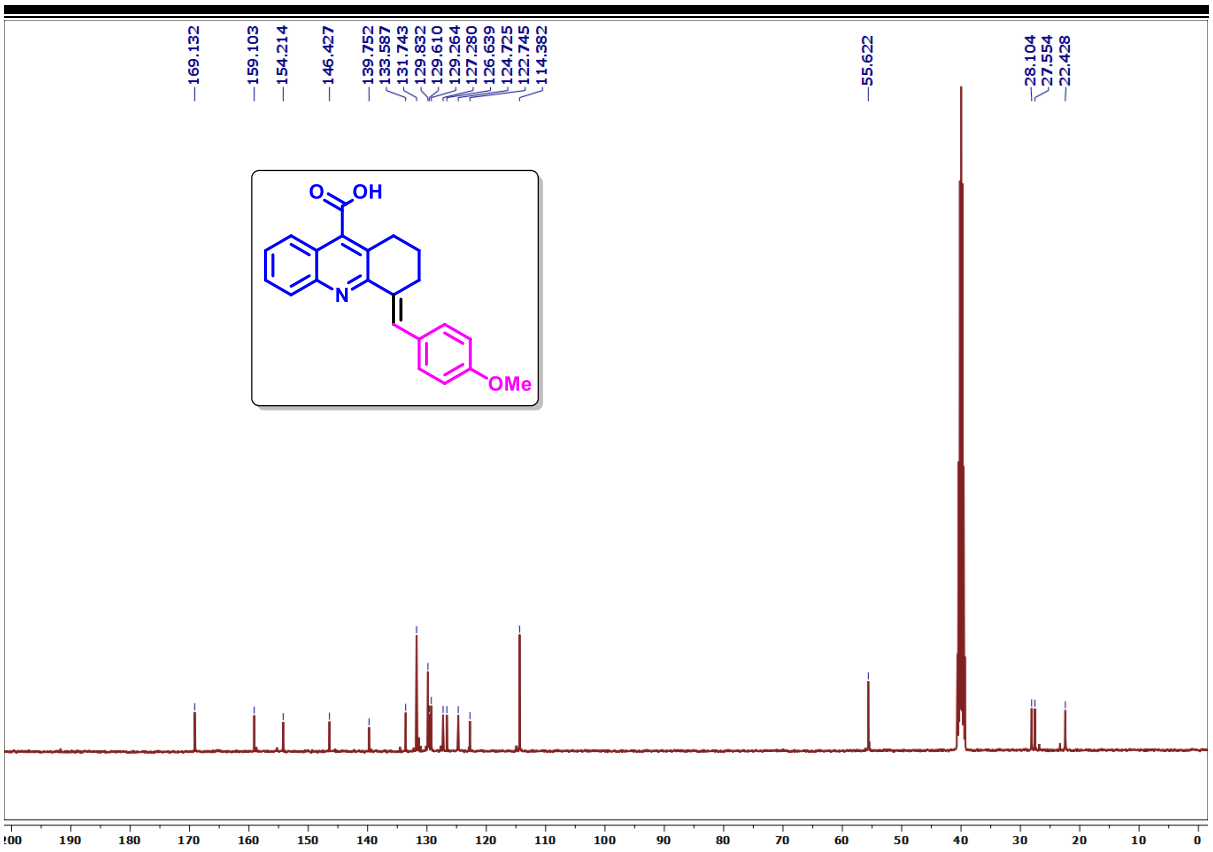
169.132
159.103
154.214
146.427
139.752
133.587
131.743
129.832
129.610
129.264
127.280
126.639
124.725
122.745
114.382
55.622
28.104
27.554
22.428
O
OH
N
OMe

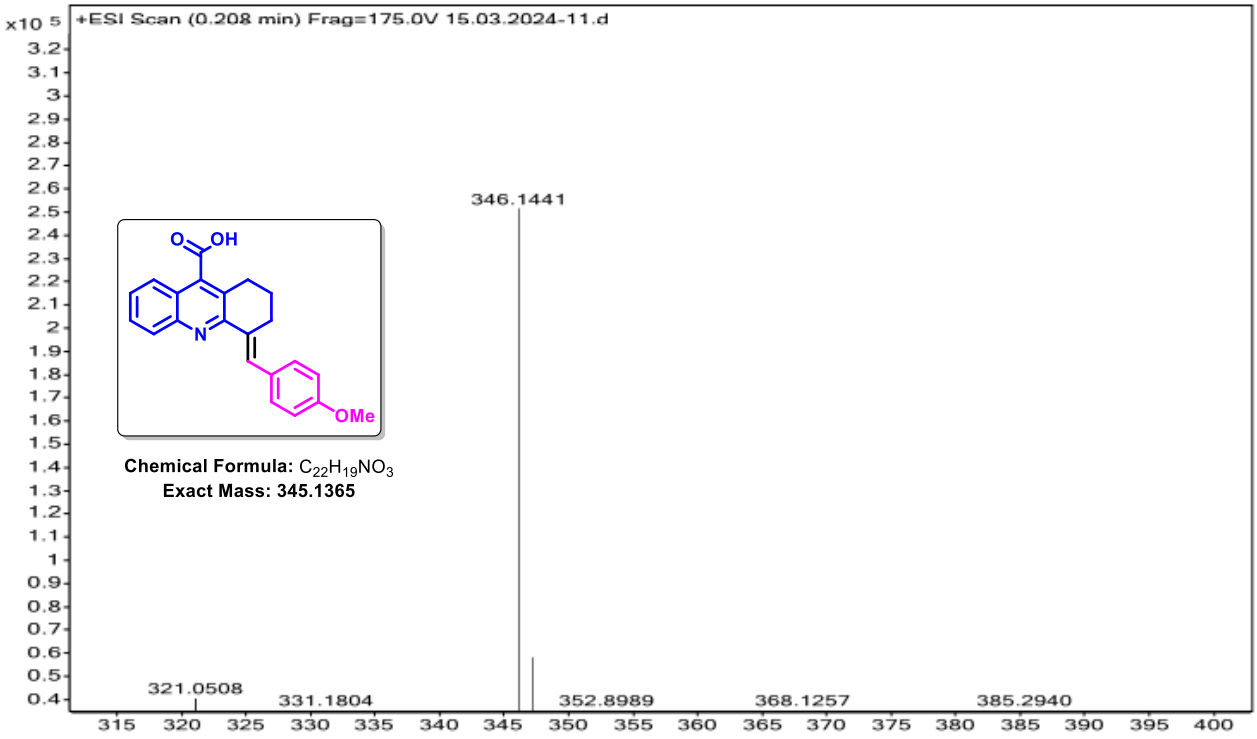
x10 5
+ESI Scan (0.208 min) Frag=175.0V 15.03.2024-11.d
346.1441
O
OH
N
OMe
Chemical Formula: C22H19NO3
Exact Mass: 345.1365
321.0508
331.1804
352.8989
368.1257
385.2940

Methyl (E)-4-(4-methylbenzylidene)-1,2,3,4-tetrahydroacridine-9-carboxylate (19c):

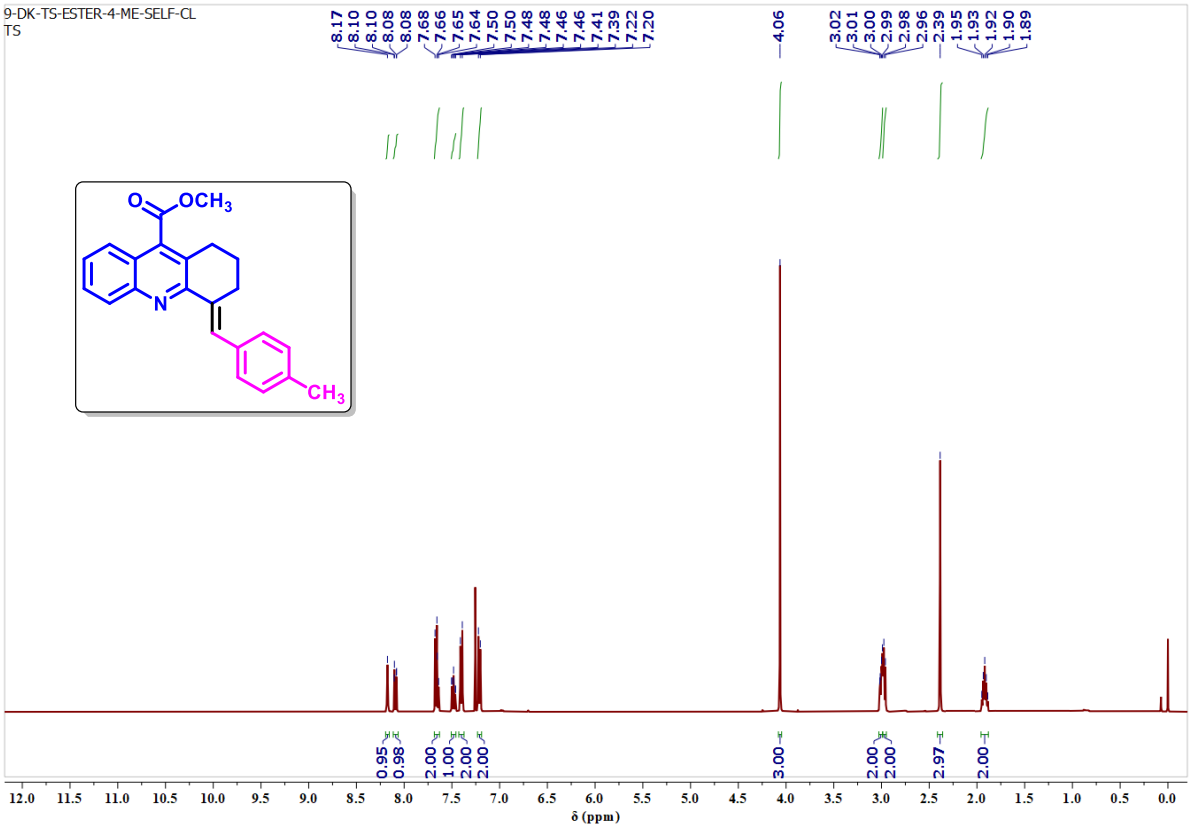

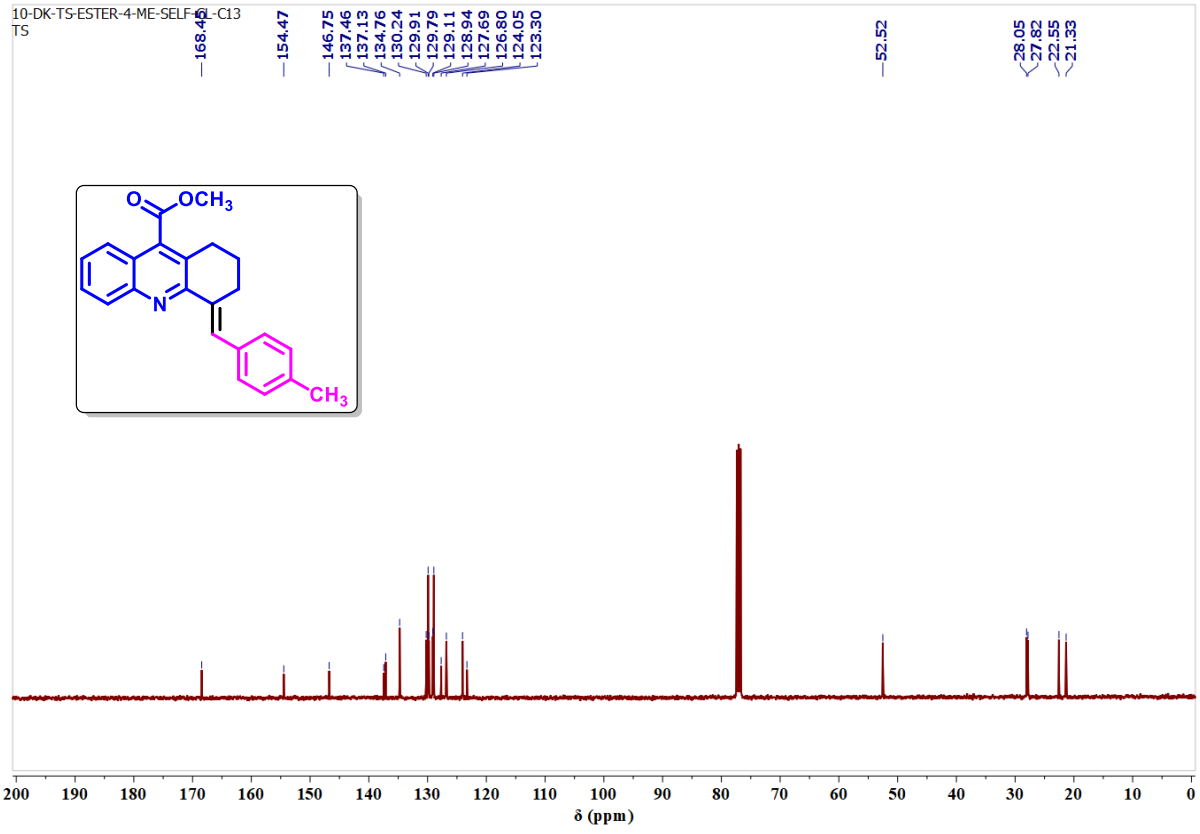

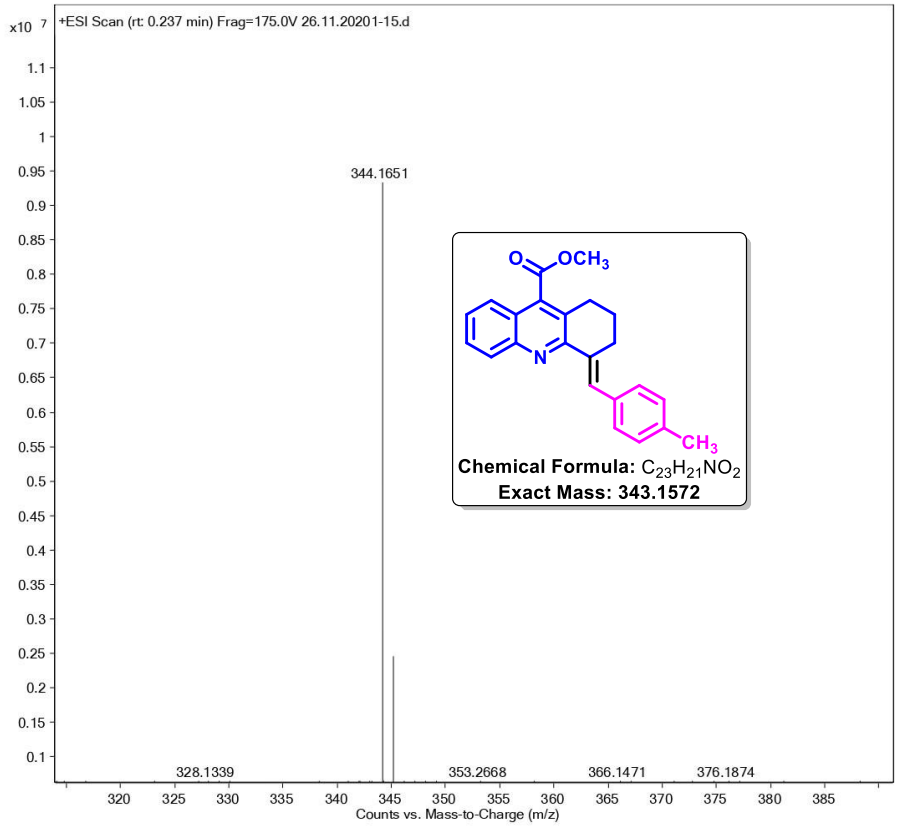

(E)-4-(4-(dimethylamino)benzylidene)-N-(p-tolyl)-1,2,3,4-tetrahydroacridine-9-carboxamide (22g):

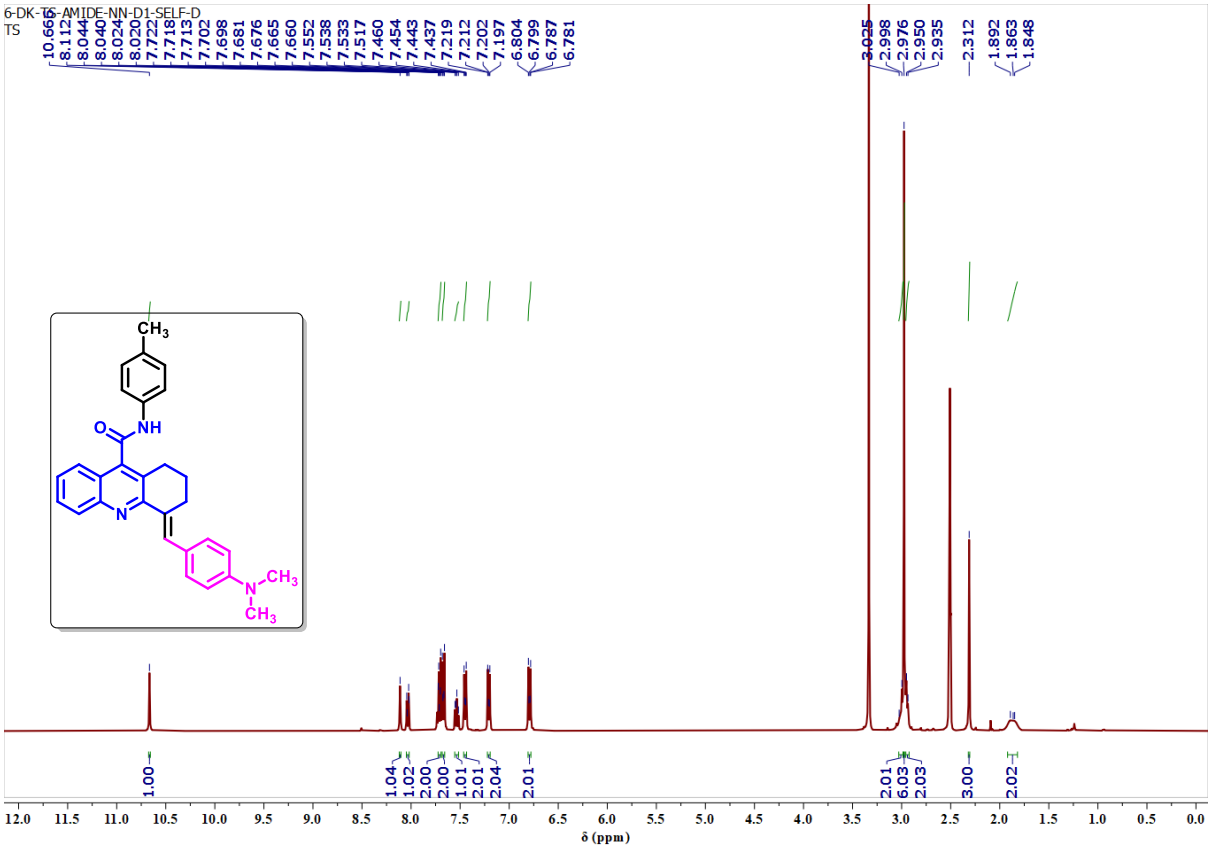

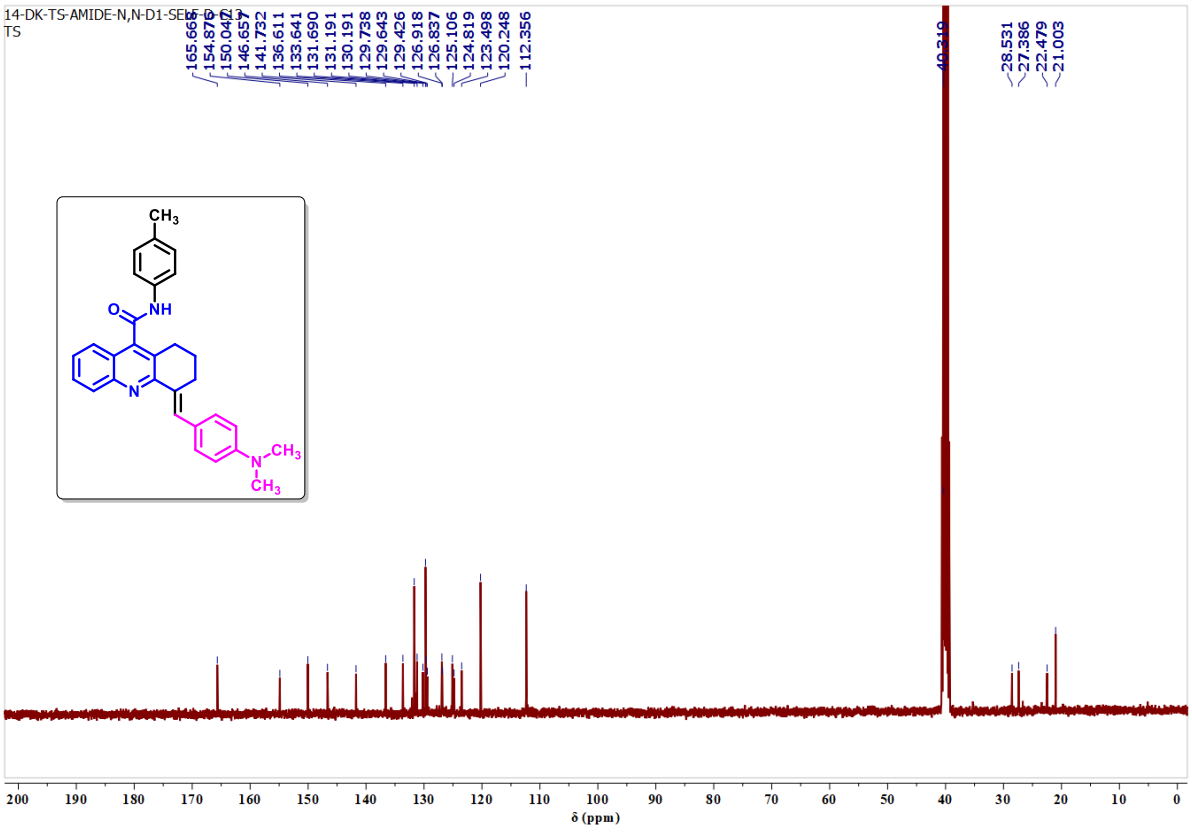
14-DK-TS-AMIDE-N,N-D1-SEQ 13
TS
165.668
154.876
150.042
146.657
141.732
136.611
133.641
131.690
131.191
130.191
129.738
129.643
129.426
126.918
126.837
125.106
124.819
123.498
120.248
112.356
40.310
28.531
27.386
22.479
21.003
δ (ppm)

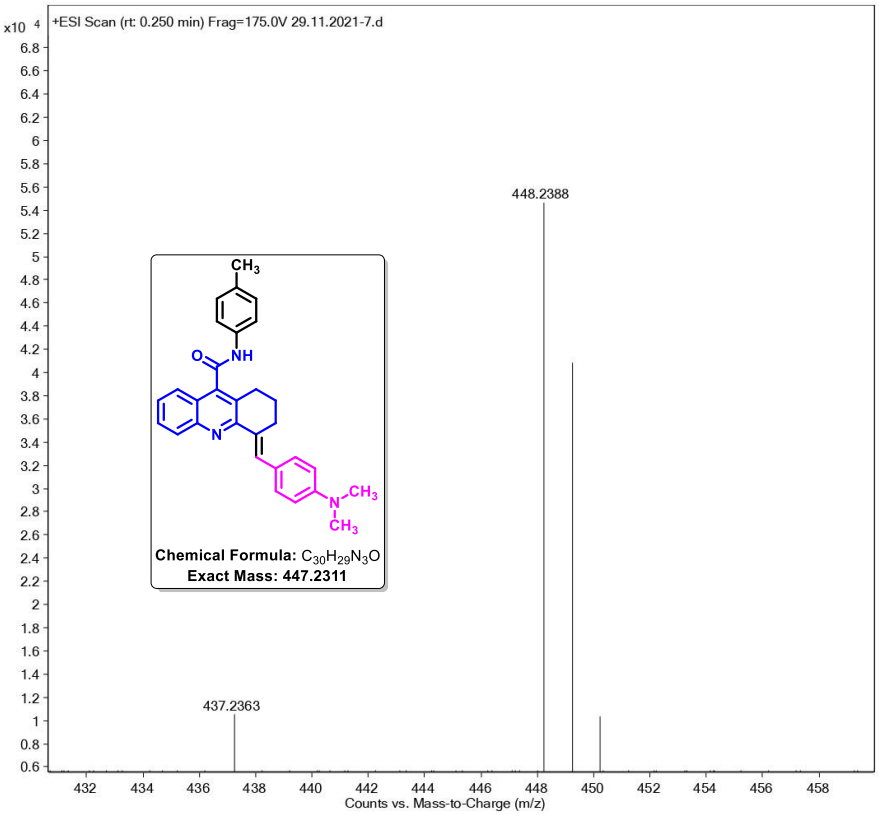
+ESI Scan (rt: 0.250 min) Frag=175.0V 29.11.2021-7.d
x10 4
448.2388
437.2363
Chemical Formula: C30H29N3O
Exact Mass: 447.2311
Counts vs. Mass-to-Charge (m/z)

(E)-N-methoxy-4-(4-methoxybenzylidene)-N-methyl-1,2,3,4-tetrahydroacridine-9-carboxamide (25b):

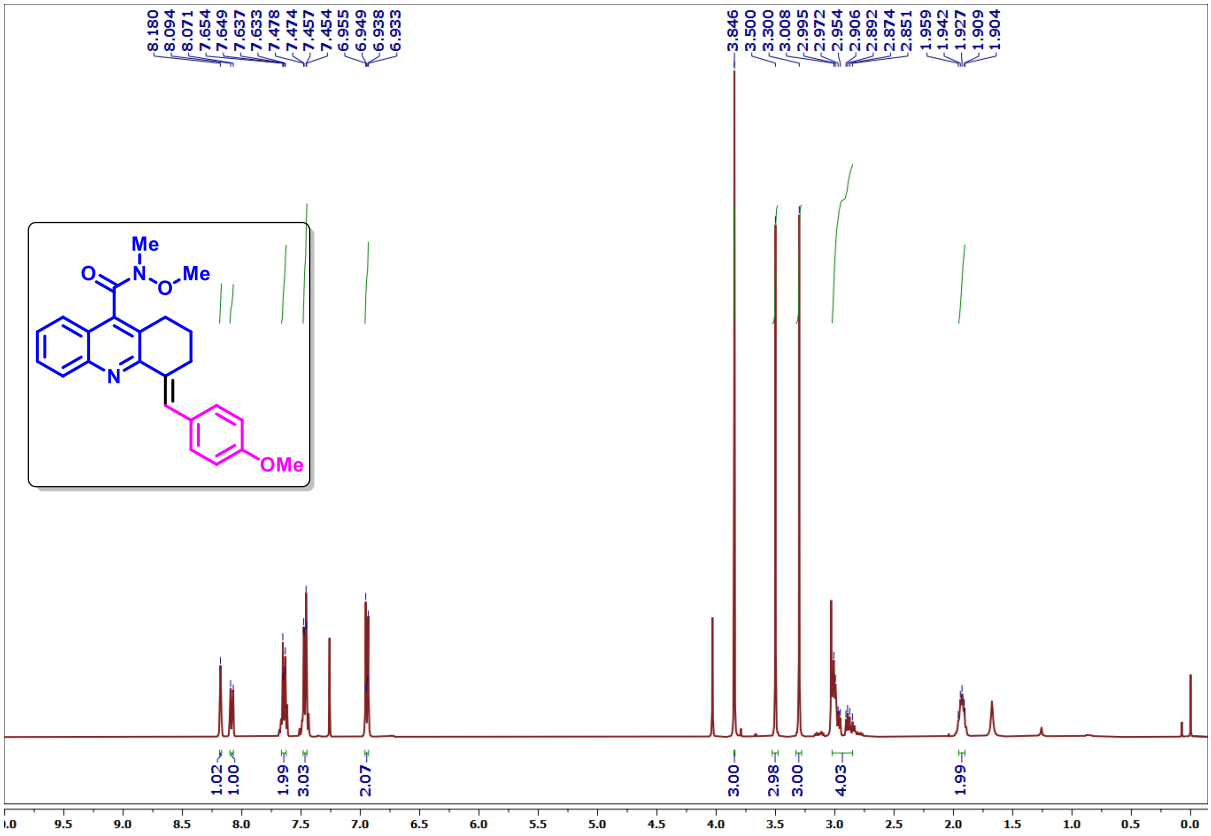

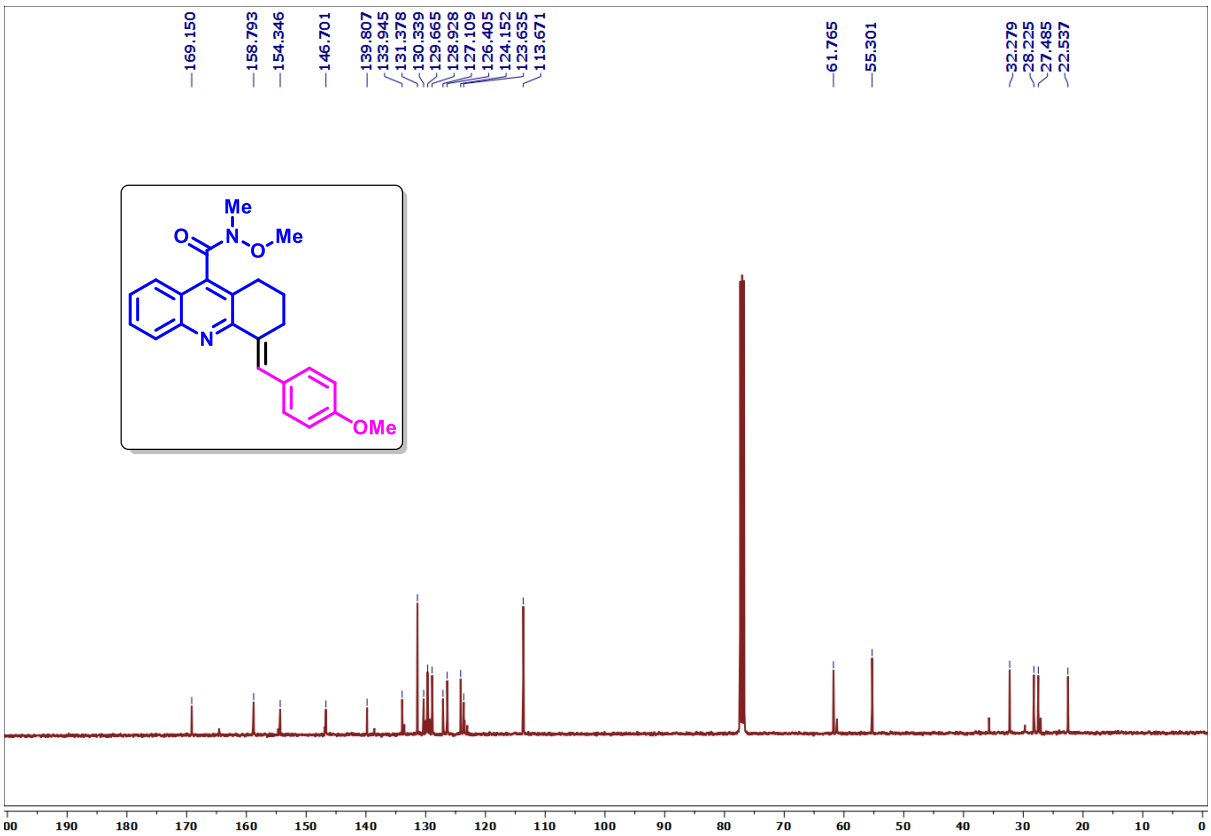

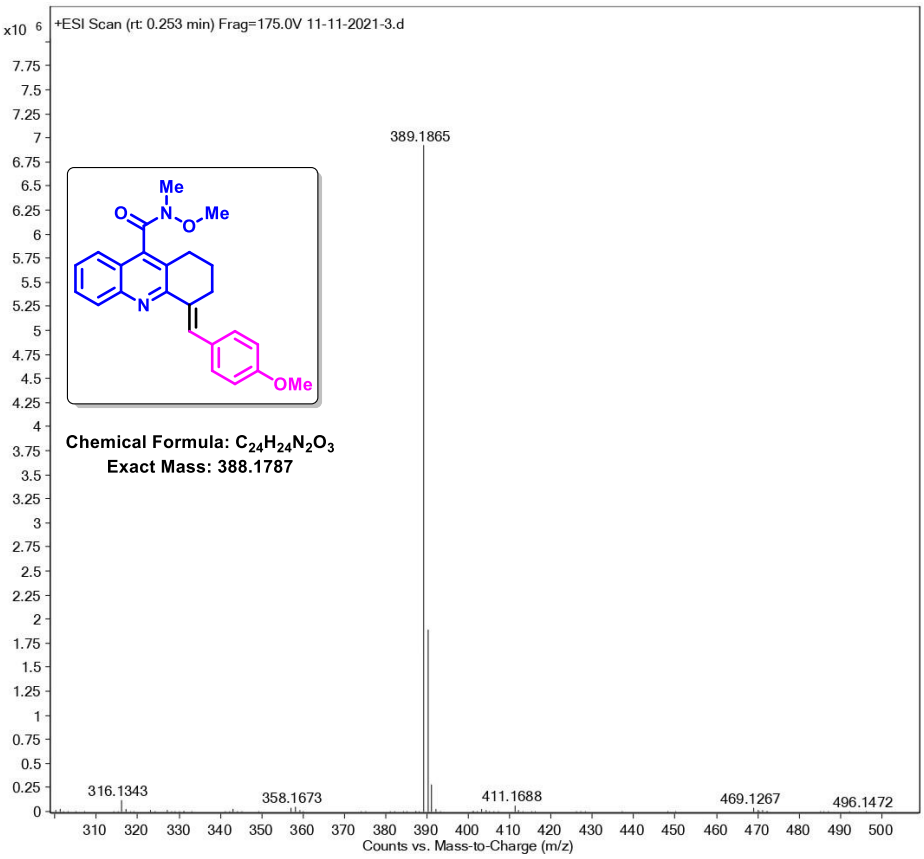
+ESI Scan (rt: 0.253 min) Frag=175.0V 11-11-2021-3.d
x10 6
389.1865
316.1343
358.1673
411.1688
469.1267
496.1472
Me
O
N
O
Me
N
OMe
Chemical Formula: C24H24N2O3
Exact Mass: 388.1787
Counts vs. Mass-to-Charge (m/z)

CHAPTER-3

Chapter-3

Part-A: Metal-free C4 C(sp^3)-H functionalization of 1,2,3,4-tetrahydroacridines using dialkyl azodicarboxylates and N-phenylmaleimide in Deep Eutectic Solvent

Part-B: TBHP-TBAI Mediated synthesis of 2,3-dihydroacridin-4(1H)-ones via C4 C(sp^3)-H sulfonylation and desulfonylation of 1,2,3,4-tetrahydroacridines

Part-C: DDQ Mediated synthesis of acridin-4-yl(aryl)methanones via aromatization-C(sp^2)-H oxidation sequence of C4-functionalized 1,2,3,4-tetrahydroacridine derivatives

Abstract

The functionalization of inactive C-H bond is one of the contemporary methods for C-C and C-X (X=O, N, S) bond formation in organic synthesis. In comparison to the cross-coupling reactions, C-H functionalisation removes the requirement for pre-functionalization of both partners. Also, C−H activation has the advantage of decreasing step count and hence offers maximum atom efficiency of chemical processes. In this context, this chapter deals with the deep eutectic solvent mediated C-C, C-N bond formation and TBAI, TBHP mediated C-S bond formation via C4 (sp^3)-H functionalization of 1,2,3,4-tetrahydroacridine derivatives and also, describes the DDQ mediated aromatization of C4 functionalised 1,2,3,4-tetrahydroacridine derivatives.

Chapter-3

Part-A: Metal-free C4 C(sp³)-H Functionalization of 1,2,3,4-Tetrahydroacridines using Dialkyl azodicarboxylates and *N*-Phenylmaleimide in Deep Eutectic Solvent

3.1.1. Introduction

Direct functionalization of inactive C–H bonds is a current topic of research and strategy for the construction of C–C and C–X (X=O, N, S) bonds in organic synthesis.[1] This method can offer a maximum atom efficiency by avoiding pre-functionalization of substrates thus widely explored in the fields of synthetic organic chemistry.[2] The C(sp³)-H functionalised 2-alkyl azaarenes are important heteroarenes, and play a crucial role in the natural compound synthesis and drug discovery. The development of mild, general, and efficient methods for direct C-H functionalisation of 2-alkyl azaarenes ~~core~~ has stimulated tremendous research efforts. This strategy has enabled the construction of various C–C bonds with great efficiency and selectivity *via* nucleophilic addition. Similarly, the development of a new catalytic system for the direct amination of inert C(sp³)–H bonds without the use of pre-functionalized substrates to construct C–N bonds remains one of the major challenges.[3] Due to the inert nature of the C(sp³)–H bond, the hydrogen atom transformation (HAT) strategy, and *N*-oxyl radicals provide a potent synthetic approach to access the desired functionalization.[4] The inert C–H bond amination has been achieved by the addition of carbon nucleophiles to N=N *via* electrophilic amination.[5]

Dialkyl azodicarboxylates serve as valuable reagents in Mitsunobu chemistry.[6] Besides this dialkyl azodicarboxylates are used as electrophiles for C–N bond formation reactions *via* nucleophilic addition.[7,8,9] Similar to dialkyl azodicarboxylates, maleimides display versatile reactivity, participating in both electrocyclic processes as dienophiles and in conjugate addition as electrophiles.[10] In addition to these, maleimides have been explored as the source for alkylation in transition metal-catalysed C(sp³)–H and C(sp²)–H bond functionalization leading to the generation of functionalized succinimides.[11] Due to the highly electrophilic nature of the unsaturated system, maleimides act as an excellent alkylating agent, because of which they participate in hydroarylation/alkylation reactions instead of oxidative Heck reactions.[12] In many cases the generated succinimides were used as precursors for the biologically active pyrrolidines and γ-lactams, thereby becoming one of the important and promising scaffolds in drug discovery.[13]

3.1.2. Previous reports

Hung[3] and Guo[5] groups reported transition metal catalysed amination of unactivated C(sp^3)–H bond of 2-alkyl azaarenes with diethyl azodicarboxylate. Similarly, Saget and co-workers also reported Zn-ProPhenol catalysed amination of un-activated aryl and vinyl ketones with di-*tert*-butyl azodicarboxylate.[14] Later, Benoit et al.[15] developed an efficient method for the amination of arenes with azodicarboxylates (**Fig. 3.1.1**).

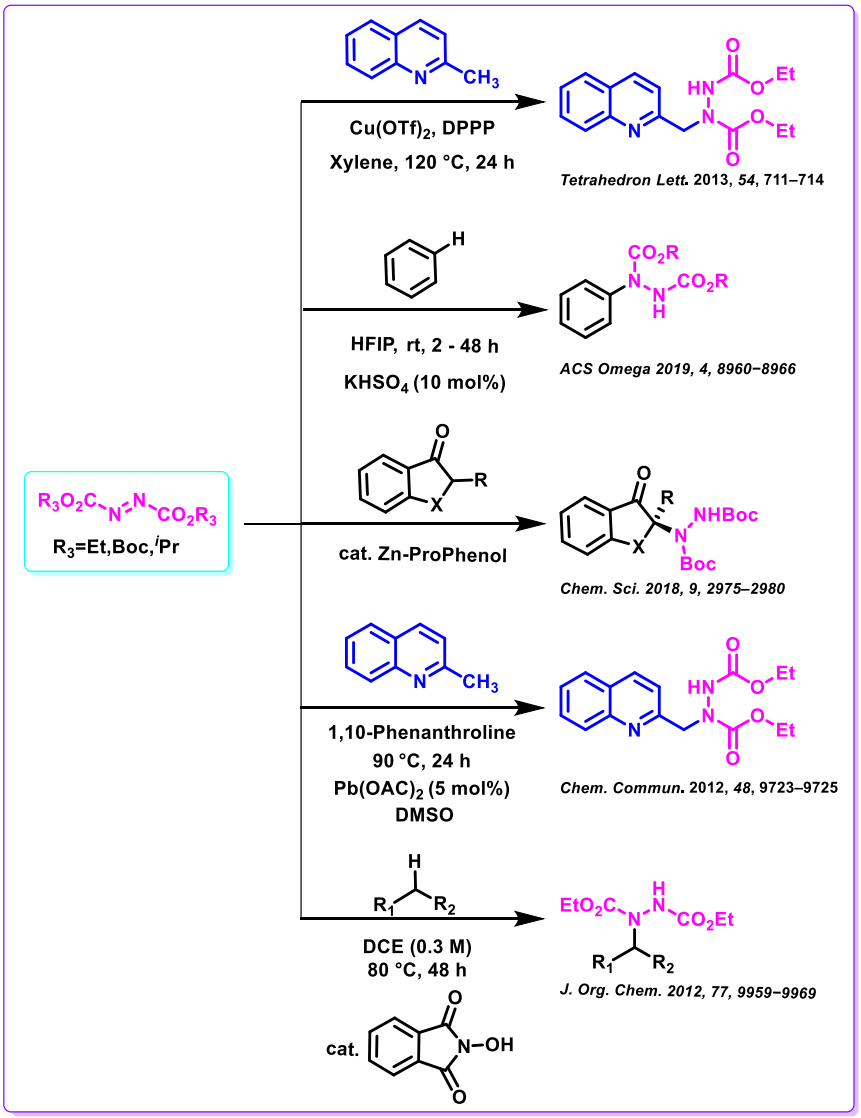

Figure 3.1.1 Reported methods for C–N bond formation *via* C(sp^3)–H functionalization

The synthetic utility of maleimide as an alkylating agent was further extended for the C(sp^3)–H functionalization of azaarenes. In this regard, Wang et al.[16] reported a catalyst-free C(sp^3) –H functionalization of 2-methyl quinoline. Similarly, Geo et al.[17] reported C(sp^3) –H functionalization of 2-methyl quinoline using pepsin, ionic liquid, and deep eutectic as reaction medium (**Figure 3.1.2**). Sharma and his group[11d] reported C(sp^3)-H alkylation of 8-methyl

quinoline with maleimides using Co(III) catalysed method. Han et al.[11e] described a Rh(III) catalysed functionalisation of C (sp^3)-H of 8-methylquinoline with maleimides. Similarly, Chen and co-workers[12e] explored Co(III) catalysed C(sp^3)-H alkylation of 8-methyl quinoline using maleimides as alkylating agents.

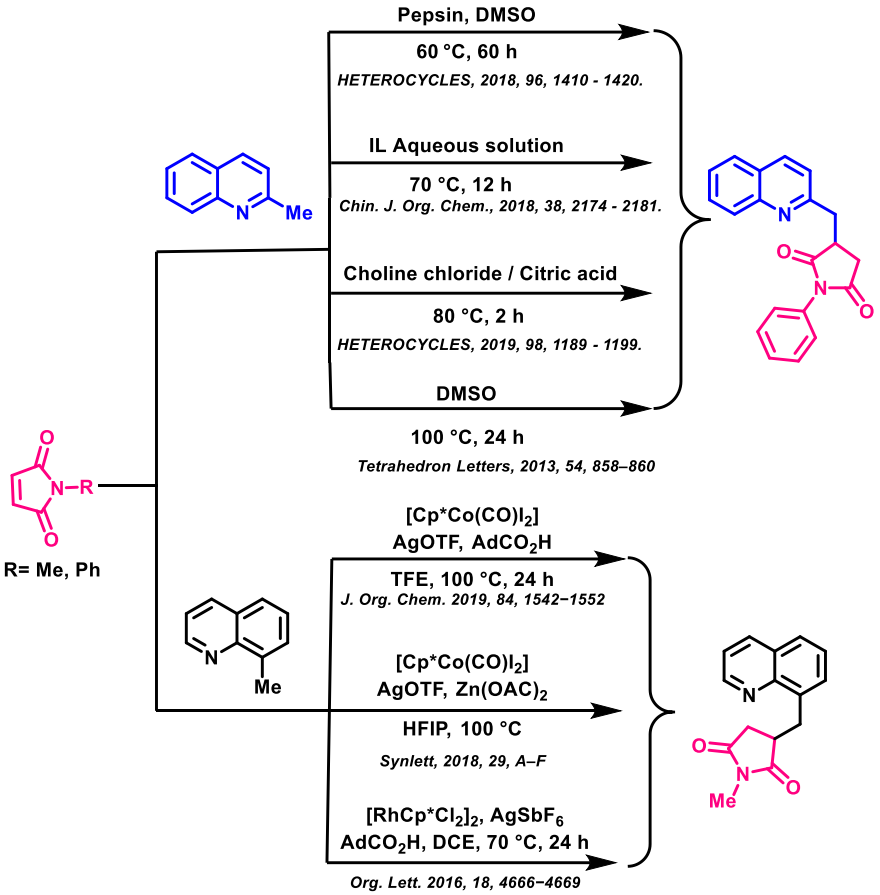

Figure 3.1.2 Reported methods and present work for C–C bond formation *via* C(sp^3)–H functionalization

3.1.3 Present work

In continuation with our efforts towards metal-free chemistry for C(sp^3) –H functionalization of 1,2,3,4-tetrahydroacrines for C-C and C-N bond formation,[18] we envisaged applying the DES strategy for the synthesis of biologically active C4 functionalised 1,2,3,4-tetrahydroacrines derivatives.

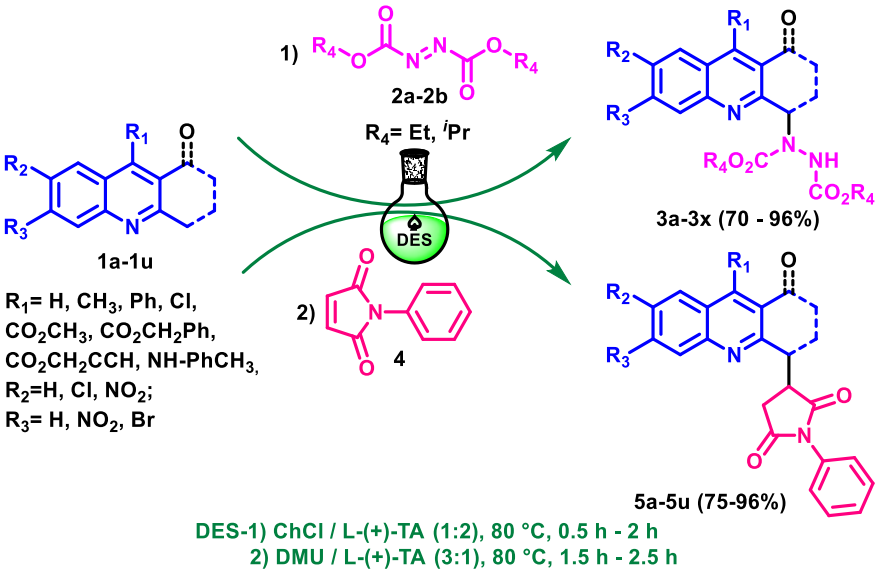

Figure 3.1.3 Present strategy for C-N, C-C bond formation at C4 position of 1,2,3,4-tetrahydroacridine

3.1.4. Results and discussion

Initially, the model reaction was conducted using 1,2,3,4-tetrahydroacridine (**1a**) and diethyl azodicarboxylate (**2a**) under DES* conditions [i.e. *N,N'*-Dimethyl Urea (DMU) + L-(+)-Tartaric Acid (L-(+)-TA) (3:1) at 80 °C; 2h]. However, the formation of the desired product was observed in only 75% (**Scheme 3.1.1)**. After confirmation of the product using complementary spectra data, and to find a better reaction condition, a series of experiments were performed in the presence of various combinations (hydrogen bond donor-acceptor) of DES systems. Among the tested DESs, a combination of ChCl/L-(+)-TA (1:2) at 80 °C (**Table 3.1.1**; entry 12) was found to be the optimum reaction condition, giving the desired product with 92% yield in 45 min. It was noticed that the temperature variations between 70 °C and 100 °C significantly influenced both the yield of the desired product and the reaction time. However, the unconsumed starting material was recovered in certain cases even after longer reaction times.

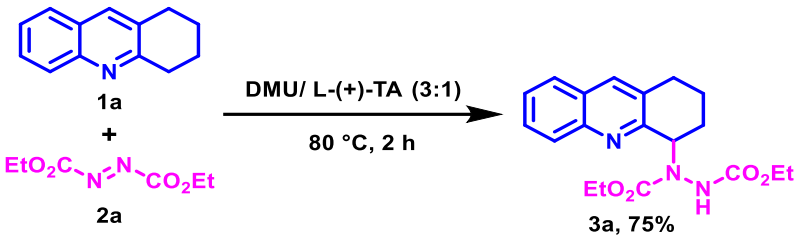

Scheme 3.1.1 Initial attempt for C –N formation *via* C (sp^3) –H functionalization.

Table 3.1.1 Optimisation table[a]

S.No.	DES	Temp (°C)	Time (h)	Yield (%) [b]
1	DMU/ L- (+)-TA (3:1)	80	2	75
2	DMU/ L-(+)-TA (3:1)	90	6	70
3	DMU/ L- (+)-TA (2:1)	80	4	55
4	ChCl/ citric acid (1:2)	80	5	10
5	ChCl/ oxalic acid ((1:2)	80	3	30
6	ChCl/ thio Urea	90	2	10
7	ChCl/ *p*-TSA	100	3	ND
8	ChCl/ DMU	80	3	20
9	ChCl/ $ZnCl_2$	80	3	ND
10	ChCl/ Urea	80	3	ND
11	ChCl/ L-proline	80	3	ND
12	**ChCl/ L-(+)-TA (1:2)**	**80**	**45 min**	**92**
13	ChCl/ L- (+)-TA (1:2)	90	3	75
14	ChCl/ L- (+)-TA (1:2)	70	6	60
15	ChCl/Glucose (1:2)	80	3	ND
16	ChCl/ L-proline (1:2)	80	3	40
17	Glucose/L-proline (1:2)	80	3	60
18	Glucose/L-(+)-TA (1:2)	80	3	70
19	L-proline/L-(+)-TA (1:2)	80	3	50

[a]Reaction condition: **1** (0.54 mmol), **2** (0.54 mmol), DES is formed by heating the hydrogen bond acceptor and hydrogen bond donor. [b]Isolated yield of the product.

Encouraged by the above results and with the optimized conditions in hand, the focus shifted towards the generation of a library of compounds. Thus, functionalized 1,2,3,4-tetrahydroacridines (**1a-1u**) were reacted with dialkyl azodicarboxylates (**2a-2b**) under optimized conditions to yield C4-functionalized 1,2,3,4-tetrahydroacridine (**3a-3x**) in good to excellent yields (70-96%) (**Scheme 3.1.2**). It is worth mentioning that a wide range of functional groups substituted on 1,2,3,4-tetrahydroacridines at C9-position tolerated reaction conditions, with significant effect shown by the electronic nature of the substituents. Interestingly, substituents like methyl and phenyl at the 9th position (**3b and 3c**) on acridine gave good results with dialkyl azodicarboxylates. In addition to this, the substitution on the 7th

carbon of the aromatic ring (-Cl and –NO_2) played an important role in obtaining variable yields as shown in **Scheme 3.1.2**. Other notable observations were the tolerance of the terminal alkyne (**3m, 3n**) and hierarchical selectivity of sp^3–carbon (between C2 and C4 positions) (**3q-3s**) worth mentioning.

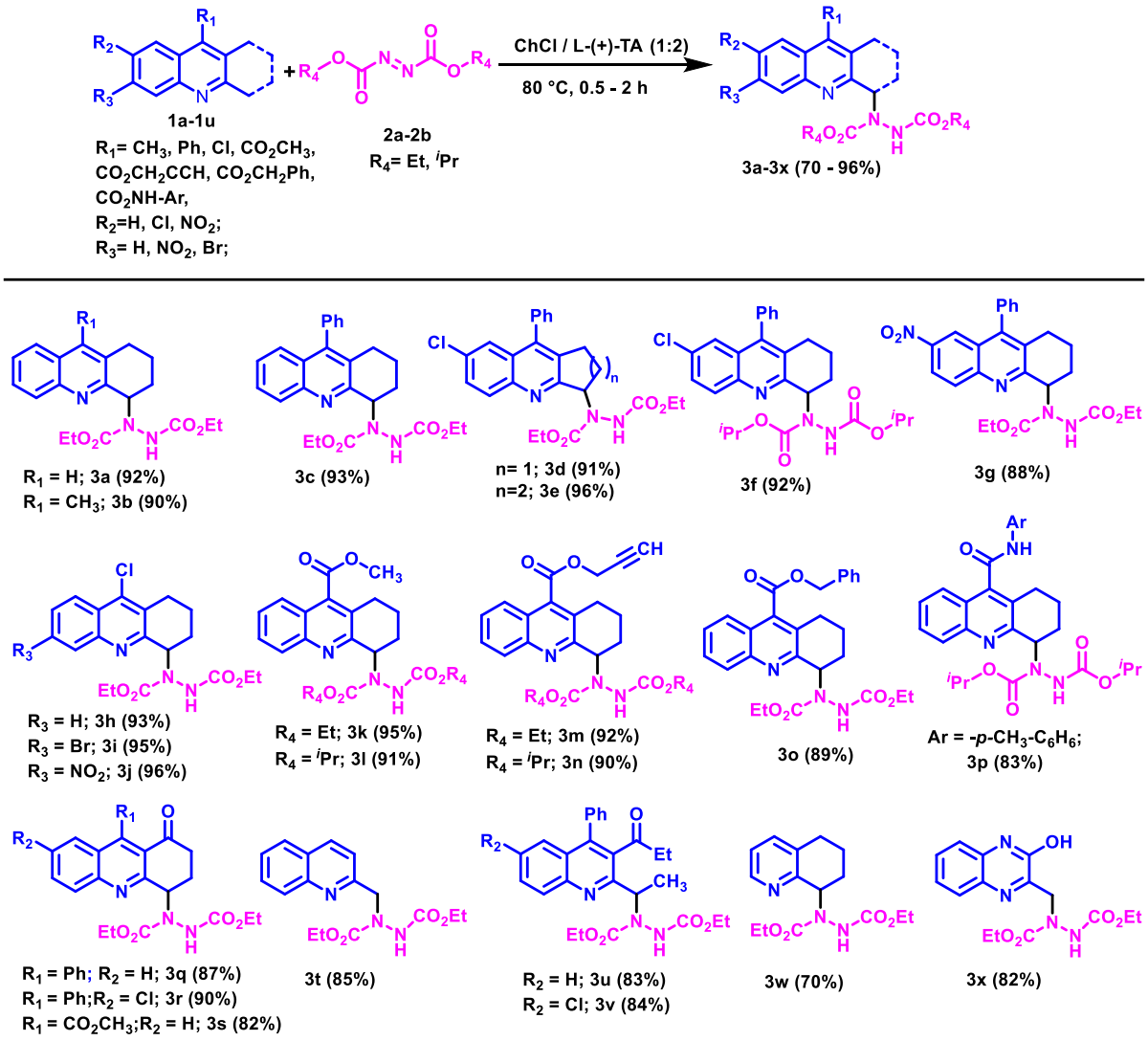

Scheme 3.1.2 Synthesis of C4-substituted 1,2,3,4-tetrahydroacridine derivatives

Having demonstrated the C(sp^3)–H amination of 1,2,3,4-tetrahydroacridine at the C4-position, we investigated the applicability of the present conditions for C–C bond formation using *N*-phenylmaleimide. Towards this, 1,2,3,4-tetrahydroacridine (**1a**) was reacted with *N*-phenylmaleimide (**4**) at 80 °C for 3 h using ChCl/L-(+)-TA (1:2) as DES to obtain the corresponding product in 70% yield (**Scheme 3.1.3**). Encouraged by the result, and to improve product yield, further investigation was carried out using various combinations of DESs at variable temperatures as shown in **Table 3.1.2**.

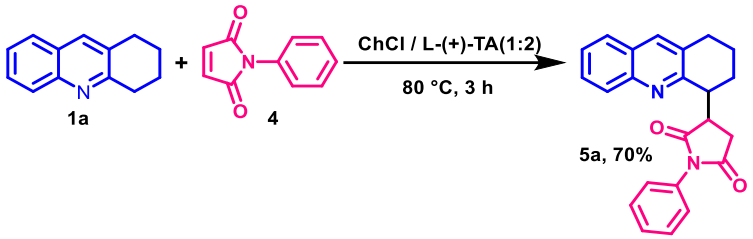

Scheme 3.1.3 Initial attempt for C–C bond formation *via* C(sp³)–H functionalisation

Table 3.1.2 Optimization table[a]

S.No.	DES	Temp (°C)	Time (h)	yield (%)[b]
1	ChCl/ L-(+)-TA (1:2)	80	3	70
2	ChCl/ oxalic acid (1:2)	80	3	ND
3	ChCl/ citric acid (1:1)	80	2	50
4	ChCl/Glucose (1:2)	80	3	ND
5	ChCl/ *p*-TSA (1:1)	80	3	ND
6	ChCl/ thio Urea (1:1)	90	2	10
7	ChCl/ L-proline (1:2)	80	3	ND
8	ChCl/ DMU (1:2)	80	3	80
9	ChCl/ $ZnCl_2$ (1:2)	80	3	ND
10	ChCl/ Urea (1:1)	80	3	78
11	**DMU/ L-(+)-TA (3:1)**	**80**	**2**	**90**
12	DMU/ L-(+)-TA (3:1)	70	6	60
13	DMU/ L-(+)-TA (2:1)	80	3	79
14	DMU/ L-(+)-TA (3:1)	90	3	75
15	DMU/ L-(+)-TA (3:1)	100	6	50
16	Glucose/ L-proline (1:2)	80	5	ND
17	Glucose/ L-(+)-TA (1:2)	80	5	40
18	L-Proline/ L-(+)-TA (1:2)	80	5	50

[a]Reaction condition: **1** (0.54 mmol), **4** (0.54 mmol), DES is formed by heating the hydrogen bond donor and hydrogen bond acceptor. [b]Isolated yield of the final product.

Interestingly, the desired product was obtained in 90% yield with DMU/ L-(+)-TA (3:1) as DES at 80 °C in 2 h (**Table 3.1.2**; entry 11). With a simple and efficient optimized solvent system in hand, the next task was to check the feasibility of the reaction for the substrate scope. Thus, various substituted 1,2,3,4-tetrahydroacridines (**1a-1u**) were reacted with *N*-phenylmaleimide (**4**) to give the respective products (**5a-5u**) in good to excellent yields, as shown in **Scheme 3.1.4**. Similar to C(sp³)–N bond formation results (**Scheme 3.1.2**), in this case also, it was observed that the presence of methyl and phenyl substitution at C9-position of 1,2,3,4-tetrahydroacridine which afforded the desired products in good yields.

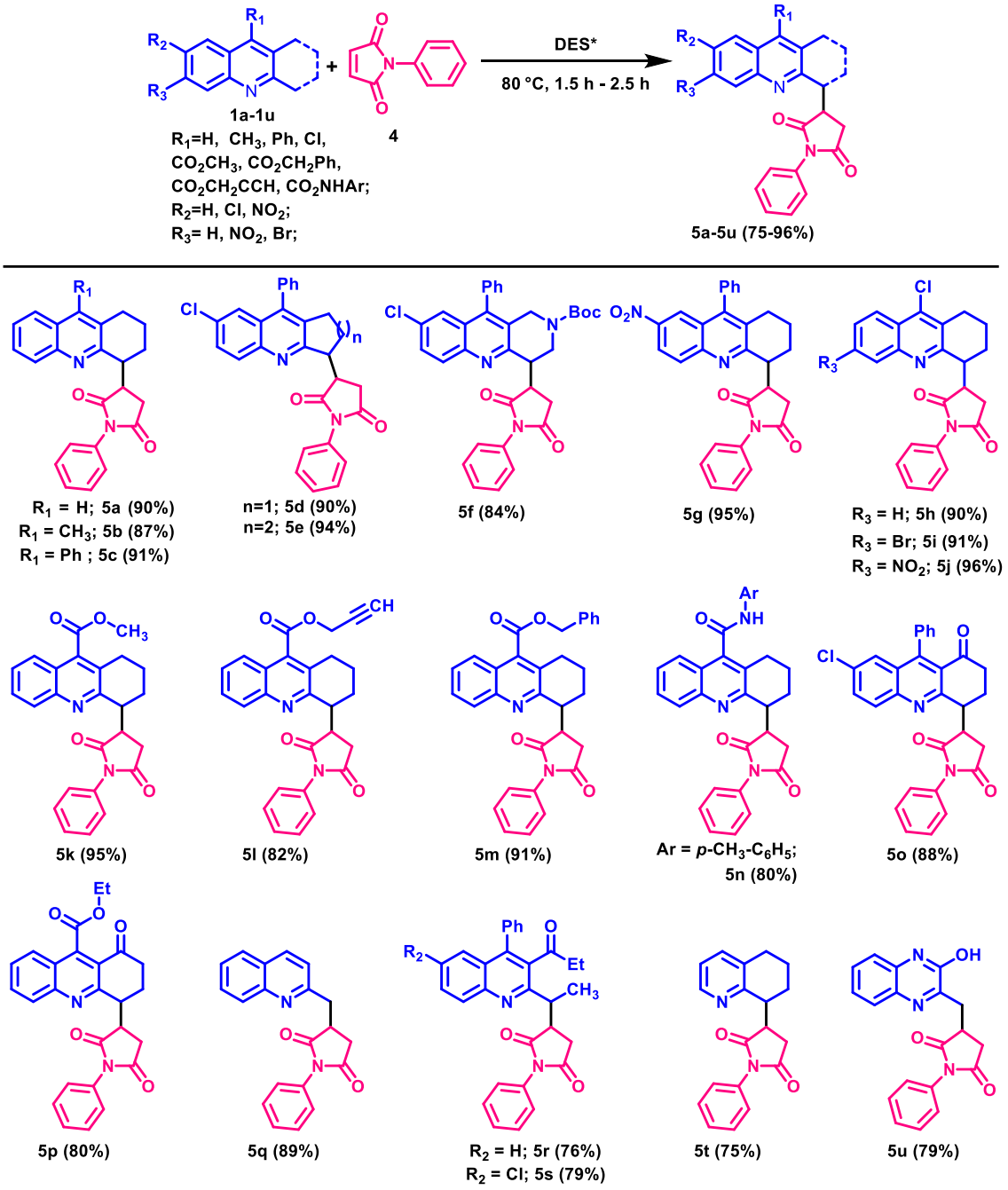

Scheme 3.1.4 Synthesis of *N*–phenyl maleimide substituted 1,2,3,4-tetrahydroacridine derivatives

The –Cl and –NO_2 substitution at the 7th position and –Ph at the 9th position shows very good reactivity with a good yield of the desired product (**5e, 5g**). Also, –Br and –NO_2 at the 6th position with –Cl at the 9th position and –COOR groups at the 9th position on acridine afforded the corresponding products in good to excellent yields (**5h-5m**). However, the ring size (5-membered ring) and the presence of a hetero atom in the aliphatic ring influence the reduction of yields along with Ph at the 9th position (**5d, 5f**). The presence of amide (-CONHR) at the 9th

position and 3,4-dihydroacridin-1(2*H*)-one derivative had little impact on the addition of *N*-phenylmaleimide leading to low yields (**5n, 5o, and 5p**). Similarly, 2-methylquinoline reacted well with *N*-phenylmaleimide to yield the corresponding product **5q** in good yield (89%). Low yield was obtained with 5,6,7,8-tetrahydroquinoline derivative (**5t**). 3-Methylquinoxalin-2-ol reacted moderately with *N*-phenylmaleimide to afford the desired product (**5u**) in moderate yield (79%). The synthesized compounds were confirmed by ^{1}H-NMR, ^{13}C-NMR, and mass spectral data.

The ^{1}H-NMR spectrum of compound **5i** showed a peak at 4.06–4.01 δ ppm (m, 1H) which represents C–H proton of *N*-phenyl succinimide, while the peak at 3.30 δ ppm (m, 1H) represents the C–H proton of 1,2,3,4-tetrahydroacridine attached to *N*-phenyl succinimide. The observed HRMS mass m/z of **5i** is 469.0317 (M+H$^+$) confirming the formation of the desired product. Further, the structure of compound 5i was confirmed by single crystal X-ray diffraction analysis **Figure 3.1.4** (**CCDC 2294878**).

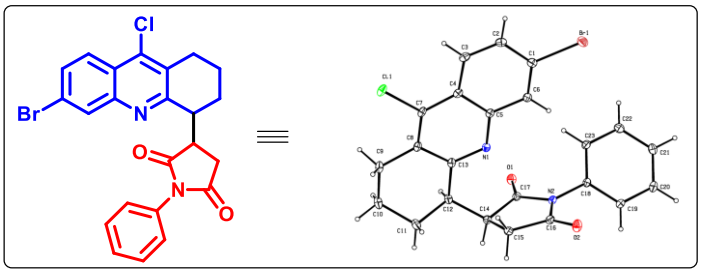

Figure 3.1.4 ORTEP Diagram of compound **5i** (**CCDC 2294878**)

The scalability of the protocol was effectively demonstrated by the gram-scale synthesis of **3e** and **5e**, which yielded 89% and 87%, respectively, under optimized reaction conditions (**Scheme 3.1.5**).

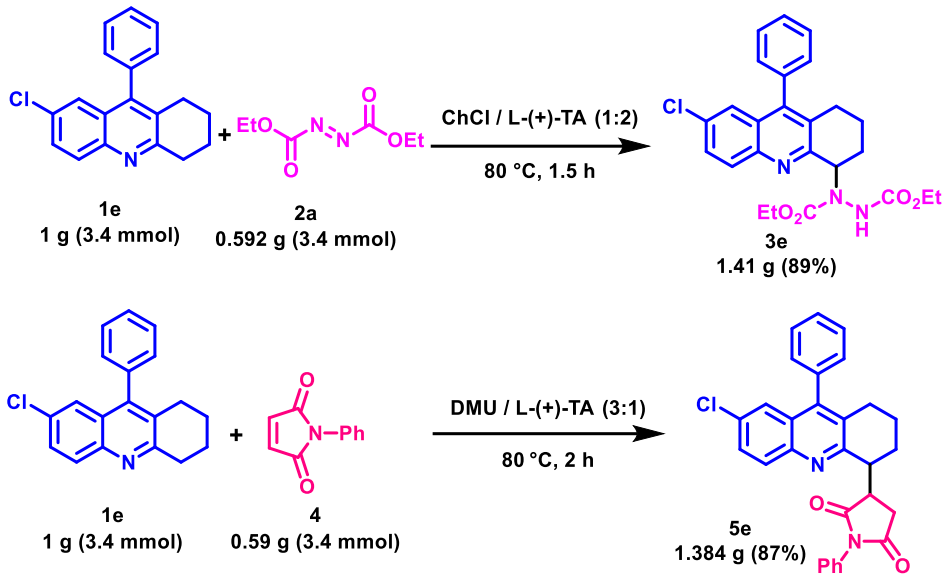

Scheme 3.1.5 Gram-scale synthesis of compounds **3e** and **5e** under optimized conditions

3.1.5 Green metrics Calculation

Metrics are important for any reaction that is performed using green approaches. Towards this, we have evaluated the green chemistry parameters[19] for the chemical transformation and final compounds. **Table 3.1.3** summarizes the green metrics used in this evaluation for compounds **5j** and **3j**, which include simple *E*-factor, mass intensity, atom economy, reaction mass efficiency, and carbon efficiency. All calculations and calculated values are provided in the electronic supporting information. The atom economy efficiency of the transformation is high, the conversion being high in most of the cases. However, to know better the environmental impact of the process, the simple *E*-factor was calculated by taking into account only starting materials. Pleasingly, an *E*-factor ranging from 0.042 (**5j**) to 0.42 (**3w**) was obtained. Although the DES used in this report is recyclable; by including DES in the *E*-factor calculation we obtained *E*- factor of 1.062 for compound **5j** and 1.27 for compound **3j**.

Table 3.1.3 Calculated green metrics values for compound **5j** and **3j**

S. No.	Green metrics	Ideal values	Calculated values for compound 5j	Calculated values for compound 3j
1	Environmental (*E*) factor	0	0.042	0.044
2	Mass Intensity (MI)	1	1.042	1.044
3	Atom Economy (AE %)	100	100	100
4	Reaction Mass Efficiency (RME %)	100	95.9	95.78
5	Carbon Efficiency (CE %)	100	96	95.78

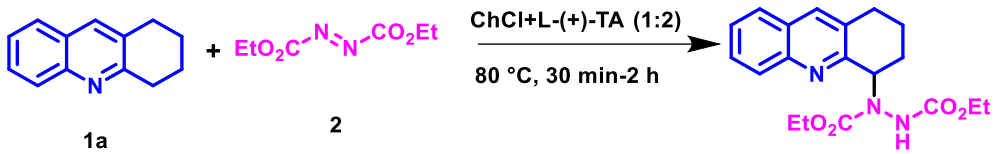

	1a	2	3a
MW:	183.25	174.1560	357.4100
mmol	0.545	0.545	0.5
Amount	0.1g	0.095g	0.179g

S. No.	Parameters	Formula	Characteristics	Ideal Value	Calculated value for compound 3a
1	Environmental (*E*) factor	Amount of waste/ Amount of product	E-factor signifies the total amount of waste generated in a chemical reaction.	0	0.0166 / 0.179 = 0.09
2.	Atom economy (AE %)	[MW of product] / Sum of MW of reactants) × 100	Atom economy signifies the percentage of atoms wasted in chemical reactions. Higher the value of AE, greener is the reaction.	100%	[357.41/ (183.254+174.156)]×100 = 100
3.	Mass intensity (MI)	∑ (mass of stoichiometric reactants)/[mass of stoichiometry product]	Mass intensity (MI), defined as the mass ratio of total input of materials (excluding water) to final product. MI takes into account reaction efficiency.	1	(0.1+0.095)/0.179 = 1.09
4.	Reaction mass efficiency (RME %)	[mass of product/∑ (mass of stoichiometric reactants)] × 100	RME accounts into atom economy, chemical yield and stoichiometry.	100%	[0.179/ (0.1+0.095)]×100 = 91.79
5.	Carbon efficiency (CE %)	[Amount of carbon in product/ Total carbon present in reactants] x 100	CE signifies the percentage of carbons in the reactants that is remain in the product.	100%	[0.5 × 19/ (0.545 × 13 + 0.545 × 6)] × 100 = [3.401/ (7.085+3.27) = 91.74%

S. No.	Compound No.	*E*-Factor	Atom economy (%)	Mass intensity	Reaction mass efficiency (%)	Carbon efficiency (%)
1	3a	0.09	100	1.09	91.79	91.74
2	3b	0.11	100	1.11	89.89	89.9
3	3c	0.075	100	1.075	92.9	92.9
4	3d	0.096	100	1.096	90.7	90.5
5	3e	0.046	100	1.046	95.59	95.5

6	3f	0.089	100	1.089	91.8	91.8
7	3g	0.139	100	1.139	87.78	87.3
8	3h	0.074	100	1.074	92.9	93
9	3i	0.058	100	1.058	94.5	94.55
10	**3j**	**0.044**	**100**	**1.044**	**95.78**	**95.78**
11	3k	0.052	100	1.052	95	95
12	3l	0.099	100	1.099	90.9	90.8
13	3m	0.087	100	1.087	91.96	91.9
14	3n	0.11	100	1.11	89.77	89.6
15	3o	0.129	100	1.129	88.5	88.5
16	3p	0.2	100	1.2	82.9	82.8
17	3q	0.15	100	1.15	86.7	86.68
18	3r	0.1	100	1.11	90	90
19	3s	0.219	100	1.219	82	81.9
20	3t	0.17	100	1.17	85	84.94
21	3u	0.2	100	1.2	83	83
22	3v	0.19	100	1.19	83.9	83.7
23	3w	0.42	100	1.42	70	70
24	3x	0.216	100	1.216	82	82

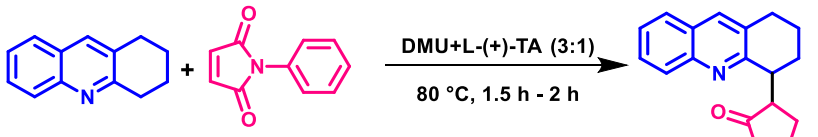

	1a	4	5a
MW:	183.25	173.1710	356.4250
mmol	0.545	0.545	0.49
Amount	0.1g	0.0945g	0.175g

S. No.	Compound No.	*E*-Factor	Atom economy (%)	Mass intensity	Reaction mass efficiency (%)	Carbon efficiency (%)
1	**5a**	0.11	100	1.11	89.97	89.9
2	**5b**	0.149	100	1.149	87	87
3	**5c**	0.098	100	1.098	91	90.9
4	**5d**	0.11	100	1.11	90	89.6
5	**5e**	0.063	100	1.063	94	93.8
6	**5f**	0.19	100	1.19	83.9	83.4
7	**5g**	0.053	100	1.053	94.9	94.8
8	**5h**	0.11	100	1.11	90	89.3
9	**5i**	0.098	100	1.098	91	90.8
10	**5j**	**0.042**	**100**	**1.042**	**95.9**	**96**

11	**5k**	0.053	100	1.053	94.9	94.9
12	**5l**	0.2	100	1.2	82	81.9
13	**5m**	0.1	100	1.1	90.9	90.4
14	**5n**	0.25	100	1.25	79.9	79.7
15	**5o**	0.13	100	1.13	87.9	87.8
16	**5p**	0.25	100	1.25	79.8	79.7
17	**5q**	0.12	100	1.12	89	88.9
18	**5r**	0.32	100	1.32	75.7	75.4
19	**5s**	0.26	100	1.26	79	78.8
20	**5t**	0.3	100	1.3	75	74.8
21	**5u**	0.26	100	1.26	79	78.6

3.1.6 Plausible mechanism

Based on our past experience,[18] other literature reports,[20] and experimental observations of the present investigation, a possible mechanism was proposed for C(sp^3)–H bond amination and C–C bond formation. In the amination reaction, the strong hydrogen bond network of DES helps to lower the activation energy barrier by solvating the ionic transition state. Also, the hydrogen bonding of DES [ChCl/L-(+)-TA] facilitates enolization of 1,2,3,4-tetrahydroacridine to form an enamine intermediate (**II**). This intermediate (**II**) further attacks the electrophilic centre of DEAD (N=N bond of dialkyl azodicarboxylate), which is activated by DES *via* hydrogen bonding to give an intermediate (**III**). The intermediate (**III**) later tautomerizes to provide the desired product 3a (As shown in **Figure 3.1.5**).

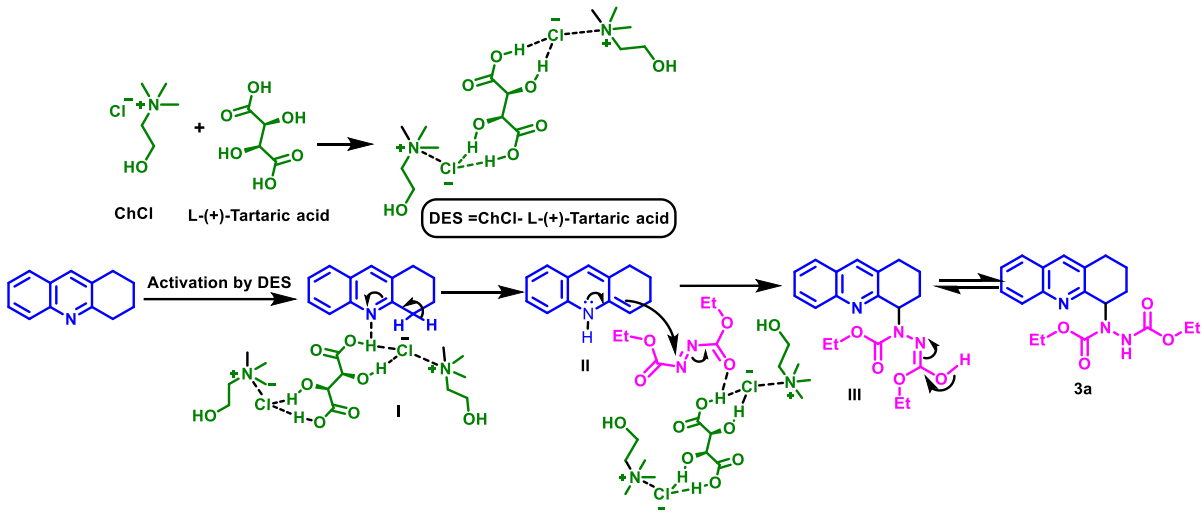

Figure 3.1.5 Proposed mechanism for the C(sp^3)–H amination of 1,2,3,4-tetrahydroacridine

Similarly, C(sp^3)–H functionalization of 1,2,3,4-tetrahydroacridine with *N*-phenyl maleimide is performed using DMU/L-(+)-TA as DES. The DES generated interacts with nitrogen atom

in the 1,2,3,4-tetrahydroacridine through hydrogen bonding to produce an enamine intermediate (**II**). Simultaneously the DES activates *N*-phenyl maleimide to facilitate the attack of enamine intermediate (**II**) on Carbon to provide the C(sp³)–H functionalized product (**III**), which on tautomerisation yields the desired product **5a** (As shown in **Figure 3.1.6**).

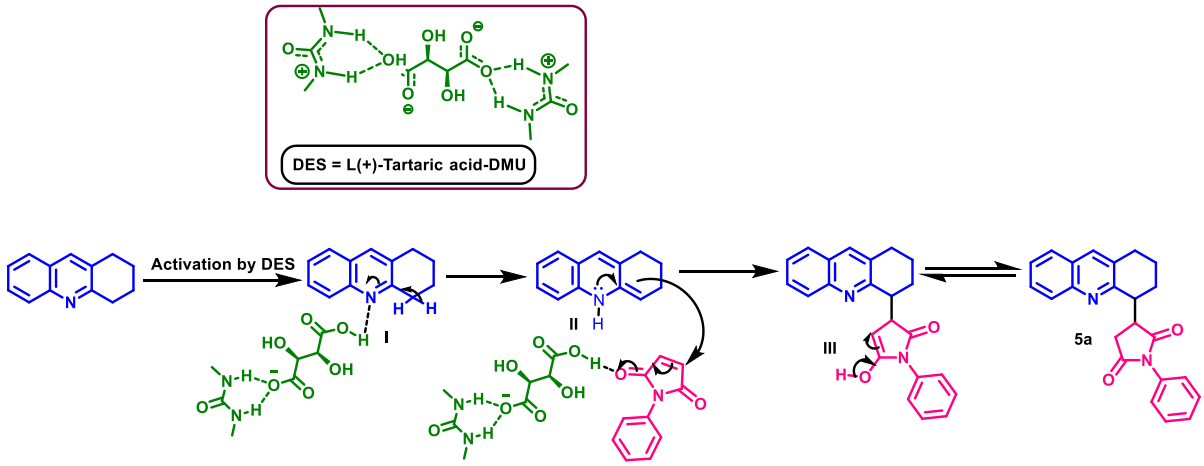

Figure 3.1.6 Proposed mechanism for the C(sp³)–H functionalization of 1,2,3,4-tetrahydroacridine

3.1.7 Conclusions

To conclude, we have successfully established an effective method for the direct C(sp³)–H amination and alkylation of 1,2,3,4-tetrahydroacridine at C-4 position using dialkyl azodicarboxylates and maleimide as coupling partners in the presence of DES serving both as catalyst and reaction medium. The versatility of this method is evident in its compatibility with a diverse range of substrates and tolerates various functional groups, demonstrating high levels of regioselectivity. Additionally, DES system offers the advantage of recyclability/reusability even at gram-scale reactions aligning with environmental considerations. Green metrics calculations reveal favourable values for atom economy, *E*-factor, reaction mass efficiency, carbon efficiency, and mass intensity, highlighting the overall efficiency of this protocol.

3.1.8 Experimental section

3.1.8.1 Synthesis of 1,2,3,4-tetrahydroacridine derivatives (1a-1p, 1r, 1s,1u)

General procedure for synthesis of compound (1a): [21]

To an RB equipped with a magnetic stir bar, 2-nitrobenzaldehyde (5.0 mmol) was dissolved in EtOH (15 mL). Iron powder (4.0 equiv.) and 0.1 N HCl (5.0 mol %, 2.5 mL) were next added after which the resulting mixture was then stirred at 95 °C for 40 min. Upon cooling, cyclohexanone (1.0 equiv.) was added followed by addition of powdered KOH (1.2 equiv.).

Heating was continued at 95 °C for another 30 min. The reaction mixture was then filtered through a pad of Celite with the resulting filtrate subsequently washed with water and extracted using dichloromethane (310 mL). The combined organic layers were further washed with brine, dried over Na_2SO_4 and concentrated under reduced pressure. Purification by silica gel chromatography (hexane/EtOAc) then afforded 1a as yellow solid in 90% yield.

General procedure for synthesis of compound (1b-1f, 1n,1o,1q,1r):

1.53g of Deep Eutectic Solvent (DES) was prepared by heating *N,N'*-dimethyl urea (0.975g) + L-tartaric acid (0.555g) at 80 °C for 30 min. To this melt, 2- aminoacetophenone/2-aminobenzophenone derivatives (0.231g, 1 mmol) and cyclohexanone/1,3-cyclohexadione/ 1,3-diketone was added and heating continued for another 1-2 h at 80 °C to give the (**1b-1f**,**1n**,**1o**,**1q**,**1r**)

General procedure for synthesis of compound (1g-1i): [22]

$POCl_3$ (25 mL) was added dropwise using a constant pressure dropping funnel to an ice-cooled mixture of anthranilic acid (3.2 g, 23.3 mmol) and cyclohexanone (2.65 mL, 27 mmol). Then, the reaction mixture was heated at 100 °C for 3 h. After the reaction was completed, the reaction mixture was cold to rt. Then the solvent was reduced in a vacuum and the ethyl acetate was added to residue and neutralized with 1 N K_2CO_3 solution, and brine, and the organic layer was dried over anhydrous Na_2SO_4. The residue was purified by silica gel chromatography to yield the desired product (**4**) as a yellow solid.

General procedure for synthesis of compound (1j-1l): [23]

1,2,3,4-tetrahydroacridine-9-carboxylic acid (0.98 g, 3 mmol) and potassium carbonate (2.07 g, 15 mmol) were weighed into a round-bottom flask. Methyl iodide / propargyl bromide/ benzyl bromide (3 equiv.) and acetone (4 mL) were added. The reaction mixture was stirred at room temperature. The progress of the reaction was monitored by TLC. The reaction was completed after 5 h. The solvent was evaporated in vacuo and water was added to the remaining mixture. The product was collected by suction filtration and air-dried. The crude product was separated on a silica gel column to obtain desired product (**1j**-**1l**).

General procedure for synthesis of compound (1m): [24]

To a solution of 1,2,3,4-tetrahydroacridine-9-carboxylic acid (3.2 mmol) in DMF (10 mL) DMAP (9.7 mmol) was added and cooled to 0 °C. Then EDC.HCl (6.5 mml), HOBt (6.5 mmol)

and toluidine (4.9 mmol) were added and resulting mixture was stirred at room temperature for 30 minutes.

General procedure for synthesis of compound (1p): [25]

In a 25-mL round bottom flask, the mixture of isatins (1.0 g, 6.8 mmol), cyclohexanone (2.15 g, 13.6 mmol), conc.H_2SO_4 (1.0 mL, l8.4 mmol), and EtOH (10 mL) was stirred at 80 °C for 1.5 h, and monitored by thin layer chromatography (TLC) until the staring material to show complete consumption. The mixture was cooled to room temperature, the alcohols were evaporated in vacuo, and then water was added. The mixture was extracted with ethyl acetate (EtOAc). The organic phase was washed with brine, dried with sodium sulphate (Na_2SO_4), and concentrated. The residue was purified by column chromatography on silica gel (5–25% ethyl acetate in petroleum ether) to get the desired product.

General procedure for synthesis of compound (3):

Deep eutectic solvent was prepared by heating Choline chloride + L-tartaric acid (1:2 ratio) at 80 °C for 30 min. To this, 1,2,3,4-tetrahydroacridine **1** (0.545 mmol) and dialkylazodicarboxylate **2** (0.545 mmol) were added and heating continued for another 30 min to 2 hours at 80 °C. The completion of reaction was monitored by TLC. After completion of reaction the crude products obtained were purified by column chromatography on silica gel using petroleum ether-ethyl acetate as eluent to give the compound **3**.

General procedure for synthesis of compound (5):

Deep eutectic solvent was prepared by heating *N,N'*-dimethyl urea + L-tartaric acid (3:1 ratio) at 80 °C for 30 min. To this, compound **1** (0.545 mmol) and *N*- phenyl maleimide (0.545 mmol) were added and heating continued 2 hours at 80 °C. The completion of reaction was monitored by TLC. After completion of reaction the crude products obtained were purified by column chromatography on silica gel using petroleum ether-ethyl acetate as eluent to give the compound **5**.

3.1.9 Characterization data for synthesized compounds

Diethyl 1-(1,2,3,4-tetrahydroacridin-4-yl)hydrazine-1,2-dicarboxylate(3a): Yield= 92%, white solid; M. P: 99.2 -99.8 °C; **IR (KBr, cm^{-1})**: 3055, 2928, 2862, 1757, 1623, 1545, 1247, 1141, 1056, 945, 742; **^{1}H NMR (400 MHz, CDCl$_3$) δ** 7.94 (d, *J* = 10.6 Hz, 1H), 7.86 (d, *J* = 9.0 Hz, 1H), 7.73 (dd, *J* = 13.6, 7.5 Hz, 1H), 7.64 – 7.58 (m, 1H), 7.51 – 7.42 (m, 1H), 6.61 (m, 1H), 4.24 (d, *J* = 7.1 Hz, 2H), 4.21 – 4.02 (m, 2H), 3.04 – 2.87 (m, 2H), 2.44 (d, *J* = 33.5 Hz, 1H), 2.04 (d, *J* = 32.4 Hz, 2H), 1.72 (s, 1H), 1.39 – 1.25 (m, 6H). **^{13}C NMR (100 MHz, DMSO) δ** 156.85, 156.30, 152.37, 146.60, 135.32, 132.02, 129.21, 128.81, 127.37, 127.09, 126.53, 63.65, 62.02, 61.14, 28.64, 27.69, 21.24, 14.74, 14.35. **HRMS (ESI-MS):** m/z Calculated for $C_{19}H_{23}N_3O_4$ $[M+H]^+$: 358.1761; Observed: 358. 1766.

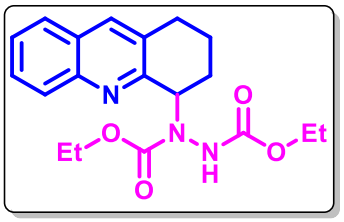

Diethyl 1-(9-methyl-1,2,3,4-tetrahydroacridin-4-yl)hydrazine-1,2-dicarboxylate (3b): Yield= 90%, White solid; M. P: 119-119.9 °C; **IR (KBr, cm^{-1})**: 3025, 2948, 2884, 1753, 1645, 1510, 1275, 1112, 1071, 954, 798; **^{1}H NMR (400 MHz, CDCl$_3$) δ** 7.96 (d, *J* = 8.4 Hz, 1H), 7.93 (d, *J* = 8.0 Hz, 1H), 7.60 (t, *J* = 8.4 Hz, 1H), 7.49 (t, *J* = 8.4 Hz, 1H), 6.73 – 6.38 (m, 1H), 5.51 (m, 1H), 4.30 (q, *J* = 7.2 Hz, 4H), 2.99 (d, *J* = 16.8 Hz, 1H), 2.84 – 2.75 (m, 1H), 2.54 (s, 3H), 2.51 – 2.41 (m, 1H), 2.17 (s, 1H), 1.96 (d, *J* = 6.0 Hz, 2H), 1.32 (t, *J* = 7.2 Hz, 6H). **^{13}C NMR (100 MHz, CDCl$_3$) δ** 158.43, 157.66, 156.90, 155.23, 152.23, 145.85, 142.02, 129.88, 129.25, 128.20, 127.20, 126.03, 123.28, 64.08, 62.61, 62.48, 61.66, 26.99, 26.58, 21.43, 14.58, 14.40, 14.13, 13.77. **HRMS (ESI-MS):** m/z Calculated for $C_{20}H_{25}N_3O_4$ $[M+H]^+$: 372.1918; Observed: 372.1920.

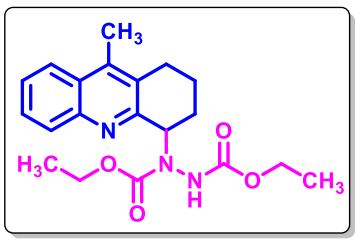

Diethyl 1-(9-phenyl-1,2,3,4-tetrahydroacridin-4-yl)hydrazine-1,2-dicarboxylate (3c): Yield= 93%, white solid; M. P: 121.9 – 121.5 °C; **IR (KBr, cm^{-1})**: 3055, 2984, 2873, 1756, 1672, 1531, 1274, 1142, 1049, 959, 763; **^{1}H NMR (400 MHz, CDCl$_3$) δ** 7.99 (d, *J* = 8.8 Hz, 1H), 7.59 (d, *J* = 5.6 Hz, 1H), 7.54 – 7.50 (m, 2H), 7.49 – 7.46 (m, 1H), 7.34 (d, *J* = 5.6 Hz, 2H), 7.22 (d, *J* = 6.8 Hz, 2H), 6.87 – 6.50 (m, 1H), 5.58 (m, 1H), 4.35 (s, 2H), 4.20 (q, *J* = 7.2 Hz, 2H), 2.62 (d, *J* = 8.4 Hz, 2H), 2.46 (s, 1H), 1.97 (s, 3H), 1.43 – 1.25 (m, 6H). **^{13}C NMR (100 MHz, DMSO) δ** 156.88, 156.18, 146.59, 146.23, 136.84, 130.62, 129.59, 129.40, 129.34, 129.27, 129.17, 129.07, 128.72, 128.39, 126.90, 126.64,

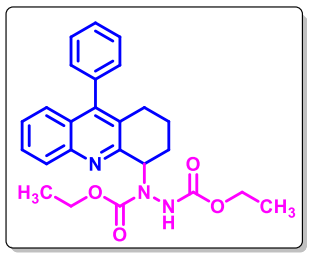

125.58, 62.05, 61.15, 27.52, 27.18, 21.16, 14.85, 14.79. **HRMS (ESI-MS):** m/z Calculated for $C_{25}H_{27}N_3O_4$ $[M+H]^+$: 434.2075; Observed: 434.2068.

Diethyl1-(7-chloro-9-phenyl-2,3-dihydro-1H-cyclopenta[b]quinolin-3-yl)hydrazine-1,2-dicarboxylate (3d): Yield= 91%, White solid; M. P: 198.1- 198.4 °C; **IR (KBr, cm^{-1})**: 3255, 2978, 2928, 2852, 1743, 1682, 1522, 1228, 1159, 1060, 942, 759; **^{1}H NMR (400 MHz, CDCl$_3$+DMSO-d6) δ** 8.04 (d, *J* = 8.8 Hz, 1H), 7.73 (s, 1H), 7.59 (dd, *J* = 6.4, 2.3 Hz, 2H), 7.56 (d, *J* = 2.4 Hz, 2H), 7.52 (d, *J* = 7.1 Hz, 1H), 7.35 (q, *J* = 7.5 Hz, 2H), 5.84 (s, 1H), 4.31 – 4.22 (m, 2H), 4.18 – 4.07 (m, 2H), 2.84 (t, *J* = 7.3 Hz, 2H), 2.55 – 2.48 (m, 1H), 2.26 (s, 1H), 1.31 (t, *J* = 6.8 Hz, 3H), 1.21 (t, *J* = 7.0 Hz, 3H). **^{13}C NMR (100 MHz, CDCl$_3$+DMSO-d6) δ** 163.73, 156.85, 156.00, 152.31, 146.91, 142.39, 135.51, 134.21, 131.68, 131.46, 129.35, 129.13, 129.05, 128.81, 127.60, 124.21, 63.49, 62.12, 61.16, 27.81, 27.40, 14.68, 14.29. **HRMS (ESI-MS):** m/z Calculated for $C_{24}H_{24}ClN_3O_4$ $[M+H]^+$: 454.1528; Observed: 454.1529.

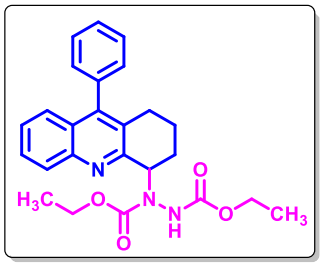

Diethyl 1-(7-chloro-9-phenyl-1,2,3,4-tetrahydroacridin-4-yl)hydrazine-1,2-dicarboxylate (3e): Yield= 96%, White solid; M. P: 186.9 – 187.3 °C; **IR (KBr, cm^{-1})**: 3367, 2979, 1801, 1759, 1516, 1240, 1173, 1050, 837, 762; **^{1}H NMR (400 MHz, CDCl$_3$) δ** 7.94 (d, *J* = 8.8 Hz, 1H), 7.58 – 7.53 (m, 3H), 7.52 (dt, *J* = 6.8, 1.6 Hz, 1H), 7.30 (d, *J* = 1.6 Hz, 1H), 7.22 (d, *J* = 7.2 Hz, 2H), 6.84 – 6.50 (m, 1H), 5.57 (m, 1H), 4.41 – 4.30 (m, 2H), 4.27 – 4.16 (m, 2H), 2.66 – 2.58 (m, 2H), 2.46 (s, 1H), 2.05 – 1.85 (m, 3H), 1.43 – 1.27 (m, 6H). **^{13}C NMR (100 MHz, DMSO-d6) δ** 157.03, 156.91, 145.71, 144.75, 136.11, 131.98, 131.28, 130.54, 129.38, 129.32, 129.23, 128.73, 127.68, 124.07, 62.06, 61.14, 27.60, 27.07, 21.01, 14.85, 14.80. **HRMS (ESI-MS):** m/z Calculated for $C_{25}H_{26}ClN_3O_4$$[M+H]^+$: 468.1685; Observed: 468.1686.

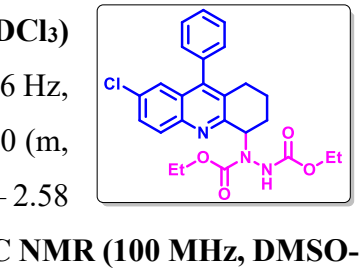

Diisopropyl 1-(7-chloro-9-phenyl-1,2,3,4-tetrahydroacridin-4-yl)hydrazine-1,2-dicarboxylate (3f): Yield= 92%, White solid; M. P: 150.9-151.3 °C; **IR (KBr, cm^{-1})**: 3304, 2981, 2934, 1730, 1674, 1469, 1262, 1097, 831, 762; **^{1}H NMR (400 MHz, CDCl$_3$) δ** 8.19 (d, *J* = 9.2 Hz, 1H), 7.90 (d, *J* = 9.2 Hz, 1H), 7.71 – 7.65 (m, 1H), 7.62 (m, 1H), 7.55 – 7.50 (m, 2H), 7.49 – 7.41 (m, 1H), 7.20 (d, *J* = 6.6 Hz, 1H), 6.78 – 6.24 (m, 1H), 5.52 (m, 1H), 5.11 – 5.03 (m, 1H), 4.99 (q, *J* = 6.0 Hz, 1H), 2.52 (m, 2H), 2.19 (m, 1H), 2.02 – 1.72 (m, 3H), 1.30 (dd, *J* = 16.4,

6.0 Hz, 12H). **^{13}C NMR (100 MHz, DMSO-d6) δ** 157.18, 156.54, 155.67, 152.01, 145.68, 144.75, 136.11, 135.02, 132.68, 131.84, 131.56, 131.28, 130.56, 128.68, 127.67, 124.78, 124.09, 71.64, 69.59, 27.60, 27.12, 22.27, 22.21, 22.15, 21.86, 21.06. **HRMS (ESI-MS):** m/z Calculated for $C_{27}H_{30}ClN_3O_4[M+H]^+$: 496.1998; Observed: 496.1999.

Diethyl 1-(7-nitro-9-phenyl-1,2,3,4-tetrahydroacridin-4-yl)hydrazine-1,2-dicarboxylate (3g): Yield= 88%, Yellow solid; M. P: 176.2 – 177.0 °C; **IR (KBr, cm^{-1})**: 3420, 2924, 2853, 1751, 1715, 1545, 1374, 1292, 1054, 706; **^{1}H NMR (400 MHz, CDCl$_3$) δ** 8.37 (dd, *J* = 9.2, 2.4 Hz, 1H), 8.29 (d, *J* = 2.4 Hz, 1H), 8.10 (d, *J* = 9.0 Hz, 1H), 7.59 (d, *J* = 2.4 Hz, 1H), 7.58 – 7.55 (m, 2H), 7.25 – 7.23 (m, 1H), 7.22 (m, 1H), 6.81 – 6.47 (m, 1H), 5.57 (m, 1H), 4.34 (s, 2H), 4.27 – 4.19 (m, 2H), 2.66 (m, 2H), 2.50 (s, 1H), 2.03 (m, 3H), 1.40 (s, 2H), 1.32 – 1.26 (m, 4H). **^{13}C NMR (100 MHz, CDCl$_3$) δ** 156.70, 150.96, 148.76, 148.10, 146.94, 135.28, 134.44, 133.37, 130.97, 130.30, 129.32, 129.18, 129.00, 128.86, 127.76, 122.83, 62.89, 62.28, 61.97, 40.08, 28.02, 22.25, 14.42. **HRMS (ESI-MS):** m/z Calculated for $C_{25}H_{26}N_4O_6[M+H]^+$: 479.1925; Observed: 479.1930.

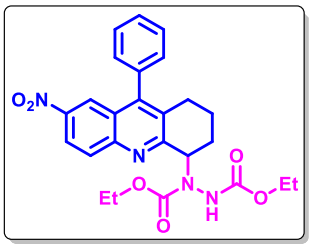

Diethyl 1-(9-chloro-1,2,3,4-tetrahydroacridin-4-yl)hydrazine-1,2-dicarboxylate (3h): Yield= 93%, White solid; M. P: 153.8 – 154.9 °C; **IR (KBr, cm^{-1})**: 3251, 2979, 2934, 2868, 1749, 1682, 1512, 1317, 1217, 1132, 1056, 915,753; **^{1}H NMR (400 MHz, CDCl$_3$) δ** 8.19 (dd, *J* = 8.8, 1.8 Hz, 1H), 7.97 (d, *J* = 8.8 Hz, 1H), 7.69 (ddd, *J* = 8.4, 6.8, 1.6 Hz, 1H), 7.60 (ddd, *J* = 8.4, 6.8, 1.6 Hz, 1H), 6.68 – 6.33 (m, 1H), 5.54 (m, 1H), 4.34 (s, 2H), 4.25 – 4.11 (m, 2H), 3.20 (d, *J* = 16.0 Hz, 1H), 2.90 (m, 1H), 2.49 (s, 1H), 2.22 (s, 1H), 2.01 (s, 2H), 1.40 – 1.23 (m, 6H). **^{13}C NMR (100 MHz, DMSO-d6) δ** 158.38, 156.87, 156.78, 147.19, 140.59, 131.97, 130.95, 130.75, 125.61, 124.35, 123.00, 62.08, 61.09, 27.28, 26.87, 20.42, 14.82, 14.78. **HRMS (ESI-MS):** m/z Calculated for $C_{19}H_{22}ClN_3O_4[M+H]^+$: 392.1372; Observed: 392.1372.

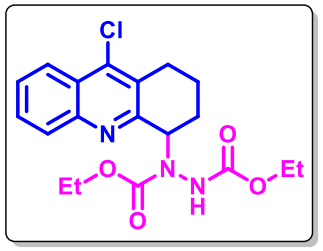

Diethyl 1-(6-bromo-9-chloro-1,2,3,4-tetrahydroacridin-4-yl)hydrazine-1,2-dicarboxylate (3i): Yield= 95%, white solid; M. P: 169.4-169.9 °C; **IR (KBr, cm^{-1})**: 3253, 3062, 2977, 2933, 2869, 1750, 1682, 1509, 12290, 1094, 805; **^{1}H NMR (400 MHz, CDCl$_3$) δ** 8.11 (s, 1H), 7.98 (d, *J* = 8.8 Hz, 1H), 7.62 (d, *J* = 7.2 Hz, 1H), 6.76 – 6.30 (m, 1H), 5.48 (m, 1H), 4.38 – 4.26 (m, 2H), 4.23 – 4.10 (m, 2H), 3.19 – 3.13 (m, 1H), 2.89 – 2.77

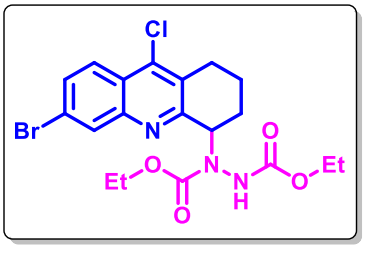

(m, 1H), 2.46 (s, 1H), 2.20 (s, 1H), 2.01 – 1.94 (m, 2H), 1.40 – 1.21 (m, 6H). **^{13}C NMR (100 MHz, DMSO-d6) δ** 156.82, 146.72, 140.43, 130.03, 129.98, 129.82, 128.01, 125.42, 123.49, 62.06, 61.13, 27.30, 27.00, 20.48, 14.81, 14.76. **HRMS (ESI-MS):** m/z Calculated for $C_{19}H_{21}BrClN_3O_4[M+H]^+$: 470.0477; Observed: 470.0477.

Diethyl 1-(9-chloro-6-nitro-1,2,3,4-tetrahydroacridin-4-yl)hydrazine-1,2-dicarboxylate (3j): Yield= 96%, light Yellow solid; M. P: 158.2 – 158.9 °C; **IR (KBr, cm^{-1})**:3246, 3021, 2931, 1749, 1677, 1528, 1346, 1226, 1163, 1068, 901, 885;**^{1}H NMR (400 MHz, CDCl$_3$) δ** 8.83 (s, 1H), 8.32 (s, 2H), 6.70 – 6.25 (m, 1H), 5.53 (m, 1H), 4.39 – 4.26 (m, 2H), 4.25 – 4.09 (m, 2H), 3.23 (m, 1H), 2.93 (m, 1H), 2.51 (s, 1H), 2.25 (s, 1H), 2.04 (d, *J* = 6.4 Hz, 2H), 1.25 (d, *J* = 6.0 Hz, 6H). **^{13}C NMR (100 MHz, CDCl$_3$) δ** 159.54, 157.13, 156.31, 148.05, 145.39, 141.86, 133.25, 128.85, 125.76, 125.58, 120.59, 62.97, 62.01, 27.46, 26.46, 20.74, 14.55, 14.42. **HRMS (ESI-MS):** m/z Calculated for $C_{19}H_{21}ClN_4O_6[M+H]^+$: 437.1223; Observed: 437.1228.

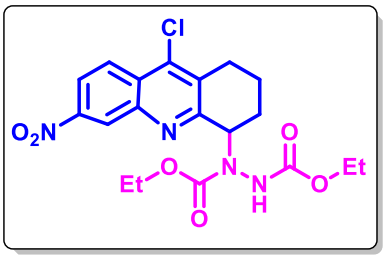

Diethyl 1-(9-(methoxycarbonyl)-1,2,3,4-tetrahydroacridin-4-yl)hydrazine-1,2-dicarboxylate (3k): Yield= 95%, white solid; M. P: 147.8 -148.6 °C; **IR (KBr, cm^{-1})**: 3253, 2978, 2933, 1744, 1683, 1435, 1316, 1194, 1059, 957, 758; **^{1}H NMR (400 MHz, CDCl$_3$) δ** 7.98 (d, *J* = 8.4 Hz, 1H), 7.70 – 7.63 (m, 2H), 7.55 – 7.49 (m, 1H), 6.60 (m, 1H), 5.52 (m, 1H), 4.32 (s, 2H), 4.24 – 4.11 (m, 2H), 4.06 (s, 3H), 2.94 (q, *J* = 5.2 Hz, 2H), 2.30 (m, 2H), 2.02 (m, 2H), 1.41 – 1.21 (m, 6H). **^{13}C NMR (100 MHz, CDCl$_3$) δ** 172.56, 161.67, 161.57, 161.22, 151.00, 142.81, 134.66, 134.21, 132.92, 132.55, 129.13, 127.94, 66.78, 65.85, 57.81, 31.96, 31.31, 25.47, 19.57, 19.53. **HRMS (ESI-MS):** m/z Calculated for $C_{21}H_{25}N_3O_6[M+H]^+$: 416.1816; Observed: 416.1839.

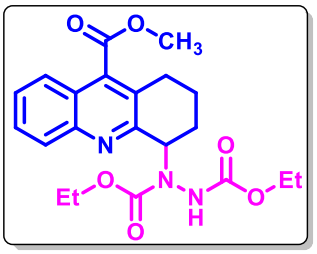

Diisopropyl 1-(9-(methoxycarbonyl)-1,2,3,4-tetrahydroacridin-4-yl)hydrazine-1,2-dicarboxylate (3l): Yield= 91%, White solid; M. P: 119.2 -119.9 °C; **IR (KBr, cm^{-1})**:3273, 2977, 2938, 1728, 1671, 1231, 1026, 962, 761; **^{1}H NMR (400 MHz, CDCl$_3$) δ** 7.96 (d, *J* = 8.4 Hz, 1H), 7.66 (m, 2H), 7.55 – 7.49 (m, 1H), 6.47 (s, 1H), 5.50 (m, 1H), 5.02 (m, 2H), 4.05 (s, 3H), 2.98 – 2.92 (m, 2H), 2.53 – 1.95 (m, 4H), 1.44 – 1.18 (m, 12H). **^{13}C NMR (100 MHz, CDCl$_3$) δ** 172.56, 161.37, 161.29, 161.15, 151.00,

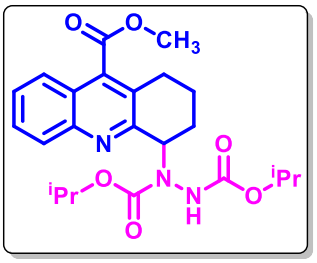

142.76, 134.60, 134.21, 132.89, 132.52, 129.14, 127.93, 74.27, 73.32, 57.82, 31.99, 31.33, 27.01, 26.99, 26.96, 26.93, 25.48. **HRMS (ESI-MS):** m/z Calculated for $C_{23}H_{29}N_3O_6$ $[M+H]^+$: 444.2129; Observed: 444.2127.

Diethyl 1-(9-((prop-2-yn-1-yloxy)carbonyl)-1,2,3,4-tetrahydroacridin-4-yl)hydrazine-1,2-dicarboxylate (3m): Yield= 92%, White solid; M. P: 110.1-110.5 °C; **IR (KBr, cm^{-1})**:3273, 2977, 2938, 1728, 1671, 1231, 1026, 962, 761; **^{1}H NMR (400 MHz, $CDCl_3$) δ** 7.98 (d, *J* = 8.8 Hz, 1H), 7.73 (d, *J* = 8.4 Hz, 1H), 7.69 – 7.64 (m, 1H), 7.56 – 7.52 (m, 1H), 6.55 (s, 1H), 5.53 (m, 1H), 5.06 (s, 2H), 4.31 (dd, *J* = 6.8, 2.0 Hz, 2H), 4.20 (dd, *J* = 6.8, 2.4 Hz, 2H), 3.02 – 2.95 (m, 2H), 2.62 (t, *J* = 2.4 Hz, 1H), 2.49 (s, 1H), 2.06 (m, 3H), 1.35 – 1.25 (m, 6H). **^{13}C NMR (100 MHz, DMSO-d6) δ** 166.65, 156.95, 156.88, 156.80, 156.55, 146.26, 136.99, 129.96, 129.56, 128.40, 127.89, 124.09, 123.14, 78.68, 78.26, 62.03, 61.11, 60.91, 53.69, 27.18, 26.45, 20.66, 14.89, 14.77. **HRMS (ESI-MS):** m/z Calculated for $C_{23}H_{25}N_3O_6$ $[M+H]^+$: 440.1816; Observed: 440.1816.

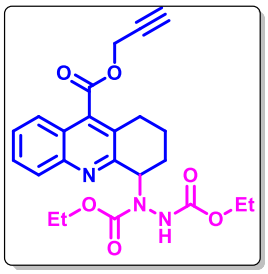

Diisopropyl 1-(9-((prop-2-yn-1-yloxy)carbonyl)-1,2,3,4-tetrahydroacridin-4-yl)hydrazine-1,2-dicarboxylate (3n) : Yield= 90%, White solid; M. P: 94.8-95.2 °C; **IR (KBr, cm^{-1})**:3273, 2977, 2938, 1728, 1671, 1231, 1026, 962, 761;**^{1}H NMR (400 MHz, $CDCl_3$) δ** 7.97 (d, *J* = 8.4 Hz, 1H), 7.73 (d, *J* = 8.4 Hz, 1H), 7.66 (ddd, *J* = 8.4, 6.8, 1.6 Hz, 1H), 7.53 (ddd, *J* = 8.4, 6.8, 1.2 Hz, 1H), 6.45 (s, 1H), 5.62 (s, 1H), 5.06 (d, *J* = 2.4 Hz, 2H), 5.03 – 4.89 (m, 2H), 3.01 – 2.95 (m, 2H), 2.62 (t, *J* = 2.4 Hz, 1H), 2.49 (s, 1H), 2.08 (m, 3H), 1.31 – 1.23 (m, 12H). **^{13}C NMR (100 MHz, $CDCl_3$) δ** 166.80, 166.21, 156.14, 146.19, 137.11, 132.46, 131.83, 129.58, 129.26, 127.47, 124.05, 123.97, 123.33, 77.24, 76.85, 75.97, 70.24, 69.51, 52.99, 29.69, 27.19, 26.29, 21.98, 21.95. **HRMS (ESI-MS):** m/z Calculated for $C_{25}H_{29}N_3O_6$ $[M+H]^+$: 468.2129; Observed: 468.2126.

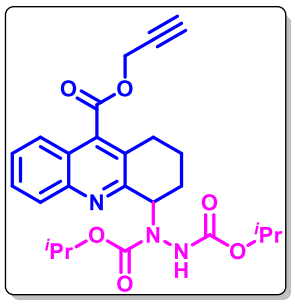

Diethyl 1-(9-((benzyloxy)carbonyl)-1,2,3,4-tetrahydroacridin-4-yl)hydrazine-1,2-dicarboxylate (3o): Yield= 89%, white solid; M. P: 145.5 – 146.3 °C; **IR (KBr, cm^{-1})**:3250, 2979, 2933, 1745, 1683, 1513, 1093, 956; **^{1}H NMR (400 MHz, DMSO-d6) δ** 8.54 (s, 1H), 7.71 (s, 1H), 7.48 (t, *J* = 8.4 Hz, 1H), 7.44 (d, *J* = 7.0 Hz, 1H), 7.33 (t, *J* = 8.4 Hz, 1H), 7.30 – 7.24 (m, 2H), 7.21 – 7.11 (m, 3H), 5.29 (s, 2H), 5.15 (s, 1H), 4.03 – 3.70 (m, 4H), 3.13 (s, 3H), 2.57 (t, *J* = 6.4 Hz, 2H), 1.86 (m, 2H), 1.67 (m, 2H), 1.02 – 0.84

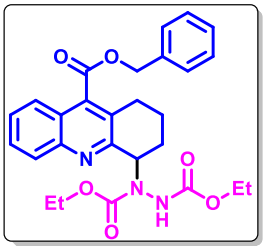

(m, 6H). **^{13}C NMR (100 MHz, DMSO-d6) δ** 167.22, 156.87, 156.81, 156.53, 146.27, 137.80, 135.81, 129.94, 129.46, 129.14, 129.00, 128.94, 128.16, 127.78, 124.19, 123.20, 67.87, 62.03, 61.11, 27.16, 26.47, 20.69, 14.80, 14.76. **HRMS (ESI-MS):** m/z Calculated for $C_{27}H_{29}N_3O_6$ $[M+H]^+$: 492.2129; Observed: 492.2129.

Diisopropyl 1-(9-(p-tolylcarbamoyl)-1,2,3,4-tetrahydroacridin-4-yl)hydrazine-1,2-dicarboxylate (3p): Yield= 83%, White solid; M. P: 238.4- 238.9 °C; **^{1}H NMR (400 MHz, DMSO-d6) δ** 10.98 (s, 1H), 10.13 (s, 1H), 8.21 (s, 1H), 8.12 (s, 1H), 8.01 (d, *J* = 8.0 Hz, 1H), 7.92 (t, *J* = 7.6 Hz, 2H), 7.71 (d, *J* = 8.8 Hz, 2H), 7.24 (d, *J* = 8.8 Hz, 2H), 4.94 – 4.88 (m, 2H), 4.88 – 4.75 (m, 2H), 4.35 (s, 1H), 2.33 (s, 3H), 1.79 (m, 2H), 1.54 (s, 1H), 1.22 (d, *J* = 6.4 Hz, 12H). **^{13}C NMR (100 MHz, DMSO-d6) δ** 164.91, 155.41, 153.92, 147.94, 142.07, 140.13, 139.90, 136.58, 134.05, 130.97, 130.31, 129.67, 127.89, 125.59, 122.75, 122.48, 120.74, 71.12, 70.22, 69.04, 22.27, 22.14, 22.01, 20.91. **HRMS (ESI-MS):** m/z Calculated for $C_{29}H_{34}N_4O_5$ $[M+H]^+$: 519.2602; Observed: 519.2596.

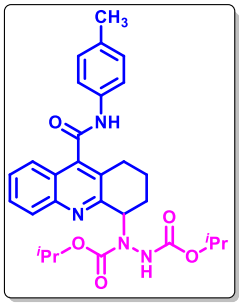

Diethyl 1-(1-oxo-9-phenyl-1,2,3,4-tetrahydroacridin-4-yl)hydrazine-1,2-dicarboxylate (3q): Yield= 87%, light Yellow solid; M. P: 121.3 – 122.1 °C; **IR (KBr, cm^{-1})**: 3275, 2988, 1750, 1682, 1610, 1505, 1387, 1221, 1061, 952, 757; **^{1}H NMR (400 MHz, DMSO-d6) δ** 8.89 (s, 1H), 8.08 (d, *J* = 8.4 Hz, 1H), 7.87 (ddd, *J* = 8.4, 6.8, 1.6 Hz, 1H), 7.55 (t, *J* = 6.8 Hz, 1H), 7.52 – 7.46 (m, 3H), 7.36 (d, *J* = 6.8 Hz, 1H), 7.18 (d, *J* = 5.6 Hz, 2H), 5.79 (s, 1H), 4.13 (m, 4H), 2.99 – 2.64 (m, 2H), 2.32 (m, 2H), 1.29 – 1.16 (m, 6H). **^{13}C NMR (100 MHz, DMSO-d6) δ** 196.32, 158.79, 156.91, 150.78, 148.41, 137.62, 131.89, 129.81, 128.82, 128.30, 127.81, 127.65, 127.57, 124.40, 62.25, 61.24, 38.30, 29.36, 25.62, 14.85, 14.78. **HRMS (ESI-MS):** m/z Calculated for $C_{25}H_{25}N_3O_5$[M+H] $^+$: 448.1867; Observed: 448.1869.

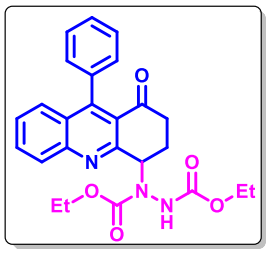

Diethyl 1-(7-chloro-1-oxo-9-phenyl-1,2,3,4-tetrahydroacridin-4-yl)hydrazine-1,2-dicarboxylate (3r): Yield= 90%, light Yellow solid; M. P: 181.2 – 181.6 °C; **IR (KBr, cm^{-1})**: 3309, 2982 1750, 1678, 1548, 1482,1312, 1284, 1024, 945,856; **^{1}H NMR (400 MHz, $CDCl_3$) δ** 8.00 (s, 1H), 7.71 (dd, *J* = 8.8, 2.0 Hz, 1H), 7.52 (m, 3H), 7.44 (d, *J* = 2.0 Hz, 1H), 7.22 – 7.16 (m, 1H), 7.14 – 7.09 (m, 1H), 6.56 (s, 1H), 5.74 (m, 1H), 4.43 – 4.31 (m, 2H), 4.22 (m, 2H), 2.83 (m, 2H), 2.62 (s, 1H), 2.39 (s, 1H), 1.42 (m, 2H), 1.28 (m, 4H). **^{13}C NMR (100 MHz, $CDCl_3$) δ** 195.82, 158.70, 156.75, 151.58, 146.73, 136.27,

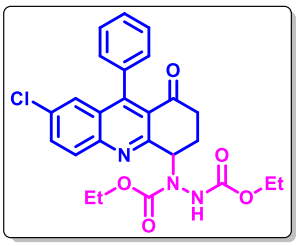

133.26, 132.83, 130.86, 128.65, 128.46, 128.35, 128.21, 128.13, 127.73, 126.74, 63.05, 62.22, 38.92, 25.63, 14.59, 14.43. **HRMS (ESI-MS):** m/z Calculated for $C_{25}H_{24}ClN_3O_5[M+H]^+$: 482.1477; Observed: 482.1479.

Diethyl 1-(9-(ethoxycarbonyl)-1-oxo-1,2,3,4-tetrahydroacridin-4-yl)hydrazine-1,2-dicarboxylate (3s): Yield= 82%, white solid; M. P: 170.3 – 170.9 °C; **IR (KBr, cm^{-1})**: 3350, 2924, 1725, 1689, 1356, 1227, 1024, 759; **^{1}H NMR (400 MHz, DMSO-d6) δ** 8.93 (s, 1H), 8.11 (d, *J* = 8.8 Hz, 1H), 7.98 (ddd, *J* = 8.4, 6.8, 1.4 Hz, 1H), 7.83 (d, *J* = 6.8 Hz, 1H), 7.76 (ddd, *J* = 8.4, 6.8, 1.2 Hz, 1H), 5.89 (s, 1H), 4.53 (q, *J* = 7.2 Hz, 2H), 4.20 (q, *J* = 7.0 Hz, 2H), 4.09 – 3.98 (m, 2H), 3.15 – 2.79 (m, 2H), 2.46 – 2.19 (m, 2H), 1.38 (t, *J* = 7.2 Hz, 3H), 1.28 – 1.20 (m, 3H), 1.12 (t, *J* = 7.0 Hz, 3H). **^{13}C NMR (100 MHz, DMSO) δ** 195.89, 167.26, 158.78, 156.88, 156.74, 149.12, 141.55, 132.99, 130.08, 128.83, 126.14, 123.28, 121.91, 62.25, 62.22, 61.22, 36.89, 25.70, 14.80, 14.74, 14.24. **HRMS (ESI-MS):** m/z Calculated for $C_{22}H_{25}N_3O_7[M+H]^+$: 444.1766; Observed: 444.1764.

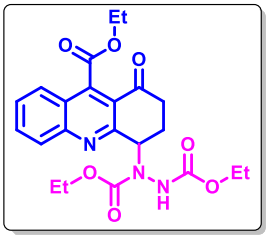

Diethyl 1-(quinolin-2-ylmethyl)hydrazine-1,2-dicarboxylate (3t): Yield= 85%, white solid; M. P: 77.9- 78.2 °C; **IR (KBr, cm^{-1})**: 3263, 2978, 2874, 1754, 1645, 1502, 1325, 1219, 1132, 1058, 915; **^{1}H NMR (400 MHz, CDCl$_3$) δ** 8.18 – 8.04 (m, 1H), 7.99 (s, 1H), 7.74 (s, 2H), 7.65 (s, 1H), 7.51 – 7.47 (m, 1H), 7.33 (d, *J* = 8.4 Hz, 1H), 5.01 (s, 2H), 4.24 – 4.15 (m, 4H), 1.23 (t, *J* = 7.2 Hz, 6H). **^{13}C NMR (100 MHz, DMSO-d6) δ** 157.88, 156.57, 156.19, 147.61, 136.90, 129.85, 129.08, 128.12, 127.58, 126.62, 120.47, 62.35, 61.23, 56.81, 14.75, 14.46. **HRMS (ESI-MS):** m/z Calculated for $C_{16}H_{19}N_3O_4[M+H]^+$: 318.1449; Observed: 318.1454.

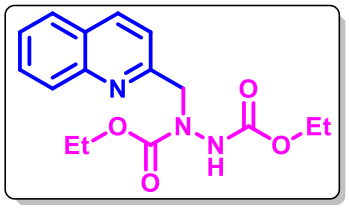

Diethyl 1-(1-(4-phenyl-3-propionylquinolin-2-yl)ethyl)hydrazine-1,2-dicarboxylate (3u): Yield= 83%, white solid; M. P: 127.1 – 127.6 °C;**IR (KBr, cm^{-1})**: 3351, 2978, 2934, 1744, 1707, 1559, 1314, 1257, 1140, 1028, 954, 755; **^{1}H NMR (400 MHz, DMSO-d6) δ** 8.86 (s, 1H), 7.94 (s, 1H), 7.57 (t, *J* = 7.2 Hz, 1H), 7.39 (s, 1H), 7.33 (d, *J* = 8.8 Hz, 2H), 7.31 – 7.28 (m, 2H), 7.23 (s, 1H), 6.92 (s, 1H), 5.52 – 5.13 (m, 1H), 3.81 (m, 4H), 1.84 (s, 2H), 1.27 (s, 3H), 0.90 (m, 6H), 0.42 – 0.38 (m, 3H). **^{13}C NMR (100 MHz, DMSO-d6) δ** 207.81, 156.60, 155.93, 147.03, 135.35, 130.45, 130.34, 129.90, 129.31, 129.22, 128.90,

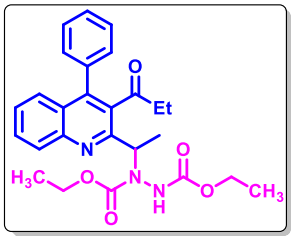

127.84, 126.00, 125.68, 62.18, 61.08, 37.74, 16.84, 14.70, 7.51. **HRMS (ESI-MS):** m/z Calculated for $C_{26}H_{29}N_3O_5[M+H]^+$: 464.218; Observed: 464.2183.

Diethyl 1-(1-(6-chloro-4-phenyl-3-propionylquinolin-2-yl)ethyl)hydrazine-1,2-dicarboxylate (3v): Yield= 84%, white solid; M. P: 129.2 - 130 °C;**IR (KBr, cm^{-1})**: 3274, 2981, 2929, 1749, 1731, 1702, 1682, 1226, 1058, 768; **^{1}H NMR (400 MHz, DMSO-d6) δ** 9.15 (s, 1H), 8.23 (s, 1H), 7.83 (dd, *J* = 8.8, 2.4 Hz, 1H), 7.66 – 7.62 (m, 1H), 7.56 (td, *J* = 4.0, 2.0 Hz, 2H), 7.49 – 7.43 (m, 2H), 7.16 (s, 1H), 5.56 (m, 1H), 4.02 (s, 4H), 2.08 (s, 1H), 1.50 (m, 3H), 1.22 – 1.07 (m, 6H), 0.64 (m, 4H). **^{13}C NMR (100 MHz, DMSO-d6) δ** 207.41, 156.62, 155.88, 145.49, 143.51, 134.63, 132.61, 132.10, 131.01, 130.40, 130.18, 129.62, 129.39, 129.09, 126.64, 124.57, 62.22, 61.08, 37.67, 16.70, 14.71, 14.68, 7.43. **HRMS (ESI-MS):** m/z Calculated for $C_{26}H_{28}ClN_3O_5[M+H]^+$: 498.179; Observed: 498.1799.

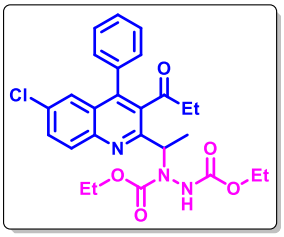

Diethyl 1-(5,6,7,8-tetrahydroquinolin-8-yl)hydrazine-1,2-dicarboxylate (3w): Yield= 70%, colourless oil; **IR (KBr, cm^{-1})**: 3274, 2981, 2929, 1749, 1731, 1702, 1682, 1226, 1058, 768 **^{1}H NMR (400 MHz, CDCl$_3$) δ** 8.38 (d, *J* = 5.2 Hz, 1H), 7.40 (d, *J* = 7.6 Hz, 1H), 7.09 (dd, *J* = 7.8, 4.8 Hz, 1H), 6.53 (s, 1H), 5.58 – 5.26 (m, 1H), 4.23 (q, *J* = 7.2 Hz, 4H), 2.83 – 2.71 (m, 2H), 2.04 – 1.81 (m, 4H), 1.28 (m, 6H). **^{13}C NMR (100 MHz, CDCl$_3$) δ** 156.36, 154.24, 147.18, 137.27, 122.21, 63.10, 62.61, 61.77, 31.88, 28.32, 21.32, 14.45. **HRMS (ESI-MS):** m/z Calculated for $C_{15}H_{21}N_3O_4[M+H]^+$: 308.1605; Observed: 308.1605.

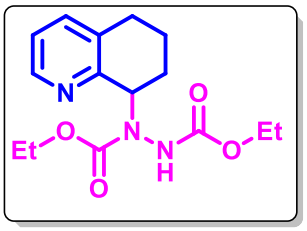

Diethyl 1-((3-hydroxyquinoxalin-2-yl)methyl)hydrazine-1,2-dicarboxylate (3x): Yield= 82%, white solid; M. P: 128.5 – 128.9 °C; **IR (KBr, cm^{-1})**: 3274, 2982, 2929, 1728, 1481, 1380, 1236, 1060, 763; **^{1}H NMR (400 MHz, DMSO-d6) δ** 12.39 (s, 1H), 8.99 (m, 1H), 7.85 – 7.58 (m, 1H), 7.55 – 7.48 (m, 1H), 7.36 – 7.21 (m, 2H), 4.15 – 3.98 (m, 4H), 1.23 – 1.08 (m, 6H). **^{13}C NMR (100 MHz, DMSO-d6) δ** 155.99, 155.46, 154.04, 132.79, 131.54, 130.95, 129.26, 123.43, 115.71, 62.61, 61.32, 14.56, 14.53. **HRMS (ESI-MS):** m/z Calculated for $C_{15}H_{18}N_4O_5[M+H]^+$: 335.135; Observed: 335.1349.

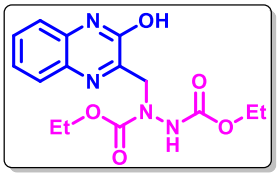

1-Phenyl-3-(1,2,3,4-tetrahydroacridin-4-yl)pyrrolidine-2,5-dione (5a): Yield= 90%, white solid; M. P: 154.5 – 155.1 °C; **IR (KBr, cm^{-1})**: 3034, 2982, 2855, 1759, 1699, 1454, 1392, 1132, 758; **^{1}H NMR (400 MHz, CDCl$_3$) δ** 7.83 (s, 1H), 7.70 – 7.63 (m, 2H), 7.63 – 7.51 (m,

4H), 7.50 – 7.28 (m, 3H), 4.04 (m, 1H), 3.26 (s, 1H), 3.00 (m, 2H), 2.84 (m, 1H), 2.51 – 2.40 (m, 1H), 2.24 (m, 1H), 2.03 (m, 2H), 1.74 (m, 1H). **^{13}C NMR (101 MHz, $CDCl_3$) δ** 179.33, 176.53, 157.47, 146.13, 135.19, 132.95, 131.20, 129.07, 128.75, 128.70, 128.09, 127.33, 126.80, 126.31, 126.15, 44.02, 43.16, 31.23, 29.32, 28.75, 22.56. **HRMS (ESI-MS):** m/z Calculated for $C_{23}H_{20}N_2O_2[M+H]^+$: 357.1598; Observed: 357.1597.

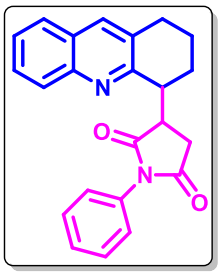

3-(9-Methyl-1,2,3,4-tetrahydroacridin-4-yl)-1-phenylpyrrolidine-2,5-dione (5b): Yield= 87%, white solid; M. P: 180.9 – 181.9 °C; **IR (KBr, cm^{-1})**: 3068, 2924, 2858, 1770, 1705, 1498, 1181, 785; **^{1}H NMR (400 MHz, $CDCl_3$) δ** 7.96 (dd, *J* = 8.4, 2.0 Hz, 1H), 7.83 (dd, *J* = 8.4, 2.0 Hz, 1H), 7.56 (ddd, *J* = 8.4, 6.8, 1.6 Hz, 1H), 7.47 (ddd, *J* = 8.3, 6.8, 1.6 Hz, 1H), 7.41 – 7.33 (m, 2H), 7.33 – 7.28 (m, 1H), 7.17 – 7.08 (m, 2H), 3.96 – 3.86 (m, 1H), 3.69 – 3.60 (m, 1H), 3.16 – 3.06 (m, 2H), 3.06 – 2.99 (m, 1H), 2.90 – 2.80 (m, 1H), 2.55 (s, 3H), 2.22 – 2.15 (m, 2H), 2.11 (m, 1H), 1.90 – 1.82 (m, 1H).

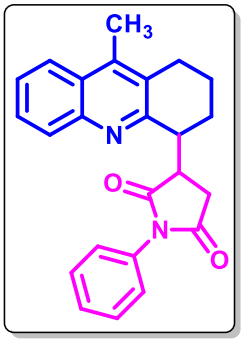

^{13}C NMR (101 MHz, $CDCl_3$) δ 179.31, 176.99, 157.85, 145.52, 141.40, 132.36, 129.58, 128.98, 128.85, 128.29, 128.17, 127.04, 126.64, 125.82, 123.30, 44.75, 43.89, 35.15, 29.72, 27.10, 22.80, 13.74. **HRMS (ESI-MS):** m/z Calculated for $C_{24}H_{22}N_2O_2[M+H]^+$: 371.1754; Observed: 371.1754.

1-Phenyl-3-(9-phenyl-1,2,3,4-tetrahydroacridin-4-yl)pyrrolidine-2,5-dione (5c): Yield= 91%, white solid; M. P: 208.4 - 209.2 °C; **IR (KBr, cm^{-1})**: 3060, 2927, 2861, 1702, 1572, 1485, 1186, 770; **^{1}H NMR (400 MHz, $CDCl_3$) δ** 7.71 (d, *J* = 8.4 Hz, 1H), 7.65 – 7.60 (m, 2H), 7.59 – 7.54 (m, 2H), 7.54 – 7.50 (m, 2H), 7.48 (dd, *J* = 8.4, 4.4 Hz, 2H), 7.45 – 7.41 (m, 1H), 7.29 (dd, *J* = 4.4, 1.2 Hz, 2H), 7.22 (dt, *J* = 6.4, 1.2 Hz, 2H), 4.13 – 4.08 (m, 1H), 3.29 (m, 1H), 2.89 (m, 1H), 2.73 – 2.62 (m, 2H), 2.61 – 2.56 (m, 1H), 2.25 – 2.19 (m, 1H), 1.98 – 1.87 (m, 2H), 1.78 – 1.70 (m, 1H). **^{13}C NMR (101 MHz, $CDCl_3$) δ** 179.42, 176.67, 157.30, 146.77, 145.75, 136.92, 132.99, 129.11, 129.08, 129.00, 128.84, 128.71, 128.68, 128.53, 128.08, 127.88, 126.77, 126.34, 125.99, 125.75, 44.08, 43.52, 31.34, 28.87, 27.41, 22.53. **HRMS (ESI-MS):** m/z Calculated for $C_{29}H_{24}N_2O_2[M+H]^+$: 433.1911; Observed: 433.1910.

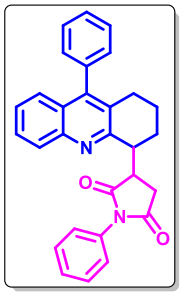

3-(7-Chloro-9-phenyl-2,3-dihydro-1H-cyclopenta[b]quinolin-3-yl)-1-phenylpyrrolidine-2,5-dione (5d): Yield= 90%, white solid; M. P: 198.9-199.4 °C; **IR (KBr, cm^{-1})**: 3072, 2954, 1706, 1556, 1475, 1150, 945, 762; **^{1}H NMR (400 MHz, CDCl$_3$) δ** 7.81 (d, *J* = 8.8 Hz, 1H), 7.59 (d, *J* = 3.5 Hz, 3H), 7.58 (d, *J* = 1.6 Hz, 2H), 7.54 (dd, *J* = 8.8, 4.4 Hz, 2H), 7.51 (d, *J* = 1.6 Hz, 1H), 7.50 – 7.44 (m, 2H), 7.37 – 7.32 (m, 2H), 4.24 (m, 1H), 3.47 – 3.41 (m, 1H), 2.99 – 2.79 (m, 3H), 2.51 (m, 2H), 1.94 – 1.85 (m, 1H). **^{13}C NMR (101 MHz, CDCl$_3$) δ** 178.65, 176.01, 164.98, 146.46, 142.55, 135.53, 134.38, 132.68, 131.96, 130.86, 129.32, 129.20, 128.51, 127.18, 126.58, 124.54, 46.74, 41.72, 31.30, 29.43, 28.74. **HRMS (ESI-MS):** m/z Calculated for $C_{28}H_{21}ClN_2O_2$[M+H] $^{+}$: 453.1359; Observed: 453.1359.

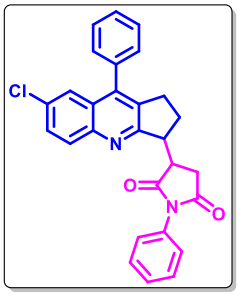

3-(7-Chloro-9-phenyl-1,2,3,4-tetrahydroacridin-4-yl)-1-phenylpyrrolidine-2,5-dione (5e): Yield= 94%, white solid; M. P: 200 – 200.8 °C; **IR (KBr, cm^{-1})**: 3065, 2957, 2874, 1734, 1589, 1498, 1167, 860, 770; **^{1}H NMR (400 MHz, CDCl$_3$) δ** 7.63 (d, *J* = 8.8 Hz, 1H), 7.60 (s, 1H), 7.58 (s, 2H), 7.56 (s, 1H), 7.55 – 7.49 (m, 3H), 7.48 – 7.44 (m, 1H), 7.42 (dd, *J* = 8.8, 2.0 Hz, 1H), 7.26 (s, 1H), 7.20 (dt, *J* = 6.4, 2.0 Hz, 2H), 4.08 (m, 1H), 3.34 – 3.28 (m, 1H), 2.91 (m, 1H), 2.69 – 2.64 (m, 1H), 2.64 – 2.59 (m, 1H), 2.59 – 2.52 (m, 1H), 2.27 – 2.20 (m, 1H), 1.98 – 1.94 (m, 1H), 1.94 – 1.69 (m, 2H). **^{13}C NMR (101 MHz, CDCl$_3$) δ** 179.32, 176.59, 157.77, 146.08, 144.07, 136.10, 132.87, 131.89, 130.40, 129.86, 129.53, 129.14, 128.98, 128.94, 128.90, 128.24, 128.18, 127.51, 126.21, 124.56, 43.94, 43.51, 31.31, 28.70, 27.45, 22.38. **HRMS (ESI-MS):** m/z Calculated for $C_{29}H_{23}ClN_2O_2$[M+H] $^{+}$: 467.1521; Observed: 467.1527.

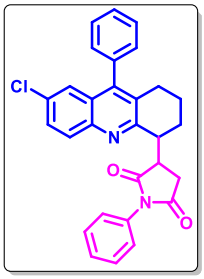

tert-Butyl 8-chloro-4-(2,5-dioxo-1-phenylpyrrolidin-3-yl)-10-phenyl-3,4-dihydrobenzo[b][1,6]naphthyridine-2(1H)-carboxylate (5f): Yield= 84%, white solid; M. P: 202.1- 202.7 °C; **IR (KBr, cm^{-1})**: **^{1}H NMR (400 MHz, CDCl$_3$) δ** 7.70 (d, *J* = 8.8 Hz, 1H), 7.58 (s, 2H), 7.56 (s, 1H), 7.54 (s, 3H), 7.53 – 7.47 (m, 2H), 7.45 (t, *J* = 8.4 Hz, 1H), 7.36 (s, 1H), 7.23 (d, *J* = 7.6 Hz, 2H), 4.54 (m, 2H), 4.30 – 4.19 (m, 2H), 3.32 (m, 2H), 2.99 – 2.82 (m, 1H), 2.74 – 2.53 (m, 1H), 1.43 (m, 9H). **^{13}C NMR (101 MHz, CDCl$_3$) δ** 178.33, 176.05, 154.37, 144.64, 134.40, 132.68, 132.61, 130.53, 130.38, 129.20, 128.87, 128.38, 127.34, 126.27, 124.73, 80.73, 44.04, 41.21, 31.13,

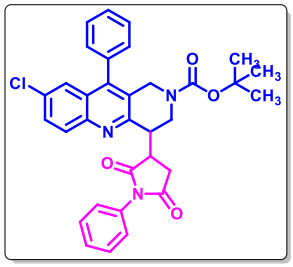

29.71, 28.35. **HRMS (ESI-MS):** m/z Calculated for $C_{33}H_{30}ClN_3O_4[M+H]^+$: 568.1998; Observed: 568.1995.

3-(7-Nitro-9-phenyl-1,2,3,4-tetrahydroacridin-4-yl)-1-phenylpyrrolidine-2,5-dione (5g): Yield= 95%, light Yellow solid; M. P: 201.4 - 202.2 °C; **IR (KBr, cm^{-1})**: 3032, 1770, 1704, 1596, 1344, 1283, 1182, 1092, 781; **^{1}H NMR (400 MHz, CDCl$_3$) δ** 8.30 – 8.21 (m, 2H), 7.81 (d, *J* = 8.8 Hz, 1H), 7.58 (d, *J* = 4.0 Hz, 5H), 7.57 – 7.50 (m, 2H), 7.46 (dt, *J* = 8.8, 4.0 Hz, 1H), 7.23 (m, 2H), 4.14 – 4.08 (m, 1H), 3.36 (m, 1H), 2.96 (m, 1H), 2.76 – 2.63 (m, 2H), 2.58 (m, 1H), 2.27 (m, 1H), 1.98 (m, 2H), 1.81 – 1.74 (m, 1H). **^{13}C NMR (101 MHz, CDCl$_3$) δ** 179.07, 176.38, 161.82, 148.79, 147.58, 145.32, 135.08, 132.76, 131.28, 130.46, 129.21, 129.15, 128.92, 128.85, 128.83, 128.30, 126.10, 122.91, 122.18, 43.81, 43.76, 31.35, 28.36, 27.41, 22.15. **HRMS (ESI-MS):** m/z Calculated for $C_{29}H_{23}N_3O_4[M+H]^+$: 478.1762; Observed: 478.1689.

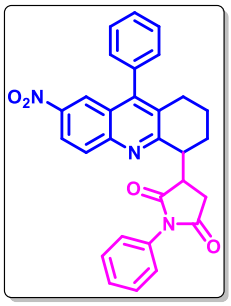

3-(9-Chloro-1,2,3,4-tetrahydroacridin-4-yl)-1-phenylpyrrolidine-2,5-dione (5h): Yield= 90%, White solid; M. P: 166.2 – 167.0 °C; **IR (KBr, cm^{-1})**: 3063, 2923, 2854, 1770, 1705, 1595, 1480, 1158, 919, 857; **^{1}H NMR (400 MHz, CDCl$_3$) δ** 8.14 (dd, *J* = 8.0, 3.2 Hz, 1H), 7.67 (dd, *J* = 7.2, 1.6 Hz, 1H), 7.60 (dd, *J* = 8.8, 1.6 Hz, 2H), 7.58 – 7.55 (m, 2H), 7.55 – 7.50 (m, 2H), 7.47 – 7.40 (m, 1H), 4.06 (m, 1H), 3.30 – 3.26 (m, 1H), 3.26 – 3.19 (m, 1H), 2.96 – 2.80 (m, 2H), 2.38 (m, 1H), 2.23 (m, 2H), 2.05 – 1.95 (m, 1H), 1.73 (td, *J* = 12.8, 9.4 Hz, 1H). **^{13}C NMR (101 MHz, CDCl$_3$) δ** 179.09, 176.31, 157.60, 146.13, 141.86, 132.85, 129.54, 129.10, 128.12, 127.17, 126.18, 125.45, 123.66, 44.04, 43.69, 31.09, 28.97, 27.34, 22.30. **HRMS (ESI-MS):** m/z Calculated for $C_{23}H_{19}ClN_2O_2[M+H]^+$: 391.1208; Observed: 391.1214.

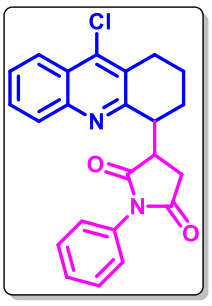

3-(6-Bromo-9-chloro-1,2,3,4-tetrahydroacridin-4-yl)-1-phenylpyrrolidine-2,5-dione (5i): Yield= 91%, white solid; M. P: 186.5 – 187.2 °C; **IR (KBr, cm^{-1})**: 3054, 2924, 2853, 1710, 1599, 1458, 1382, 1179, 821, 816; **^{1}H NMR (400 MHz, CDCl$_3$) δ** 8.00 (d, *J* = 8.8 Hz, 1H), 7.88 (d, *J* = 2.0 Hz, 1H), 7.63 – 7.59 (m, 1H), 7.58 (d, *J* =6.0 Hz, 4H), 7.49 – 7.41 (m, 1H), 4.06 – 4.01 (m, 1H), 3.30 (m, 1H), 3.25 – 3.17 (m, 1H), 2.86 (m, 2H), 2.38 – 2.32 (m, 1H), 2.27 – 2.21 (m, 2H), 2.01 – 1.95 (m, 1H), 1.77 – 1.71 (m, 1H). **^{13}C NMR (101 MHz, CDCl$_3$) δ** 178.82, 176.03, 158.87, 146.53, 142.00, 132.68, 131.28, 130.68, 129.71,

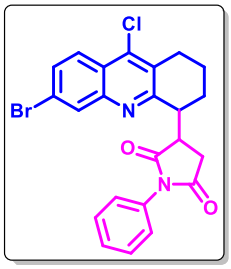

129.15, 128.27, 126.06, 125.19, 124.23, 123.80, 43.89, 43.64, 31.11, 28.72, 27.39, 22.14. **HRMS (ESI-MS):** m/z Calculated for $C_{23}H_{18}BrClN_2O_2[M+H]^+$: 469.0313; Observed: 469.0317.

3-(9-Chloro-6-nitro-1,2,3,4-tetrahydroacridin-4-yl)-1-phenylpyrrolidine-2,5-dione (5j): Yield= 96%, white solid; M. P: 184.2 – 185.2 °C; **IR (KBr, cm^{-1})**: 3069, 2953, 2824, 1732, 1549, 1452, 1361, 1182, 825; **^{1}H NMR (400 MHz, CDCl$_3$) δ** 8.63 (s, 1H), 8.30 (s, 2H), 7.63 (s, 1H), 7.62 (d, *J* = 2.6 Hz, 3H), 7.48 (dd, *J* = 6.2, 3.4 Hz, 1H), 4.08 (m, 1H), 3.40 – 3.36 (m, 1H), 3.33 – 3.27 (m, 1H), 2.90 (m, 2H), 2.32 (d, *J* = 5.6 Hz, 1H), 2.28 (t, *J* = 5.6 Hz, 2H), 2.04 – 1.99 (m, 1H), 1.78 (m, 1H). **^{13}C NMR (101 MHz, CDCl$_3$) δ** 178.67, 175.80, 160.71, 148.13, 144.86, 142.04, 132.86, 132.49, 129.37, 128.57, 128.45, 125.93, 125.76, 125.17, 120.59, 43.77, 31.14, 29.71, 28.45, 27.78, 21.97. **HRMS (ESI-MS):** m/z Calculated for $C_{23}H_{18}ClN_3O_4[M+H]^+$: 436.1059; Observed: 436.1056.

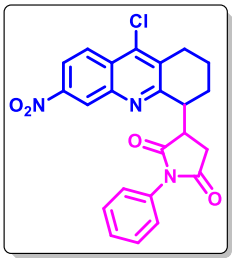

Methyl-4-(2,5-dioxo-1-phenylpyrrolidin-3-yl)-1,2,3,4-tetrahydroacridine-9-carboxylate (5k): Yield= 95%, White solid; M. P: 134.6 - 135.2 °C; **IR (KBr, cm^{-1})**: 3045, 2937, 1770, 1736, 1596, 1440, 1384, 1228, 1182, 1092, 985, 781; **^{1}H NMR (400 MHz, CDCl$_3$) δ** 7.88 (d, *J* = 8.0 Hz, 1H), 7.67 (d, *J* = 9.2 Hz, 1H), 7.62 (ddd, *J* = 8.0, 6.8, 1.6 Hz, 1H), 7.51 (ddd, *J* = 8.0, 6.8, 1.6 Hz, 1H), 7.41 – 7.36 (m, 2H), 7.34 (d, *J* = 7.2 Hz, 1H), 7.16 (d, *J* = 1.6 Hz, 1H), 7.14 (s, 1H), 4.05 (s, 3H), 3.94 (d, *J* = 8.0 Hz, 1H), 3.70 – 3.64 (m, 1H), 3.13 (m, 1H), 3.01 (m, 2H), 2.97 (d, *J* = 4.8 Hz, 1H), 2.22 – 2.14 (m, 2H), 2.14 – 2.08 (m, 1H), 1.95 – 1.85 (m, 1H). **^{13}C NMR (101 MHz, CDCl$_3$) δ** 178.91, 176.68, 168.13, 158.43, 145.83, 137.88, 132.25, 129.26, 129.20, 129.04, 128.40, 127.54, 127.20, 126.57, 124.13, 123.12, 52.58, 44.37, 43.51, 34.77, 29.70, 26.71, 22.17. **HRMS (ESI-MS):** m/z Calculated for $C_{25}H_{22}N_2O_4[M+H]^+$: 415.1653; Observed: 415.1654.

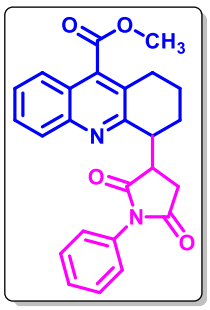

Prop-2-yn-1-yl 4-(2,5-dioxo-1-phenylpyrrolidin-3-yl)-1,2,3,4-tetrahydroacridine-9-carboxylate (5l): Yield= 82%, white solid; M. P: 170.1-171 °C; **IR (KBr, cm^{-1})**: 3229, 2932, 2865, 1741, 1701, 1498, 1397, 1206,1026, 947, 769; **^{1}H NMR (400 MHz, CDCl$_3$) δ** 7.71 (m, 1H), 7.69 (m,1H), 7.59 – 7.56 (m, 3H), 7.54 (dd, *J* = 7.2, 1.6 Hz, 2H), 7.51 – 7.47 (m, 1H), 7.45 – 7.41 (m, 1H), 5.05 (s, 2H), 4.09 – 4.04 (m, 1H), 3.30 – 3.26 (m, 1H), 3.04 – 2.98 (m, 2H), 2.86 (m, 1H), 2.61 (s, 1H), 2.44 (m, , 1H), 2.28 – 2.22 (m,

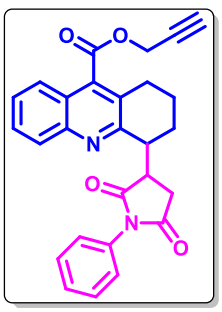

1H), 2.16 – 2.10 (m, 1H), 2.05 – 1.97 (m, 1H), 1.81 – 1.74 (m, 1H). **^{13}C NMR (100 MHz, $CDCl_3$) δ** 179.03, 176.27, 166.82, 157.43, 145.68, 137.05, 132.84, 129.41, 129.09, 128.13, 127.86, 127.38, 126.20, 123.95, 123.01, 76.89, 75.95, 52.99, 43.98, 43.41, 31.12, 28.79, 26.38, 22.13. **HRMS (ESI-MS):** m/z Calculated for $C_{27}H_{22}N_2O_4[M+H]^+$: 439.1653; Observed: 439.1658.

Benzyl 4-(2,5-dioxo-1-phenylpyrrolidin-3-yl)-1,2,3,4-tetrahydroacridine-9-carboxylate (5m): Yield= 91%, white solid; M. P: 138.7- 139.3 °C; **IR (KBr, cm^{-1})**: 3060, 2935, 2852, 1730, 1705, 1498, 1337, 1178, 1023, 766; **^{1}H NMR (400 MHz, $CDCl_3$) δ** 7.68 (d, *J* = 8.0 Hz, 1H), 7.59 (d, *J* = 2.0 Hz, 1H), 7.57 (d, *J* = 2.0 Hz, 3H), 7.55 – 7.53 (m, 1H), 7.53 – 7.50 (m, 1H), 7.47 (dd, *J* = 8.0, 2.0 Hz, 2H), 7.45 – 7.42 (m, 2H), 7.41 – 7.37 (m, 3H), 5.50 (s, 2H), 4.04 (dd, *J* = 5.2, 2.4 Hz, 1H), 3.26 (dd, *J* = 5.2, 2.4 Hz, 1H), 2.96 – 2.88 (m, 2H), 2.84 (m, 1H), 2.42 (m, 1H), 2.26 – 2.19 (m, 1H), 2.08 (m, 1H), 2.01 – 1.92 (m, 1H), 1.75 (m, 1H). **^{13}C NMR (101 MHz, $CDCl_3$) δ** 179.06, 176.30, 167.47, 157.39, 145.69, 137.97, 135.00, 132.84, 129.29, 129.09, 128.79, 128.12, 127.52, 127.23, 126.20, 124.01, 123.06, 67.67, 43.98, 43.41, 31.12, 28.80, 26.35, 22.14. **HRMS (ESI-MS):** m/z Calculated for $C_{31}H_{26}N_2O_4[M+H]^+$: 491.1966; Observed: 491.1966.

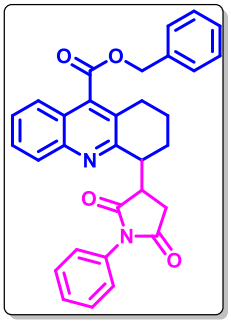

4-(2,5-Dioxo-1-phenylpyrrolidin-3-yl)-N-(p-tolyl)-1,2,3,4-tetrahydroacridine-9-carboxamide (5n): Yield= 80%, white solid; M. P: 227.9 – 228.3 °C; **IR (KBr, cm^{-1})**: 3441, 3296, 2926, 2858, 1706, 1670, 1534, 1392, 1185, 819, 763; **^{1}H NMR (400 MHz, $CDCl_3$) δ** 8.66 (s, 1H), 7.80 (q, *J* = 8.4 Hz, 2H), 7.59 (d, *J* = 7.6 Hz, 1H), 7.54 (m, 3H), 7.52 (d, *J* = 2.4 Hz, 2H), 7.50 (m, 2H), 7.42 (t, *J* = 7.2 Hz, 2H), 7.15 (d, *J* = 8.4 Hz, 2H), 3.05 (m, 3H), 2.82 (s, 1H), 2.62 (s, 2H), 2.35 (s, 3H), 2.06 (m, 2H), 1.84 (s, 1H), 1.58 (s, 1H). **^{13}C NMR (101 MHz, $CDCl_3$) δ** 176.43, 165.52, 157.49, 145.66, 141.56, 135.17, 134.73, 132.71, 129.69, 129.56, 129.29, 129.10, 128.87, 128.26, 127.13, 126.19, 124.39, 123.40, 120.00, 43.85, 43.23, 30.88, 28.64, 26.04, 22.03, 20.96. **HRMS (ESI-MS):** m/z Calculated for $C_{31}H_{27}N_3O_3[M+H]^+$: 490.2125; Observed: 490.2124.

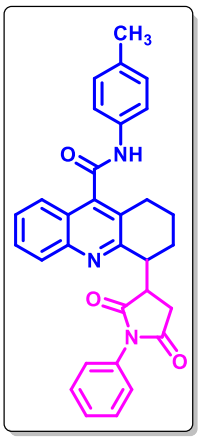

3-(7-Chloro-1-oxo-9-phenyl-1,2,3,4-tetrahydroacridin-4-yl)-1-phenylpyrrolidine-2,5-dione (5o): Yield= 88%, white solid; M. P: 241.2-241.9 °C; **IR (KBr, cm^{-1})**: 3072, 2954, 1706, 1556, 1475, 1386, 1150, 945, 762; **^{1}H NMR (400 MHz, $CDCl_3$) δ** 7.85 (d, *J* = 8.8 Hz, 1H), 7.67 (dd, *J* = 8.8, 2.4 Hz, 1H), 7.58 – 7.51 (m, 3H), 7.49 – 7.45 (m, 2H), 7.45 – 7.38 (m, 2H), 7.26 (s, 1H), 7.25 – 7.19 (m, 2H), 7.19 – 7.13 (m, 1H), 3.85 – 3.74 (m, 2H), 3.36 – 3.20 (m, 2H), 2.88 (m, 1H), 2.82 – 2.70 (m, 2H), 2.35 (m, 1H). **^{13}C NMR (101 MHz, $CDCl_3$) δ** 196.55, 178.51, 176.47, 161.04, 151.09, 146.15, 136.37, 133.14, 132.80, 132.24, 130.50, 129.15, 128.55, 128.53, 128.47, 128.37, 128.26, 128.10, 127.71, 126.81, 126.47, 124.38, 44.62, 43.28, 40.31, 35.15, 26.59. **HRMS (ESI-MS):** m/z Calculated for $C_{29}H_{21}ClN_2O_3[M+H]^+$: 481.1314; Observed: 481.1312.

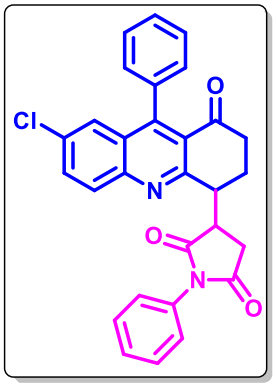

Ethyl 4-(2,5-dioxo-1-phenylpyrrolidin-3-yl)-1-oxo-1,2,3,4-tetrahydroacridine-9-carboxylate (5p): Yield= 80%, light Yellow solid; M. P: 204.1- 204.5 °C; **IR (KBr, cm^{-1})**: 3084, 2924, 1731, 1708, 1691, 1571, 1498, 1287, 1181, 784, 755; **^{1}H NMR (400 MHz, $CDCl_3$) δ** 7.94 (d, *J* = 8.0 Hz, 1H), 7.87 – 7.80 (m, 2H), 7.65 (t, *J* = 7.2 Hz, 1H), 7.46 – 7.41 (m, 2H), 7.39 (d, *J* = 7.2 Hz, 1H), 7.24 – 7.18 (m, 2H), 4.66 (q, *J* = 7.2 Hz, 2H), 3.87 (d, *J* = 2.4 Hz, 1H), 3.87 – 3.82 (m, 1H), 3.29 (m, 1H), 3.13 (m, 1H), 3.07 – 3.00 (m, 1H), 2.90 – 2.81 (m, 1H), 2.77 – 2.67 (m, 1H), 2.41 – 2.35 (m, 1H), 1.50 (t, *J* = 7.2 Hz, 3H). **^{13}C NMR (100 MHz, $CDCl_3$) δ** 195.79, 178.27, 176.30, 167.64, 160.42, 148.66, 142.40, 132.89, 132.15, 129.31, 129.11, 128.52, 128.22, 126.49, 126.37, 123.35, 121.44, 62.54, 44.01, 43.07, 39.11, 34.78, 29.70, 26.40, 14.08. **HRMS (ESI-MS):** m/z Calculated for $C_{26}H_{22}N_2O_5[M+H]^+$: 443.1602; Observed: 443.1603.

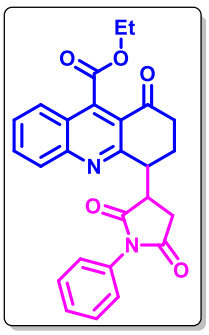

1-Phenyl-3-(quinolin-2-ylmethyl)pyrrolidine-2,5-dione (5q): Yield= 89%, white solid; M. P: 123.4 -124 °C; **IR (KBr, cm^{-1})**: 3084, 2924, 1731, 1708, 1691, 1571, 1498, 1287, 1181, 784, 755; **^{1}H NMR (400 MHz, $CDCl_3$) δ** 8.04 (d, *J* = 8.4 Hz, 1H), 7.85 (d, *J* = 8.8 Hz, 1H), 7.74 (d, *J* = 8.4 Hz, 1H), 7.61 (t, *J* = 7.6 Hz, 1H), 7.49 – 7.45 (m, 2H), 7.43 (s, 1H), 7.39 – 7.35 (m, 2H), 7.34 (s, 1H), 7.25 (t, *J* = 2.4 Hz, 1H), 3.69 (m, 1H), 3.53 – 3.44 (m, 2H), 3.05 – 2.90 (m, 2H). **^{13}C NMR (100 MHz, $CDCl_3$) δ** 179.24, 176.47, 157.42, 147.47, 136.60, 132.57, 129.69, 129.13, 129.04, 128.39, 127.56, 126.84, 126.55,

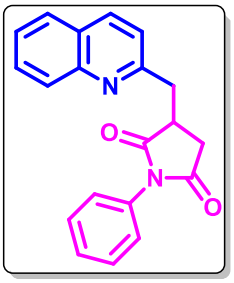

126.28, 121.59, 38.34, 37.23, 34.09. **HRMS (ESI-MS):** m/z Calculated for $C_{20}H_{16}N_2O_2$[M+H]$^+$: 317.1285; Observed: 317.1284.

1-Phenyl-3-(1-(4-phenyl-3-propionylquinolin-2-yl)ethyl)pyrrolidine-2,5-dione (5r): Yield= 76%, white solid; M. P: 172.1-172.8 °C; **IR (KBr, cm^{-1})**: 3060, 2927, 2861, 1702, 1572, 1498, 1186, 770, 756; **^{1}H NMR (400 MHz, $CDCl_3$) δ** 7.95 (dd, *J* = 9.0, 1.2 Hz, 1H), 7.67 (ddd, *J* = 8.4, 6.8, 1.6 Hz, 1H), 7.61 (dd, *J* = 9.0, 1.6 Hz, 1H), 7.51 – 7.46 (m, 3H), 7.46 – 7.43 (m, 1H), 7.39 – 7.35 (m, 1H), 7.35 – 7.30 (m, 3H), 7.30 – 7.26 (m, 1H), 7.07 – 7.00 (m, 2H), 4.15 – 3.88 (m, 1H), 3.75 – 3.63 (m, 1H), 3.41 (m, 1H), 3.01 (m, 1H), 2.48 (m, 1H), 2.24 – 2.09 (m, 1H), 1.55 (t, *J* = 7.2 Hz, 3H), 0.83 (t, *J* = 7.2 Hz, 3H). **^{13}C NMR (100 MHz, $CDCl_3$) δ** 208.59, 179.11, 177.20, 158.49, 146.97, 144.65, 135.06, 134.68, 132.30, 130.65, 130.17, 129.99, 129.22, 129.04, 128.92, 128.83, 128.40, 128.37, 126.99, 126.60, 126.12, 125.25, 45.17, 38.59, 38.36, 33.05, 20.08, 7.59. **HRMS (ESI-MS):** m/z Calculated for $C_{30}H_{26}N_2O_3$[M+H]$^+$: 463.2016; Observed: 463.2027.

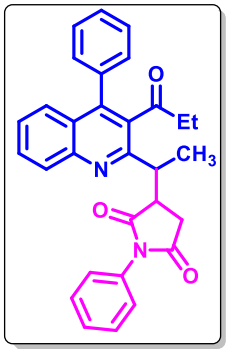

3-(1-(3-Acetyl-6-chloro-4-phenylquinolin-2-yl)ethyl)-1-phenylpyrrolidine-2,5-dione (5s): Yield= 79%, White solid; M. P: 162.3-163 °C; **IR (KBr, cm^{-1})**:3057, 2973, 2925, 1775, 1705, 1478, 1392, 1184, 1074, 965, 835; **^{1}H NMR (400 MHz, $CDCl_3$) δ** 7.90 (d, *J* = 8.8 Hz, 1H), 7.64 (dd, *J* = 8.8, 2.4 Hz, 1H), 7.60 (d, *J* = 2.4 Hz, 1H), 7.57 – 7.52 (m, 3H), 7.52 – 7.49 (m, 1H), 7.39 – 7.35 (m, 3H), 7.34 (d, *J* = 7.6 Hz, 1H), 7.33 – 7.30 (m, 1H), 7.04 (dd, *J* = 4.8, 2.4 Hz, 1H), 3.90 (d, *J* = 4.8 Hz, 1H), 3.76 – 3.67 (m, 1H), 3.46 – 3.40 (m, 1H), 3.05 (d, *J* = 8.1 Hz, 1H), 2.50 (m, 1H), 2.15 (m, 1H), 1.57 (d, *J* = 7.2 Hz, 3H), 0.85 (t, *J* = 7.2 Hz, 3H). **^{13}C NMR (100 MHz, $CDCl_3$) δ** 208.15, 178.95, 177.08, 158.94, 145.33, 143.91, 135.41, 134.32, 133.03, 132.16, 131.11, 130.75, 130.59, 129.81, 129.25, 129.10, 129.03, 128.65, 128.45, 126.45, 126.09, 124.94, 45.08, 38.59, 38.26, 32.95, 20.01, 7.49. **HRMS (ESI-MS):** m/z Calculated for $C_{30}H_{25}ClN_2O_3$[M+H]$^+$: 497.1627; Observed: 497.1627.

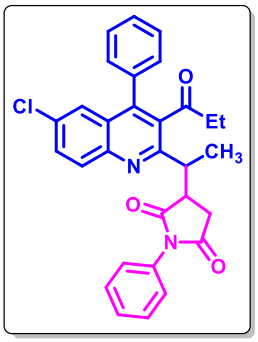

1-Phenyl-3-(5,6,7,8-tetrahydroquinolin-8-yl)pyrrolidine-2,5-dione (5t): Yield= 75%, light Yellow solid; M. P: 129.1-130.2 °C; **IR (KBr, cm^{-1})**: 3010, 2967, 2903, 2852, 1714, 1665, 1598, 1215, 1177, 1094, 880, 760; **^{1}H NMR (400 MHz, $CDCl_3$) δ** 8.34 (dd, *J* = 4.6, 1.8 Hz, 1H), 7.47 – 7.43 (m, 2H), 7.38 (dd, *J* = 7.6, 2.3 Hz, 2H), 7.24 (d, *J* = 1.3 Hz, 1H), 7.23 – 7.21 (m, 1H), 7.07 (ddd, *J* = 7.7, 4.6, 1.0 Hz, 1H), 4.06 (ddd, *J* = 9.7, 4.8, 3.4 Hz, 1H), 3.67 – 3.60 (m, 1H), 2.93 (dd, *J* = 18.5, 9.6 Hz, 1H), 2.83 – 2.80 (m, 2H), 2.67 (dd, *J* = 18.5, 4.7 Hz, 1H), 2.10 – 2.02 (m, 2H), 1.83 – 1.75 (m, 2H). **^{13}C NMR (100 MHz, $CDCl_3$) δ** 179.12, 176.47, 156.44, 146.76, 136.91, 133.18, 129.11, 128.47, 126.53, 121.75, 43.11, 42.51, 33.28, 28.82, 25.63, 22.06. **HRMS (ESI-MS):** m/z Calculated for $C_{19}H_{18}N_2O_2$ $[M+H]^+$: 307.1441; Observed: 307.1441.

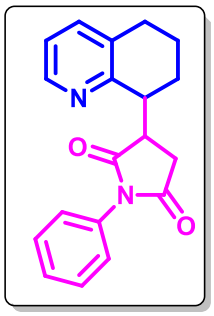

3-((3-Hydroxyquinoxalin-2-yl)methyl)-1-phenylpyrrolidine-2,5-dione (5u): Yield= 79%, white solid; M. P: 234.5-234.9 °C; **IR (KBr, cm^{-1})**: 3010, 2967, 2903, 2852, 1714, 1665, 1598, 1215, 1177, 1094, 880, 760; **^{1}H NMR (400 MHz, DMSO-d6) δ** 12.41 (s, 1H), 7.57 – 7.52 (m, 2H), 7.49 (d, *J* = 8.8 Hz, 2H), 7.42 (t, *J* = 7.6 Hz, 1H), 7.32 (t, *J* = 8.0 Hz, 3H), 7.27 (t, *J* = 7.6 Hz, 1H), 3.56 (q, *J* = 5.0 Hz, 1H), 3.43 (d, *J* = 4.4 Hz, 1H), 3.30 (m, 1H), 3.04 (m, 1H), 2.77 (m, 1H). **^{13}C NMR (100 MHz, DMSO-d6) δ** 179.58, 176.79, 159.26, 155.14, 133.36, 132.29, 131.65, 130.17, 129.30, 128.53, 127.33, 123.65, 115.86, 37.02, 34.43, 33.03. **HRMS (ESI-MS):** m/z Calculated for $C_{19}H_{15}N_3O_3[M+H]^+$: 334.1186; Observed: 334.1188.

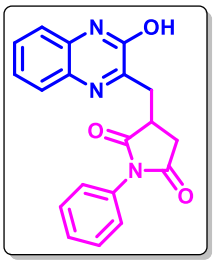

3.1.10 References

(1) Shukla, R. D.; Rai, B. *Spectrum of Emerging Sciences* **2021**,*1*, 21–28.

(2) (a) Latha, D. S.; Yaragorla, S. *Eur. J. Org. Chem.* **2020**, *15*, 2155–2179. (b) Yaragorla, S.; Singh, G.; Dada, R. *Tetrahedron Lett.* **2015,** *56*, 5924–5929. (c) Kumar, A.; Gupta, L. P.; Kumar, M. *RSC Adv.* **2013**, *3*, 18771–18774.

(3) (a) Liu, J. Y.; Niu, H. Y.; Wu, S.; Qu, G. R.; Guo, H. M. *Chem. Commun*. **2012**, *48*, 9723–9725. (b) Zhirov A. M.; Aksenov, A. V. *Russ. Chem. Rev*. **2014**, *83*, 502–522.

(4) (a) Zheng, H.; Fan, Y.; Blenko, A. L.; Lin, W. *J. Am. Chem. Soc.* **2023**, *145*, 9994–10000. (b) Chen, H.; Wang, L.; Xu, S.; Liu, X.; He, Q.; Song, L.; Ji, H. *ACS Catal.* **2021**, *11*, 6810–6815. (c) Amaoka, Y.; Kamijo, S.; Hoshikawa, T.; Inoue, M. *J. Org. Chem*. **2012**, *77*, 9959–9969.

(5) Qian, B.; Yang, L.; Huang, H. *Tetrahedron Lett.* **2013**, *54*, 711–714.

(6) (a) Fletcher, S. *Org. Chem. Front.* **2015**, *2*, 739–752. (b) Furkert, D. P.; Breitenbach, B.; Juen, L.; Sroka, I.; Pantin, M.; Brimble, M. A. *Eur. J. Org. Chem*. **2014**, 7806–7809. (c) Beddoe, R. H.; Sneddon, H. F.; Denton, R. M. *Org. Biomol. Chem*. **2018**, *16*, 7774–7781. (d) Usman, M.; Zhang, X. W.; Wu, D.; Guan, V.; Liu, W. B. *Org. Chem. Front.* **2019**, *6*, 1905–1928.

(7) (a) Nair, V.; Biju, A. T.; Mathew, S. C.; Babu, B. P.; *Chem. Asian J.* **2008**, *3*, 810–820. (b) Qian, B.; Guo, S.; Shao, J.; Zhu, Q.; Yang, L.; Xia, C.; Huang, H.; *J. Am. Chem. Soc.* **2010**, *132*, 3650–3651.

(8) (a) Manoharan, R.; Jeganmohan, M. *Asian J. Org. Chem.* **2019**, *11*, 1949–1969. (b) Singh, P.; Mritunjay, *Asian J. Org. Chem.* **2021**, *10*, 964–979. (c) Rueping, M.; Tolstoluzhsky, N. *Org. Lett.* **2011**,*13*, 1095–1097.

(9) (a) Janey, J. M. *Angew. Chem. Int. Ed.* **2005**, *44*, 4292–4300. (b) Stini, N. A.; Poursaitidis, E. T.; Nikitas, N. F.; Kartsinis, M.; Spiliopoulou, N.; Dasenaki, P. A.; Kokotos, C. G. *Org. Biomol. Chem.* **2023**, *21*, 1284–1293.

(10) Bettadapur, K. R.; Sherikar, M. S.; Lanke, V.; Prabhu, K. R. *Asian J. Org. Chem.* **2018**, *7*, 1338–1342

(11) (a) Nale, S. D.; Aslam, M.; Lee, Y. R. *ChemistrySelect* **2021**, *6*, 8244–8248. (b) Liu, S. L.; Shi, Y.; Xue, C.; Zhang, L.; Zhou, L.; Song, M. P. *Eur. J. Org. Chem.* **2021**, 5862–5879. (c) Thakur, A.; Dhiman, A. K.; Sumit, Kumar, R.; Sharma, U. *J. Org. Chem.* **2021**, *86*, 6612–6621. (d) Kumar, R.; Kumar, R.; Chandra, D.; Sharma, U. *J. Org. Chem.* **2019**, *84*, 1542–1552. (e) Han, S.; Park, J.; Kim, S.; Lee, S. H.; Sharma, S.; Mishra, N. K.; Jung, Y. H.; Kim, I. S. *Org. Lett.* **2016**, *18*, 4666–4669. (f) Kumar, S. V.; Banerjee, S.; Punniyamurthy, T. *Org. Chem. Front.* **2020**, *7*, 1527–1569.

(12) (a)Lanke, V.; Bettadapur, K. R.; Prabhu, K. R. *Org. Lett.* **2015**, *17*, 4662–4665. (b) Bettadapur, K. R.; Lanke, V.; Prabhu, K. R. *Org. Lett.* **2015**, *17*, 4658–4661. (c) Keshri, P.; Bettadapur, K. R.; Lanke, V.; Prabhu, K. R. *J. Org. Chem.* **2016**, *81*, 6056–6065. (d) Bettadapur, K. R.; Lanke, V.; Prabhu, K. R. *Chem. Commun*. **2017**, *53*, 6251–6254. (e) Chen, X. X.; Ren, J. T.; Xu, J. L.; Xie, H.; Sun, W.; Li, Y. M.; Sun, M. *Synlett.* **2018**, *29*, A–F.

(13) (a) Zhao, Z.; Yue, J.; Ji, X.; Nian, M.; Kang, K.; Qiao, H.; Zheng, X. *Bioorg. Chem.* **2021**, *108*,104557. (b) Zhang, L.; Tan, Y.; Wang, N. X.; Wu, Q. Y.; Xi, Z.; Yang, G. F. *Bioorg. Med. Chem.* **2010**, *18*,7948–7956.

(14)Trost, B. M.; Tracy, J. S.; Saget, T. *Chem. Sci*. **2018**, *9*, 2975–2980.

(15) Tang, R. J.; Retailleau, P.; Milcent, T.; Crousse, B. *ACS Omega* **2019**, *4*, 8960–8966.

(16) Li, H. Y.; Xing, L. J.; Xu, T.; Wang, P.; H. R.; Liu; Wang, B. *Tetrahedron Lett.* **2013**, *54*, 858–860.

(17) (a) Ai, F.; Chen, G. Q.; Ji, J. J.; Zhu, Z. Q.; Le, Z. G.; Xie, Z. B. *Heterocycles* **2018**, *96*, 1410–1420. (b) Ai, F.; Xie, Z. B.; Guofang, J.; Ji, J. J.; Le, C. *Chin. J. Org. Chem.* **2018**, *38*, 2174–2181. (c) Chen, G. Q.; Xie, Z. B.; Ai, F.; Chen, Z. S.; Lan, J.; Hu, Z. Y.; Le, Z. G. *Heterocycles* **2019**, *98*, 1189–1199.

(18)Shirisha, T.; Majhi, S.; Divakar, K.; Kashinath, D. *Org. Biomol. Chem*. **2024**, *22*, 790–804.

(19) (a) Sheldon, R. A. *ACS Sustain. Chem. Eng.* **2018**, *6*, 32–48. (b) Gisbert, P.; Albert-Soriano, M.; Pastor, I. M. *Eur. J. Org. Chem.* **2019**, 4928–4940. (c) Singh, P.; Yadav, P.; Mishra, A.; Awasthi, SK. *ACS omega* **2020**, *5*, 4223–4232.

(20) (a) Rather, I. A.; Alotaibi, S. H.; Alotaibi, M. T.; Altaf, M.; Ali, R. *ACS Omega* **2022**, *7*, 35825−35833. (b) Azizi, N.; Qomi, M.; Asghari, M.; Farhadi, E. *Sustain. Chem. and Pharm.* **2021**, *22*, 100457.

(21) Jamal, Z.; Teo, Y. C.; Lim, G. S. *Tetrahedron* **2016**, *72*, 2132–2138.

(22) Wang, D.; Hu, M.; Li, X.; Zhang, D.; Chen, C.; Fu, J.; Shao, S.; Shi, G.; Zhou, Y.; Wu, S.; Zhang, T. *Eur. J. Med. Chem*. **2019**, *168*, 207–220.

(23) Wu, Y.; Chen, Z.; Liu, Y.; Yu, L.; Zhou, L.; Yang, S.; Lai, L. *Bioorg. Med. Chem.* **2011**, *19*, 3361–3366.

(24) Lu, X.; Zhang, H.; Li, X.; Chen, G.; Li, Q. S.; Luo, Y.; Ruan, B. F.; Chen, X.-W.; Zhu, H.-L. *Bioorg. Med. Chem.* **2011**, *19*, 6827–6832.

(25) Ge, Y.; Yu, N.; *Synth. Commun*. **2021**, *51*, 379–387.

3.1.11 Selected Spectra

Diethyl 1-(7-chloro-9-phenyl-1,2,3,4-tetrahydroacridin-4-yl)hydrazine-1,2-dicarboxylate (3e):

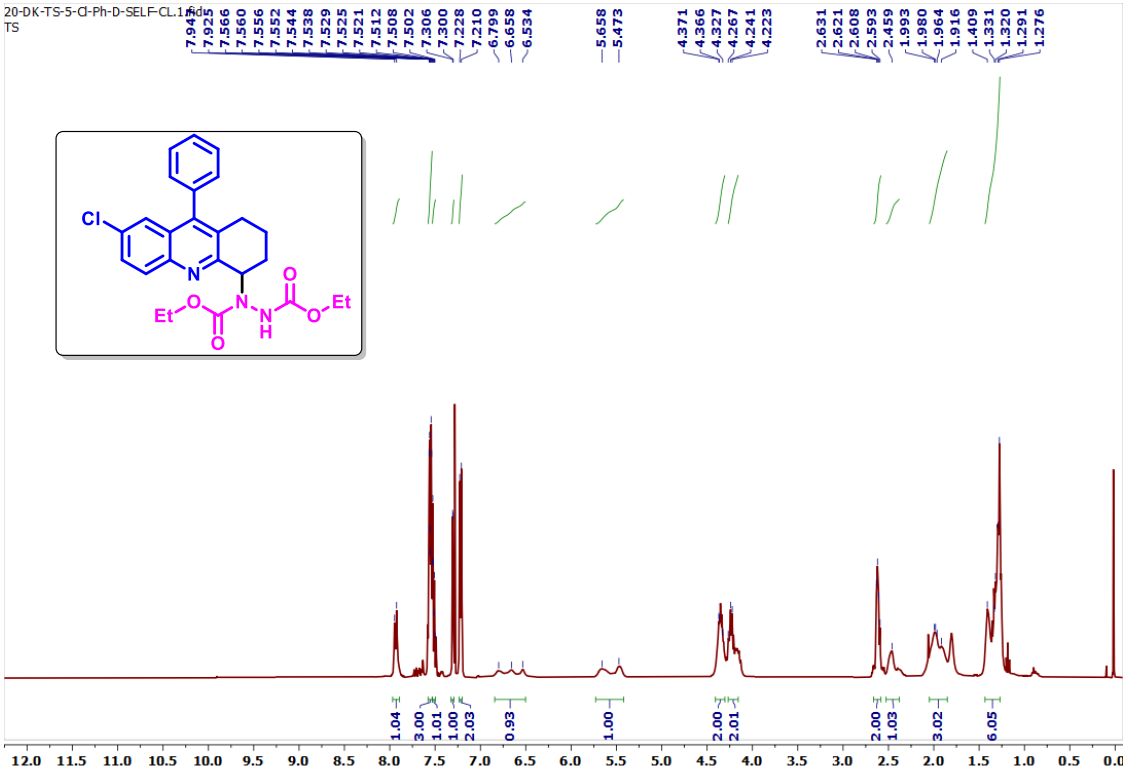

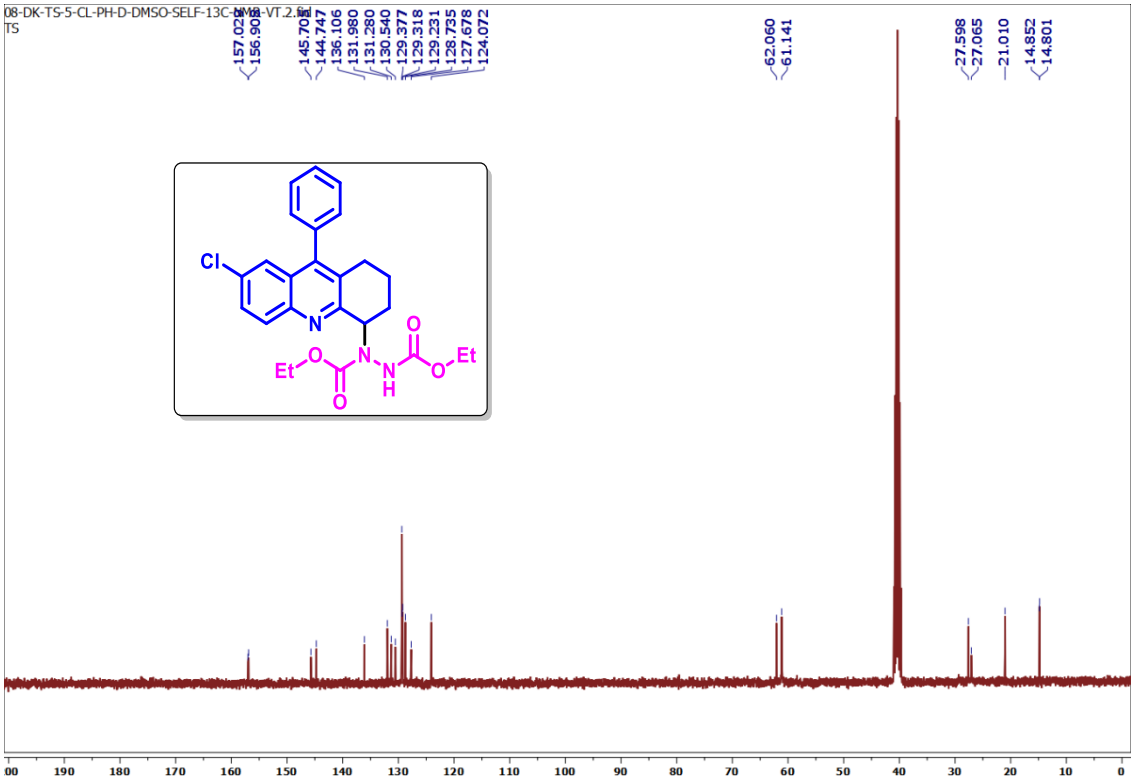

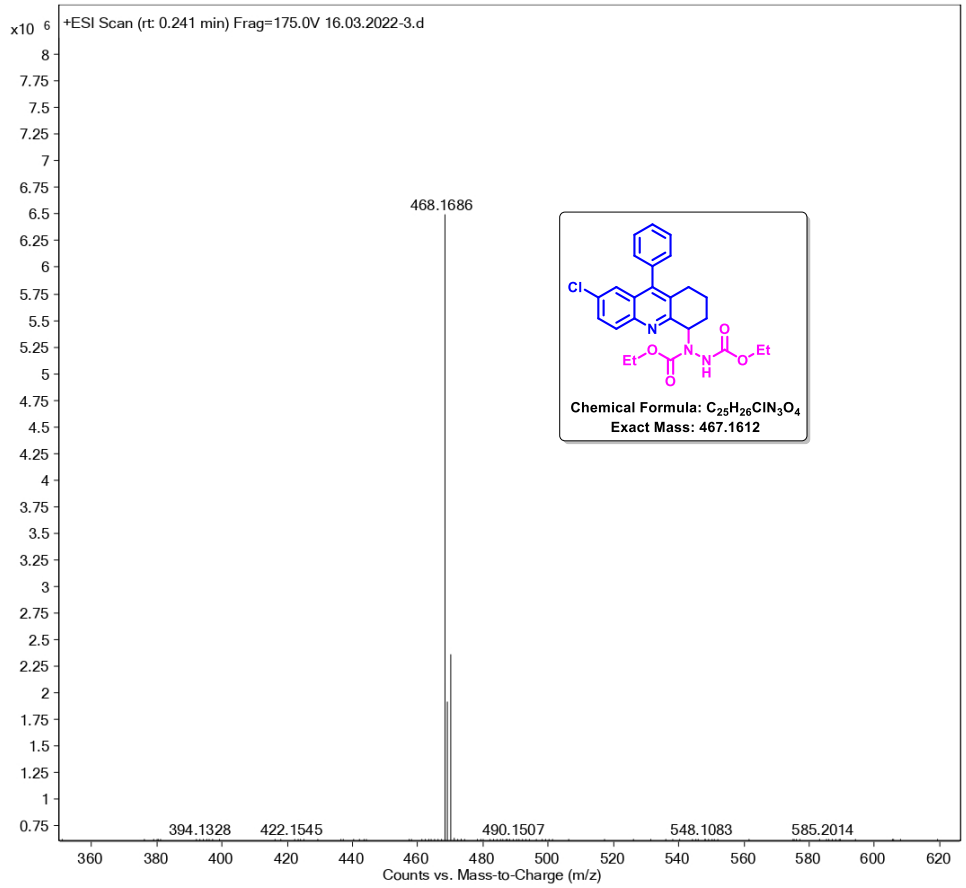

Diethyl 1-(9-chloro-1,2,3,4-tetrahydroacridin-4-yl)hydrazine-1,2-dicarboxylate (3h):

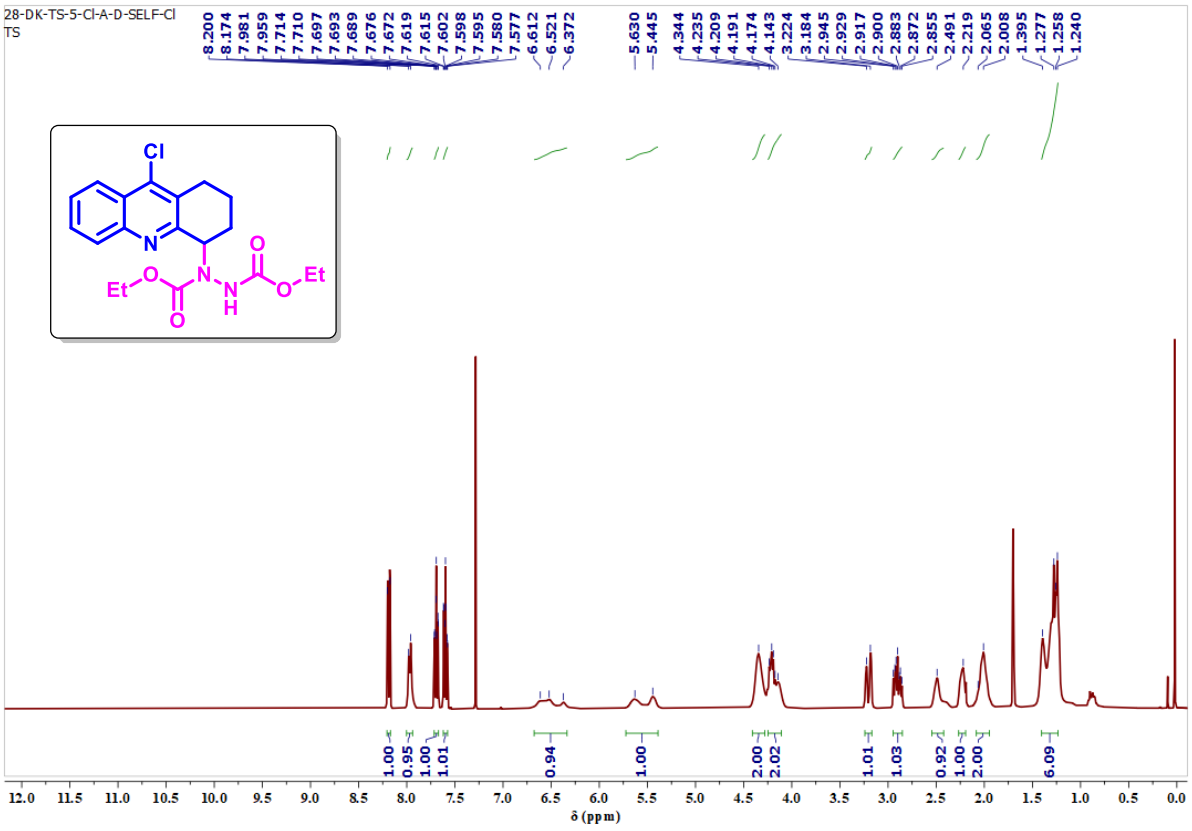

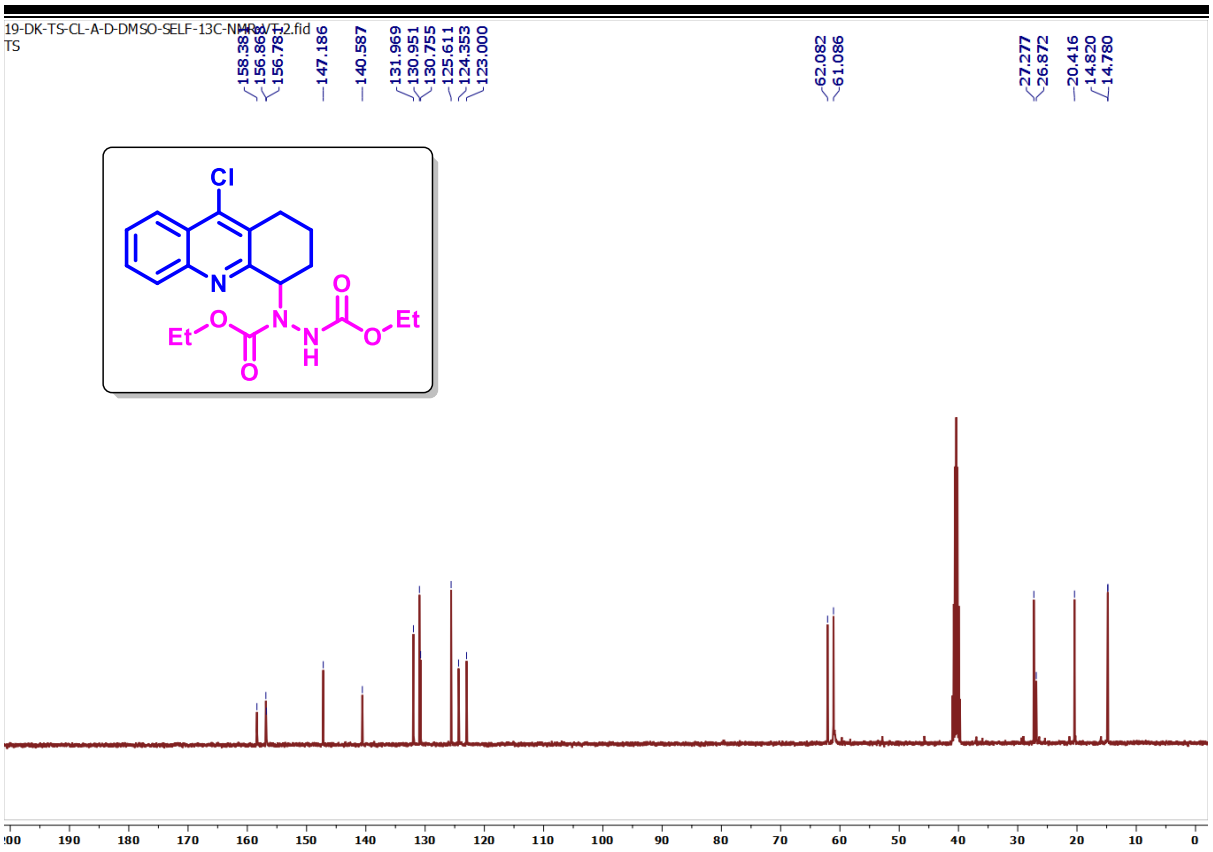
19-DK-TS-CL-A-D-DMSO-SELF-13C-NMR-01-F2.fid
TS
158.383
156.866
156.787
147.186
140.587
131.969
130.951
130.755
125.611
124.353
123.000
62.082
61.086
27.277
26.872
20.416
14.820
14.780
Cl
N
O
Et
O
N
N
H
O
Et
O

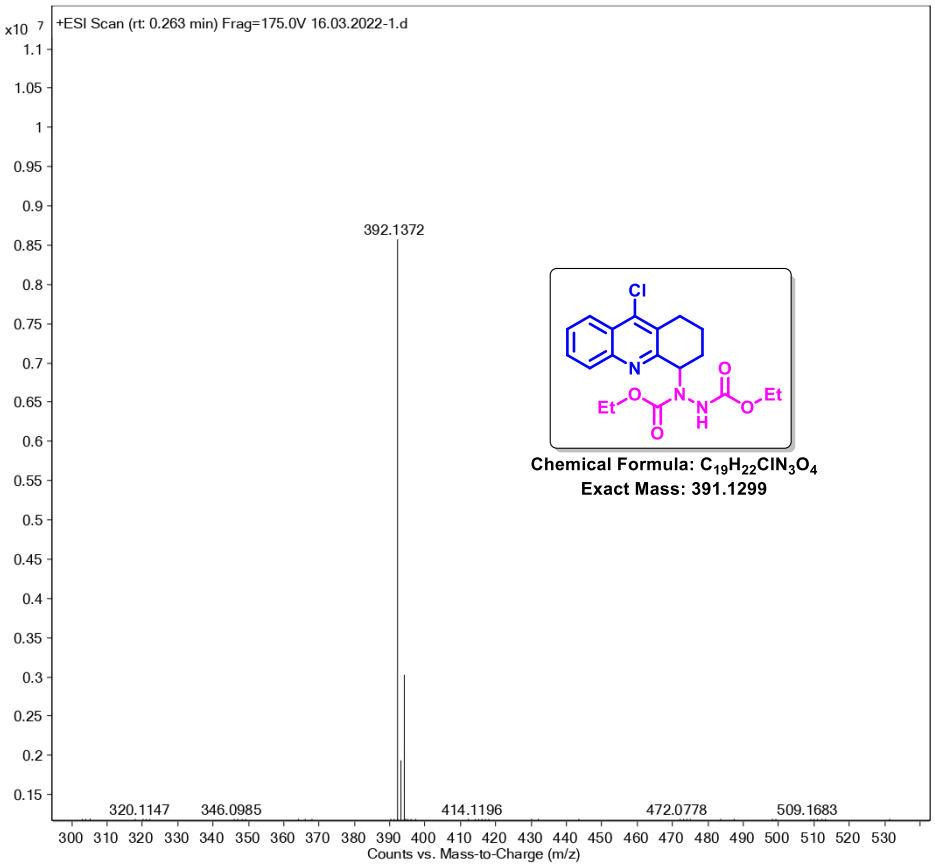
x10 7
+ESI Scan (rt: 0.263 min) Frag=175.0V 16.03.2022-1.d
392.1372
320.1147
346.0985
414.1196
472.0778
509.1683
Counts vs. Mass-to-Charge (m/z)
Cl
N
O
Et
O
N
N
H
O
Et
O
Chemical Formula: C19H22ClN3O4
Exact Mass: 391.1299

Diisopropyl 1-(9-(methoxycarbonyl)-1,2,3,4-tetrahydroacridin-4-yl)hydrazine-1,2-dicarboxylate (3l):

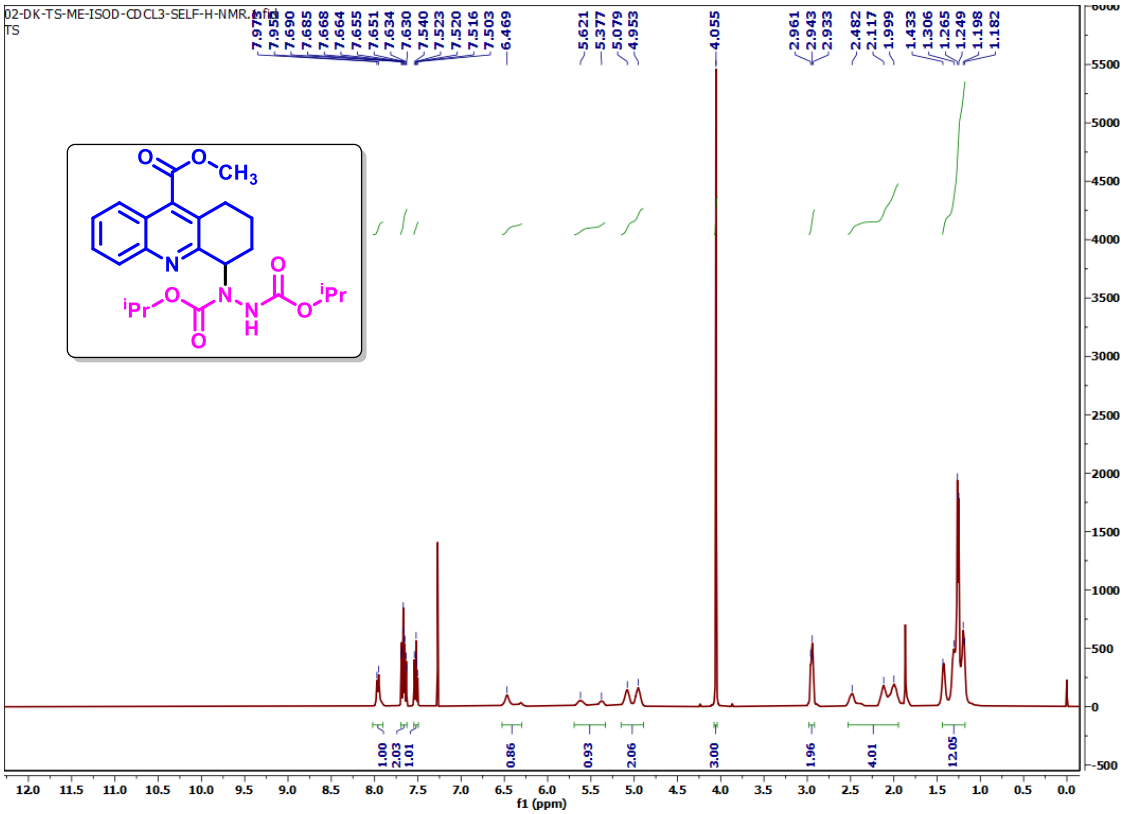

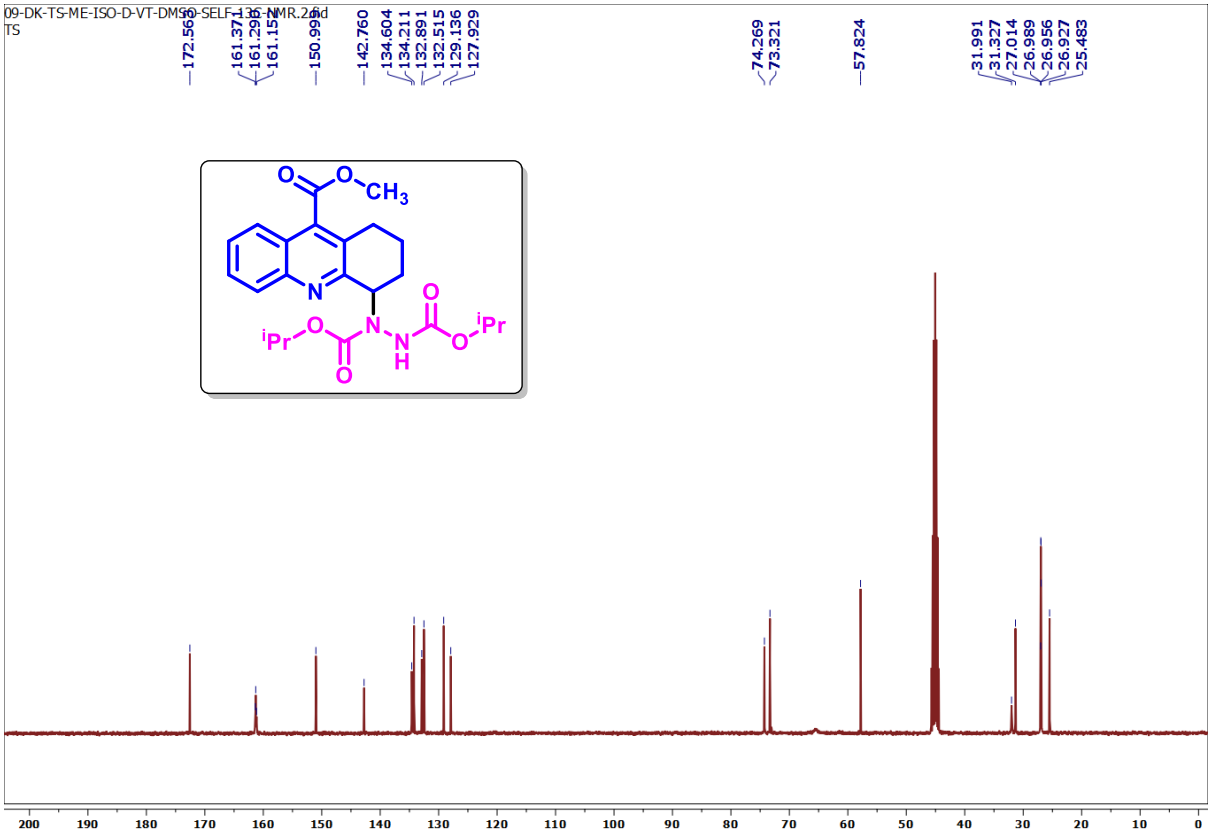

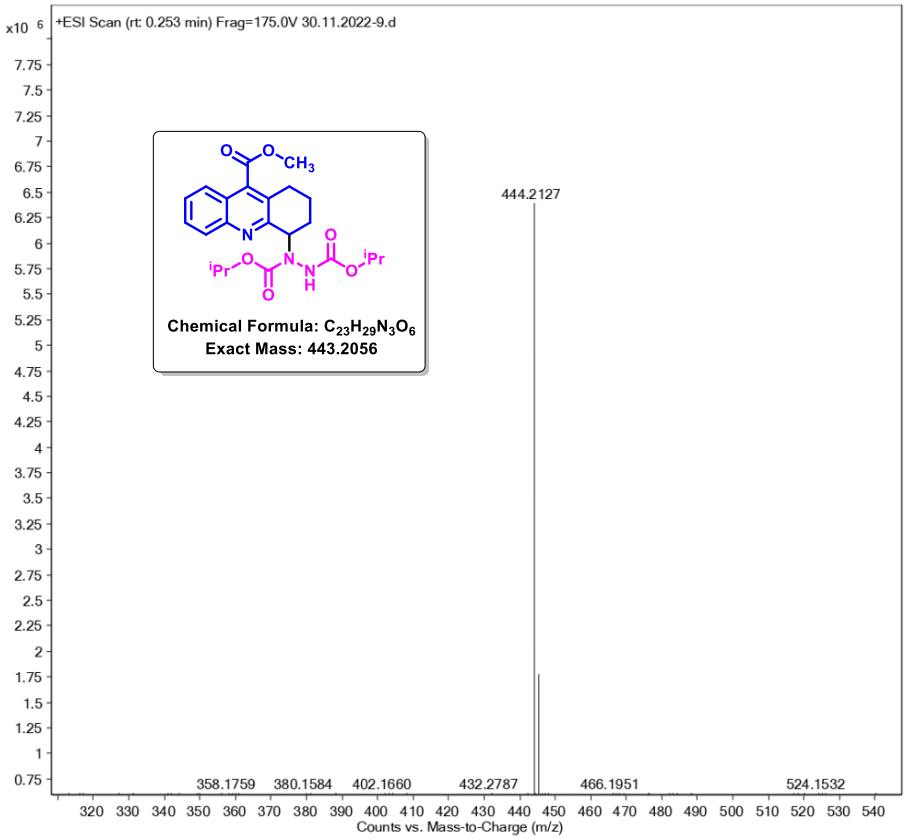

3-(9-Chloro-1,2,3,4-tetrahydroacridin-4-yl)-1-phenylpyrrolidine-2,5-dione (5h):

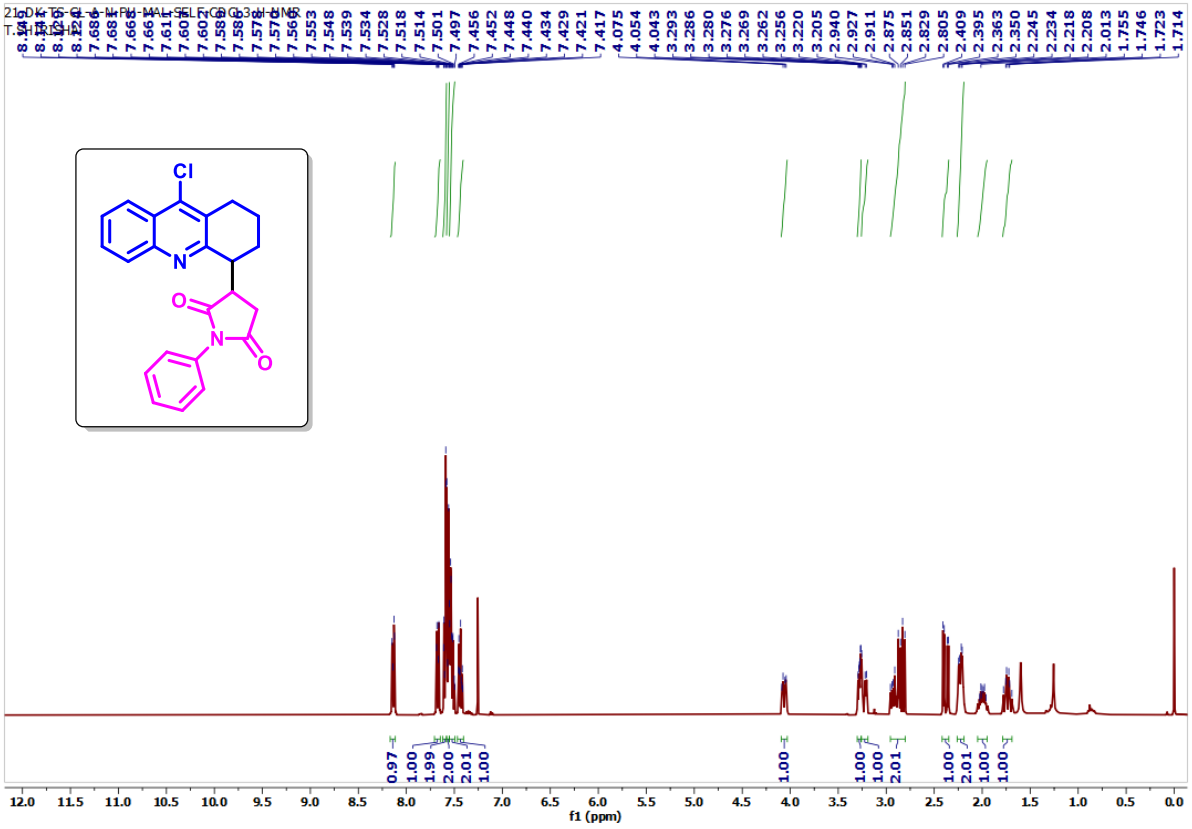

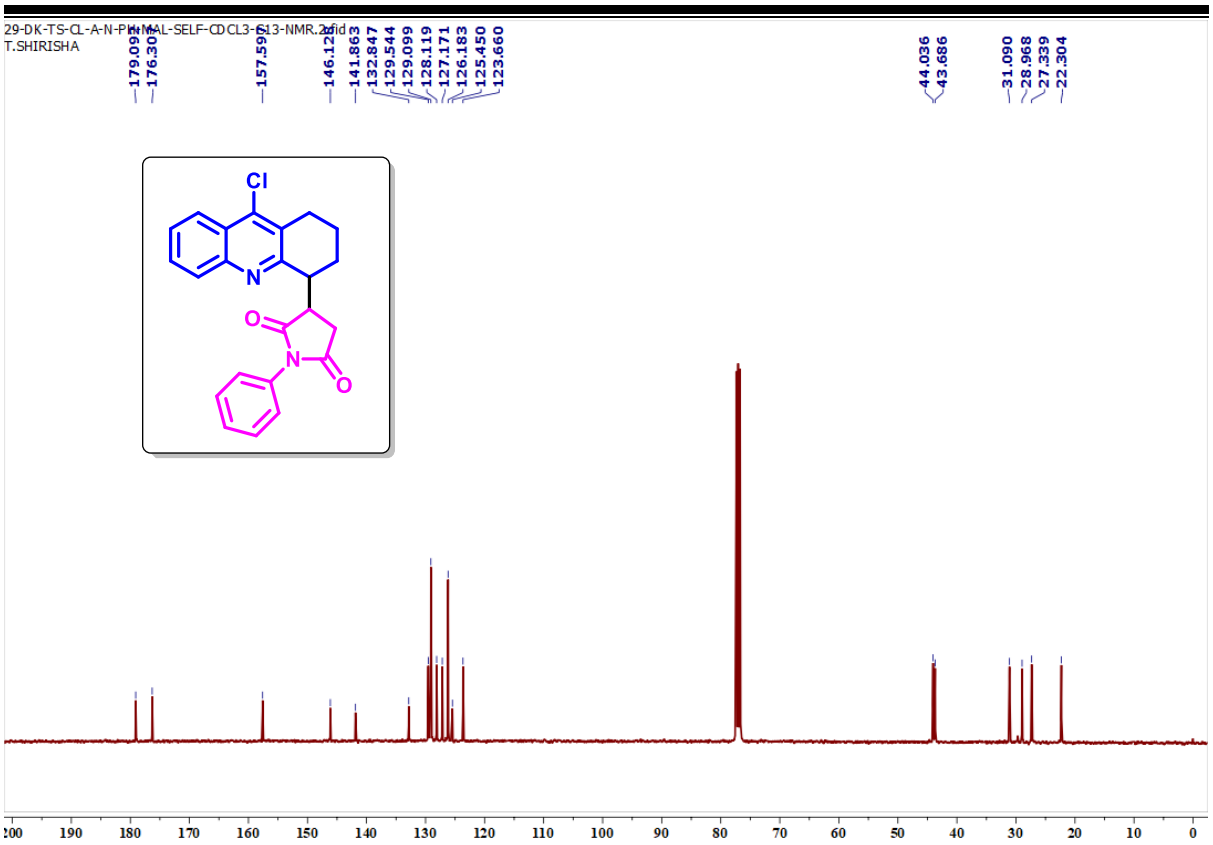
29-DK-TS-CL-A-N-PH-MAL-SELF-CDCL3-C13-NMR.2.fid
T.SHIRISHA
179.094
176.305
157.591
146.121
141.863
132.847
129.544
129.099
128.119
127.171
126.183
125.450
123.660
44.036
43.686
31.090
28.968
27.339
22.304
Cl
N
O
N
O

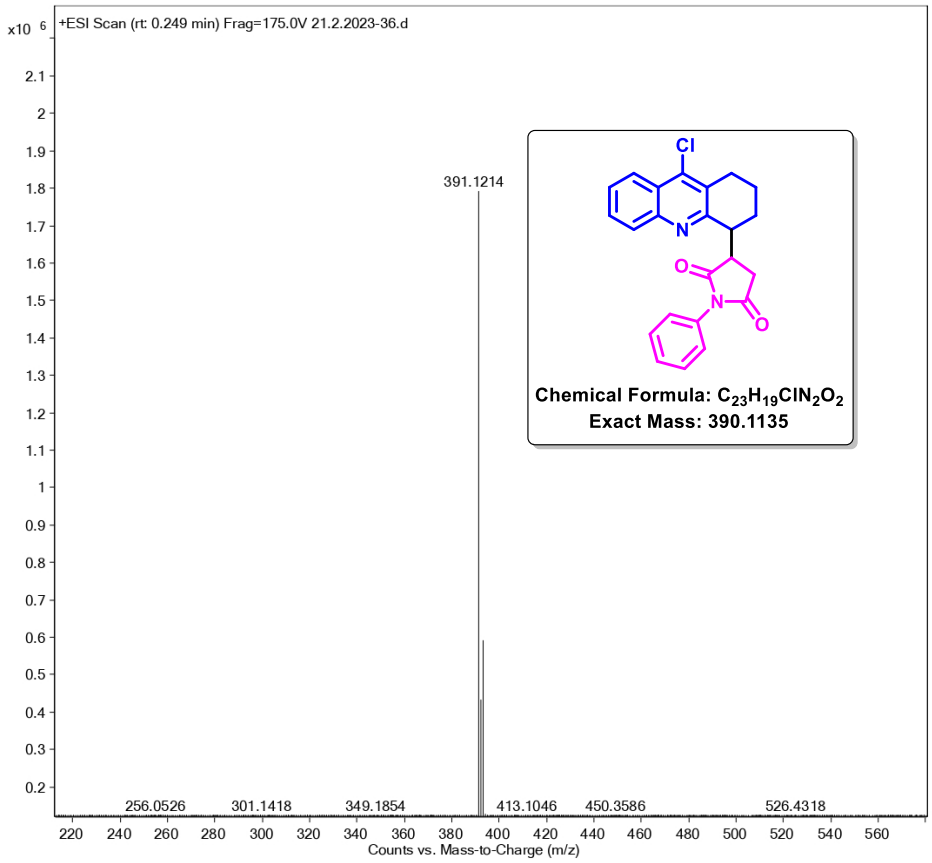
x10 6
+ESI Scan (rt: 0.249 min) Frag=175.0V 21.2.2023-36.d
391.1214
256.0526
301.1418
349.1854
413.1046
450.3586
526.4318
Counts vs. Mass-to-Charge (m/z)
Cl
N
O
N
O
Chemical Formula: C23H19ClN2O2
Exact Mass: 390.1135

Methyl 4-(2,5-dioxo-1-phenylpyrrolidin-3-yl)-1,2,3,4-tetrahydroacridine-9-carboxylate (5k):

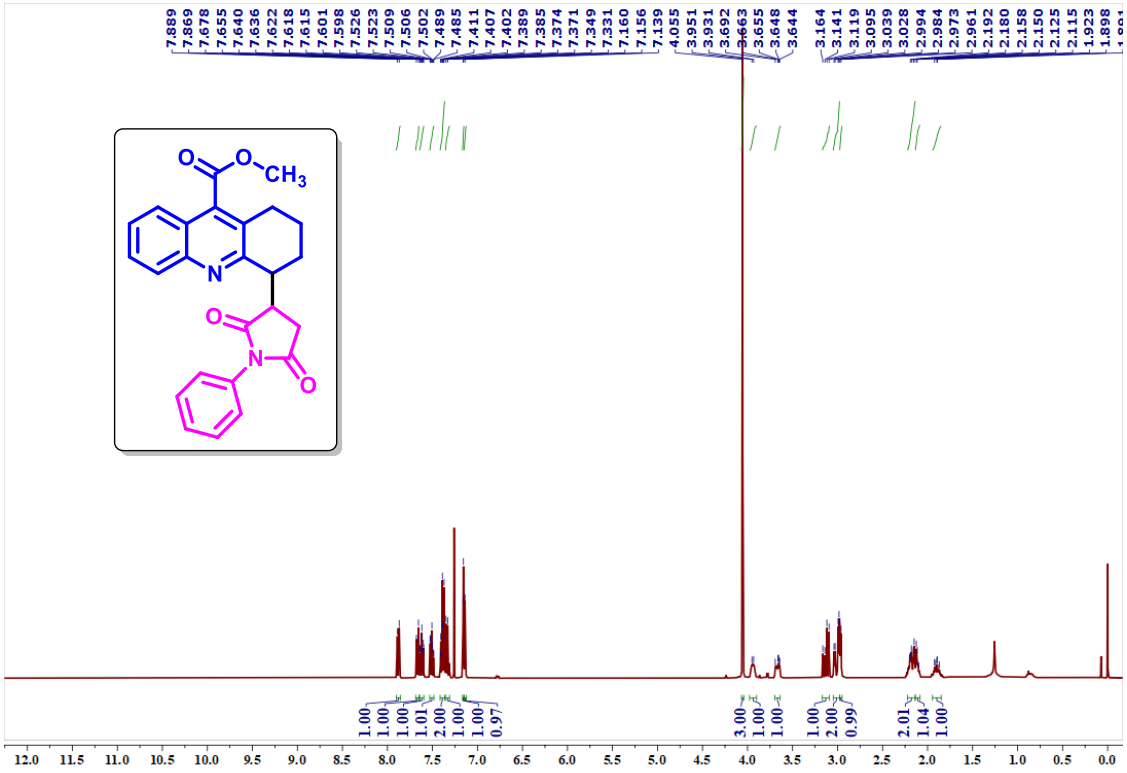

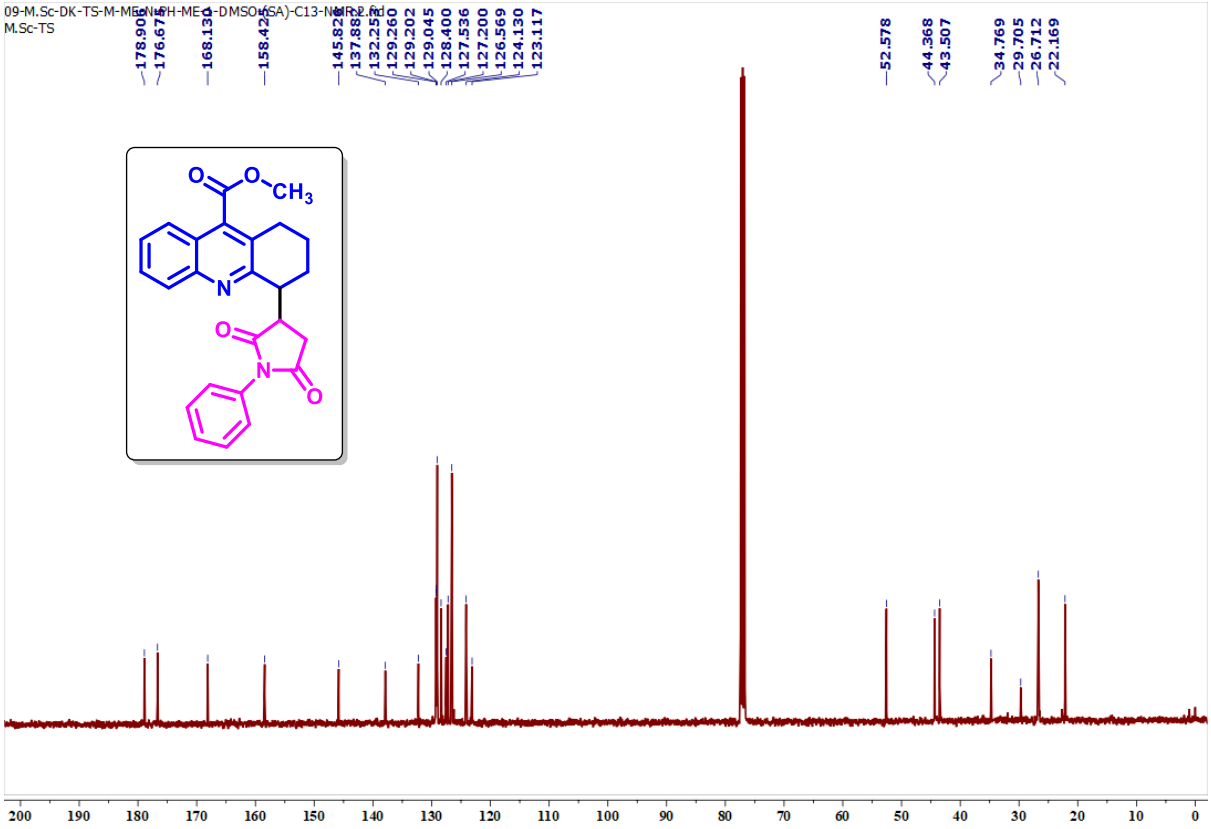

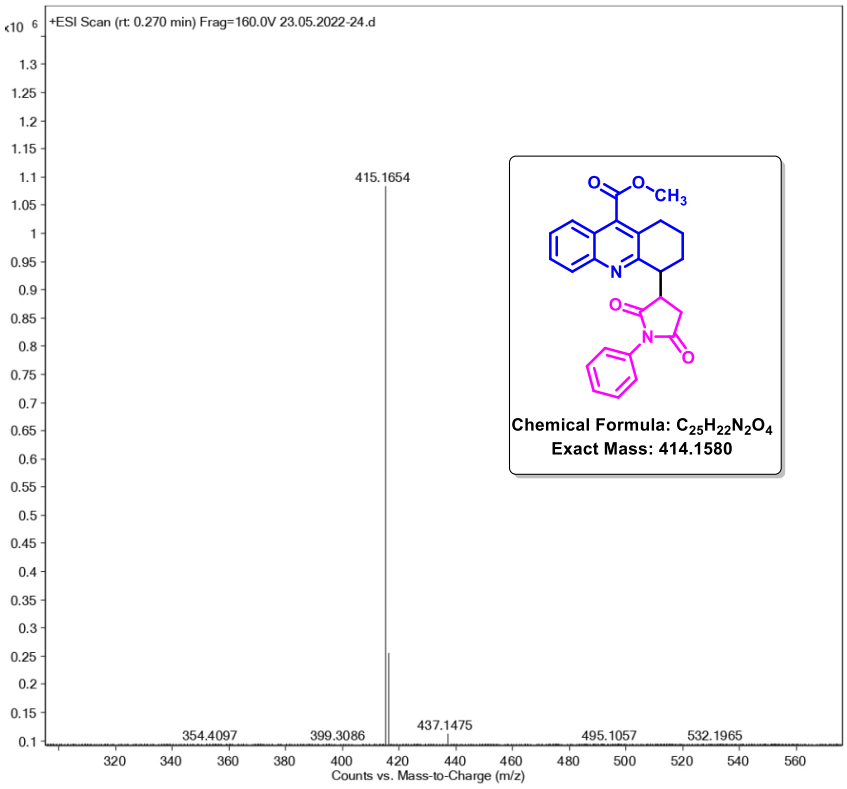
+ESI Scan (rt: 0.270 min) Frag=160.0V 23.05.2022-24.d
x10 6
1.3
1.25
1.2
1.15
1.1
1.05
1
0.95
0.9
0.85
0.8
0.75
0.7
0.65
0.6
0.55
0.5
0.45
0.4
0.35
0.3
0.25
0.2
0.15
0.1
415.1654
354.4097
399.3086
437.1475
495.1057
532.1965
320
340
360
380
400
420
440
460
480
500
520
540
560
Counts vs. Mass-to-Charge (m/z)
Chemical Formula: C25H22N2O4
Exact Mass: 414.1580

Part-B: TBHP-TBAI Catalysed Synthesis of 2,3-Dihydroacridin-4(1H)-ones via C4 C(sp^3)-H Sulfonylation and Desulfonylation of 1,2,3,4-tetrahydroacridines

3.2.1 Introduction

Sulfone motifs are prevalent in a wide range of bioactive molecules, including natural products, pharmaceuticals, and agrochemical compounds.[1] Diaryl/aryl or alkyl sulfones exhibit diverse pharmacological properties, such as antibacterial,[2] antibiotic,[3] and γ-secretase inhibitor activity.[4] Notably, 2-sulfolmethyl quinoline scaffolds are components of various medicinally significant compounds due to their broad spectrum of pharmacological activity, such as the treatment of Alzheimer's disease[5] and show anti-hepatitis B activity[6] and anti-proliferative activity[7] (**Figure 3.2.1**). Beyond drug design, sulfonyl moiety serves as a versatile tool in organic synthesis, employed in reactions like Julia olefination,[8] fluoroalkylation[9] and Smiles rearrangement.[10]

Generally, benzylic sulfones were synthesized by the oxidation of sulfide or sulfonylation with sulfonyl precursors, such as sulfonyl chlorides, sulfonic acid, sodium sulfonates, sulfonyl hydrazides, and sulfur dioxide surrogates. Compared with other sulfonic precursors sulfonyl hydrazides are easy to handle, stable, moisture-compatible, and noncorrosive.[11]

In recent years, direct sulfonylation *via* C–H functionalization has attracted great interest since this method can potentially lead to more efficient synthesis with fewer synthetic operations.[12] In this connection, Xiao et al., [13a] Dong et al., [13b] and Li et al.[13c] reported transition metal-free C(sp^3)-H sulfonylation for the synthesis of 2-sulfomethyl quinoline from 2-methylquinoline (**Figure 3.2.2**). As part our continuing efforts in C(sp^3)-H functionalization of 1,2,3,4-tetrahydroacridine,[14] herein we have described a TBAI-TBHP catalysed direct sulfonylation of 1,2,3,4-tetrahydroacridine with sulfonyl hydrazide under mild conditions, affording 4-sulfonyl substituted 1,2,3,4-tetrahydroacridine in good to high yields (**Figure 3.2.3**). In recent years, the combination of tetrabutylammonium iodide (TBAI) with ^{t}butyl hydroperoxide (TBHP) has garnered significant attention as a transition metal-free oxidation process.[15]

Acridine and 1,2,3,4-tetrahydroacridine derivatives form a significant class of nitrogen-containing heterocycles because of their plethora of biological activities, encompassing anti-cancer,[16] anti-inflammatory,[17] anti-malarial,[18] and potent inhibitors of acetylcholinesterase,[19] α-glucosidase enzyme.[20] Owing to pronounced therapeutic applications of acridine derivatives and sulfone derivatives, we intended to synthesis C4 sulfonyl 1,2,3,4-tetrahydroacridine under transition metal-free conditions.

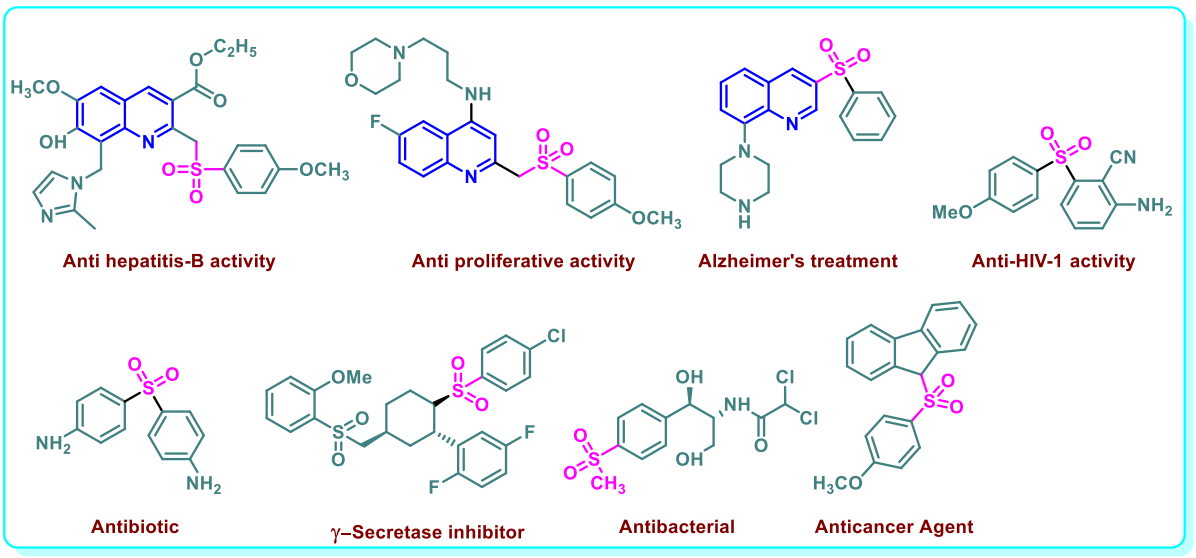

Figure 3.2.1 Drugs containing organo sulfone compounds

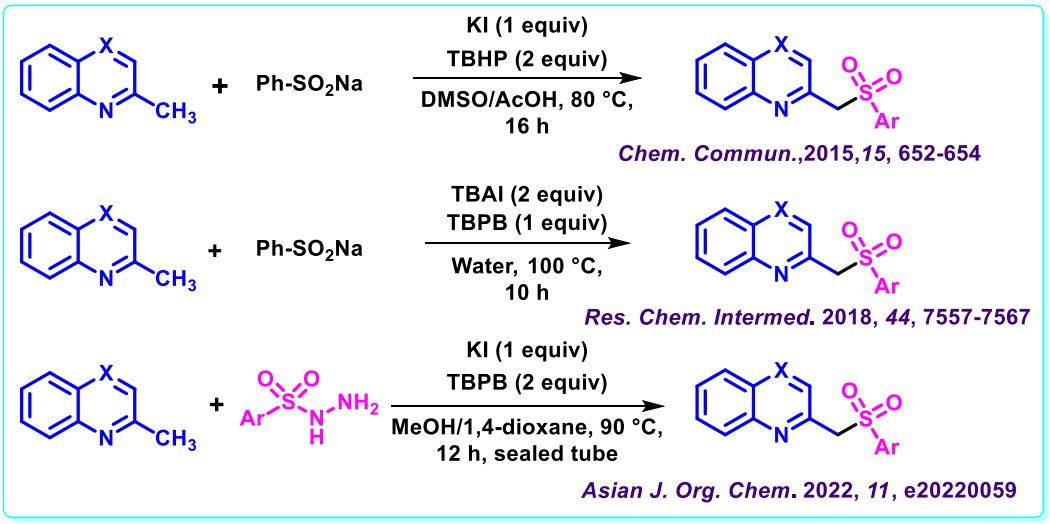

Figure 3.2.2 Previous reports for the C(sp^3)-H sulfonylation of 2-methylquinoline

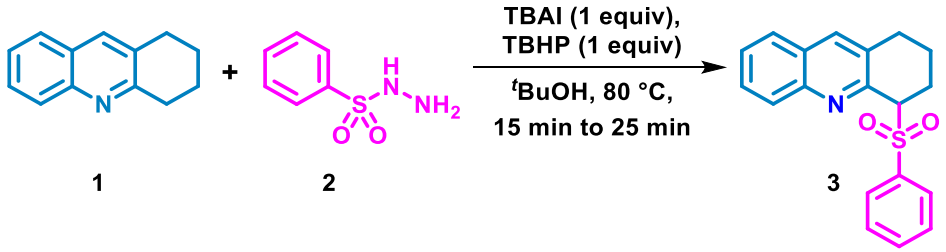

Figure 3.2.3 Present work for the C(sp^3)-H sulfonylation of 1,2,3,4-tetrahydroacridine derivatives

3.2.2 Results and Discussion

To explore C(sp^3)–H sulfonylation of 1,2,3,4-tetrahydroacridine derivatives, initially 1,2,3,4-tetrahydroacridine (**1a**) and benzene sulfonyl hydrazide (**2a**) were reacted according to literature reports in the presence of KI and TBHP as an oxidant in MeOH/1,4-dioxane solvent (1:1) at 90 °C and DMSO/AcOH at 80 °C. However, only 10% and 20% of sulfonylated 1,2,3,4-tetrahydracridine product (**3a**) was observed (**Table 3.2.1**; entry 1,2). Gratifyingly, when the reaction was performed in water, the yield of the sulfonated product increased significantly to 79% (**Table 3.2.1**; entry 3). To our delight, the corresponding product was obtained in 94% when TBHP was used as the oxidant in the presence of TBAI and ^{t}BuOH at 80 °C (**Table 3.2.1**; entry 4). Other oxidants like H_2O_2, $K_2S_2O_8$, and *m*-CPBA were also evaluated but showed less efficiency (**Table 3.2.1**; entries 5-7). Later, various iodine-containing additives such as KI, NaI, I_2, NIS, CuI were also screened but they didn't work well (**Table 3.2.1**; entries 8-12). However other organic solvents such as DMSO, MeOH, EtOH, ^{i}PrOH and 1,4-dioxane were tested and found less promising for this kind of transformation (**Table 3.2.1**; entries 13–17). We next investigated the influence of catalyst loading on the sulfonation reaction, interestingly decreasing the amount of TBAI to 0.2 equiv. did not significantly affect the yield (**Table 3.2.1**; entries 18, 19). Although the desired product formation not observed without TBAI (**Table 3.2.1**; entry 21) and in the absence TBHP a trace amount was detected (**Table 3.2.1**; entry 22). Therefore, after exploring the various reaction conditions, the optimised reaction condition for sulfonylation is TBAI (0.2 equiv) and TBHP (1 equiv) in ^{t}BuOH at 80 °C.

Table 3.2.1 Optimisation Table[a]

S.No.	Additive (1 equiv)	Oxidant (1 equiv)	solvent	Temp (°C)	Time(h)	Yield (%) [b]
1	KI	TBHP	MeOH/1,4-Dioxane	90	12	10
2	KI	TBHP	DMSO/AcOH	80	12	20
3	TBAI	TBHP	H_2O	80	30 min	79
4	TBAI	TBHP	^{t}BuOH	80	15 min	94
5	TBAI	H_2O_2	^{t}BuOH	80	1	50
6	TBAI	*m*-CPBA	^{t}BuOH	80	3	ND
7	TBAI	$K_2S_2O_8$	^{t}BuOH	80	2	30
8	KI	TBHP	^{t}BuOH	80	2	ND
9	NaI	TBHP	^{t}BuOH	80	2	ND

10	NIS	TBHP	^{t}BuOH	80	2	20
11	I_2	TBHP	^{t}BuOH	80	2	30
12	CuI	TBHP	^{t}BuOH	80	2	ND
13	TBAI	TBHP	MeOH	80	3	30
14	TBAI	TBHP	EtOH	80	3	ND
15	TBAI	TBHP	^{i}PrOH	80	3	ND
16	TBAI	TBHP	DMSO	80	3	ND
17	TBAI	TBHP	1,4-Dioxane	80	3	ND
18	TBAI (0.5 equiv.)	TBHP	^{t}BuOH	80	15 min	94
19	**TBAI (0.2 equiv.)**	TBHP	^{t}BuOH	**80**	**15 min**	**94**
20	**TBAI (0.2 equiv.)**	TBHP	^{t}BuOH	**70**	**30 min**	**88**
21	-	TBHP	^{t}BuOH	80	2	Trace
22	TBAI (0.2 equiv.)	-	^{t}BuOH	80	2	ND

[a] Reaction condition: **1** (0.54 mmol), **2** (0.54 mmol). [b] Isolated yield of the final product.

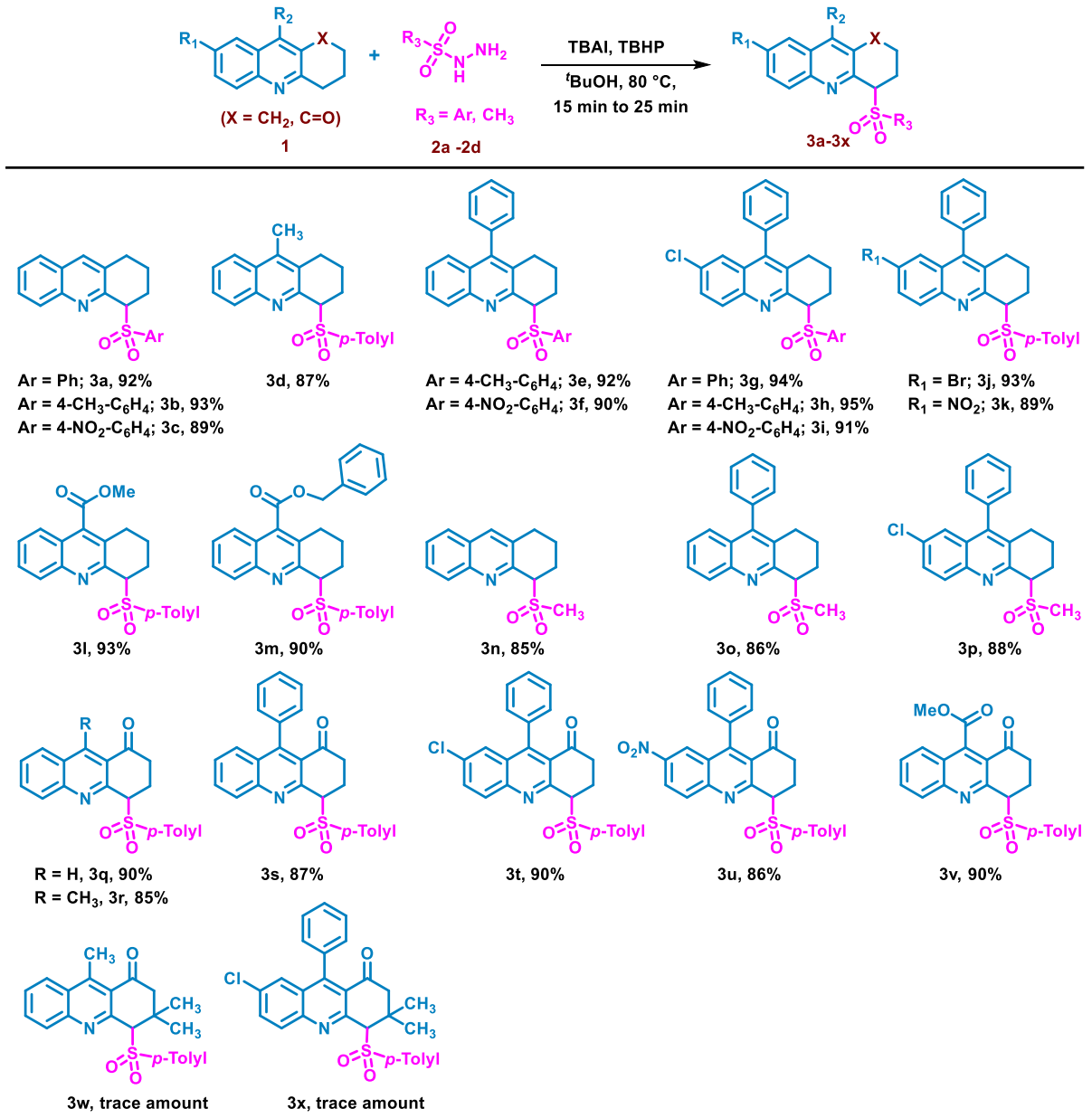

Scheme 3.2.1 Substrate scope for C(sp^3)-H sulfonylation of 1,2,3,4-tetrahydroacridine derivatives

Under the optimized conditions, we assessed the efficiency and substrate scope of TBAI catalysed C(sp^3)-H sulfonylation (**Scheme 3.2.1**). First, the aryl sulfonyl hydrazides (**2a-2c**) were investigated in the reaction of 1,2,3,4-tetrahydroacridine (**1a**) and it was found that this sulfonylative process showed good tolerance with *p*-tolyl and *p*-NO_2 sulfonyl hydrazides and provide the corresponding product in excellent yield. Compared to *p*-NO_2 benzene sulfonyl hydrazide, *p*-tolyl sulfonyl hydrazide affords the corresponding derivative in high yield. Then the influence of substitution on 1,2,3,4-tetrahydroacridine was also evaluated. It is worth mentioning that, a series of substituents including methyl, phenyl, and ester were tolerated under optimised conditions and the desired products were obtained in high yields. For example,

substrates with methyl and phenyl groups at the C9 position (**3d-3f**) afforded good yields (87%-92%). In addition, the substitution at C7 (phenyl at the C9 position) of the aromatic ring i.e. Cl, Br, NO_2 reacted smoothly with aryl sulfonyl hydrazides to yield the corresponding product (**3g-3k**) in good to excellent yield. Similarly, a strong electron-withdrawing group like ester (methyl and benzyl ester) at the C9 position was found compatible with the protocol and affords the desired product (**3l,3m**) in good yield. Interestingly, methylsulfonyl hydrazides also went well to afford the corresponding sulfone derivative (**3n-3p**) with good yield under optimised condition.

We further extended to showcase more flexibility for the present protocol where various substituted 3,4-dihydroacridin-1(2*H*)-ones (**1i-1n**) were also estimated for the C(sp^3)-H sulfonylation. Gratifyingly, the corresponding C4 sulfonylation products (**3q-3v**) were isolated in good to excellent yields (**Scheme 3.2.1**). Similar to 1,2,3,4-tetrahydroacridine C4 sulfonylation, in this case also it was observed that various substituents like methyl, phenyl, and ester at C9 position tolerated the optimal reaction condition and showed hierarchical selectivity of sp^3-carbon (between C2 and C4 positions). Unfortunately, when we envisioned 3,3-dimethyl-2,3-dihydroacridin-4(1*H*)-one sulfonylation (**1o,1p**) at C4 position a trace amount of the corresponding sulfonated product (**3w,3x**) was observed (Confirmed by LC-HRMS).

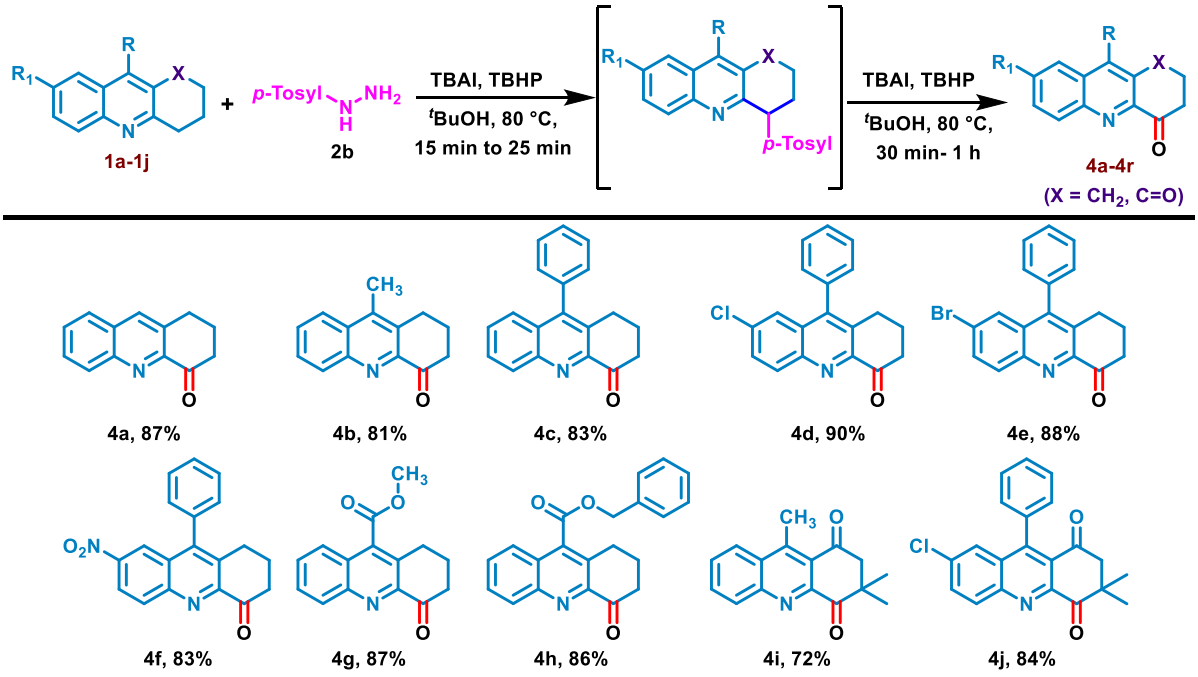

Scheme 3.2.2 Substrate scope for oxidative desulfonation of diaryl sulfones

To our surprise, it was found that at an extended reaction time, the C4 sulfonated 1,2,3,4-tetrahydroacridines undergo oxidative desulfonylation followed by keto formation at the same

C4 position. This resulted in the undesired product, 2,3-dihydroacridin-4(1*H*)-ones (**4a-4h**) (**Scheme 3.2.2**). This unforeseen side reaction significantly reduced the yield of the desired sulfonylated product. Consequently, careful monitoring and precise control of reaction time are crucial in preventing the oxidative desulfonylation and keto formation processes from occurring (**Scheme 3.2.2**). Perhaps unsurprisingly, typically the sulfones can act as a leaving group. These sulfonyl moieties can be easily removed through homolytic cleavage of S−C bond under oxidative, reductive or redox-neutral conditions.[21]

We investigated the suitability of various sulfonyl hydrazides for oxidative desulfonylation followed by keto formation under optimal conditions. On thorough investigation with different sulfonyl hydrazides, we observed that *p*-tosyl hydrazide underwent rapid desulfonation, affording the corresponding keto in high yield whereas phenyl sulfonylhyrazide exhibited slower desulfonation and provided keto compound in lower yield. Interestingly, no keto formation was noticed with *p*-NO_2 phenylsulfonyl hydrazide or methyl sulfonyl hydrazide. To our surprise 3,4-dihydroacridin-1(2*H*)-one displayed poor desulfonylation, only trace amounts of diketone were formed, detectable by LC-HRMS spectra. Additionally, the presence of dimethyl groups at the C3 position resulted in a rapid desulfonylation for the formation of the corresponding diketone (**4i,4j**) with good yield with a trace amount of sulfonated product.

Much to our surprise, an unusual reaction was encountered when Cl substituted (at C9 position) 1,2,3,4-tetrahydroacridine (**1q**) was subjected to C(sp^3)-H sulfonylation with benzene sulfonyl hydrazide (**2a**). Though our expected sulfonated product (**5a**) was afforded in good yield but this transformation was not entirely selective as alongside the desired sulfonated product, C9 sulfonated derivative (**5a'**) and C4, C9-disulfonylation products (**5a''**) (**Scheme 3.2.3**) were also formed (which may be occurred *via* dechlorination followed by sulfonylation). All the products were isolated and confirmed using spectrum analysis data such as ^{1}H, ^{13}C and LC-HRMS spectra. To check substrate scope of C(sp^3)-H sulfonylation of 9-chloro-1,2,3,4-tetrahydroacridine derivatives, different aryl sulfonyl hydrazides (**2a-2d**) were treated with 9-chloro-tetrahydroacridine (**1q,1r**) under optimised condition and the corresponding sulfonylation products were obtained along with dechlorinated sulfonation and di-sulfonylation derivatives.

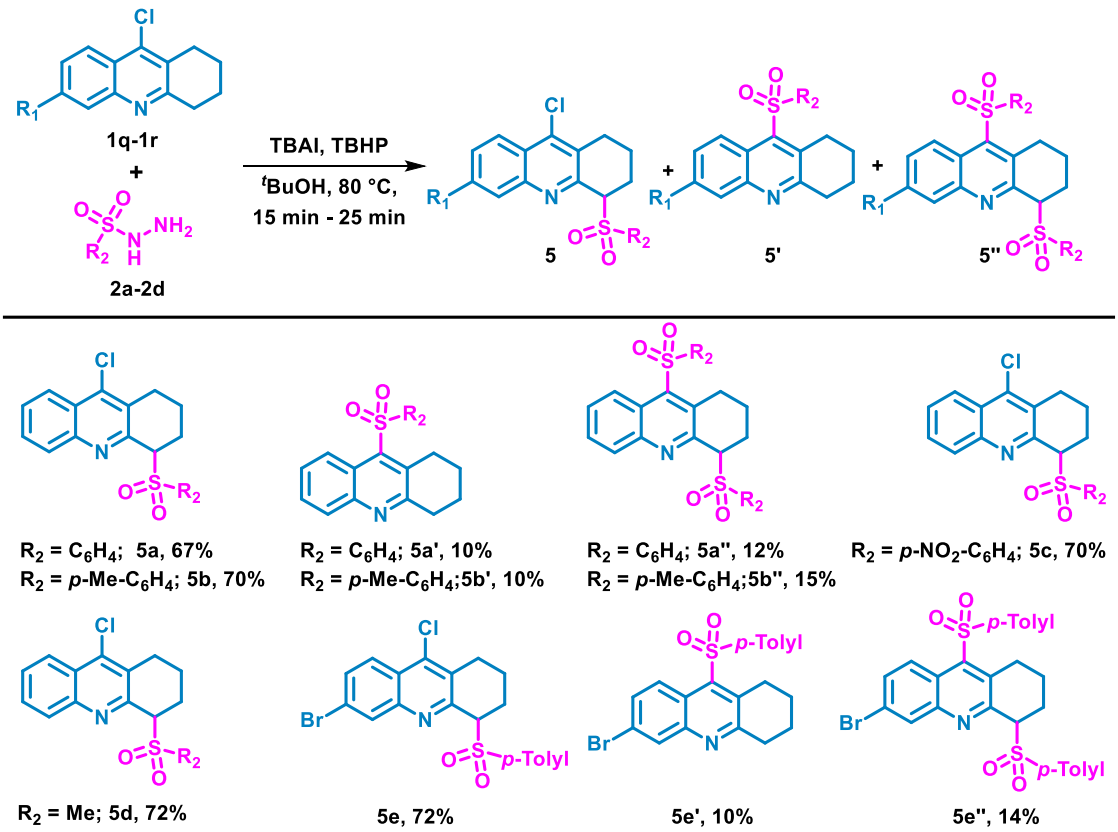

Scheme 3.2.3 Substrate scope for Dechlorination-Sulfonation

In our investigation of the oxidative desulfonylation followed by keto formation for the 9-Cl substituted compounds, we observed the formation of both the expected C4 keto product (**6a,6d**) and C9 sulfonylated C4 keto product (**6b,6c,6d**). The corresponding C9 sulfonated 2,3-dihydroacridin-4(1*H*)-ones were isolated in yields of 30-35% (**Scheme 3.2.4**).

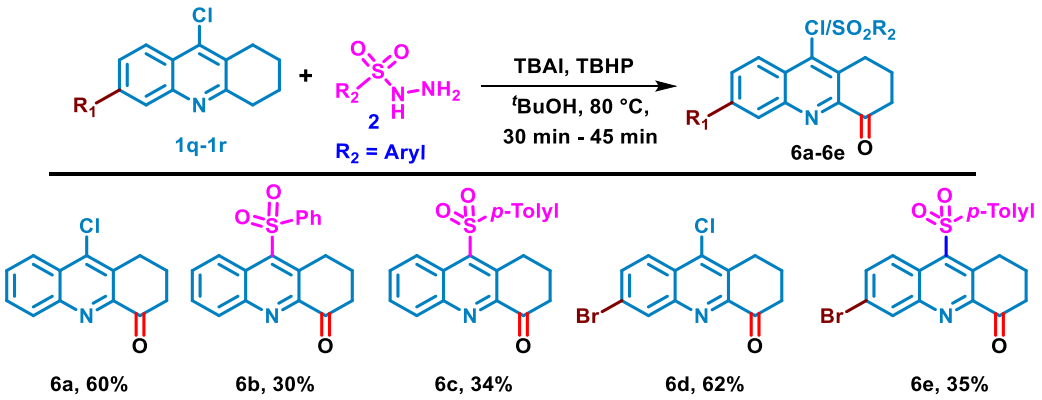

Scheme 3.2.4 Substrate scope for oxidative-desulfonation

3.2.3 Control experiments

In order to get a better understanding of the reaction mechanism, controlled experiments were performed (**Scheme 3.2.5**). In our first investigation, we observed that no desired product formation when 2 equiv. of radical scavengers such as 2,2,6,6-tetramethyl-1-piperidinyloxy

(TEMPO) was added to the reaction mixture under standard conditions suggesting a possibility of free radical mechanism. To provide further support for the reaction pathway, the reaction was carried out without the use of aq. TBHP, the sulfonated product was not detected. On the other hand, omitting TBAI from the reaction still produced a trace amount of desired product which indicates the radical initiator TBHP plays a pivotal role in this transformation.

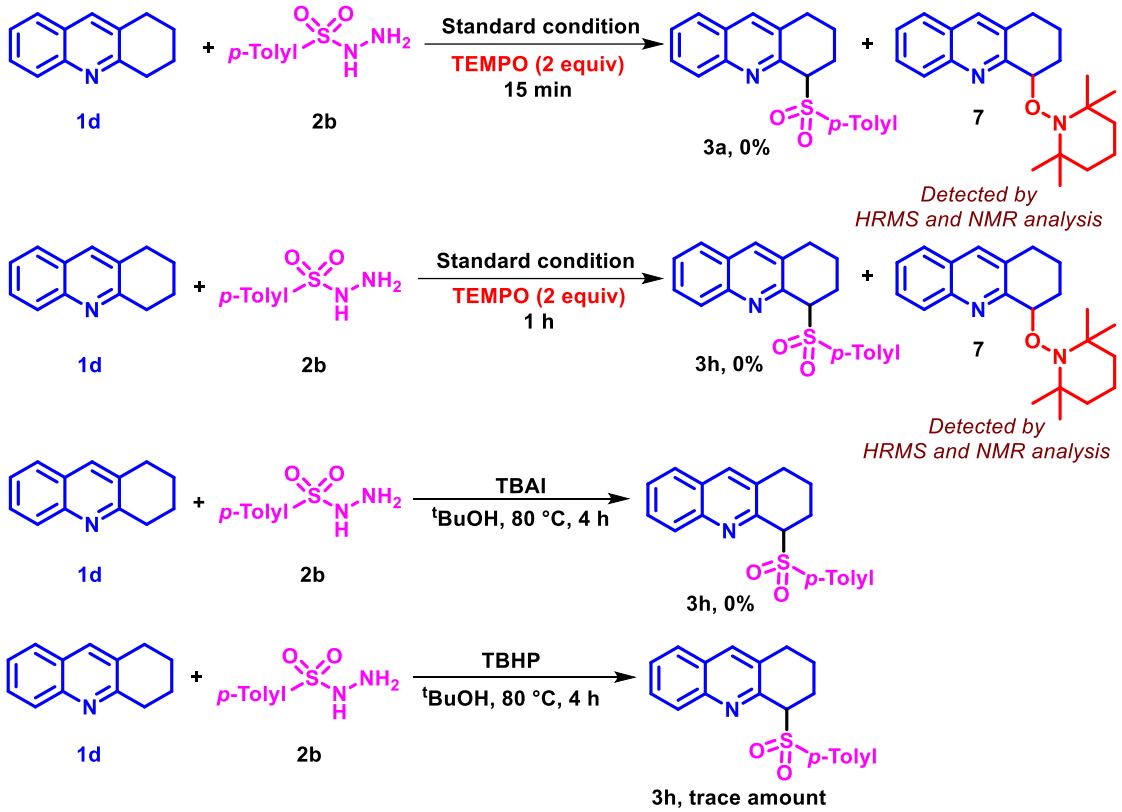

Scheme 3.2.5 Control experiments

3.2.4 Plausible mechanism

Based on the experiment outcomes from controlled experiments and literature reports [13,22] a tentative mechanism to rationalise this transformation is illustrated in (**Figure 3.2.3**). Initially, ^{t}butoxyl and ^{t}butyl peroxy radicals were generated from oxidant TBHP in the presence of TBAI catalyst. Then, these radicals sequentially abstract H-atom from sulfonylhydrazides to yield initially arylsulfonyl diazene radical (**I**). Then this arylsulfonyl diazene radical generate sulfonyl radical (**II**). The generated sulfonyl radical undergoes an addition reaction with intermediate (**III**), which is generated from **1a** to afford an intermediate (**IV**). Which can be further oxidised by an iodide radical to generate the desired product **3a** and release HI. The released HI is used to participate in the next catalytic reaction cycle.

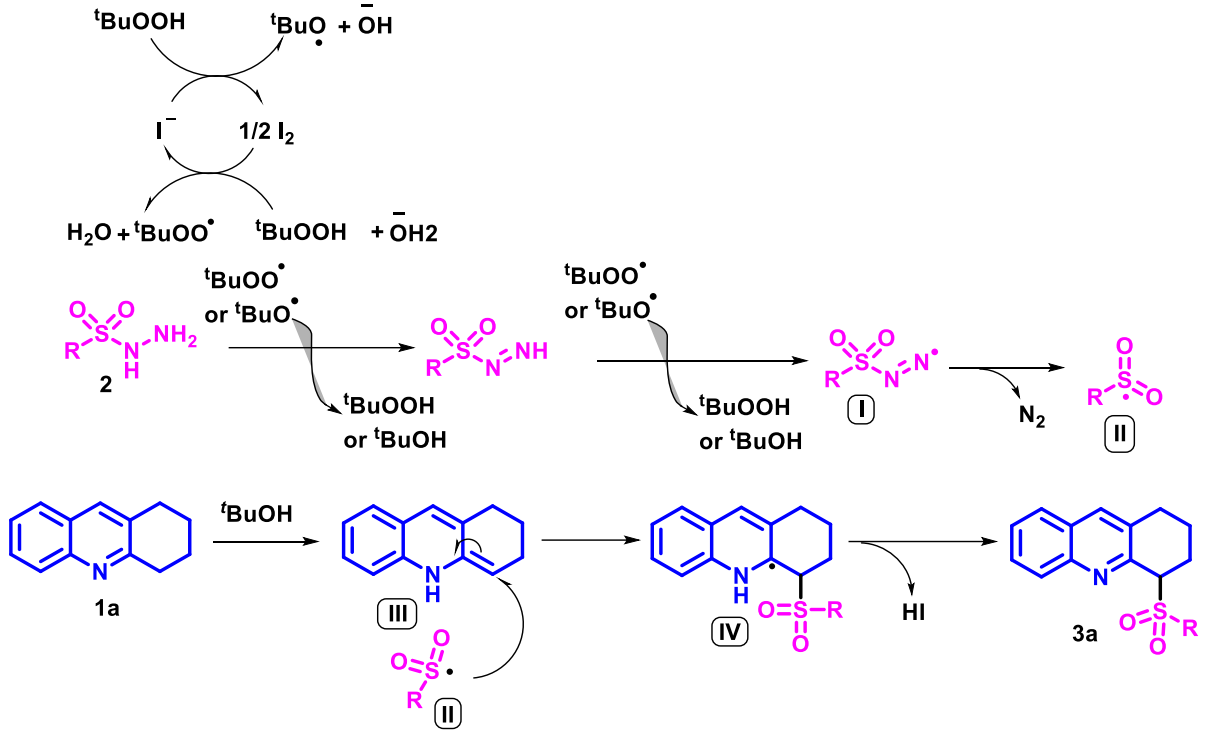

Figure 3.2.3 Proposed mechanism for C(sp^3)-H sulfonylation

We suspect that the formed C(sp^3)-H sulfonylation product (**3a)** then undergoes homolytic cleavage at the C-S bond in the presence of TBHP and releases *p*-TSA and intermediate (**V**), which could then couple with another ^{t}butyl peroxy radical to give the peroxy species (**VI**) (**Figure 3.2.4**). Further oxidation process might collapse the peroxy species to give keto product **4a** along with ^{t}BuOH.[23]

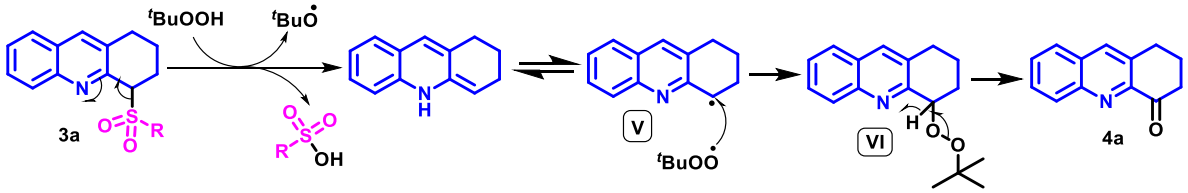

Figure 3.2.4 Proposed mechanism for oxidative desulfonation and keto formation

3.2.5 Conclusions

In conclusion, we have developed a versatile and efficient approach for the C(sp^3)–H functionalization of tetrahydroacridines. This method offers remarkable flexibility, allowing direct and selective synthesis of 4-sulfonyl-tetrahydroacridine derivatives or, with extended time, in-situ oxidative desulfonylation to yield 2,3-dihydroacridinones. The protocol demonstrates excellent tolerance towards a wide range of substrates, consistently delivering good to excellent yields for both products. This streamlined approach holds significant promise for the synthesis of diversely functionalized tetrahydroacridines. The proposed radical reaction mechanism provides valuable insight into these intriguing time-dependent transformations.

3.2.6 Experimental procedures

3.2.6.1 General procedure for the synthesis of product (3 or 5): An oven dried round bottom flask was charged with 1,2,3,4-tetrahydroacridine derivative (1) (0.54 mmol), benzenesulfonylhydrazide (2) (0.54 mmol), TBAI (0.2 equiv.) and tert-butyl hydrogenperoxide (1 equiv.) followed by 2 mL of tert-butanol solvent, then the resulting mixture was stirred under air at 80 °C for 15-20 min. After completion, the mixture was cooled to room temperature, then hypo solution was added to quench the reaction mixture. The quenched mixture was distributed between ethyl acetate (15 mL) and water (15 mL). After the organic phase was isolated, the aqueous phase was further extracted with ethyl acetate (3×15 mL), and then the extracted organic phase was dried with sodium sulphate and concentrated. Finally, the residue was purified by column chromatography (petroleum ether/ethyl acetate 8:2) to give the desired product **3 or 5**.

3.2.6.2 General procedure for the synthesis of product (4 or 6): An oven dried round bottom flask was charged with 1,2,3,4-tetrahydroacridine derivative (1) (0.54 mmol), benzenesulfonylhydrazide (2) (0.54 mmol), TBAI (0.2 equiv.) and tert-butyl hydrogenperoxide (1 equiv.) followed by 2 mL of tert-butanol solvent, then the resulting mixture was stirred under air at 80 °C for 45 min. After completion, the mixture was cooled to room temperature, then hypo solution was added to quench the reaction mixture. The quenched mixture was distributed between ethyl acetate (15 mL) and water (15 mL). After the organic phase was isolated, the aqueous phase was further extracted with ethyl acetate (3×15 mL), and then the extracted organic phase was dried with sodium sulphate and concentrated. Finally, the residue was purified by column chromatography (petroleum ether/ethyl acetate 8:2) to give the desired product **4 or 6**.

3.2.7 Characterization data for synthesized compounds

4-(Phenylsulfonyl)-1,2,3,4-tetrahydroacridine (3a): Yield = 92%, White solid; M. P: 167.5-168 °C; **IR (KBr, cm^{-1})**: 2965, 2854, 1501, 1198, 732; **^{1}H NMR (400 MHz, $CDCl_3$) δ** 7.90 (s, 1H), 7.71 (d, *J* = 8.8 Hz, 1H), 7.67 (s, 1H), 7.66 – 7.62 (m, 2H), 7.54 (ddd, *J* = 8.4, 6.8, 1.6 Hz, 1H), 7.48 (m, 1H), 7.47 (m, 2H), 7.44 (m, 1H), 4.73 (dd, *J* = 7.2, 3.6 Hz, 1H), 3.14 (m, 1H), 3.04 – 2.92 (m, 2H), 2.50 – 2.41 (m, 1H), 2.37 – 2.29 (m, 1H), 1.90 – 1.84 (m, 1H). **^{13}C NMR (100 MHz, $CDCl_3$) δ** 149.93, 145.92, 139.16, 135.73, 133.35, 132.30, 129.52, 128.90, 128.61, 127.85, 126.96, 66.76, 28.44, 22.93, 19.79. **HRMS (ESI-MS):** m/z Calculated for $C_{19}H_{17}NO_2S$ $[M+H]^+$: 324.1053; Observed: 324.1053.

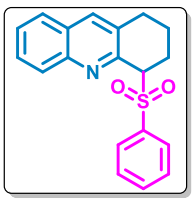

4-Tosyl-1,2,3,4-tetrahydroacridine (3b): Yield = 93%, White solid; M. P: 172.3-172.9 °C; **IR (KBr, cm^{-1})**: 2920, 2895, 1480, 1297, 705; **^{1}H NMR (400 MHz, $CDCl_3$) δ** 7.89 (s, 1H), 7.72 (d, *J* = 8.0 Hz, 1H), 7.60 – 7.55 (m, 1H), 7.54 (d, *J* = 8.0 Hz, 3H), 7.47 (t, *J* = 8.0 Hz, 1H), 7.25 (d, *J* = 8.4 Hz, 2H), 4.70 (dd, *J* = 7.2, 3.6 Hz, 1H), 3.17 – 3.11 (m, 1H), 3.00 – 2.92 (m, 2H), 2.46 (s, 3H), 2.42 (m, 1H), 2.31 (m, 1H), 1.85 (m, 1H). **^{13}C NMR (100 MHz, $CDCl_3$) δ** 150.19, 146.08, 144.25, 136.20, 135.59, 132.30, 129.57, 129.24, 128.78, 128.63, 127.86, 127.00, 126.86, 66.97, 28.46, 23.08, 21.69, 19.77. **HRMS (ESI-MS):** m/z Calculated for $C_{20}H_{19}NO_2S$ $[M+H]^+$: 338.1209; Observed: 338.1210.

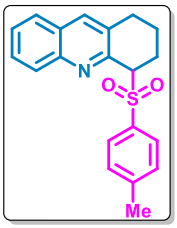

4-((4-Nitrophenyl)sulfonyl)-1,2,3,4-tetrahydroacridine(3c): Yield = 89%, White solid; M. P: 191.8-192.3 °C; **IR (KBr, cm^{-1})**: 2959, 2873, 1336, 1134, 705; **^{1}H NMR (400 MHz, $CDCl_3$) δ** 8.33 – 8.29 (m, 2H), 7.94 (s, 1H), 7.88 – 7.85 (m, 2H), 7.73 (dd, *J* = 8.4, 1.6 Hz, 1H), 7.56 (ddd, *J* = 8.4, 6.8, 1.6 Hz, 1H), 7.52 – 7.47 (m, 1H), 7.29 (d, *J* = 8.4 Hz, 1H), 4.78 – 4.74 (m, 1H), 3.18 (m, 1H), 3.10 – 3.03 (m, 1H), 3.02 – 2.94 (m, 1H), 2.49 – 2.37 (m, 2H), 1.97 – 1.90 (m, 1H). **^{13}C NMR (100 MHz, $CDCl_3$) δ** 150.59, 149.38, 145.87, 145.67, 136.04, 132.05, 130.98, 129.34, 128.12, 127.90, 127.25, 127.16, 123.57, 66.90, 28.42, 22.62, 19.95. **HRMS (ESI-MS):** m/z Calculated for $C_{19}H_{16}N_2O_4S$ $[M+H]^+$: 369.0904; Observed: 369.0904.

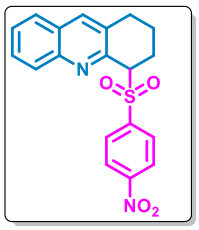

9-Methyl-4-tosyl-1,2,3,4-tetrahydroacridine(3d): Yield = 87%, White solid; M. P: 183.6-184 °C; **IR (KBr, cm^{-1})**: 2952, 2865, 1575, 1080, 813; **^{1}H NMR (400 MHz, $CDCl_3$) δ** 7.99 (d, *J* = 10.0 Hz, 1H), 7.64 – 7.59 (m, 1H), 7.56 (m, 1H), 7.54 (m, 1H), 7.52 – 7.50 (m, 1H), 7.46 (d, *J* =10.0 Hz, 1H), 7.28 (s, 1H), 7.26 (s, 1H), 4.67 (dd, *J* = 6.8, 3.6 Hz, 1H), 3.16 – 3.08 (m, 1H), 3.01 – 2.93 (m, 2H), 2.86 (q, *J* = 6.8 Hz, 1H), 2.59 (s, 3H), 2.47 (s, 3H), 2.30 – 2.19 (m, 2H), 1.97 (m, 1H). **^{13}C NMR (100 MHz, $CDCl_3$) δ** 149.54, 145.35, 144.13, 142.15, 136.63, 129.57, 129.33, 129.19, 128.32, 127.64, 127.12, 126.51, 123.48, 122.72, 67.64, 26.07, 22.73, 21.70, 19.47, 13.82. **HRMS (ESI-MS):** m/z Calculated for $C_{21}H_{21}NO_2S$ $[M+H]^+$: 352.1366; Observed: 352. 1367.

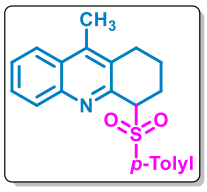

9-Phenyl-4-tosyl-1,2,3,4-tetrahydroacridine (3e): Yield = 92%, White solid; M. P: 222.7-223.5 °C; **IR (KBr, cm^{-1})**: 3035, 2979, 1450, 1145, 796; **^{1}H NMR (400 MHz, CDCl$_3$) δ** 7.62 – 7.59 (m, 2H), 7.58 – 7.55 (m, 2H), 7.55 – 7.53 (m, 1H), 7.49 (m, 2H), 7.36 (m, 2H), 7.34 – 7.31 (m, 1H), 7.28 (d, J = 8.0 Hz, 2H), 7.18 – 7.15 (m, 1H), 4.81 – 4.76 (m, 1H), 2.92 (m, 1H), 2.80 – 2.73 (m, 1H), 2.60 – 2.53 (m, 1H), 2.48 (s, 3H), 2.34 – 2.27 (m, 2H), 1.77 – 1.70 (m, 1H). **^{13}C NMR (100 MHz, CDCl$_3$) δ** 150.36, 146.59, 144.37, 143.94, 139.28, 136.24, 135.65, 133.40, 132.76, 131.13, 130.32, 129.76, 129.54, 129.49, 129.31, 129.02, 128.88, 128.83, 128.67, 128.43, 127.94, 124.69, 67.28, 27.19, 22.77, 21.71, 19.79. **HRMS (ESI-MS):** m/z Calculated for $C_{26}H_{23}NO_2S$ $[M+H]^+$: 414.1522; Observed: 414.1527.

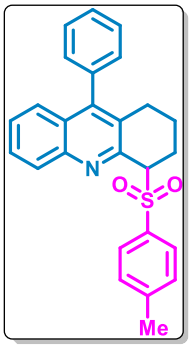

4-((4-Nitrophenyl)sulfonyl)-9-phenyl-1,2,3,4-tetrahydroacridine (3f): Yield = 90%, White solid; M. P: 234.8-235.2 °C; **IR (KBr, cm^{-1})**: 3048, 2994, 1470, 1190, 782; **^{1}H NMR (400 MHz, CDCl$_3$) δ** 8.38 – 8.33 (m, 2H), 7.98 – 7.93 (m, 2H), 7.56 (ddd, *J* = 8.4, 4.4, 3.2 Hz, 2H), 7.53 – 7.47 (m, 2H), 7.39 – 7.36 (m, 2H), 7.33 (td, *J* = 8.4, 1.2 Hz, 2H), 7.16 (m, 1H), 4.85 (dd, *J* = 6.8, 4.8 Hz, 1H), 3.07 – 2.99 (m, 1H), 2.85 – 2.77 (m, 1H), 2.65 – 2.57 (m, 1H), 2.43 – 2.29 (m, 2H), 1.85 – 1.77 (m, 1H). **^{13}C NMR (100 MHz, CDCl$_3$) δ** 150.60, 149.28, 147.73, 146.01, 145.57, 136.19, 131.01, 129.66, 129.32, 129.13, 128.94, 128.87, 128.68, 128.21, 127.30, 127.05, 126.11, 123.61, 67.54, 27.19, 22.39, 20.13. **HRMS (ESI-MS):** m/z Calculated for $C_{25}H_{20}N_2O_4S$ $[M+H]^+$: 445.1217; Observed: 445.1228.

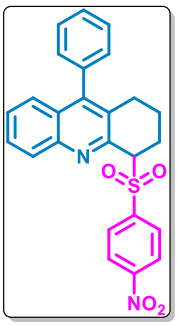

7-Chloro-9-phenyl-4-(phenylsulfonyl)-1,2,3,4-tetrahydroacridine (3g): Yield =94%, White solid; M. P: 201.5-202 °C; **IR (KBr, cm^{-1})**: 3055, 2999, 1480, 1290, 697; **^{1}H NMR (400 MHz, CDCl$_3$) δ** 7.73 – 7.68 (m, 1H), 7.68 – 7.57 (m, 2H), 7.57 – 7.50 (m, 3H), 7.49 (m, 2H), 7.47 – 7.39 (m, 1H), 7.33 – 7.27 (m, 3H), 7.17 – 7.11 (m, 1H), 4.77 (m, 1H), 2.99 – 2.88 (m, 1H), 2.75 (m, 1H), 2.59 – 2.51 (m, 1H), 2.36 – 2.26 (m, 2H), 1.72 (m, 1H). **^{13}C NMR (100 MHz, CDCl$_3$) δ** 150.36, 146.59, 144.37, 143.94, 139.28, 136.24, 135.65, 133.40, 132.76, 131.13, 130.32, 129.76, 129.54, 129.49, 129.31, 129.02, 128.88, 128.83, 128.67, 128.43, 127.94, 124.69, 67.28, 27.19, 22.77, 19.79. **HRMS (ESI-MS):** m/z Calculated for $C_{25}H_{20}ClNO_2S$ $[M+H]^+$: 434.0976; Observed: 434.0980.

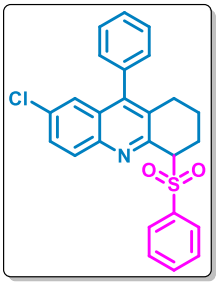

7-Chloro-9-phenyl-4-tosyl-1,2,3,4-tetrahydroacridine (3h): Yield = 95%, White solid; M. P: 183.2-184 °C; **IR (KBr, cm^{-1})**: 3027, 2944, 1290, 1118, 765; **^{1}H NMR (400 MHz, CDCl$_3$) δ** 7.59 (m, 1H), 7.58 (m, 1H), 7.57 – 7.53 (m, 1H), 7.53 – 7.50 (m, 2H), 7.49 (s, 2H), 7.32 (m, 1H), 7.30 (s, 1H), 7.28 (d, *J* = 5.6 Hz, 2H), 7.16 – 7.12 (m, 1H), 4.75 (dd, *J* = 6.8, 3.2 Hz, 1H), 2.95 – 2.88 (m, 1H), 2.75 (m, 1H), 2.59 – 2.52 (m, 1H), 2.49 (s, 3H), 2.34 – 2.25 (m, 2H), 1.73 – 1.69 (m, 1H). **^{13}C NMR (100 MHz, CDCl$_3$) δ** 150.49, 146.31, 144.32, 144.17, 136.33, 135.74, 132.62, 131.02, 130.44, 129.60, 129.54, 129.37, 129.29, 128.99, 128.91, 128.81, 128.37, 127.91, 124.68, 67.55, 27.22, 22.79, 21.72, 19.85. **HRMS (ESI-MS):** m/z Calculated for $C_{26}H_{22}ClNO_2S$ $[M+H]^+$: 448.1133; Observed: 448.1132.

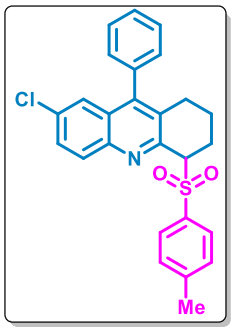

7-Chloro-4-((4-nitrophenyl)sulfonyl)-9-phenyl-1,2,3,4-tetrahydroacridine(3i): Yield = 91%, White solid; M. P: 206.5-207 °C; **IR (KBr, cm^{-1})**: 3057, 2955, 1523, 1348, 1145, 736; **^{1}H NMR (400 MHz, CDCl$_3$) δ** 8.39 – 8.34 (m, 2H), 7.97 – 7.92 (m, 2H), 7.60 – 7.56 (m, 1H), 7.55 – 7.51 (m, 2H), 7.49 (dd, *J* = 8.8, 2.4 Hz, 1H), 7.34 – 7.31 (m, 2H), 7.27 (d, *J* = 7.2 Hz, 1H), 7.16 – 7.12 (m, 1H), 4.82 (dd, *J* = 6.8, 4.0 Hz, 1H), 3.05 – 2.98 (m, 1H), 2.80 (m, 1H), 2.63 – 2.55 (m, 1H), 2.42 – 2.29 (m, 2H), 1.85 – 1.77 (m, 1H). **^{13}C NMR (100 MHz, CDCl$_3$) δ** 150.65, 149.67, 147.01, 145.87, 143.90, 135.44, 133.08, 130.96, 130.77, 130.18, 129.83, 129.22, 129.10, 128.92, 128.83, 128.56, 128.01, 124.88, 123.66, 67.37, 27.25, 22.33, 19.97. **HRMS (ESI-MS):** m/z Calculated for $C_{25}H_{19}ClN_2O_4S$ $[M+H]^+$: 479.0827; Observed: 479.0831.

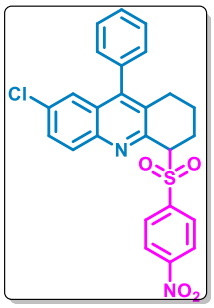

7-Bromo-9-phenyl-4-tosyl-1,2,3,4-tetrahydroacridine (3j): Yield = 93%, White solid; M. P: 198.8-199.2 °C; **IR (KBr, cm^{-1})**: 3026, 2898, 1562, 1073, 765; **^{1}H NMR (400 MHz, CDCl$_3$) δ** 7.63 (dd, *J* = 9.2, 2.4 Hz, 1H), 7.60 – 7.57 (m, 2H), 7.55 (d, *J* = 2.4 Hz, 1H), 7.55 – 7.50 (m, 2H), 7.49 (d, *J* = 2.4 Hz, 1H), 7.42 (d, *J* = 9.2 Hz, 1H), 7.32 – 7.30 (m, 1H), 7.30 – 7.27 (m, 2H), 7.14 (dq, *J* = 5.2, 2.4 Hz, 1H), 4.74 (dd, *J* = 6.4, 4.0 Hz, 1H), 2.95 – 2.87 (m, 1H), 2.75 (m, 1H), 2.59 – 2.52 (m, 1H), 2.49 (s, 3H), 2.30 (m, 2H), 1.75 – 1.69 (m, 1H). **^{13}C NMR (100 MHz, CDCl$_3$) δ** 150.63, 146.26, 144.33, 136.31, 135.68, 132.17, 131.06, 130.51, 129.53, 129.37, 129.29, 129.00, 128.91, 128.82, 128.39, 128.01, 120.98, 67.56, 27.20, 22.77, 21.70, 19.84. **HRMS (ESI-MS):** m/z Calculated for $C_{26}H_{22}BrNO_2S$ $[M+H]^+$: 492.0627; Observed: 492.0639.

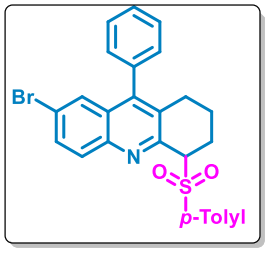

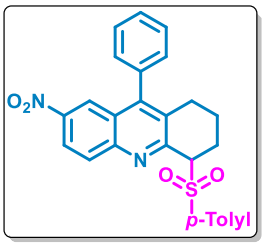

7-Nitro-9-phenyl-4-tosyl-1,2,3,4-tetrahydroacridine (3k): Yield = 89%, White solid; M. P: 223.8-224.5 °C; **IR (KBr, cm^{-1})**: 3027, 2985, 1329, 1170, 826; **^{1}H NMR (400 MHz, CDCl$_3$) δ** 8.34 – 8.30 (m, 2H), 7.68 – 7.65 (m, 1H), 7.62 – 7.58 (m, 3H), 7.57 – 7.54 (m, 2H), 7.33 (dd, *J* = 8.8, 1.6 Hz, 3H), 7.19 – 7.15 (m, 1H), 4.80 (dd, *J* = 6.4, 3.6 Hz, 1H), 2.98 – 2.91 (m, 1H), 2.81 (m, 1H), 2.66 – 2.59 (m, 1H), 2.51 (s, 3H), 2.36 – 2.28 (m, 2H), 1.76 (m, 1H).**^{13}C NMR (100 MHz, CDCl$_3$) δ** 154.31, 149.20, 147.54, 145.74, 144.60, 136.19, 134.76, 132.28, 130.59, 130.00, 129.47, 129.40, 129.32, 129.24, 129.06, 128.98, 128.85, 126.27, 123.04, 122.08, 67.65, 27.29, 22.69, 21.74, 19.73. **HRMS (ESI-MS):** m/z Calculated for $C_{26}H_{24}N_2O_4S$ $[M+H]^+$: 459.1373; Observed: 459.1373.

Methyl 4-tosyl-1,2,3,4-tetrahydroacridine-9-carboxylate (3l): Yield = 93%, White solid; M. P: 182.2-183.1 °C; **IR (KBr, cm^{-1})**: 2958, 2912, 1738, 1308, 1217, 1135, 759,670; **^{1}H NMR (400 MHz, CDCl$_3$) δ** 7.70 (dd, *J* = 8.0, 2.0 Hz, 1H), 7.60 (ddd, *J* = 8.0, 6.8, 1.6 Hz, 1H), 7.56 – 7.52 (m, 3H), 7.52 – 7.49 (m, 1H), 7.28 – 7.24 (m, 2H), 4.70 (dd, *J* = 6.8, 3.6 Hz, 1H), 4.06 (s, 3H), 3.07 (m, 1H), 3.01 – 2.88 (m, 2H), 2.47 (s, 3H), 2.46 – 2.40 (m, 1H), 2.33 – 2.25 (m, 1H), 1.87 (m, 1H). **^{13}C NMR (100 MHz, CDCl$_3$) δ** 167.76, 150.25, 145.73, 144.37, 138.18, 136.07, 129.56, 129.29, 129.25, 129.10, 128.84, 127.90, 124.30, 123.62, 67.07, 52.66, 26.17, 22.62, 21.69, 19.26. **HRMS (ESI-MS):** m/z Calculated for $C_{22}H_{21}NO_4S$ $[M+H]^+$: 396.1264; Observed: 396.1261.

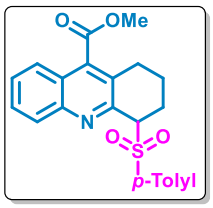

Benzyl 4-tosyl-1,2,3,4-tetrahydroacridine-9-carboxylate (3m): Yield = 90%, Semi solid (liquid); **IR (KBr, cm^{-1})**: 3045, 2945, 2887, 1730, 1423, 1172, 808; **^{1}H NMR (400 MHz, CDCl$_3$) δ** 7.63 (dd, *J* = 7.8, 1.6 Hz, 1H), 7.60 – 7.56 (m, 1H), 7.55 – 7.52 (m, 2H), 7.50 – 7.48 (m, 2H), 7.47 (m, 2H), 7.44 – 7.40 (m, 2H), 7.39 (s, 1H), 7.26 (s, 1H), 7.24 (s, 1H), 5.51 (d, *J* = 3.6 Hz, 2H), 4.68 (dd, *J* = 6.8, 3.6 Hz, 1H), 3.04 – 2.94 (m, 2H), 2.90 – 2.83 (m, 1H), 2.46 (s, 3H), 2.44 – 2.37 (m, 1H), 2.31 – 2.24 (m, 1H), 1.83 (m, 1H). **^{13}C NMR (100 MHz, CDCl$_3$) δ** 167.11, 150.14, 145.54, 144.39, 138.22, 136.04, 134.92, 129.58, 129.35, 129.30, 128.93, 128.87, 128.80, 127.96, 124.22, 123.66, 67.79, 66.90, 26.01, 22.58, 21.69, 19.17. **HRMS (ESI-MS):** m/z Calculated for $C_{28}H_{24}NO_4S$ $[M+H]^+$: 472.1577; Observed: 472.1569.

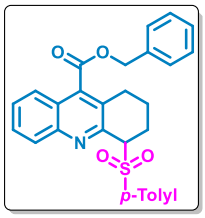

4-(Methylsulfonyl)-1,2,3,4-tetrahydroacridine (3n): Yield = 85%, White solid; M. P: 168.4-169 °C; **IR (KBr, cm^{-1})**: 2952, 2874, 1595, 1490, 1291, 1138, 668; **^{1}H NMR (400 MHz, CDCl$_3$) δ** 7.98 (d, *J* = 8.4 Hz, 1H), 7.96 (s, 1H), 7.76 (d, *J* = 8.0 Hz, 1H), 7.66 (ddd, *J* = 8.4, 6.8, 1.6 Hz, 1H), 7.53 (ddd, *J* = 8.0, 6.8, 1.2 Hz, 1H), 4.58 (dd, *J* = 6.8, 4.4 Hz, 1H), 3.32 (s, 3H), 3.17 – 3.09 (m, 1H), 3.00 – 2.89 (m, 2H), 2.37 – 2.22 (m, 2H), 1.92 – 1.83 (m, 1H). **^{13}C NMR (100 MHz, CDCl$_3$) δ** 150.74, 146.46, 136.21, 132.06, 129.19, 128.70, 128.01, 127.15, 65.20, 41.78, 28.61, 21.91, 19.80. **HRMS (ESI-MS):** m/z Calculated for $C_{14}H_{15}NO_2S$ $[M+H]^+$: 262.0896; Observed: 262.0896.

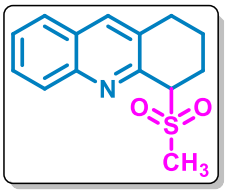

4-(Methylsulfonyl)-9-phenyl-1,2,3,4-tetrahydroacridine (3o): Yield =86%, White solid; M. P: 203.5-204.2 °C; **IR (KBr, cm^{-1})**:2944, 2920, 1596, 1211, 769; **^{1}H NMR (400 MHz, CDCl$_3$) δ** 8.02 (d, *J* = 8.4 Hz, 1H), 7.66 (ddd, *J* = 8.4, 5.6, 2.4 Hz, 1H), 7.57 – 7.51 (m, 2H), 7.50 – 7.46 (m, 1H), 7.43 – 7.37 (m, 2H), 7.31 (d, *J* = 7.2 Hz, 1H), 7.19 (d, *J* = 7.6 Hz, 1H), 4.67 (dd, *J* = 6.7, 4.3 Hz, 1H), 3.38 (s, 3H), 2.94 – 2.86 (m, 1H), 2.76 (m, 1H), 2.64 – 2.55 (m, 1H), 2.30 – 2.19 (m, 2H), 1.78 – 1.72 (m, 1H). **^{13}C NMR (100 MHz, CDCl$_3$) δ** 150.59, 147.80, 146.13, 136.40, 129.73, 129.33, 128.99, 128.92, 128.86, 128.79, 128.64, 128.12, 127.45, 126.92, 126.09, 65.87, 41.99, 27.39, 21.64, 19.94. **HRMS (ESI-MS):** m/z Calculated for $C_{20}H_{19}NO_2S$ $[M+H]^+$: 338.1209; Observed: 338.1217.

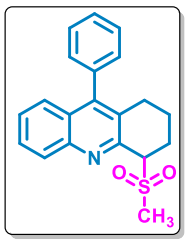

7-Chloro-4-(methylsulfonyl)-9-phenyl-1,2,3,4-tetrahydroacridine (3p): Yield = 88%, White solid; M. P: 230.4-231 °C; **IR (KBr, cm^{-1})**: 3027, 2999, 2944, 1562, 1290, 1118, 697; **^{1}H NMR (400 MHz, CDCl$_3$) δ** 7.96 (d, *J* = 9.2 Hz, 1H), 7.59 (dd, *J* = 9.2, 2.4 Hz, 1H), 7.58 – 7.52 (m, 2H), 7.52 – 7.48 (m, 1H), 7.35 (d, *J* = 2.4 Hz, 1H), 7.31 – 7.27 (m, 1H), 7.19 – 7.16 (m, 1H), 4.64 (dd, *J* = 6.4, 4.0 Hz, 1H), 3.37 (s, 3H), 2.92 – 2.85 (m, 1H), 2.74 (m, 1H), 2.58 (m, 1H), 2.30 – 2.18 (m, 2H), 1.79 – 1.71 (m, 1H). **^{13}C NMR (100 MHz, CDCl$_3$) δ** 151.02, 147.05, 144.50, 135.66, 132.89, 130.78, 130.46, 130.01, 129.22, 129.08, 128.86, 128.80, 128.45, 128.13, 124.82, 65.77, 42.05, 27.46, 21.59, 19.80. **HRMS (ESI-MS):** m/z Calculated for $C_{20}H_{18}ClNO_2S$ $[M+H]^+$: 372.0820; Observed: 372.0822.

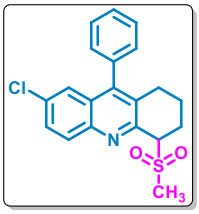

4-Tosyl-3,4-dihydroacridin-1(2H)-one (3q): Yield = 90%, White solid; M. P: 185.7-186.4 °C; **IR (KBr, cm^{-1})**:2920, 1723, 1212, 1136, 769; **^{1}H NMR (400 MHz, $CDCl_3$) δ** 8.93 (s, 1H), 7.98 (dd, *J* = 8.4, 1.2 Hz, 1H), 7.80 – 7.76 (m, 1H), 7.69 (dt, *J* = 8.4, 1.2 Hz, 1H), 7.61 (ddd, *J* = 8.0, 6.8, 1.2 Hz, 1H), 7.54 – 7.49 (m, 2H), 7.28 (s, 1H), 7.26 (s, 1H), 4.73 (dd, *J* = 5.2, 2.4 Hz, 1H), 3.55 (m, 1H), 3.20 – 3.13 (m, 1H), 2.85 – 2.78 (m, 1H), 2.68 – 2.58 (m, 1H), 2.47 (s, 3H). **^{13}C NMR (100 MHz, $CDCl_3$) δ** 195.73, 152.80, 148.95, 145.02, 137.60, 134.95, 132.50, 129.78, 129.53, 129.32, 128.89, 127.90, 127.55, 126.89, 66.20, 34.13, 21.88, 21.72. **HRMS (ESI-MS):** m/z Calculated for $C_{20}H_{17}NO_3S$ $[M+H]^+$: 352.1002; Observed: 352.1007.

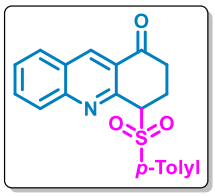

9-Methyl-4-tosyl-3,4-dihydroacridin-1(2H)-one (3r): Yield = 85%, White solid; M. P: 240.5-241 °C; **IR (KBr, cm^{-1})**: 2945, 2865, 1685, 1298, 740; **^{1}H NMR (400 MHz, $CDCl_3$) δ** 8.29 (d, *J* = 8.4 Hz, 1H), 7.77 (ddd, *J* = 8.4, 7.2, 1.2 Hz, 1H), 7.68 (m, 2H), 7.66 – 7.64 (m, 2H), 7.50 – 7.47 (m, 2H), 7.30 (d, *J* = 7.8 Hz, 2H), 7.24 (d, *J* = 7.8 Hz, 2H), 4.71 – 4.68 (m, 1H), 3.29 – 3.21 (m, 1H), 3.00 – 2.93 (m, 1H), 2.58 – 2.51 (m, 1H), 2.44 (s, 3H), 2.43 (s, 3H), 2.43 – 2.38 (m, 1H). **^{13}C NMR (100 MHz, $CDCl_3$) δ** 197.92, 152.83, 148.20, 145.15, 134.72, 132.12, 129.81, 129.58, 128.65, 126.17, 67.15, 35.34, 21.70, 20.50. **HRMS (ESI-MS):** m/z Calculated for $C_{21}H_{19}NO_3S$ $[M+H]^+$: 366.1165; Observed: 366.1168.

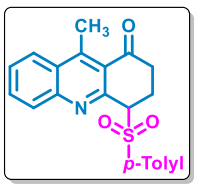

9-Phenyl-4-tosyl-3,4-dihydroacridin-1(2H)-one (3s): Yield = 87%, White solid; M. P: 220.8-221.4 °C; **IR (KBr, cm^{-1})**: 3041, 2965, 2895, 1656, 1298, 1136, 769; **^{1}H NMR (400 MHz, $CDCl_3$) δ** 7.75 – 7.69 (m, 2H), 7.59 (dd, *J* = 8.4, 3.2 Hz, 2H), 7.56 – 7.49 (m, 3H), 7.49 – 7.45 (m, 2H), 7.34 (dd, *J* = 7.2, 2.4 Hz, 1H), 7.29 (d, *J* = 8.4 Hz, 2H), 7.08 (m, 1H), 4.83 – 4.80 (m, 1H), 3.45 – 3.35 (m, 1H), 3.11 – 3.04 (m, 1H), 2.70 – 2.59 (m, 2H), 2.47 (s, 3H). **^{13}C NMR (100 MHz, $CDCl_3$) δ** 189.98, 151.92, 146.67, 145.36, 135.17, 134.72, 134.14, 133.07, 130.56, 129.68, 129.31, 128.72, 128.23, 127.03, 126.73, 123.94, 67.69, 32.53, 23.70, 21.76. **HRMS (ESI-MS):** m/z Calculated for $C_{26}H_{21}NO_3S$ $[M+H]^+$: 428.1315; Observed: 428.1316.

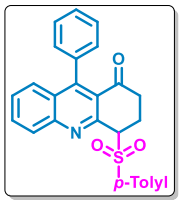

7-Chloro-9-phenyl-4-tosyl-3,4-dihydroacridin-1(2H)-one(3t): Yield = 90%, White solid; M. P: 228.5-229.2 °C; **IR (KBr, cm^{-1})**: 3021, 2956, 2920, 1636, 1215, 1137, 740; **^{1}H NMR (400 MHz, $CDCl_3$) δ** 7.67 – 7.64 (m, 2H), 7.59 – 7.57 (m, 2H), 7.56 – 7.53 (m, 1H), 7.53 – 7.51 (m, 1H), 7.51 – 7.48 (m, 1H), 7.47 (m, 1H), 7.34 – 7.31 (m, 1H), 7.30 (d, *J* = 8.0 Hz, 2H), 7.08 – 7.04 (m, 1H),

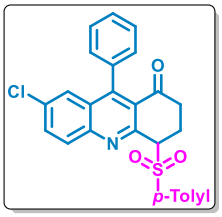

4.79 (m, 1H), 3.47 – 3.37 (m, 1H), 3.11 – 3.04 (m, 1H), 2.70 – 2.58 (m, 2H), 2.48 (s, 3H). **^{13}C NMR (100 MHz, $CDCl_3$) δ** 195.07, 153.53, 151.05, 146.39, 145.06, 136.27, 135.09, 133.81, 132.80, 130.47, 129.60, 129.27, 129.06, 128.82, 128.37, 128.16, 127.53, 126.83, 125.09, 67.28, 35.54, 21.74, 21.29. **HRMS (ESI-MS):** m/z Calculated for $C_{26}H_{20}ClNO_3S$ $[M+H]^+$: 462.0925; Observed: 462.0878.

7-Nitro-9-phenyl-4-tosyl-3,4-dihydroacridin-1(2H)-one (3u): Yield = 86%, White solid; M. P: 199.6-200.3 °C; **IR (KBr, cm^{-1})**: 3024, 2989, 2874, 1628, 1276, 1171, 769; **^{1}H NMR (400 MHz, $CDCl_3$) δ** 8.49 – 8.45 (m, 2H), 7.86 – 7.83 (m, 1H), 7.61 – 7.58 (m, 3H), 7.58 – 7.50 (m, 2H), 7.38 – 7.35 (m, 1H), 7.33 (m, 1H), 7.32 – 7.30 (m, 1H), 7.11 – 7.07 (m, 1H), 4.86 – 4.83 (m, 1H), 3.49 – 3.39 (m, 1H), 3.13 – 3.07 (m, 1H), 2.75 – 2.68 (m, 1H), 2.68 – 2.59 (m, 1H), 2.49 (s, 3H). **^{13}C NMR (100 MHz, $CDCl_3$) δ** 194.51, 157.01, 153.89, 149.63, 146.25, 145.34, 135.26, 134.91, 129.71, 129.23, 128.86, 128.59, 127.61, 125.00, 67.37, 35.46, 21.77, 21.21. **HRMS (ESI-MS):** m/z Calculated for $C_{26}H_{20}N_2O_5S$ $[M+H]^+$: 473.1136; Observed: 473.1172

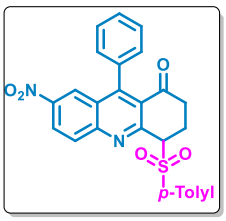

Methyl 1-oxo-4-tosyl-1,2,3,4-tetrahydroacridine-9-carboxylate (3v): Yield = 90%, White solid; M. P: 200.1-200.6 °C; **IR (KBr, cm^{-1})**: 3024, 2989, 2874, 1754, 1628, 1431, 1217, 719; **^{1}H NMR (400 MHz, $CDCl_3$) δ** 7.85 – 7.82 (m, 1H), 7.82 – 7.78 (m, 1H), 7.69 – 7.63 (m, 2H), 7.54 – 7.49 (m, 2H), 7.27 (s, 1H), 7.26 (d, *J* = 2.0 Hz, 1H), 4.76 – 4.73 (m, 1H), 4.13 (s, 3H), 3.56 (m, 1H), 3.22 – 3.14 (m, 1H), 2.86 – 2.79 (m, 1H), 2.68 – 2.58 (m, 1H), 2.47 (s, 3H). **^{13}C NMR (100 MHz, $CDCl_3$) δ** 194.85, 167.94, 152.80, 148.69, 145.13, 141.91, 134.74, 132.82, 129.56, 129.35, 129.21, 128.82, 126.46, 123.94, 122.38, 66.33, 53.32, 34.21, 21.72, 21.44. **HRMS (ESI-MS):** m/z Calculated for $C_{22}H_{19}NO_5S$ $[M+H]^+$: 410.1057; Observed: 410.1059.

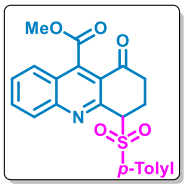

2,3-Dihydroacridin-4(1H)-one (4a): Yield: 87%, Brown Solid; M.P: 195.5-197.0 °C; **IR (KBr, cm^{-1}):** 3058, 2943, 1706, 1561, 1484, 1174, 1019, 916, 768: **^{1}H NMR (400 MHz, $CDCl_3$):** ^{1}H NMR (400 MHz, $CDCl_3$) δ 8.33 (d, *J* = 8.4 Hz, 1H), 8.11 (s, 1H), 7.80 (d, *J* = 8.4 Hz, 1H), 7.73 (m, 1H), 7.61 (t, *J* = 7.4 Hz, 1H), 3.21 (t, *J* = 6.4 Hz, 2H), 2.93 (t, *J* = 6.4, 2H), 2.26 (p, *J* = 6.4 Hz, 2H). **^{13}C NMR (100 MHz, $CDCl_3$)** δ 197.29, 148.54, 147.42, 136.35, 135.96, 131.28, 129.77, 129.50, 128.87, 126.81, 40.49, 29.53, 22.76. **HRMS (ESI-MS):** m/z calculated for $C_{13}H_{11}NO$ $(M+H)^+$ 198.0913, found 198.0916.

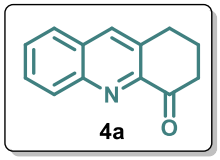

9-Methyl-2,3-dihydroacridin-4(1H)-one (4b): Yield: 81%, Red Solid; M.P: 76.7-77.3 °C; **IR (KBr, cm^{-1}):** 2924, 2854, 1703, 1598, 1381, 1113, 1032, 757: **^{1}H NMR (400 MHz, $CDCl_3$).** ^{1}H NMR (400 MHz, $CDCl_3$) δ 8.32 (dd, *J* = 8.4, 2.0 Hz, 1H), 8.05 – 7.99 (m, 1H), 7.71 (ddd, *J* = 8.4, 6.8, 1.6 Hz, 1H), 7.63 (ddd, *J* = 8.4, 6.8, 1.6 Hz, 1H), 3.16 (t, *J* = 6.0 Hz, 2H), 2.89 (m, 2H), 2.69 (s, 3H), 2.30 – 2.24 (m, 2H). **^{13}C NMR (101 MHz, $CDCl_3$) δ** 197.74, 148.01, 146.59, 143.16, 133.68, 132.17, 129.24, 129.06, 128.52, 123.36, 39.84, 26.83, 22.06, 14.16. **HRMS (ESI-MS):** m/z calculated for $C_{14}H_{13}NO$ $(M+H)^+$ 212.1070, found 212.1073.

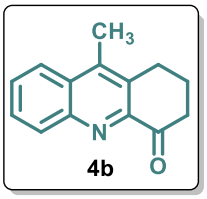

9-Phenyl-2,3-dihydroacridin-4(1H)-one (4c): Yield: 83%, Red Solid; M.P. 186.5-188.3 °C; **IR (KBr, cm^{-1}):** 3058, 2944, 1706, 1485, 1305, 1140, 1020, 916, 768: **^{1}H NMR (400 MHz, $CDCl_3$) δ** 8.40 (d, *J* = 8.8 Hz, 1H), 7.72 (ddd, *J* = 8.4, 6.8, 1.6 Hz, 1H), 7.60 – 7.55 (m, 2H), 7.54 – 7.42 (m, 3H), 7.32 – 7.27 (m, 2H), 2.98 – 2.90 t, *J* = 6.0 Hz, 2H), 2.87 (t, *J* = 6.0 Hz, 2H), 2.15 (p, *J* = 6.4 Hz, 2H).^{13}C NMR (101 MHz, $CDCl_3$) δ 197.66, 148.35, 148.20, 147.15, 136.12, 133.98, 133.48, 131.47, 129.55, 129.16, 128.84, 128.75, 128.38, 125.85, 40.22, 27.99, 22.60. **HRMS (ESI-MS):** m/z calculated for $C_{19}H_{15}NO$ $(M+H)^+$ 274.1226, found 274.1229.

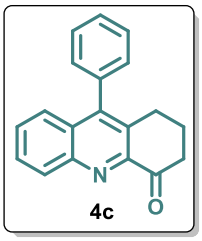

7-Chloro-9-phenyl-2,3-dihydroacridin-4(1H)-one (4d): Yield: 90%, Red Solid; M.P. 218.2-219.8 °C ; **IR (KBr, cm^{-1}):** 3045, 2948, 1708, 1599, 1476, 1166, 845, 709; **^{1}H NMR (400 MHz, $CDCl_3$) δ** 8.32 (d, *J* = 9.2 Hz, 1H), 7.68 – 7.52 (m, 4H), 7.40 (s, 1H), 7.27 (s, 1H), 7.25 (s, 1H), 2.91 (t, *J* = 6.4 Hz, 2H), 2.89 – 2.81 (t, *J* = 6.4 Hz, 2H), 2.14 (p, *J* = 6.4 Hz, 2H).**^{13}C NMR (100 MHz, $CDCl_3$) δ** 197.31, 148.50, 147.48, 145.50, 135.38, 135.04, 134.45, 133.07, 130.77, 129.38, 129.08, 129.05, 128.73, 124.62, 40.13, 28.03, 22.44. **HRMS (ESI-MS):** m/z calculated for $C_{19}H_{14}ClNO$ $(M+H)^+$ 308.0837, found 308.0839.

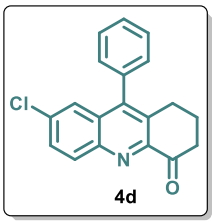

7-Bromo-9-phenyl-2,3-dihydroacridin-4(1H)-one (4e): Yield: 88%, Off White Solid; M.P. 228.2-229.0 °C; **IR (KBr, cm^{-1}**): 3046, 2948,2863, 1705, 1568, 1476, 1166, 845, 649, 709; **^{1}H NMR (400 MHz, $CDCl_3$) δ** 8.32 (d, *J* = 9.2 Hz, 1H), 7.65 (d, *J* = 9.2 Hz, 1H), 7.62 – 7.56 (m, 2H), 7.54 (s, 1H), 7.40 (s, 1H), 7.26 (d, *J* = 4.0 Hz, 2H), 2.91 (t, *J* = 6.4 Hz, 2H), 2.88 – 2.82 (m, 2H). **^{13}C NMR (100 MHz, $CDCl_3$) δ** 207.00, 155.99, 147.36, 144.99, 135.80, 132.54, 130.83, 129.06, 128.97, 128.86, 128.83, 128.73, 128.41, 128.33, 127.87, 121.12, 59.87, 31.98, 30.94,

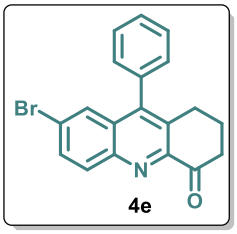

27.19, 17.43. **HRMS (ESI-MS):** m/z calculated for $C_{19}H_{15}BrNO$ $(M+H)^+$ 352.0332, found 352.0332.

7-Nitro-9-phenyl-2,3-dihydroacridin-4(1H)-one (4f): Yield: 83%, Green Solid; M.P. 73.8-76.7 °C ; **IR (KBr, cm^{-1})**: 2924, 2853, 1708, 1530, 1339, 1170, 1030, 704: **^{1}H NMR (400 MHz, $CDCl_3$) δ** 8.53 (dd, *J* = 9.2, 0.8 Hz, 1H), 8.46 (dd, *J* = 9.2, 2.4 Hz, 1H), 8.40 (dd, *J* = 2.4, 0.8 Hz, 1H), 7.65 – 7.60 (m, 3H), 7.32 – 7.28 (m, 2H), 2.96 (dd, *J* = 6.4, 5.6 Hz, 2H), 2.93 (dd, *J* = 6.4, 5.6 Hz, 2H), 2.22 – 2.16 (m, 2H).**^{13}C NMR (100 MHz, $CDCl_3$) δ** 196.77, 150.94, 148.78, 146.95, 135.26, 134.45, 133.39, 129.32, 129.00, 127.77, 122.83, 40.09, 28.03, 22.26. **HRMS (ESI-MS):** m/z calculated for $C_{19}H_{14}N_2O_3$ $(M+H)^+$ 319.1077, found 319.1087.

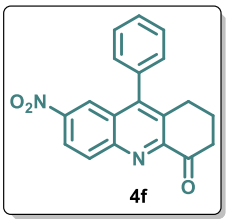

Methyl 4-oxo-1,2,3,4-tetrahydroacridine-9-carboxylate (4g): Yield: 87%: Yellow Solid M.P. 133.0-134.5 °C; **IR (KBr, cm^{-1})**: 2943, 1723, 1707, 1458, 1283, 1224, 1032, 975, 752; **^{1}H NMR (400 MHz, $CDCl_3$) δ** 8.37 (dd, *J* = 9.2, 2.4 Hz, 1H), 7.82 – 7.74 (m, 2H), 7.73 – 7.64 (m, 1H), 4.11 (s, 3H), 3.17 (t, *J* = 6.4 Hz, 2H), 2.95 (t, *J* = 6.4 Hz, 2H), 2.27 (p, *J* = 6.4 Hz, 2H).; ^{13}C NMR (100 MHz, $CDCl_3$) δ 196.28, 167.39, 148.31, 147.11, 138.97, 132.25, 131.76, 130.20, 130.01, 125.15, 124.21, 52.89, 40.10, 27.28, 22.13. **HRMS (ESI-MS):** m/z calculated for $C_{15}H_{13}NO_3$ $(M+H)^+$ 256.0968, found 256.0972.

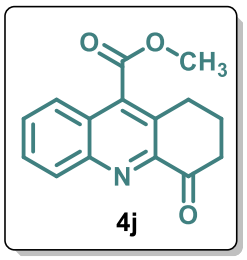

Benzyl 4-oxo-1,2,3,4-tetrahydroacridine-9-carboxylate (4h): Yield: 86%, Red Liqiud; **IR (KBr, cm^{-1})**: 3064, 2926, 1729, 1456, 1211, 1078, 960, 758; **^{1}H NMR (400 MHz, $CDCl_3$) δ** 8.36 (d, *J* = 8.4 Hz, 1H), 7.77 – 7.71 (m, 2H), 7.64 – 7.60 (m, 1H), 7.49 (dd, *J* = 7.2, 2.4 Hz, 2H), 7.45 – 7.39 (m, 3H), 5.55 (s, 2H), 3.10 (t, *J* = 6.4 Hz, 2H), 2.91(t, *J* = 6.4 Hz 2H), 2.25 – 2.18 (m, 2H). **^{13}C NMR (100 MHz, $CDCl_3$) δ** 196.28, 166.84, 148.29, 147.12, 138.84, 134.76, 132.18, 131.78, 130.19, 130.03, 128.98, 128.88, 128.86, 125.16, 124.11, 68.02, 40.08, 27.15, 22.11. **HRMS (ESI-MS):** m/z calculated for $C_{21}H_{17}NO_3$ $(M+H)^+$ 332.1281, found 332.1280.

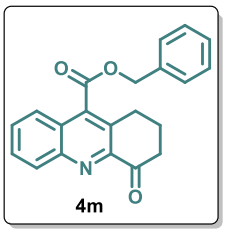

3,3,9-trimethyl-2,3-dihydroacridine-1,4-dione (4i): Yield: 72%, White Solid; M. P: 167.9-170.6 °C; **IR (KBr, cm^{-1})**: 2925, 2853, 1716, 1703, 1367, 1075, 699; **^{1}H NMR (400 MHz, CDCl3) δ** 8.14 – 8.11 (m, 1H), 8.09 – 8.06 (m, 1H), 7.89 – 7.85 (m, 1H), 7.69 – 7.66 (m, 1H), 3.28 (s, 2H), 2.72 (s, 3H), 1.16 (s, 6H).

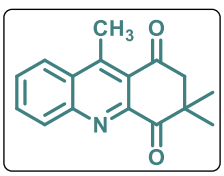

^{13}C NMR (100 MHz, CDCl3) δ 200.44, 194.01, 161.25, 149.53, 135.83, 132.35, 129.82, 128.20, 126.33, 123.97, 123.75, 54.14, 48.18, 32.28, 28.21.

7-Chloro-3,3-dimethyl-9-phenyl-2,3-dihydroacridine-1,4-dione (4j): Yield: 84%, Yellow Solid; M. P: 167.9-170.6 °C; **IR (KBr, cm^{-1})** 2925, 2853, 1716, 1703, 1367, 1075, 699; **^{1}H NMR (400 MHz, CDCl$_3$):** δ 8.39 (d, *J* = 9.2 Hz, 1H), 7.81 (dd, *J* = 9.2, 2.4 Hz, 1H), 7.58 – 7.54 (m, 4H), 7.24 – 7.19 (m, 2H), 2.99 (s, 2H), 1.40 (s, 6H); **^{13}C{^{1}H} NMR (100 MHz, CDCl$_3$) δ** 199.27, 194.89, 150.36, 148.93, 148.06, 135.98, 135.29, 133.50, 132.94, 130.08, 128.55, 128.52, 128.32, 126.84, 126.64, 53.56, 45.44, 25.22; **HRMS *m/z* (ESI):** calculated for $C_{21}H_{16}ClNO_2$ $(M+H)^+$ 350.0942, found 350.0942.

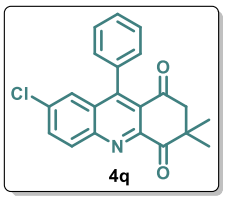

9-Chloro-4-(phenylsulfonyl)-1,2,3,4-tetrahydroacridine (5a): Yield = 67%, White solid; M. P: 109.6-110.2 °C; **IR (KBr, cm^{-1})**: 3045, 2984, 2832, 1423, 1089, 801; **^{1}H NMR (400 MHz, CDCl$_3$) δ** 9.07 (dd, *J* = 8.8, 1.6 Hz, 1H), 8.12 (dd, *J* = 8.4, 1.6 Hz, 1H), 7.91 (t, *J* = 1.6 Hz, 1H), 7.89 (d, *J* = 1.6 Hz, 1H), 7.74 – 7.70 (m, 1H), 7.64 – 7.60 (m, 1H), 7.60 – 7.57 (m, 1H), 7.53 – 7.49 (m, 2H), 5.57 – 5.52 (m, 1H), 3.80 – 3.73 (m, 1H), 3.37 – 3.30 (m, 1H), 2.50 – 2.43 (m, 1H), 2.35 – 2.24 (m, 2H), 1.97 (m, 1H). **^{13}C NMR (100 MHz, CDCl$_3$) δ** 156.35, 147.57, 142.17, 141.84, 133.69, 132.18, 130.36, 129.64, 129.40, 129.13, 126.43, 124.58, 123.89, 60.32, 31.09, 27.05, 17.36. **HRMS (ESI-MS):** m/z Calculated for $C_{19}H_{16}ClNO_2S$ $[M+H]^+$: 358.0663; Observed: 358. 066.

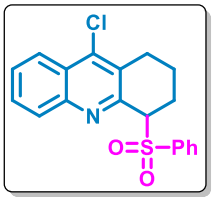

9-(Phenylsulfonyl)-1,2,3,4-tetrahydroacridine (5a'): Yield = 10%, White solid; M. P: 118.2-119 °C; **IR (KBr, cm^{-1})**: 3052, 2965, 2789, 1125, 1089, 767; **^{1}H NMR (400 MHz, CDCl$_3$) δ** 9.04 (dd, *J* = 8.8, 2.0 Hz, 1H), 8.02 (d, *J* = 8.8 Hz, 1H), 7.92 – 7.86 (m, 2H), 7.71 – 7.67 (m, 1H), 7.60 – 7.56 (m, 1H), 7.56 – 7.53 (m, 1H), 7.51 – 7.47 (m, 2H), 3.46 (t, *J* = 6.4 Hz, 2H), 3.19 (t, *J* = 6.4 Hz, 2H), 1.98 – 1.91 (m, 2H), 1.86 – 1.80 (m, 2H). **^{13}C NMR (100 MHz, CDCl$_3$) δ** 160.16, 147.20, 142.56, 140.71, 133.45, 129.47, 129.27, 129.20, 128.65, 127.66, 126.37, 124.60, 122.84, 34.58, 27.87, 22.31, 21.55. **HRMS (ESI-MS):** m/z Calculated for $C_{19}H_{17}NO_2S$ $[M+H]^+$: 324.1053; Observed: 324.1054.

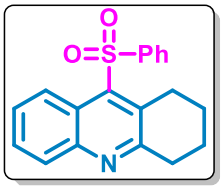

4,9-bis(Phenylsulfonyl)-1,2,3,4-tetrahydroacridine (5a"): Yield = 12%, White solid; M. P: 172.8-173.2 °C; **IR (KBr, cm^{-1})**: 3021, 2998, 2875, 1541, 1245, 1023, 812; **^{1}H NMR (400 MHz, $CDCl_3$) δ** 9.05 – 9.00 (m, 1H), 7.91 – 7.88 (m, 2H), 7.64 – 7.59 (m, 4H), 7.58 – 7.57 (m, 2H), 7.55 – 7.50 (m, 2H), 7.43 (qd, *J* = 7.2, 2.0 Hz, 3H), 4.84 (dd, *J* = 7.6, 4.4 Hz, 1H), 3.65 – 3.58 (m, 1H), 3.46 – 3.39 (m, 1H), 2.95 – 2.88 (m, 1H), 2.39 – 2.28 (m, 2H), 1.75 – 1.69 (m, 1H). **^{13}C NMR (100 MHz, $CDCl_3$) δ** 151.00, 146.63, 142.29, 141.28, 138.71, 134.99, 133.69, 133.49, 129.86, 129.42, 129.29, 129.03, 128.74, 126.42, 124.66, 123.24, 67.84, 27.19, 21.71, 20.00. **HRMS (ESI-MS):** m/z Calculated for $C_{19}H_{23}N_3O_4$ $[M+H]^+$: 464.0985; Observed: 464.0983.

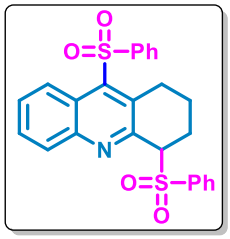

9-Chloro-4-tosyl-1,2,3,4-tetrahydroacridine (5b): Yield = 70%, White solid; M. P: 170.8-171°C; **IR (KBr, cm^{-1})**: 2959, 2920, 2873, 1527, 1480, 1339, 705; **^{1}H NMR (400 MHz, $CDCl_3$) δ** 9.10 (dd, *J* = 9.2, 2.0 Hz, 1H), 8.12 (dd, *J* = 8.4, 2.0 Hz, 1H), 7.80 – 7.77 (m, 2H), 7.73 – 7.70 (m, 1H), 7.64 – 7.60 (m, 1H), 7.29 (d, *J* = 8.4 Hz, 2H), 5.55 – 5.53 (m, 1H), 3.80 – 3.73 (m, 1H), 3.37 – 3.29 (m, 1H), 2.47 – 2.43 (m, 1H), 2.40 (s, 3H), 2.33 – 2.23 (m, 2H), 2.00 – 1.96 (m, 1H). **^{13}C NMR (100 MHz, $CDCl_3$) δ** 156.33, 147.58, 144.79, 142.24, 139.23, 131.98, 130.33, 129.99, 129.56, 129.03, 126.55, 124.67, 123.89, 60.38, 31.11, 27.03, 21.64, 17.38. **HRMS (ESI-MS):** m/z Calculated for $C_{20}H_{18}ClNO_2S$ $[M+H]^+$: 372.0820; Observed: 372.0822.

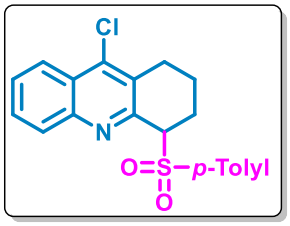

9-Tosyl-1,2,3,4-tetrahydroacridine (5b'): Yield = 10%, White solid; M. P: 125.2-125.9 °C; **IR (KBr, cm^{-1})**: 3012, 2965, 2862, 1432, 1243, 765; ^{1}H NMR (400 MHz, $CDCl_3$) δ 8.01 (dd, *J* = 8.4, 1.6 Hz, 1H), 7.78 (d, *J* = 6.8 Hz, 1H), 7.66 (dt, *J* = 6.8, 1.6 Hz, 1H), 7.59 – 7.55 (m, 3H), 7.30 (s, 1H), 7.28 (s, 1H), 3.46 (t, *J* = 6.4 Hz, 2H), 3.19 (t, *J* = 6.4 Hz, 2H), 2.48 (s, 3H), 1.96 – 1.91 (m, 2H), 1.83 (m, 2H). **^{13}C NMR (101 MHz, $CDCl_3$) δ** 160.15, 150.51, 144.37, 139.66, 136.39, 133.48, 129.86, 129.55, 129.50, 129.29, 127.79, 127.56, 126.49, 124.69, 123.87, 27.84, 26.60, 22.79, 22.34, 21.57. **HRMS (ESI-MS):** m/z Calculated for $C_{20}H_{19}NO_2S$ $[M+H]^+$: 338.1209; Observed: 338.1209.

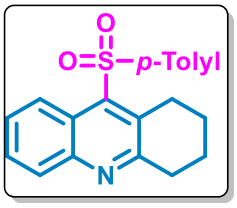

4,9-Ditosyl-1,2,3,4-tetrahydroacridine (5b"): Yield = 15%, White solid; M. P: 119-119.9 °C; **IR (KBr, cm^{-1})**: 2994, 2983, 1543, 1145, 760; ^{1}H NMR (400 MHz, $CDCl_3$) δ 9.05 (dd, *J* = 8.4, 1.4 Hz, 1H), 7.78 (d, *J* = 8.4 Hz, 2H), 7.64 – 7.57 (m, 2H), 7.52 (dd, *J* = 7.6, 2.0 Hz, 1H),

7.45 (d, *J* = 8.4 Hz, 2H), 7.30 (d, *J* = 8.0 Hz, 2H), 7.21 (d, *J* = 8.4 Hz, 2H), 4.80 (dd, *J* = 7.6, 4.4 Hz, 1H), 3.65 – 3.57 (m, 1H), 3.40 (m, 1H), 2.92 – 2.84 (m, 1H), 2.44 (s, 3H), 2.40 (s, 3H), 2.37 – 2.28 (m, 2H), 1.72 (m, 1H). ^{13}C NMR (101 MHz, $CDCl_3$) δ 151.16, 146.66, 144.77, 144.50, 141.63, 139.34, 135.66, 134.86, 130.01, 129.78, 129.37, 129.28, 128.90, 126.53, 124.76, 123.26, 68.01, 27.17, 21.87, 21.66, 20.00. **HRMS (ESI-MS):** m/z Calculated for $C_{27}H_{25}NO_4S_2$ $[M+H]^+$: 492.1298; Observed: 492.1296.

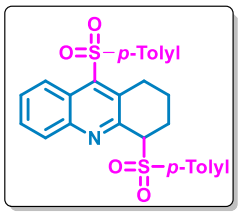

9-Chloro-4-((4-nitrophenyl)sulfonyl)-1,2,3,4-tetrahydroacridine (5c): Yield = 70%, White solid; M. P: 186.3-186.9 °C; **IR (KBr, cm^{-1})**: 3051, 2996, 2856, 1432, 1256, 1085, 782; **^{1}H NMR (400 MHz, $CDCl_3$) δ** 8.37 – 8.32 (m, 2H), 8.22 – 8.17 (m, 1H), 7.93 – 7.88 (m, 2H), 7.66 – 7.59 (m, 2H), 7.33 – 7.29 (m, 1H), 4.74 (dd, *J* = 6.4, 4.0 Hz, 1H), 3.33 – 3.26 (m, 1H), 3.10 – 3.05 (m, 1H), 3.02 – 2.93 (m, 1H), 2.55 – 2.45 (m, 1H), 2.36 – 2.27 (m, 1H), 2.09 – 2.02 (m, 1H). **^{13}C NMR (100 MHz, $CDCl_3$) δ** 150.66, 149.68, 145.84, 145.69, 142.48, 130.98, 130.08, 129.91, 128.49, 128.20, 126.19, 124.05, 123.66, 67.02, 26.60, 22.33, 19.11. **HRMS (ESI-MS):** m/z Calculated for $C_{19}H_{23}N_3O_4$ $[M+H]^+$: 403.0514; Observed: 403.0510.

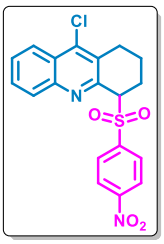

9-Chloro-4-(methylsulfonyl)-1,2,3,4-tetrahydroacridine (5d): Yield = 72%, White solid; M. P: 166.5-167.2 °C; **IR (KBr, cm^{-1})**: 2984, 2865, 1523, 1245, 1012, 756; **^{1}H NMR (400 MHz, $CDCl_3$) δ** 8.23 (d, *J* = 8.4 Hz, 1H), 7.99 (d, *J* = 7.6 Hz, 1H), 7.75 – 7.71 (m, 1H), 7.64 (ddd, *J* = 8.4, 6.8, 1.2 Hz, 1H), 4.57 (dd, *J* = 6.4, 4.0 Hz, 1H), 3.33 (s, 3H), 3.27 – 3.22 (m, 1H), 3.00 – 2.92 (m, 2H), 2.39 – 2.32 (m, 1H), 2.24 – 2.16 (m, 1H), 2.01 – 1.95 (m, 1H). **^{13}C NMR (100 MHz, $CDCl_3$) δ** 151.02, 146.41, 142.63, 129.92, 129.08, 128.05, 126.27, 124.02, 65.38, 42.03, 26.80, 21.63, 18.95. **HRMS (ESI-MS):** m/z Calculated for $C_{14}H_{14}ClNO_2S$ $[M+H]^+$: 296.0507; Observed: 296.0519.

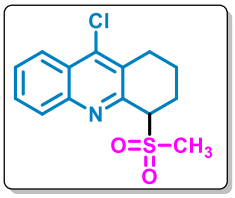

6-Bromo-9-chloro-4-tosyl-1,2,3,4-tetrahydroacridine (5e): Yield = 72%, White solid; M. P: 138.2-138.7 °C; **IR (KBr, cm^{-1})**: 2995, 2875, 1456, 1189, 1029, 809; **^{1}H NMR (400 MHz, $CDCl_3$) δ** 8.12 (dd, *J* = 8.4, 2.0 Hz, 1H), 7.80 – 7.77 (m, 2H), 7.73 – 7.70 (m, 1H), 7.64 – 7.60 (m, 1H), 7.31 – 7.28 (m, 2H), 5.56 – 5.53 (m, 1H), 3.80 – 3.73 (m, 1H), 3.38 – 3.30 (m, 1H), 2.40 (s, 3H), 2.34 – 2.24 (m, 2H), 2.00 – 1.92 (m, 2H). **^{13}C NMR (100 MHz, $CDCl_3$) δ** 160.15, 150.51, 144.37, 136.39, 133.48, 129.86, 129.55, 129.44, 129.29, 129.00, 127.79,

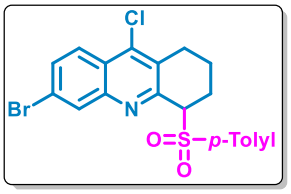

126.49, 124.69, 123.87, 67.11, 27.84, 26.60, 22.79, 21.57. **HRMS (ESI-MS):** m/z Calculated for $C_{20}H_{17}BrClNO_2S$ $[M+H]^+$: 449.9925; Observed: 449.9930.

6-Bromo-9-tosyl-1,2,3,4-tetrahydroacridine (5e'): Yield = 10%, White solid; M. P: 140.2-141 °C; **IR (KBr, cm^{-1})**: 3065, 2937, 1423, 1156, 1024, 732; **^{1}H NMR (400 MHz, CDCl$_3$) δ** 8.19 (s, 1H), 7.75 (dt, *J* = 8.8, 2.0 Hz, 2H), 7.64 (dd, *J* = 9.0, 2.0 Hz, 1H), 7.61 – 7.55 (m, 1H), 7.32 – 7.27 (m, 2H), 3.41 (t, *J* = 6.2 Hz, 2H), 3.16 (t, *J* = 6.2 Hz, 2H), 2.40 (s, 3H), 1.95 – 1.89 (m, 2H), 1.85 – 1.79 (m, 2H). **^{13}C NMR (100 MHz, CDCl$_3$) δ** 161.57, 147.87, 144.75, 141.40, 139.28, 133.77, 131.62, 130.86, 129.96, 129.46, 126.52, 126.19, 125.36, 123.39, 34.63, 27.83, 22.20, 21.64, 21.44. **HRMS (ESI-MS):** m/z Calculated for $C_{20}H_{18}BrNO_2S$ $[M+H]^+$: 416.0314; Observed: 416.0312.

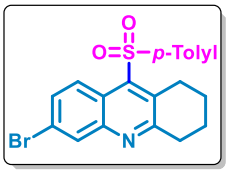

6-Bromo-4,9-ditosyl-1,2,3,4-tetrahydroacridine (5e"): Yield = 14%, White solid; M. P: 153.8-154.1 °C; **IR (KBr, cm^{-1})**: 3078, 2995, 1563, 1123, 789; **^{1}H NMR (400 MHz, CDCl$_3$) δ** 9.05 (d, *J* = 6.8 Hz, 1H), 7.80 – 7.76 (m, 2H), 7.64 – 7.57 (m, 2H), 7.51 (dd, *J* = 7.6, 1.8 Hz, 1H), 7.45 – 7.43 (m, 1H), 7.29 (d, *J* = 8.0 Hz, 2H), 7.23 – 7.17 (m, 2H), 4.80 (dd, *J* = 8.0, 4.4 Hz, 1H), 3.65 – 3.56 (m, 1H), 3.45 – 3.35 (m, 1H), 2.92 – 2.83 (m, 1H), 2.43 (s, 3H), 2.39 (s, 3H), 2.36 – 2.26 (m, 2H), 1.73 – 1.70 (m, 1H). **^{13}C NMR (101 MHz, CDCl$_3$) δ** 149.27, 147.76, 142.95, 134.09, 133.73, 133.37, 132.15, 131.93, 130.10, 129.45, 129.29, 126.55, 126.31, 125.26, 124.87, 39.63, 29.70, 27.30, 21.66, 21.56. **HRMS (ESI-MS):** m/z Calculated for $C_{27}H_{24}BrNO_4S_2$ $[M+H]^+$: 570.0403; Observed: 570.0405

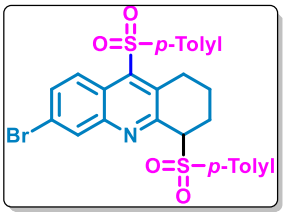

9-Chloro-2,3-dihydroacridin-4(1H)-one (6a): Yield=60%: M.P. 138.0-139.7 °C ; **IR (KBr, cm^{-1})**: 2951, 1706, 1547, 1479, 1293, 1022, 913, 768; **^{1}H NMR (400 MHz, CDCl$_3$) δ** 8.36 (dd, *J* = 8.4, 2.0 Hz, 1H), 8.24 (dd, *J* = 8.4, 1.6 Hz, 1H), 7.79 (ddd, *J* = 8.4, 6.8, 1.6 Hz, 1H), 7.73 (ddd, *J* = 8.4, 6.8, 1.4 Hz, 1H), 3.31 (t, *J* = 6.4 Hz, 2H), 2.98 – 2.87 (m, 2H), 2.30 (p, *J* = 6.8 Hz, 2H). **^{13}C NMR (100 MHz, CDCl$_3$) δ** 196.71, 148.63, 147.47, 142.83, 133.86, 131.96, 130.66, 130.14, 127.76, 124.01, 39.90, 27.50, 21.89. **HRMS (ESI-MS):** m/z calculated for $C_{13}H_{10}ClNO$ $(M+H)^+$ 232.0524, found 232.0522.

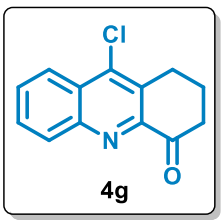

9-(Phenylsulfonyl)-2,3-dihydroacridin-4(1H)-one (6b): Yield = 30%, White solid; M. P: 172.8-173.2 °C; **IR (KBr, cm^{-1})**: 3045, 2921, 2856, 1658, 1235, 1021, 782; **^{1}H NMR (400 MHz, $CDCl_3$) δ** 8.24 (d, *J* = 8.4 Hz, 1H), 7.85 (m, 1H), 7.83 (s, 1H), 7.79 (ddd, *J* = 8.4, 6.8, 1.6 Hz, 1H), 7.76 – 7.71 (m, 1H), 7.43 (dd, *J* = 8.4, 0.8 Hz, 3H), 3.31 (t, *J* = 6.4 Hz, 2H), 2.93 (m, 2H), 2.51 (s, 3H), 2.34 – 2.27 (m, 2H). **^{13}C NMR (100 MHz, $CDCl_3$) δ** 196.46, 148.51, 148.13, 147.32, 142.62, 133.67, 131.82, 131.52, 130.42, 129.93, 128.00, 127.58, 123.83, 39.72, 27.33, 22.05, 21.72. **HRMS (ESI-MS):** m/z Calculated for $C_{19}H_{15}NO_3S$ $[M+H]^+$: 338.0845; Observed: 338.0845.

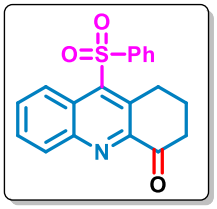

9-Tosyl-2,3-dihydroacridin-4(1H)-one (6c): Yield = 34%, White solid; M. P: 165.3-166.2 °C; **IR (KBr, cm^{-1})**: 3013, 2991, 2812, 1678, 1589, 1128, 805; **^{1}H NMR (400 MHz, $CDCl_3$) δ** 8.36 (d, *J* = 7.2 Hz, 1H), 8.25 (dd, *J* = 8.4, 2.0 Hz, 1H), 7.85 (s, 1H), 7.83 (s, 1H), 7.79 (ddd, *J* = 8.4, 6.8, 1.6 Hz, 1H), 7.76 – 7.71 (m, 1H), 7.43 (d, *J* = 8.0 Hz, 3H), 3.31 (t, *J* = 5.6 Hz, 2H), 2.96 – 2.89 (t, *J* = 5.6 Hz, 2H), 2.51 (s, 3H), 2.34 – 2.27 (m, 2H). **^{13}C NMR (100 MHz, $CDCl_3$) δ** 196.46, 148.51, 148.13, 147.32, 142.62, 133.67, 131.82, 131.52, 129.93, 128.00, 127.58, 123.83, 39.72, 27.33, 22.05, 21.72. **HRMS (ESI-MS):** m/z Calculated for $C_{20}H_{17}NO_3S$ $[M+H]^+$: 352.1002; Observed: 352.1010.

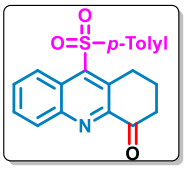

6-Bromo-9-chloro-2,3-dihydroacridin-4(1H)-one (6d): Yield: 62%: Brick Red Solid; M.P. 120.0-121.5 °C ; **IR (KBr, cm^{-1})**: 2926, 2854, 1699, 1620, 1574, 1456, 1059, 915, 833: **^{1}H NMR (400 MHz, CDCl3) δ** 8.54 (d, J = 2.0 Hz, 1H), 8.10 (d, J = 9.2 Hz, 1H), 7.79 (dd, J = 9.2, 2.0 Hz, 1H), 3.28 (t, J = 6.4 Hz, 2H), 2.93 (dd, J = 7.8, 5.5 Hz, 2H), 2.35 – 2.26 (m, 3H). **^{13}C NMR (100 MHz, CDCl3) δ** 195.98, 149.25, 147.73, 142.95, 134.09, 133.70, 133.36, 126.30, 125.25, 124.87, 39.62, 27.29, 21.56. **HRMS (ESI-MS):** m/z Calculated for $C_{13}H_9BrClNO$ $[M+H]^+$: 309.9629; Observed: 309.9621.

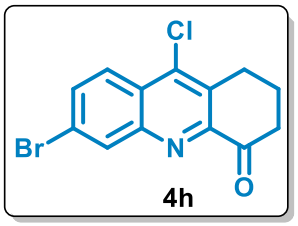

6-Bromo-9-tosyl-2,3-dihydroacridin-4(1H)-one (6e): Yield = 35%, White solid; M. P: 159.7-160.4 °C; **IR (KBr, cm^{-1})**: 3011, 2999, 1678, 1545, 1214, 1085, 723;**^{1}H NMR (400 MHz, $CDCl_3$) δ** 9.07 (d, *J* = 9.6 Hz, 1H), 8.57 (d, *J* = 2.0 Hz, 1H), 7.82 (m, 1H), 7.78 – 7.75 (m, 2H), 7.33 – 7.31 (m, 2H), 3.64 (t, *J* = 6.2 Hz, 2H), 2.91 (t, *J* =6.2 Hz, 2H), 2.42 (s, 3H), 2.21 – 2.16 (m, 2H). **^{13}C NMR (100 MHz, $CDCl_3$) δ** 195.11, 150.03, 148.52, 145.41, 138.63, 136.75, 134.38, 134.22, 130.22, 129.69, 126.65, 126.44, 125.95, 124.78, 123.65, 39.43, 27.96, 21.69, 21.59.

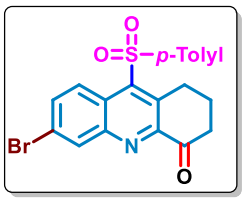

HRMS (ESI-MS): m/z Calculated for $C_{20}H_{16}BrNO_3S$ $[M+H]^+$: 430.0107; Observed: 430.0105.

3.2.8 References

(1) Gairola, D.; Peddinti, R. K. *Asian J. Org. Chem.* **2022**, *11*, e202200517. (b) Gong, X.; Chen, J.; Li, X.; Xie, W.; Wu, J. *Asian J. Org. Chem.* **2018**, *13*, 2543–2548.

(2) Cutler, R. A.; Stenger, R. J.; Suter, C. M. *J. Am. Chem. Soc.* **1952**, *74*, 5475–5481.

(3) (a) Gong, X.; Shen, Z.; Wang, G.; Qu, L.; Zhu, C. *Org. Biomol. Chem*. **2021**, *19*, 10662. (b) Zhu, Y. I.; Stiller, M. J. *J. Am. Acad. Dermatol.* **2001**, *45*, 420–434.

(4) Churcher, I.; Beher, D.; Best, J. D.; Castro, J. L.; Clarke, E. E.; Gentry, A.; Harrison, T.; Hitzel, L.; Kay, E.; Kerrad, S.; Lewis, H. D.; Morentin-Gutierrez, P.; Russell Mortishire-Smith; Oakley, P. J.; Reilly, M.; Shaw, D. E.; Shearman, M. S.; Teall, M. R.; Jonathan, S. W.; Wrigley, D. J. *Bioorg. Med. Chem. Lett.* **2006**, *16*, 280–284.

(5) (a) Liu, Y.; Wang, Q. L.; Chen, Z.; Zhou, Q.; Zhou, C. S.; Xiong, B. Q.; Zhang, P.L.; Yang, C. A.; Tang, K. W. *Org. Biomol. Chem.* **2019**, *17*, 1365–1369. (b) Lang, F. M.; Mo, Y.; Sabbagh, M.; Solomon, P.; Boada, M.; Giovanni, R. W. J.; Grimmer, B. F. T.; Dubois, B.; Harnett, M.; Friedhoff, R. S.; Coslett, S.; Cummings, J. L. *Alzheimer's Dement*. **2021**, *7*, 12136.

(6) Liu, Y.; Zhao, Y.; Zhai, X.; Liu, X.; Sun, L.; Ren, Y.; Gong, P. *Arch. Pharm. Chem. Life Sci*. **2008**, *341*, 446–452.

(7) (a) Harrak, Y.; Casula, G.; Basset, J.; Rosell, G.; Plescia, S.; Raffa, D.; Cusimano, M. G.; Pouplana, R.; Pujol, M. D. *J. Med. Chem.* **2010**, *53*, 6560–571. (b) Jiang, N.; Zhai, X.; Li, T.; Liu, D.; Zhang, T.; Wang, B.; Gong, P. *Molecules* **2012**, *17*, 5870–5881.

(8) (a) Řehová, L.; Dračínský, M.; Jahn, U. *Org. Biomol. Chem*. **2016**, *14*, 9612–9621. (b) Wang, W.; Wang, B. *Chem. Commun*. **2017**, *53*, 10124–10127. (c) Oka, N.; Mori, A.; Suzuki, K.; Ando, K. *J. Org. Chem*. **2021**, *86*, 657–673.

(9) (a) Prakash, G. K. S.; Hu, J. *Asc. Chem. Res*. **2007**, *40*, 921–930. (b) Miao, W.; Zhao, Y.; Ni, C.; Gao, B.; Zhang, W.; Hu, J.; Am. J. *Chem. Soc*. **2018**, *140*, 880–883.

(10) (a) Bujok, R.; Mąkosza, M. *Synthesis* **2019**, *51*, A–H. (b) Sephton, T.; Large, J. M.; Butterworth, S.; Greaney, M. F. *Org. Lett*. **2022**, *24*, 1132–1135.

(11) (a) Yang, F. L.; Tian, S.K. *Tetrahedron Lett*. **2017**, *58*, 487–504. (b) Zhao, S.; Chen, K.; Zhang, L.; Yang, W.; Huang, D. *Adv. Synth. Catal*., **2020**, *362*, 3516–3541. (c) Xu, Z. Q.; Wang, W. B.; Zheng, L. C.; Li, L.; Duan, L.; Li, Y. M. *Org. Biomol. Chem*. **2019**, *17*, 9026–9038.

(12) Li, B.; Li, Y.; Yu, L.; Wu, X.; Wei, W. *Tetrahedron* **2017**, *73*, 2760–2765.

(13) (a) Xiao, F.; Chen, S.; Chen, Y.; Huang, H.; Deng, G. J. *Chem. Commun*. **2015**, *51*, 652–654. (b) Dong, D. Q.; Gao, X.; Li, L. X.; Hao, S. H.; Wang, Z. L. *Rev. Chem. Intermed.* **2018**, *44*, 7557–7567. (c) Zhu, Q. Li, H.; Yang, L.; Meng, J.; Xie, Z.; Le, Z. G. *Asian J. Org. Chem.* **2022**, *11*, e202200509.

(14) Shirisha, T.; Majhi, S.; Balasubramanian, S.; Kashinath, D. *Org. Biomol. Chem.* **2024**, *22*, 1434–1440.

(15) (a) Wu, X. F.; Gong, J. L.; Qi, X. *Org. Biomol. Chem*. **2014**, *12*, 5807–5817. (b) Sofi, F. A.; Sharma, R.; Masoodi, M. H.; Tabassum, N. *Synth. Commun*. **2021**, *51*, 3657–3693. (c) Chen, R.; Chen, J.; Zhang, J.; Wan, X. *Chem. Rec*. **2018**, *18*, 1–15

(16) Sondhi, S. M.; Singh, J.; Rani, R.; Gupta, P. P.; Agrawal, S. K.; Saxena, A. K. *Eur. J. Med. Chem*. **2010**, *45*, 555–563.

(17) Chen, Y. L.; Lu, C. M.; Chen, I. L.; Tsao, L. T.; Wang, J. P. *J. Med. Chem*. **2002**, *45*, 4689–4694.

(18) Cross, R. M.; Maignan, J. R.; Mutka, T. S.; Luong, L.; Sargent, J.; Kyle, D. E.; Manetsch, R. *J. Med. Chem*. **2011**, *54*, 4399–4426.

(19) Sameem, B.; Saeedi, M.; Mahdavi, M.; Shafiee, A. *Eur. J. Med. Chem*. **2017**, *128*, 332–345.

(20) Sepehri, N.; Asemanipoor, N.; Mousavianfard, S. A.; Hoseini, S.; Faramarzi, M. A.; Adib, M.; Biglar, M.; Larijani, B.; Hamedifar, H.; Khanaposhtani, M. M.; Mahdavi, M. *Med. Chem. Res*. **2020**, *29*,1836–1845.

(21) (a) Chu, X. Q.; Ge, D.; Cui, Y. Y.; Shen, Z. L.; Li, C. J. *Chem. Rev*., **2021**, *121*, *20*, 12548–12680. (b) Trost, B. M.; Kalnmals, C. A. *Chem. Eur. J*. **2019**, *25*, 1193–11213.

(22) Liu, Z.; Zhang, J.; Chen, S.; Shi, E.; Xu, Y.; Wan, X.; *Angew, Chem. Int. Ed*. **2012**, *51*, 3231–3235.

(23) Lam, Y. P.; Yeung, Y. Y. *Chem. Asian J. l.* **2018**, *13*, 2369–2372.

3.2.9 Selected spectra

4-(Phenylsulfonyl)-1,2,3,4-tetrahydroacridine(3a):

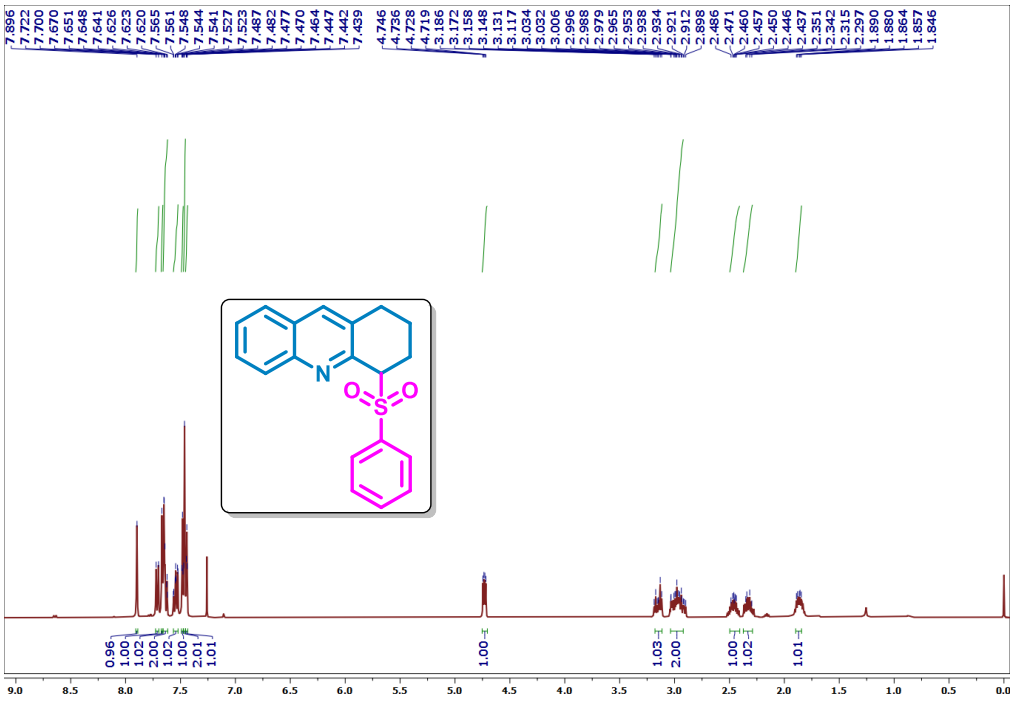

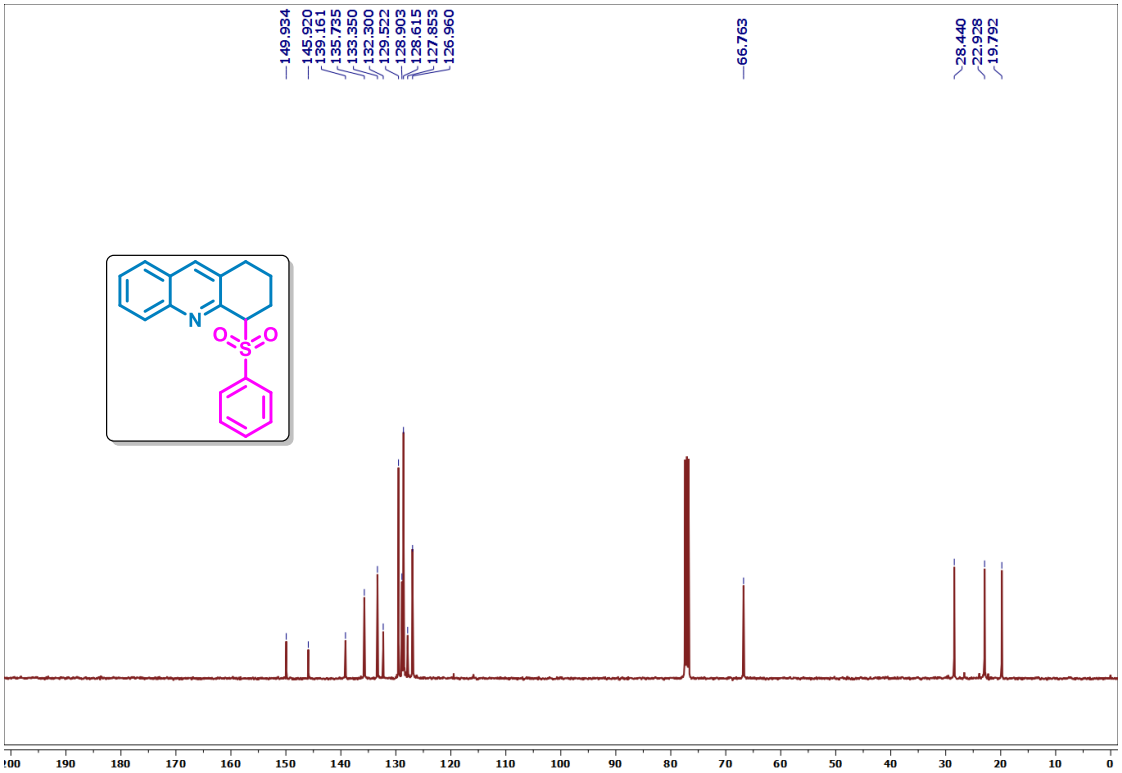

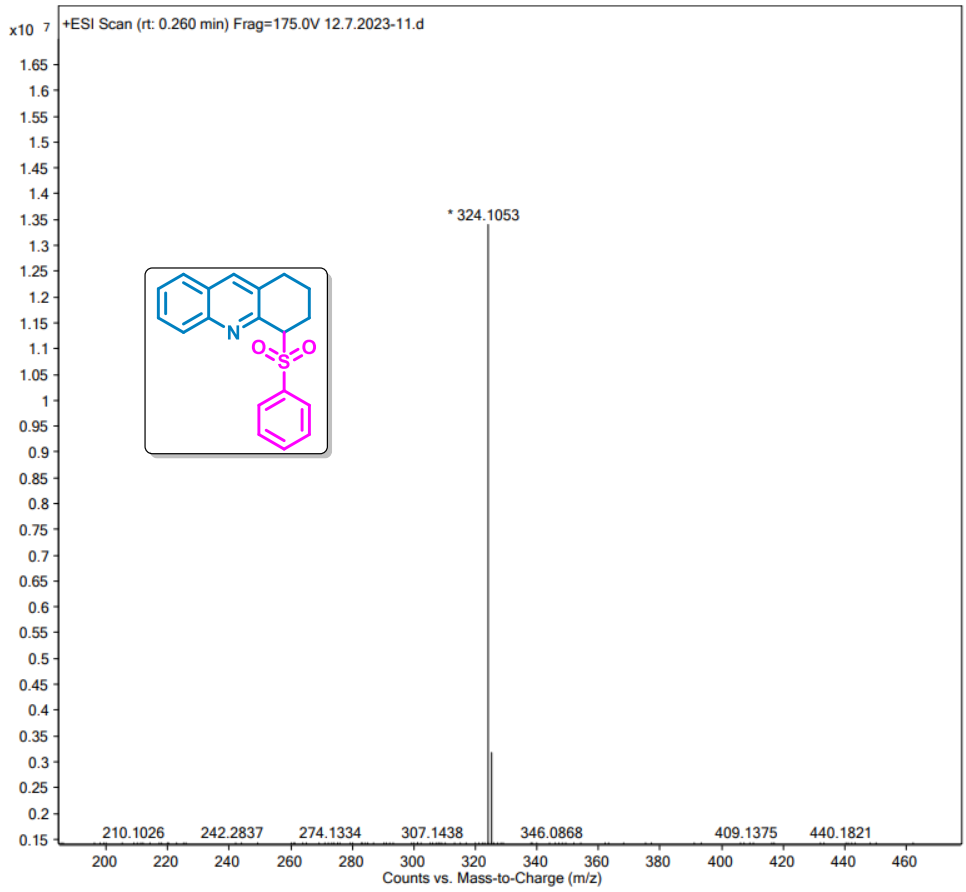

4-Tosyl-1,2,3,4-tetrahydroacridine(3b):

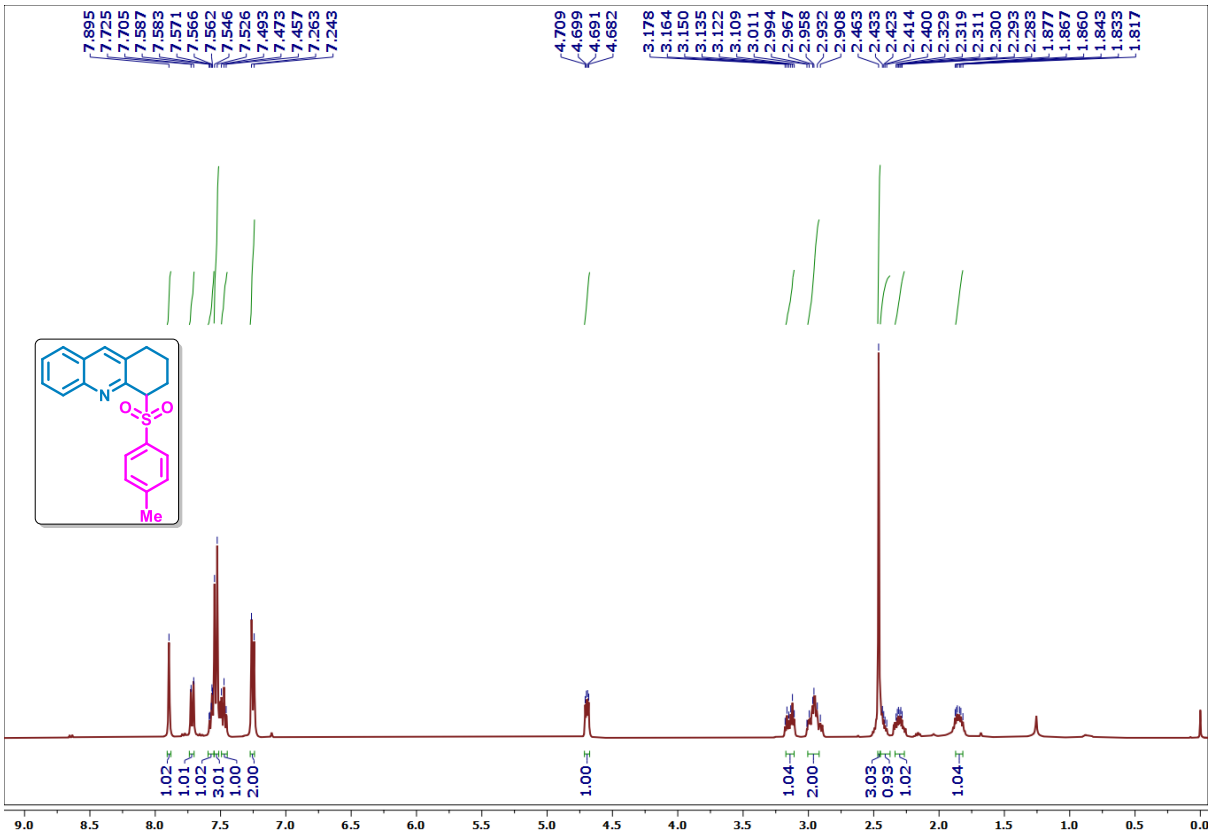

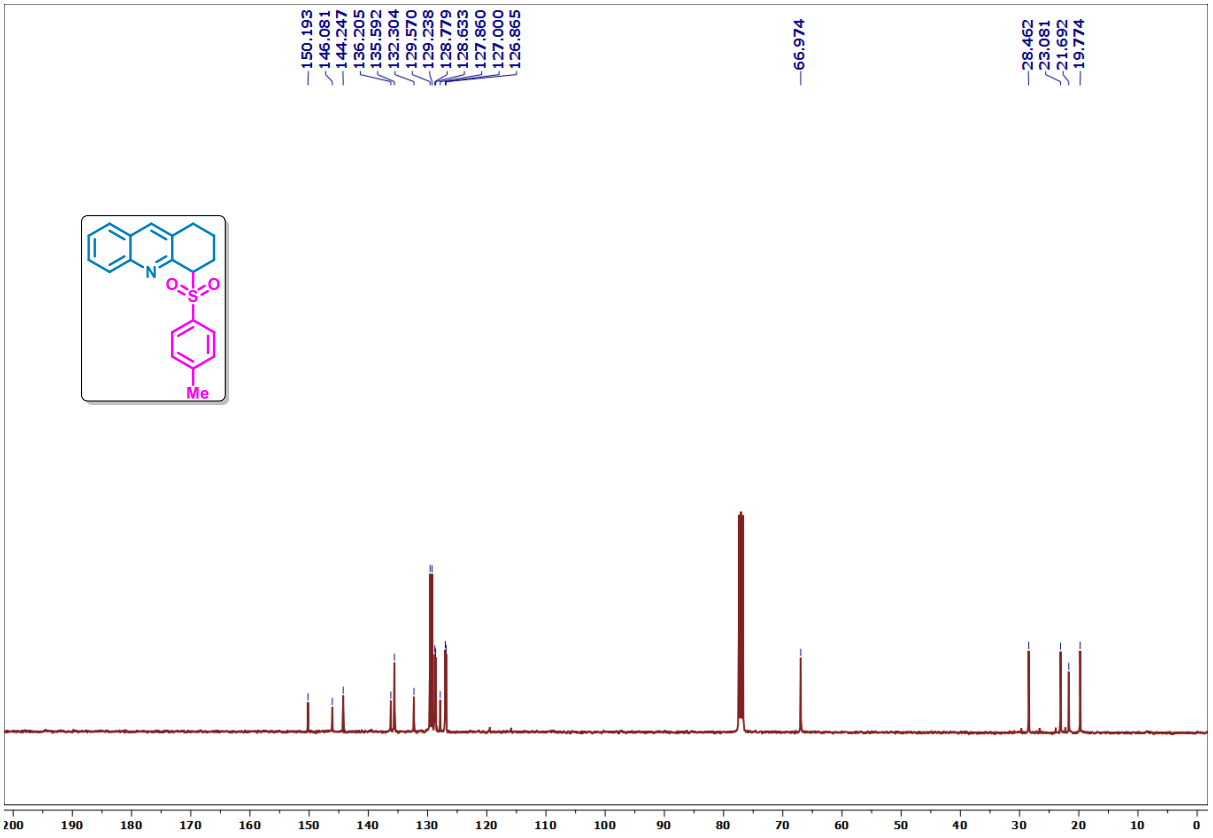
150.193
146.081
144.247
136.205
135.592
132.304
129.570
129.238
128.779
128.633
127.860
127.000
126.865
66.974
28.462
23.081
21.692
19.774
N
O
S
O
Me
200 190 180 170 160 150 140 130 120 110 100 90 80 70 60 50 40 30 20 10 0

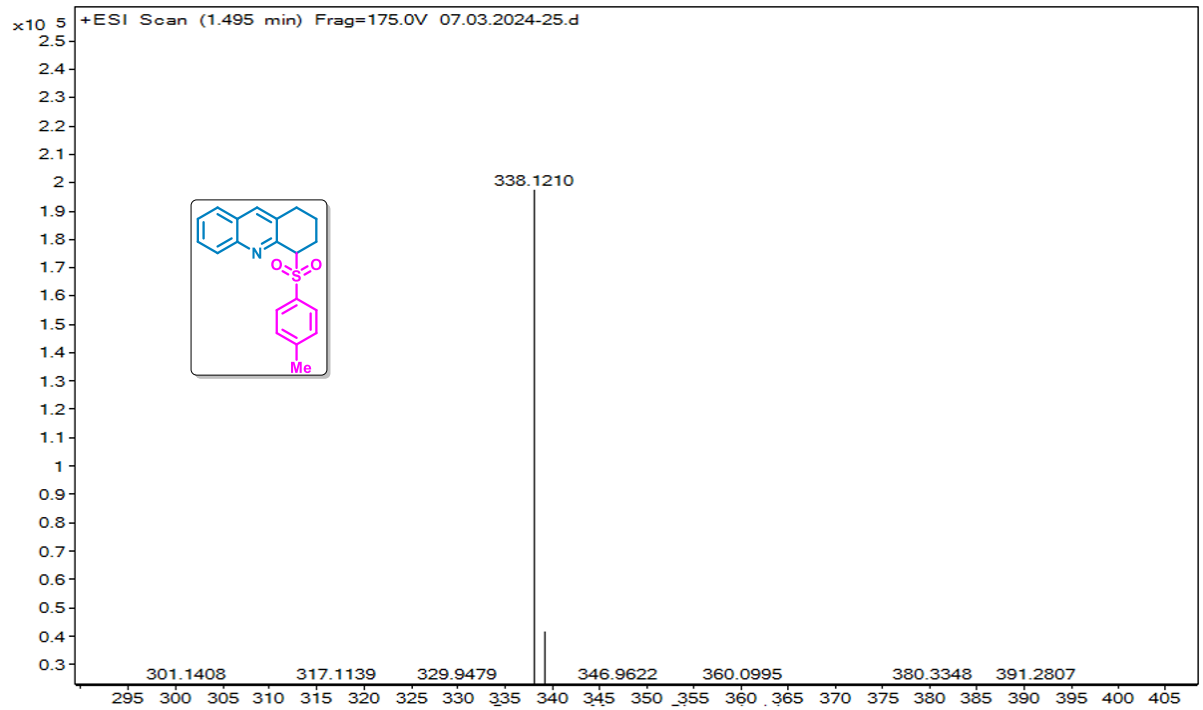
x10 5
+ESI Scan (1.495 min) Frag=175.0V 07.03.2024-25.d
338.1210
301.1408
317.1139
329.9479
346.9622
360.0995
380.3348
391.2807
N
O
S
O
Me
2.5 2.4 2.3 2.2 2.1 2 1.9 1.8 1.7 1.6 1.5 1.4 1.3 1.2 1.1 1 0.9 0.8 0.7 0.6 0.5 0.4 0.3
295 300 305 310 315 320 325 330 335 340 345 350 355 360 365 370 375 380 385 390 395 400 405

4-((4-Nitrophenyl)sulfonyl)-9-phenyl-1,2,3,4-tetrahydroacridine(3f):

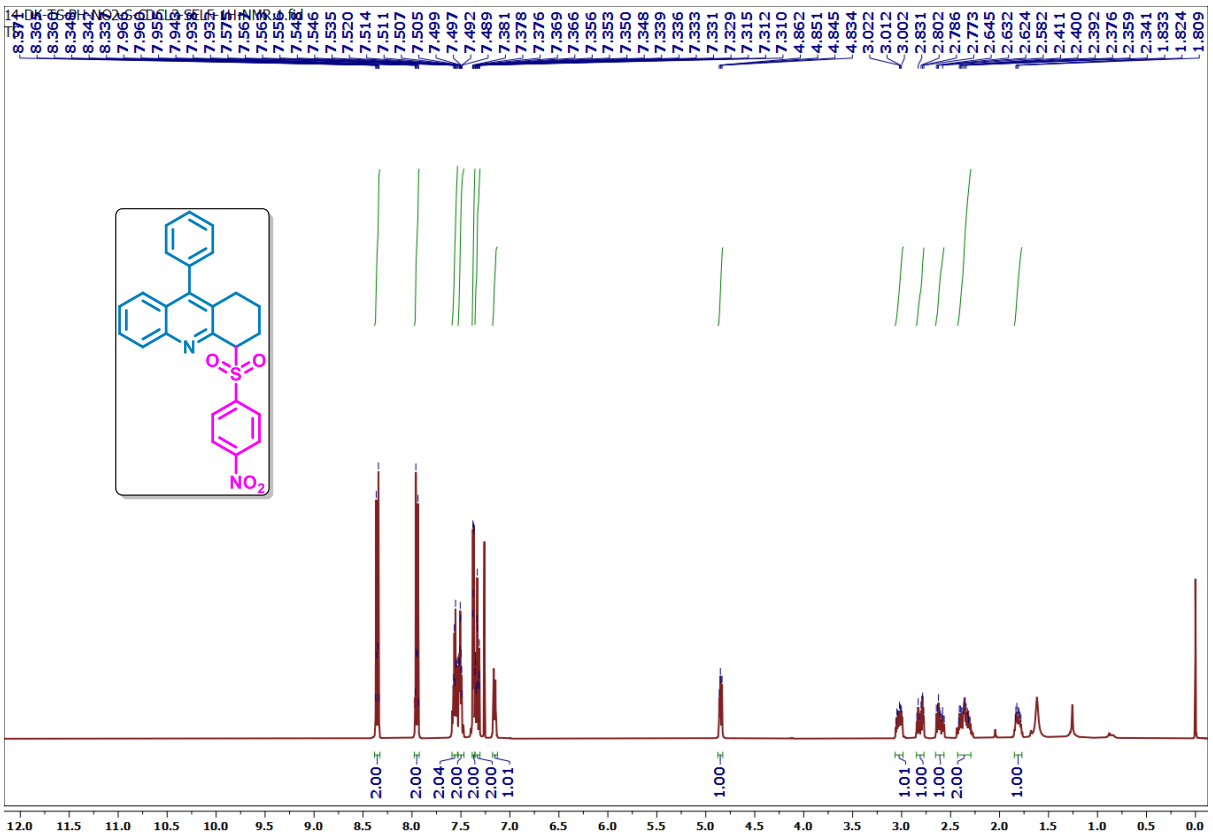

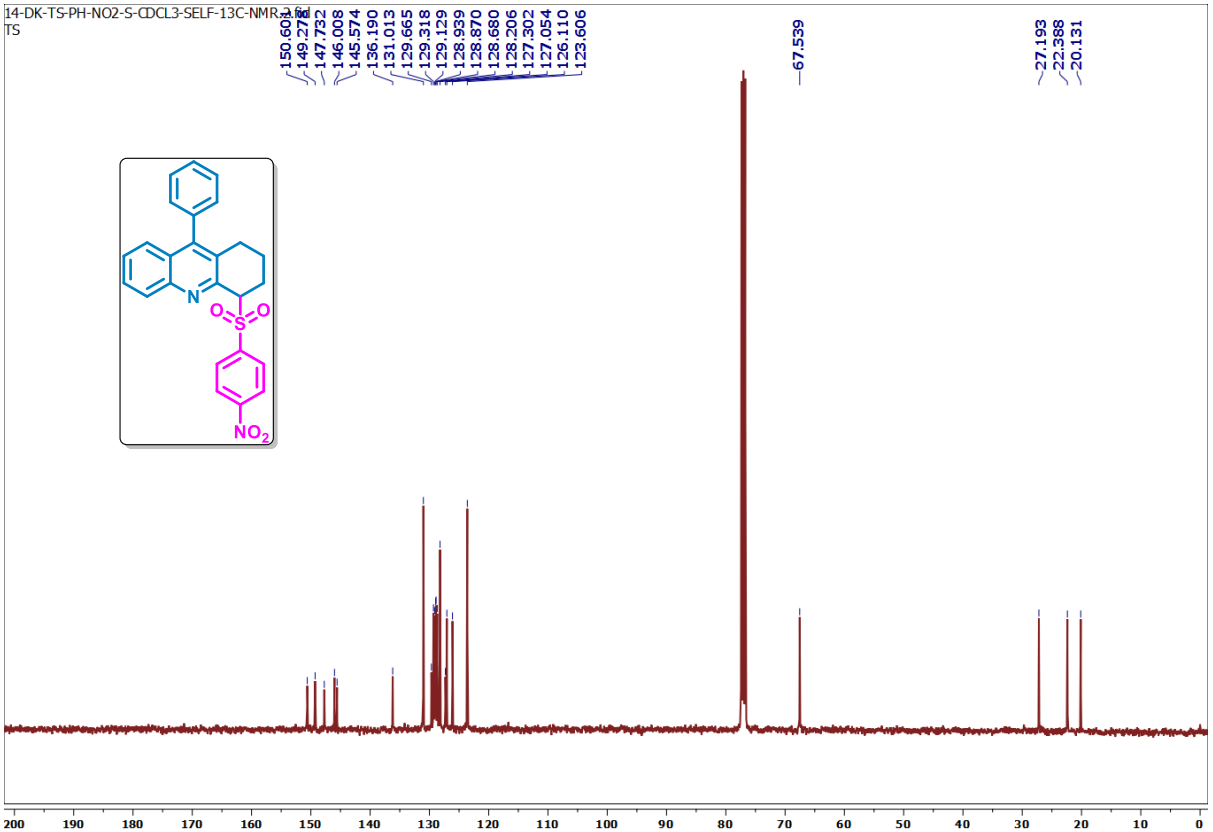

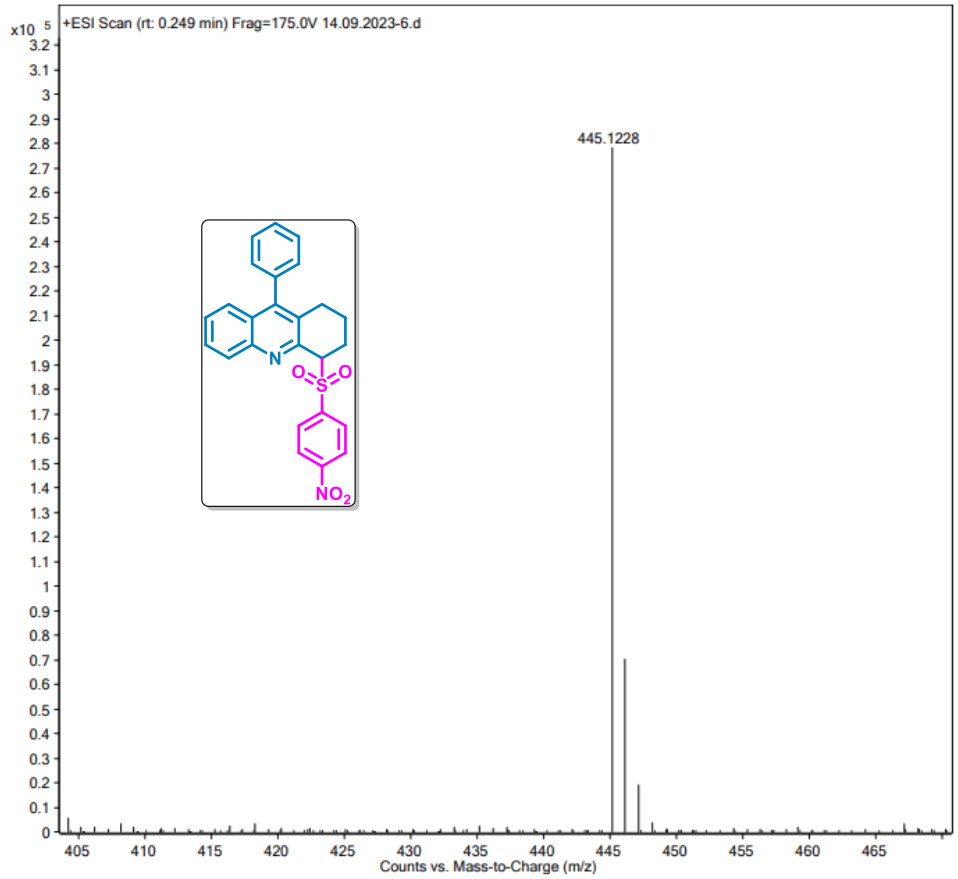

7-Chloro-9-phenyl-2,3-dihydroacridin-4(1H)-one (4d):

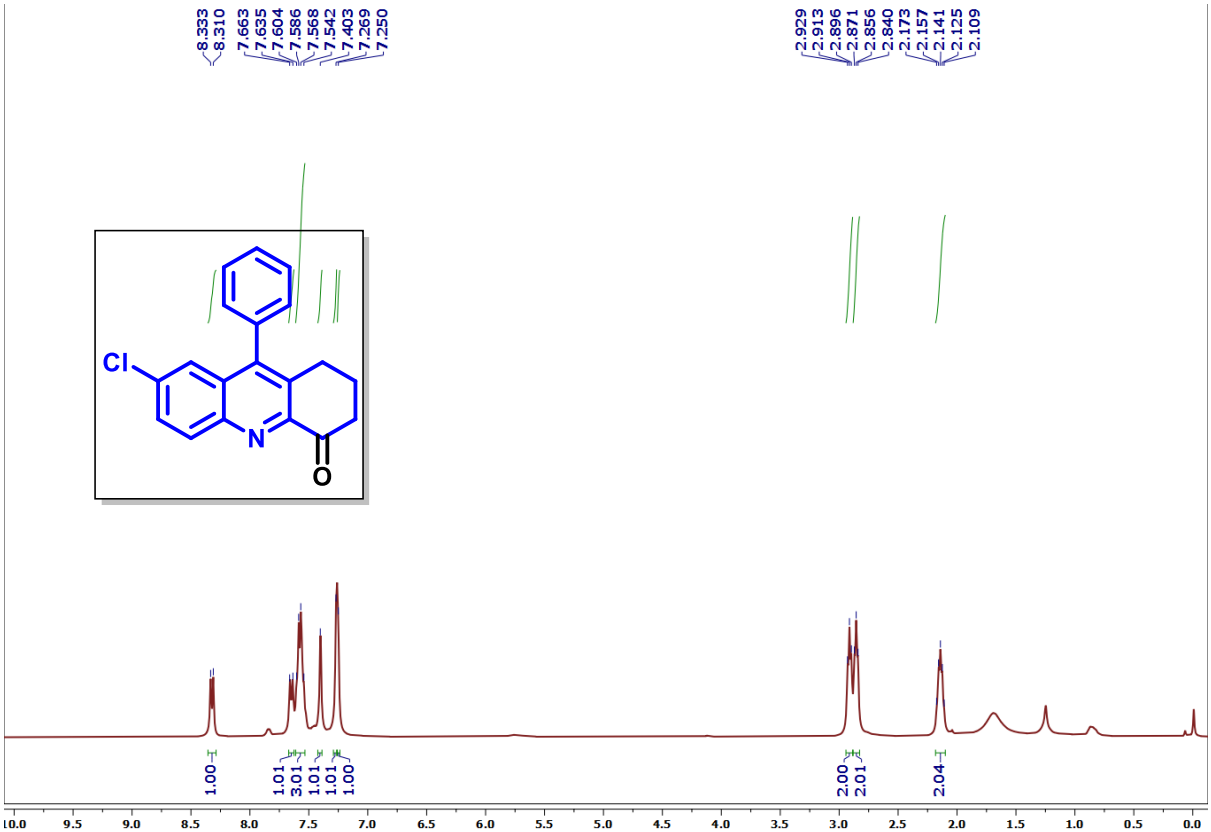

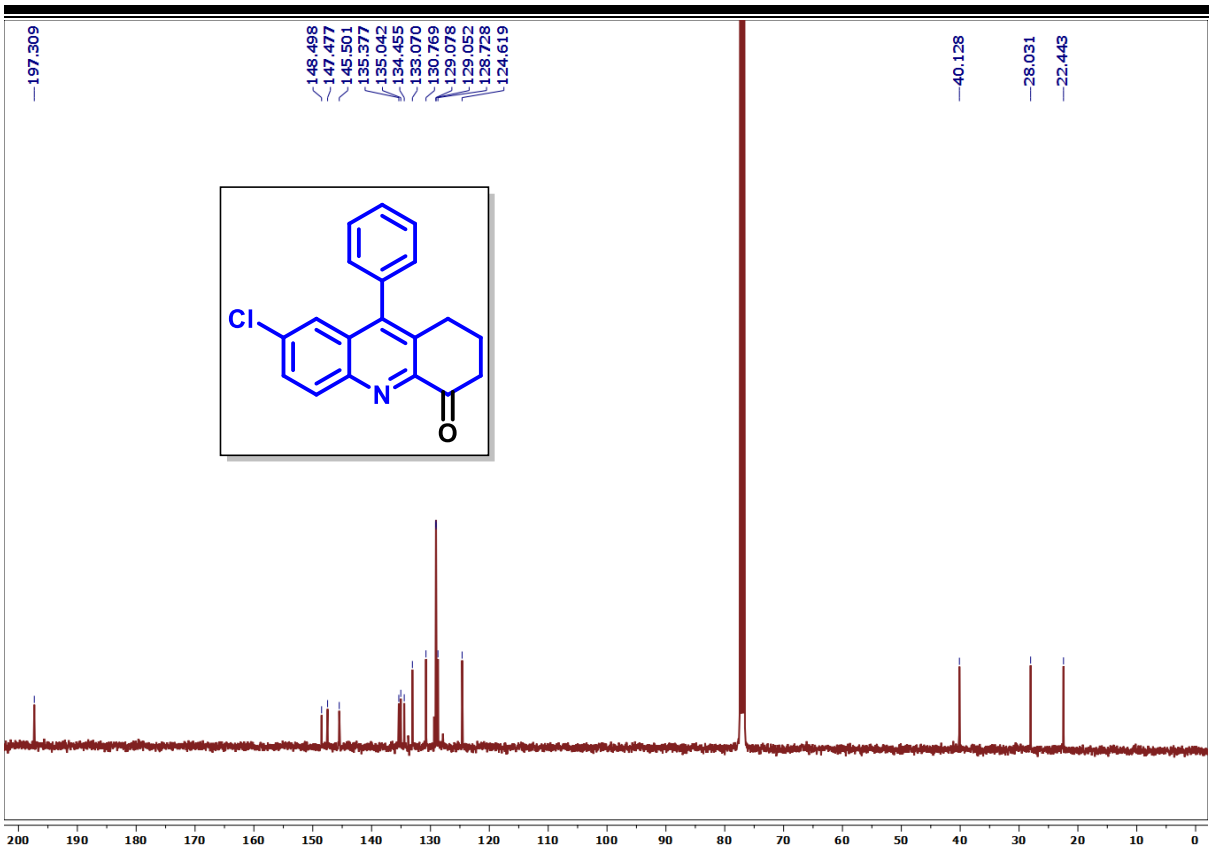
197.309
148.498
147.477
145.501
135.377
135.042
134.455
133.070
130.769
129.078
129.052
128.728
124.619
40.128
28.031
22.443
Cl
N
O
200 190 180 170 160 150 140 130 120 110 100 90 80 70 60 50 40 30 20 10 0

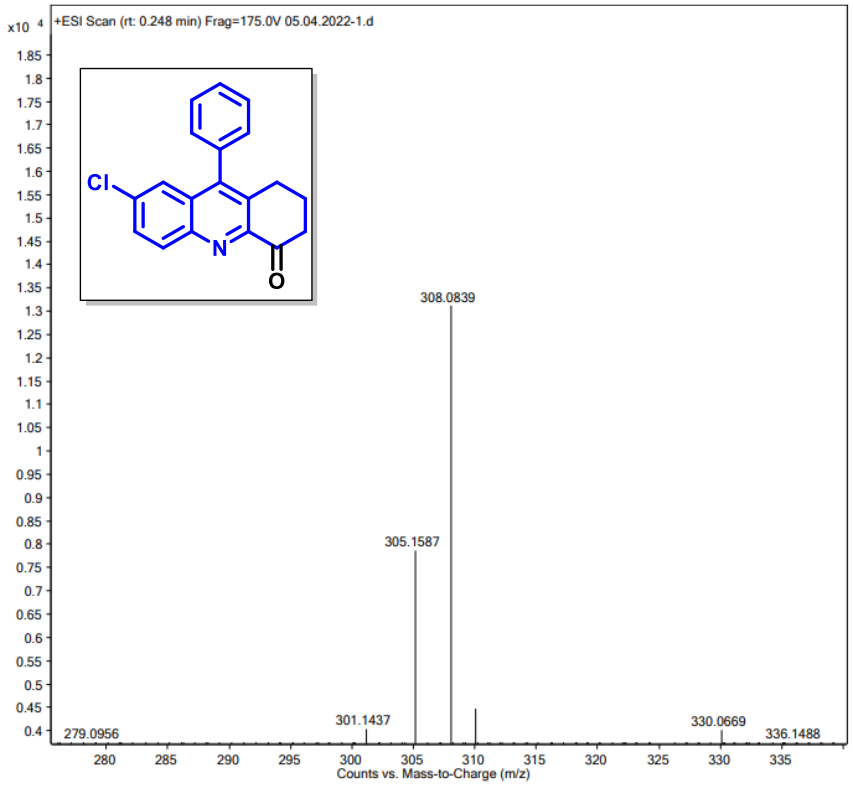
x10 4
+ESI Scan (rt: 0.248 min) Frag=175.0V 05.04.2022-1.d
Cl
N
O
308.0839
305.1587
301.1437
279.0956
330.0669
336.1488
Counts vs. Mass-to-Charge (m/z)

9-Chloro-4-(phenylsulfonyl)-1,2,3,4-tetrahydroacridine (5a):

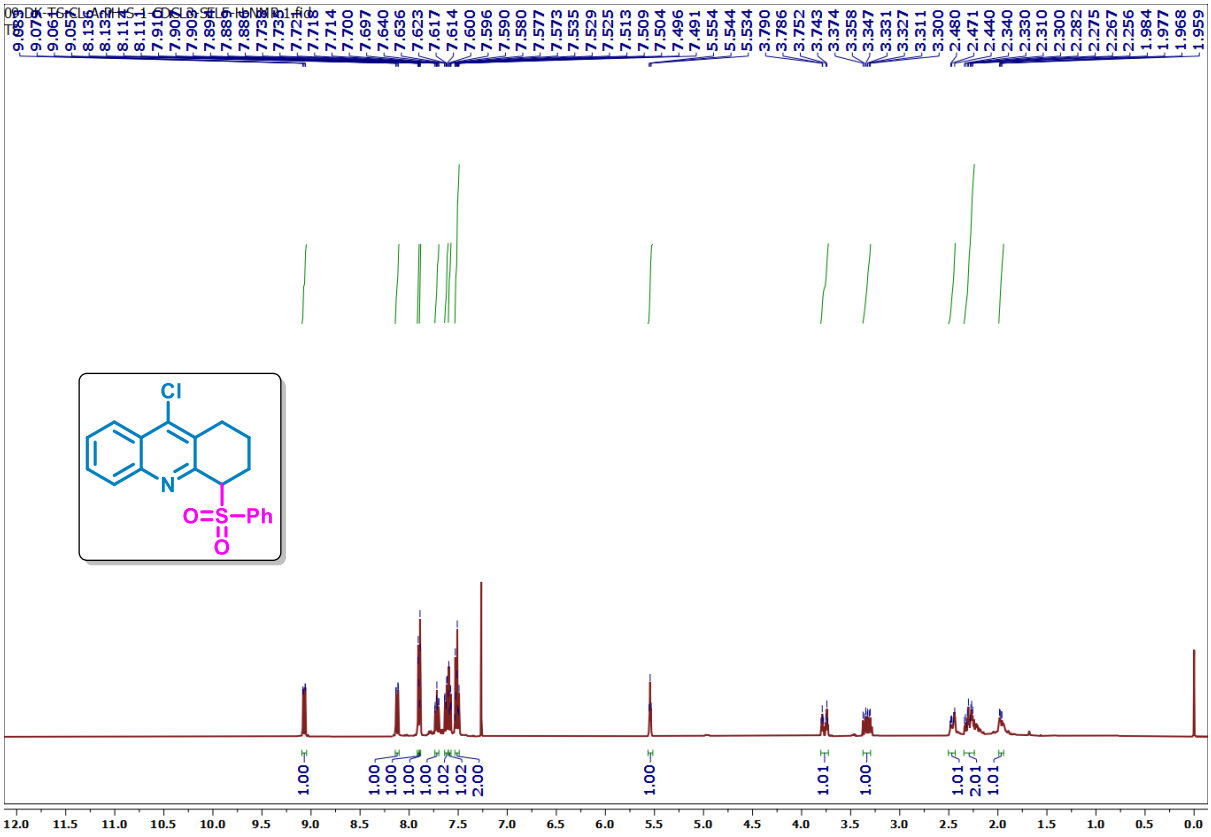

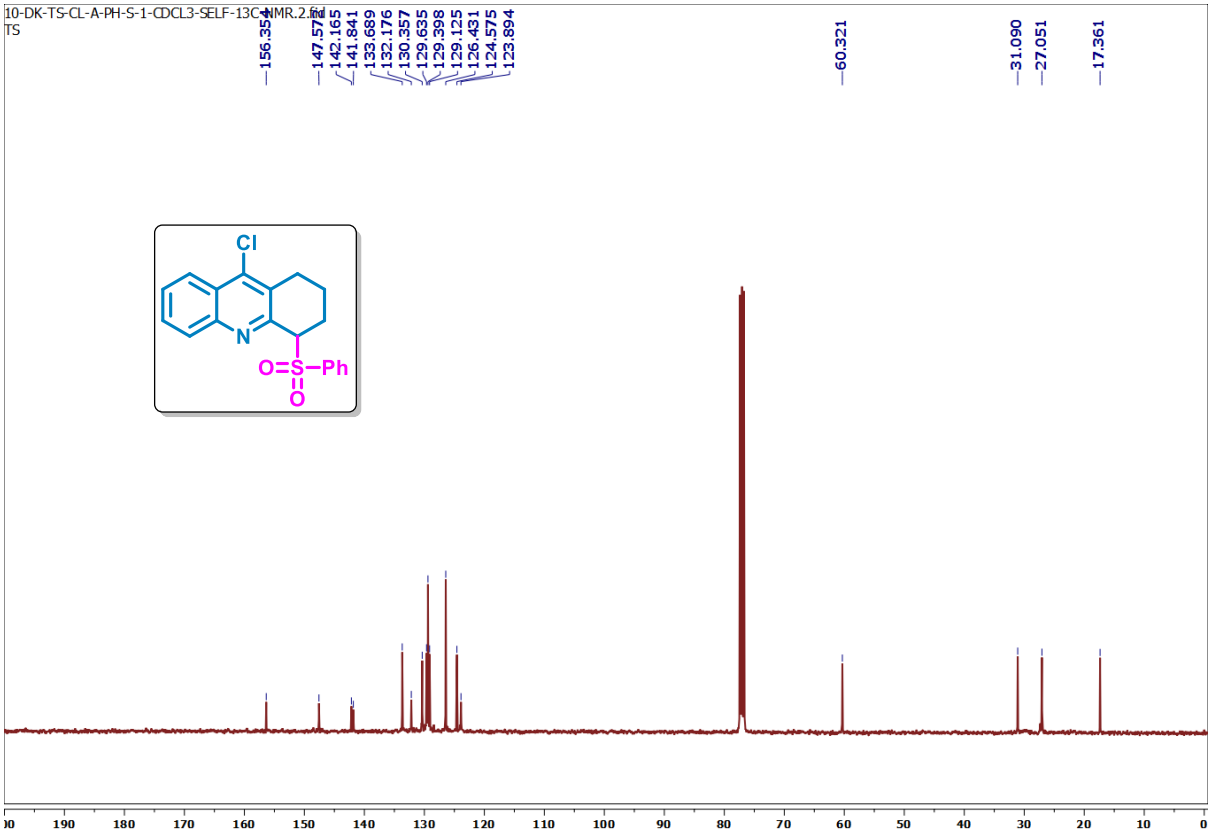

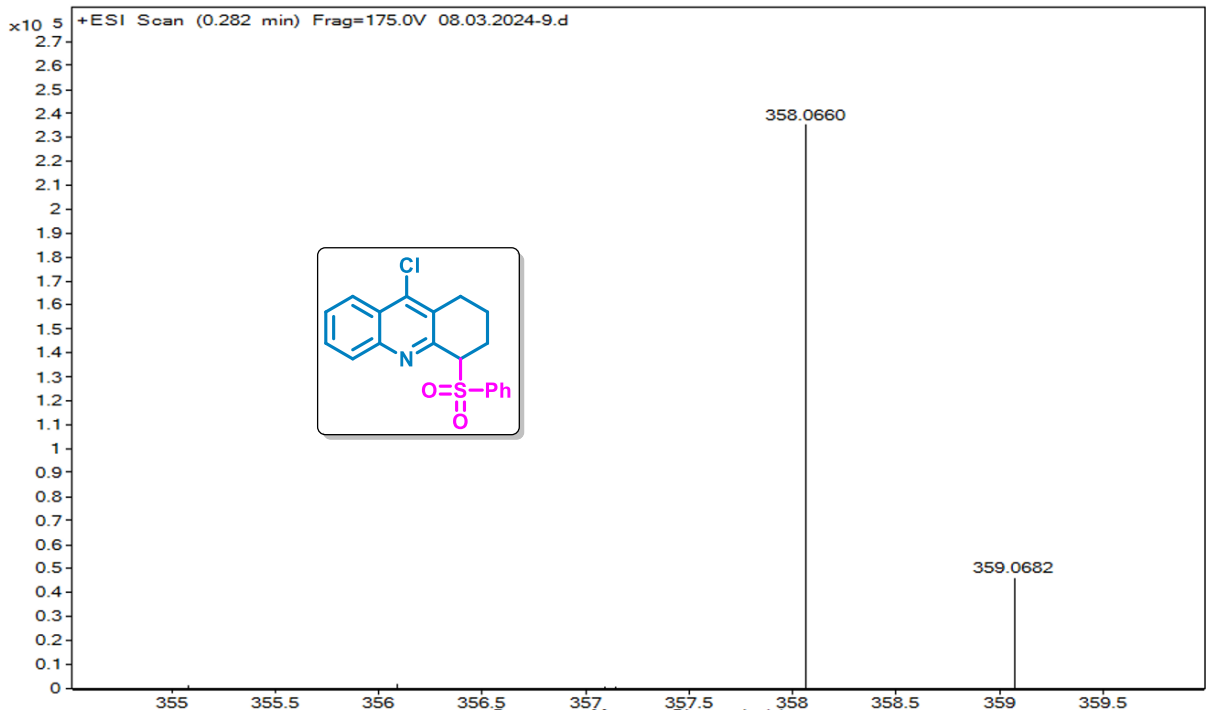
+ESI Scan (0.282 min) Frag=175.0V 08.03.2024-9.d
x10 5
358.0660
359.0682
Cl
N
O=S–Ph
O

Part-C: DDQ Mediated Synthesis of Acridin-4-yl(aryl)methanones *via* Aromatization-C(sp^2)-H Oxidation-sequence of C4 Functionalized 1,2,3,4-Tetrahydroacridine derivatives

3.3.1 Introduction

Owing to significant progress in medicinal chemistry, the synthesis and biological assessment of structurally diverse *N*-heterocycles have emerged as prominent research areas in recent years. Acridines, a typical *N*-heterocycles structurally similar to anthracene, have a long history of use as pigments and dyes.[1] However, recent years have unveiled a significantly more captative potential for these molecules. This newfound potential stems from the discovery of wide-ranging biological properties in acridine derivatives, including antimalarial,[2] antibacterial,[3] antiviral,[4] anticancer,[5] and antileukemic activities,[6] as well as their ability to inhibit the enzyme acetylcholinesterase[7] (**Figure-3.3.1**). Furthermore, they also show interesting photo-physical and electrochemical properties. As a result, they are used in material science as potential organic electronic devices and organic light-emitting diodes.[8]

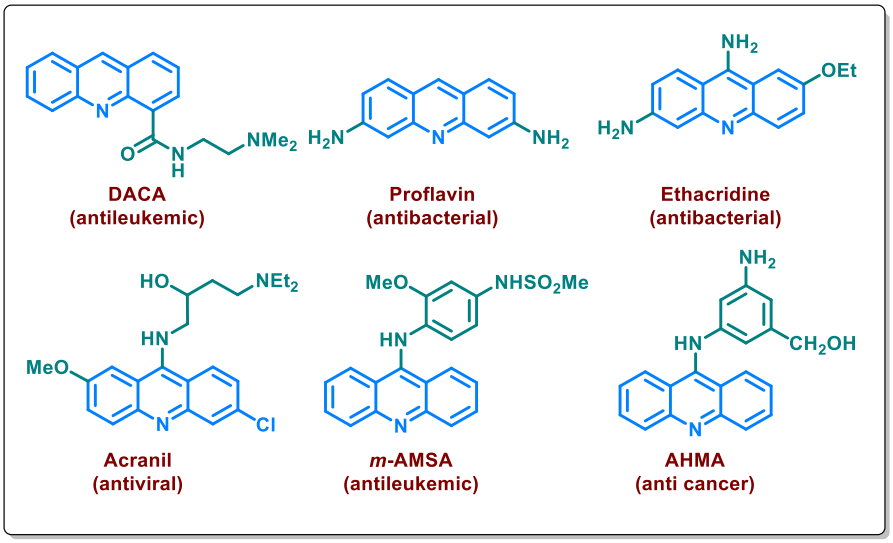

Figure 3.3.1 Biologically active Acridine derivatives

DDQ (2,3-Dichloro-5,6-dicyano-1,4-benzoquinone) is a versatile, mild and eco-friendly oxidant in organic synthesis and exhibits three available oxidation states i.e., oxidized quinone, one electron reduced semiquinone and two-electron reduced hydroquinone.[9] In the synthetic organic chemistry, DDQ has found broad applications in the oxidation of various organic compounds like alcohols,[10] phenols,[11] ketones,[12] aromatic compounds,[13] imines[14] and heterocyclics.[15] Besides, it is used as an oxidant for the C-H bond functionalisation,[16] and C-C

bond formation reaction,[17] the dehydrogenation of saturated C-C,[18] C-O,[19] C-N bond,[20] cross-coupling reactions.[21] Apart from that, it may also behave as a potential chlorinating agent as well as an oxidant simultaneously.[22] It can also be used to remove protecting groups during deprotection reaction,[23] and several other organic transformations such as DDQ initiative visible light reaction.[24]

3.3.2 Literature Reports

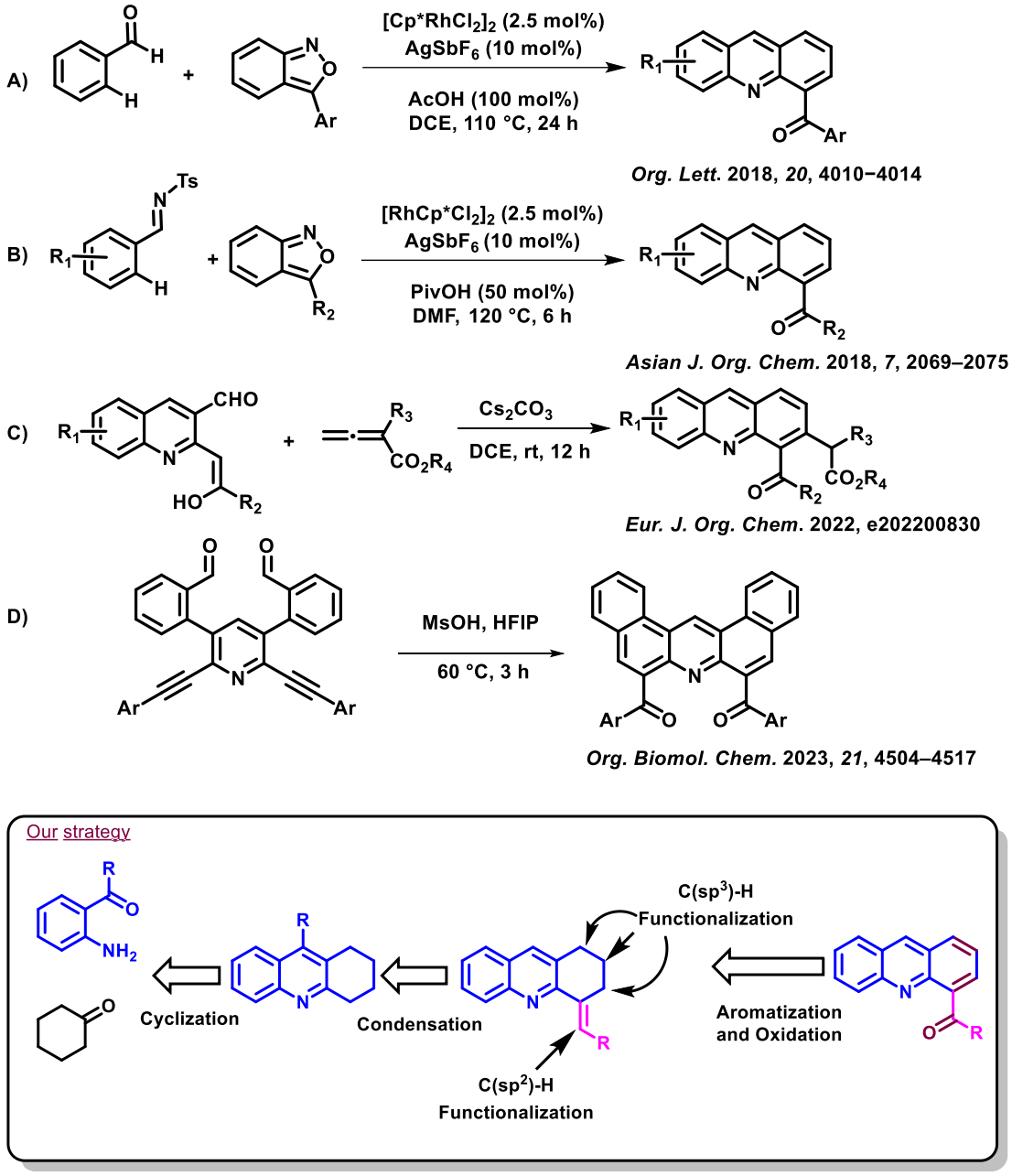

Figure 3.3.2 Literature reports for the synthesis of acridin-4-yl(phenyl)methanones derivatives and our strategy

Kim et al. disclosed the transient directing group promoted Rh(III) catalysed C(sp^2)-H functionalisation followed by intramolecular electrophilic cyclisation of benzaldehyde with anthranils. Notably, anthranil has a dual role as a transient directing group and amination source to afford 2-acyl acridine (**Figure 3.3.2A**).[25] The same group reported Rh(III) catalysed C-H amination aldimines with anthranils followed by intramolecular cyclization for the synthesis of 2-acyl acridine (**Figure 3.3.2B**).[26] Balalaie et al. established a base-promoted formal [4+2]-cycloaddition reaction of allenoates and (Z)-2-(2-hydroxy-2- alkylvinyl) quinoline-3-carbaldehydes in the presence of Cs_2CO_3 for the synthesis of functionalised acridines in the mild condition through a sequential Michael addition, aldol condensation and isomerisation process (**Figure 3.3.2C**).[27] Recently, Langer et al. synthesised Dibenzo[*a,j*]acridines and regioisomeric dibenzo[*c,h*]acridines derivatives by combination of site-selective Pd catalysed cross-coupling reaction and ring-closing alkyne-carbonyl metathesis (**Figure 3.3.2D**).[28]

3.3.3 Present work

Considering the importance and in continuation of our research goal on the synthesis of biologically relevant acridine molecules, herein we reported the synthesis of acridin-4-yl(aryl)methanones *via* DDQ Mediated aromatization followed by C(sp^2)-H oxidation of C4 functionalized 1,2,3,4-tetrahydroacridine derivatives (**Scheme 3.3.1**).

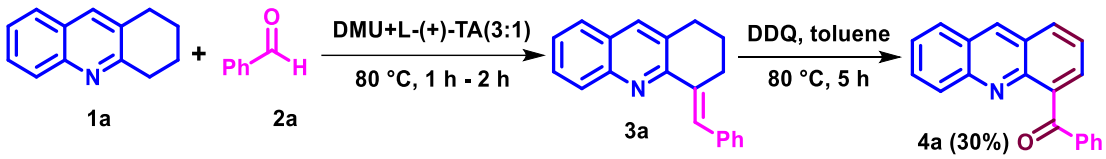

Scheme 3.3.1 Present strategy for the dehydrogenating aromatisation, C(sp^2)-H oxidation of C4 functionalized 1,2,3,4-tetrahydroacridine derivatives

3.3.4 Results and Discussion

Towards this objective, we commenced our studies by synthesising the C4 functionalised 1,2,3,4-tetrahydroacridines (**3**) as starting materials under DES condition. Then compound (**3**) was treated with DDQ (2 equiv.) in toluene at 80 °C to afford acridine derivatives. To our delight, this reaction condition helps dehydrogenative aromatisation and oxidation of vinylic C(sp^2)-H leading to the formation of acridin-4-yl(phenyl)methanones (**4**) in 30% yields (Scheme-3.3.1). After confirmation of the product using complementary spectra data, we next commenced the optimisation studies to improve the reaction yield. The investigated reaction conditions for the dehydrogenative oxidative functionalisation of compound (**3**) are summarised in **Table 3.3.1**. The solvent screening revealed that toluene was an effective solvent

in comparison to other solvents screened for dehydrogenative aromatisation and oxidation. By increasing the reaction temperature from 80 °C to 100 °C, a little improvement in yield (40%) was observed (**Table 3.3.1;** entry-8). Further increasing the DDQ load from 2 equiv. to 4 equiv., 5 equiv. or 6 equiv. there is no significant improvement in the yield of the desired product (**Table 3.3.1;** entries-9-11). Gratifyingly, in O_2 atmosphere with DDQ 2 equiv. in toluene at 100 °C furnished the desired product in a yield of 78% (**Table 3.3.1;** entry-12). Further, additives like TBN, $NaNO_2$, *m*-CPBA, TBHP, DMP, $Ph(IOAc)_2$ along with DDQ were screened to check the role in improving the yield (**Table 3.3.1;** entries-13-18). However, to our disappointment the results were not encouraging.

Table 3.3.1 Optimisation table[a]

S. No.	Oxidant (2 equiv.)	Additive (20 mol%)	Solvent	Temp (°C)	Time (h)	Yield (%)[b]
1	DDQ		Toluene	80	5	30
2	DDQ		CH_3CN	80	6	10
3	DDQ		DCE	80	5	20
4	DDQ		THF	80	7	Trace
5	DDQ		1,4-Dioxane	80	7	ND
6	DDQ		DMSO	100	7	ND
7	DDQ		DMF	100	5	ND
8	DDQ		Toluene	100	2	40
9	DDQ (4 equiv.)		Toluene	100	2	40
10	DDQ (5 equiv.)		Toluene	100	2	40
11	DDQ (6 equiv.)		Toluene	100	2	40
12	**DDQ (O_2 atm)**		**Toluene**	**100**	**1**	**78**
13	DDQ	TBN	Toluene	100	3	ND
14	DDQ	$NaNO_2$	Toluene	100	4	ND
15	DDQ	*m*-CPBA	Toluene	100	4	ND
16	DDQ	TBHP	Toluene	100	4	ND
17	DDQ	DMP	Toluene	100	4	40
18	DDQ	$Ph(IOAc)_2$	Toluene	100	5	ND

[a]Reaction condition: **3a** (0.25mmol). [b]Isolated yield of the final product

Having the established optimised condition, we proceed to explore the scope and versatility of substrate towards the developed strategy. Initially, we synthesised various substituted C4 functionalised 1,2,3,4-tetrahydroacridine derivatives, then subjected to dehydrogenative aromatisation with DDQ and provided the corresponding derivatives in good yields (**Scheme 3.3.2**). It is worth mentioning that a wide range of functional groups substituted on 1,2,3,4-tetrahydracridines at C9 position tolerated the reaction condition.

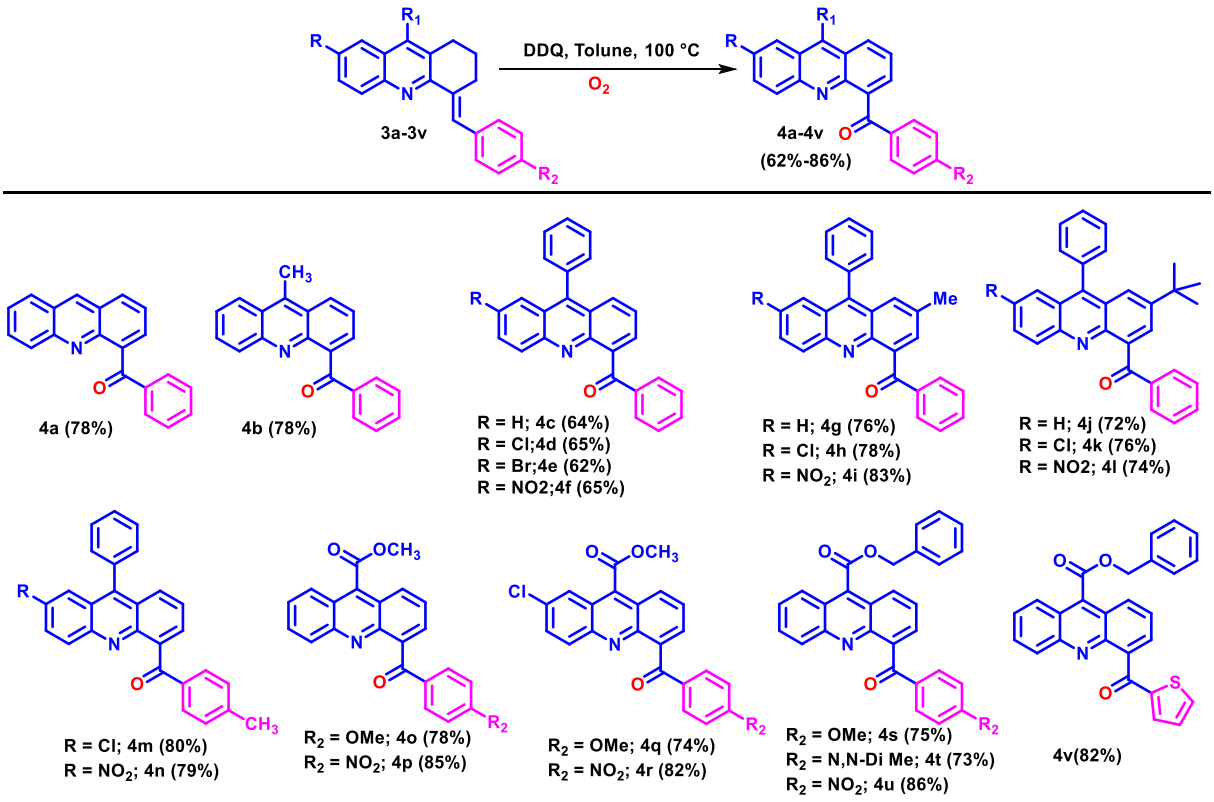

Scheme 3.3.2 Scope of acridin-4-yl(aryl)methanones derivatives

3.3.5 Control Experiments and Mechanistic Studies

Next, to confirm the radical mechanism for the reaction, the DDQ-mediated dehydrogenative aromatisation reaction is conducted in the presence of TEMPO a radical quencher. Notably, the formation of TEMPO adduct (**5**) was confirmed by HRMS (**Scheme 3.3.3**), this indicates the radical mechanism of the reaction pathway. Next, to gain more insight into the mechanism of the reaction, the DDQ-catalysed dehydrogenative aromatisation of compound 3a was first executed using MeOH as the nucleophile, and the reactions were stopped midway (after 20 min) in the quest for the possible intermediates leading to 4a. Interestingly, nucleophile attached adduct (**6**) was confirmed through HRMS (**Scheme 3.3.3b**). This indeed confirms the possibility of the formation of an electrophilic intermediate. Further, we found the HRMS data for the TEMPO attached (**7**) product when 3a was subjected to radical scavenger TEMPO in

the presence of DDQ which strongly recommits the radical nature of the mechanism over the mechanistic pathways, especially after the formation of the acridine core. After the formation of the acridine core, the stable carbocation, acridin-4-yl(phenyl)methylium cation was trapped by adding MeOH in the reaction mixture and the methoxy attached product detected by HRMS obviates the need for isolation. Finally, the confirmation of the intermediate **9**, hydroxyl attached acridine core suggests the oxidation of the OH group to the ketone which leads to the desired product.

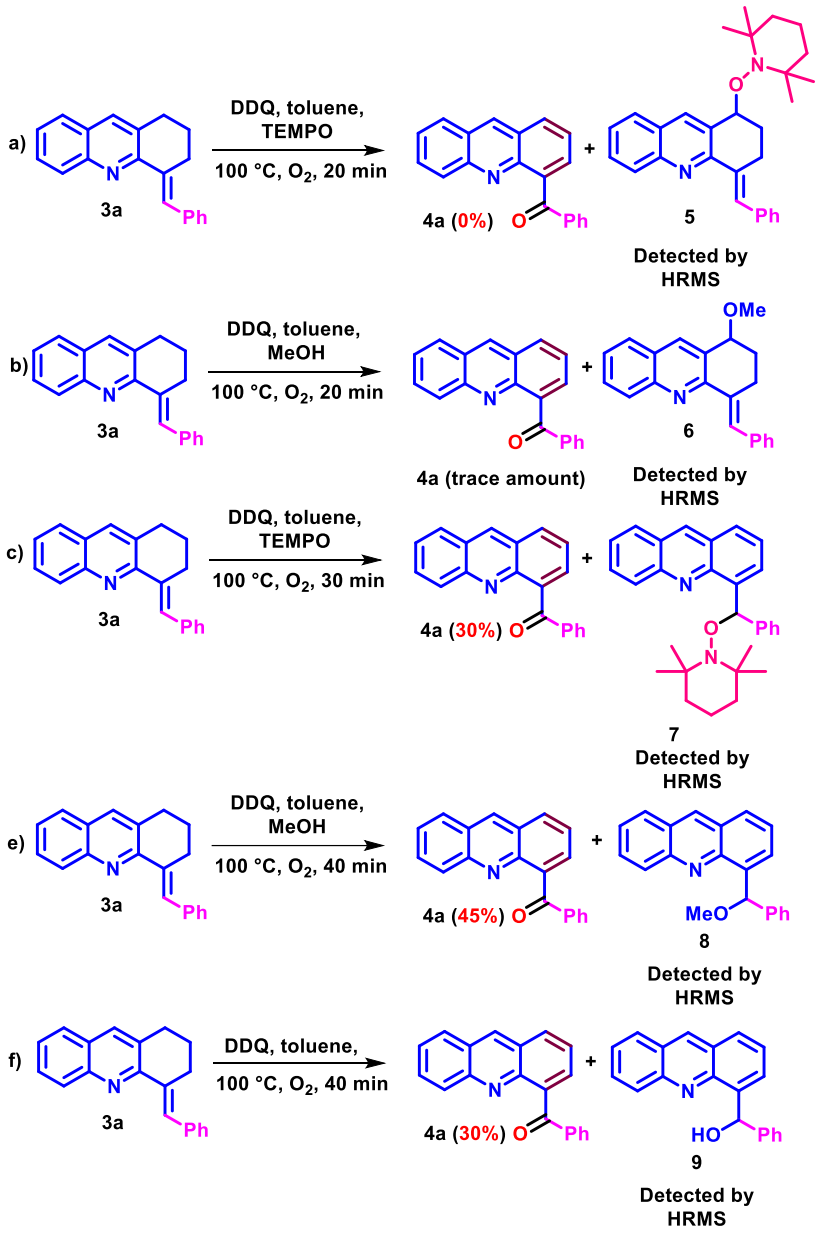

Scheme 3.3.3 Control experiments

3.3.6 Plausible mechanism

In the light of the aforementioned mechanistic investigation and literature reports [9,29] a plausible mechanism for the present DDQ-mediated dehydrogenative aromatisation, C(sp^2)-H oxidation of 1,2,3,4-tetrhydroacridine is as described in **Figure 3.3.4**. A hydrogen atom transfer (HAT) from 1,2,3,4-tetrhydroacridine to DDQ, followed by single electron transfer (SET) along route B instead of going *via* route A (SET and then HAT process) is presumed to be the predominant pathway for the formation of resonance stabilised benzyl carbocation (**II**). Subsequently, carbocation (**II**) undergoes DDQH-assisted H-elimination to afford the dihydroacridine derivative (**III**), this then undergoes another HAT and SET sequence to deliver stable acridinyl carbocation (**VI**) while eliminating another competitive pathway which is first SET and then HAT process. Finally, nucleophilic attack by the H_2O molecule on (**VI**), followed by the DDQ-mediated dehydrogenation closing cycle, delivers the corresponding product **4a**.

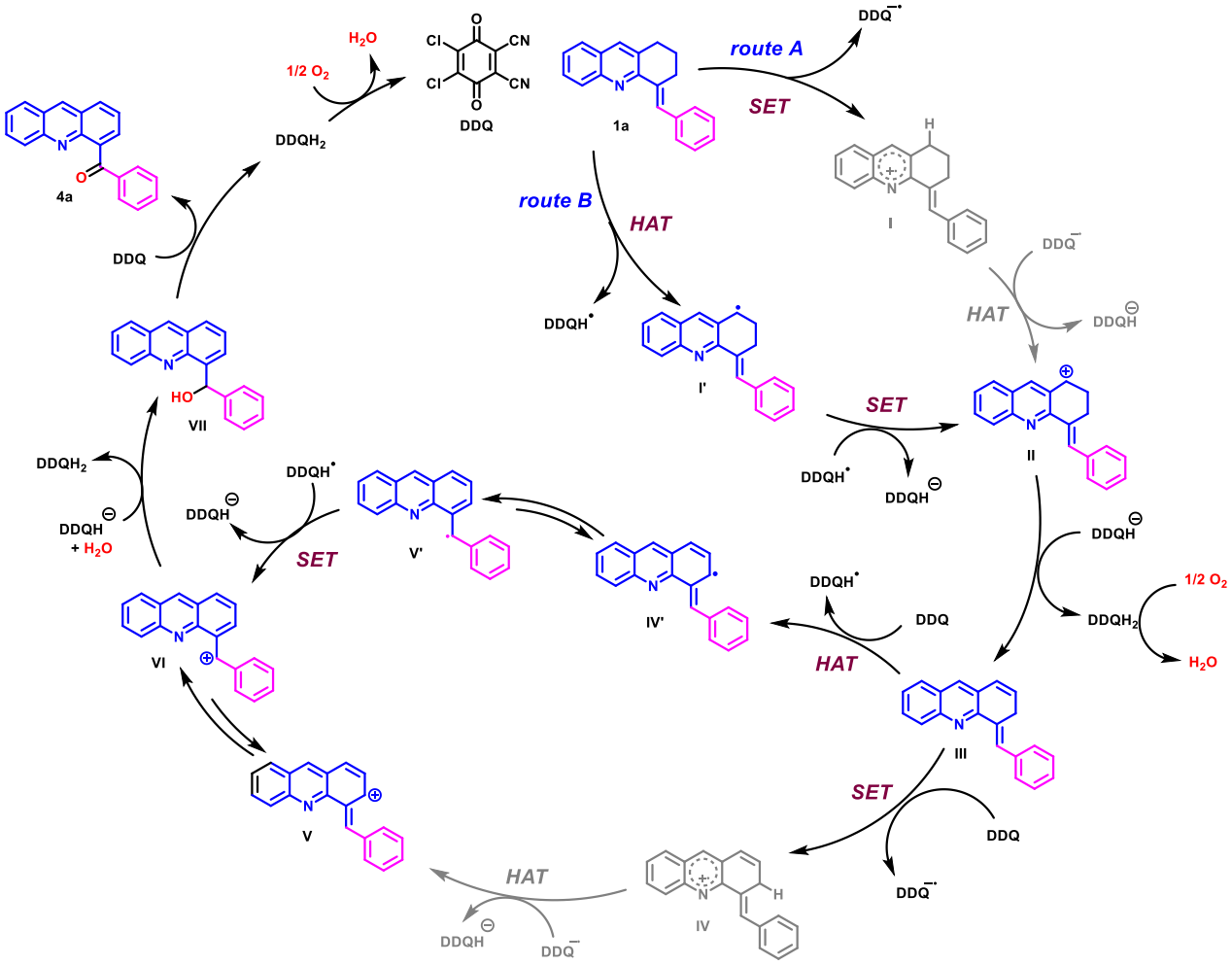

Figure 3.3.4 Plausible mechanism for the DDQ mediated dehydrogenative aromatisation, C(sp^2)-H oxidation of C4 functionalised 1,2,3,4-tetrahydroacridine derivatives

3.3.7 Conclusions

In conclusion, we have demonstrated a mild and efficient strategy for the synthesis of acridin-4-yl(aryl)methanones *via* DDQ-mediated dehydrogenative aromatisation, C(sp^2)-H oxidation of C4 functionalised 1,2,3,4-tetrahydroacridine derivatives. This strategy has shown compatibility with a diverse range of substrates and tolerates various functional groups, with good yields. The developed methodology holds promises for the synthesis of various acridine-based derivatives with potential applications in medicinal chemistry and material sciences.

3.3.8 Experimental section

3.3.8.1 General procedure for the synthesis of compound (3a-3v):

Deep eutectic solvent was prepared by heating *N, N*'-Dimethyl urea + L-(+)-Tartaric acid (3:1 ratio) at 80 °C for 30 min. To this, various substituted 1,2,3,4-tetrahydroacridines (1.0 mmol) and aromatic aldehyde (1.0 mmol) were added and heating continued for another 2- 3 hours at 80 °C. The completion of the reaction was monitored by TLC. After completion of the reaction the crude products obtained were purified by column chromatography on silica gel using petroleum ether-ethyl acetate as eluent to give the final compound**.**

3.3.8.2 General procedure for the DDQ-mediated C(sp^3)-H and C(sp^2)-H funtionalization of C4 condensed tetrahydroacridine to access acridin-4-yl(aryl)methanones *(4a-4v):*

To a solution of various substituted (E)-4-benzylidene-1,2,3,4-tetrahydroacridines in toluene was added (*2 equiv.*), and the mixture was stirred under O_2 atmosphere (O_2 ballon) for 2-6 h at 100 °C. After complete consumption of starting material checked by TLC analysis, the reaction was worked up by removing up the solvent under reduced pressure, and the resultant residue was further purified by SiO_2 gel column chromatography to give the desired product.

3.3.9 Characterization Data for synthesized compounds:

Acridin-4-yl(phenyl)methanone (4a): Yield= 78%,Pale Yellow solid; M. P: 151.2 – 151.6 °C; **IR (KBr, cm^{-1})**: 3041, 2920, 2850, 1725, 1654, 1618, 1429, 1350, 1275, 1231, 1038, 901, 805; **^{1}H NMR (400 MHz, $CDCl_3$) δ** 8.98 (t, *J* = 2.0 Hz, 1H), 8.08 – 7.89 (m, 3H), 7.83 – 7.71 (m, 2H), 7.66 (t, *J* = 8.8 Hz, 1H), 7.59 – 7.45 (m, 3H). **^{13}C NMR (100 MHz, $CDCl_3$) δ** 196.24, 148.52, 146.62, 137.33, 133.20, 132.68, 131.62, 131.17, 130.27, 130.06, 128.89, 128.83, 128.70, 127.59, 127.45, 126.70, 126.64. **HRMS (ESI-MS): m/z Calculated for** $C_{20}H_{13}NO$ $[M+H]^+$: 284.1070; Observed: 284.1068.

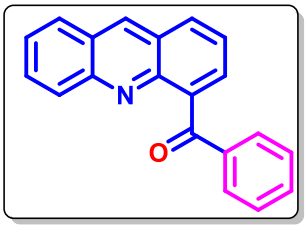

(9-Methylacridin-4-yl)(phenyl)methanone (4b): Yield= 78%, Pale Yellow solid; M. P: 176.2 – 177.0 °C; **IR (KBr, cm^{-1})**: 3034, 2991, 2853, 1725, 1644, 1605, 1549, 1526, 1425, 1345, 1270, 1220, 1039, 985; **^{1}H NMR (400 MHz, CDCl$_3$) δ** 8.20 (dd, *J* = 8.8, 1.2 Hz, 1H), 8.12 (dd, *J* = 8.4, 1.6 Hz, 1H), 8.00 (dd, *J* = 7.6, 1.2 Hz, 1H), 7.94 (dd, *J* = 8.8, 1.2 Hz, 1H), 7.77 – 7.71 (m, 2H), 7.62 – 7.41 (m, 5H), 2.92 (s, 2H). **^{13}C NMR (100 MHz, CDCl$_3$) δ** 196.11, 147.98, 147.63, 137.72, 137.36, 132.68, 131.08, 130.92, 130.27, 130.02, 128.83, 128.52, 127.86, 127.38, 126.70, 126.04, 125.23, 123.27, 15.44. **HRMS (ESI-MS): m/z Calculated for** $C_{21}H_{15}NO$ $[M+H]^+$: 298.1226; Observed: 298.1226.

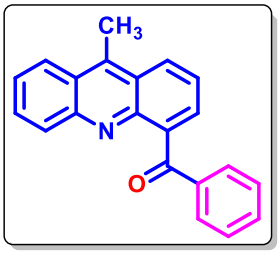

Phenyl(9-phenylacridin-4-yl)methanone (4c): Yield= 64%, Pale Yellow solid; M. P: 151.2 – 151.7 °C; **IR (KBr, cm^{-1})**: 3040, 2918, 2854,1725, 1645, 1605, 1554, 1513, 1421, 1348, 1273, 1219, 1039, 981, 920, 810; **^{1}H NMR (400 MHz, CDCl$_3$) δ** 8.75 (dd, *J* = 8.8, 1.2 Hz, 1H), 8.23 (dd, *J* = 7.4, 1.6 Hz, 1H), 7.95 (dt, *J* = 8.8, 1.6 Hz, 2H), 7.80 (td, *J* = 7.2, 1.2 Hz, 1H), 7.77 – 7.71 (m, 2H), 7.74 – 7.68 (m, 1H), 7.61 (ddd, *J* = 8.4, 7.2, 1.2 Hz, 1H), 7.58 – 7.49 (m, 6H), 7.52 – 7.45 (m, 1H), 7.41 – 7.34 (m, 1H). **^{13}C NMR (100 MHz, CDCl$_3$) δ** 196.07, 149.39, 147.55, 141.41, 138.56, 137.82, 132.68, 131.49, 131.06, 130.51, 130.37, 130.23, 130.11, 129.29, 128.83, 128.43, 128.37, 127.94, 127.08, 126.56, 125.68, 125.36. **HRMS (ESI-MS): m/z Calculated for** $C_{26}H_{17}NO$ $[M+H]^+$: 360.1383; Observed: 360.1385.

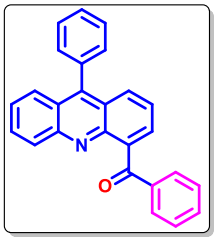

(7-Chloro-9-phenylacridin-4-yl)(phenyl)methanone (4d): Yield= 65%, Yellow solid; M. P: 156.4 – 157.0 °C; **IR (KBr, cm^{-1})**: 2924, 2850, 1725, 1654, 1530, 1451, 1265, 1165, 1067, 819,; **^{1}H NMR (400 MHz, CDCl$_3$) δ** 8.75 (dd, *J* = 8.8, 1.2 Hz, 1H), 8.10 (d, *J* = 8.4 Hz, 1H), 7.95 (dd, *J* = 8.8, 1.2 Hz, 1H), 7.80 (d, *J* = 2.4 Hz, 1H), 7.77 – 7.66 (m, 3H), 7.59 – 7.45 (m, 7H), 7.41 – 7.34 (m, 1H). **^{13}C NMR (100 MHz, CDCl$_3$) δ** 196.20, 147.86, 147.32, 141.22, 137.82, 137.66, 132.68, 131.46, 131.23, 130.35, 130.23, 130.10, 129.70, 129.29, 128.83, 128.66, 128.39, 127.94, 127.08, 126.60, 125.86, 125.31. **HRMS (ESI-MS): m/z Calculated for** $C_{26}H_{16}ClNO$ $[M+H]^+$: 394.0993; Observed: 394.0991.

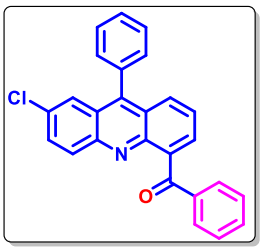

(7-Bromo-9-phenylacridin-4-yl)(phenyl)methanone (4e): Yield= 62%, Yellow solid; M. P: 176.2 – 177.0 °C; **IR (KBr, cm^{-1})**: 2920, 2845, 1720, 1645, 1531, 1450, 1268, 1156, 1057, 823; **^{1}H NMR (400 MHz, CDCl$_3$) δ** 8.75 (dd, J = 8.8, 1.2 Hz, 1H), 8.59 (d, J = 2.4 Hz, 1H), 8.10 (d, *J* = 8.0 Hz, 1H), 7.95 (dd, *J* = 8.8, 1.2 Hz, 1H), 7.77 – 7.71 (m, 2H), 7.73 – 7.64 (m, 1H), 7.59 – 7.45 (m, 7H), 7.41 – 7.34 (m, 1H). **^{13}C NMR (100 MHz, CDCl$_3$) δ** 196.20, 148.18, 147.75, 140.33, 137.82, 137.27, 134.06, 132.68, 131.46, 130.35, 130.23, 130.10, 129.29, 128.83, 128.39, 127.94, 127.50, 127.30, 127.08, 126.45, 125.85, 122.49. **HRMS (ESI-MS): m/z Calculated for** $C_{26}H_{16}BrNO$ $[M+H]^+$: 438.0488; Observed: 438.0490.

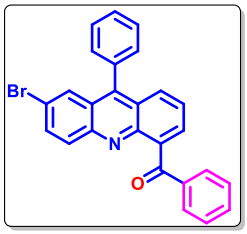

(7-Nitro-9-phenylacridin-4-yl)(phenyl)methanone (4f): Yield= 65%, Yellow solid; M. P: 176.2 – 177.0 °C; **IR (KBr, cm^{-1})**: 3044, 2921, 2857,1727, 1654, 1559, 1516, 1429, 1350, 1277, 1221, 1040, 980; **^{1}H NMR (400 MHz, CDCl$_3$) δ** 8.93 (d, *J* = 2.0 Hz, 1H), 8.77 (dd, J = 8.8, 1.2 Hz, 1H), 8.42 (dd, *J* = 9.2, 2.4 Hz, 1H), 8.30 (d, *J* = 8.8 Hz, 1H), 7.95 (dd, *J* = 8.8, 1.2 Hz, 1H), 7.77 – 7.69 (m, 2H), 7.59 – 7.45 (m, 6H), 7.41 – 7.34 (m, 1H). **^{13}C NMR (100 MHz, CDCl$_3$) δ** 196.20, 150.25, 147.68, 144.97, 140.79, 137.82, 137.04, 132.68, 131.46, 130.23, 130.15, 130.11, 129.28, 128.83, 128.43, 127.94, 127.08, 126.98, 126.97, 126.93, 124.88, 121.59. **HRMS (ESI-MS): m/z Calculated for** $C_{26}H_{16}N_2O_3$ $[M+H]^+$: 405.1234; Observed: 405.1237.

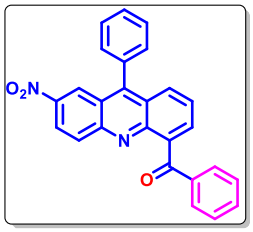

(2-Methyl-9-phenylacridin-4-yl)(phenyl)methanone (4g): Yield= 76%, Yellow solid; M. P: 176.2 – 177.0 °C; **IR (KBr, cm^{-1})**: 3060, 2920, 2859, 1729, 1655, 1621, 1553, 1504, 1459, 1075, 901, 831;**^{1}H NMR (400 MHz, CDCl$_3$) δ** 8.23 (dd, *J* = 7.6, 1.2 Hz, 1H), 8.04 (d, *J* = 2.0 Hz, 1H), 7.99 (d, *J* = 2.0 Hz, 1H), 7.95 (dd, *J* = 8.6, 1.4 Hz, 1H), 7.80 (td, *J* = 7.2, 1.4 Hz, 1H), 7.77 – 7.71 (m, 2H), 7.61 (ddd, *J* = 8.4, 7.2, 1.2 Hz, 1H), 7.58 – 7.45 (m, 7H), 7.41 – 7.34 (m, 1H); **^{13}C NMR (100 MHz, CDCl$_3$) δ** 195.75, 149.25, 147.26, 139.89, 137.11, 136.59, 136.51, 132.68, 131.06, 130.87, 130.51, 130.21, 130.10, 130.09, 129.29, 128.83, 128.43, 127.94, 127.55, 126.39, 125.52, 125.34, 21.14. **HRMS (ESI-MS): m/z Calculated for** $C_{27}H_{19}NO$ $[M+H]^+$: 373.1469; Observed: 373.1470.

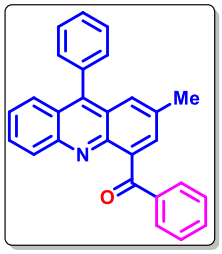

(7-Chloro-2-methyl-9-phenylacridin-4-yl)(phenyl)methanone (4h): Yield= 78%, Yellow solid; M. P: 165.3-166.2 °C; **IR (KBr, cm^{-1})**: 2920, 2855, 1730, 1659, 1533, 1454, 1070; **^{1}H NMR (400 MHz, CDCl$_3$) δ** 8.11 (d, *J* = 8.0 Hz, 1H), 8.05 (d, J = 2.0 Hz, 1H), 7.99 (d, *J* = 2.0

Hz, 1H), 7.79 (d, *J* = 2.4 Hz, 1H), 7.77 – 7.71 (m, 2H), 7.69 (dd, *J* = 8.0, 2.4 Hz, 1H), 7.59 – 7.45 (m, 8H), 7.41 – 7.34 (m, 1H), 2.53 (s, 3H); **^{13}C NMR (100 MHz, $CDCl_3$) δ** 195.84, 147.74, 146.82, 140.24, 136.59, 136.51, 136.17, 132.68, 131.23, 130.87, 130.21, 130.09, 129.70, 129.29, 128.83, 128.65, 127.94, 127.56, 125.92, 125.57, 125.30, 21.14. **HRMS (ESI-MS): m/z Calculated for** $C_{27}H_{18}ClNO$ $[M+H]^+$: 284.1070; Observed: 284.1068.

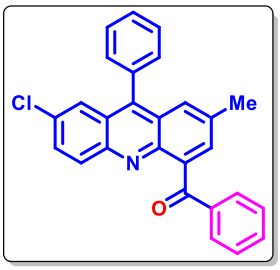

(2-Methyl-7-nitro-9-phenylacridin-4-yl)(phenyl)methanone (4i): Yield= 83%, Yellow solid; M. P: 195.3-195.7 °C; **IR (KBr, cm^{-1})**: 3064, 2919, 2855, 1981, 1918, 1663, 1625, 1507, 1383, 1273, 907, 867, 827; **^{1}H NMR (400 MHz, $CDCl_3$) δ** ^{1}H NMR (400 MHz, $CDCl_3$) δ 8.64 (d, *J* = 2.4 Hz, 1H), 8.32 (dd, *J* = 9.6, 2.4 Hz, 1H), 8.08 (d, *J* = 9.6 Hz, 1H), 7.90 (d, *J* = 7.6 Hz, 2H), 7.77 (d, *J* = 2.4 Hz, 1H), 7.70 (d, *J* = 1.2 Hz, 1H), 7.69 (d, *J* = 2.4 Hz, 2H), 7.62 – 7.57 (m, 2H), 7.48 (d, *J* = 3.6 Hz, 1H), 7.47 – 7.42 (m, 3H), 2.53 (s, 3H);**^{13}C NMR (100 MHz, $CDCl_3$) δ** 197.66, 149.82, 148.72, 147.67, 145.13, 139.66, 138.07, 136.43, 134.32, 133.54, 133.31, 132.31, 130.39, 130.14, 129.39, 129.00, 128.39, 127.01, 125.50, 124.55, 123.56, 122.32, 22.07. **HRMS (ESI-MS): m/z Calculated for** $C_{27}H_{18}N_2O_3$ $[M+H]^+$: 419.1390; Observed: 419.1393.

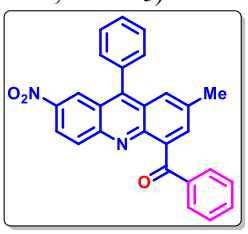

(2-(Tert-butyl)-9-phenylacridin-4-yl)(phenyl)methanone (4j): Yield= 72%, Pale Yellow solid; M. P: 192.1-192.9 °C; **IR (KBr, cm^{-1})**: 3063, 2919, 2858, 1725, 1660, 1569, 1503, 1269, 1069, 902, 867; **^{1}H NMR (400 MHz, $CDCl_3$) δ** 8.23 (dd, *J* = 7.5, 1.4 Hz, 1H), 8.18 (d, *J* = 2.2 Hz, 1H), 8.08 (d, *J* = 2.2 Hz, 1H), 7.95 (dd, *J* = 8.6, 1.5 Hz, 1H), 7.80 (td, *J* = 7.1, 1.3 Hz, 1H), 7.77 – 7.71 (m, 2H), 7.65 – 7.45 (m, 8H), 7.41 – 7.34 (m, 1H), 1.34 (s, 9H). **^{13}C NMR (100 MHz, $CDCl_3$) δ** 195.89, 149.33, 148.65, 147.01, 140.37, 137.08, 136.58, 132.68, 131.16, 131.06, 130.51, 130.21, 130.10, 129.29, 128.83, 128.43, 128.36, 127.94, 125.53, 125.34, 125.04, 124.00, 35.16, 31.5. **HRMS (ESI-MS): m/z Calculated for** $C_{30}H_{25}NO$ $[M+H]^+$: 416.2009; Observed: 416.2010.

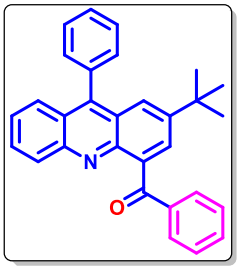

(2-(Tert-butyl)-7-chloro-9-phenylacridin-4-yl)(phenyl)methanone (4k): Yield= 76%, Pale Yellow solid; M. P: 178.1-179 °C; **IR (KBr, cm^{-1})**: 3060, 2920, 2859, 1735, 1661, 1622, 1570, 1510, 1172, 870;**^{1}H NMR (400 MHz, $CDCl_3$) δ** 8.18 (d, *J* = 2.2 Hz, 1H), 8.14 – 8.06 (m, 2H), 7.77 – 7.71 (m, 2H), 7.69 (s, 1H), 7.71 – 7.66 (m, 1H), 7.59 – 7.47 (m, 7H), 7.51 – 7.45 (m,

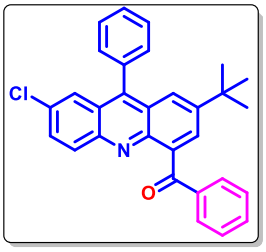

1H), 7.41 – 7.34 (m, 1H), 1.36 (s, 9H).**^{13}C NMR (101 MHz, $CDCl_3$) δ** 195.91, 148.65, 147.80, 146.74, 139.75, 136.58, 136.11, 132.68, 131.38, 131.23, 130.21, 130.09, 129.70, 129.29, 128.83, 128.65, 128.36, 127.94, 125.82, 125.30, 124.61, 123.98, 35.16, 31.56. **HRMS (ESI-MS): m/z Calculated for** $C_{30}H_{24}ClNO$ $[M+H]^+$: 450.1619; Observed: 450.1621.

(2-(Tert-butyl)-7-nitro-9-phenylacridin-4-yl)(phenyl)methanone (4l): Yield= 74%, Yellow solid; M. P: 222.5-223.2 °C; **IR (KBr, cm^{-1})**: 3065, 2921, 2860, 1731, 1662, 1460, 1344, 1073, 833; **^{1}H NMR (400 MHz, $CDCl_3$) δ** ^{1}H NMR (400 MHz, $CDCl_3$) δ 8.68 (dd, *J* = 2.4, 0.8 Hz, 1H), 8.34 (dd, *J* = 9.6, 2.4 Hz, 1H), 8.03 (d, *J* = 2.4 Hz, 1H), 7.92 (d, *J* = 1.2 Hz, 1H), 7.90 (t, *J* = 1.6 Hz, 1H), 7.78 (d, *J* = 2.4 Hz, 1H), 7.70 (dd, *J* = 5.2, 2.0 Hz, 3H), 7.62 – 7.58 (m, 1H), 7.50 (s, 1H), 7.48 (d, *J* = 2.0 Hz, 1H), 7.46 (s, 1H), 1.34 (s, 9H).**^{13}C NMR (101 MHz, $CDCl_3$) δ** ^{13}C NMR (100 MHz, $CDCl_3$) δ 197.94, 149.02, 148.95, 145.09, 138.11, 134.26, 133.33, 132.26, 130.38, 130.22, 129.47, 128.96, 128.42, 124.60, 35.41, 30.68. **HRMS (ESI-MS): m/z Calculated for** $C_{30}H_{24}N_2O_3$ $[M+H]^+$: 461.1860; Observed: 461.1863.

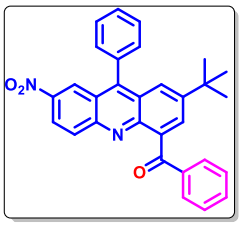

(7-Chloro-9-phenylacridin-4-yl)(p-tolyl)methanone (4m): Yield= 80%, Pale Yellow solid; M. P: 176.2 – 177.0 °C; **IR (KBr, cm^{-1})**: 3065, 2919, 2850, 1730, 1655, 1620, 1573, 1506, 1455, 1333, 1270, 854; **^{1}H NMR (400 MHz, $CDCl_3$) δ** 8.75 (dd, *J* = 8.8, 1.2 Hz, 1H), 8.10 (d, *J* = 8.4 Hz, 1H), 7.96 (dd, *J* = 8.4, 1.2 Hz, 1H), 7.82 – 7.71 (m, 3H), 7.73 – 7.66 (m, 1H), 7.59 – 7.49 (m, 4H), 7.41 – 7.34 (m, 1H), 7.23 – 7.17 (m, 2H), 2.31 (s, 3H). **^{13}C NMR (100 MHz, $CDCl_3$) δ** 196.08, 147.86, 147.32, 142.97, 141.22, 137.66, 135.37, 131.46, 131.23, 130.30, 130.16, 130.10, 129.70, 129.36, 129.29, 128.66, 128.39, 127.94, 127.08, 126.60, 125.86, 125.31, 21.37. **HRMS (ESI-MS): m/z Calculated for** $C_{27}H_{18}ClNO$ $[M+H]^+$: 408.1150; Observed: 408.1147.

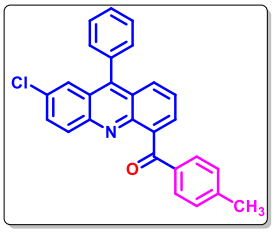

(7-Nitro-9-phenylacridin-4-yl)(p-tolyl)methanone (4n): Yield= 79%, Yellow solid; M. P: 153.4 – 155.0 °C; **IR (KBr, cm^{-1})**: 3091, 2987, 2842, 1745 1359, 1145, 1014,845; **^{1}H NMR (400 MHz, $CDCl_3$) δ** 8.64 (d, *J* = 2.4 Hz, 1H), 8.32 (dd, *J* = 9.6, 2.4 Hz, 1H), 8.08 (d, *J* = 9.6 Hz, 1H), 7.90 (d, *J* = 7.6 Hz, 2H), 7.77 (d, *J* = 2.0 Hz, 1H), 7.70 (d, *J* = 1.2 Hz, 1H), 7.69 (d, *J* = 2.4 Hz, 2H), 7.62 – 7.57 (m, 2H), 7.48 (d, *J* = 3.6 Hz, 1H), 7.47 – 7.42 (m, 3H), 2.53 (s, 3H). **^{13}C NMR (100 MHz, $CDCl_3$) δ** 197.66, 149.82, 148.72, 147.67, 145.13, 139.66, 138.07, 136.43, 134.32, 133.54, 133.31, 132.31, 130.39, 130.14, 129.39,

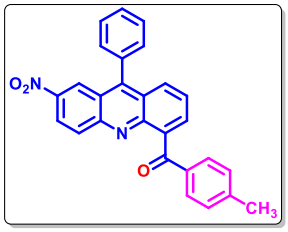

129.00, 128.39, 127.01, 125.50, 124.55, 123.56, 122.32, 22.07. **HRMS (ESI-MS): m/z Calculated for** $C_{27}H_{18}N_2O_3$ $[M+H]^+$: 413.1390; Observed: 413.1392.

Methyl 4-(4-methoxybenzoyl)acridine-9-carboxylate (4o): Yield= 74%, Yellow solid; M. P: 114.2-115.1 °C; **IR (KBr, cm^{-1})**: 3024, 2978, 2832, 1742, 1349, 1224, 1112, 1054, 920; **^{1}H NMR (400 MHz, $CDCl_3$) δ** 8.07 (dd, *J* = 8.8, 1.3 Hz, 1H), 7.92 (d, *J* = 0.7 Hz, 1H), 7.90 (d, *J* = 0.6 Hz, 1H), 7.75 (d, *J* = 1.3 Hz, 1H), 7.74 – 7.71 (m, 2H), 7.62 (dd, *J* = 8.7, 6.8 Hz, 1H), 7.55 (dd, *J* = 9.3, 2.3 Hz, 1H), 6.82 – 6.79 (m, 2H), 4.17 (s, 3H), 3.78 (s, 3H). **^{13}C NMR (100 MHz, CDCl3) δ** 195.86, 167.27, 163.74, 146.90, 146.50, 140.32, 135.63, 133.85, 132.51, 132.32, 131.61, 131.10, 128.94, 126.98, 126.69, 123.34, 122.67, 122.42, 113.60, 55.48, 53.28. **HRMS (ESI-MS): m/z Calculated for** $C_{27}H_{18}NO_3$ $[M+H]^+$: 372.1230; Observed: 372.1238.

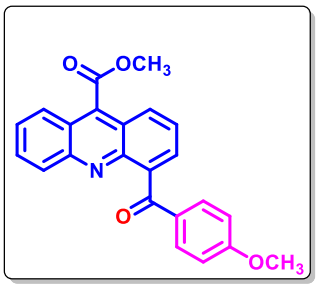

Methyl 4-(4-nitrobenzoyl)acridine-9-carboxylate (4r): Yield= 82%, Yellow solid; M. P: 125.2-126.1 °C; **IR (KBr, cm^{-1})**: 3074, 2923, 2854, 1719, 1630, 1349, 1278, 1175, 1129, 1075, 879; **^{1}H NMR (400 MHz, $CDCl_3$) δ** 8.28 – 8.26 (m, 1H), 8.25 (d, *J* = 4.8 Hz, 2H), 8.03 (d, *J* = 2.4 Hz, 1H), 8.03 – 8.00 (m, 1H), 7.95 – 7.92 (m, 2H), 7.79 (d, *J* = 6.8 Hz, 1H), 7.78 (s, 1H), 7.64 (dd, *J* = 9.2, 2.0 Hz, 1H), 4.28 (s, 3H).**^{13}C NMR (100 MHz, $CDCl_3$) δ** 196.04, 166.97, 150.09, 146.73, 146.13, 143.24, 138.45, 135.97, 134.27, 132.23, 131.79, 130.57, 130.53, 128.35, 127.09, 123.50, 122.79, 122.40, 53.41. **HRMS (ESI-MS): m/z Calculated for** $C_{22}H_{15}N_2O_5$ $[M+H]^+$: 387.0975; Observed: 387.0987.

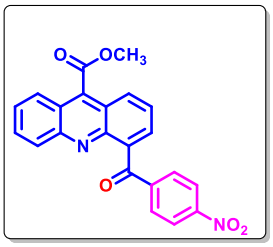

Methyl 2-chloro-5-(4-methoxybenzoyl)acridine-9-carboxylate (4q): Yield= 79%, Yellow solid; M. P: 208.5-209.1 °C; **IR (KBr, cm^{-1})**: 3081, 2931, 2874, 1735, 1278, 1175, 1129, 1045, 817; **^{1}H NMR (400 MHz, $CDCl_3$) δ** 8.07 (dd, *J* = 8.8, 1.3 Hz, 1H), 7.92 (d, *J* = 0.7 Hz, 1H), 7.90 (d, *J* = 0.6 Hz, 1H), 7.75 (d, *J* = 1.3 Hz, 1H), 7.74 – 7.71 (m, 2H), 7.62 (dd, *J* = 8.7, 6.8 Hz, 1H), 7.55 (dd, *J* = 9.3, 2.3 Hz, 1H), 6.82 – 6.79 (m, 2H), 4.17 (s, 3H), 3.78 (s, 3H). **^{13}C NMR (100 MHz, CDCl3) δ** 195.86, 167.27, 163.74, 146.90, 146.50, 140.32, 135.63, 133.85, 132.51, 132.32, 131.61, 131.10, 128.94, 126.98, 126.69, 123.34, 122.67, 122.42, 113.60, 55.48, 53.28. **HRMS (ESI-MS): m/z Calculated for** $C_{23}H_{17}ClNO_4$ $[M+H]^+$: 406.0841; Observed: 406.0849.

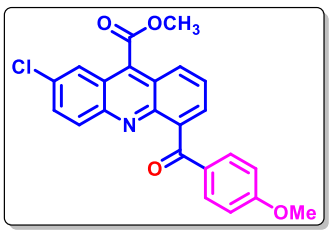

Methyl 2-chloro-5-(4-nitrobenzoyl)acridine-9-carboxylate (4r): Yield= 82%, Yellow solid; M. P: 198.1-198.5 °C; **IR (KBr, cm^{-1})**: 3068, 2925, 2867, 1735, 1662, 1630, 1349, 1278, 1129, 1075, 910;**^{1}H NMR (400 MHz, CDCl$_3$) δ** 8.28 – 8.26 (m, 1H), 8.25 (d, *J* = 4.8 Hz, 2H), 8.03 (d, *J* = 2.4 Hz, 1H), 8.03 – 8.00 (m, 1H), 7.95 – 7.92 (m, 2H), 7.79 (d, *J* = 6.8 Hz, 1H), 7.78 (s, 1H), 7.64 (dd, *J* = 9.2, 2.0 Hz, 1H), 4.28 (s, 3H).**^{13}C NMR (100 MHz, CDCl$_3$) δ** 196.04, 166.97, 150.09, 146.73, 146.13, 143.24, 138.45, 135.97, 134.27, 132.23, 131.79, 130.57, 130.53, 128.35, 127.09, 123.50, 122.79, 122.40, 53.41. **HRMS (ESI-MS): m/z Calculated for** $C_{22}H_{13}N_2ClO_5$ $[M+H]^+$: 420.0586; Observed: 421.059.

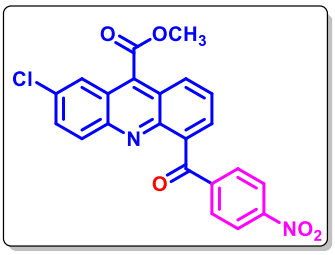

Benzyl 4-(4-methoxybenzoyl)acridine-9-carboxylate (4s): Yield= 75%, Yellow solid; M. P: 125.4-125.9 °C; **IR (KBr, cm^{-1})**: 3025, 2954, 2878,1758, 1626, 1559, 1429, 1350, 1277, 1054, 980; **^{1}H NMR (400 MHz, CDCl$_3$) δ** 8.05 (dd, *J* = 8.8, 1.2 Hz, 1H), 8.01 (dt, *J* = 8.8, 1.2 Hz, 1H), 7.91 (ddd, *J* = 8.8, 1.6, 0.8 Hz, 1H), 7.82 – 7.77 (m, 3H), 7.67 (ddd, *J* = 8.8, 6.4, 1.2 Hz, 1H), 7.61 (dd, *J* = 8.8, 6.8 Hz, 1H), 7.57 – 7.54 (m, 2H), 7.54 – 7.50 (m, 1H), 7.47 – 7.44 (m, 1H), 7.44 – 7.39 (m, 2H), 6.88 – 6.84 (m, 2H), 5.69 (s, 2H), 3.84 (s, 3H). **^{13}C NMR (100MHz, CDCl$_3$) δ** 196.23, 167.29, 163.63, 148.63, 146.43, 140.22, 136.55, 134.99, 132.54, 131.26, 130.70, 130.20, 128.91, 128.87, 128.83, 128.73, 127.64, 126.64, 126.29, 124.75, 122.34, 122.02, 113.53, 68.16, 55.47. **HRMS (ESI-MS): m/z Calculated for** $C_{29}H_{21}NO_4$ $[M+H]^+$: 448.1543; Observed: 448.1548.

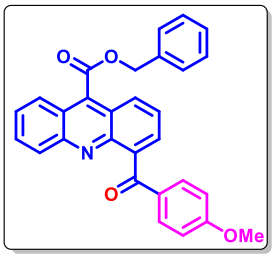

Benzyl 4-(4-methoxybenzoyl)acridine-9-carboxylate (4t): Yield= 73%, Yellow solid; M. P: 132.4-132.8 °C; **IR (KBr, cm^{-1})**: 3021, 2934, 2821,1724, 1608, 1559, 1277, 1221, 1040, 921, 815, **^{1}H NMR (400 MHz, CDCl$_3$) δ** 8.05 (dd, *J* = 8.8, 1.2 Hz, 1H), 8.01 (dt, *J* = 8.8, 1.2 Hz, 1H), 7.91 (ddd, *J* = 8.8, 1.6, 0.8 Hz, 1H), 7.82 – 7.77 (m, 3H), 7.67 (ddd, *J* = 8.8, 6.4, 1.2 Hz, 1H), 7.61 (dd, *J* = 8.8, 6.8 Hz, 1H), 7.57 – 7.54 (m, 2H), 7.54 – 7.50 (m, 1H), 7.47 – 7.44 (m, 1H), 7.44 – 7.39 (m, 2H), 6.88 – 6.84 (m, 2H), 5.69 (s, 2H), 3.84 (s, 3H). **^{13}C NMR (100MHz, CDCl$_3$) δ** 196.23, 167.29, 163.63, 148.63, 146.43, 140.22, 136.55, 134.99, 132.54, 131.26, 130.70, 130.20, 128.91, 128.87, 128.83, 128.73, 127.64, 126.64, 126.29, 124.75, 122.34, 122.02, 113.53, 68.16, 55.47. **HRMS (ESI-MS): m/z Calculated for** $C_{30}H_{24}N_2O_3$ $[M+H]^+$: 461.1860; Observed: 461.1860.

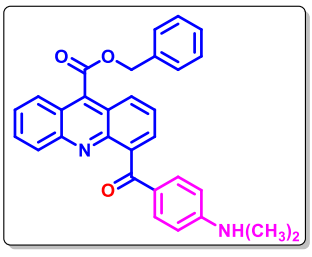

Benzyl 4-(4-methoxybenzoyl)acridine-9-carboxylate (4u): Yield= 86%, Yellow solid; M. P: 116.5-116.9 °C; **IR (KBr, cm^{-1})**: 3064, 2985, 2866,1730, 1645, 1022, 921; **^{1}H NMR (400 MHz, $CDCl_3$) δ** 8.05 (dd, *J* = 8.8, 1.2 Hz, 1H), 8.01 (dt, *J* = 8.8, 1.2 Hz, 1H), 7.91 (ddd, *J* = 8.8, 1.6, 0.8 Hz, 1H), 7.82 – 7.77 (m, 3H), 7.67 (ddd, *J* = 8.8, 6.4, 1.2 Hz, 1H), 7.61 (dd, *J* = 8.8, 6.8 Hz, 1H), 7.57 – 7.54 (m, 2H), 7.54 – 7.50 (m, 1H), 7.47 – 7.44 (m, 1H), 7.44 – 7.39 (m, 2H), 6.88 – 6.84 (m, 2H), 5.69 (s, 2H). **^{13}C NMR (100MHz, $CDCl_3$) δ** 196.23, 167.29, 163.63, 148.63, 146.43, 140.22, 136.55, 134.99, 132.54, 131.26, 130.70, 130.20, 128.91, 128.87, 128.83, 128.73, 127.64, 126.64, 126.29, 124.75, 122.34, 122.02, 113.53, 68.16. **HRMS (ESI-MS): m/z Calculated for** $C_{28}H_{18}N_2O_5$ $[M+H]^+$: 463.1288; Observed: 463.1292.

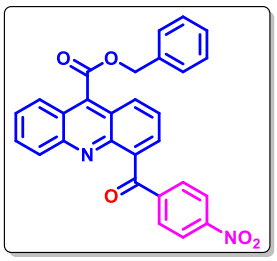

Benzyl 4-(thiophene-2-carbonyl)acridine-9-carboxylate (4v): Yield= 82%, Yellow solid; M. P: 120.1-120.6 °C; **IR (KBr, cm^{-1})**: 3044, 2921, 2857,1727, 1654, 1608, 1559, 1516, 1429, 1350, 1277, 1221, 1040, 980, 921, 815, 749, 629, 546; **^{1}H NMR (400 MHz, $CDCl_3$) δ** 8.11 (dt, *J* = 8.8, 1.2 Hz, 1H), 8.07 (dd, *J* = 8.8, 1.2 Hz, 1H), 7.94 – 7.91 (m, 1H), 7.87 (dd, *J* = 6.8, 1.2 Hz, 1H), 7.73 – 7.69 (m, 2H), 7.62 – 7.59 (m, 1H), 7.57 – 7.56 (m, 1H), 7.54 (dt, *J* = 2.4, 1.2 Hz, 2H), 7.45 – 7.42 (m, 2H), 7.33 (dd, *J* = 3.6, 1.2 Hz, 1H), 7.03 (dd, *J* = 5.2, 3.6 Hz, 1H), 5.69 (s, 2H). **^{13}C NMR (100 MHz, $CDCl_3$) δ** 189.25, 167.20, 148.75, 146.12, 145.45, 139.43, 136.62, 135.41, 134.98, 134.56, 130.72, 130.38, 128.96, 128.92, 128.87, 128.83, 128.00, 127.75, 127.23, 126.06, 124.81, 122.44, 122.13, 68.18. **HRMS (ESI-MS): m/z Calculated for** $C_{26}H_{18}NO_3S$ $[M+H]^+$: 424.1002; Observed: 424.1007.

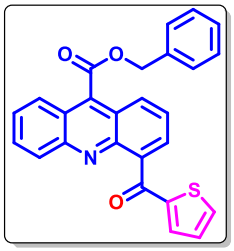

3.3.10 References

(1) Adhikari, S.; Mitra, A. K. *J. Iran. Chem. Soc.* **2023**, *20*, 2399–2455.

(2) (a) Kumar, A.; Srivastava, K.; Raja Kumar, S.; Puri, S. K.; Chauhan, P. M. S. *Bioorg. Med. Chem. Lett.* **2009**, *19*, 6996–6999. (b) Yu, X.; Ramiandrasoa, F.; Guetzoyan, L.; Pradines, B.; Quintino, E.; Gadelle, D.; Forterre, P.; Cresteil, T.; Mahy, J.; Pethe, S. *Chem MedChem* **2012**, *7*, 587–605. (c) Tomar, V.; Bhattacharjee, G.; Kamaluddin; Rajakumar, S.; Srivastava, K.; Puri, S. K. *Eur. J. Med. Chem.* **2010**, *45*, 745–751.

(3) (a) Demeunynck, M.; Charmantray, F.; Martelli, A. *Curr. Pharm. Des.* **2001**, *7*. (b) Anderson, M. O.; Sherrill, J.; Madrid, P. B.; Liou, A. P.; Weisman, J. L.; DeRisi, J. L.; Guy, R. K. *Bioorg. Med. Chem.* **2006**, *14*, 334–343

(4) Tonelli, M.; Vettoretti, G.; Tasso, B.; Novelli, F.; Boido, V.; Sparatore, F.; Busonera, B.; Ouhtit, A.; Farci, P.; Blois, S.; Giliberti, G.; La Colla, P. *Antiviral Res.* **2011**, *91*, 133–141.

(5) (a) Chen, C.-H.; Lin, Y.-W.; Zhang, X.; Chou, T.-C.; Tsai, T.-J.; Kapuriya, N.; Kakadiya, R.; Su, T.-L. *Eur. J. Med. Chem.* **2009**, *44*, 3056–3059. (b) Lang, X.; Li, L.; Chen, Y.; Sun, Q.; Wu, Q.; Liu, F.; Tan, C.; Liu, H.; Gao, C.; Jiang, Y. *Bioorg. Med. Chem.* **2013**, *21*, 4170–4177. (c) Gamage, S. A.; Spicer, J. A.; Atwell, G. J.; Finlay, G. J.; Baguley, B. C.; Denny, W. A. *J. Med. Chem.* **1999**, *42*, 2383–2393.

(6) Gensicka-Kowalewska, M.; Cholewiński, G.; Dzierzbicka, K. *RSC Adv.* **2017**, *7*, 15776–15804.

(7) Makhaeva, G. F.; Lushchekina, S. V.; Boltneva, N. P.; Serebryakova, O. G.; Rudakova, E. V.; Ustyugov, A. A.; Bachurin, S. O.; Shchepochkin, A. V.; Chupakhin, O. N.; Charushin, V. N.; Richardson, R. J. *Bioorg. Med. Chem.* **2017**, *25*, 5981–5994.

(8) Tka, N.; Ayed, M.A.H.; Braiek, M. B.; Jabli, M.; Langer, P. *Beilstein J. Org. Chem.* **2021**, *17*, 2450-2461.

(9) Alsharif, M. A.; Raja, Q. A.; Majeed, N. A.; Jassas, Rabab. S.; Alsimaree, A. A.; Sadiq, A.; Naeem, N.; Mughal, E. U.; Alsantali, R. I.; Moussa, Z.; Ahmed, S. A. *RSC Adv.* **2021**, *11*, 29826–29858.

(10) Huang, Q.; Zheng, B.-Z.; Long, Q. *J. Chem. Sci.* **2010**, *122*, 203–207.

(11) Tomakinian, T.; Guillot, R.; Kouklovsky, C.; Vincent, G. *Angew. Chem.* **2014**, *126*, 12075–12079.

(12) (a) Katsina, T.; Clavier, L.; Giffard, J.-F.; Macedo Portela Da Silva, N.; Fournier, J.; Tamion, R.; Copin, C.; Arseniyadis, S.; Jean, A. *Org. Process Res. Dev.* **2020**, *24*, 856–860. (b) Bouquet, M.; Guy, A.; Lemaire, M.; Guetté, J. P. *Synth. Commun.* **1985**, *15*, 1153–1157.

(13) Dilek, Ö.; Patir, S.; Tilki, T.; Ertürk, E. *Tetrahedron Lett.* **2023**, *124*, 154603.

(14) Bortolotti, B.; Leardini, R.; Nanni, D.; Zanardi, G. *Tetrahedron* **1993**, *49*, 10157–10174.

(15) (a) Shariati, M.; Imanzadeh, G.; Rostami, A.; Ghoreishy, N.; Kheirjou, S. *Comptes Rendus Chim.* **2019**, *22*, 337–346. (b) Wang, Z.-L.; Li, H.-L.; Ge, L.-S.; An, X.-L.; Zhang, Z.-G.; Luo, X.; Fossey, J. S.; Deng, W.-P. *J. Org. Chem.* **2014**, *79*, 1156–1165. (c) Jang, Y. H.; Youn, S. W. *Org. Lett.* **2014**, *16*, 3720–3723.

(16) (a) Batista, V. S.; Crabtree, R. H.; Konezny, S. J.; Luca, O. R.; Praetorius, J. M. *New J. Chem.* **2012**, *36*, 1141. (b) Cui, Y.; Floreancig, P. E. *Org. Lett.* **2012**, *14*, 1720–1723.

(17) Zhai, L.; Shukla, R.; Rathore, R. *Org. Lett.* **2009**, *11*, 3474–3477.

(18) (a) Röse, P.; Emge, S.; König, C. A.; Hilt, G. *Adv. Synth. Catal.* **2017**, *359*, 1359–1372. (b) Zhang, W.; Ma, H.; Zhou, L.; Sun, Z.; Du, Z.; Miao, H.; Xu, J. *Molecules* **2008**, *13*, 3236–3245.

(19) (a) Wang, Z.-L.; An, X.-L.; Ge, L.-S.; Jin, J.-H.; Luo, X.; Deng, W.-P. *Tetrahedron* **2014**, *70*, 3788–3792. (b) Chen, C.-H.; Lin, Y.-W.; Zhang, X.; Chou, T.-C.; Tsai, T.-J.; Kapuriya, N.; Kakadiya, R.; Su, T.-L. *Eur. J. Med. Chem.* **2009**, *44*, 3056–3059.

(20) Hati, S.; Holzgrabe, U.; Sen, S. *Beilstein J. Org. Chem.* **2017**, *13*, 1670–1692.

(21) (a) Cheng, D.; Yu, C.; Pu, Y.; Xu, X. *Tetrahedron Lett.* **2022**, *90*, 153609. (b) Zhang, Y.; Li, C.-J. *J. Am. Chem. Soc.*, **2006**, *128*, 4242–4243. (c) Shariati, M. *Mol. Catal.* **2018**.

(22) Ali, A.; Cheng, F.; Wen, W.-H.; Ying, X.; Kandhadi, J.; Wang, H.; Liu, H.-Y.; Chang, C.-K. *Chin. Chem. Lett.* **2018**, *29*, 1888–1892.

(23) (a) Rahim, M. A.; Matsumura, S.; Toshima, K. *Tetrahedron Lett.* **2005**, *46*, 7307– 7309. (b) Liu, L.; Floreancig, P. E. *Org. Lett.* **2010**, *12*, 4686–4689.

(24) (a) Nakayama, K.; Okada, Y. *J. Org. Chem.* **2023**, *88*, 5913–5922. (b) Natarajan, P.; König, B. *Eur. J. Org. Chem.* **2021**, 2145–2161.

(25) Kim, S.; Han, S. H.; Mishra, N. K.; Chun, R.; Jung, Y. H.; Kim, H. S.; Park, J. S.; Kim, I. S. *Org. Lett.* **2018**, *20*, 4010–4014.

(26) Kim, S.; Kundu, A.; Chun, R.; Han, S. H.; Pandey, A. K.; Yoo, S.; Junghyun, P.; Hyung, S.; Ku, J. M.; Kim, I. S. *Asian J. Org. Chem*. **2018**, *7*, 2069–2075.

(27) Shirazian, T. S.; Tejeneki, H. Z.; Nikbakht, A.; Rominger, F.; Balalaie, S. *Eur. J. Org. Chem*. **2022**, e202200830.

(28) Ammon, E.; Heine, P.; Cordero, M. A. A.; Lochbrunner, S.; Villinger, A.; Ehlers, P.; Langer, P. *Org. Biomol. Chem.* **2023**, *21*, 4504–4517.

(29) (a) Kumar, D.; Salam, A.; Sahu, T. K.; Sahoo, S. S.; Khan, T. *J. Org. Chem.* **2021**, *86*, 15096–15116; (b) Kim, H. P.; Yu, H.; Kim, H.; Kim, S.-H.; Lee, D. *Molecules* **2018**, *23*, 3223.

3.3.11 Selected Spectra

Methyl 4-(4-nitrobenzoyl)acridine-9-carboxylate (4p):

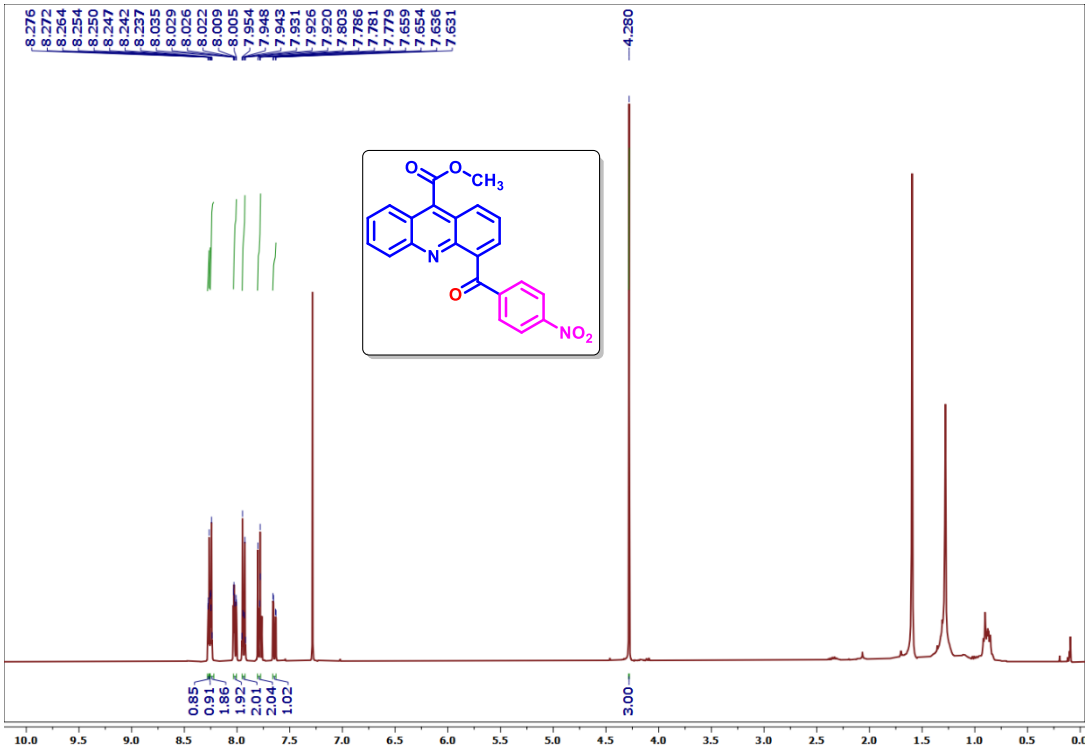

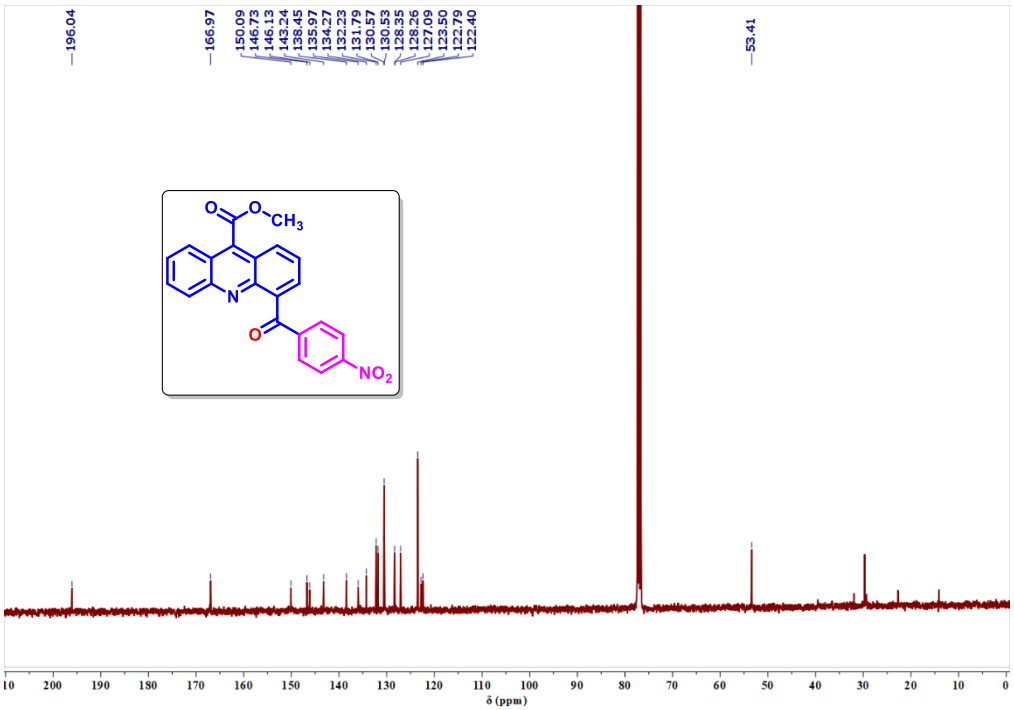

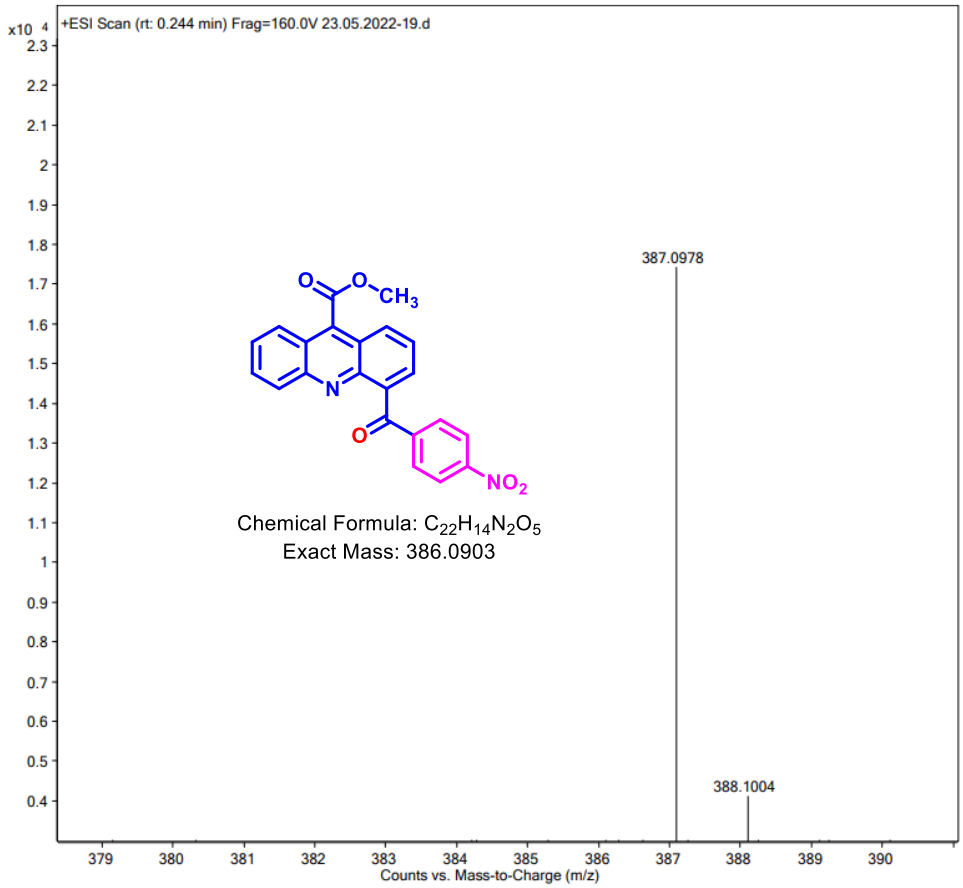

Methyl 2-chloro-5-(4-methoxybenzoyl)acridine-9-carboxylate (4q):

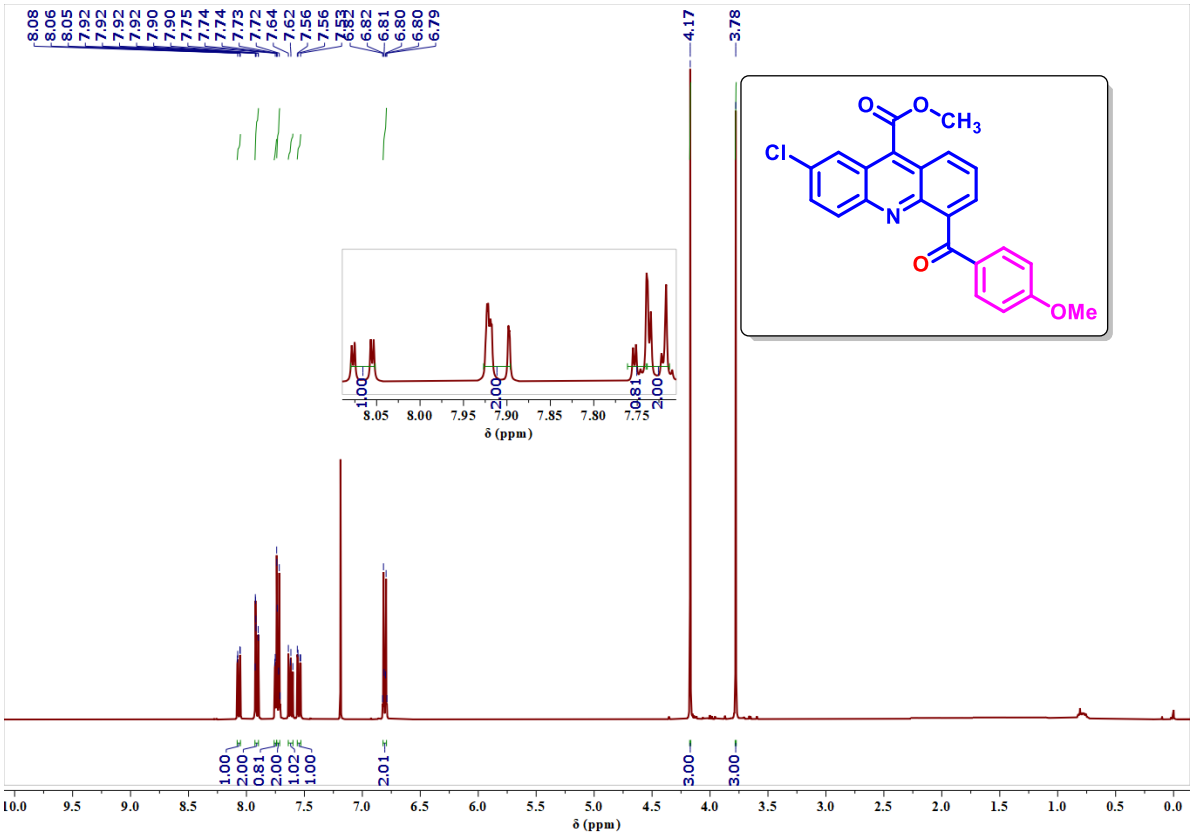

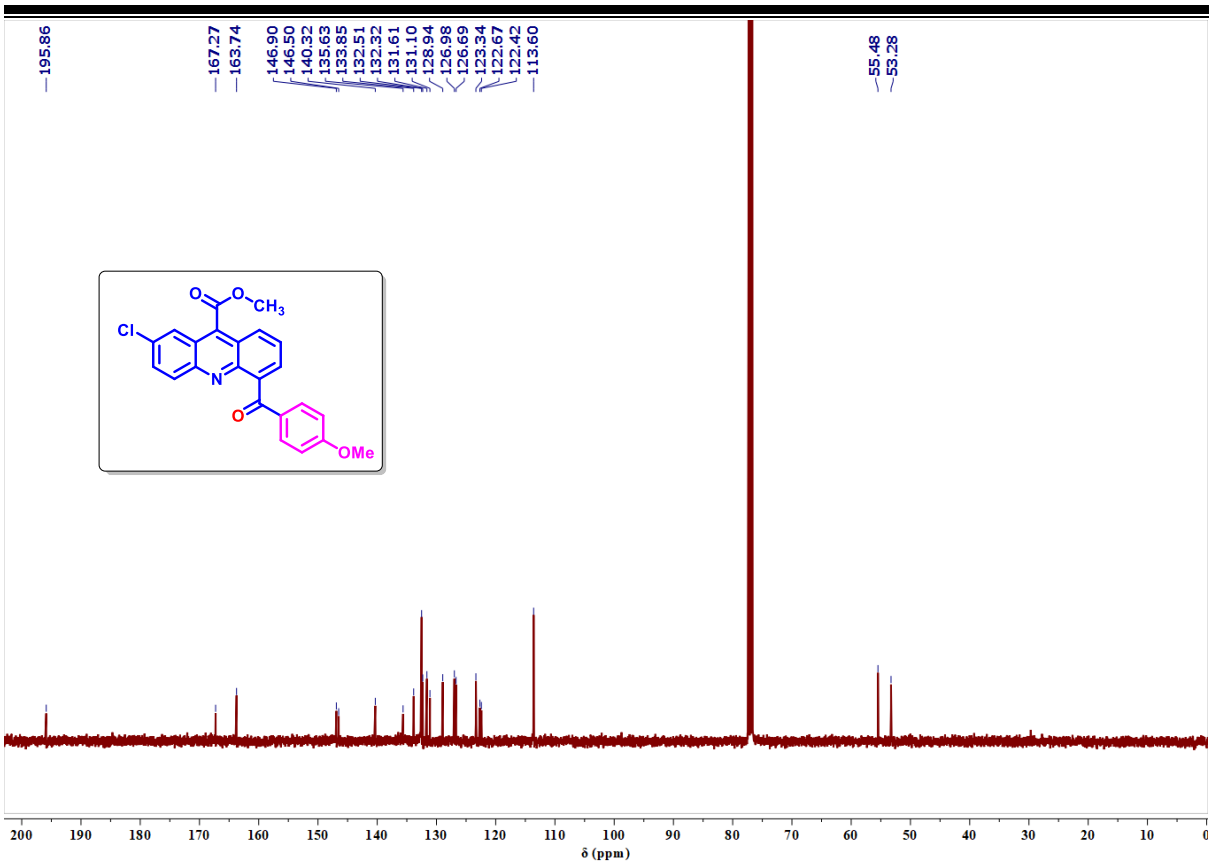
195.86
167.27
163.74
146.90
146.50
140.32
135.63
133.85
132.51
132.32
131.61
131.10
128.94
126.98
126.69
123.34
122.67
122.42
113.60
55.48
53.28
Cl
N
O
O
CH3
OMe
δ (ppm)

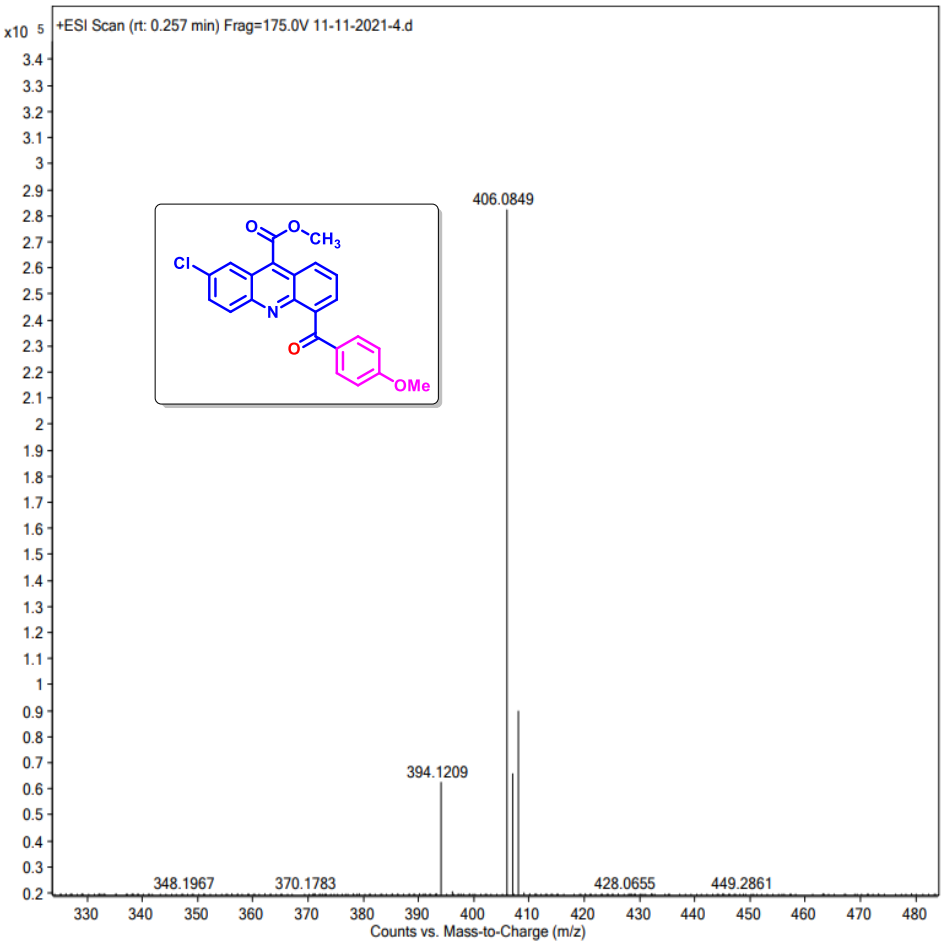
x10 5
+ESI Scan (rt: 0.257 min) Frag=175.0V 11-11-2021-4.d
406.0849
394.1209
348.1967
370.1783
428.0655
449.2861
Cl
N
O
O
CH3
OMe
Counts vs. Mass-to-Charge (m/z)

Methyl 2-chloro-5-(4-nitrobenzoyl)acridine-9-carboxylate (4r):

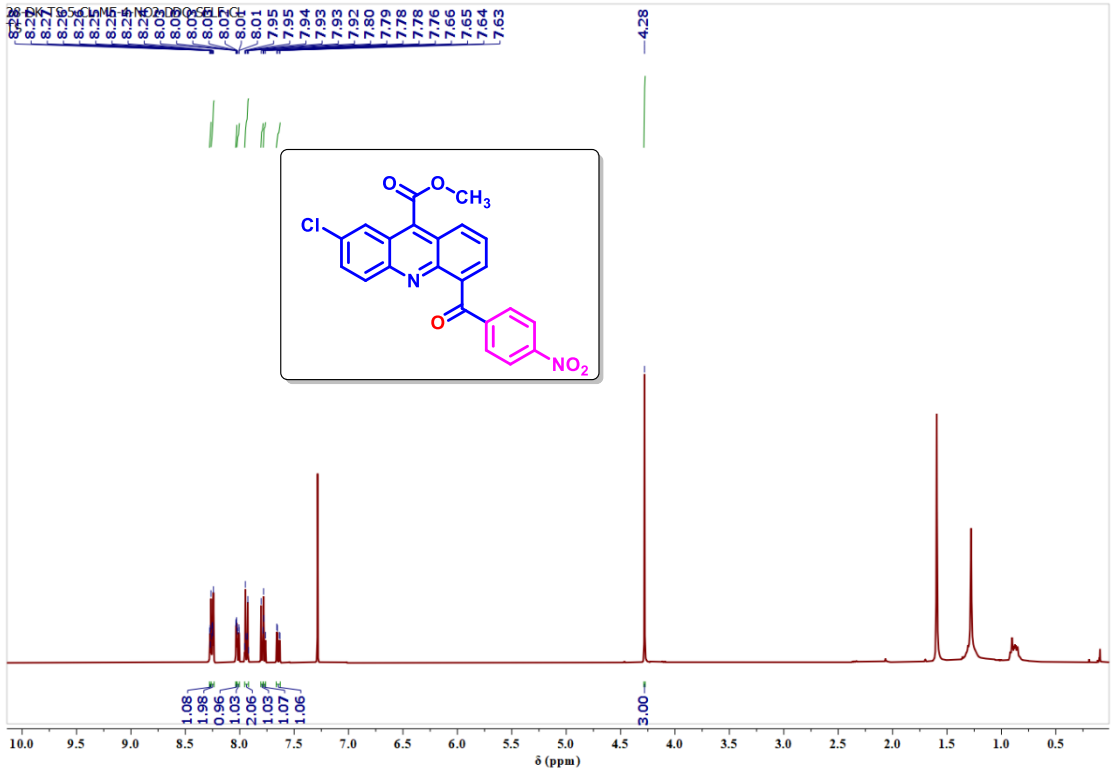

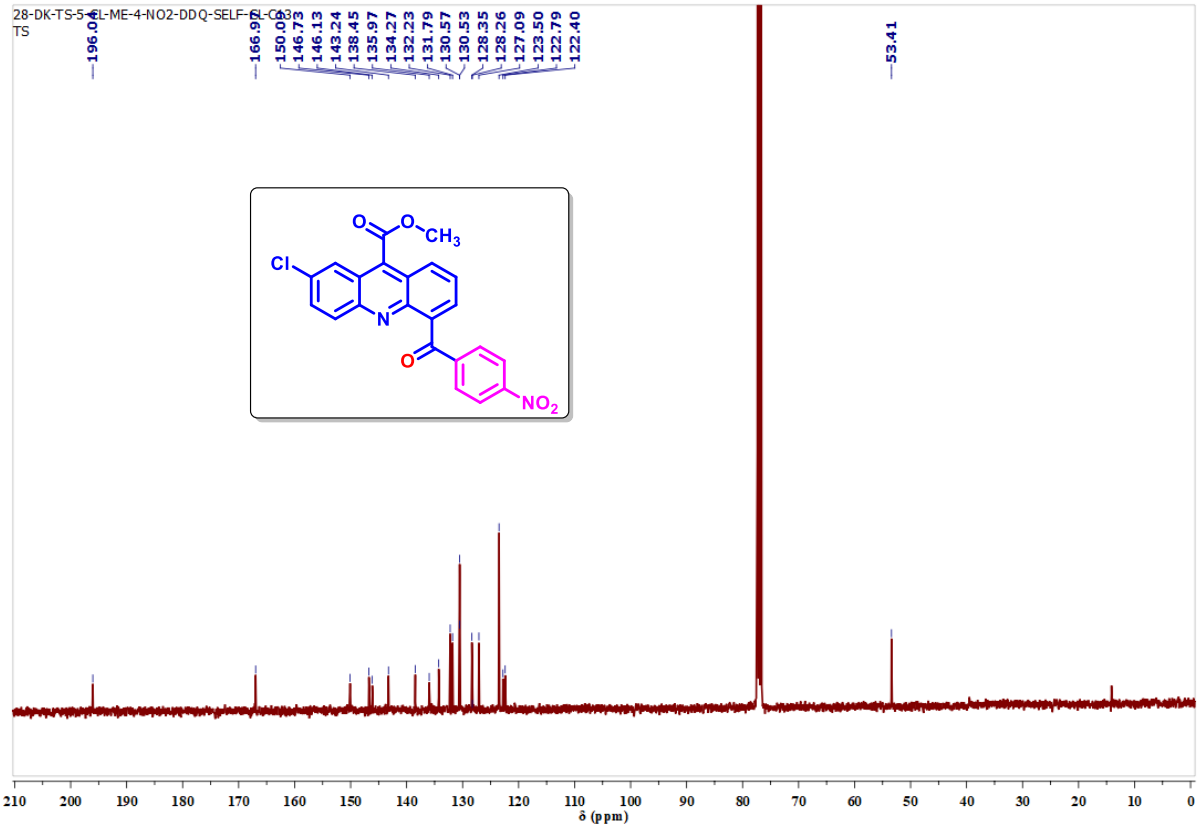

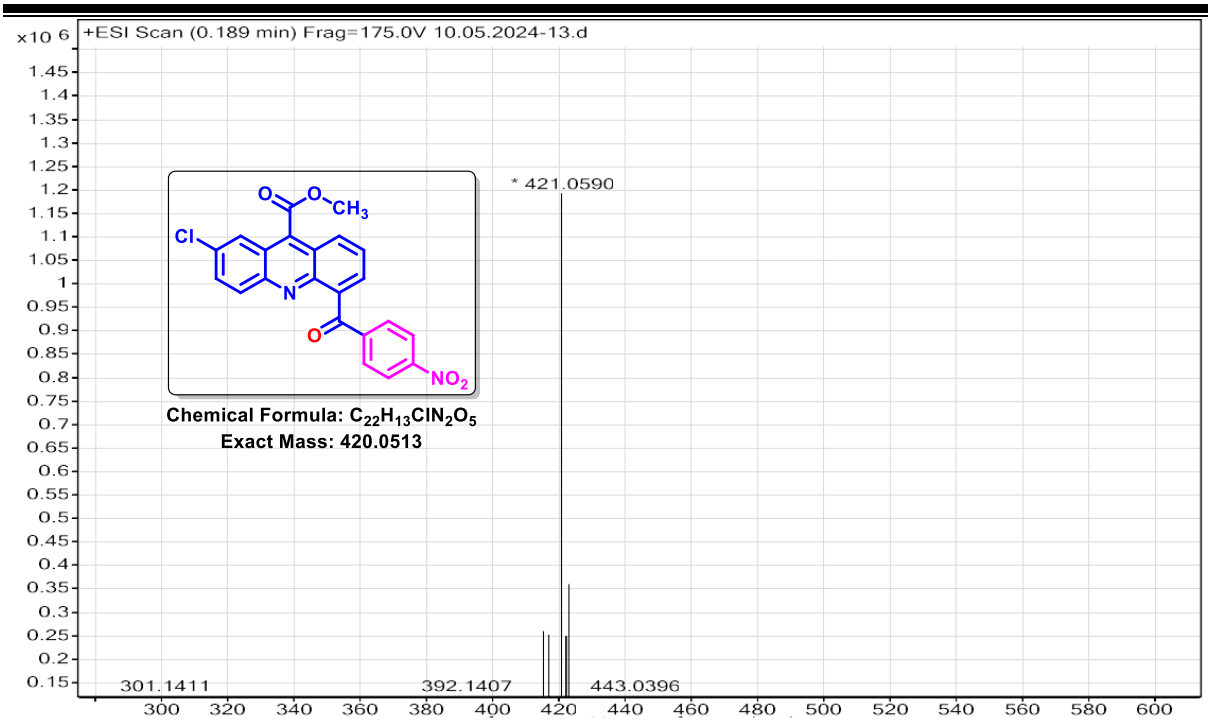

Benzyl 4-(4-methoxybenzoyl)acridine-9-carboxylate (4s):

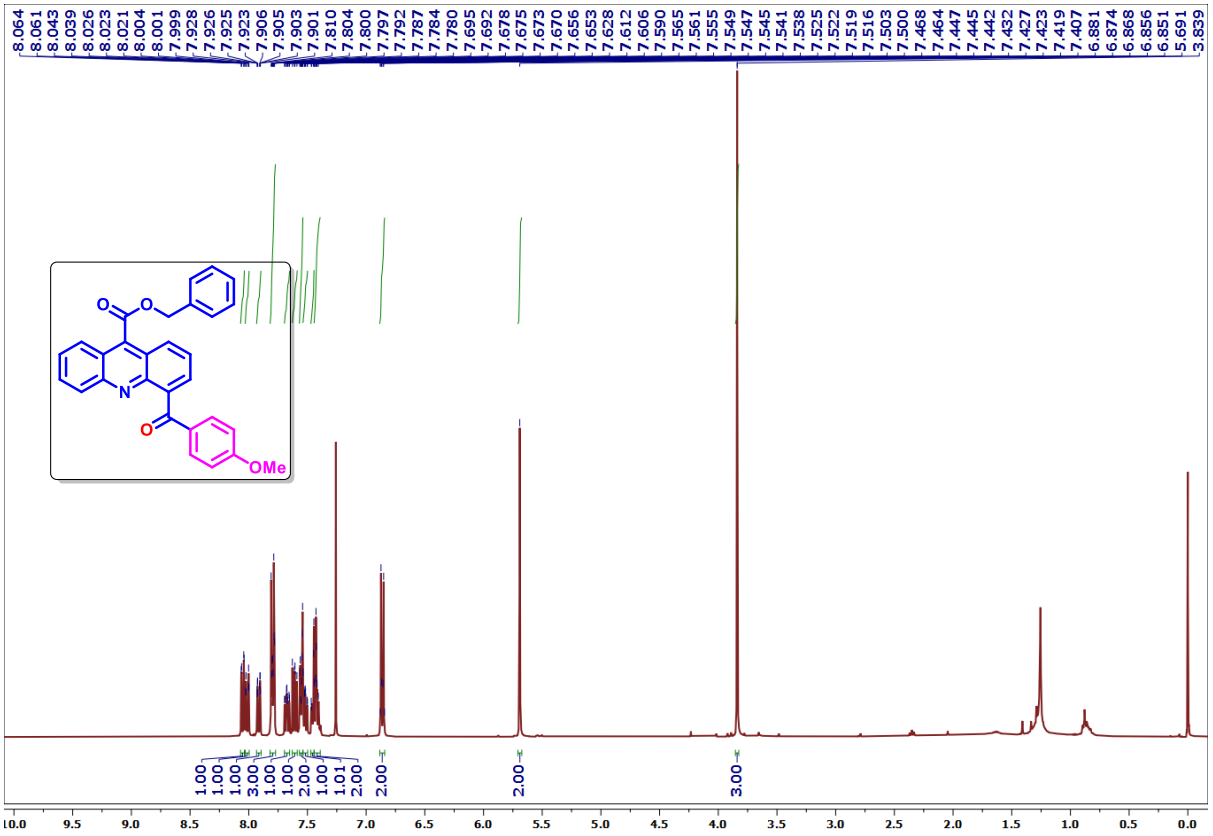

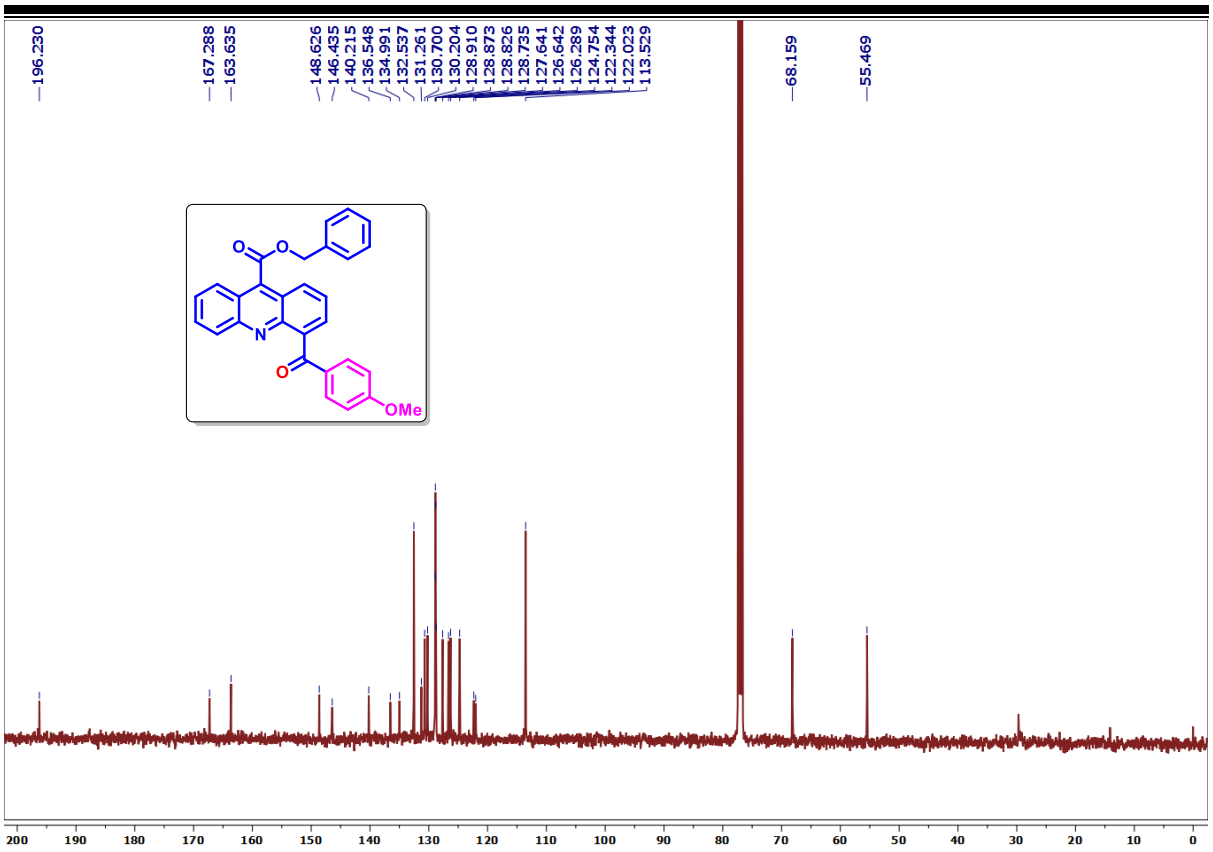
196.230
167.288
163.635
148.626
146.435
140.215
136.548
134.991
132.537
131.261
130.700
130.204
128.910
128.873
128.826
128.735
127.641
126.642
126.289
124.754
122.344
122.023
113.529
68.159
55.469
OMe

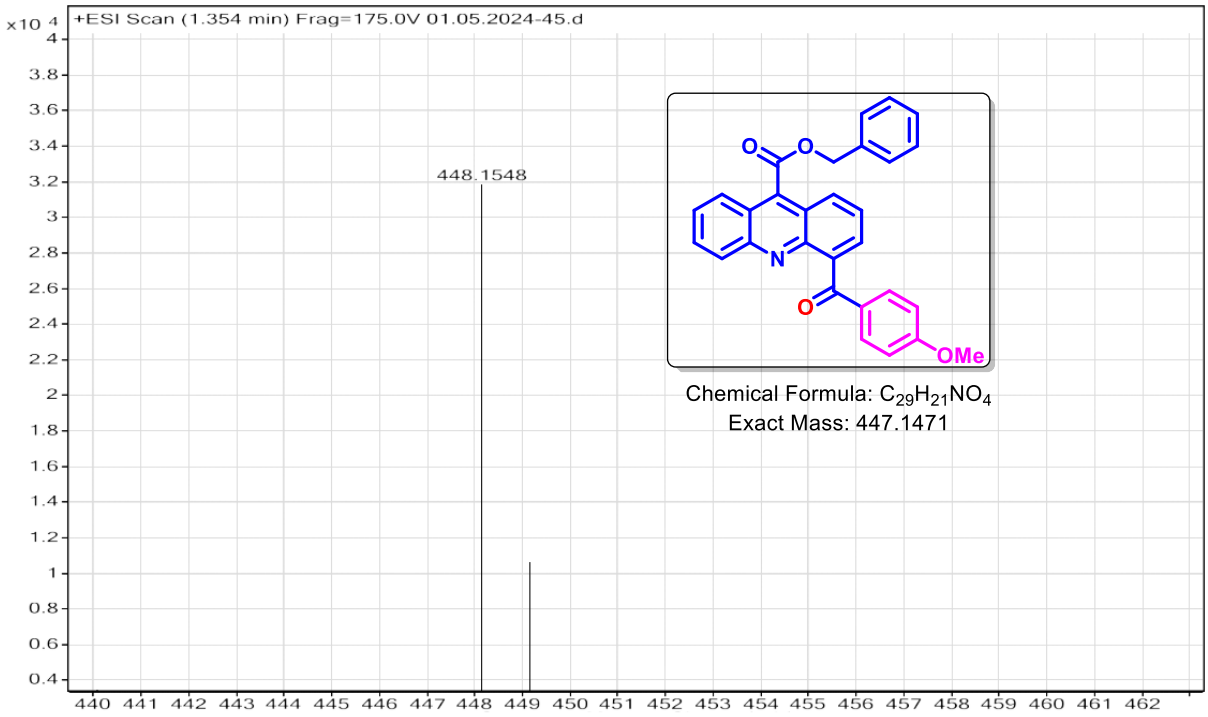
+ESI Scan (1.354 min) Frag=175.0V 01.05.2024-45.d
x10 4
448.1548
OMe
Chemical Formula: C29H21NO4
Exact Mass: 447.1471

Benzyl 4-(thiophene-2-carbonyl)acridine-9-carboxylate (4v):

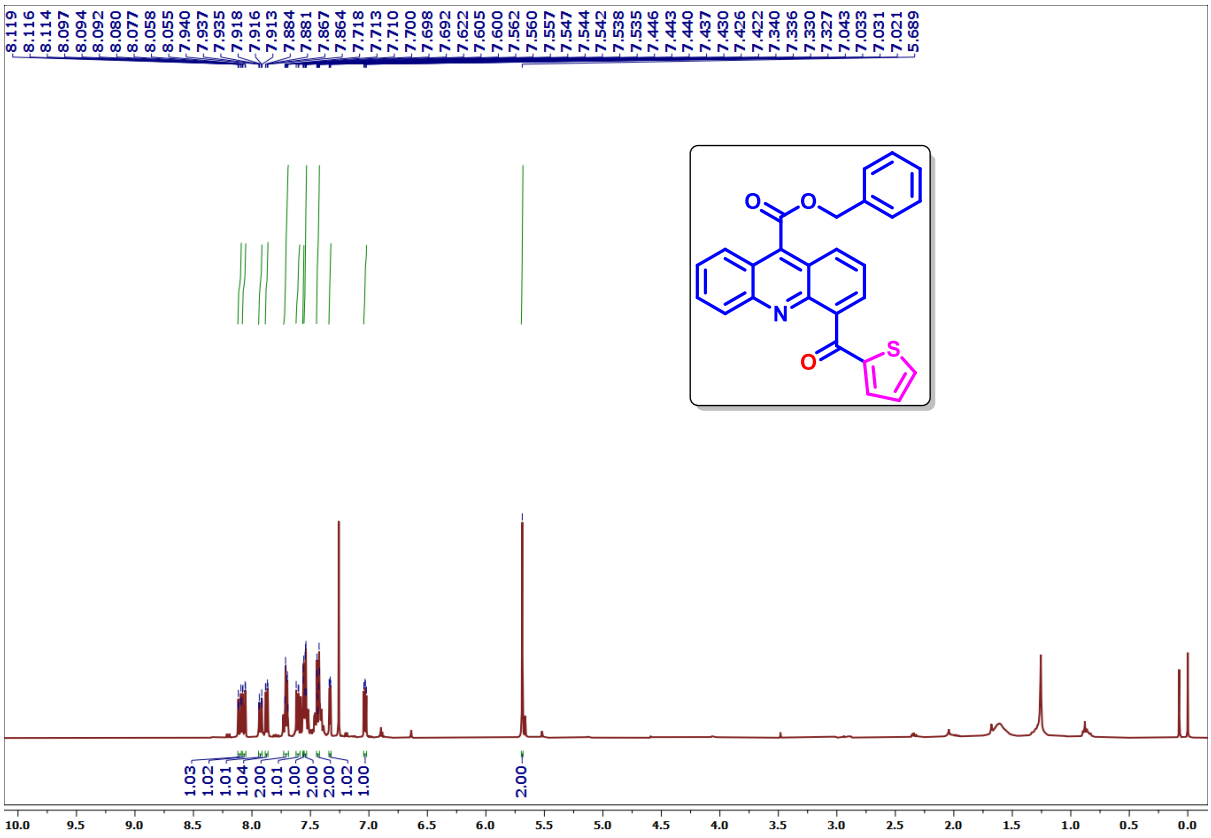

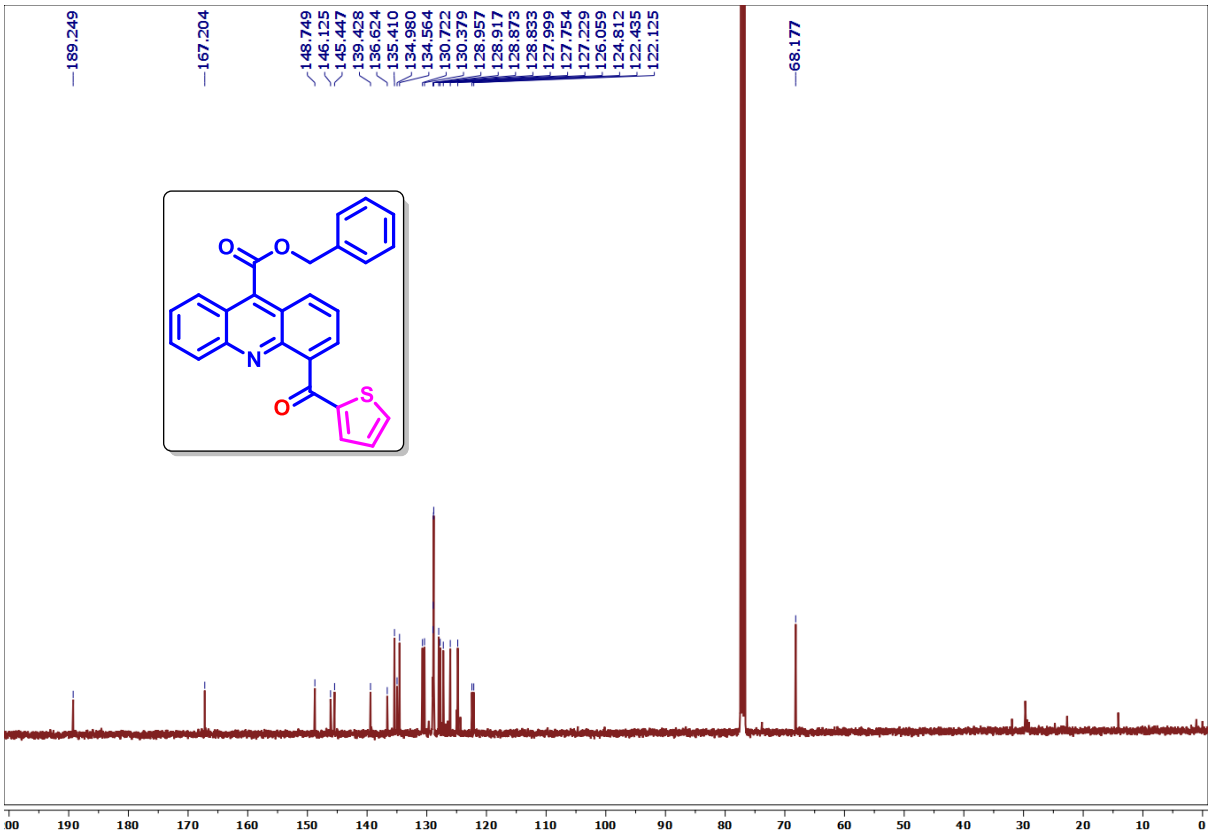

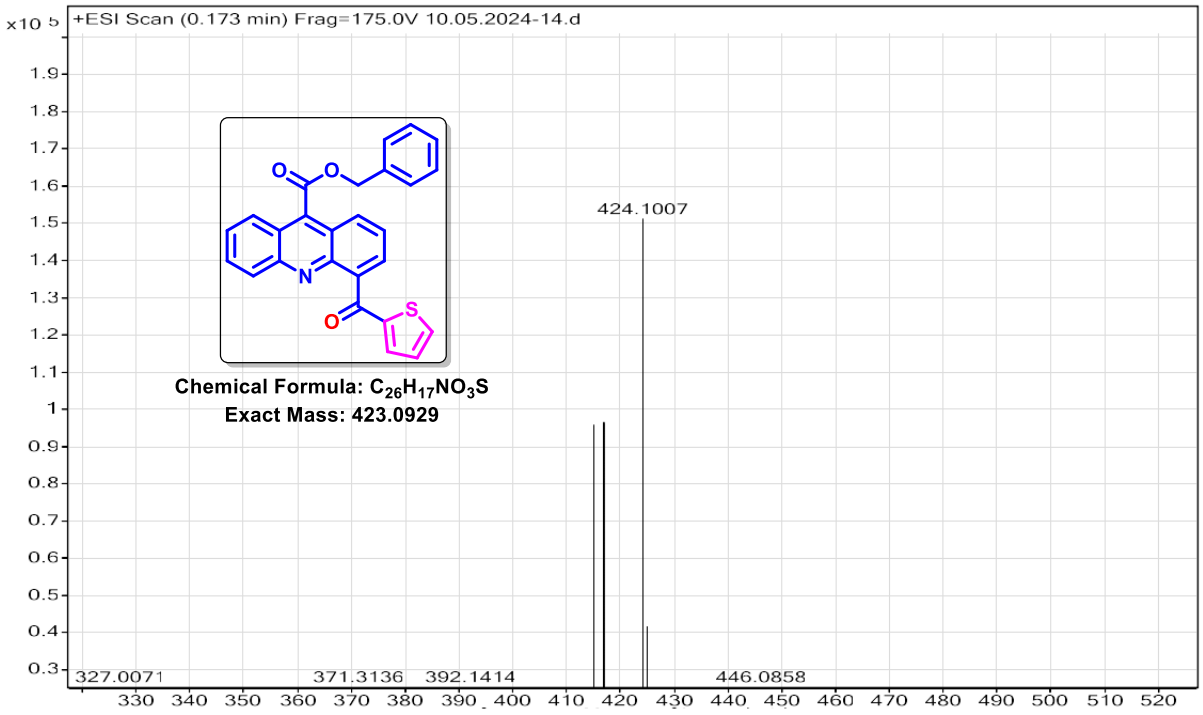

HRMS spectrum for control experiment intermediate (5):

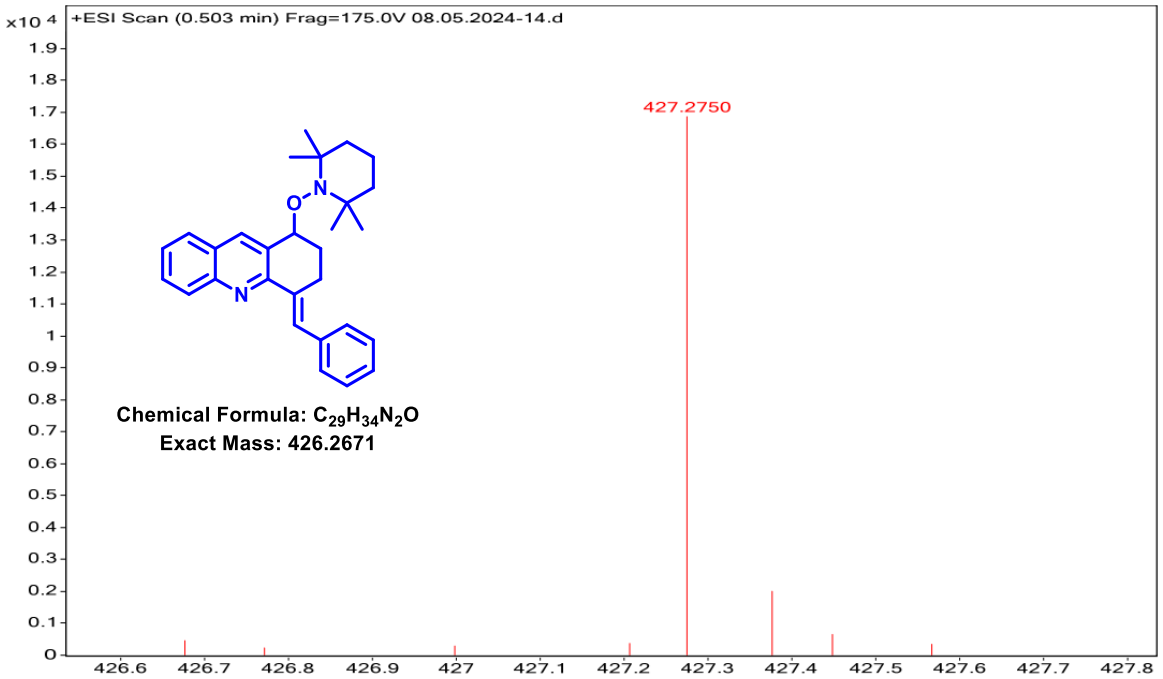

HRMS spectrum for control experiment intermediate (6):

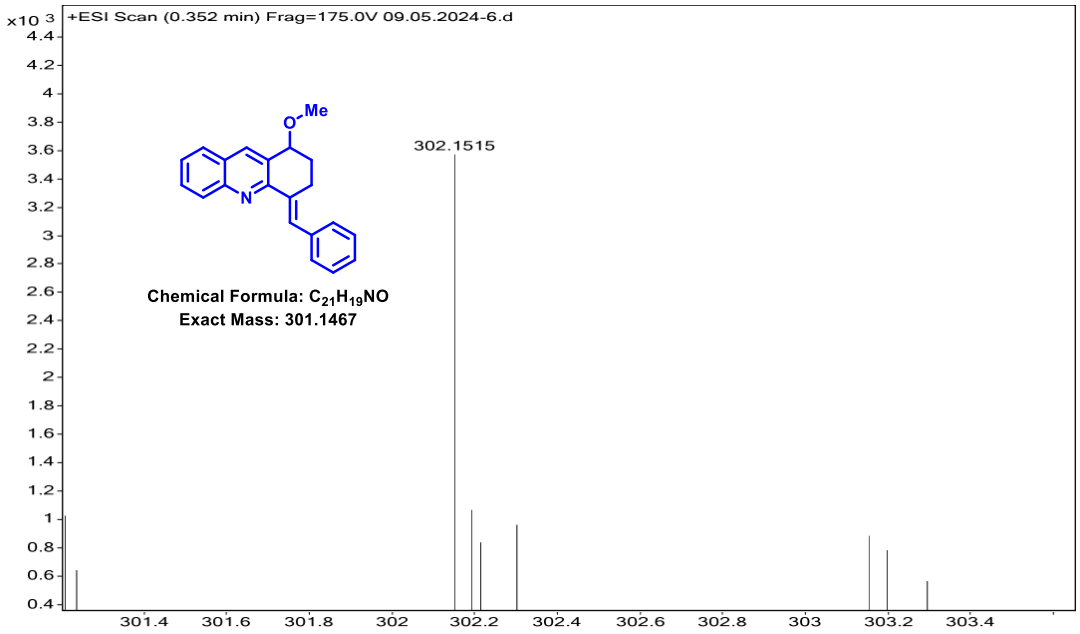

HRMS spectrum for control experiment intermediate (7):

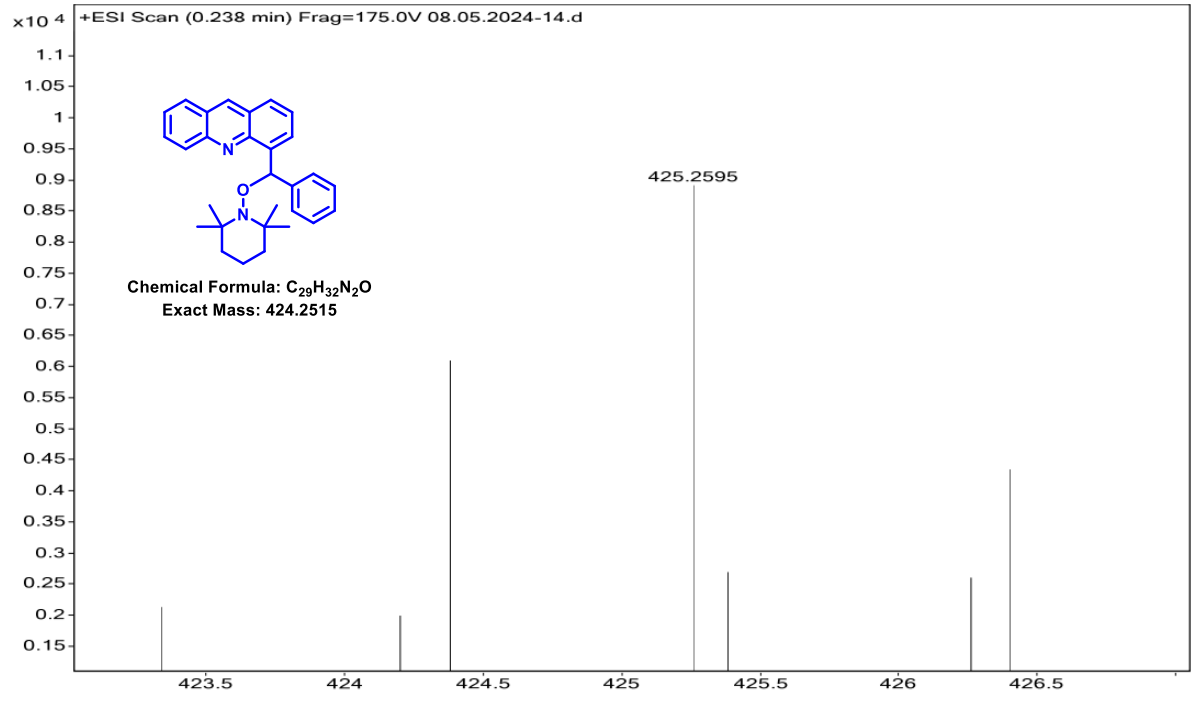

HRMS spectrum for control experiment intermediate (8):

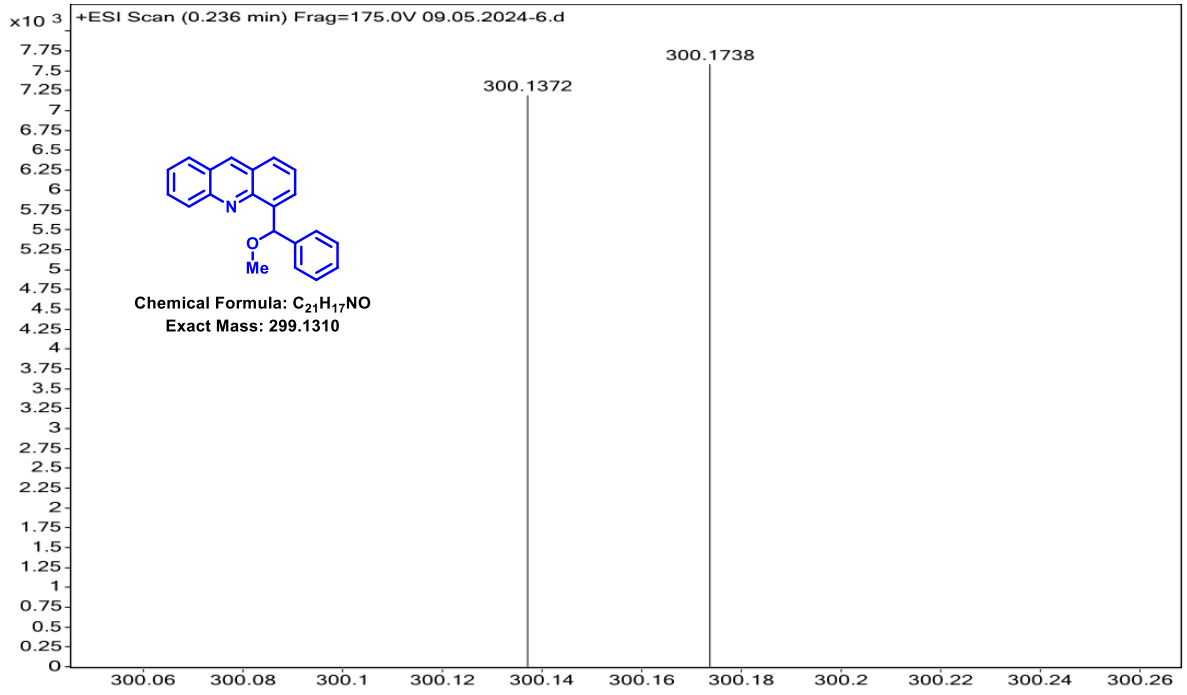

HRMS spectrum for control experiment intermediate (9):

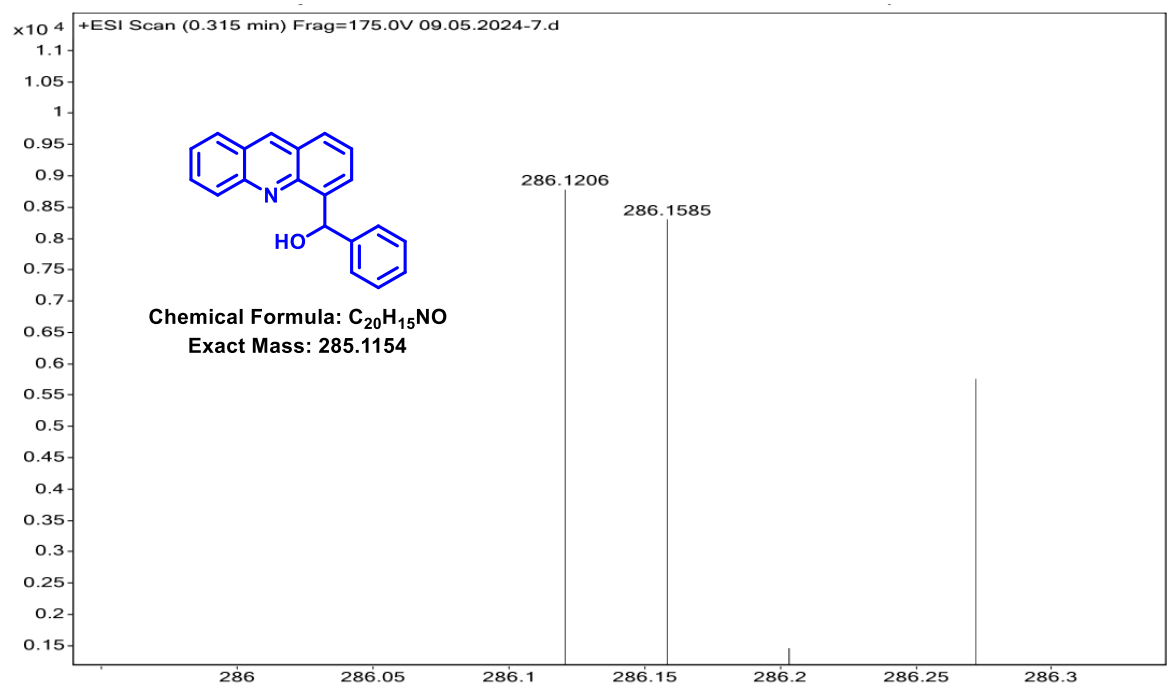

CHAPTER-IV

Chapter-IV

One-Pot Synthesis of functionalized Carbazoles and β-Carbolines *via* Diethyl Azodicarboxylate mediated dehydrogenative aromatization in Deep Eutectic Solvent

Abstract

Carbazoles and β-Carbolines structures can be found in a diverse array of natural and synthetic molecules and display a wide range of biological activities. In addition, many carbazoles exhibit photo-physical properties, allowing them to be employed in the development of fluorescent materials. In recognition of the diverse biological functions associated with carbazole and β-carbolines, various synthetic methods are reported in the literature for the construction of carbazole architectures. Considering the biological, material importance of these molecules in this chapter we envisaged a green protocol for one-pot synthesis of carbazoles and β-carbolines using Diethyl azodicarboxylate (DEAD) as dehydrogenating agent in Deep Eutectic Solvent (DES).

4.1 Introduction

Carbazole, a fused [6-5-6] tricyclic system with nitrogen in the five-membered ring constitutes the core structure of a diverse array of alkaloids (**Figure 4.1**) found in many natural and pharmaceutical ingredients.[1] These alkaloids exhibit a plethora of bioactivities and therapeutic properties, including antitumor,[2] antiviral,[3] psychotropic,[4] anti-Alzheimer's,[5] anti-inflammatory,[6] antibiotic,[7] anti-oxidative,[8] anti-TB activities.[9] Furthermore many derivatives of carbazole are known to show remarkable electrical,[10] thermal,[11] optical,[12] organic light emitting properties,[13] and proved as important functional group in the development of organic photo/electroluminescent materials and organic solar cells.[14]

β-Carboline is another intriguing alkaloid (an indole-based heterocyclic moiety/a fused [6-5-6] tricyclic system with a nitrogen in the five-membered ring and a 1*H*-pyrrolo[2,3-c] pyridine system) found in various pharmaceutical drugs and natural products[15] (**Figure 4.1**). Specifically, aromatic β-carboline derivatives exhibit excellent biological properties, such as antitumor,[16] anti-tubercular,[17] anti-viral activities,[18] and anti-malarial.[19] In addition, some β-carboline derivatives can also inhibit acetylcholinesterase and human monoamine oxidase and are useful in the treatment of neurodegenerative disorders (Alzheimer's and Parkinson's disease).[20]

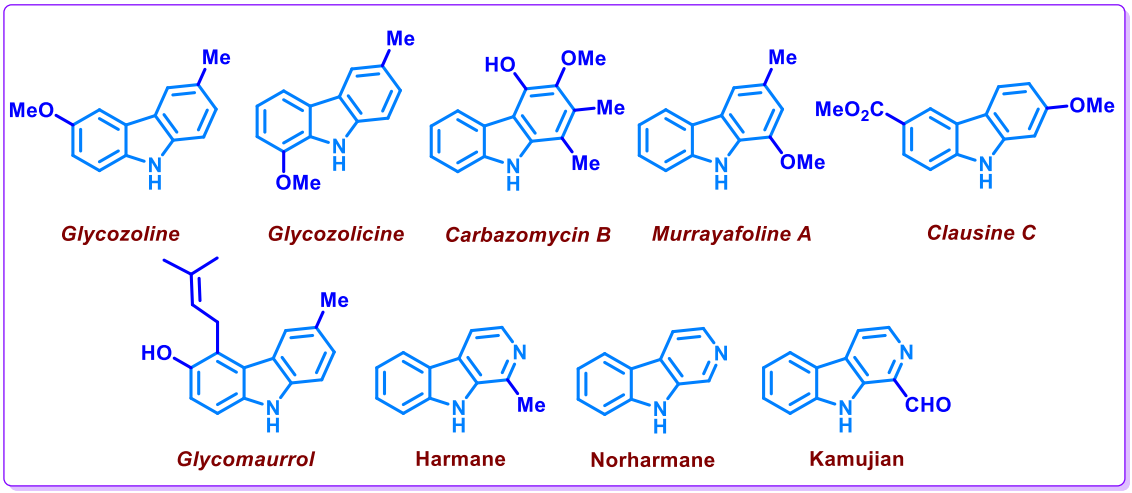

Figure 4.1 Bioactive natural carbazole and β-carboline compounds

4.2 Literature Reports

Several strategies are available for the synthesis of carbazoles *via* C–C or C–N coupling/cyclization reactions in the presence of transition metals such as Iron,[21] palladium,[22] rhodium,[23] copper [24] and iridium [25] or without transition metal catalyst,[26] in the presence of visible light,[27] and electrochemical anodic oxidation.[28] Besides these sophisticated methods,

aromatisation of the Fischer-Borsche ring approach for carbazole synthesis is an established process. This involves the condensation of arylhydrazine with cyclohexanone followed by oxidative aromatization to yield the corresponding carbazole. Recently this method has been reported under modified conditions using a low melting mixture as catalyst and reaction medium,[29] and reagents like Pd/C,[30] $CuCl_2$/DMSO,[31] I_2/DMSO,[32] DDQ,[33] V_2O_5[34a] NMP/O_2[34b] (**Figure 4.2**) for dehydrogenative aromatization of tetrahydrocarbazoles to produce carbazoles. While existing methodologies offer efficient access to carbazoles, some suffer from limitations such as the requirement for expensive catalysts with high loading, elevated reaction temperatures, and the need for additional protection of the central ring nitrogen.

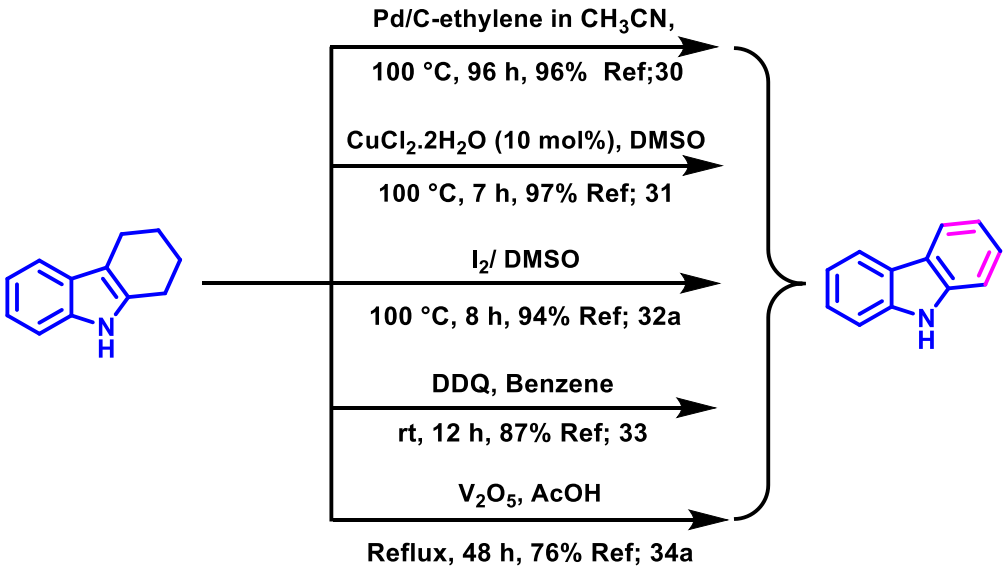

Figure 4.2 Previous reports for the dehydrogenative aromatisation of tetrahydrocarbazole

β-Carboline, like carbazoles, possess significant biological potential. This has driven the development of various methods for synthesizing their derivatives. A general method used for this purpose is Pictet-Spengler reaction [35] of tryptamine derivatives and an aldehyde followed by dehydrogenation to access β-carboline. Often, oxidative dehydrogenation requires special conditions like elemental sulfur,[36] palladium on carbon,[37] MnO_2,[38] *n*Bu_4NBr-CHP,[39] DDQ,[40] trichloroisocyanuric acid,[41] $PhI(OAc)_2$,[42] *N*-chlorosuccinimide,[43] IBX,[44a] (**Figure 4.3**) I_2/DMSO[44b] and DBN/Air,[45a] $FeCl_3$,[45b] and activated carbon.[45c] In addition to these, NMP/O_2,[45d] trityl tetrakis-(pentafluorophenyl)-borate catalysed SET,[46] water-mediated[47] one-pot synthesis of β-carboline were reported. However, these methods require longer times for the completion of the reaction or special catalyst/starting material.

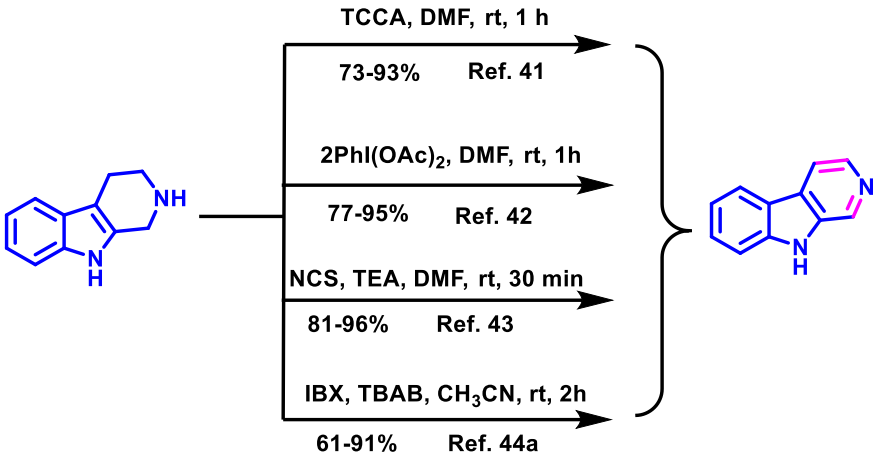

Figure 4.3 Previous reports for the dehydrogenative aromatisation of tetrahydro-β-carboline

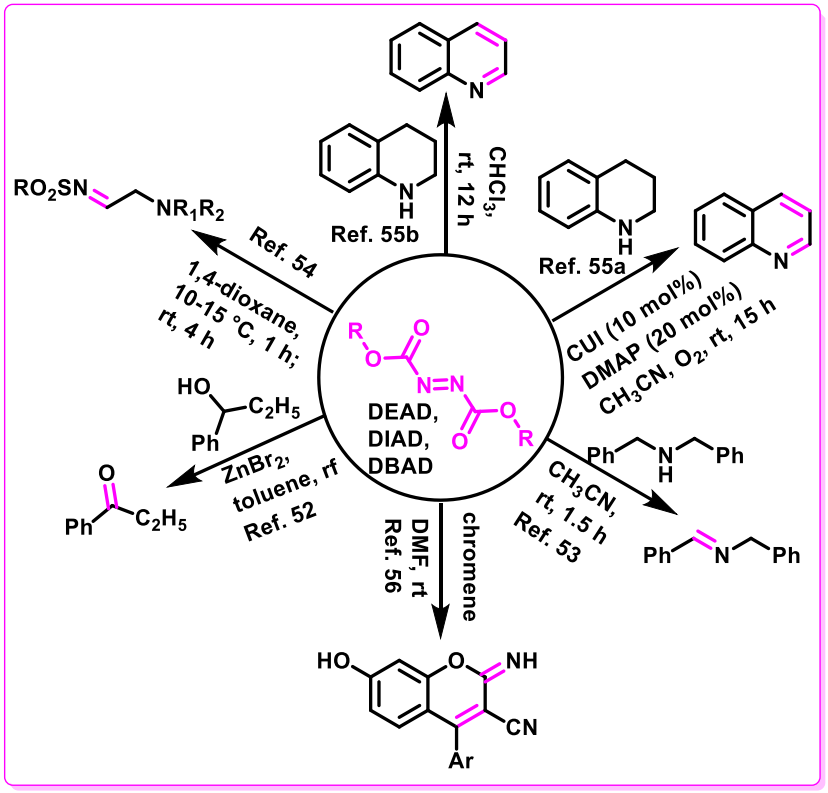

Figure 4.4 Previous reports for DEAD as dehydrogenating agent

Dialkyl azodicarboxylates such as diethyl azodicarboxylate (DEAD), diisopropyl azodicarboxylate (DIAD), and di-*tert*-butyl azodicarboxylate (DBAD) are well-known in the Mitsunobu chemistry. [48,49] Beyond this, the electrophilic nature of azo dicarboxylates allows them to participate in reactions like amination,[50] cycloaddition reactions [51] as dienophiles. Apart from this, the azodicarboxylates also known to participate in dehydrogenation reactions

such as dehydrogenation of alcohols,[52] secondary/tertiary amines, [53,54] tetrahydroquinolines,[55] 2-amino-3-cyano 4*H*-chromenes (**Figure 4.4**).[56]

4.3 Present study

In continuation with our interest in the development of green methods, herein we report an efficient, simple route for one-pot synthesis of carbazole and β-carbolines using Deep Eutectic Solvent (DES) as reaction medium and Diethyl azodicarboxylate (DEAD) as the dehydrogenating agent (**Figure 4.5**). The advantage of this method is to avoid strong oxidizing agents under eco-friendly/green conditions to achieve both the title compounds (i.e. functionalized carbazoles and β-Carbolines).[57]

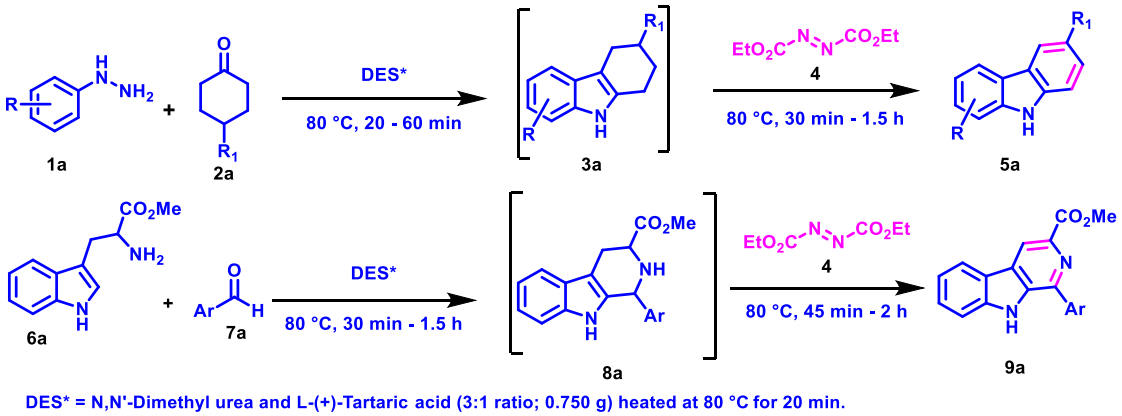

Figure 4.5 Present work for the dehydrogenative aromatisation of tetrahydrocarbazole and tetrahydro-β-carboline

4.4 Results and Discussion

Building upon our prior success in activating C(sp^3)–H bonds of 1,2,3,4-tetrahydroacridine for C–N bond formation, [50b] we aimed to react 1,2,3,4-tetrahydrocarbazole (1 mmol) with diethyl azodicarboxylate (2 mmol) at 80 °C under *N,N'*-dimethyl urea (DMU) and L-(+)-tartaric acid (L-(+)-TA) (3:1 ratio; heated at 80 °C for 20 min) as DES* to get hydrazine substituted tetrahydrocarbazole. Surprisingly, the reaction led to the direct aromatization of tetrahydrocarbazole, yielding carbazole itself in an exceptional yield of 96% within just 30 min (**Scheme 4.1**). Spectroscopic analysis using ^{1}H, ^{13}C-NMR, and HRMS confirmed the successful formation of the carbazole.

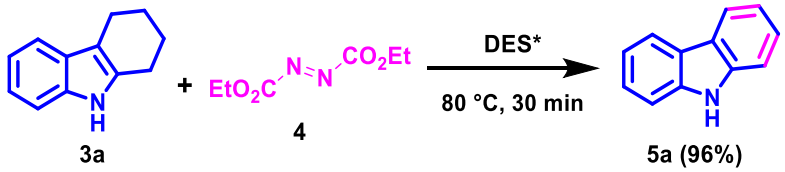

Scheme 4.1 Dehydrogenation of 1,2,3,4-tetrahydrocarbazole **5a**

To check the applicability of DES* as a reaction medium for one-pot synthesis of carbazole, phenylhydrazine (1 mmol) was treated with cyclohexanone (1 mmol) in DMU/L-(+)-TA at 80 °C for 30 min to give the 1,2,3,4-tetrahydrocarbazole (**3a**; complete conversion checked with TLC). To the same reaction pot, DEAD was added and heating was continued for 30 min. to deliver the dehydrogenated product i.e., carbazole (**5a**) in excellent yield (96%) (Scheme 4.2). Different combinations of DES and reaction temperature were scrutinized to establish the best reaction conditions for the one-pot synthesis of carbazole (**5a**). Among all, a combination of DMU/L-(+)-TA in a 3:1 ratio at 80 °C was found to be the best suitable for the conversion of hydrazine into carbazole. Though the other combinations of DESs were able to give the desired product, the yields were poor and the reaction time was more for the completion of the reaction (**Table 4.1**; entries 2-11). In addition, it was observed that the yield of (**5a**) is temperature-dependent. Lower reaction temperatures resulted in a significant decrease in yield, while elevated temperatures (beyond 90 °C) did not lead to any further change in the yield (**Table 4.1**; entries 12-13). Additionally, the influence of the DMU+L-(+)-TA (DES) ratio on reaction outcome was also investigated. Interestingly, a decrease in the product yield was observed with decreased amounts of L-(+)-TA in the DES (**Table 4.1**; entry 14-15). This suggests a specific role of L-(+)-TA beyond acting as a reaction medium. To enquire about the effect of the azodicarboxylates, the reaction was repeated at 80 °C with diisopropyl azodicarboxylate (DIAD), and di *tert*-butyl azodicarboxylate (DBAD) instead of DEAD. This substitution resulted in a longer reaction time and a decrease in the yield of corresponding carbazole (**5a**) to 70% and 65% (**Table 4.1**; entry 18-19).

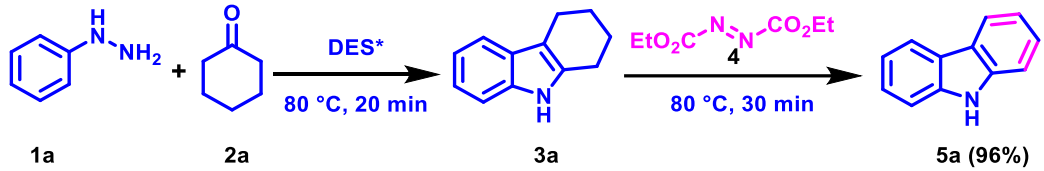

Scheme 4.2 One-pot synthesis of carbazole **5a**

Table 4.1 Optimization of reaction condition[a]

S. No.	DES	Temp(°C)[b]	Time (h) 1st step	Time (h) 2nd step	yield (%)[c]
1	**DMU + L-(+)-TA (3:1)**	**80**	**20 min**	**30 min**	**96**
2	ChCl + oxalic acid (1:2)	80	3	3	30
3	ChCl + thio Urea (1:2)	80	2	3	10
4	ChCl + citric acid (1:2)	80	2	3	10

5	ChCl + DMU (1:2)	80	3	4	20
6	ChCl + Urea (1:2)	80	3	6	ND
7	ChCl + p-TSA (1:2)	100	3	6	40
8	ChCl + ZnCl2 (1:2)	80	3	6	40
9	Citric acid + DMU	80	4	5	40
10	Urea + L-(+)-TA	80	2	4	50
11	ChCl + L-proline (1:2)	80	3	5	ND
12	DMU + L-(+)-TA (3:1)	70	4	3	60
13	DMU + L-(+)-TA (3:1)	90	2	2	80
14	DMU + L-(+)-TA (2:1)	80	4	3	50
15	DMU + L-(+)-TA (1:1)	80	4	6	30
16	ChCl + Glucose (1:2)	80	4	6	ND
17	Glucose + L-proline (1:2)	80	6	5	20
18[d]	DMU + L-(+)-TA (3:1)	80	20 min	4	70
19[e]	DMU + L-(+)-TA (3:1)	80	20 min	4	65

[a]Reaction condition: 1a (1.0 mmol), 2a (1.0 mmol), 4 (DEAD) (2.0 mmol), DES is formed by heating the hydrogen bond donor and hydrogen bond acceptor. [b]Temperature for steps 1 and 2. [c]Isolated yield. [d]1a (1.0 mmol), 2a (1.0 mmol), DIAD (2.0 mmol). [e]1a (1 mmol), 2a (1.0 mmol), DBAD (2.0 mmol).

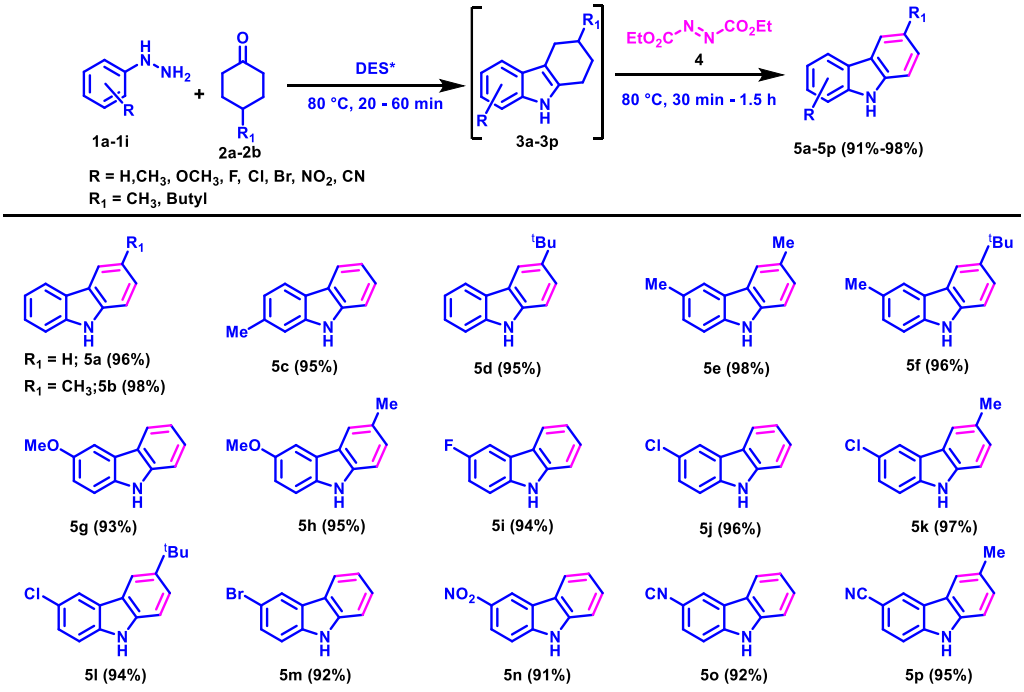

Scheme 4.3 One-pot synthesis of carbazole derivatives (**5a-5p**)

Further, the substrate scope and functional group tolerance were investigated under the established conditions for one-pot synthesis of carbazoles using substituted phenylhydrazines and cyclohexanones. The developed protocol works well with electron-donating and electron-withdrawing groups on the aromatic ring of the hydrazine producing various carbazoles in high yields (**Scheme 4.3**). It is noteworthy to mention that all the substrates are equally reactive in the first step. However, faster reaction rates were observed with the electron-donating groups. In contrast, longer reaction times were needed for NO_2, CN substituted hydrazine's due to the strong deactivation effect on the aromatic ring (**5n**-**5o**). Moreover, di-substitution on both the benzene ring with the competitive substituents also suited well to afford the desired product **5p** with 95% yield. This sustainable protocol demonstrates its utility in the synthesis of naturally occurring carbazole alkaloids like 3-methylcarbazole (**5b**),[58]glycozoline (**5h**) [59] with excellent yields and significantly reduced reaction time.

Encouraged by the above method, we shifted our attention to applying the same strategy for the synthesis β-carbolines *via* dehydrogenative aromatization (**Scheme 4.4**). To initiate one-pot synthesis of β-carboline, L-tryptophan methyl ester (**6**) and benzaldehyde (**7a**) were heated in DES* at 80 °C for 30 min to afford 1,2,3,4-tetrahydro-β-carboline (**8a**) *via* Pictet-Spengler reaction. To the same reaction pot diethyl azodicarboxylate was added and heating was continued for 45 min to yield β-carboline (**9a**) in 94%. Later, the substrate scope was tested with many aromatics and heteroaromatic aldehydes with electron-donating and withdrawing groups to offer corresponding β-carbolines (**9b-9i**) in excellent yields (91%-96%).

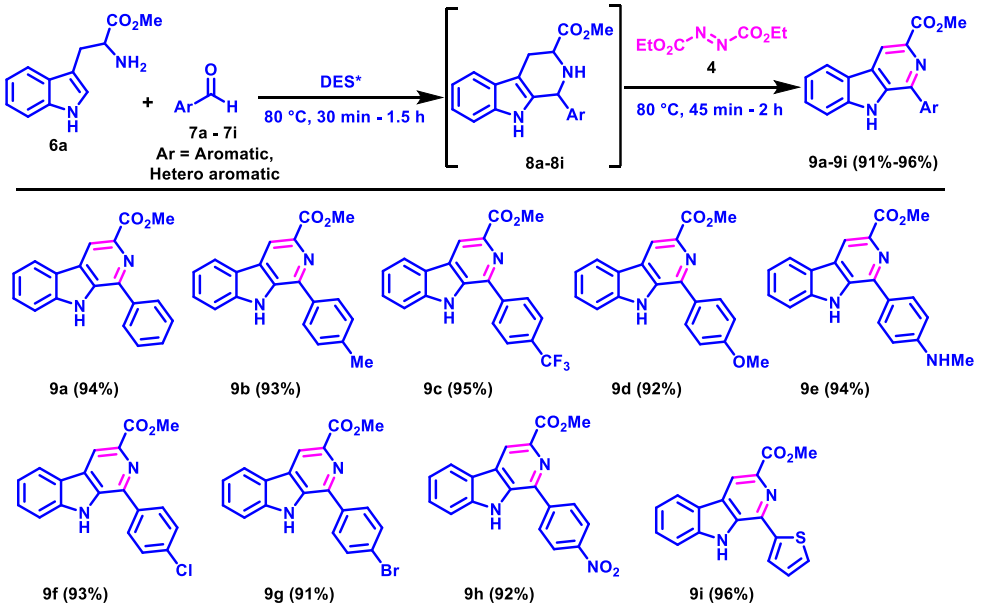

Scheme 4.4 One-pot synthesis of β-carboline (**9a-9i**)

We continued the dehydrogenative aromatization strategy for *N*-alkylated tetrahydrocarbazoles and tetrahydroquinolone and isoquinoline under standard reaction conditions to obtain corresponding fully aromatic products in good to excellent yields (90%-94%) (**Schemes 4.5 and 4.6**, **11a-11g** and **14-15**). It is interesting to note that the unsaturated systems like allyl and propargyl groups sustained the reaction giving the desired products in 92% (**11c**) and 93% (**11d**) respectively.

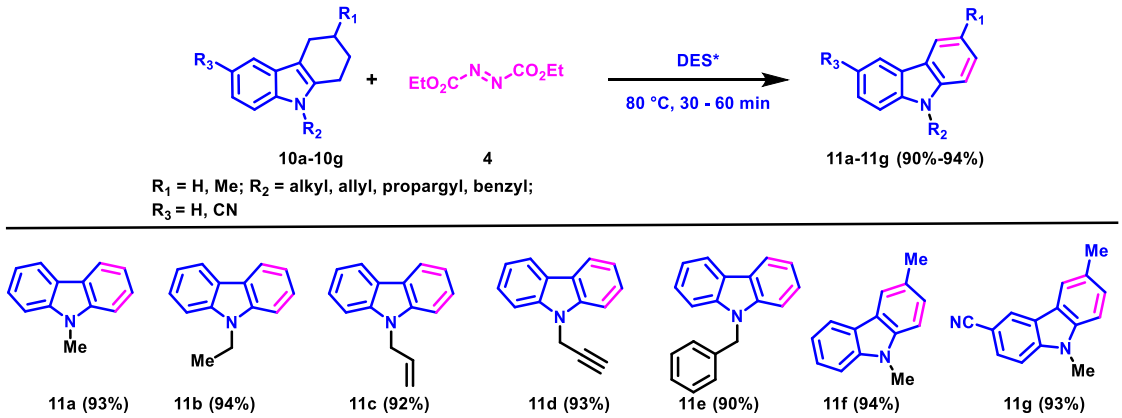

Scheme 4.5 Dehydrogenative aromatisation of *N*-substituted tetrahydrocarbazoles

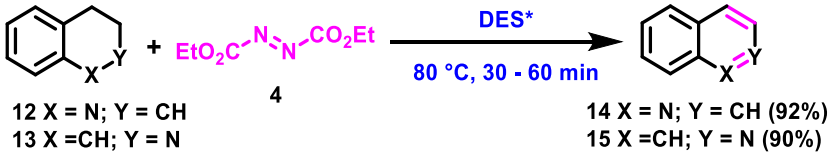

Scheme 4.6 Dehydrogenative aromatisation of 1,2,3,4-tetrahydroquinoline (**12**) and 1,2,3,4-tetrahydroisoquinoline (**13**)

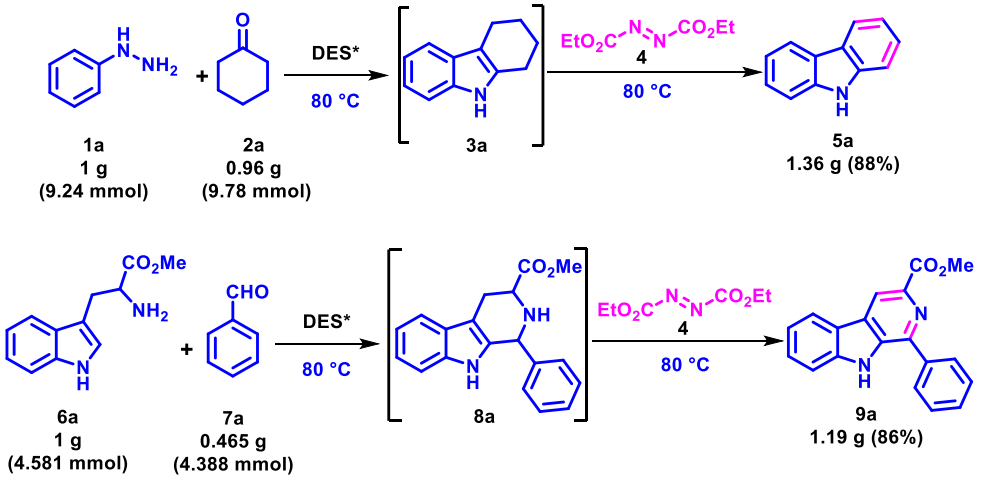

Scheme 4.7 Gram scale synthesis of compounds 5a and 9a under optimized condition

The scalability of the dehydrogenation protocol was effectively demonstrated by the gram scale synthesis of (**5a)** and (**9a**), which yielded 88% and 86% respectively under optimized reaction conditions (**Scheme. 4.7**). Also, the by-product i.e. diethyl hydrazine-1,2-dicarboxylate was recovered to the maximum extent. [55b]

To assess the reusability of DES*, the reaction mixture was subjected to liquid-liquid extraction to recover DES* followed by evaporation of the aqueous layer.[60] The recovered DES* was then vacuum-dried and reused for a subsequent run. Notably, the DES* remained stable after four consecutive runs, consistently delivering the desired product **5a** with good yield (above 85% after the 4th cycle) (**Figure 4.6**).

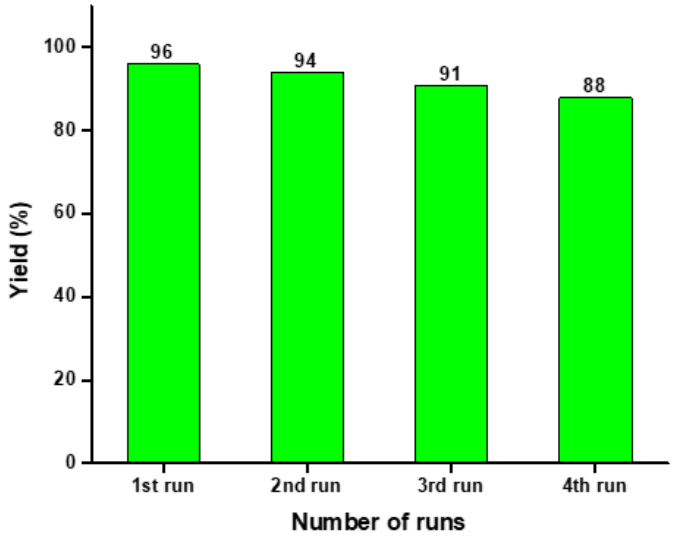

Figure 4.6 Bar graph showing the reusability of DES* for the synthesis of compound **5a**.

Having demonstrated the synthetic utility of diethyl azodicarboxylate for effective dehydrogenative aromatization of tetrahydrocarbazoles and tetrahydro-β-carbolines in DES as a reaction medium, the next task was to reduce the stoichiometric amounts of DEAD. To address this, the procedure reported by Jung et al.[55a] was adopted for the regeneration of DEAD under aerobic conditions. Thus, compounds (**3a** and **6a**; 1 mmol) were reacted with DEAD (**4**; 20 mol%) in the presence of CuI/DMAP (a co-catalyst system), and O_2 in DMU/L-(+)-TA at 80 °C to give the corresponding products **5a** and **9a** in good yields (92% and 91%) (**Scheme 4.8**). Other attempts to improve the reaction conditions (**Table 4.2**) were futile.

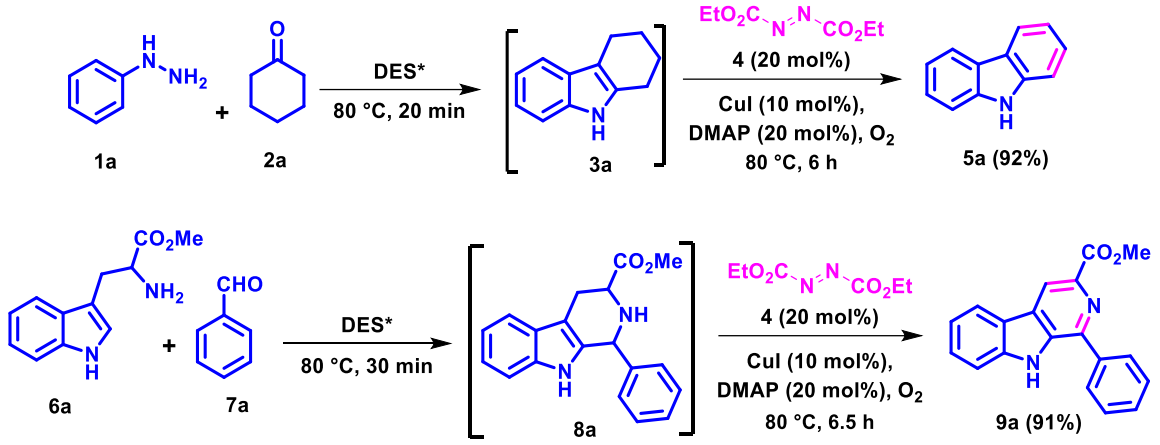

Scheme 4.8. A catalytic approach to regenerate DEAD

Table 4.2 Optimisation of reaction condition for regeneration of diethyl azodicarboxylate [a].

S.No.	Cu source (10 mol%)	Additive (20 mol%)	Time	Yield (%)[b]
1[c]	-	-	20 min	96
2	CuI	DMAP	6 h	92
3[d]	CuI	DMAP	12 h	85
4[e]	CuI	DMAP	16 h	70
5	CuBr	DMAP	10 h	78
6	CuI	1,10-Phenanthroline	9 h	84
7	CuI	DABCO	11 h	72
8	CuI	K_2CO_3	10 h	45

[a]Reaction condition: 1a (1.0 mmol), 2a (1.0 mmol) 4 (20 mol%), DES* is prepared by heating the hydrogen bond donor and hydrogen bond acceptor at 80 °C. [b] isolated yield. [c] 4 (2.0 mmol). [d] 4 (15 mol%). [e] (10 mol%).

4.5 Proposed mechanism

Based on previous reports, [53,55b] we proposed mechanisms for one-pot synthesis of carbazole using DEAD as a dehydrogenating agent, facilitated by deep eutectic solvent (**Figure 4.7**). Initially the DES* is formed through H-bonding between the carbonyl group of DMU and hydroxyl groups of L-(+)-TA. In the 1st step phenylhydrazine and cyclohexanone undergo a Fischer indole-type reaction in the presence of DES* leading to the formation 1,2,3,4-tetrahydrocarbazole (**3a**). Then in the 2nd step DEAD (**4**) acts as a dehydrogenating agent, converting tetrahydrocarbazole (**3a**) into aromatic carbazole (**5a**). According to mechanism, the process proceeds through the formation of triazane intermediate, [53,55b] facilitated by the

DES* interacting with the oxygen of the ester carbonyl through H-bonding and enhancing the electrophilicity of the N=N of DEAD. This promotes the nucleophilic attack by the lone pair of electrons of nitrogen of tetrahydrocarbazole, forming the triazane intermediate (**I**). This intermediate then undergoes an intramolecular elimination and subsequent proton transfer to produce an intermediate (**III**) and diethyl 1,2-hydrazinedicarboxylate. The resulting intermediate (**III**) undergoes the second dehydrogenation to provide aromatized carbazole (**5a**). There is a possibility for the dehydrogenation proceeding through electrophilic substitution of 1,2,3,4-tetrahydrocarbazole with DEAD to form intermediate (**Ia**) which undergo intramolecular proton transfer to produce intermediate (**IIIa**) and diethyl 1,2-hydrazinedicarboxylate. The resulting intermediate (**IIIa**) undergoes a second dehydrogenation to provide carbazole (**5a**).

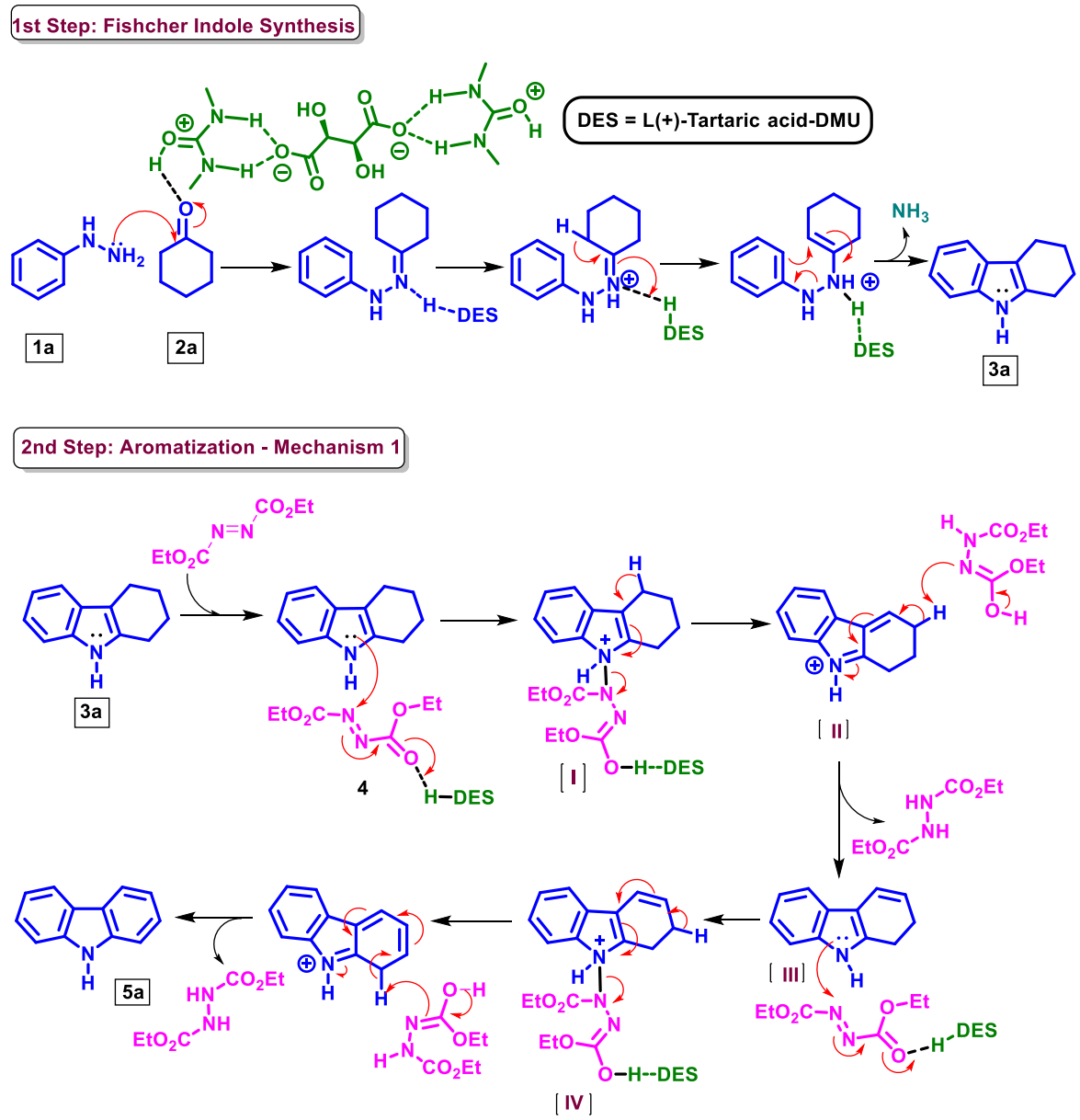

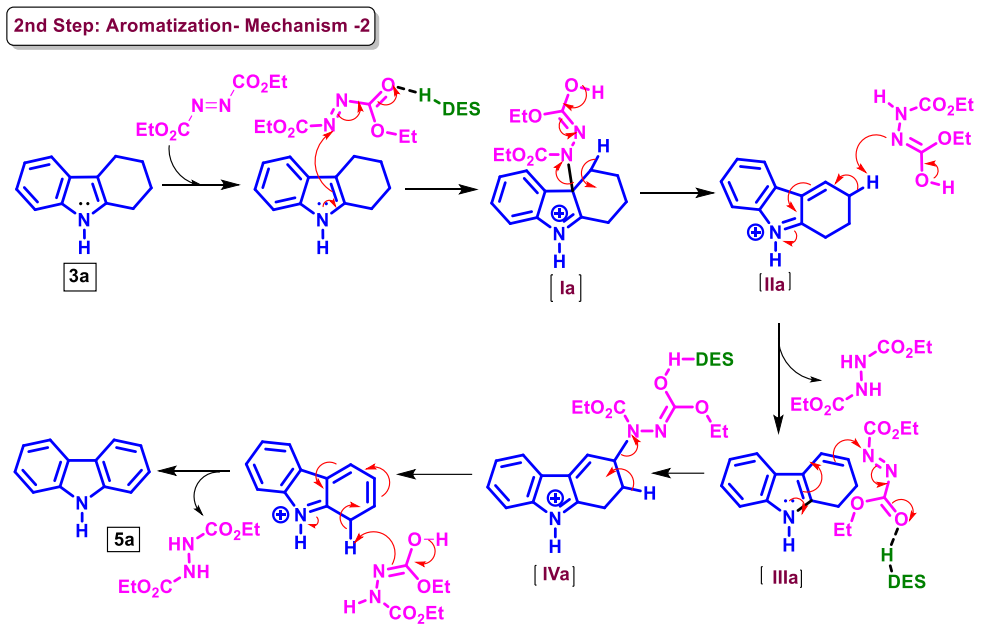

Figure 4.7 Proposed mechanism for one-pot synthesis of carbazole

Similarly, the one-pot synthesis of β-carboline using DEAD as a dehydrogenating agent can be explained by a two-step mechanism involving Pictet-Spengler cyclization and a triazane intermediate (**Figure 4.8**). First, DES is formed by heating DMU and L-(+)-Tartaric Acid. The DES* activates the carbonyl group of the aldehyde, allowing it to react with primary amine to form an imine (**I**). This imine then undergoes a Pictet-Spengler reaction to produce tetrahydro-β-carboline. In the second step, tetrahydro-β-carboline (**8a**) is dehydrogenated *via* a triazane intermediate (**II**). This intermediate is generated by the addition of activated DEAD (**4**) to the amine of tetrahydro-β-carboline. The triazane (**II**) undergoes elimination and proton transfer, resulting in the formation of an imine derivative (**IV**) and diethyl 1,2-hydrazinedicarboxylate. Finally, tautomerization of the imine derivative (**IV**) leads to intermediate (**VI**), which then undergoes second dehydrogenation to yield the aromatized β-carboline (**9a**).

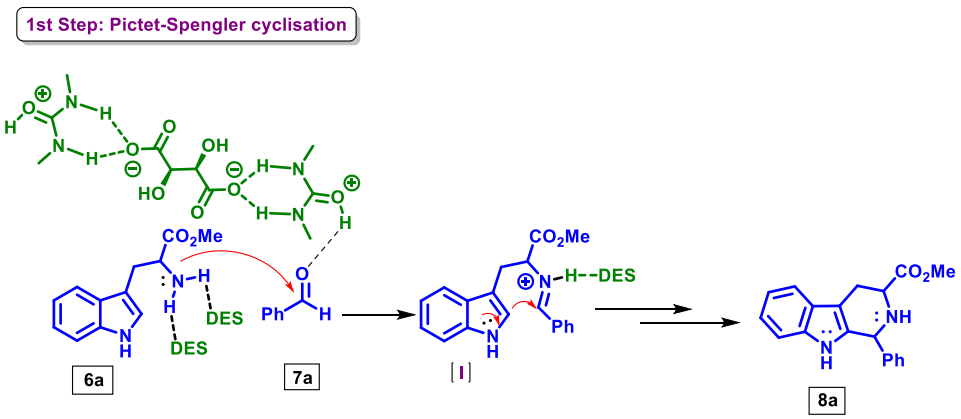

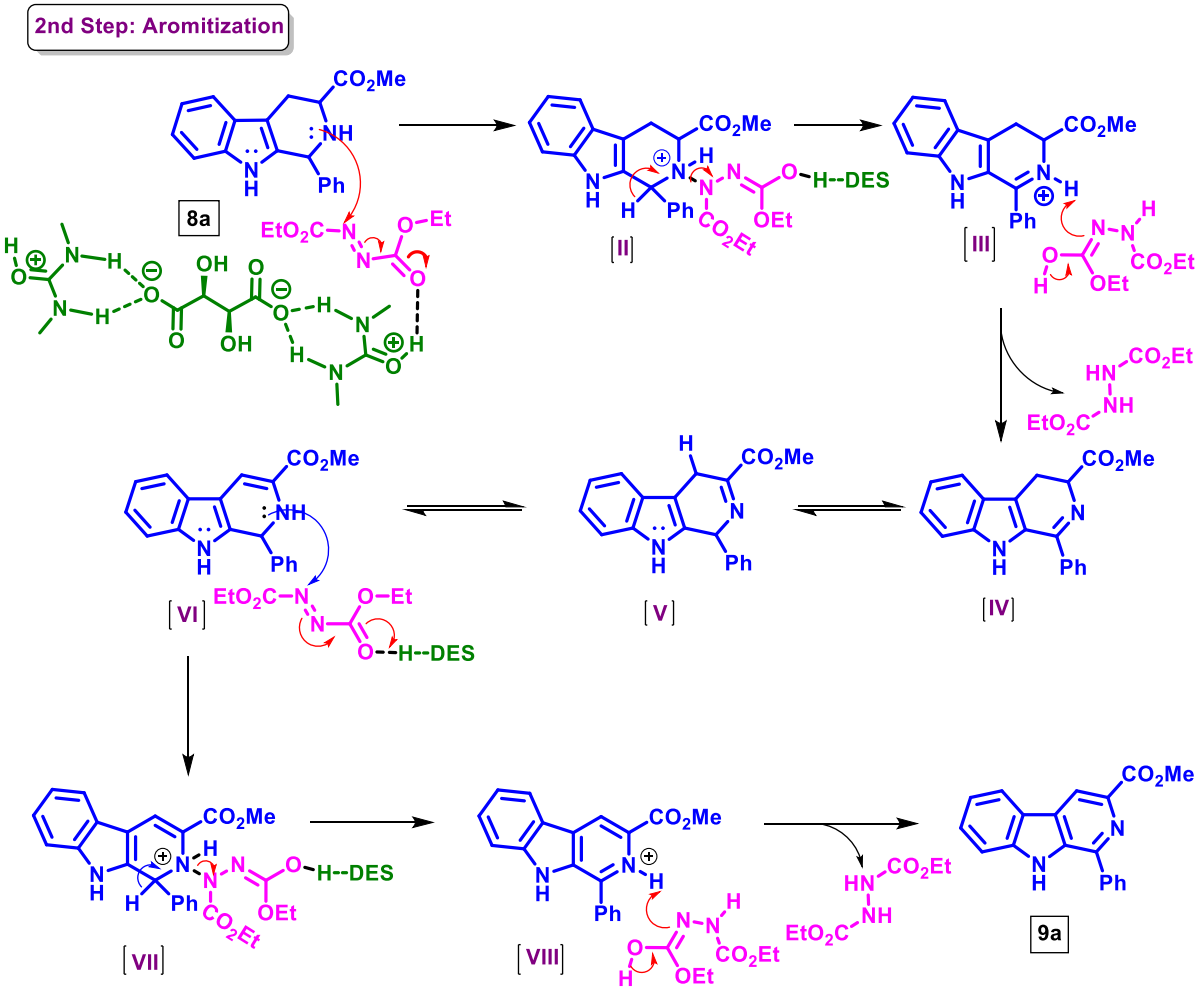

Figure 4.8 Proposed mechanism for one-pot synthesis of β-carboline

4.6 Conclusions

In conclusion, we have demonstrated a simple and efficient one-pot method for the synthesis of carbazoles and β-carbolines derivatives. The key to success lies in the strategic utilization of a combination of readily available diethyl azodicarboxylate and a sustainable Deep Eutectic Solvent. This method gave a library of title compounds with good to excellent yields.

4.7 Experimental section

4.7.1 General procedure for synthesis of compound (5)

Deep eutectic solvent was prepared by heating *N, N*'-dimethyl urea + L-tartaric acid (3:1 ratio) at 80 °C for 20 min (Total weight 0.75 g). To this, phenyl hydrazine (**1**) (1.0 mmol) and cyclohexanone (**2**) (1 equiv.) was added and heating continued for another 20 minutes at 80 °C to afford the 1,2,3,4-tetrahydrocarbazole (**3**). To the same reaction pot Diethyl azodicarboxylate (**4**) (2 equiv.) was added and continued heating. The completion of reaction was monitored by TLC. After completion of the reaction, the reaction mixture was cooled to room temperature.

Water was added to it and stirred for 10 min if a solid was obtained, the solid was collected through filtration or extracted by EtOAc. Crude products obtained were purified by column chromatography on silica gel using petroleum ether-ethyl acetate as eluent to give the compound.

4.4.2 General procedure for synthesis of compound (6)

To a stirred solution of (*tert*-butoxycarbonyl) tryptophan (1 g, 3.28) in MeOH (10 mL) at 0 °C, $SOCl_2$(4 eq.) was added dropwise, resulting reaction mixture stirred at 80 °C for 16 h. Reaction mixture was cooled to room temperature, concentrated under reduced pressure to afford the solid compound. The resulting solid was neutralized with 1N $NaHCO_3$ solution to afford compound (6).

4.7.3 General procedure for synthesis of compound (9)

Deep eutectic solvent was prepared by heating *N, N*'-dimethyl urea + L-tartaric acid (3:1 ratio) at 80 °C for 30 min. To this, compound (**6**) (0.46 mmol) and aromatic aldehyde (**7**) (1 equiv.) were added and heating continued for another 30 minutes at 80 °C to afford the 1,2,3,4-tetrahydro-β-carboline (**8**). To the same reaction pot Diethyl azodicarboxylate (**4**) (2 equiv.) was added and continued heating. The completion of reaction was monitored by TLC. After completion of the reaction, the reaction mixture was cooled to room temperature. Water was added to it and stirred for 10 min if a solid was obtained, the solid was collected through filtration or extracted by EtOAc. Crude products obtained were purified by column chromatography on silica gel using petroleum ether-ethyl acetate as eluent to give the compound.

4.8 Characterization data for synthesized compounds

9H-Carbazole (5a): Yield= 96%, white solid; M. P: 246-247 °C; **IR (KBr, cm^{-1})**: 3398, 3024, 2958, 1619, 1128, 1034, 932, 875; **^{1}H NMR (400 MHz, DMSO-*d6*) δ** 11.25 (s, 1H), 8.11 (dd, *J* = 7.6, 1.2 Hz, 2H), 7.49 (dt, *J* = 8.0, 1.2 Hz, 2H), 7.41 – 7.36 (m, 2H), 7.16 (ddd, *J* = 8.0, 7.2, 1.2 Hz, 2H). **^{13}C NMR (100 MHz, DMSO-*d6*) δ** 140.17, 125.96, 122.85, 120.59, 118.94, 111.38. **HRMS (ESI-MS):** m/z Calculated for $C_{12}H_9N$ $[M-H]^-$: 166.0662; Observed: 166.0673.

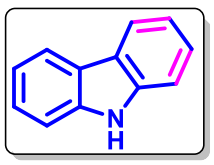

3-Methyl-9H-carbazole (5b): Yield= 98%, white solid; M. P: 206-207 °C (Lit. 205-210 °C)[61]; **IR (KBr, cm^{-1})**: **^{1}H NMR (400 MHz, DMSO-*d6*) δ** 11.08 (s, 1H), 8.05 (d, *J* = 7.6 Hz, 1H), 7.89 (s, 1H), 7.45 (d, *J* = 8.0 Hz, 1H), 7.37 (m, 1H), 7.34 (d, *J* = 7.2 Hz, 1H), 7.20 (d, *J* = 8.4 Hz, 1H), 7.12 (t, *J* = 7.6 Hz, 1H), 2.46 (s, 3H). **^{13}C NMR (100 MHz, DMSO-*d6*) δ** 140.42, 138.40, 127.56, 127.29, 125.77, 122.99, 122.67, 120.47, 120.35, 118.71, 111.31, 111.09, 21.56. **HRMS (ESI-MS):** m/z Calculated for $C_{13}H_{11}N$ [M-H]$^-$: 180.0818; Observed: 180.0816.

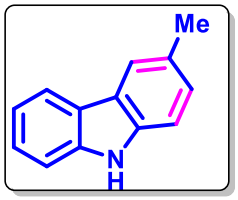

2-Methyl-9H-carbazole (5c): Yield= 95%, white solid; M. P: 242-242 °C (Lit. 245-247 °C) [62]; **IR (KBr, cm^{-1})**: **^{1}H NMR (400 MHz, DMSO-*d6*) δ** 11.15 (s, 1H), 8.08 (d, *J* = 8.0 Hz, 1H), 7.92 (d, *J* = 8.0 Hz, 1H), 7.51 (dt, *J* = 8.4, 1.2 Hz, 1H), 7.38 (ddd, *J* = 8.0, 7.2, 1.2 Hz, 1H), 7.19 (dt, *J* = 7.2, 1.2 Hz, 1H), 7.14 (ddd, *J* = 8.0, 7.2, 1.2 Hz, 1H), 7.07 (t, *J* = 7.2 Hz, 1H), 2.55 (s, 3H). **^{13}C NMR (100 MHz, DMSO-*d6*) δ** 140.25, 139.50, 126.41, 125.77, 123.24, 122.41, 120.64, 120.52, 119.10, 118.94, 118.08, 111.49, 17.46. **HRMS (ESI-MS):** m/z Calculated for $C_{13}H_{11}N$ [M-H]$^-$: 180.0818; Observed: 180.0816.

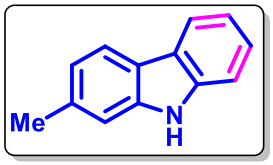

3-(tert-Butyl)-9H-carbazole (5d): Yield= 95%, white solid; M. P: 127-128 °C; **IR (KBr, cm^{-1})**: 3398, 3024, 2958, 1619, 1128, 1034, 932, 875; **^{1}H NMR (400 MHz, DMSO-*d6*) δ** 11.09 (s, 1H), 8.14 – 8.10 (m, 2H), 7.46 (dd, *J* = 8.4, 1.2 Hz, 2H), 7.41 (d, *J* = 8.4 Hz, 1H), 7.37 – 7.33 (m, 1H), 7.13 (t, *J* = 7.4 Hz, 1H), 1.40 (s, 9H). **^{13}C NMR (100 MHz, DMSO-*d6*) δ** 141.42, 140.56, 138.31, 125.65, 123.82, 123.14, 122.58, 120.48, 118.66, 116.47, 111.31, 110.86, 34.83, 32.36. **HRMS (ESI-MS):** m/z Calculated for $C_{16}H_{17}N$ [M-H]$^-$: 222.1288; Observed: 222.1277.

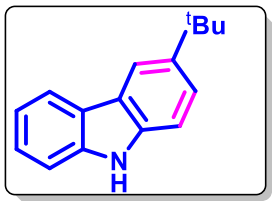

3,6-Dimethyl-9H-carbazole (5e): Yield= 98%, white solid; M. P: 224-225 °C; **IR (KBr, cm^{-1})**: 3400, 3012, 2964, 1479, 1246, 1084, 856; **^{1}H NMR (400 MHz, DMSO-*d6*) δ** 10.93 (s, 1H), 7.83 (s, 2H), 7.33 (d, *J* = 8.4 Hz, 2H), 7.17 (dd, *J* = 8.4, 2.0 Hz, 2H), 2.45 (s, 6H). **^{13}C NMR (100 MHz, DMSO-*d6*) δ** 138.73, 127.26, 127.11, 122.85, 120.26, 111.05, 21.59.

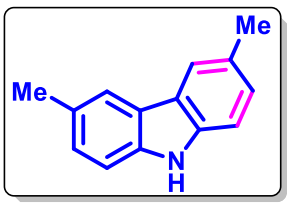

3-(tert-Butyl)-6-methyl-9H-carbazole (5f): Yield= 96%, white solid; M. P: 124-124 °C; **IR (KBr, cm^{-1})**: 3398, 3024, 2958, 1619, 1128, 1034, 932, 875; **^{1}H NMR (400 MHz, DMSO-*d6*) δ** 10.92 (s, 1H), 8.05 (s, 1H), 7.91 (s, 1H), 7.42 (dd, *J* = 8.4, 2.0 Hz, 1H), 7.34 (dd, *J* = 10.8, 8.4 Hz, 2H), 7.16 (dd, *J* = 8.4, 2.0 Hz, 1H), 2.46 (s, 3H), 1.39 (s, 9H). **^{13}C NMR**

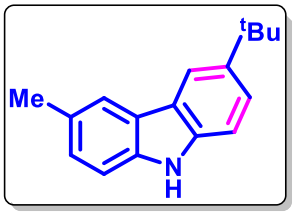

(100 MHz, DMSO-*d6*) δ 141.16, 138.80, 138.59, 127.23, 126.98, 123.62, 123.28, 122.41, 120.30, 116.39, 111.01, 110.79, 34.80, 32.36, 21.56.

3-Methoxy-9H-carbazole (5g): Yield= 93%, white solid; M. P: 151-152 °C (Lit. 152-158 °C) [61]; **IR (KBr, cm^{-1})**: 3403, 2965, 1607, 1463, 1019, 821, 757; **^{1}H NMR (400 MHz, DMSO-*d6*) δ** 11.02 (s, 1H), 8.09 (dd, *J* = 8.0, 1.2 Hz, 1H), 7.67 (d, *J* = 2.4 Hz, 1H), 7.46 – 7.43 (m, 1H), 7.39 (d, *J* = 8.4 Hz, 1H), 7.37 – 7.33 (m, 1H), 7.13 – 7.09 (m, 1H), 7.03 (dd, *J* = 8.8, 2.4 Hz, 1H), 3.85 (s, 3H). **^{13}C NMR (100 MHz, DMSO-*d6*) δ** 153.43, 140.81, 134.97, 125.85, 123.22, 122.89, 120.70, 118.47, 115.23, 112.07, 111.44, 103.40, 56.06.

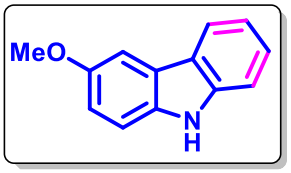

3-Methoxy-6-methyl-9H-carbazole (5h): Yield= 95%, white solid; M. P: 152-153 °C (Lit. 148-150 °C) [62]; **IR (KBr, cm^{-1})**: 3393, 2973, 1569, 1423, 1120, 1029, 834; **^{1}H NMR (400 MHz, DMSO-*d6*) δ** 10.87 (s, 1H), 7.88 (s, 1H), 7.63 (d, *J* = 2.8 Hz, 1H), 7.34 (t, *J* = 8.4 Hz, 2H), 7.17 (dd, *J* = 8.4, 2.0 Hz, 1H), 7.00 (dd, *J* = 8.8, 2.8 Hz, 1H), 3.84 (s, 3H), 2.45 (s, 3H). **^{13}C NMR (100 MHz, MeOD) δ** 153.48, 140.82, 135.03, 125.04, 123.28, 122.95, 119.55, 117.85, 114.46, 110.97, 110.39, 102.48, 55.10, 20.73.

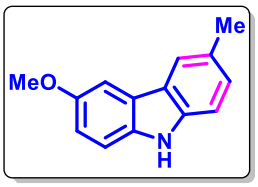

3-Fluoro-9H-carbazole (5i): Yield= 94%, white solid; M. P: 208-209 °C; **IR (KBr, cm^{-1})**: 3325, 2865, 1536, 1234, 11028, 1096, 873; **^{1}H NMR (400 MHz, DMSO-*d6*) δ** 11.28 (s, 1H), 8.12 (d, *J* = 7.6 Hz, 1H), 7.95 (dd, *J* = 9.6, 2.8 Hz, 1H), 7.51 – 7.46 (m, 2H), 7.40 (t, *J* = 7.6 Hz, 1H), 7.25 – 7.20 (m, 1H), 7.15 (t, *J* = 7.6 Hz, 1H). **^{13}C NMR (100 MHz, DMSO-*d6*) δ** 157.98, 155.68, 141.22, 136.62, 126.58, 123.34, 123.24, 122.59, 121.10, 118.90, 113.73, 113.47, 112.26, 112.17, 111.66, 106.29, 106.05. **^{19}F NMR (376 MHz, DMSO-*d6*) δ** -125.17. **HRMS (ESI-MS):** m/z Calculated for $C_{12}H_8FN$ [M-H]$^-$: 184.0568; Observed: 184.0558.

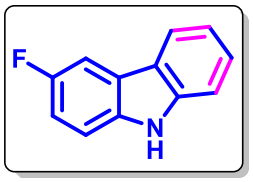

3-Chloro-9H-carbazole (5j): Yield= 96%, white solid; M. P: 198 - 199 °C; **IR (KBr, cm^{-1})**: 3296, 2956, 1463, 1235, 1145, 1096, 892, 789; **^{1}H NMR (400 MHz, DMSO-*d6*) δ** 11.42 (s, 1H), 8.22 (s, 1H), 8.16 (d, *J* = 7.2 Hz, 1H), 7.51 (dd, *J* = 8.4, 1.6 Hz, 2H), 7.45 – 7.41 (m, 1H), 7.39 (dd, *J* = 8.8, 2.0 Hz, 1H), 7.20 – 7.16 (m, 1H). **^{13}C NMR (100 MHz, DMSO-*d6*) δ** 140.78, 138.58, 126.78, 125.74, 124.20, 123.29, 122.03, 121.15, 120.23, 119.34, 112.85, 111.68. **HRMS (ESI-MS):** m/z Calculated for $C_{12}H_8ClN$ [M-H]$^-$: 200.0272; Observed: 200.0241.

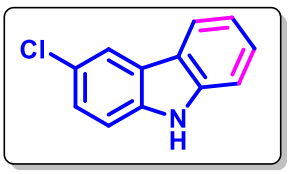

3-Chloro-6-methyl-9H-carbazole (5k): Yield= 97%, white solid; M. P: 163-164 °C; **IR (KBr, cm^{-1})**: 3400, 2920, 1611, 1449, 1059, 874, 805; **^{1}H NMR (400 MHz, DMSO-*d6*) δ** 11.28 (s, 1H), 8.15 (d, *J* = 2.0 Hz, 1H), 7.94 (s, 1H), 7.47 (d, *J* = 8.8 Hz, 1H), 7.40 (d, *J* = 8.4 Hz, 1H), 7.36 (dd, *J* = 8.8, 2.0 Hz, 1H), 7.25 (dd, *J* = 8.4, 2.0 Hz, 1H), 2.46 (s, 3H). **^{13}C NMR (100 MHz, DMSO-*d6*) δ** 139.06, 138.84, 128.17, 128.05, 125.54, 124.01, 123.05, 122.18, 120.78, 120.08, 112.79, 111.41, 21.54. **HRMS (ESI-MS):** m/z Calculated for $C_{13}H_{10}ClN$ [M-H]$^{-}$: 214.0429; Observed: 214.0419.

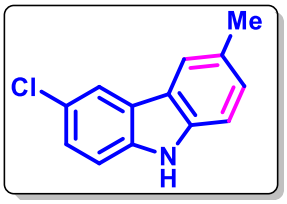

3-(tert-Butyl)-6-chloro-9H-carbazole (5l): Yield= 94%, white solid; M. P: 135-136 °C; **IR (KBr, cm^{-1})**: 3398, 3028, 2962, 1489, 1246, 1034, 932, 875, 804; **^{1}H NMR (400 MHz, DMSO-*d6*) δ** 11.26 (s, 1H), 8.25 (d, *J* = 2.0 Hz, 1H), 8.18 (d, *J* = 2.0 Hz, 1H), 7.50 (dd, *J* = 8.4, 2.0 Hz, 1H), 7.48 – 7.40 (m, 2H), 7.35 (dd, *J* = 8.4, 2.0 Hz, 1H), 1.39 (s, 9H). **^{13}C NMR (100 MHz, DMSO-*d6*) δ** 141.92, 138.94, 125.40, 124.69, 124.51, 123.03, 121.80, 120.17, 117.12, 112.73, 111.12, 34.89, 32.28. **HRMS (ESI-MS):** m/z Calculated for $C_{16}H_{16}ClN$ [M-H]$^{-}$: 256.0898; Observed: 256.0888.

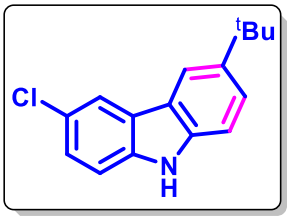

3-Bromo-9H-carbazole (5m): Yield= 92%, white solid; M. P: 199-200 °C; **IR (KBr, cm^{-1})**: 3267, 2932, 1640, 1532, 1260, 1178, 1033, 885; **^{1}H NMR (400 MHz, DMSO-*d6*) δ** 11.43 (s, 1H), 8.36 (d, *J* = 2.0 Hz, 1H), 8.17 (d, *J* = 6.4 Hz, 1H), 7.51 (ddd, *J* = 8.4, 2.4, 1.2 Hz, 2H), 7.46 (dd, *J* = 8.4, 0.8 Hz, 1H), 7.45 – 7.41 (m, 1H), 7.18 (ddd, *J* = 8.0, 7.2, 0.8 Hz, 1H). **^{13}C NMR (100 MHz, DMSO-*d6*) δ** 140.59, 138.84, 128.32, 126.81, 124.86, 123.20, 121.91, 121.16, 119.41, 113.35, 111.66, 111.01. **HRMS (ESI-MS):** m/z Calculated for $C_{12}H_{8}BrN$ [M-H]$^{-}$: 243.9767; Observed: 243.9757.

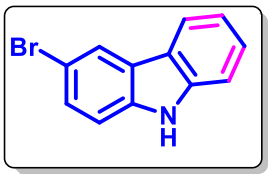

3-Nitro-9H-carbazole (5n): Yield= 91%, pale yellow solid; M. P: 216-217 °C (Lit. 215-216 °C) [63]; **IR (KBr, cm^{-1})**: 3278, 2927, 1468, 1236, 1098, 876; **^{1}H NMR (400 MHz, DMSO-*d6*) δ** 11.06 (s, 1H), 9.32 (s, 1H), 8.41 (s, 1H), 8.39 (s, 1H), 8.13 (m, 1H), 8.12 (m, 1H), 7.81 (s, 1H), 7.79 (m, 1H). **^{13}C NMR (100 MHz, DMSO-*d6*) δ** 164.37, 157.08, 156.08, 154.87, 148.72, 140.08, 126.64, 125.43, 123.44, 116.26. **HRMS (ESI-MS):** m/z Calculated for $C_{12}H_{8}N_{2}O_{2}$ [M-H]$^{-}$: 211.0513; Observed: 211.0513.

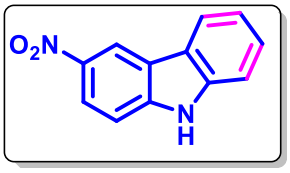

9H-Carbazole-3-carbonitrile (5o): Yield= 92%, white solid; M. P: 189-190 °C (Lit. 181-186 °C) [61]; **IR (KBr, cm^{-1})**: 3294, 2920, 2217, 1596, 1121, 838; **^{1}H NMR (400 MHz, DMSO-*d6*) δ** 11.87 (s, 1H), 8.71 (s, 1H), 8.25 (d, *J* = 8.0 Hz, 1H), 7.76 (dd, *J* = 8.4, 1.6 Hz, 1H), 7.64 (d, *J* = 8.4 Hz, 1H), 7.59 (d, *J* = 8.0 Hz, 1H), 7.53 – 7.48 (m, 1H), 7.27 (t, *J* = 7.2 Hz, 1H). **^{13}C NMR (100 MHz, DMSO-*d6*) δ** 142.15, 140.73, 129.06, 127.45, 126.04, 123.11, 122.06, 121.41, 121.05, 120.34, 112.49, 112.04, 100.67.

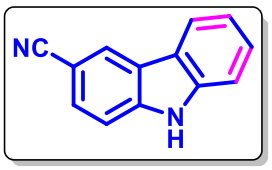

6-Methyl-9H-carbazole-3-carbonitrile (5p): Yield= 95%, pale yellow solid; M. P: 175-176 °C (Lit. 180-183 °C)[61]; **IR (KBr, cm^{-1})**: 3382, 2918, 2219, 1463, 1133, 963, 885; **^{1}H NMR (400 MHz, DMSO-*d6*) δ** 11.75 (s, 1H), 8.63 (s, 1H), 8.03 (s, 1H), 7.73 (dd, *J* = 8.4, 1.6 Hz, 1H), 7.61 (d, *J* = 8.4 Hz, 1H), 7.48 (d, *J* = 7.6 Hz, 1H), 7.32 (dd, *J* = 8.4, 2.4 Hz, 1H), 2.49 (s, 3H). **^{13}C NMR (100 MHz, DMSO-*d6*) δ** 142.33, 138.95, 129.19, 128.80, 125.84, 122.91, 122.19, 121.03, 112.40, 111.73, 100.39, 21.54.

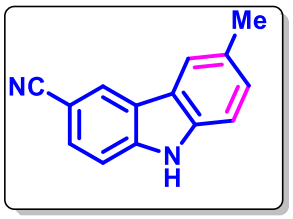

Methyl 1-phenyl-9H-pyrido[3,4-b]indole-3-carboxylate (9a): Yield= 94%, white solid; M. P: 251-252 °C; **IR (KBr, cm^{-1})**: 3289, 2965, 1764, 1589, 1236, 1149, 896; **^{1}H NMR (400 MHz, DMSO-*d6*) δ** 11.94 (s, 1H), 9.00 (s, 1H), 8.94 (s, 1H), 8.44 (d, *J* = 8.0 Hz, 1H), 8.05 – 8.02 (m, 2H), 7.71 (d, *J* = 8.0 Hz, 1H), 7.65 (dd, *J* = 8.0, 1.2 Hz, 2H), 7.61 (dt, *J* = 6.8, 1.2 Hz, 1H), 7.34 (ddd, *J* = 8.0, 6.8, 1.2 Hz, 1H), 3.95 (s, 3H). **^{13}C NMR (100 MHz, DMSO-*d6*) δ** 166.56, 157.08, 155.85, 142.61, 141.93, 137.94, 137.15, 135.04, 129.28, 129.18, 129.05, 122.42, 121.56, 120.93, 117.12, 113.24, 52.53. **HRMS (ESI-MS):** m/z Calculated for $C_{19}H_{14}N_2O_2$ $[M+H]^+$: 303.1128; Observed: 303.1137.

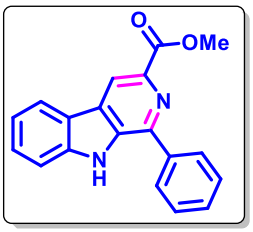

Methyl 1-(p-tolyl)-9H-pyrido[3,4-b]indole-3-carboxylate (9b): Yield= 93%, pale yellow solid; M. P: 191-192 °C; **IR (KBr, cm^{-1})**: 3352, 2965, 1742, 1521, 1245, 1098, 899, 754; **^{1}H NMR (400 MHz, DMSO-*d6*) δ** 11.89 (s, 1H), 8.91 (s, 1H), 8.43 (d, *J* = 8.0 Hz, 1H), 7.94 (d, *J* = 8.0 Hz, 2H), 7.71 (d, *J* = 8.0 Hz, 1H), 7.64 – 7.58 (m, 1H), 7.46 (d, *J* = 8.0 Hz, 2H), 7.33 (t, *J* = 8.0 Hz, 1H), 3.95 (s, 3H), 2.46 (s, 3H). **^{13}C NMR (100 MHz, DMSO-*d6*) δ** 166.58, 142.65, 141.91, 138.98, 137.11, 135.22, 134.99, 129.82, 129.53, 129.08, 128.98, 122.44, 121.62, 120.85, 116.95, 113.25, 52.50, 21.44. **HRMS (ESI-MS):** m/z Calculated for $C_{20}H_{16}N_2O_2$ $[M+H]^+$: 317.1285; Observed: 317.1290.

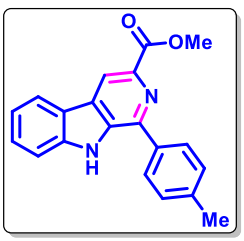

Methyl 1-(4-(trifluoromethyl)phenyl)-9H-pyrido[3,4-b]indole-3-carboxylate (9c): Yield= 95%, white solid; M. P: 293-294 °C; **IR (KBr, cm^{-1})**: 3262, 2365, 1731, 1621, 1256, 1119, 896, 746; **^{1}H NMR (400 MHz, DMSO-*d6*) δ** 12.08 (s, 1H), 8.99 (s, 1H), 8.47 (d, *J* = 8.0 Hz, 1H), 8.33 (d, *J* = 7.2 Hz, 1H), 8.28 – 8.27 (m, 1H), 7.96 – 7.93 (m, 1H), 7.90 (t, *J* = 7.6 Hz, 1H), 7.71 (dt, *J* = 8.0, 1.0 Hz, 1H), 7.66 – 7.62 (m, 1H), 7.38 – 7.34 (m, 1H), 3.95 (s, 3H). **^{13}C NMR (100 MHz, DMSO-*d6*) δ** 166.34, 142.04, 140.84, 138.90, 137.23, 135.16, 133.04, 130.42, 130.09, 129.39, 126.05, 125.59, 122.59, 121.57, 121.05, 117.70, 113.20, 52.59. **^{19}F NMR (376 MHz, DMSO-*d6*) δ** -60.97. **HRMS (ESI-MS):** m/z Calculated for $C_{20}H_{13}F_3N_2O_2$ $[M+H]^+$: 371.1002; Observed: 371.1003.

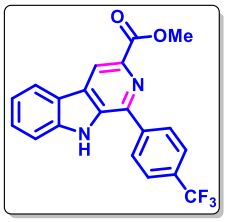

Methyl 1-(4-methoxyphenyl)-9H-pyrido[3,4-b]indole-3-carboxylate (9d): Yield= 92%, pale yellow solid; M. P: 232-233 °C; **IR (KBr, cm^{-1})**: 3362, 2974, 1756, 1629, 1236, 1019, 878, 759; **^{1}H NMR (400 MHz, DMSO-*d6*) δ** 11.89 (s, 1H), 8.88 (s, 1H), 8.41 (d, *J* = 8.0 Hz, 1H), 8.01 – 7.98 (m, 2H), 7.71 (d, *J* = 8.0 Hz, 1H), 7.63 – 7.59 (m, 1H), 7.33 (t, *J* = 7.6 Hz, 1H), 7.22 – 7.19 (m, 2H), 3.94 (s, 3H), 3.89 (s, 3H). **^{13}C NMR (100 MHz, DMSO-*d6*) δ** 166.60, 160.43, 142.49, 141.88, 137.08, 134.83, 130.43, 129.45, 129.04, 122.41, 121.64, 120.85, 116.65, 114.68, 113.25, 55.83, 52.50. **HRMS (ESI-MS):** m/z Calculated for $C_{20}H_{16}N_2O_3$ $[M+H]^+$: 333.1234; Observed: 333.1239.

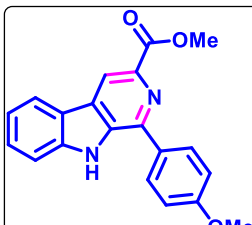

Methyl 1-(4-(methylamino)phenyl)-9H-pyrido[3,4-b]indole-3-carboxylate (9e): Yield= 94%, pale brown solid; M. P: 224-225 °C; **IR (KBr, cm^{-1})**: 3300, 2921, 1710, 1524, 1253, 1105, 826, 744; **^{1}H NMR (400 MHz, DMSO-*d6*) δ** 11.78 (s, 1H), 8.79 (s, 1H), 8.38 (d, *J* = 7.6 Hz, 1H), 7.88 – 7.85 (m, 2H), 7.71 (d, *J* = 8.4 Hz, 1H), 7.61 – 7.57 (m, 1H), 7.33 – 7.29 (m, 1H), 6.80 – 6.77 (m, 2H), 6.13 (s, 1H), 3.93 (s, 3H), 2.80 (s, 3H). **^{13}C NMR (100 MHz, DMSO-*d6*) δ** 166.74, 151.14, 143.53, 141.75, 137.00, 134.51, 129.97, 129.04, 128.75, 125.11, 122.23, 121.74, 120.67, 115.75, 113.26, 111.98, 52.42, 30.09. **HRMS (ESI-MS):** m/z Calculated for $C_{20}H_{17}N_3O_2$ $[M+H]^+$: 332.1394; Observed: 332.1395.

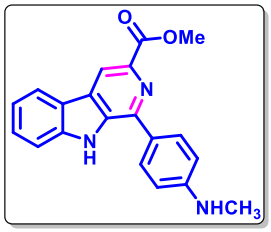

Methyl 1-(4-chlorophenyl)-9H-pyrido[3,4-b]indole-3-carboxylate (9f): Yield= 93%, pale yellow solid; M. P: 282-283 °C (Lit. 282-283 °C) [65]; **IR (KBr, cm^{-1})**: 3321, 2928, 1724, 1535, 1125, 1024, 826, 806, 744; **^{1}H NMR (400 MHz, DMSO-*d6*) δ** 11.99 (s, 1H), 8.94 (s,

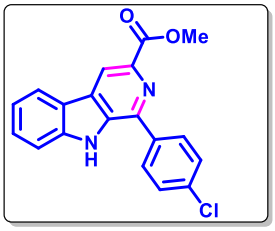

1H), 8.43 (d, *J* = 8.0 Hz, 1H), 8.06 – 8.03 (m, 2H), 7.75 – 7.69 (m, 3H), 7.63 (t, *J* = 8.0 Hz, 1H), 7.35 (t, *J* = 7.5 Hz, 1H), 3.94 (s, 3H). **^{13}C NMR (100 MHz, DMSO-*d6*) δ** 166.46, 141.95, 141.28, 137.16, 136.69, 135.01, 134.25, 131.63, 130.87, 129.86, 129.30, 129.16, 128.80, 122.51, 121.53, 121.05, 117.39, 113.20, 52.59.

Methyl 1-(4-bromophenyl)-9H-pyrido[3,4-b]indole-3-carboxylate (9g): Yield= 91%, pale yellow solid; M. P: 191-192 °C; **IR (KBr, cm^{-1})**: 3315, 2965, 1754, 1500, 1102, 758; **^{1}H NMR (400 MHz, DMSO-*d6*) δ** 11.98 (s, 1H), 8.95 (s, 1H), 8.44 (dd, *J* = 8.0, 4.8 Hz, 1H), 7.98 (dd, *J* = 8.0, 3.2 Hz, 2H), 7.86 – 7.83 (m, 2H), 7.70 (d, *J* =8.0 Hz, 1H), 7.62 (t, *J* = 8.0 Hz, 1H), 7.35 (dt, *J* = 8.0, 3.2 Hz, 1H), 3.94 (s, 3H). **^{13}C NMR (100 MHz, DMSO-*d6*) δ** 166.43, 141.96, 141.31, 137.19, 135.00, 132.21, 131.16, 129.89, 129.32, 122.94, 122.55, 121.55, 121.01, 117.43, 113.20, 52.57. **HRMS (ESI-MS):** m/z Calculated for $C_{19}H_{13}BrN_2O_2$ $[M+H]^+$: 381.0233; Observed: 381.0225.

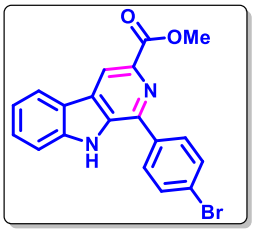

Methyl 1-(4-nitrophenyl)-9H-pyrido[3,4-b]indole-3-carboxylate (9h): Yield= 92%, yellow solid; M. P: 268-269 °C; **IR (KBr, cm^{-1})**: 3321, 2985, 1741, 1517, 1267, 1102, 768; **^{1}H NMR (400 MHz, DMSO-*d6*) δ** 12.14 (s, 1H), 9.02 (s, 1H), 8.50 (m, 1H), 8.48 (m, 2H), 8.33 – 8.30 (m, 2H), 7.71 (dt, *J* = 8.4, 1.2 Hz, 1H), 7.67 – 7.63 (m, 1H), 7.39 – 7.35 (m, 1H), 3.96 (s, 3H). **^{13}C NMR (100 MHz, DMSO-*d6*) δ** 166.30, 147.99, 144.14, 142.09, 139.97, 137.40, 135.34, 130.43, 129.60, 124.40, 122.72, 121.49, 121.21, 118.16, 113.23, 52.66. **HRMS (ESI-MS):** m/z Calculated for C19H13N3O4 $[M+H]^+$: 347.0979; Observed: 347.0968.

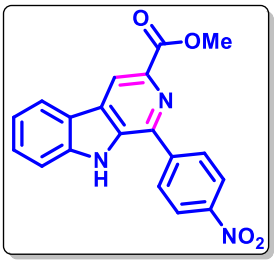

Methyl 1-(thiophen-2-yl)-9H-pyrido[3,4-b]indole-3-carboxylate (9i): Yield= 96%, yellow solid; M. P: 179-180 °C; **^{1}H NMR (400 MHz, DMSO-*d6*) δ** 11.91 (s, 1H), 8.88 (s, 1H), 8.43 (d, *J* = 8.0 Hz, 1H), 8.16 (dd, *J* = 4.0, 1.2 Hz, 1H), 7.82 – 7.77 (m, 2H), 7.67 – 7.62 (m, 1H), 7.37 (m, 2H), 3.95 (s, 3H). **^{13}C NMR (100 MHz, DMSO-*d6*) δ** 166.12, 142.81, 142.01, 136.81, 132.92, 130.24, 129.39, 129.35, 128.94, 127.15, 122.48, 121.53, 121.24, 116.97, 113.41, 52.63. **HRMS (ESI-MS):** m/z Calculated for $C_{17}H_{12}N_2O_2S$ $[M+H]^+$: 309.0692; Observed: 309.0687.

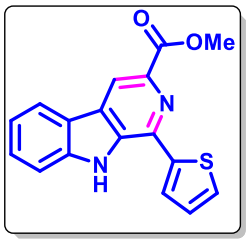

9-Methyl-9H-carbazole (11a): Yield= 93%, white solid; M. P: 80-81 °C (Lit. 80-84 °C) [62]; **IR (KBr, cm^{-1})**: **^{1}H NMR (400 MHz, DMSO-*d6*) δ** 8.15 (dt, *J* = 8.0, 0.8 Hz, 2H), 7.59 (dt, *J* = 8.4, 0.8 Hz, 2H), 7.47 (ddd, *J*

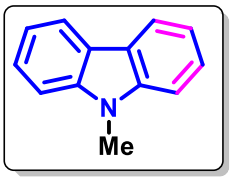

= 8.4, 7.2, 1.2 Hz, 2H), 7.21 (ddd, *J* = 8.0, 7.2, 1.2 Hz, 2H), 3.87 (s, 3H). **^{13}C NMR (100 MHz, DMSO-*d6*) δ** 141.05, 126.16, 122.41, 120.65, 119.16, 109.54, 29.40.

9-Ethyl-9H-carbazole (11b): Yield= 94%, white solid; M. P: 107-108 °C (Lit. 110-112 °C) [62]; **IR (KBr, cm^{-1}): ^{1}H NMR (400 MHz, DMSO-*d6*) δ** 8.14 (dt, *J* = 8.0, 1.2 Hz, 2H), 7.58 (dt, *J* = 8.4, 1.0 Hz, 2H), 7.45 (ddd, *J* = 8.4, 7.2, 1.2 Hz, 2H), 7.19 (ddd, *J* = 8.0, 7.2, 1.2 Hz, 2H), 4.41 (q, *J* = 7.2 Hz, 2H), 1.29 (t, *J* = 7.2 Hz, 3H). **^{13}C NMR (100 MHz, DMSO-*d6*) δ** 139.97, 126.15, 122.63, 120.78, 119.13, 109.46, 37.34, 14.09.

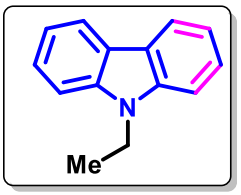

9-Allyl-9H-carbazole (11c): Yield= 92%, white solid; M. P: 89-90 °C; **IR (KBr, cm^{-1})**: 3054, 2922, 1869, 1592, 1455, 1324, 1129, 993, 839; **^{1}H NMR (400 MHz, DMSO-*d6*) δ** 8.15 (dt, *J* = 8.0, 1.2 Hz, 2H), 7.54 (dt, *J* = 8.4, 1.2 Hz, 2H), 7.44 (ddd, *J* = 8.4, 7.2, 1.2 Hz, 2H), 7.20 (ddd, *J* = 8.0, 7.2, 1.2 Hz, 2H), 6.07 – 5.88 (m, 1H), 5.09 (dq, *J* = 10.4, 1.6 Hz, 1H), 5.01 (dt, *J* = 5.2, 1.6 Hz, 2H), 4.92 (dq, *J* = 10.4, 1.6 Hz, 1H). **^{13}C NMR (100 MHz, DMSO-*d6*) δ** 140.43, 133.61, 126.17, 122.62, 120.75, 119.35, 116.84, 109.85, 45.02.

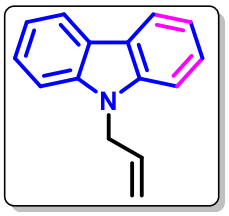

9-(Prop-2-yn-1-yl)-9H-carbazole (11d): Yield= 93%, white solid; M. P: 108-109 °C; **IR (KBr, cm^{-1})**: 3261, 3052, 2925, 2115,1897, 1592, 1259, 1144, 1056, 920; **^{1}H NMR (400 MHz, DMSO-*d6*) δ** 8.15 (dt, *J* = 8.0, 1.2 Hz, 2H), 7.65 (dt, *J* = 8.0, 1.2 Hz, 2H), 7.48 (ddd, *J* = 8.4, 7.2, 1.2 Hz, 2H), 7.24 (td, *J* = 7.6, 1.2 Hz, 2H), 5.27 (d, *J* = 2.8 Hz, 2H), 3.17 (t, *J* = 2.4 Hz, 1H). **^{13}C NMR (100 MHz, DMSO-*d6*) δ** 140.09, 126.35, 122.96, 120.82, 119.88, 110.00, 79.65, 74.87, 32.30.

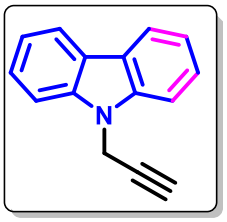

9-Benzyl-9H-carbazole (11e): Yield= 90%, white solid; M. P: 118.5-118.9 °C (Lit. 122-125 °C) [62]; **IR (KBr, cm^{-1})**: 3053, 2928, 1593, 1452, 1147, 1056, 925, 840; **^{1}H NMR (400 MHz, DMSO-*d6*) δ** 8.18 (dt, *J* = 8.0, 1.2 Hz, 2H), 7.61 (d, *J* = 8.4 Hz, 2H), 7.43 (ddd, *J* = 8.4, 7.2, 1.2 Hz, 2H), 7.26 (d, *J* = 7.2 Hz, 1H), 7.24 – 7.21 (m, 3H), 7.20 – 7.15 (m, 3H), 5.65 (s, 2H). **^{13}C NMR (100 MHz, DMSO-*d6*) δ** 140.63, 138.28, 129.03, 127.72, 127.18, 126.33, 122.71, 120.81, 119.52, 109.97, 46.03.

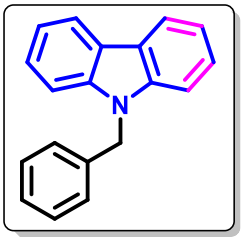

3,9-Dimethyl-9H-carbazole (11f): Yield= 94%, white solid; M. P: 74-75 °C; **IR (KBr, cm^{-1}):** **^{1}H NMR (400 MHz, CDCl$_3$) δ** 8.07 – 8.04 (m, 1H), 7.89 (m, 1H), 7.44 (ddd, *J* = 8.4, 6.8, 1.2 Hz, 1H), 7.36 (dt, *J* = 8.4, 1.2 Hz, 1H), 7.28 (m,2H), 7.20 (ddd, *J* = 8.0, 7.2, 1.2 Hz, 1H), 3.81 (s, 3H), 2.53 (s, 3H). **^{13}C NMR (100 MHz, CDCl$_3$) δ** 141.25, 139.37, 128.11, 127.00, 125.49, 122.89, 122.62, 120.29, 120.23, 118.57, 108.36, 108.12, 29.10, 21.42.

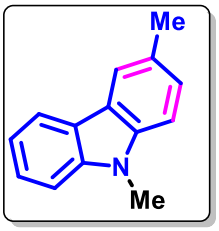

6,9-Dimethyl-9H-carbazole-3-carbonitrile (11g): Yield= 93%, white solid; M. P: 119-120 °C; **IR (KBr, cm^{-1})**: 2923, 2211, 1598, 1248, 1141, 1041, 943, 797; ^{1}H NMR (**400 MHz, CDCl$_3$**) **δ** 8.26 (dd, *J* = 1.6, 0.8 Hz, 1H), 7.83 (dt, *J* = 1.6, 0.8 Hz, 1H), 7.63 (dd, *J* = 8.4, 1.6 Hz, 1H), 7.37 – 7.32 (m, 2H), 7.30 (dd, *J* = 8.4, 0.8 Hz, 1H), 3.80 (s, 3H), 2.54 (s, 3H). **^{13}C NMR (100 MHz, CDCl$_3$) δ** 142.65, 139.79, 129.90, 128.68, 128.53, 124.99, 122.69, 121.88, 120.78, 120.53, 108.98, 108.78, 101.10, 29.30, 21.41. **HRMS (ESI-MS):** m/z Calculated for $C_{15}H_{12}N_2$ $[M+H]^+$: 221.1073; Observed: 221.1074.

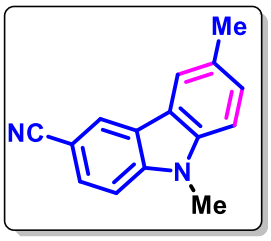

Quinoline (14): Yield= 92%; colourless oil; **^{1}H NMR (400 MHz, CDCl$_3$) δ** 8.91 (dd, *J* = 4.0, 1.6 Hz, 1H), 8.15 – 8.10 (m, 2H), 7.80 (d, *J* = 8.0 Hz, 1H), 7.71 (ddd, *J* = 8.4, 6.8, 1.2 Hz, 1H), 7.55 – 7.51 (m, 1H), 7.37 (dd, *J* = 8.3, 4.2 Hz, 1H). **^{13}C NMR (100 MHz, CDCl$_3$) δ** 150.35, 148.22, 136.06, 129.45, 129.38, 128.26, 127.78, 126.53, 121.05.

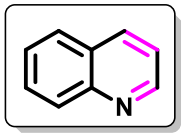

Isoquinoline (15): Yield= 90%; light brown oil; **^{1}H NMR (400 MHz, CDCl$_3$) δ** 9.24 (s, 1H), 8.52 (dd, *J* = 5.7, 1.5 Hz, 1H), 7.93 (dd, *J* = 8.0, 2.0 Hz, 1H), 7.79 (dd, *J* = 8.0, 2.0 Hz, 1H), 7.66 (ddd, *J* = 8.4, 6.4, 2.0 Hz, 1H), 7.63 – 7.55 (m, 2H). **^{13}C NMR (100 MHz, CDCl$_3$) δ** 152.52, 142.97, 135.76, 130.34, 128.67, 127.61, 127.24, 126.46, 120.47.

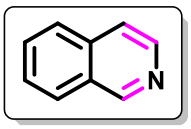

4.9 Reference

(1) (a) Naykode, M. S.; Tambe, S. D.; Lokhande, P. D. *ChemistrySelect* **2017**, *2*, 567–570.
(b) Schmidt, A. W.; Reddy, K. R.; Knölker, H. J. *Chem. Rev.* **2012**, *112*, 3193–3328.
(c) Knölker, H. J.; Bauermeister, M. *J. Chem. Soc. Chem. Commun.* **1990**, 664–665.

(2) Padmaja, P.; Koteswara Rao, G.; Indrasena, A.; Subba Reddy, B. V.; Patel, N.; Shaik, A. B.; Reddy, N.; Dubey, P. K.; Bhadra, M. P. *Org. Biomol. Chem.* **2015**, *13*, 1404–1414.

(3) Caruso, A.; Ceramella, J.; Iacopetta, D.; Saturnino, C.; Mauro, M. V.; Bruno, R.; Aquaro, S.; Sinicropi, M. S. *Molecules* **2019**, *24*, 1912.

(4) Pieper, A. A.; McKnight, S. L. ; Ready, J. M. *Chem. Soc. Rev.* **2014**, *43*, 6716–6726.

(5) Wu, X.; Kosaraju, J.; Zhou, W.; Tam, K. Y. *ACS Chem. Neurosci*. **2017**, *8*, 676–685.

(6) Nalli, Y.; Khajuria, V.; Gupta, S.; Arora, P.; Riyaz-Ul-Hassan, S.; Ahmed, Z.; Ali, A. *Org. Biomol. Chem.* **2016**, *14*, 3322–3332.

(7) T. Nagappan, P. Ramasamy, M. E. A. Wahid, T. C. Segaran, C. S. Vairappan, *Molecules* **2011**, *16*, 9651–9664.

(8) Narayana Reddy, P.; Padmaja, P.; Ramana Reddy, B.; Singh Jadav, S. *Med. Chem. Res.* **2017**, *26*, 2243–2259.

(9) Börger, C.; Brütting, C.; Julich-Gruner, K. K.; Hesse, R.; Pavan Kumar, V.; Kutz, S. K.; Rönnefahrt, M.; Thomas, C.; Wan, B.; Franzblau, S. G.; Knölker, H. J. *Bioorg. Med. Chem.* **2017**, *25*, 6167–6174.

(10) Ree, B. J.; Kwon, W.; Kim, K.; Ko, Y. G.; Kim, Y. Y.; Lee, H.; Ree, M. *ACS Appl. Mater. Interfaces* **2014**, *6*, 21692–21701.

(11) Zhu, J.; Zhang, T.; Ding, Y.; Zhou, H.; Huang, J.; Guo, L.; Su, J. *New. J. Chem.* **2022**, *46*, 22633–22638.

(12) Liu, Y.; Ye, X.; Liu, G.; Lv, Y.; Zhang, X.; Chen, S.; Lam, Kwok, Y. J. W.; Tao, S. H. X.; Tang, B. Z. *J. Mater. Chem.* **2014**, *2*, 1004–1009.

(13) (a) Tsuboi, T.; Liu, S.-W.; Wu, M.-F.; Chen, C.-T. *Org. Electron.* **2009**, *10*, 1372–1377. (b) Van Dijken, A.; Bastiaansen, J. J. A. M.; Kiggen, N. M. M.; Langeveld, B. M. W.; Rothe, C.; Monkman, A.; Bach, I.; Stössel, P.; Brunner, K. *J. Am. Chem. Soc.* **2004**, *126*, 7718–7727.

(14) Sathiyan, G.; Sivakumar, E. K. T.; Ganesamoorthy, R.; Thangamuthu, R.; Sakthivel, P. *Tetrahedron Lett.* **2016**, *57*, 243–252.

(15) Inman, W. D.; Bray, W. M.; Gassner, N. C.; Lokey, R. S.; Tenney, K.; Shen, Y. Y.; TenDyke, K.; Suh, T.; Crews, P. *J. Nat. Prod*. **2010**, *73*, 255–257.

(16) Aaghaz, S.; Sharma, K.; Jain, R.; Kamal, A. *Eur. J. Med. Chem*. **2021**, *216*, 113321.

(17) Tewari, U.; Sharma, D.; Srivastava, S.; Kumar, B. K.; Faheem,; Murugesan, S. *ChemistrySelect* **2021**, *6*, 2428–2445.

(18) Nazari Formagio, A. S.; Santos, P. R.; Zanoli, K.; Ueda-Nakamura, T.; Düsman Tonin, L. T.; Nakamura, C. V.; Sarragiotto, M. H. *Eur. J. Med. Chem*. **2009**, *44*, 4695–4701.

(19) Winkler, J. D.; Londregan, A. T.; Hamann, M. T. *Org. Lett*. **2006**, *8*, 2591–2594.

(20) Beato, A.; Gori, A.; Boucherle, B.; Peuchmaur, M.; Haudecoeur, R.; *J. Med. Chem.* **2021**, *64*, 1392–1422.

(21) (a) Das, S. K.; Das, S.; Ghosh, S.; Roy, S.; Pareek, M.;. Roy, B.; Sunoj, R. B.; Chattopadhyay, *B. Chem. Sci*. **2022**, *13*, 11817–11828. (b) Knölker, H. J.; Fröhner, W. *Tetrahedron Lett.* **1997**, *38*, 1535–1538. (c) Knott, K. E.; Auschill, S.; Jäger, A.; Knölker, H. J. *Chem. Commun.* **2009**, 1467–1469.

(22) (a) Tsang, W. C. P.; Zheng N.;. Buchwald, S. L, *J. Am. Chem. Soc.* **2005**, *127*, 14560–14561. (b) Jordan-Hore, J. A.; Johansson, C. C. C.; Gulias, M.; Beck, E. M.; Gaunt, M. J. *J. Am. Chem. Soc.* **2008**, *130*, 16184–16186. (c) Gensch, T.; Rönnefahrt, M.; Czerwonka, R.; Jäger, A.; Kataeva, O.; Bauer, I.; Knölker, H. J. *Chem. Eur. J.* **2012**, *18*, 770–776. (d) Gruner, K. K. J.; Kataeva, O.; Schmidt, A. W.; Knölker, H. J. *Chem. Eur. J.* **2014**, *20*, 8536–8540. (e) Hesse, R.; Kataeva, O.; Schmidt, A. W.; Knölker, H. J.; *Chem. Eur. J.* **2014**, *20*, 9504–9509.

(23) Fan, W.; Jiang, S.; Feng, B. *Tetrahedron* **2015**, *71*, 4035–4038.

(24) (a) Niu, Y.N., Qiao, Y.; Wang, K.Y.; Sha, B.X.; Li, G.Q. *RSC Adv.* **2022**, *12*, 24232–24236. (b) Börger, C.; Kataeva, O.; Knölker, H. J. *Org. Biomol. Chem.* **2012**, *10*, 7269–7273.

(25) Suzuki, C.; Hirano, K.; Satoh, T.; Miura, M. *Org. Lett.* **2015**, *17*, 1597–1600.

(26) Natarajan, P.; Priya, P.; Chuskit, D. *Green Chem.* **2017**, *19*, 5854–5861.

(27) Chatterjee, T.; Roh, G.; Shoaib, M. A.; Suhl, C.-H.; Kim, J. S.; Cho, C.-G.; Cho, E. J. *Org. Lett.* **2017**, *19*, 1906–1909.

(28) Sato, E.; Yukiue, A.; Mitsudo, K.; Suga, S. *Org. Lett.* **2023**, *25*, 5339–5344.

(29) Gore, S.; Baskaran, S.; König, B. *Org. Lett*. **2012**, *14*, 4568.

(30) Tanaka, T.; Okunaga, K.; Hayashi, M. *Tetrahedron Lett*. **2010**, *51*, 4633–4635.

(31) Dalvi, A.; Lokhande, B. P. D. *Tetrahedron Lett.* **2018**, *59*, 2145–2149.

(32) (a) Naykode, M. S.; Humne, V. T.; Lokhande, P. D. *J. Org. Chem.* **2015**, *80*, 2392–2396. (b) Humne, V.; Dangat, Y.; Vanka, K.; Lokhande, P. *Org. Biomol. Chem.* **2014**, *12*, 4832– 4836.

(33) Park, I.K.; Suh, S.E.; Lim, B.Y.; Cho, C.G. *Org. Lett.* **2009**, *11*, 5454–5456.

(34) (a) Karki, M.; Araujo, H. C.; Magolan, J. *Synlett* **2013**, *24*, 1675–1678. (b) Xiao, F.; Liao, Y.; Wu, M.; Deng, G. J. *Green Chem.* **2012**,*14*, 3277–3280.

(35) Handy, S.; Wright, M. *Tetrahedron Lett*. **2014**, *55*, 3440–3442.

(36) (a) Szabó, T.; Volk, B.; Milen, M. *Molecules* **2021**, *26*, 663. (b) Szabó, T.; Hazai, V.; Volk, B.; Simig, G.; Milen, M. *Tetrahedron Lett*. **2019**, *60*, 1471–1475.

(37) Kulkarni, A.; Abid, M.; Török, B.; Huang, X. *Tetrahedron Lett*. **2009**, *50*, 1791–1794.

(38) Yin, W.; Majumder, S.; Clayton, T.; Petrou, S.; VanLinn, M. L.; Namjoshi, A. O.; Ma, C.; Cromer, B. A.; Roth, B. L.; Platt, D. M.; Cook, J. M. *Bioorg. Med. Chem*. **2010**, *18*, 7548–7564.

(39) Wang, Z.; Yu, Z.; Yao, Y.; Zhang, Y.; Xiao, X.; Wang, B. *Chin. Chem. Lett*. **2019**, *30*, 1541–1544.

(40) Bai, B.; Li, X.Y.; Liu, L.; Li, Y.; Zhu, H.J. *Bioorg. Med. Chem. Lett*. **2014**, *24*, 96–98.

(41) Manasa, K. L.; Tangella, Y.; Ramu, G.; Nagendra Babu, B. *ChemistrySelect*. **2017**, *2*, 9162–9167.

(42) Kamal, A.; Tangella, Y.; Manasa, K. L.; Sathish, M.; Srinivasulu, V.; Chetna, J.; Alarifi, A. *Org. Biomol. Chem.* **2015**, *13*, 8652–8662.

(43) Kamal, A.; Sathish, M.; Prasanthi, A. V. G.: Chetna, J.; Tangella, Y.; Srinivasulu, V.; Shankaraiah, N.; Alarifi, A. *RSC Adv*. **2015**, *5*, 90121–90126.

(44) (a) Panarese, J. D.; Waters, S.P. *Org. Lett*. **2010**, *12*, 4086–4089. (b) Battini, N.; Padala, A. K.; Mupparapu, N.; Vishwakarma, R. A.; Ahmed, Q. N. *RSC Adv*. **2014**, *4*, 26258.

(45) (a) Zhao, Z.; Sun, Y.; Wang, L.; Chen, X.; Sun, Y.; Lin, L.; Tang, Y.; Li, F.; Chen, D. *Tetrahedron Lett*. **2019**, *60*, 800–804. (b) Mohamad Arshad, A. S.: Meesala, R.; Hanapi, N. A.; Mordi, M. N. *Tetrahedron* **2021**, *83*, 131960. (c) Enders, L.; Casadio, D. S.; Aikonen, S.; Lenarda, A.; Wirtanen, T.; Hu, T.; Hietala, S.; Ribeiro, L. S.; Pereira, M. F. R.; Helaja, J. *Catal. Sci. Technol*. **2021**, *11*, 5962–5972. (d) Ramu, S.; Srinath, S.; Kumar, A. A.; Baskar, B.; Ilango, K.; Balasubramanian, K. K. *Mol. Catal*. **2019**, *468*, 86–93.

(46) Zhang, Z.; Gu, J.; Lv, Y.; Ji, L.; Liu, X.; Wu, B.; Liu, F.; Jia, Z.; Loh, T.P. C*ell Rep. Phys. Sci.* **2023**, *4*, 101246.

(47) (a) Gunjan,; Sharma, P.; Kumar, P.; Sharma, N.; Bhagat, S. *ChemistrySelect* **2023**, *8*, e202300080 (1 of 7). (b) Byeon, H.J.; Jung, K. H.; Moon, G. S.; Moon, S.K.; Lee, H.Y. *Sci. Rep*. **2020**, *10*, 1057.

(48) (a) Singh, P.; Mritunjay, *Asian J. Org. Chem*. **2021**, *10*, 964–979. (b) Usman, M.; Zhang, X.W.; Wu, D.; Guan, Z.H.; Liu, W.B. *Org. Chem. Front*. **2019**, *6*, 1905–1928.

(49) Mitsunobu, O.; Yamada, M.; Bull. *Chem. Soc. Jpn*. **1967**, *40*, 2380-2382.

(50) (a) Cheng, L.; Liu, L.; Wang, D.; Chen, Y. J. *Org. Lett*. **2009**, *11*, 3874–3877. (b) Shirisha, T.; Majhi, S.; Balasubramanian, S.; Kashinath, D. *Org. Biomol. Chem*. **2024**, *22*, 1434–1440.

(51) Xu, Y.W.; Wang, J.; Wang, G.; Zhen, L. *J. Org. Chem*. **2021**, *86*, 91–102.

(52) Cao, H. T.; Grée, R. *Tetrahedron Lett*. **2009**, *50*, 1493–1494.

(53) Wang, G.; Piva De Silva, G.; Wiebe, N. E.; Fehr, G. M.; Davis, R. L. *RSC Adv*. **2017**, *7*, 48848-48852.

(54) Xu, X.; Li, X.; Ma, L.; Ye, N.; Weng, B. *J. Am. Chem. Soc*. **2008**, *130*, 14048–14049.

(55) (a) Jung, D.; Kim, M. H.; Kim, J. *Org. Lett.* **2016**, *18*, 6300–6303. (b) Bang, S. B.; Kim, J.; *Synth. Commun.* **2018**, *48*, 1291–1298.

(56) Sharma, H.; Mourya, M.; Guin, D.; Joshi, Y. C.; Dobhal, M. P.; Basak, A. K. *Tetrahedron Lett*. **2017**, *58*, 1727–1732.

(57) (a) Hooshmand, S. E.; Afshari, R.; Ramón, D. J.; Varma, R. S. *Green Chem*. **2020**, *22*, 3668–3692. (b) Liu, P.; Hao, J. W.; Mo, L.P.; Zhang, Z. H. *RSC Adv*. **2015**, *5*, 48675–48704. (c) Alonso, D. A.; Baeza, A.; Chinchilla,; Guillena, G.; Pastor, I. M.; Ramón, D. J. *Eur. J. Org Chem.* **2016**, 612–632. (d) Smith, E. L.; Abbott, A. P.; Ryder, K. S. *Chem. Rev*. **2014**, *114*, 11060–11082.

(58) Knölker, H. J.; Bauermeister, M.; Pannek, J. B. *Chem. Ber*. **1992**, *125*, 2783–2793.

(59) Forke, R.; Krahl, M. P.; Krause, T.; Schlechtingen, G.; Knölker H. J. *Synlett*. **2007**, *2*, 268–272.

(60) Isci, A.; Kaltschmitt, M. *Biomass Convers. Biorefin*. **2022**, *12*, S197–S226.

(61) Humne, V.; Dangat, Y.; Vanka, K.; Lokhande, P. *Org. Biomol. Chem.* **2014**, *12*, 4832–4836.

(62) Suzuki, C.; Hirano, K.; Satoh, T.; Miura, M. *Org. Lett.* **2015**, *17*, 1597–1600.

(63) Nagarajan, R.; Muralidharan, D.; Perumal P.T. *Synth. Commun.* **2004**, *34*, 1259–1264.

(64) Wang, Z.; Yu, Z.; Yao, Y.; Zhang, Y.; Xiao, X.; Wang, B. *Chin. Chem. Lett.* **2019**, *30*, 1541–1544.

4.9 Selected Spectra

3-(tert-Butyl)-9H-carbazole (5d):

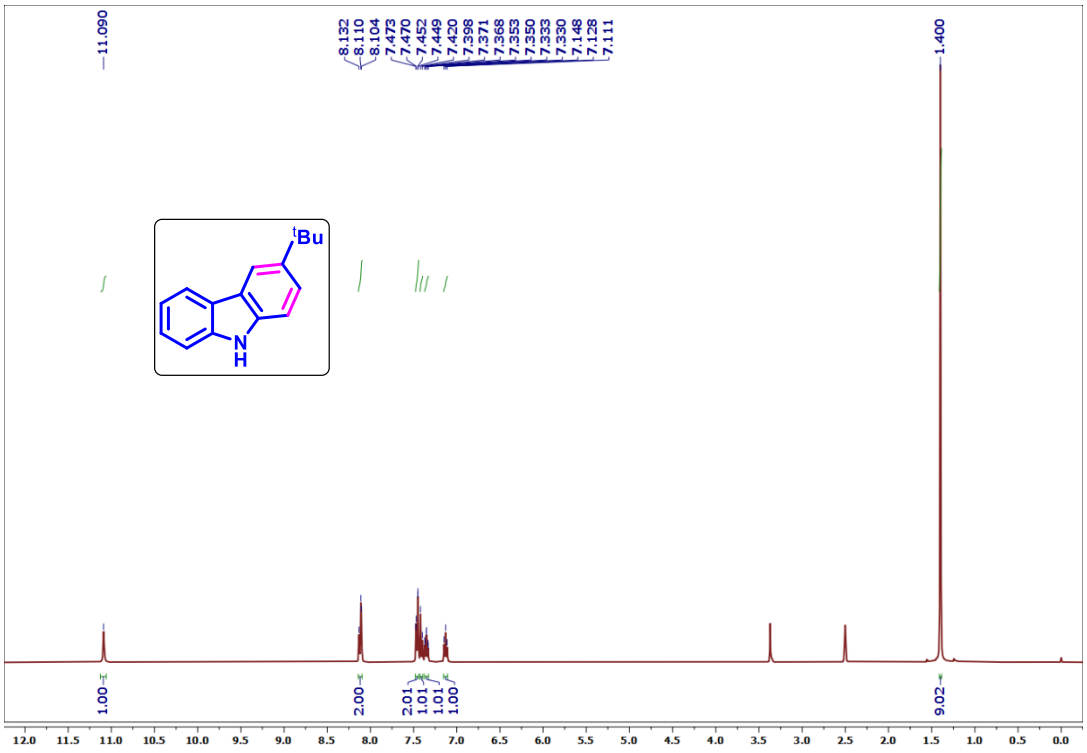

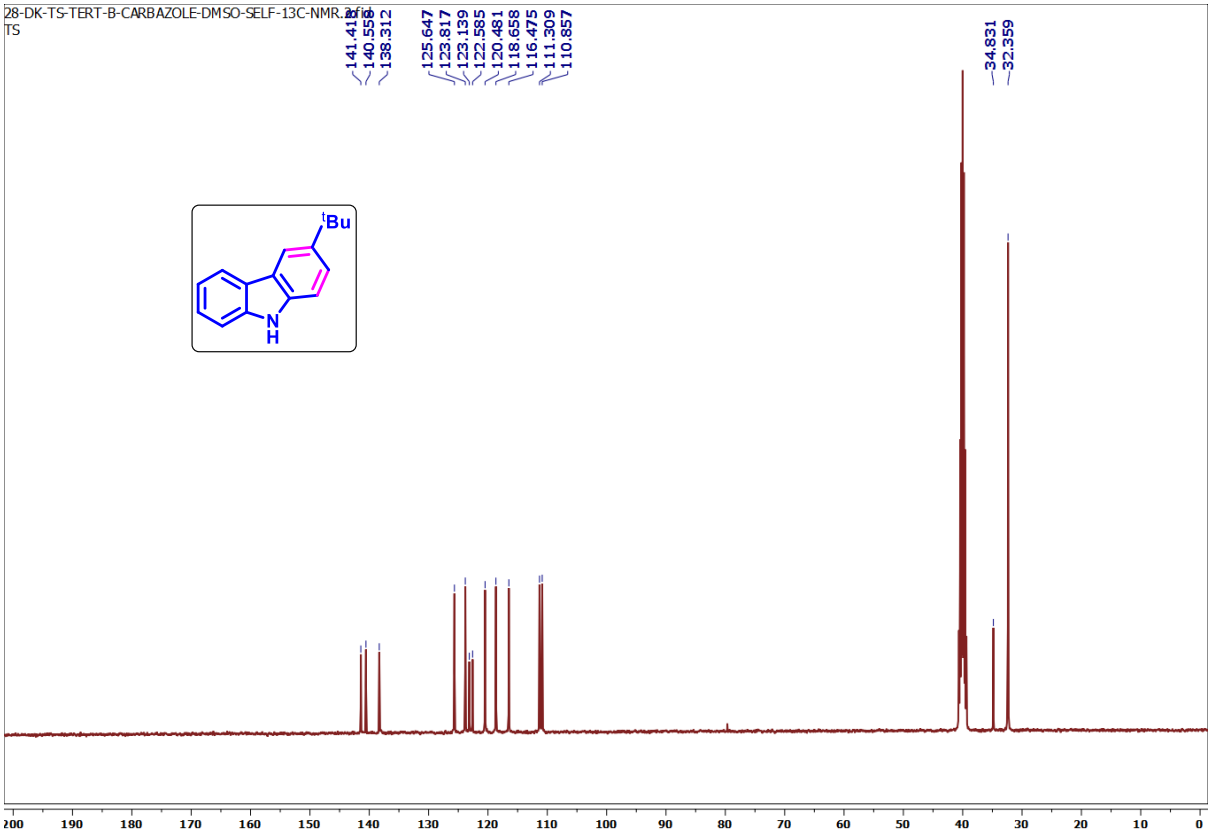

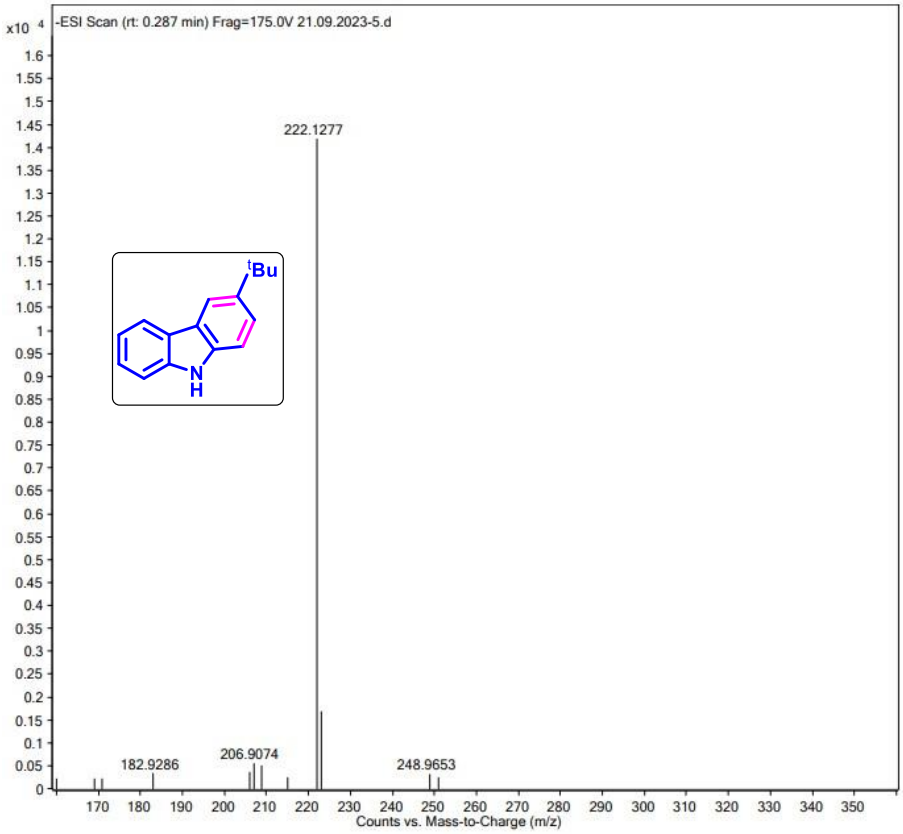

3-Chloro-9H-carbazole (5j):

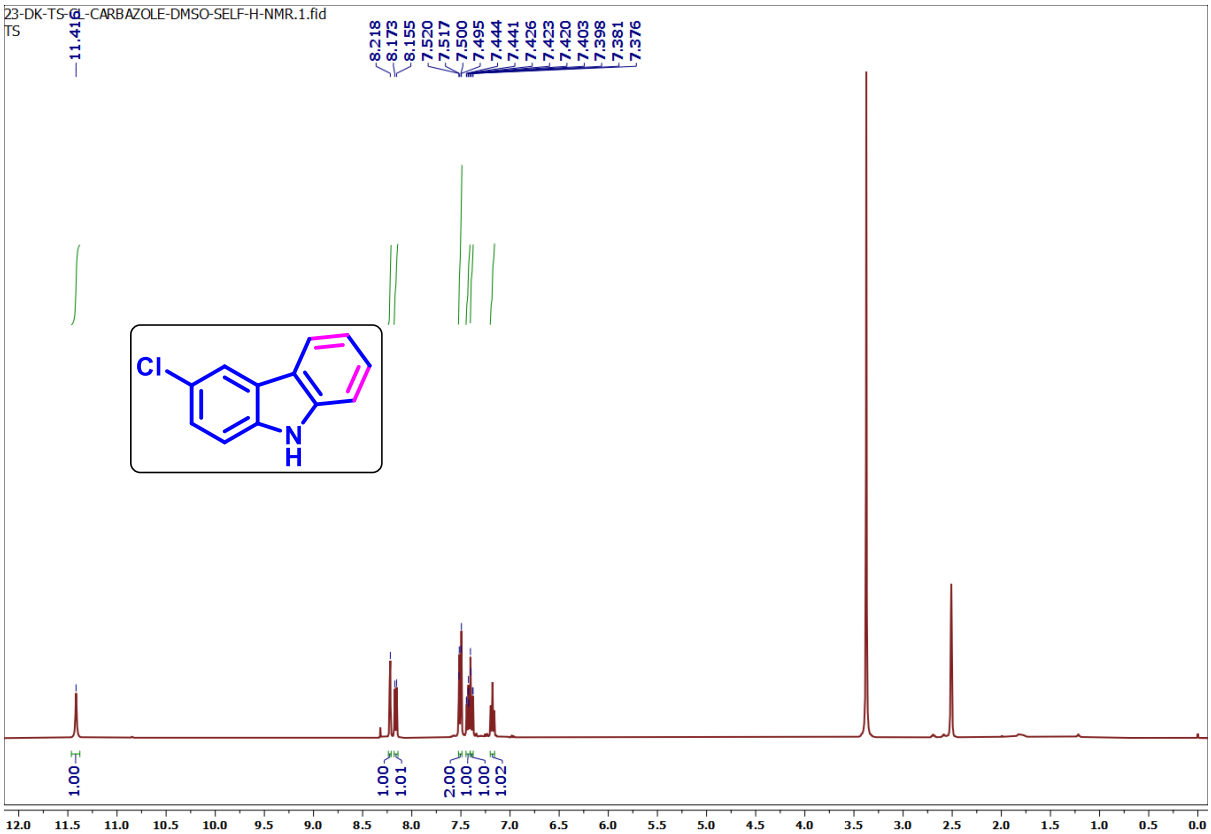

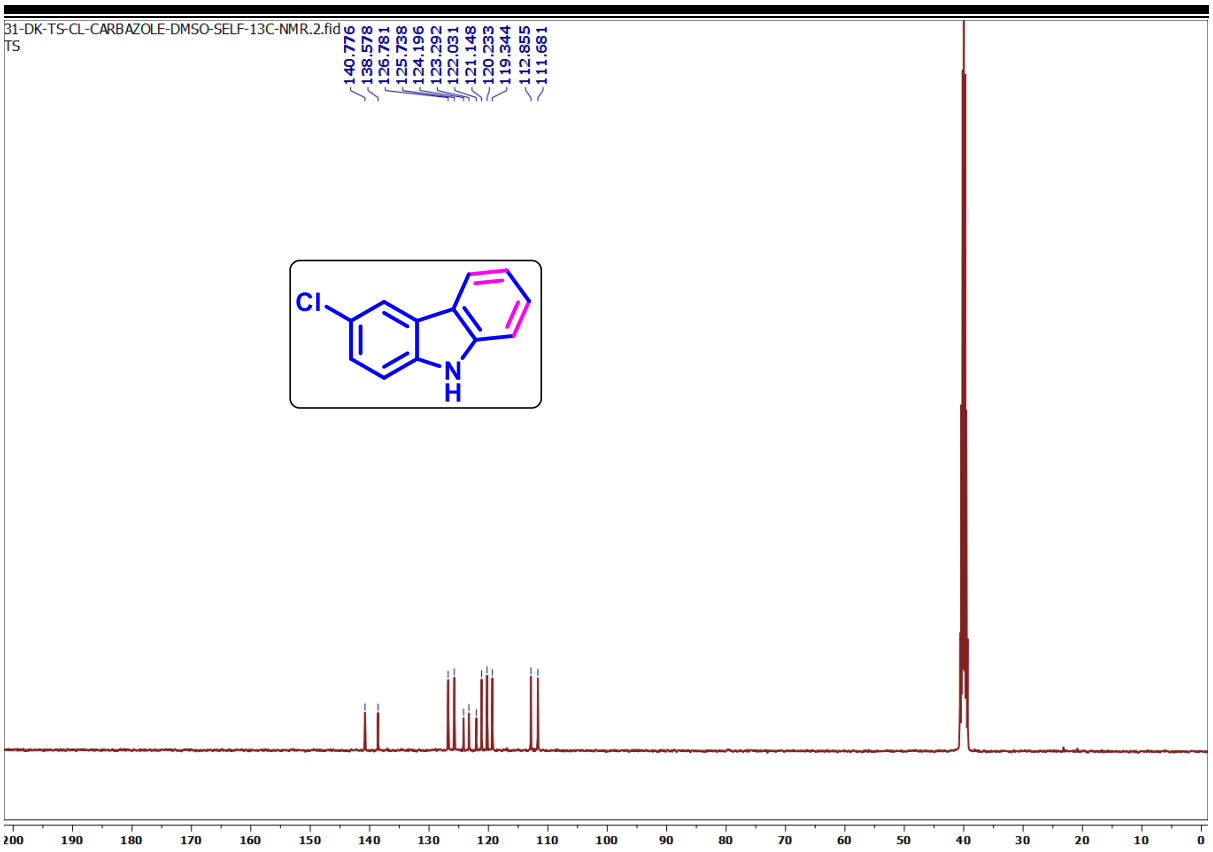
31-DK-TS-CL-CARBAZOLE-DMSO-SELF-13C-NMR.2.fid
TS
140.776
138.578
126.781
125.738
124.196
123.292
122.031
121.148
120.233
119.344
112.855
111.681
Cl
N
H
200 190 180 170 160 150 140 130 120 110 100 90 80 70 60 50 40 30 20 10 0

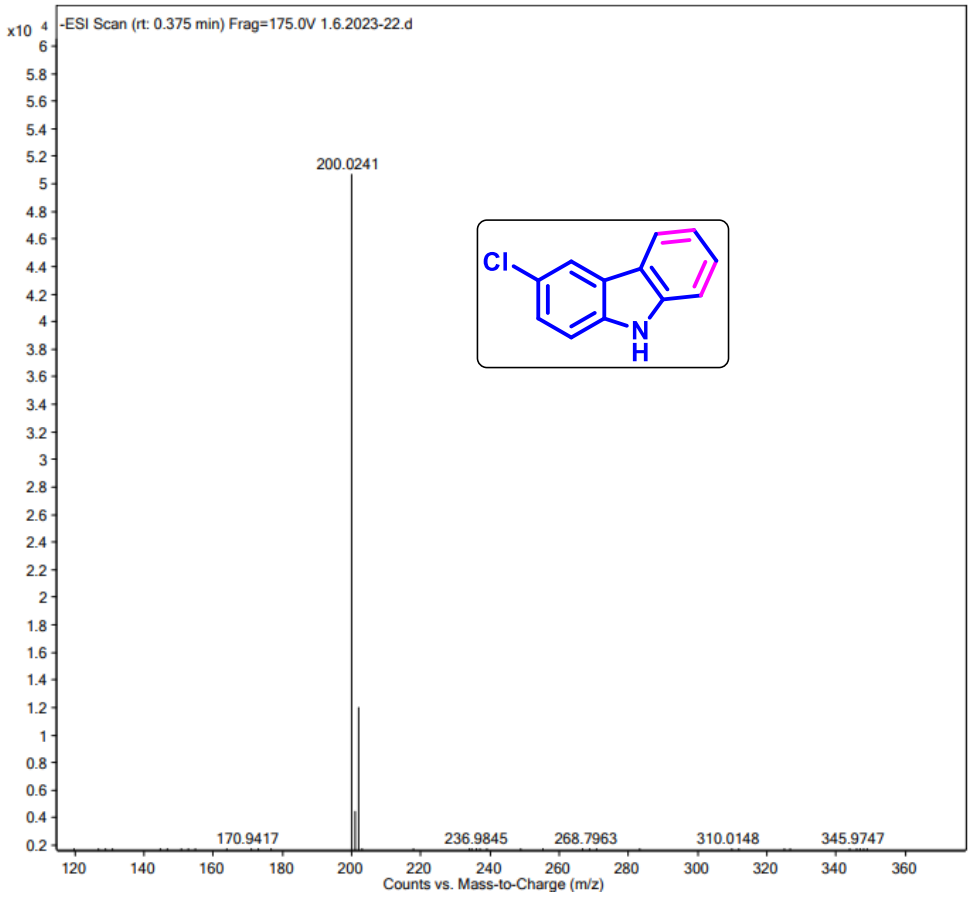
x10 4
-ESI Scan (rt: 0.375 min) Frag=175.0V 1.6.2023-22.d
200.0241
Cl
N
H
170.9417
236.9845
268.7963
310.0148
345.9747
Counts vs. Mass-to-Charge (m/z)

6-Methyl-9H-carbazole-3-carbonitrile (5p):

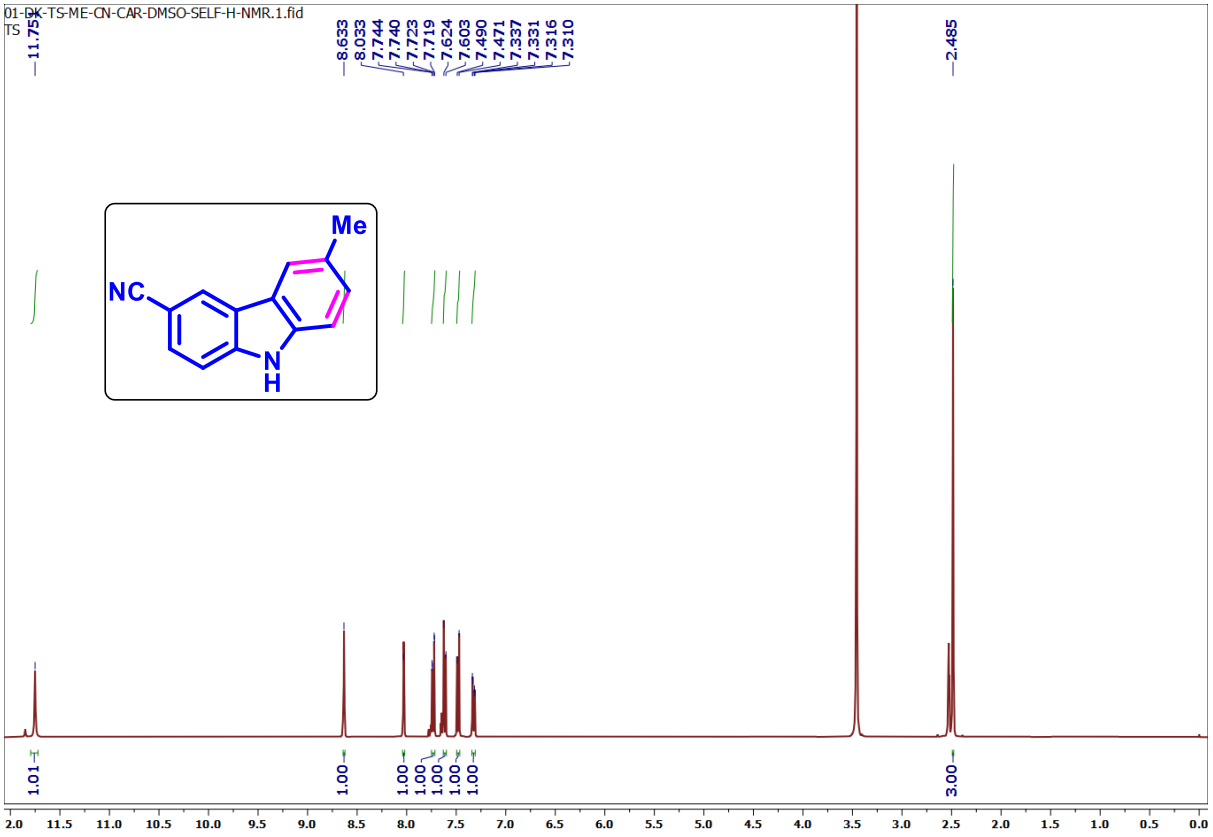

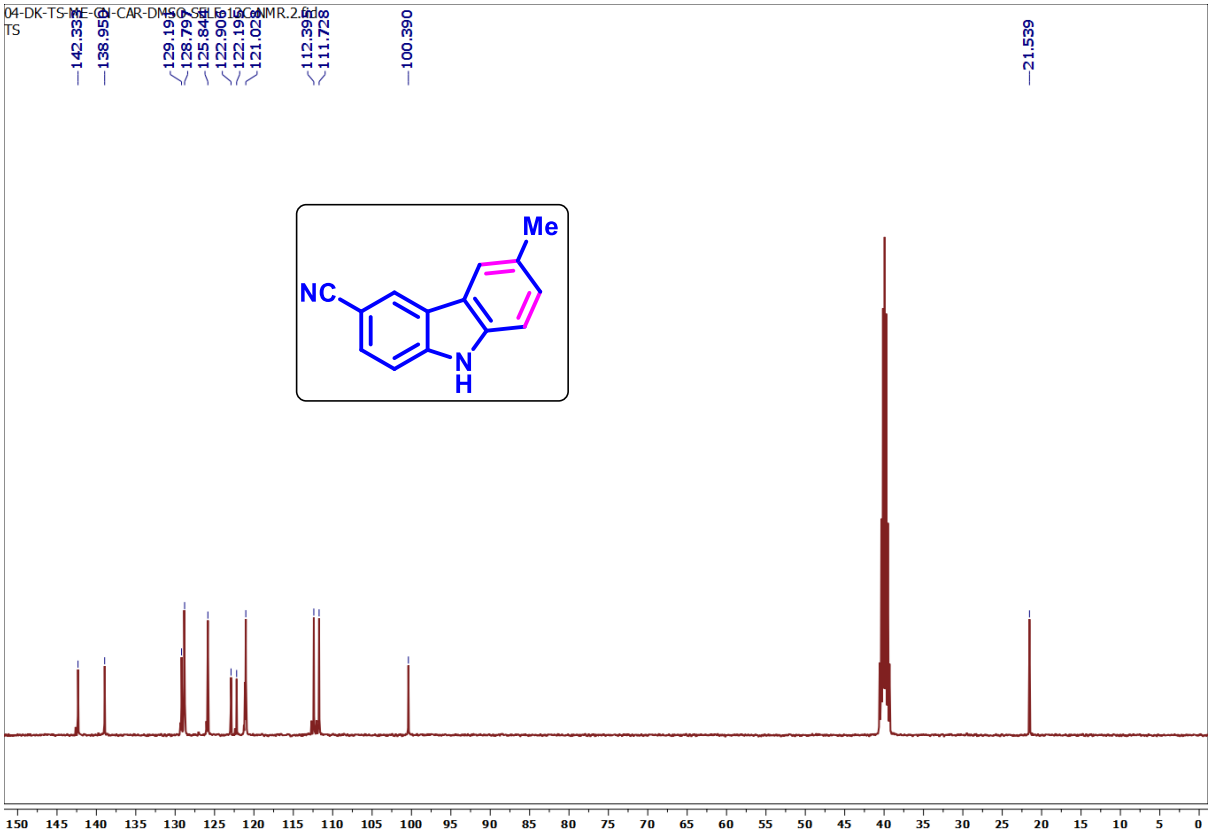

Methyl 1-phenyl-9H-pyrido[3,4-b]indole-3-carboxylate (9a):

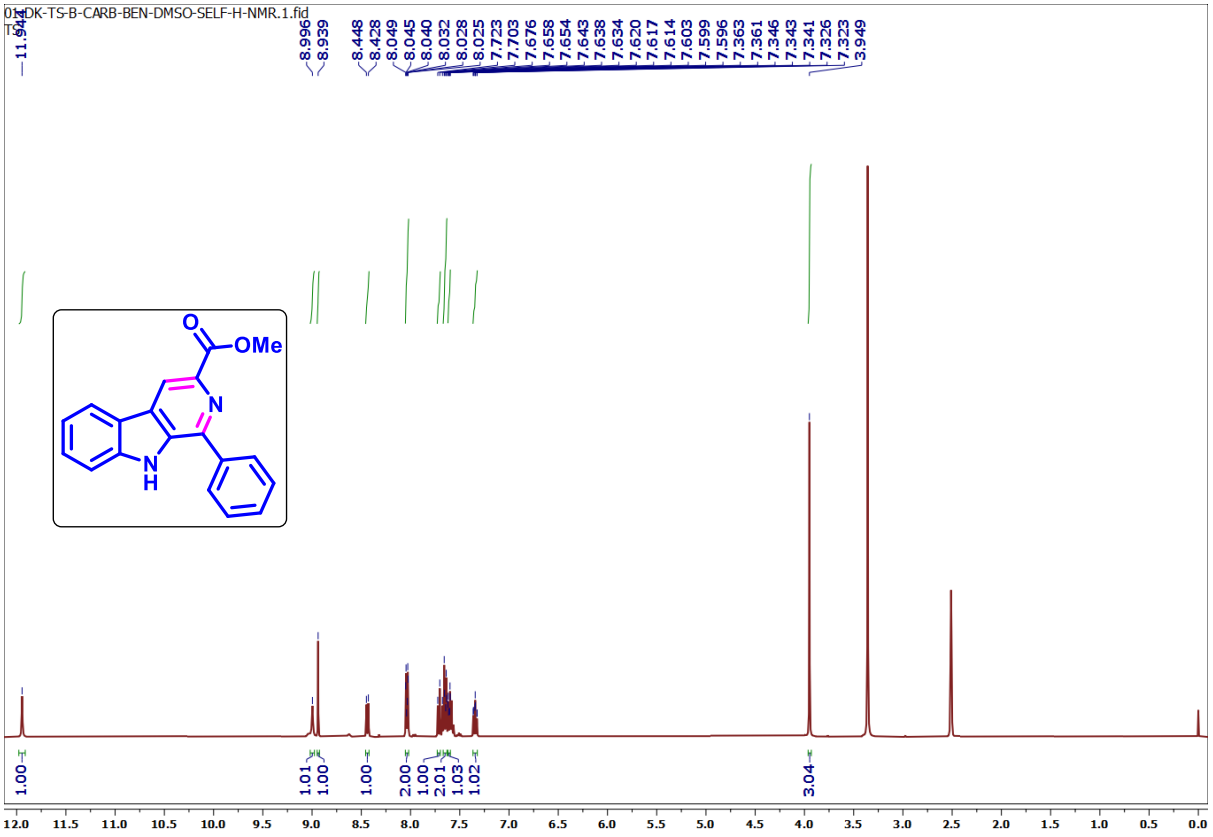

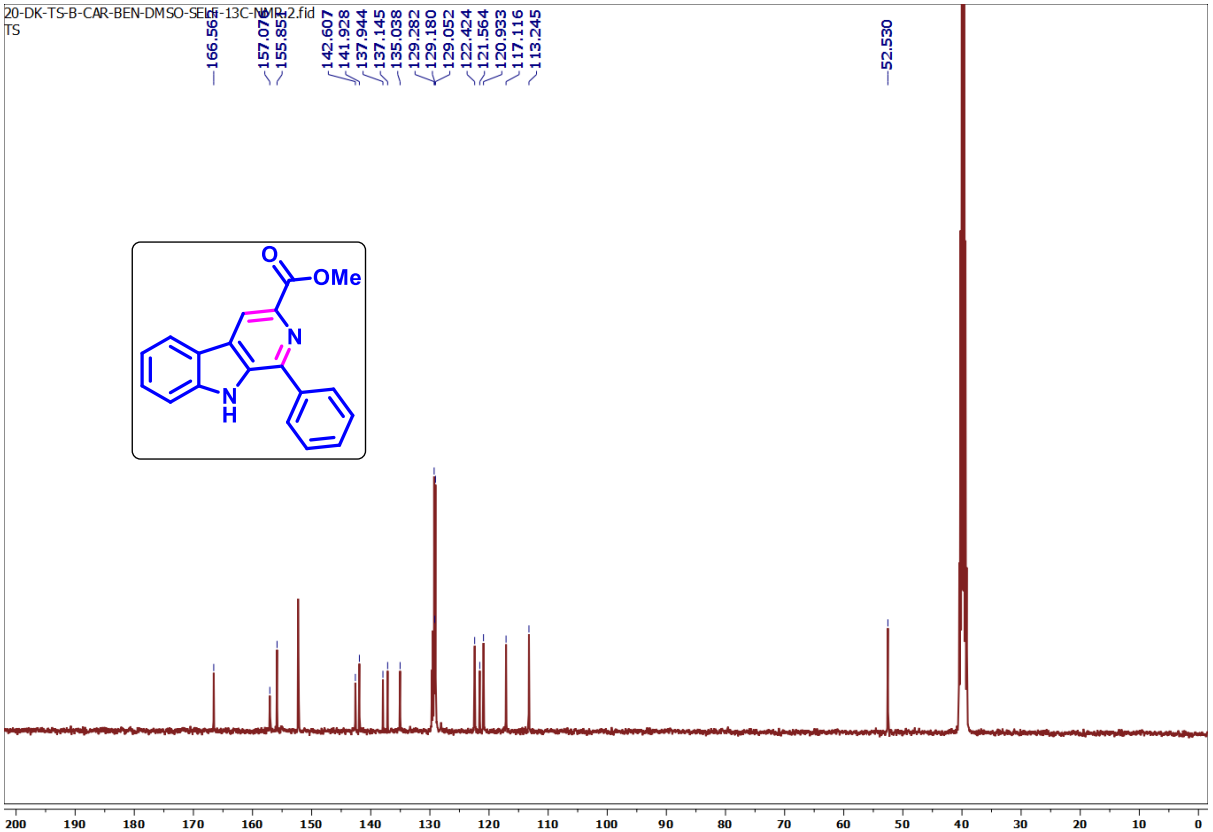

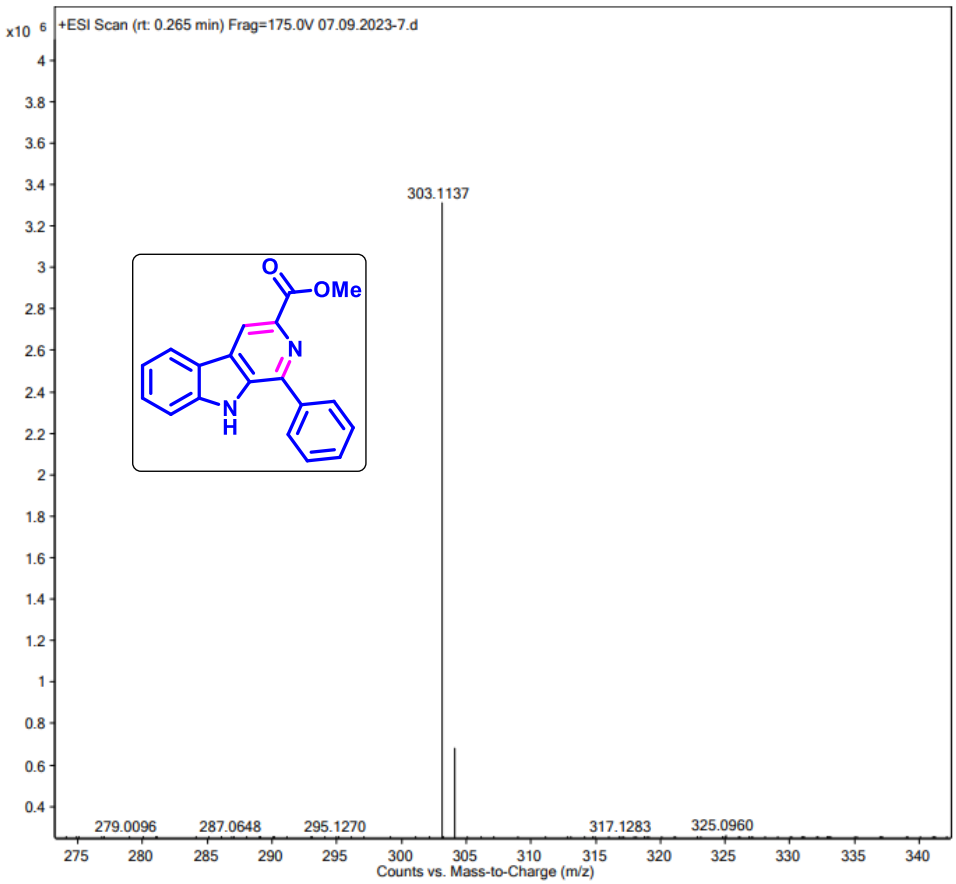

Methyl 1-(p-tolyl)-9H-pyrido[3,4-b]indole-3-carboxylate (9b):

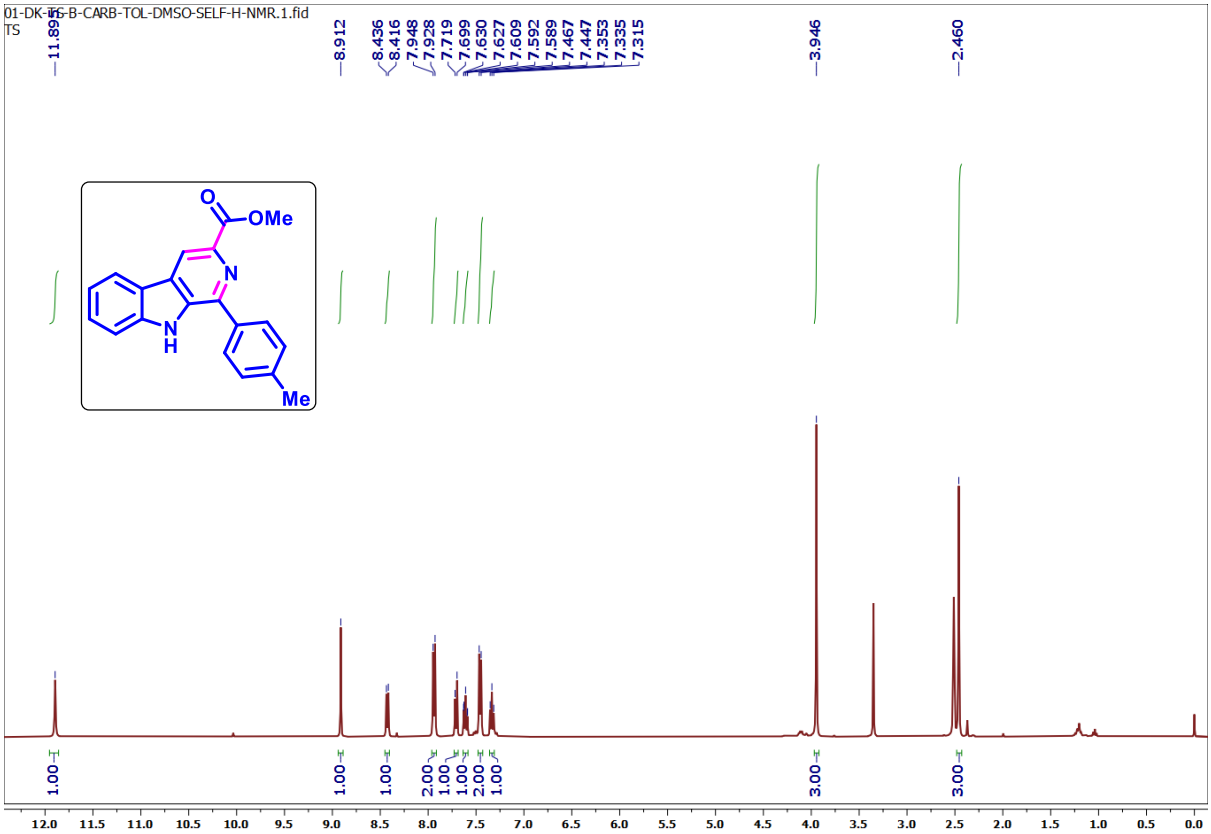

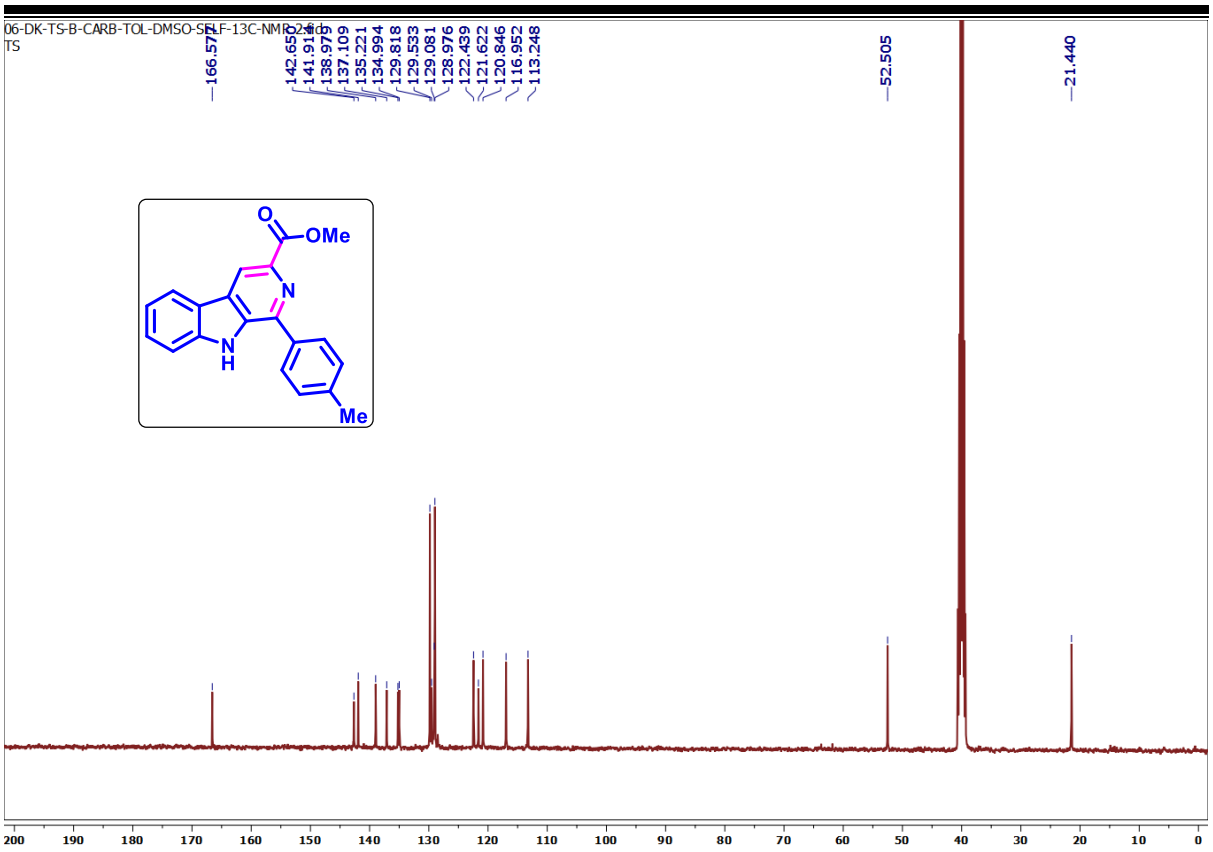
06-DK-TS-B-CARB-TOL-DMSO-SELF-13C-NMR-2.fid
TS
166.571
142.655
141.918
138.978
137.109
135.221
134.994
129.818
129.533
129.081
128.976
122.439
121.622
120.846
116.952
113.248
52.505
21.440
O
OMe
N
N
H
Me
200 190 180 170 160 150 140 130 120 110 100 90 80 70 60 50 40 30 20 10 0

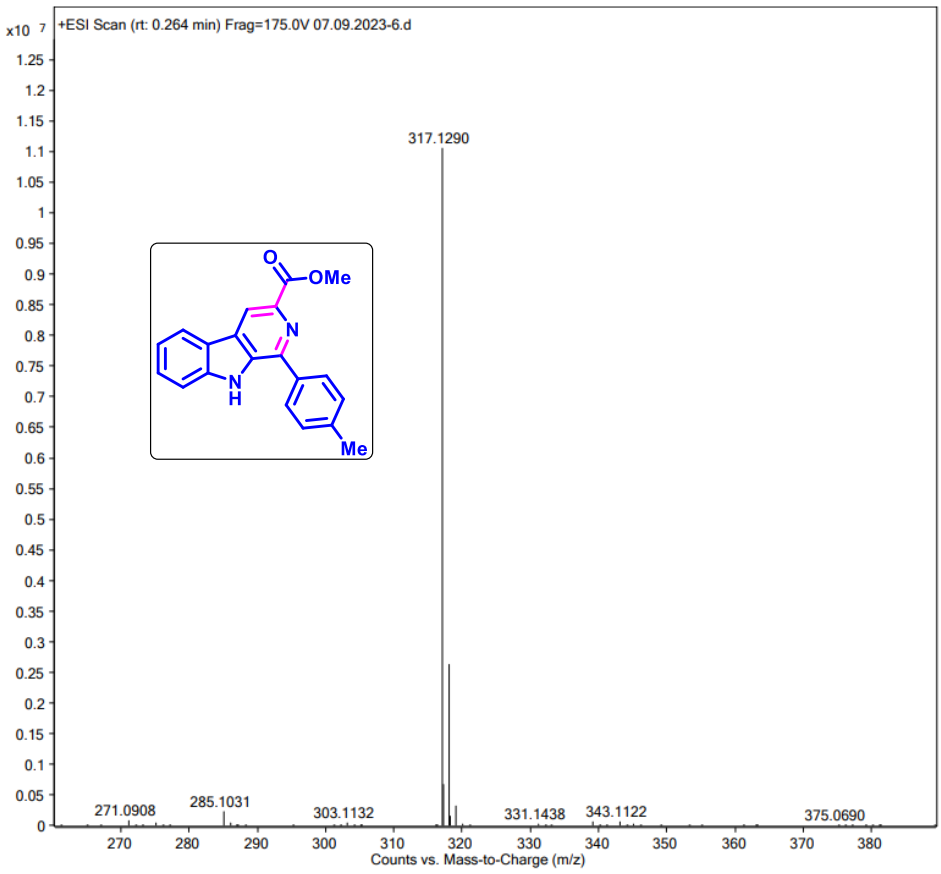
x10 7
+ESI Scan (rt: 0.264 min) Frag=175.0V 07.09.2023-6.d
317.1290
271.0908
285.1031
303.1132
331.1438
343.1122
375.0690
O
OMe
N
N
H
Me
Counts vs. Mass-to-Charge (m/z)

Summary of the thesis

The thesis entitled ***"Development of synthetic methods for the functionalized Tacrines, 1,2,3,4-Tetrahydroacridines, Acridin-4-yl(aryl)methanones, Carbazoles, and β-Carbolines"*** has been divided into **four chapters** with following titles. These titles have been decided based on the objectives and results obtained in the present investigation. In correlation with the titles, a brief discussion on the biologically active molecules of respective chapters, the synthetic methods reported in the literature along a detailed discussion of the results obtained along with the biological activity is discussed in the thesis.

Chapter-I: Introduction

Introduction of Cholinesterase Inhibitors

Cholinesterase inhibitors are used in the treatment of Alzheimer's disease (AD) and dementia symptoms. The primary neuropathological feature of the brain of AD patients is the misfolding and intracellular accumulation of neurofibrillary tangles or senile plaques of amyloid-β-peptide. These pathological changes contribute to a loss of cholinergic neurons in the basal forebrain, resulting in decreased levels of neurotransmitter acetylcholine, which plays a crucial role in cognitive function. Among the approaches explored for the treatment of AD, i.e., inhibition of cholinesterase (AChE and BChE) using cholinesterase inhibitors was approved as a therapeutic strategy to alleviate the symptoms of AD and delay its progression. Tacrine, Galantamine, rivastigmine, and donepezil are the four acetylcholinesterase inhibitors that have been approved for commercial use.

Introduction of Glucosidase Inhibitors:

α-Glucosidase is an intestinal enzyme that plays a major role in the degradation of carbohydrates to glucose so inhibiting it can reduce the release of glucose into the bloodstream. For example, α-Glucosidase inhibitors like acarbose, miglitol, and voglibose are used effectively for the treatment of type 2 diabetes.

Introduction of C(sp^3)-H activation:

The construction of C–C and C–X (X = O, N, *etc*.) bonds is the key task in organic synthesis. Traditionally, these goals were mainly approached through the transformation of pre-existing functional groups leaving C–H bonds untouched, which are ubiquitous in organic compounds. With recently much more attention to the atom-economical process and green chemistry goal, transition metal-catalysed direct C–H activation has emerged as the most powerful and straight forward strategy for the production of organic molecules from easily available chemicals.

Introduction of Deep Eutectic solvent:

Deep eutectic solvents (DESs) exhibit distinct physical and chemical characteristics such as non-toxicity, biodegradability, and use of inexpensive/ readily available reagents for the preparation. Considering this, DESs have been widely used in the field of organic synthesis as catalysts, and green and sustainable reaction medium. Formation of the new C–C, C–N bonds is a significant transformation in organic synthesis and well established using catalytic/green methods. Still, there is a demand in this area to develop new green chemical approaches for C–C, C–N bond formation for the active pharmaceutical intermediates and drug-like molecules.

<u>Chapter-II:</u> Synthesis of functionalized tacrine/1,2,3,4-tetrahydroacridine, Pfitzinger acid derivatives and their evaluation for dual cholinesterase and α-glucosidase inhibition

Tacrine (9-amino-1,2,3,4-tetrahydroacridine THA), a competitive cholinesterase inhibitor, is the first drug for the treatment of AD. Proctor and Harvey demonstrated that complex forms between tacrine and AChE due to vander Waals interactions and charge transfer involving π electrons at the peripheral site on the enzyme. The catalytic site of AChE participates in electrostatic π–π stacking interactions with the amino acid tryptophan and phenylamine. Tacrine also forms hydrogen bonds with histidine.

Unfortunately, THA administration is associated with a significant rate of hepatotoxicity. This effect constrained the administration of tacrine in the medicinal application. Therefore, significant efforts have been directed toward the development of tacrine derivatives that exhibit enhanced inhibitory activity while lacking hepatotoxic effects. To enhance the inhibitory activity and produce multi-targeted AChE inhibitors, a range of tacrine derivatives with similar structures were designed and synthesized.

The majority of these molecules are based on the modification of benzene ring in to pyrano, pyrano[2,3-*c*]pyrazole, pyridine, dihydropyridine using multi-component approaches. Along with these, the $–NH_2$ moiety of tacrine was used to generate an array of hybrid molecules with tacrine, 8-hydroxyquinoline, coumarin, chromene, cysteine, benzothiazole, melatonin, triazole at the other end (Fig. 2.1).

The above discussion indicates that there are many variations of *N*-alkyl/aryl derivatives and aromatic ring modifications and only a couple of reports for the cyclohexane modification at the C2 position of tacrine. However, there are no reports found in the literature for the functionalization of the C4 position of the tacrine. To fill the gap in the SAR of tacrine analogues, we decided to carry on our work on 9-amino-1,2,3,4-tetrahydroacridine-based AChE inhibitors by synthesizing and testing a series of tacrine derivatives substituted in positions C4, C6 and C7 of the acridine nucleus and modification at C9 $-NH_2$ position. Considering this, we performed molecular docking analysis for *in vitro* studies of tacrine to the active site of the AChE or BChE and observed a void space below the C4 position of tacrine after binding. This could be used for designing and synthesizing new compounds to improve the binding between the compound and protein in its active site. Based on the substitutions that gave better interaction/dock scores, compounds were synthesized and tested for *in vitro* activities. So, in this report, an attempt was made to introduce substitutions in the C4 position of tacrine, 1,2,3,4-tetrahydroacridine using metal-free C–C bond formation *via* $C(sp^3)$–H functionalization in the presence of DES. Along with C4 activation, we aim to describe a more economical and environmentally friendly approach for the synthesis of *N*-aryl tacrine through a metal-free C–N bond formation reaction, facilitated by deep eutectic solvent. As well as we synthesised 1,2,3,4-tetrahydroacridine derivatives by incorporating triazole moiety, ester, amide at C9 position along with C4 activation and performed molecular docking analysis for *in vitro* studies.

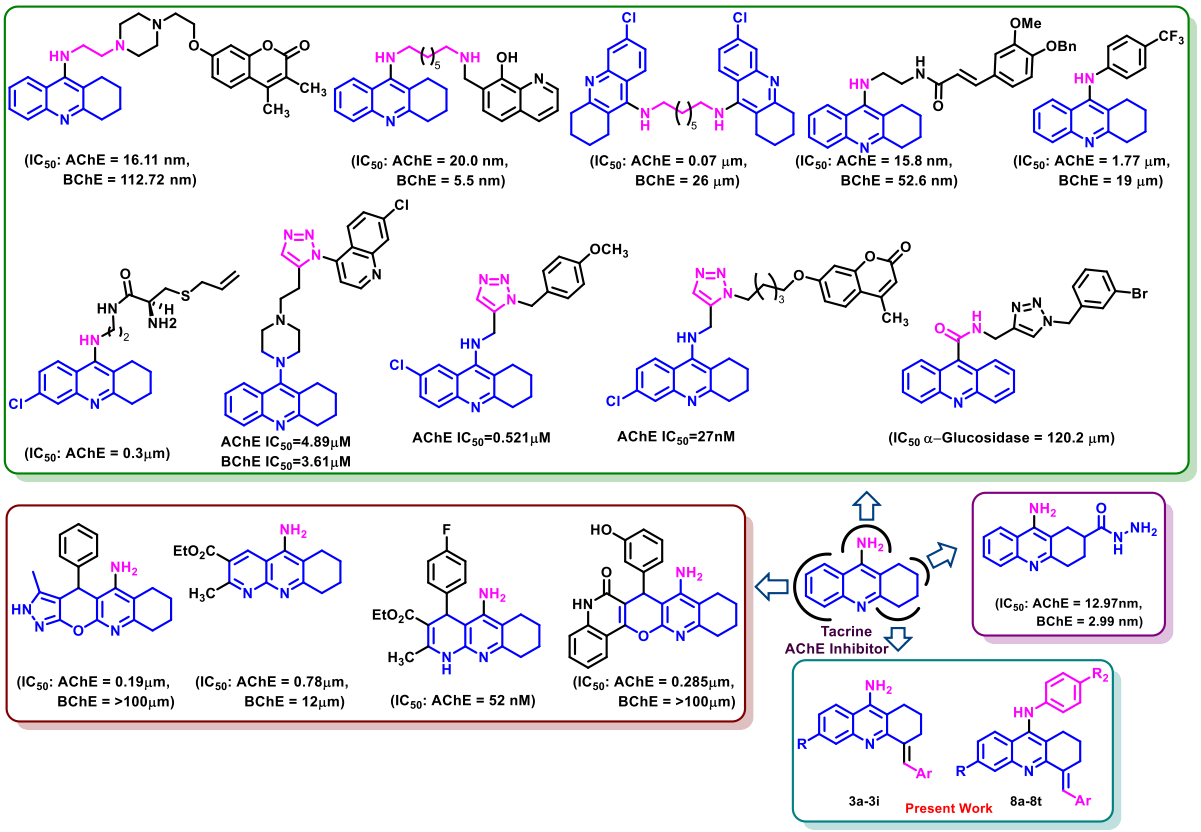

Fig-2.1. Reported Tacrine-based AChE and BChE inhibitors and newly synthesised compounds (**3a-3i and 8a-8t**).

<u>Part-A:</u> ***Metal-free synthesis of functionalized tacrine derivatives using deep eutectic solvent and their evaluation for dual cholinesterase and α-glucosidase inhibition***

Thus, with the background about various tacrine based AChE, BChE inhibitors, with our previous experience in C(sp^3)-H azaarenes activation, we initially planned directly to synthesis C4 activated tacrine derivatives (**3a**) through activation of tacrine (**1**) with aromatic aldehyde (**2a**). However, there was no product formation was observed. Later, an alternative method was envisaged, according to that 9-chloro-1,2,3,4-tetrahydroacridine derivatives (**4a-4f**) was reacted with aromatic aldehyde (**2a**) to provide the C4 activated 1,2,3,4-tetrahydracridine derivatives(**5a**). The DES *N,N'*-dimethylurea (DMU), and L(+)-tartaric acid ((L-(+)-TA) (in a 3:1 ratio at 80 °C) was found to be optimised condition for synthesis of desired derivatives (**5a-5ae**) in 73%-94%.

The C4 functionalisation of tacrine derivatives was achieved by converting C4 activated 9-chloro-1,2,3,4-tetrahydroacridine derivatives (**5a-5i**) into 9-azido-1,2,3,4-tetrahydroacridines **(6a–6i)** in the presence of DES i.e., DMU+L-(+)-TA (3:1) and then reduced into amines **(3a–3i)** using Staudinger conditions in moderate to good yields (50%-72%). Inspired by successful synthesis of functionalised tacrine derivatives, next we synthesised *N*-aryl tacrine scaffolds by the reaction of compound (**5a-5j**) with aniline derivatives (**7a-7e**) under optimised DES condition i.e., DMU+L-(+)-TA (3:1) at 80 °C, and afford the desired products (**8a-8t**) in 71%-90% yield.

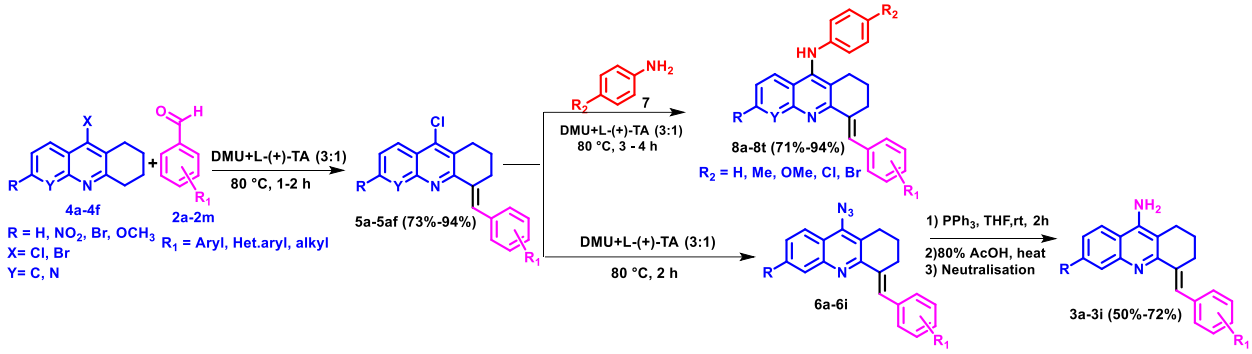

Scheme-2.1. Synthesis of C4 functionalised 9-Chloro-1,2,3,4-tetrhydroacridine, tacrine, *N*-aryl tacrine.

Biological activity

In vitro and *in silico* studies performed for the synthesised compounds (**3a-3i, 5a-5af, 8a-8t**) showed improved AChE (PDB ID: 1DX6) and BChE (PDB ID: 6EMI) inhibitory activity and binding efficiency. By studying the inhibition pattern and kinetics of inhibition of AChE and BChE, majority of the compounds reported here were significantly more potent inhibitors than the standard inhibitor Tacrine (AChE IC_{50} = **203.51 nM**; BChE IC_{50} = **204.01 nM**). Among the compounds screened, **8m** was found to be more potent with IC_{50} = **125.06 nM** and **119.68 nM** towards AChE and BChE inhibition respectively. The α-glucosidase inhibitory activity of the compounds was tested using acarbose as a standard drug (IC_{50} = **23100 nM**) and compound **8j** was found to be active with IC_{50} = **19400 nM**.

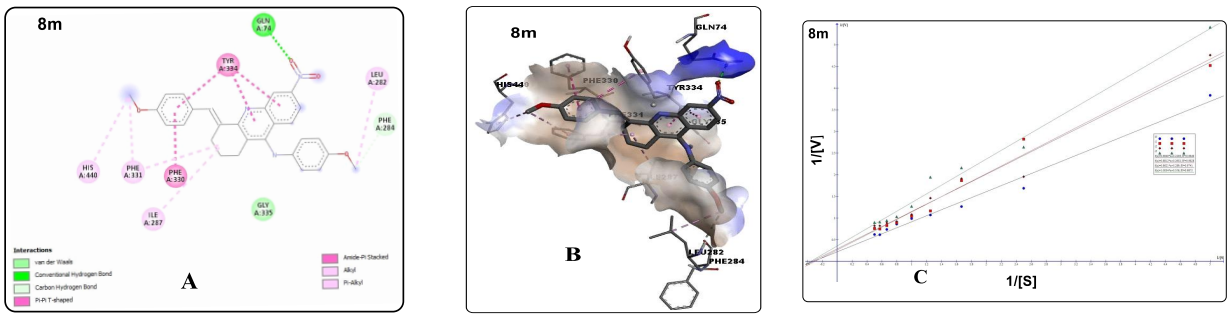

Fig. 2.2. A) 2D interaction of compound **8m** with protein 1DX6. **B)** 3D interaction of compound **8m** with protein 1DX6. **C)** Lineweaver–Burk plot for understanding the interaction of AChE with compound **8m.**

Molecular dynamics simulations analysis providing stability of ligand-protein complexes and corresponding apo-protein system over the simulated time course, extending up to 200 nanoseconds. It was observed that the compounds **8m** and **8o**, exhibited an average RMSD value consistently below 2 Å. This observation underscores the increased stability of these specific compounds within the complex with the target protein compared to the apo-protein. From Blood Brain Barrier (BBB) analysis it was shows that the tested compounds are BBB permeable can cross blood brain barrier and also, do not violate the Lipinski Rule of Five, showing drug-like properties.

<u>Part-B:</u> ***Synthesis of 1,2,3,4-tetrahydroacridine based-1,2,3-triazole derivatives and their evaluation as dual cholinesterase, α-glucosidase inhibitors***

In the present study by considering tacrine to be the basic AChE inhibitory moiety, we aimed to replace the substitution of its -NH_2 by a 1,2,3-triazole moiety.

The desired compounds **10a-10n** were obtained by the reaction sequence illustrated in Scheme 2.2. According to previous chapter C (sp^3)-H functionalized 1,2,3,4-tetrahydroacridine derivatives (**3a)** was synthesized under DES at 80 °C. To the same reaction pot sodium azide (**4**) was added to obtain 9-azido-1,2,3,4-tetrahydracridine derivatives (**6a-6h**). Finally, desired product **10a** was prepared by click reaction of azide derivative (**6a-6h**) with phenylacetylenes (**6**) in H_2O: ^{t}BuOH (1:1) in the presence of Et_3N along with a catalytic amount of $CuSO_4$ and sodium ascorbate at room temperature for 2–4 h in good to excellent yield. In continuation of this, we synthesized tacrine triazole hybrids (**13a-13h**) by adopting click chemistry conditions in good to excellent yield (87%-94%).

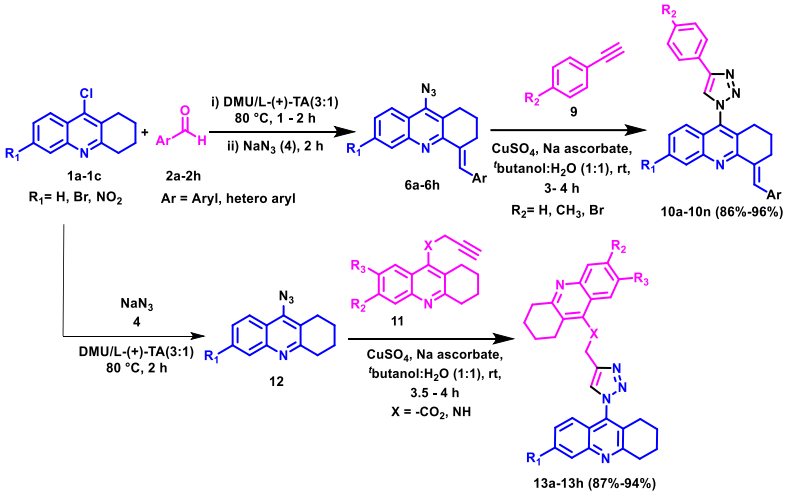

Scheme-2.2. Synthesis of Tacrine-triazole hybrids.

Biological activity

In vitro and *in silico* studies were performed for the tacrine triazole derivatives. Majority of tacrine-triazole hybrids show better activity than standard tacrine (AChE IC_{50} = **201.05 nM**; BChE IC_{50} = **202.14 nM)**. Among the synthesized compounds compound **10j** showed maximum inhibitory activity for AChE (IC_{50} = **120.67 nM)**, compound **13e** exhibited minimum IC_{50} i.e. **124.94 nM** value for BChE, and the α-glucosidase inhibitory activity of the compounds was tested using acarbose as a standard drug (IC_{50} = **23100 nM**) and compound **13b** exhibiting potent inhibitory activity for α-glucosidase (IC_{50} = **22390 nM**).

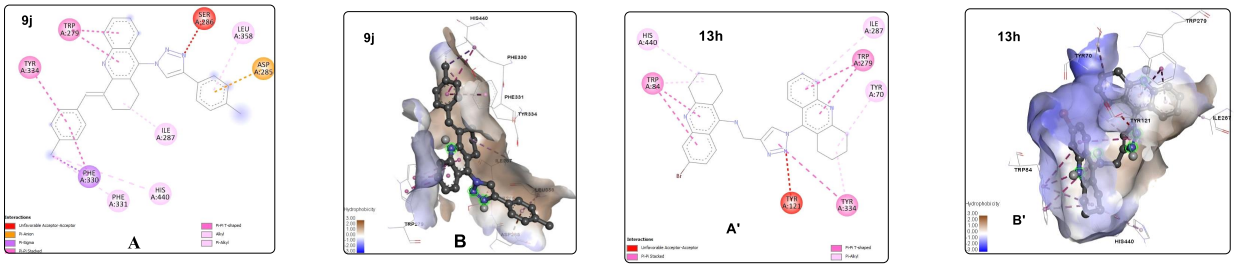

Fig-2.3. A) 2D interaction of compound **10j** with protein 1DX6. **B)** 3D interaction of compound **10j** with protein 1DX6. **A)** 2D interaction of compound **13h** with protein 1DX6. **B)** 3D interaction of compound **13h** with protein 1DX6

All the tested compounds selected based on their *in vitro* inhibitory activity against AChE and BChE were determined to be BBB+. This indicates that these molecules possess BBB permeability and can traverse the blood-brain barrier and do not violate the Lipinski Rule of Five, hence having drug-like properties.

Part-C: ***Deep Eutectic Solvent mediated synthesis of C4 functionalized Pfitzinger acid derivatives and their evaluation as dual cholinesterase and α-glucosidase inhibitors***

Encouraged by the promising cholinesterase inhibitory activity of 1,2,3,4-tetrahydroacridine in our previous studies, we aimed to synthesize a series of 1,2,3,4-tetrahydroacridine derivatives. Specifically, we targeted the 9th position ($-NH_2$) for derivatization with carboxylic acid (-COOH), ester (-COOR), or amide (-COONHR) functionalities. Additionally, substitutions at the C4 and C7 positions were incorporated to explore their influence on cholinesterase inhibitory activity and α-glucosidase inhibitory activity.

The C(sp^3)-H functionalization of 1,2,3,4-tetrahydroacridine-9-carboxylic acid (**15**), its derivatives (**18, 21,24**) is carried out by treating with aromatic aldehyde (**2a**) was performed using a combination of *N, N'*- dimethyl urea and L-(+) tartaric acid (3:1) ratio at 80 °C. The reaction proceeds smoothly, affording the intended products (**16a-16d, 19a-19y, 22a-22m, 25a-25d**) with good to excellent yield (Scheme-2.3).

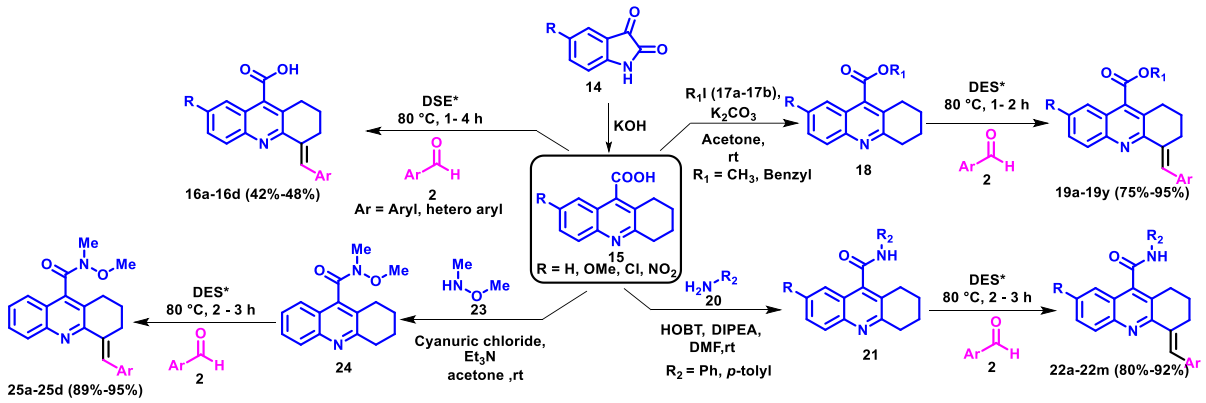

Scheme-2.3. synthesis of C4, C9 substituted 1,2,3,4-tetrahydroacridine derivatives

Biological activity

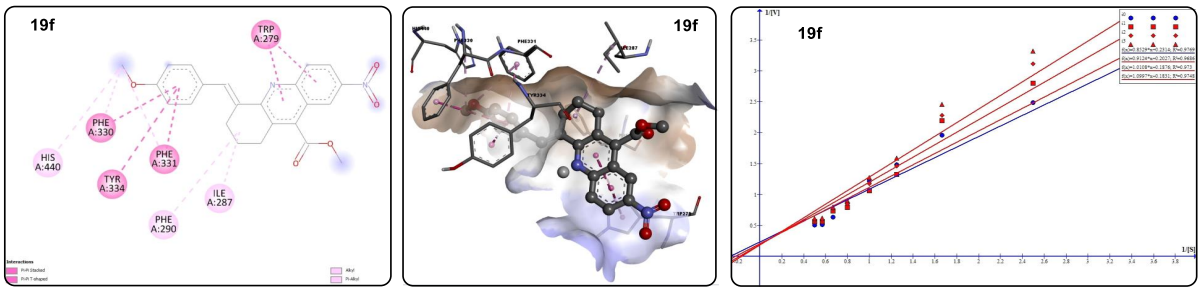

Fig. 2.4. 2D, 3D interaction of compound **19f** with protein 1DX6, Lineweaver–Burk plot for understanding the interaction of AChE with compound **19f**

In vitro and *in silico* studies performed for the synthesised compounds (**16a-16d, 19a-19y, 22a-22m, 25a-25d**) showed improved AChE and BChE inhibitory activity and binding efficiency. By studying the inhibition pattern and kinetics of inhibition of AChE and BChE, compounds **19f, 19t,** and **19v** were found to exhibit maximum inhibitory activity with IC_{50} values for AChE **119.45 nM, 119.65 nM, 124.65 nM** and for BChE **121.58 nM, 118.69 nM, 118.25 nM** respectively. Among the tested compounds, **22g** compound showed good inhibitory activity against α-D-glucosidase (IC_{50}= **21442 nM**).

<u>Chapter-III:</u> Part-A: ***Metal-free C4 C(sp^3)-H functionalization of 1,2,3,4-tetrahydroacridines using dialkyl azodicarboxylates and N-phenylmaleimide in Deep Eutectic Solvent***

Direct functionalization of inactive C–H bonds is a current topic of research and strategy for the construction of C–C and C–X (X=O, N, S) bonds in organic synthesis. This method can offer a maximum atom efficiency by avoiding pre-functionalization of substrates thus widely explored in the fields of synthetic organic chemistry. The development of a new catalytic system for the direct amination of inert C(sp^3)–H bonds without the use of pre-functionalized substrates to construct C–N bonds remain one of the major challenges. Dialkyl azodicarboxylates are used as electrophiles for C–N bond formation reactions *via* nucleophilic addition. Similarly, maleimides have been explored as the source for alkylation in C(sp^3)–H and C(sp^2)–H bond functionalization leading to the generation of functionalized succinimides. In this regard, we wish to report a very simple, efficient, and metal-free approach for the C4(sp^3)-H amination and alkylation of 1,2,3,4-tetrahydroacridine using deep eutectic solvent as a catalyst and reaction medium.

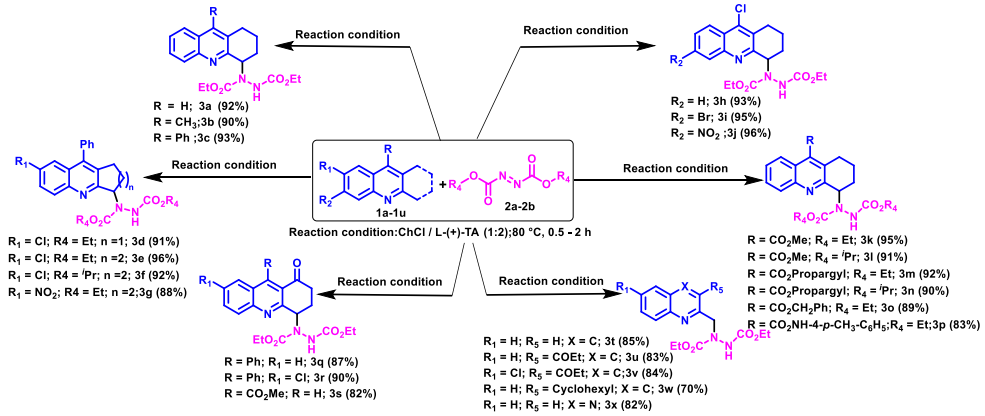

Scheme-3.1. Synthesis of C4-substituted 1,2,3,4 tetrahydroacridine derivatives

Thus, 1,2,3,4-tetrahydroacridine (**1a-1u**) and dialkyl azodicarboxylate (**2a-2b**) was treated under Choline chloride and L-(+)-tartaric acid in 1:2 ratio at 80 °C provided the desired products (**3a-3x**) in 70%-96% yield.

Then we extended the C4(sp^3)-H functionalization strategy for alkylation of 1,2,3,4-tetrahydroacridine at C4 position. For C4 alkylation 1,2,3,4-tetrahydroacridine (**1a-1u**) reacted with *N*-phenyl maleimide (**4**) in DES DMU and L-(+)-tartaric acid in 3:1 ratio at 80 °C to afford the corresponding alkylated products (**5a-5u**) in 75%-96%.

The scalability of the protocol was effectively demonstrated by the gram-scale synthesis of **3e** and **5e**, which yielded 89% and 87%, respectively, under optimized reaction conditions.

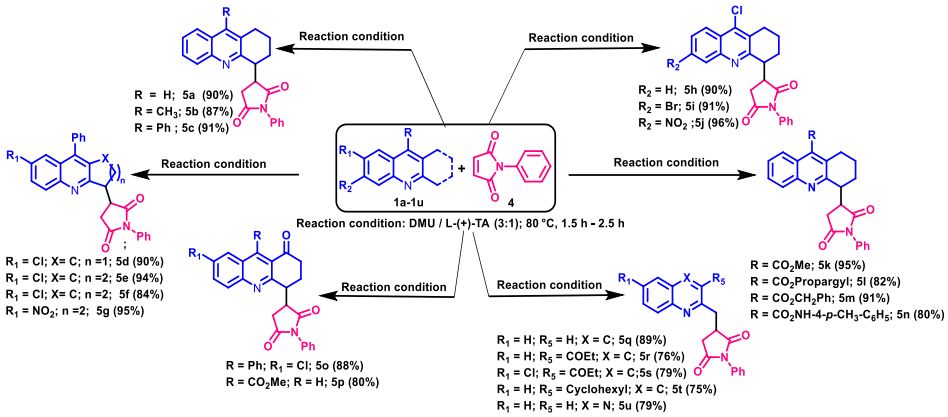

Scheme-3.2. Synthesis of C4 alkylated 1,2,3,4-tetrahydroacridine derivatives

Part-B: *TBHP-TBAI Catalyzed synthesis of 2,3-Dihydroacridin-4(1H)-ones via C4 C(sp^3)-H sulfonylation and desulfonylation of 1,2,3,4-tetrahydroacridines*

Sulfone motifs are widely found in a broad scope of bioactive natural products, pharmaceuticals, agrochemical compounds. Organo sulfones exhibit a diverse range of pharmacological properties, including antibacterial, antibiotic, γ-secretase inhibitor. Among numerous organo sulfone derivatives, 2-sulfolmethyl quinoline scaffolds are component of various medicinally significant compounds.

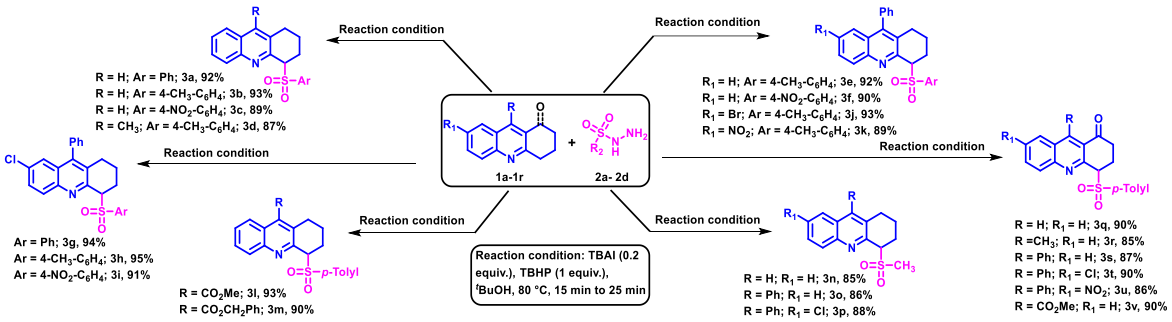

Scheme-3.3. C4(sp^3)-H sulfonylation of 1,2,3,4-tetrahydroacridine

As part our continuing efforts in C(sp^3)-H functionalisation of 1,2,3,4-tetrahydroacridine, herein we describe a TBAI-mediated direct sulfonylation of 1,2,3,4-tetrahydroacridine (**1a-1r**) with sulfonyl hydrazide (**2a-2d**) under mild conditions, affording 4-sulfonyl substituted 1,2,3,4-tetrahydroacridine (**3a-3v**) in good to high yields (Scheme-3.3).

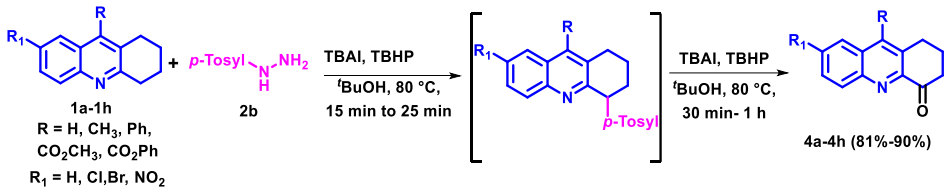

Scheme-3.4. Oxidative desulfonylation followed by keto formation at the C4 position of 1,2,3,4-tetrahydroacridine

When *p*-tolyl sulfonylhydrazine was used as the substrate for the C(sp^3)-H sulfonylation of 1,2,3,4-tetrahydroacridine, it was found that at an extended reaction time the C4 sulfonated 1,2,3,4-tetrahydroacridine undergoes oxidative desulfonylation followed by keto formation at

the C4 position i.e. 2,3-dihydroacridin-4(1H)-one derivatives (**4a-4r**) in 81%-90% yield (Scheme-3.4).

Part-C: ***DDQ Mediated synthesis of Acridin-4-yl(aryl)methanones via aromatization-C(sp^2)-H oxidation sequence of C4 functionalized 1,2,3,4-Tetrahydroacridine derivatives***

Acridine derivatives form an important class of heterocycles containing nitrogen due to their broad range of pharmaceutical properties. The numerous biological activities of acridine derivatives encompass roles as anti-inflammatory, anti-cancer, antitubercular agents, and potent inhibitors of acetylcholinesterase. However, though these naturally occurring compounds were used as pigment and dyes in the nineteenth-century researchers have found that along with the antitumor activity, it could be also effective as inhibitors of acetylcholinesterase for the treatment of Alzheimer's disease. Owing to the pronounced biological effects by the acridine derivatives, we intended to synthesis acridine derivatives through dehydrogenative aromatization of 1,2,3,4-tetrahydroacridine derivatives.

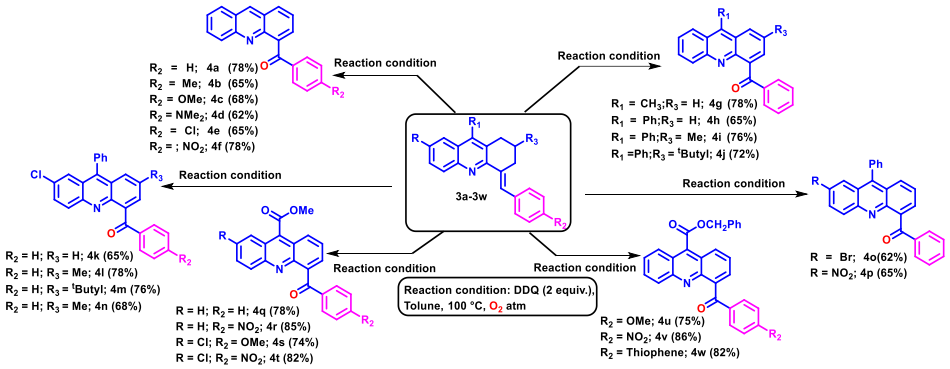

Scheme-4.1. Synthesis of Acridine derivatives

Towards this objective, the C4 functionalised 1,2,3,4-tetrahydroacridine (**3a-3x**) was treated with 2 equiv. of DDQ in toluene under O_2 atmosphere at 100 °C to afford acridine derivatives *via* dehydrogenative aromatisation and C(sp^2)-H oxidation (Scheme-4.1). The synthesis of various acridin-4-yl(phenyl)methanones was achieved from differently functionalized tetrahydroacridine and the corresponding substituted aromatic aldehyde in moderate to good yields under mild condition.

<u>Chapter-4:</u> ***One-Pot Synthesis of functionalized Carbazoles and β-Carbolines via Diethyl Azodicarboxylate mediated dehydrogenative aromatization in Deep Eutectic Solvent***

Carbazole, β-Carboline with a nitrogen in the five-membered ring constitute core structure of a diverse array of alkaloids found in many natural and pharmaceutical ingredients. These alkaloids exhibit a plethora of bioactivities and therapeutic properties, including antitumor, antiviral, psychotropic, anti-Alzheimer's, anti-inflammatory, antibiotic, and anti-oxidative, anti-TB activities.

In continuation with our interest in the development of green methods, herein we report an efficient, simple route for one-pot synthesis of carbazole and β-carbolines using Deep Eutectic Solvent (DES) as reaction medium and Diethyl azodicarboxylate (DEAD) as the dehydrogenating agent. The advantage of this method is to avoid strong oxidizing agents under eco-friendly/green conditions to achieve both the title compounds (i.e. functionalized carbazoles and β-Carbolines). For the one-pot synthesis of carbazole, phenylhydrazine (**1a-1i**) (1 mmol)

was treated with cyclohexanone (**2a-2c**) (1 mmol) in DMU/L-(+)-TA (3:1) (DES) at 80 °C for 30 min to give the 1,2,3,4-tetrahydrocarbazole (**3a-3p**). To this mixture, DEAD was added and heating was continued for 30 min. to give the dehydrogenated product i.e., carbazole (**5a-5p**) in excellent yield (91%-98%) scheme-4.2.

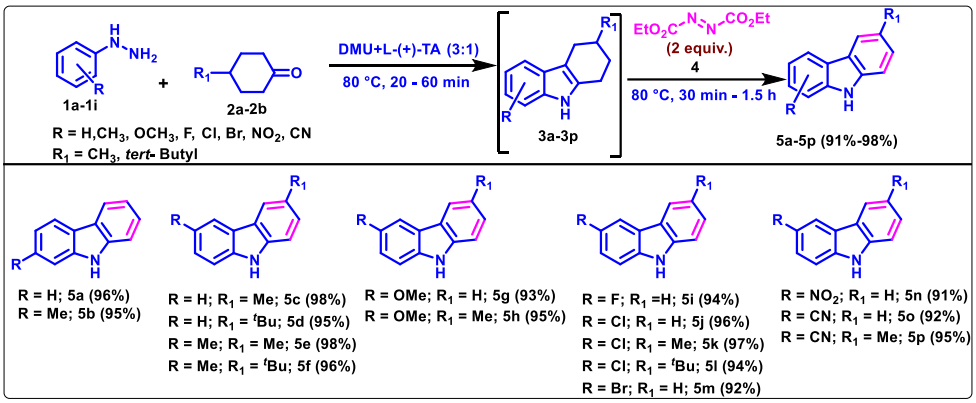

Scheme-4.2. One-pot synthesis of carbazole derivatives (5a-5p)

Encouraged by the above method, we applied the same strategy for the one-pot synthesis β-carbolines derivatives *via* dehydrogenative aromatization. To initiate one-pot synthesis of β-carboline, L-tryptophan methyl ester (**6**) and aromatic aldehyde (**7a**) were heated in DES at 80 °C for 30 min to afford 1,2,3,4-tetrahydro-β-carboline (**8a-8i**) *via* Pictet-Spengler reaction. To the same reaction pot DEAD (**4**) was added and heating was continued for 45 min to yield β-carboline derivatives (**9a-9i**) in 91%-96% (scheme-4.3).

While diethyl azodicarboxylate are effective dehydrogenating agents for aromatizing tetrahydrocarbazoles and tetrahydro-β-carbolines under DES conditions, their stoichiometric use and byproduct formation make them less atom-economical. Seeking to address to this, we explored Jung et al.'s reported method for aerobic azocarboxylate regeneration. We applied this approach to the dehydrogenation of compound (**3a)** using DEAD (**4**) with a co-catalyst system of CuI, DMAP, and O_2 under DES at 80 °C. This facilitated the regeneration of DEAD from its corresponding hydrazocarboxylate intermediate. Although faster reaction times were not achieved, we successfully obtained the desired product (**5a**) in good yield.

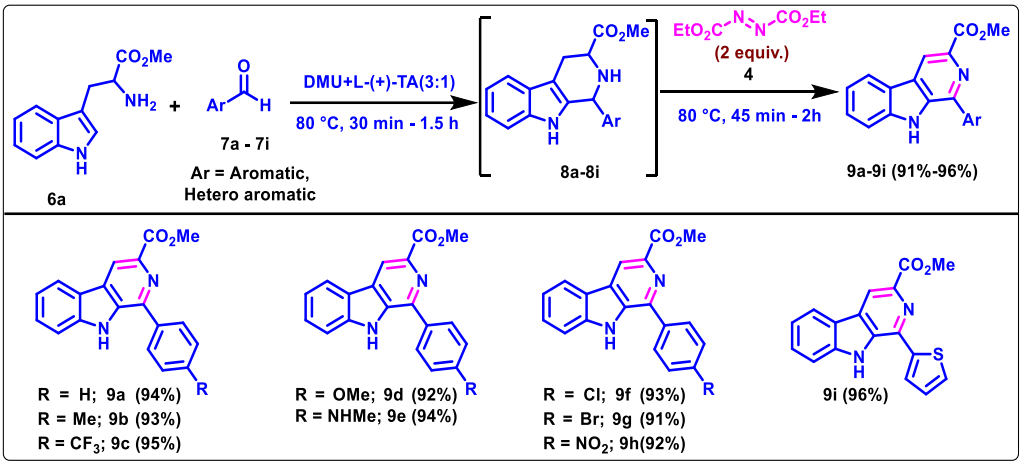

Scheme-4.3. One-pot synthesis of β-carboline (**9a-9i**)

List of publications (from the thesis)

1. **T. Shirisha**, S. Majhi, K. Divakar, D. Kashinath, "Metal-free synthesis of functionalized tacrine derivatives and their evaluation for acetyl/butyrylcholinesterase and α-glucosidase inhibition" *Org. Biomol. Chem.* **2024**, *22*, 790-804.

2. **T. Shirisha**, S. Majhi, S. Balasubramanian, and D. Kashinath, "Metal-free C (sp^3)–H functionalization (C–C and C–N bond formation) of 1, 2, 3, 4-tetrahydroacridines using deep eutectic solvents as catalyst and reaction medium" *Org. Biomol. Chem.* **2024**, *22*, 1434-1440.

3. **T. Shirisha**, S. Majhi, and D. Kashinath, "One-Pot Synthesis of Functionalized Carbazoles and *β*-Carbolines *via* Diethyl Azodicarboxylate mediated Dehydrogenative Aromatization in Deep Eutectic Solvent" manuscript accepted, *Chemistryselect* **2024**, *9*, e202401275.

4. **T. Shirisha**, S. Majhi, and D. Kashinath, "TBAI-TBHP Mediated C4-selective C(sp3)-H sulfonylation of 1,2,3,4-tetrahydroacridines and oxidative desulfonylation to 2,3-dihydro acridin-4(1H)-ones" *Chemistryselect*, Accepted Manuscript.

List of publications (as co-author)

1. N. Satyanarayana, K. Sathish, S. Nagaraju, R. Pawar, M. Faizan, M. Arumugavel, **T. Shirisha** and D. Kashinath, "Metal-free, one-pot synthesis of 2-styrylquinolines *via* Friedländer annulation and sp 3 C–H activation using 1, 3-dimethylurea and L-tartaric acid (3: 1) as a deep eutectic solvent" *New J. Chem.* **2022**, *46*, 1637-1642.
2. N. Satyanarayana, B. R. Sree, K. Sathish, S. Nagaraju, K. Divakar, R. Pawar, **T. Shirisha** and D. Kashinath, "Synthesis of 2-styryl-quinazoline and 3-styryl-quinoxaline based sulfonate esters *via* sp^3 C–H activation and their evaluation for α-glucosidase inhibition" *New J. Chem.* **2022**, *46*, 5162-5170.
3. N. Satyanarayana, S. Nagaraju, **T. Shirisha**, D. Kashinath, "One-pot synthesis of 2-thioxothiazolidin-4-one, thiazolidine-2,4-dione, 2-iminothiazolidin-4-one based spiro-thiolane and bicyclic chromene-thiolane hybrids via Knoevenagel, 1,4-sulfa-Michael and aldol Reactions" *Arkivoc* **2022**, *part vi*, 280-297.

List of publications under review

1. "Deep Eutectic Solvent mediated synthesis of C-4 functionalized Pftzinger acid derivatives and their biological evaluation as choline esterase inhibitors" **T. Shirisha,** S. Majhi, K. Divakar, D. Kashinath. *Submitted manuscript, under review*.
2. "Unveiling Boric/Boronic Acid Mediated Redox Reaction of 4-hydroxy-1,2,3,4-Tetrahydroacridine N-Oxides Through Mechanistic Studies" Subir Majhi, **Thangellapally Shirisha**, Mohmmad Faizan, Ravinder Pawar, Dhurke Kashinath. *Submitted manuscript, under revision.*
3. "Chemodivergent synthesis of (1,2,3-triazolo)chalcone and bis-1,2,3-triazolylmethanones via [3+2]-cycloaddition reactions using ZnO, Bi2WO6 nanoparticles in aqueous medium" Banoth Paplal, **Thangellapally Shirisha**, Subir Majhi, Kota Sathish, Sakkani Nagaraju, Sridhar Balasubramanian, and Dhurke Kashinath. *Submitted manuscript, under review*.

The author Mrs. T. Shirisha was born in Warangal, Telangana state, India. She received B.Sc. degree from Padmavathi Degree College for Women (affiliated to Kakatiya University), Warangal in 2004 and M.Sc. degree from Chaithanya Degree and P.G. College (affiliated to Kakatiya university), Warangal in 2006. After completing her M.Sc., she worked as lecturer at L.B. College P.G. Center. In 2018 she joined in the Ph.D. programme under the guidance of Dr. D. Kashinath, Professor in the Department of Chemistry, National Institute of Technology Warangal. Presently, she is continuing as Senior Research Fellow in the Department of Chemistry, National Institute of Technology-Warangal. Her research interests are development of synthetic methods and synthesis of biologically active compounds.

Published papers

Organic & Biomolecular Chemistry

ROYAL SOCIETY OF CHEMISTRY

PAPER

View Article Online
View Journal | View Issue

Cite this: *Org. Biomol. Chem.*, 2024, **22**, 790

Metal-free synthesis of functionalized tacrine derivatives and their evaluation for acetyl/butyrylcholinesterase and α-glucosidase inhibition†‡

Thangellapally Shirisha,[a] Subir Majhi,[a] Kalivarathan Divakar*[b] and Dhurke Kashinath *[a]

Received 27th October 2023,
Accepted 13th December 2023

DOI: 10.1039/d3ob01760e

rsc.li/obc

A mild and greener protocol was developed for C–C (C(sp^3)–H functionalization) and C–N bond formation to synthesize functionalized tacrine derivatives using a biodegradable and reusable deep eutectic solvent [(DES) formed from *N*,*N*′-dimethyl urea and L-(+)-tartaric acid in a 3 : 1 ratio at 80 °C]. The condensation of 9-chloro-1,2,3,4-tetrahydroacridines with a variety of aromatic aldehydes gave unsaturated compounds *via* C(sp^3)–H functionalization (at the C-4 position) with good yields. The substituted *N*-aryl tacrine derivatives were obtained from the condensed products of 9-chloro-1,2,3,4-tetrahydroacridine with substituted anilines *via* the nucleophilic substitution reaction (SN^2 type) in the DES with good yields. This is the first example of C4-functionalized tacrine derivatives, highlighting the dual capacity of the DES to serve as both a catalyst and a solvent for facilitating C–N bond formation on acridine. The generated compounds were evaluated for acetyl/butyrylcholinesterase (AChE/BChE) and α-glucosidase inhibitory activity. It was found that the majority of the compounds reported here were significantly more potent inhibitors than the standard inhibitor tacrine (AChE IC_{50} = 203.51 nM; BChE IC_{50} = 204.01 nM). Among the compounds screened, **8m** was found to be more potent with IC_{50} = 125.06 nM and 119.68 nM towards AChE and BChE inhibition respectively. The α-glucosidase inhibitory activity of the compounds was tested using acarbose as a standard drug (IC_{50} = 23 100 nM) and compound **8j** was found to be active with IC_{50} = 19 400 nM.

Introduction

Acridine and 1,2,3,4-tetrahydroacridine derivatives constitute a prominent group of nitrogen-containing heterocycles due to their enormous range of biological activities.[1] Numerous natural and synthetic acridines have been extensively investigated as prospective therapeutic agents for the treatment of cancer,[2] Alzheimer's disease and bacterial and protozoan infections,[3] and α-glucosidase inhibition.[4] Beyond their biological activities, these acridines have garnered significant attention in recent years in the area of materials science because of their promising photophysical and electrochemical characteristics as organic electronic devices and organic light-emitting diodes.[5]

Tacrine (9-amino-1,2,3,4-tetrahydroacridine), a competitive cholinesterase inhibitor, has been proven to be effective in treating Alzheimer's patients with low to moderate dementia.[6] Unfortunately, tacrine administration is associated with a significant rate of hepatotoxicity. This is one of the major constraints for the administration of tacrine.[7] Therefore, significant efforts have been directed towards the development of tacrine derivatives with enhanced inhibitory activity for acetyl/butyrylcholinesterase (AChE/BChE) with lower hepatotoxic effects including multi-targeted AChE inhibitors. The majority of these modifications are replacing the aromatic moiety (benzene ring) of tacrine into heterocyclic rings using multi-component reactions (MCRs).[8] Along with these, the $-NH_2$ moiety of tacrine was used to generate an array of hybrid molecules by incorporating tacrine, 8-hydroxyquinoline, coumarin, chromene, cysteine, benzothiazole, and melatonin at the other end[9] (Fig. 1). Among these, the alkylene-linked bis-tacrines (**I**) were 1000 times more potent than tacrine due to their dual interaction with cholinesterase.[10] In a similar context, *N*-aryl tacrines (**H**) were synthesized *via* metal-catalysed reactions

[a]*Department of Chemistry, National Institute of Technology, Warangal-506 004, India. E-mail: kashinath@nitw.ac.in, kashinath.dhurke@gmail.com; Tel: +91-870-2462677*
[b]*Department of Biotechnology, Sri Venkateswara College of Engineering (Autonomous), Sriperumbudur, Tamilnadu-602 117, India. E-mail: divakar@svce.ac.in, kdivak@gmail.com*

† Dedicated to Prof. Sambasivarao Kotha on the occasion of his retirement from the services.

‡ Electronic supplementary information (ESI) available. See DOI: https://doi.org/10.1039/d3ob01760e

Organic & Biomolecular Chemistry

ROYAL SOCIETY OF CHEMISTRY

PAPER

View Article Online
View Journal | View Issue

Cite this: *Org. Biomol. Chem.*, 2024, **22**, 1434

Metal-free C(sp^3)–H functionalization (C–C and C–N bond formation) of 1,2,3,4-tetrahydroacridines using deep eutectic solvents as catalyst and reaction medium†

Thangellapally Shirisha,[a] Subir Majhi,[a] Sridhar Balasubramanian[b,c] and Dhurke Kashinath *[a]

Received 26th October 2023,
Accepted 11th January 2024

DOI: 10.1039/d3ob01752d

rsc.li/obc

Herein, we report a metal-free and efficient method for the C(sp^3)–H functionalization of 1,2,3,4-tetrahydroacridines at the C4-position by the addition of azodicarboxylates (C–N bond) and maleimides (C–C bond) using deep eutectic solvents (DESs) at 80 °C. The C4-functionalized 1,2,3,4-tetrahydroacridines were achieved with high atom efficiency, precise regioselectivity, and yields ranging from 70–96%. The practicality of the developed method has been demonstrated through gram-scale synthesis. Also the green-metrics were calculated for the developed method and it was found that the metrics are near to the ideal values.

Introduction

Direct functionalization of inactive C–H bonds is a current topic of research and strategy for the construction of C–C and C–X (X = O, N, and S) bonds in organic synthesis.[1] This method can offer maximum atom efficiency by avoiding pre-functionalization of substrates, and is thus widely explored in the field of synthetic organic chemistry.[2] The development of a new catalytic system for the direct amination of inert C(sp^3)–H bonds without the use of pre-functionalized substrates to construct C–N bonds remains one of the major challenges.[3] Due to the inert nature of the C(sp^3)–H bond, the hydrogen atom transformation (HAT) strategy and *N*-oxyl radicals provide a potent synthetic approach to achieve the desired functionalization.[4] The inert C–H bond activation has been achieved by the addition of carbon nucleophiles to the N=N bond *via* electrophilic amination.[5]

Dialkyl azodicarboxylates serve as valuable reagents in Mitsunobu chemistry.[6] Besides this, dialkyl azodicarboxylates are used as electrophiles for C–N bond formation reactions *via* nucleophilic addition.[7–9] In this connection, Guo[3] and the Hung[5] groups reported transition metal catalysed amination of the un-activated C(sp^3)–H bond of 2-alkyl azaarenes using diethyl azodicarboxylate. Similarly, Saget and co-workers also reported Zn-ProPhenol catalysed amination of un-activated aryl and vinyl ketones with di-*tert*-butyl azodicarboxylate.[10] Later, Tang *et al.*[11] developed an efficient method for the amination of arenes with azodicarboxylates (Fig. 1).

Similar to dialkyl azodicarboxylates, maleimides exhibit versatile reactivity, participating in both electrocyclic processes as dienophiles and in conjugate additions as electropliles.[12] In addition to these, maleimides have been explored as the source for alkylation in transition metal-catalysed C(sp^3)–H and C(sp^2)–H bond functionalization leading to the generation of functionalized succinimides.[13] Due to the highly electrophilic nature of the unsaturated system, maleimides act as excellent alkylating agents, because of which they participate in hydroarylation/alkylation reactions instead of oxidative Heck reactions.[14] In many cases the generated succinimides were used as precursors for biologically active pyrrolidines and γ-lactams, thereby becoming one of the important and promising scaffolds in drug discovery.[15] The synthetic utility of maleimide as an alkylating agent has been further extended for the C(sp^3)–H functionalization of azaarenes. In this regard, Wang *et al.*[16] reported a catalyst-free C(sp^3)–H functionalization of 2-methyl quinoline. Similarly, Chen *et al.*[17] reported the C(sp^3)–H functionalization of 2-methyl quinoline using pepsin, an ionic liquid, and a deep eutectic solvent as the

[a]*Department of Chemistry, National Institute of Technology, Warangal-506 004, India. E-mail: kashinath@nitw.ac.in, kashinath.dhurke@gmail.com; Tel: +91-870-2462677*
[b]*Centre for X-ray Crystallography, Department of Analytical & Structural Chemistry, CSIR-Indian Institute of Chemical Technology, Tarnaka, Uppal Road, Hyderabad-500007, Telangana, India*
[c]*Academy of Scientific and Innovative Research (AcSIR), Ghaziabad-201 002, India*
† Electronic supplementary information (ESI) available. CCDC 2294878. For ESI and crystallographic data in CIF or other electronic format see DOI: https://doi.org/10.1039/d3ob01752d

ChemistrySelect

Research Article
doi.org/10.1002/slct.202401275

Chemistry Europe
European Chemical Societies Publishing

www.chemistryselect.org

One-Pot Synthesis of Functionalized Carbazoles and β-Carbolines *via* Diethyl Azodicarboxylate mediated Dehydrogenative Aromatization in Deep Eutectic Solvent

Thangellapally Shirisha,[a] Subir Majhi,[a] and Dhurke Kashinath*[a]

Herein we report a one-pot approach for the functionalized carbazoles and β-carbolines via Fischer indole/Pictet-Spengler type reactions followed by diethyl azodicarboxylate (DEAD) mediated dehydrogenative aromatization using Deep Eutectic Solvent (*N,N'*-Dimethyl urea and L-tartaric acid combination) as reaction medium. This one-pot method enables the synthesis of library of compounds of carbazoles and β-carbolines with good to excellent yields in short reaction times. The developed method was extended for the copper-mediated reaction to minimize the amounts of DEAD required. Also, the application of gram scale reaction and reusability of the DES (in both cases) is demonstrated efficiently.

Introduction

Carbazole, a fused [6-5-6] tricyclic system with a nitrogen in the five-membered ring constitute core structure of a diverse array of alkaloids (Figure 1) found in many natural and pharmaceutical ingredients.[1] These alkaloids exhibit a plethora of bioactivities and therapeutic properties, including antitumor,[2] antiviral,[3] psychotropic,[4] anti-Alzheimer's,[5] anti-inflammatory,[6] antibiotic,[7] and anti-oxidative,[8] anti-TB activities.[9] Furthermore many derivatives of carbazole are known to show remarkable electrical,[10] thermal,[11] optical,[12] organic light emitting properties,[13] and proved as important functional group in the development of organic photo/electroluminescent materials and organic solar cells.[14]

Several strategies are available for the synthesis of carbazoles *via* C–C or C–N coupling/cyclization reactions in the presence of transition metals such as Iron,[15] palladium,[16] rhodium,[17] copper[18] and iridium[19] or without transition metal catalyst,[20] in the presence of visible light,[21] and electrochemical anodic oxidation.[22] Besides these sophisticated methods, aromatisation of Fischer-Borsche ring approach for carbazole synthesis is an established process. This involves the condensation of arylhydrazine with cyclohexanone followed by oxidative aromatization to yield the corresponding carbazole. Recently this method has been reported under modified conditions using low melting mixture as catalyst and reaction medium,[23] and reagents like Pd/C,[24] $CuCl_2$/DMSO,[25] I_2/DMSO,[26] DDQ,[27] V_2O_5,[28a] NMP/O_2[28b] (Figure 1) for dehydrogenative aromatization of tetrahydrocarbazoles to produce carbazoles. Though these methods are good, a few of them require expensive catalysts with high catalyst load, elevated temperatures, and sometimes protection of the nitrogen in the central ring.

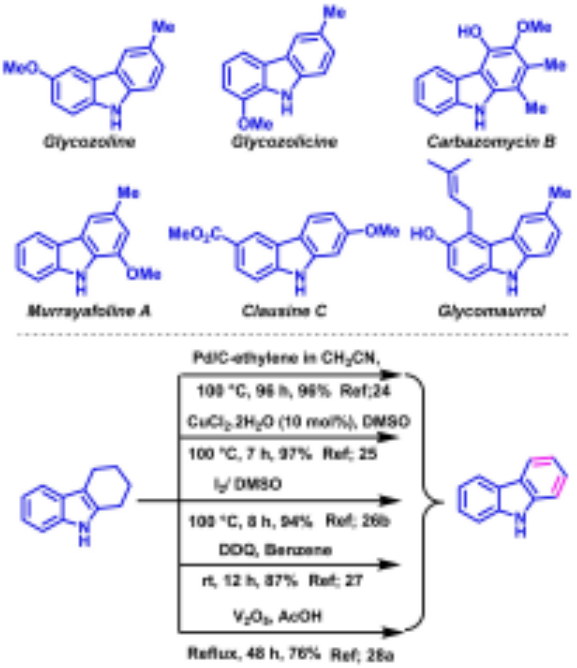

Figure 1. Bioactive natural carbazole and literature methods for the dehydrogenative aromatisation of tetrahydrocarbazoles to carbazoles β-carboline compounds.

β-Carboline is another intriguing alkaloid (an indole-based heterocyclic moiety/a fused [6-5-6] tricyclic system with a nitrogen in the five-membered ring and a 1H-pyrrolo[2,3-c] pyridine system) found in various pharmaceutical drugs and natural products[29] (Figure 2). Specifically, aromatic β-carboline derivatives exhibit excellent biological properties, such as antitumor,[30] anti-tubercular,[31] anti-viral activities,[32] and anti-

[a] T. Shirisha, S. Majhi, Prof. D. Kashinath
Department of Chemistry
National Institute of Technology Warangal
Warangal, India -506004
E-mail: kashinath@nitw.ac.in

Supporting information for this article is available on the WWW under https://doi.org/10.1002/slct.202401275

ChemistrySelect

Research Article
doi.org/10.1002/slct.202403503

Chemistry Europe
European Chemical Societies Publishing

www.chemistryselect.org

TBAI-TBHP Mediated C4-Selective C(sp^3)-H Sulfonylation of 1,2,3,4-Tetrahydroacridines and Oxidative Desulfonylation to 2,3-Dihydro Acridin-4(1H)-Ones

Thangellapally Shirisha,[a] Subir Majhi,[a] and Dhurke Kashinath*[a]

A site selective, metal-free C(sp^3)–H sulfonylation of 1,2,3,4-tetrahydroacridines is reported using sulfonyl hydrazides as sulfonyl source in the presence of a combination of tetrabutylammonium iodide (0.2 equiv.) and *tert*-butyl hydroperoxide (1 equiv.). This reaction was extended for the 2,3-dihydroacridin-4(1*H*)-ones *via* oxidative desulfonylation. Both sulfonylation and desulfonylation steps were achieved in good to excellent yields with broad substrate compatibility.

Introduction

Diaryl or alkyl-aryl sulfones are found in a wide range of bioactive molecules, natural products and agrochemical.[1] They exhibit diverse pharmacological properties, such as antibacterial,[2] antibiotic,[3] γ-secretase inhibitor activity.[4] Especially 2-sulfonylmethyl quinolines are used for the treatment of Alzheimer's disease,[5] hepatitis-B[6] and shows anti-proliferative activity[7] (Figure 1). In addition to this, the sulfonyl functional group serves as a versatile tool in organic synthesis for the Julia olefination,[8] fluoroalkylation[9] and Smiles rearrangement.[10] Generally, benzylic sulfones are synthesized by the oxidation of sulfides or sulfonylation with sulfonyl precursors, such as sulfonyl chlorides, sulfonic acids, sodium sulfonates, sulfonyl hydrazides, and sulfur dioxide as surrogates. Among these sulfonic precursors, sulfonyl hydrazides are easy to handle, stable, moisture-compatible, and non-corrosive.[11] Recently, direct C–H functionalization has attracted great interest since this method can potentially lead to more efficient synthesis with fewer number of synthetic operations.[12] In this connection, Xiao,[13a] Dong[13b] and Li[13c] groups have independently reported transition metal-free C(sp^3)–H sulfonylation of 2-methylquinolines using sodium sulfonates and tosyl hydrazides as sulfone sources (Figure 2A). In these cases, the combination of KI or tetrabutylammonium iodide (TBAI) with ^{t}butyl hydroperoxide (TBHP) has helped the transition metal-free oxidation process.[14]

Acridine, 1,2,3,4-tetrahydroacridine and quinoline derivatives form a significant class of nitrogen-containing heterocycles because of their plethora of biological activities, including anticancer,[15] anti-inflammatory,[16] anti-malarial,[17] and potent inhibitors of acetylcholinesterase,[18] α-glucosidase enzymes.[19]

Figure 1. Drugs containing organo sulfone compounds.

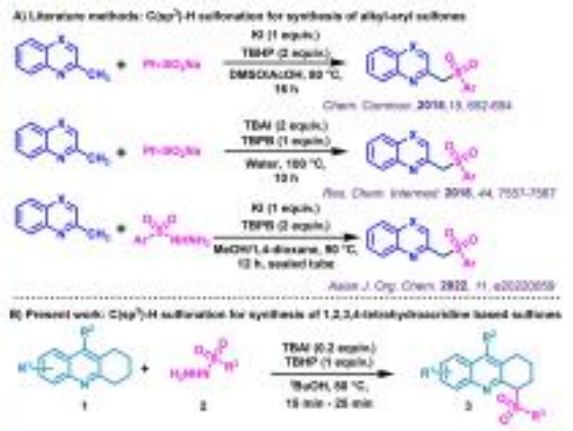

Figure 2. Previous reports for the C(sp^3)–H sulfonylation of 2-methyl quinolone and present method for the C(sp^3)–H sulfonylation of 1,2,3,4-tetrahydroacridine derivatives.

Considering the biological relevance of functionalized quinolines and 1,2,3,4-tetrahydroacridine, we have reported the metal-free C(sp^3)–H functionalization of quinolones, 1,2,3,4-tetrahydro acridines and tested their inhibitory activity towards acetylcholinesterase, α-glucosidase enzymes.[20]

[a] *T. Shirisha, S. Majhi, Prof. Dr. D. Kashinath*
Department of Chemistry, National Institute of Technology Warangal 506004, India
E-mail: kashinath@nitw.ac.in
kashinath.dhurke@gmail.com

Supporting information for this article is available on the WWW under https://doi.org/10.1002/slct.202403503